APSP 2021 MINSK

FUTURE.BY by ФЕРМЕНТ

BOOK OF ABSTRACTS

IX INTERNATIONAL SCIENTIFIC CONFERENCE

ACTUAL PROBLEMS OF SOLID STATE PHYSICS

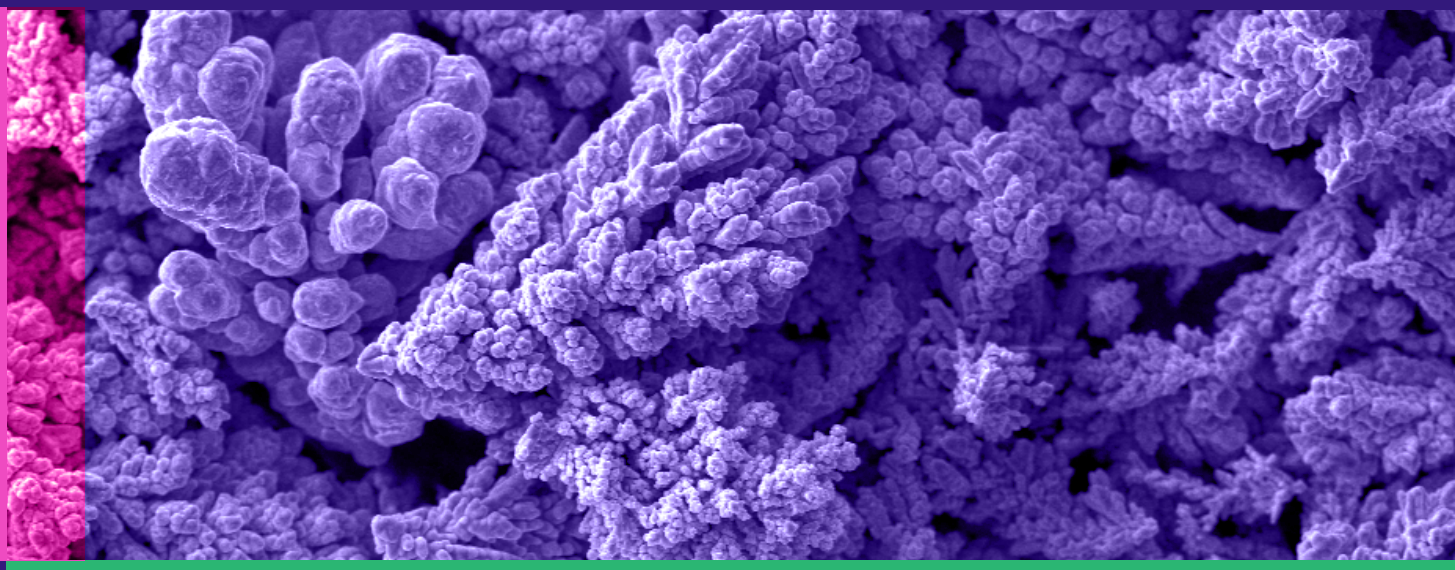

SCIENTIFIC-PRACTICAL MATERIALS RESEARCH CENTRE
OF NATIONAL ACADEMY OF SCIENCES OF BELARUS

MINSK, BELARUS

INTERNATIONAL SCIENTIFIC COMMITTEE

Dr. Valery Fedosyuk

Scientific-Practical Materials Research Centre of NAS of Belarus, Minsk, Belarus

Scientific Interests:

Dr. Valery Fedosyuk carried out studies of amorphous and nanocrystalline soft magnetic and hard magnetic films of alloys of the iron group with a number of metalloids and refractory metals. He created a direction in obtaining and researching nanoscale multilayer magnetic structures with a thickness of up to several atomic layers by means of pulsed electrolytic deposition. He discovered the effect of isotropic "giant" magnetoresistance, due to the predominant scattering of conduction electrons with different spin directions on the magnetic moments of neighboring nanolayers with repeating antiparallel orientation.

Main Publications:

V. Fedosyuk *[et al.] Giant magnetoresistance in granular electrodeposited CuCo films. Journal of Magnetism and Magnetic Materials 165 (1995) 345-346.*

V. Fedosyuk *[et al.] Granular AgCo and AgCuCo nanowires. Journal of Magnetism and Magnetic Materials 198 (1999) 246-247.*

V. Fedosyuk *[et al.] Control of growth mechanism of electrodeposited nanocrystalline NiFe films. Journal of the Electrochemical Society 166 (2019) 173-180.*

Dr. Andrey Ivanets

Institute of General and Inorganic Chemistry NAS Belarus, Minsk, Belarus

Scientific Interests:

- Physical and Colloidal Chemistry;
- Inorganic adsorbents, Ceramic membranes, Catalysts for Advanced Oxidation Processes;
- Theoretical and experimental researches in the field of water treatment.

Main Publications:

A. Ivanets *[et al.] A comparative study on the synthesis of magnesium ferrite for the adsorption of metal ions: Insights into the essential role of crystallite size and surface hydroxyl groups. Chemical Engineering Journal. 411 (2021) 128523.*

A. Ivanets *[et al.] Effect of Mg2+ ions on competitive metal ions adsorption/desorption on magnesium ferrite: mechanism, reusability and stability studies. Journal of Hazardous Materials. 411 (2021) 124902.*

A. Ivanets *[et al.] One-stage adsorption treatment of liquid radioactive wastes with complex radionuclide composition. Water, Air, & Soil Pollution. 231 (2020) 1-10.*

Prof. Sergey Aplesnin

Reshetnev Siberian State University of Science and Technology, Krasnoyarsk, Russia

Scientific Interests:

The creation of multifunctional materials that combine transport properties and multiferroics form the basis for the development of the technological base of many newest nanoelectronic devices. Influence of the orbital degrees of freedom of an electron on magnetotransport properties of disordered orbitally degenerate semiconductors with strong electronic correlations in the high-temperature range, which is important in the development and creation of an element base for microelectronics. In the region of electronic phase transitions of a metal-insulator with a strong electron-phonon interaction, it is possible to switch the sign of current carriers by ultrasound due to the electron-phonon interaction. In two-phase semiconductor-multiferroic materials, conducting channels with bistable current states are created at the interface.

Main Publications:

S. Aplesnin *[et al.] Magnetoresistance effect in anion-substituted manganese chalcogenides. Physica status solidi b, 252 (2015), 1792-1798.*

S. Aplesnin *[et al.] Bi2(Sn0.95Cr0.05)2O7: Structure, IR specture, and dielectric properties. Ceramics International, 42 (2016) 5177-5183.*

S. Aplesnin *Magnetoelectric and magnetoresistive properties of the CexMn1–xS semiconductors. Physica Status Solidi B, Vol. 253 (2016) 1771-1781.*

Prof. Abdulhadi Baykal

Department of Nanomedicine Research, Institute for Research & Medical Consultation,
Imam Abdulrahman Bin Faisal University, Dammam, Saudi Arabia

Scientific Interests:

My main research area is magnetic nanomaterials. Their synthesis, structural, magnetic, optic, Mossbauer and Microwave absorption characterizations are within my research field. I focused mainly on nanospinel ferrites (normal, inverse and mixed) and M-type nanohexaferrites (mainly on BaFe12O19 and SrFe12O19). And I am also studying on anticancer/antifungal and antibacterial activity of various types spinel nanoferrites and recyclable spinel nanocatalyst.

Main Publications:

A. Baykal *[et al.] Correlation between chemicalcomposition, electrical, magnetic and microwave properties in Dy-substituted Ni-Cu-Zn ferrites, Mat. Sci and Eng. B 270 (2021) 1152020.*

A. Baykal *[et al.] Impact of the exfoliated graphite on magnetic and microwave properties of the hexaferrite-based composites, J. Alloys Compd. 878 (2021) 160397.*

A. Baykal *[et al.] Delivery, fate, and physiological effect of engineered cobalt ferrite nanoparticles in barley (Hordeum vulgare L.), Chemosphere 265 (2021) 129138.*

Dr. Mengge Dong

Department of Resource and Environment, School of Metallurgy, Northeastern University, Shenyang, China

Scientific Interests:

Comprehensive utilization of metallurgy resources and low cost radiation protection materials; new theory and technology for radiation protection; the interactions between the shielding materials and the radiation rays; the relationship of the composition, structural and performance; the interaction between the complex shields and radiation rays.

Main Publications:

M. Dong *[et al.] A novel comprehensive utilization of vanadium slag: As gamma ray shielding material. Journal of Hazardous Materials, 318 (2016) 751-757.*

M. Dong *[et al.] A novel method of utilization of hot dip galvanizing slag using the heat waste from itself for protection from radiation. Journal of Hazardous materials, 344 (2018) 602-614.*

M. Dong *[et al.] Using Iron Concentrate in Liaoning Province, China, to Prepare Material for X-Ray Shielding. Journal of Cleaner Production, 210 (2019) 653-659.*

Prof. Sergey Gaponenko

Laboratory of the Institute of Physics named after B.I. Stepanov of the National Academy of Sciences of Belarus

Scientific Interests:

Scientific research in the field of nanostructure physics and condensed matter optics. Established the role of impurity recombination in the formation of nonlinear optical properties of semiconductor crystals. For the first time, he discovered and investigated the inhomogeneous broadening of the optical spectra of semiconductor nanocrystals in dielectric matrices and established a number of fundamental laws governing the evolution of the properties of nanoparticles during the transition from low-atomic clusters to bulk solids.

Main Publications:

S. Gaponenko *Introduction to nanophotonics. Cambridge University Press (2010) 465.*

S. Gaponenko *[et al.] Possible nanoantenna control of chlorophyll dynamics for bioinspired photovoltaics. Scientific Reports 9 (2019) 7138.*

O. Kulakovich *[et al.] Photostability enhancement of InP/ZnSe/ZnSeS/ZnS quantum dots by plasmonic nanostructures Nanotechnology 32 (2021) 035204.*

Prof. Sergey Gavrilov

Institute for Advanced Materials and Technologies of the National Research University "MIET", Moscow, Zelenograd, Russia

Scientific Interests:

-Surface physics and chemistry;
-Physicochemistry of nanostructured materials;
-Electrochemical processes in micro- and nanoelectronic technology;
-Low-temperature methods for the synthesis of nanostructured materials.

Main Publications:

S. Gavrilov *[et al.] Manifestation of the heterogeneous mechanism upon melting of low-dimensional systems. Physics of Solid State 2135, 51(10) 2009.*

S. Gavrilov *[et al.] Thermodynamic potential and phase diagram for multiferroic bismuth ferrite (BiFeO3), npj Comp. Mater. 20, 3(1) 2017.*

S. Gavrilov *[et al.] Investigation of tip-induced ultrathin Ti film oxidation kinetics Nanotechnology 273 , 12(3) 2001.*

Prof. Sakin Jabarov

Institute of Radiation Problems, Baku, Azerbaijan

Scientific Interests:

My research interests focus on condensed matter physics and material science, with main interest in phase transitions in perovskite structured ferroelectrics and multiferroics. I am also interested in experimental methods such that X-ray diffraction, neutron diffraction and Raman spectroscopy.

Main Publications:

S. Jabarov *[et al.] Probabilistic model of structural phase transition in perovskites. Modern Physics Letters B. 35 (2021) 2150211.*

S. Jabarov *[et al.] Investigation of structural and optical properties of zirconia dioxide nanoparticles by radiation and thermal methods. Modern Physics Letters B. 35 (2021) 2150050.*

S. Jabarov *[et al.] Effect of electron beam on the crystal structure of nanoscale Al particles. Modern Physics Letters B. 34 (2021) 2050531.*

Prof. Sergey Khakhomov

Francisk Skaryna Gomel State University, Gomel, Belarus

Scientific Interests:

Research interests are concentrated in the field of optics and acoustics of crystals and artificial anisotropic structures.

Main Publications:

S. Khakhomov *[et al.] Broadband Reflectionless Metasheets: Frequency-Selective Transmission and Perfect Absorption. Physical Review X 031005, 5 2015.*

S. Khakhomov *[et al.] Modeling of Spirals with Equal Dielectric, Magnetic, and Chiral Susceptibilities. Electromagnetics 476, 28(7) 2008.*

S. Khakhomov *[et al.] Reflection and transmission by a uniaxially bi-anisotropic slab under normal incidence of plane waves. Journal of Physics D: Applied Physics 2458, 31 1998.*

Prof. Andrey Kholkin

Laboratory of Advanced Microscopy of Functional Materials of CICECO -Aveiro Institute of Materials, Aveiro, Portugal

Scientific Interests:

Nanoscale properties of functional materials via scanning probe techniques; Dielectric, piezoelectric, pyroelectric and ferroelectric properties of materials and structures; Ferroelectric polymers and self-organized bioorganic materials for biology and medicine; Materials for sensors and actuators, microelectromechanical systems, and energy harvesting; Nanoscale properties of Li-battery materials; 2D materials for electronics.

Main Publications:

A. Kholkin *[et al.] Interferometric measurements of electric fieldinduced displacements in piezoelectric thin films. Rev. Sci. Instrum. 1935, 67(5) 1996.*

A. Kholkin *[et al.] Nanoscale ferroelectrics: processing, characterization and future trends. Rep. Prog. Phys. 2443, 69(8) 2006.*

A. Kholkin *[et al.] Strong Piezoelectricity in Bioinspired Peptide Nanotubes. ACS Nano. 610, 4(2) 2010.*

Prof. Konstantin Kozadaev

Belarusian State University, Minsk, Belarus

Scientific Interests:

Atmosphere Laser Deposition of Metal Nanostructures: Theory and Experiment, Photovoltaic Devises with Metal Nanostructures, SERS Substrates (Substrates for Diagnostics of Ultra Small Amounts of Substances 10-10-10-11 M). Simulation of EM Properties of Surface Metal Nanostructures, Information Technologies.

Main Publications:

K. Kozadaev *[et al.] Proposal for a photoacoustic ultrasonic generator based on Tamm plasmon structures. Optics Express, 2020, 28(18), 26161–26169.*

K. Kozadaev *[et al.] A device for atmospheric laser deposition of noble metal nanostructures. Instruments and Experimental Techniques, 2016, 59(6), 865–869.*

K. Kozadaev *[et al.] Condensation of ablation plumes in the irradiation of metals by high-intensity nanosecond laser pulses at atmospheric pressure. Quantum Electronics, 2016, 46(1), 16–22.*

Prof. Nikolay Kuleshov

Department of Laser Engineering and Technology, Belarusian National Technical University, Minsk, Belarus

Scientific Interests:

Physics of solid-state lasers based on new laser materials.

Main Publications:

N. Kuleshov *[et al.] Pulsed laser operation of Yb-doped KY(WO4)2 and KGd(WO4)2. Optics Letters 1317, 22(17) 1997;*

N. Kuleshov *[et al.] CW laser performance of Yb and Er,Yb doped tungstates. Applied Physics B 409,64 1997;*

N. Kuleshov *[et al.] 240-fs pulses with 22-W average power from a mode-locked thin-disk Yb:KY(WO4)2 laser. Optics Letters 1162, 27(13) 2002.*

Prof. Dmitry Migas

Belarusian State University of Informatics and Radioelectronics, Minsk, Belarus

Scientific Interests:

ab initio investigation of structural, electronic, optical, magnetic and transport properties of materials including bulk, thin films (including 2D structures), surfaces and nanowires of semiconducting and metal silicides, IV and III-V compounds, metal oxides.

Main Publications:

D. Migas *[et al.] Effect of polaron formation on electronic, charge and magnetic properties of Nb12O29, J. Alloys Compd. 821 (2020), 153527.*

D. Migas *[et al.] Thermodynamic driving force in the formation of hexagonal-diamond Si and Ge nanowires, App. Surf. Sci. 545 (2021), 148948.*

D. Migas *[et al.] Orientation effects in morphology and electronic properties of anatase TiO2 one-dimensional nanostructures. I. Nanowires, Phys. Chem. Chem. Phys. 16 (2014), 9479.*

Prof. Nina Mironova-Ulmane

Institute of Solid State Physics University of Latvia, Riga, Latvia

Scientific Interests:

Materials Science, Biophysics, Medical Radiation Physics, Medical Physics, Single Crystal, Raman Spectroscopy, Infrared Spectroscopy, Near Infrared Spectroscopy, Electron Spin Resonance Spectroscopy.

Main Publications:

N. Mironova-Ulmane *[et al.] Excitation and emission spectra of LaInO3-based solid solutions doped with Sm3+, Sb3+. Journal of Luminescence 182 (2017) 123-129.*

N. Mironova-Ulmane *[et al.] E xcitation and photoluminescence spectra of solid solutions based on lanthanum indate LaInO3 of a perovskite structure doped with Nd3+ and Cr3+ ions. Glass Physics and Chemistry 42 (2016) 379-385.*

N. Mironova-Ulmane *[et al.] Luminescence and EPR spectroscopy of neutron-irradiated single crystals of magnesium aluminium spinel. Radiation Measurements 90 (2016) 122-126.*

Prof. Mohammed Sayyed

Imam Abdulrahman bin Faisal University (IAU), Dammam, Saudi Arabia

Scientific Interests:

Dr. M. I. Sayyed has been actively involved in the fields of development of various radiation shielding materials including glasses doped with heavy metal oxides, glass-ceramics and alloys. He has a good experience in the experimental measurements of the attenuation factors as well as on the computer simulations related to the radiation protection field. He is also working on the fabrication of novel glasses doped with HMO nanoparticles for radiation shielding applications.

Main Publications:

M. Sayyed *[et al.] A novel method of utilization of hot dip galvanizing slag using the heat waste from itself for protection from radiation. Journal of Hazardous Materials, 344 (2018) 602–614.*

M. Sayyed *[et al.] Using Iron Concentrate in Liaoning Province, China, to Prepare Material for X-Ray Shielding. Journal of Cleaner Production, 210 (2019) 653-659.*

M. Sayyed *[et al.] Physical, optical and gamma radiation shielding competence of newly borotellurite based glasses: TeO2–B2O3–ZnO–Li2O3–Bi2O3, Ceramics International 47 (2021) 611-618.*

Dr. Vladimir Shvartsman

Institute for Material Science, Faculty of Engineering, University of Duisburg-Essen, Essen, Germany

Scientific Interests:

-Scanning force microscopy: nanoscale characterization of electroactive materials;

-Ferroelectric, dielectric, and piezoelectric properties of materials;

-Multiferroics and magnetoelectrics.

Main Publications:

V.V. Shvartsman *[et al.] Lead-Free Relaxor Ferroelectrics. J. Am. Ceram. Soc. 95(1) 1-26, 2012.*

V.V. Shvartsma *[et al.] Temperature-Insensitive (K,Na)NbO 3 -Based Lead-Free Piezoactuator. Ceramics Adv. Funct. Mater. 4079, 23(33) 2013.*

V.V. Shvartsman *[et al.], Large bulk polarization and regular domain structure in ceramic BiFeO3. Appl. Phys. Lett. 172115, 90(17) 2007.*

Dr. Vladimir Sivakov

Leibniz Institute of Photonic Technology, Head of "Silicon Nanostructures" Group, Jena, Germany

Scientific Interests:

Significant experience in the field of thin film technology (since 1996) and surface analytics (since 1999) as well as semiconductor technology and nanophysics; research foci is concerned to the top-down or bottom-up nanostructured semiconductors and functional oxides formation, surface modification and characterization for renewable energy, nanomedicine and (bio)sensor applications.

Main Publications:

V. Sivakov *[et al.] Silicon sub-oxides as driving force for efficient light-enhanced hydrogen generation on silicon nanowires, Small 17 (8), 2007650 (2021).*

V. Sivakov *[et al.] Gold nanoflowers grown in a porous Si/SiO2 matrix: the fabrication process and plasmonic properties, Appl. Surf. Sci. 507, 144989 (2020).*

V. Sivakov *[et al.], Biodegradable porous silicon nanocontainers as an effective drug carrier for regulation of the tumor cell death pathways, ACS Biomaterials Science &Engineering 5 (11), 6063-6071 (2019).*

Prof. Ozcelik Suleyman

Director of Photonics Application and Research Center, Gazi University, Ankara, Turkey

Scientific Interests:

Skilled in Materials Science, Nanomaterials, electro-optical devices, bulk and epitaxial crystal growth, thin films technologies, Physics, Spectroscopy, and Business Strategy.

Main Publications:

S. Ozcelik *[et al.] Buffer optimization for crack-free GaN epitaxial layers grown on Si(1 1 1) substrate by MOCVD. Journal of Physics D: Applied Physics 155317,41 2008.*

S. Ozcelik *[et al.] Dislocation-governed current-transport mechanism in (Ni/Au)–AlGaN/AlN/GaN heterostructures. Journal of Applied Physics 023705,105(2) 2009.*

S. Ozcelik *[et al.] A 60 GHz Wireless Home Area Network With Radio Over Fiber Repeaters. Semiconductor Science and Technology 75003, 2436(24) 2009.*

Prof. Sergio Sombra

Federal University of Ceara (UFC) Fortaleza,Brazil

Scientific Interests:

Prof. A.S.B. Sombra was born in Jaguarauana ,CE ,Brazil. He received the BSc and MSc degree in Physics from Federal University of Ceará (UFC) in 1981 and 1984, respectively, and the PhD from the Federal University of Pernambuco(UFPE) in 1990. He is head of the Telecommunications and Materials Science and Engineering Laboratory (LOCEM) at the Physics Department at Federal University of Ceara (www.locem.ufc.br). The main interest areas include research and development in optical fiber and planar devices for optical networks. He is also involved in the study of electric, dielectric and piezoelectric properties of new ceramics, glasses, polymers and films for antennas, microwave and radio-frequency (RF) applications.

Main Publications:

A.S.B. Sombra *[et al.] Investigation of structural, hysteresis and electromagnetic parameters for microwave absorption application in doped Ba–Sr hexagonal ferrites at X-band. Journal of Alloys and Compounds, 806 (2019) 1220-1229.*

A.S.B. Sombra *[et al.] Bandstop Passive Filter Characteristics of Hexagonal Ferrite Composites at X-Band. Journal of Electronic Materials, 48 (2019) 6189–6193.*

A.S.B. Sombra *[et al.] Dielectric and microwave properties of common sintering aids for the manufacture of thermally stable ceramics . Ceramics International , 45 (2019) 20446-20450.*

Prof. Atul Thakur

Amity University Haryana, India

Scientific Interests:

The leading area of research includes nanomaterials, nanocomposites, nanoelectronics, nanofabrication, nanobiotechnology, ferrites for microwave applications, high frequency applications, radar absorbing materials, water purification, DNA biosenosrs, nanosensors, diamond synthesis, metamaterials, agricultural applications of nanomaterials, renewable energy, different translational aspects of Nanotechnology viz. 3D printing and fabrication technology, agriculture applications, nanosensor development & synthesis of diamonds etc.

Main Publications:

A. Thakur *[et al.] Dielectric Resonator Negative Group Delay Circuit. Radio Science. 56 (2021).*

A. Thakur *[et al.] Diakoptics Modelling Applied to Flying Bird-Shape NGD Microstrip Circuit . IEEE Transactions on Circuits and Systems II: Express Briefs . 68 (2021) 637 - 641.*

A. Thakur *[et al.] Potential of Magnetic Nanoferrites in Removal of Heavy Metals from Contaminated Water: Mini Review. Journal of Superconductivity and Novel Magnetism 33 (2020) 3651–3665.*

Dr. Denis Vinnik

South Ural State University, Chelyabinsk, Russia

Scientific Interests:

-Synthesis of ferrite flux single crystal and powders

-Functional oxide single crystal growth (leucosapphire, ruby, lead germinates)

-Design of novel equipment for crystal growth

-High-temperature experiment and equipment

Main Publications:

D. Vinnik *[et al.] Correlation of the Fe content and entropy state in multiple substituted hexagonal ferrites with magnetoplumbite structure. Ceramics International, 2021, 47 (12), 17684–17692.*

D. Vinnik *[et al.] Structure and magnetodielectric properties of titanium substituted barium hexaferrites. Ceramics International, 2021, 47 (12), pp. 17293–17306.*

D. Vinnik *[et al.] Structure and magnetic properties of a new hexaferrite (Ba,Pb)(Fe,Ti)9O15. Ceramics International, 2021, 47 (4) 5341–5346.*

Prof. Xiangxin Xue

Department of Resource and Environment, School of Metallurgy, Northeastern University, Shenyang, China

Scientific Interests:

-Shielding materials for radiation rays;
-Energy materials;
-Catalytic materials;
-Electromagnetic shielding materials;
-The relationship of the compositions, structural and performance;
-Comprehensive utilization of solid waste;
-Industry waste water treatment and recycling.

Main Publications:

X. Xue *[et al.] Degradation of organic dyes by a new heterogeneous Fenton reagent-Fe2GeS4 nanoparticle. Journal of hazardous materials, 353, 182-189.*

X. Xue *[et al.] A novel comprehensive utilization of vanadium slag: As gamma ray shielding material. Journal of Hazardous Materials, 318 (2016) 751-757.*

X. Xue *[et al.] A novel method of utilization of hot dip galvanizing slag using the heat waste from itself for protection from radiation. Journal of Hazardous materials, 344 (2018) 602-614.*

Prof. Maxim Zdorovets

The Institute of Nuclear Physics, Nur-Sultan, Kazakhstan

Scientific Interests:

-Fundamental and applied research at the heavy ion accelerator DC-60 in the field of radiation materials science, nuclear physics and solid state physics.
-Research of polymer track-etched membranes and development of filtering elements based on them.
-Research in the field of nanotechnology and advanced materials science: synthesis of 3D nanostructures and development of nanoelectronic elements based on them.
-Preparation of magnetic nanomaterials, applicable as carriers for targeted drug delivery.
-Development of technology for creating anode materials for lithium-ion batteries based on nanostructures
-Study of radiation resistance and assessment of the applicability of nitride ceramics.

Main Publications:

M. Zdorovets *[et al.] Efficiency of magnetostatic protection using nanostructured permalloy shielding coatings depending on their microstructure. Nanomaterials. 11 (2021) 634.*

M. Zdorovets *[et al.] Study of changes in optical and heat-conducting properties of AlN ceramics under irradiation with Kr15+ and Xe22+ heavy ions. Nanomaterials 10 (2020) 2375.*

M. Zdorovets *[et al.] Ion charge influence on the molecular structure of polyethylene terephthalate films after irradiation with swift heavy ions. Crystals 10 (2020) 479.*

Prof. Di Zhou

Xi'an Jiaotong University, Xi'an, China

Main Publications:

D. Zhou *[et al.] High permittivity and low loss microwave dielectrics suitable for 5G resonators and low temperature co-fired ceramic architecture, Journal of Materials Chemistry C 5 (38), 10094-10098, 2017.*

D. Zhou *[et al.] Novel temperature stable high-εr microwave dielectrics in the Bi2O3–TiO2–V2O5 system, Journal of Materials Chemistry C 4 (23), 5357-5362, 2016.*

D. Zhou *[et al.] Microwave Dielectric Properties of Li2WO4 Ceramic with Ultra-Low Sintering Temperature, Journal of the American Ceramic Society 94 (2), 348-350, 2011.*

D. Zhou *[et al.] Microwave Dielectric Ceramics in Li2O–Bi2O3–MoO3 System with Ultra-Low Sintering Temperatures, Journal of the American Ceramic Society 93 (4), 1096-1100, 2010.*

D. Zhou *[et al.] Bi2O3–MoO3 binary system: an alternative ultralow sintering temperature microwave dielectric, Journal of the American Ceramic Society 92 (10), 2242-2246, 2009.*

Prof. Zhipeng Sun

School of Materials and Energy, Guangdong University of Technology, Guangzhou, China

Scientific Interests:

-Energy storage materials and devices;
-Structural design and functional control of catalyst materials.

Main Publications:

Z. Sun *[et al.] One-step hydrothermal synthesis of NiCo2S4 nanoplates/nitrogen-doped mesoporous carbon composites as advanced electrodes for asymmetric supercapacitors. Journal of Power Sources 439 (2019) 227082.*

Z. Sun *[et al.] Three-dimensional macroporous W2C inverse opal arrays for the efficient hydrogen evolution reaction. Nanoscale 11 (2019) 11505.*

Z. Sun *[et al.] Facile synthesis of hexagonal single-crystalline ZnCo2O4 nanosheet arrays assembled by mesoporous nanosheets as electrodes for high-performance electrochemical capacitors and gas sensors. Applied Surface Science 457 (2018) 1103–1109.*

PROGRAM COMMITTEE

Prof. Nikolay Olekhnovich – Scientific-Practical Materials Research Centre of NAS of Belarus, Minsk, Belarus

Dr. Alexander Saiko – Scientific-Practical Materials Research Centre of NAS of Belarus, Minsk, Belarus

Dr. Denis Alikin – Ural Federal University named after the 1st President of Russia B.N.Yeltsin, Yekaterinburg, Russia

Dr. Mohamed Salem – Tanta University, Physics Department, Tanta, Egypt

Prof. Valery Sobol – M.Tank Belarusian State Pedagogical University, Minsk, Belarus

Dr. Alexey Dronov – National Research University of Electronic Technology, Moscow, Russia

Dr. Sergey Dubkov – National Research University of Electronic Technology, Moscow, Russia

Prof. Anatoly Dvurechenskii – A.V. Rzhanov Institute of Semiconductor Physics of the Siberian Branch of the RAS, Novosibirsk, Russia

Prof. Ryhor Fedaruk – University of Szczecin, Szczecin, Poland

Dr. Vladimir Gaishun – Gomel State University named after F. Skaryna, Gomel, Belarus

Dr. Ilya Gavrilin – Frumkin Institute of Physical Chemistry and Electrochemistry, Moscow, Russia

Prof. Viktor Kisel – Belarusian National Technical University, Minsk, Belarus

Dr. Anna Lukowiak – Institute of Low Temperature and Structure Research, Wrocław, Poland

Prof. Munirah Abdullah Almessiere – Imam Abdulrahman Bin Faisal University, Dammam, Saudi Arabia

Dr. Maxim Silibin – National Research University of Electronic Technology, Moscow, Russia

Prof. Yassine Slimani – Imam Abdulrahman Bin Faisal University, Dammam, Saudi Arabia

Dr. Sergey Demyanov , Dr. Sergey Grabchikov , Prof. Valeriy Gremenok , Dr . Oleg Ignatenko, Dr. Dmitry Karpinsky, Dr. Stanislav Lastovskii, Dr. Sergey Leonchik, Dr. Sergey Markevich, Dr. Vladimir Merkulov, Dr. Alexander Mudryi, Dr. Ihar Razanau, Dr. Alexandra Serokurova, Dr. Sergey Sharko, Dr. Elena Stanchik, Dr. Daria Tishkevich, Dr. Ekaterina Trukhanova, Dr. Kazimir Yanushkevich, Dr. Alexander Zheludkevich, Dr. Alena Zhivulko, Dr. Vadim Zhivulko, Dr. Tatiana Zubar – Scientific-Practical Materials Research Centre of NAS of Belarus, Minsk, Belarus

PHYSICAL & CHEMICAL TECHNOLOGIES

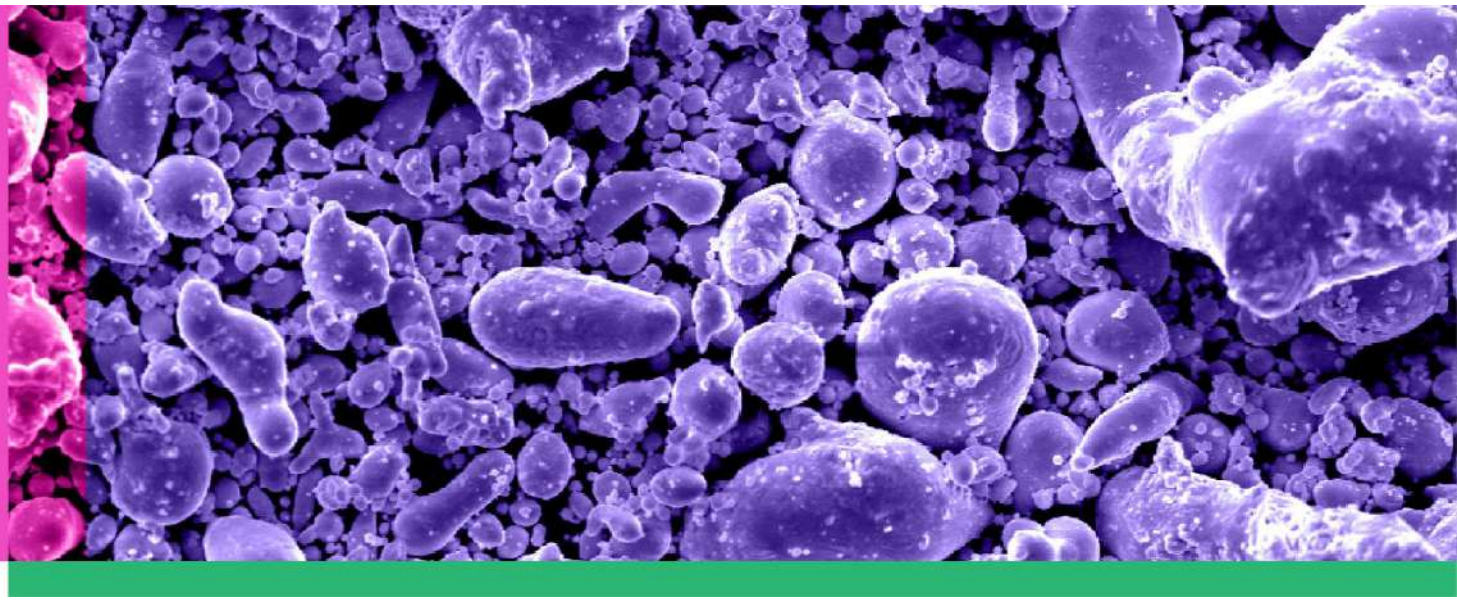

Influence of Rare Earth Ions on the Emission Properties of As_2S_3

S. Q. Asadullayeva[1]*, G.M.Fatullayeva[2], N.A. Ismayilova[1]
[1]*Institute of Physics, Azerbaijan National Academy of Sciences, Az-1143 Baku, Azerbaijan, e-mail for the corresponding author: sasadullayeva@mail.ru*
[2]*Institute of Catalysis and Inorganic Chemistry,Azerbaijan National Academy of Sciences, Az-1143 Baku, Azerbaijan*

Elementary high-purity substances were used for the synthesis of samples $(La_2O_3)_{0.05}(As_2S_3)_{0.90}(Er_2O_3)_{0.05}$: elements of 6N (As, S) and oxides Er_2O_3 (99.9 % (REO) and La_2O_3 (99.9 % (REO). The loaded ampoules were evacuated to a residual pressure of 10–5 Torr. The synthesis of glasses was performed in a shaft-type furnace with a temperature control system of ±5 K accuracy. Sealed silica ampoules was carried out at two temperature steps. The alloys for the glasses of the $(La_2O_3)_{0.05}(As_2S_3)_{0.90}(Er_2O_3)_{0.05}$ system with sample weight 3 g were presynthesized at 850 K and 3h exposure During the reaction, the furnace temperature was slowly increase to 875-1050K and continues for 4 h. Photoluminescence measurements were performed using PL/PLE/Raman spectrometer . The emission of the samples were excited by 532nm wavelength laser beams.The investigation was carried out in the visible region. Thus, at first step investigated the luminescence spectra As_2S_3:Er_2O_3 (Fig. 1). Thus, in the background of the large and intensive luminescence spectrum where maximum of As_2S_3 is in 650nm any transition of Er^{3+} ion is not observed.

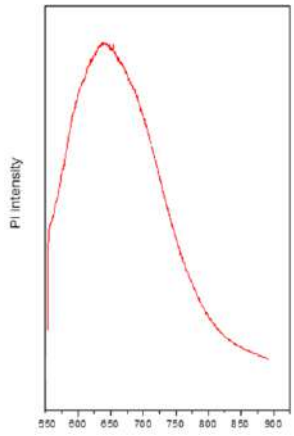

Fig.1 Photoluminescence spectrum of As_2S_3:Er_2O_3

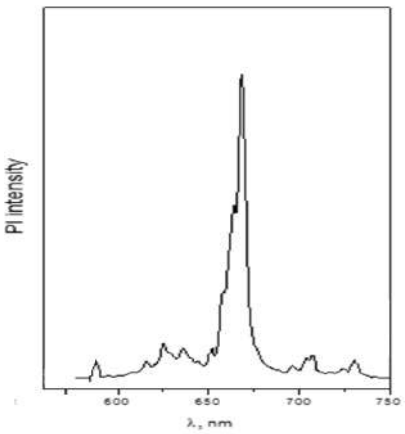

Fig.2 Photoluminescence spectrum of $(La_2O_3)_{0.05}(As_2S_3)_{0.90}(Er_2O_3)_{0.05}$

Inclusion two impurity lead to completely disappearing of maximum belonging to As_2S_3 in $(La_2O_3)_{0.05}(As_2S_3)_{0.90}(Er_2O_3)_{0.05}$ combination and to sharp increasing in the intensity of photoluminescence spectrum formed by interatomic transition of Er ions (covering 600nm-750nm region) especially increasing in intensity of photoluminescence was observed in $^4F_{9/2} \rightarrow {}^4I_{15/2}$ transition (Fig. 2). Looking at periodic literature, we can see that the lanthanum plays a sensitizer role for other rare earth elements [1-2]. From this point of view, inclusion additional La_2O_3, is lead to clearly visibility of the interatomic transitions of Er^{3+} ion.

References

[1] Chiharu Hidaka, Jun Hodotsuka, and Takeo Takizawa /Phys. Status Solidi C 6, (2009) p.1170–1173
[2] Reza Zamiri, Avito Rebelo, Hossein Abastabar Ahangar, Michael ScottBelsley, J.M.F. Ferreira Ceramics International 40,8, Part B, (2014) 12947-12951

Porous silicon as buffer layer for heteroepitaxy of GaN on silicon wafers

V. Bondarenko*, A. Dolgiy, N. Grevtsov and P. Pasikov
Belarusian State University of Informatics and Radioelectronics,
P. Brovka str. 6, 220013 Minsk, Belarus

PS layers were prepared on n+ type highly-doped silicon wafers via its galvanostatic electrochemical anodization in a room temperature and cooled electrolyte. The resulting Silicon wafers with PS buffer. After pre-treatment to sinter the uppermost parts of the PS buffer, thin GaN layers were grown via two-stage atomic-layer deposition (ALD). GaN epitaxial layers with thicknesses exceeding 0.5 microns were additionally grown via molecular beam epitaxy (MBE) with plasma activation of nitrogen

Evaluation of the X-ray diffraction patterns of the GaN/Si samples grown on substrates with single- and double-layer PS buffers has shown that for both sample types the most intense reflexes are the ones from the plane (111) of the silicon substrate and diffraction reflections (0002) and (0004) from the GaN layer, indicating the growth of GaN hexagonal wurtzite in its monocrystalline form. Reflections (0003) from the GaN layer and (222) from Si, which are forbidden for this measurement geometry, are also present. In the case of the GaN layer this can be attributed to a decrease in its crystallinity caused by the appearance of structural defects, while for Si (111) this is a matter of a slight deviation of its orientation from the (111) plane. Another characteristic feature of the resulting GaN/Si heterostructures is the presence of a GaN amorphous phase; presumably, it is formed during the nitriding stage before the epitaxial layer growth. The SEM images of the samples indicate that the GaN film had a thickness of 1.5 μm allowing a quality evaluation of the layer and the interfacial boundary between it and the PS buffer. For structures with single-layer PS serving as a buffer, the GaN film growth occurs on a substrate whose top layer adjacent to the interface has a porous structure. Depending on the type of buffer layer used, the GaN epitaxial layers also have different surface organization. The GaN film grown on single-layer PS has a rough surface with nanosized GaN phase islands 25-40 nm in height and 90-110 nm in diameter. On the other hand, the surface of the GaN layer grown on a double-layer PS buffer is made up of nanoscale blocks close to hexagonal in shape that have a more uniform and homogeneous morphological pattern. The GaN layer thickness uniformity on the substrates 76 mm in diameter did not exceed 1.5% with its refractive index being 1.90. Auger-electron spectroscopy combined with ion etching were used to determine the composition of GaN layers. It was found that the layers grown in the first stage were 300 nm thick and stoichiometric, containing 48.5 at% nitrogen and gallium and about 3 at% carbon and oxygen throughout their entire thickness. The GaN layers grown in the two-step process were 1.5 μm thick. They had a monocrystalline structure with the basic orientation [002] and very insignificant (no more than 0.5%) content of [0002]-oriented phases.

As the obtained photoluminescence spectra would indicate, for a GaN layer grown on a silicon substrate without a PS buffer layer, the primary luminescence band falls in the range of 500 to 600 nm and is mostly attributed to the layer's structural defects. For these samples, the emission that occurs around 350 nm due to the emission in GaN is very weak. At the same time, the GaN layer grown on a PS buffer layer by a combination of ALD and MBE methods is characterized by strong band-to-band emission at 350 nm, once again indicating high structural perfection of the resulting GaN layer.

It is concluded that the use of a double-layered PS buffer comprised of an upper thinner layer with a low porosity of 50%, formed in a cooled electrolyte, and a second thicker PS layer with a porosity of 65-70%, formed at room temperature, can improve the structural

perfection of GaN heteroepitaxial layers grown on silicon substrates by combining ALD and MBE.

The prospect of aluminum as a catalyst for the phase transition hBN-cBN

A. I. Alkhimenak[1]*, O. V. Ignatenko[1], V. S. Goncharov[1], I. I. Azarko[2]
[1]*SSPA "Scientific-Practical Materials Research Centre of NAS of Belarus", Belarus, Minsk, 19 P. Brovki st. * Alkhimenak@gmail.com*
[2]*Department of Semiconductor Physics and Nanoelectronics, BSU, Belarus, Minsk, 5 Bobruiskaya st.*

Cubic boron nitride(cBN) is a material similar in properties to diamond and is its heteroatomic analogue with higher chemical inertness and twice the thermal stability.

cBN is produced by a phase transition from hexagonal boron nitride (hBN) at high pressures (P) and temperatures (T) in the presence of solvent catalysts. A special place is occupied by catalysts that can be used as a binder.

In this work, samples were obtained with an aluminum content of 1, 2, 3, 5, 10, 20 wt. % at a pressure of 5 GPa and temperatures of 1500˚, 2000˚C. The samples obtained were investigated by X-ray phase analysis and electron paramagnetic resonance.

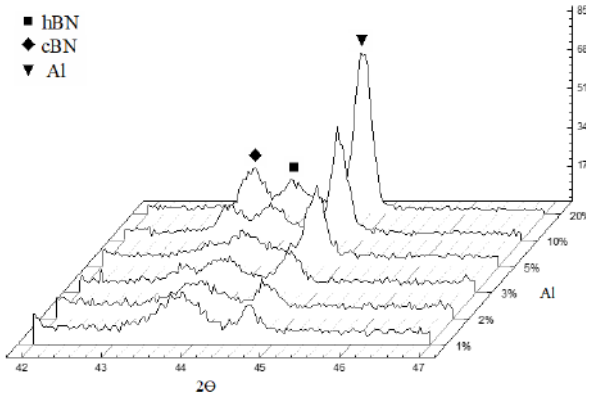

Figure 1 - X-ray diffraction patterns of samples with different Al content, sintered at a pressure of 5 GPa and a temperature of 1500° C in the 2θ range from 42 to 47

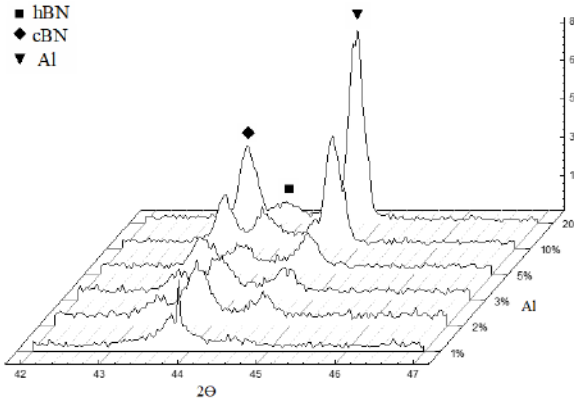

Figure 2 - X-ray diffraction patterns of samples with different Al content, sintered at a pressure of 5 GPa and a temperature of 2000° C in the 2θ range from 42 to 47

As a result of the studies performed on the sintered samples, the formation of aluminum nitride and cubic boron nitride was shown depending on the aluminum content in the samples, and additional studies using electronic paramagnetic resonance confirmed the production of cubic boron nitride in the samples.

Scanning capacitance microscopy of TGS-TGS+Cr ferroelectric crystals

A. L. Tolstikhina[1] , R. V. Gainutdinov[1], N. V. Belugina[1], A. K. Lashkova[1], V. N. Shut[2], S. E. Mozzharov[2] , I. F. Kashevich[3*]
[1] *Shubnikov Institute of Crystallography of RAS, 119333, Moscow, 59 Leninsky Prospekt, Russia*
[2]*Institute of Technical Acoustics, National Academy of Sciences of Belarus, Vitebsk, 210023, 13 general Lyudnikov avenue, Belarus*
[3]*Vitebsk State University, Vitebsk, 210038, 13 moskovsky prospect, Belarus*

Capacitance scanning microscopy was used to study the spatial distribution of capacity, the caconfiguration of domain walls and the impurity composition of TGS - TGS+Cr triglycine sulfate crystals with a periodic growth impurity structure. The concentration of chromium ions in the strips emerging on the surface is determined and the periodic character of the impurity distribution is established. It is shown that capacitive images carry information about the location of regions with an impurity gradient and domain boundaries and make it possible to establish the relationship between the defect and domain structure of the crystal.

Electrodeposition of Rhenium Thin Films via Pulse Electrolysis

N. Grevtsov*, V. Petrovich
Belarusian State University of Informatics and Radioelectronics
*220013, P. Brovki str, 6, Minsk, hrautsou@gmail.com**

The present work aims to demonstrate that pulsed electrolysis regimes pose a workaround to a number of obstacles to rhenium reduction, greatly improving its current efficiency. Experimental studies have been performed using acidic water solutions of NH_4ReO_4. For stationary electrolysis, a constant current density value of 100 mA/cm^2 was maintained. For pulsed deposition, close to rectangular cathodic current pulses of various durations were applied maintaining the same duty cycle.

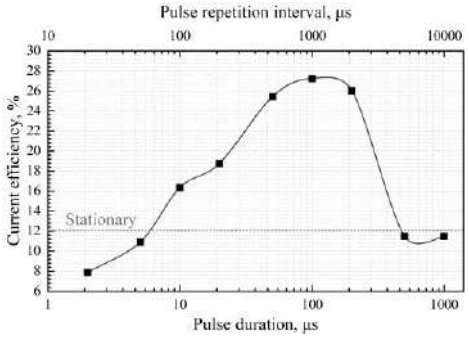

Current efficiency dependence on pulse duration for pulsed electrodeposition of rhenium

As a result of *stationary galvanostatic electrolysis*, rhenium deposition current efficiency value of 12% was obtained. This value was then used for subsequent comparison with the results of pulse-mode electrolysis. The current efficiency values in the pulse duration range of 6 to 200 μs are noticeably higher than the stationary galvanostatic deposition value of 12%, with a well-defined peak at around 100 μs. As the pulse duration values delves outside of the aforementioned range, a significant reduction of current efficiency occurs. This can be attributed to the formation of *atomic hydrogen* H^0 on the metal-solution interface over the course of each current pulse. Multiple hydrogen atoms can associate into molecular hydrogen H_2, causing hydrogenation of the rhenium deposit and bringing forward mechanical stresses, as well as causing the alkalization of the near-cathode region. In combination with the electrochemical reduction of perrhenate ions in this region, a drop in current efficiency is inevitably observed due to a drastic decrease in the primary reagents' concentration. As an alternative, atomic hydrogen H^0 present on the surface of the forming rhenium deposits, being an unstable form of hydrogen, dissociate with the formation of a hydrogen ion H^+ and a free electron, with the former helping restore the pH value in the near-cathode layer without obstructing the reduction of rhenium, and the latter contributing to it.

An *optimal charge value* needed for a single current pulse can be estimated as $Q_0 = S \cdot N_s \cdot q$, where S is electrode area, N is the number of hydrogen atoms present in a monolayer on the electrode surface, and q is the electron charge. In the cases when the charge Q concentrated in a single pulse exceeds the value of Q_0, the association reaction of H^0 atoms into H_2 molecules will be facilitated at the metal-solution interface. This also causes the aforementioned dissociation effect of H^0 to decrease, in this particular case leading to a noticeable decline in the current efficiency at pulse durations above $5 \cdot 10^2$ μs. At shorter pulse durations (corresponding to lower values of Q), the efficiency brought forward by atomic hydrogen dissociation also decreases in an approximately linear fashion. In our particular case, due to the association of atomic hydrogen after prolonged migration across the electrode surface, the effects of near-cathode layer alkalization and rhenium hydrogenation are yet to be eliminated.

During the short pause between each of the consecutive pulses rhenium reduction reactions in the DEL do not proceed, and in order to achieve thermodynamic equilibrium the solution composition in the near-cathode layer is restored to its equilibrium values, both for hydrogen ions (pH values) and the «consumed» perrhenate ions.

Title Study of the microwave properties of the SBN composite with the addition of 45% by mass of CTO

S. Saturno[1,2], F. Silva[2], R. Abreu[1,2], D. Colares[1,2], T. Abreu[2,3], J. Nascimento[2,4], F. Nobrega[2,3], S. Vasconcelos[2] and S. Sombra[1,2]*
[1] *Department of Teleinformatics Engineering Federal University of Ceará (UFC), Campus do Pici – Campus do Pici – Block 725 – CEP 60455 - 970 - Brazil*
[2] *Telecommunications and Materials Science and Engineering Laboratory (Locem), Campus do Pici – Block 930 – Fortaleza – CE, 60020-181 - Brazil*
[3] *Department of Organic and Inorganic Chemistry, Federal University of Ceará, Campus do Pici – Block 940 – Fortaleza – CE, 60020-181 – Brazil*
[4] *Federal Institute of Education, Science and Technology of Ceará, (PPGET), Benfica, Fortaleza - CE, 60040-531 - Brazil*

This paper presents the behavior of SrBi2Nb2O9 (SBN) composite added with 45% by mass of CaTiO3 (CTO) as Dielectric Resonator Antenna (DRA). The SBN was milled at 360rpm/8hours and calcined at 1000 °C/2hours. X-ray diffractometry was used in conjunction with Philips X'Pert HighScore software to determine the presence of phases present in the composite. The sample was compacted using an axial pressure of 294 MPa with a hydraulic press, and then the material was sintered at 1000°C. In addition to the evaluation as DRA, microwave property evaluation at room temperature was performed.

Study of electronic processes in a heterojunction with p-i-n-model pCdTe-iCdTe1-xSx – nCdS

Sh.B. Utamuradova, S.A. Muzafarova*, and K.M. Fayzullaev
[1]*Institute of Semiconductor Physics and Microelectronics at the National University of Uzbekistan, Tashkent, 100057, Republic of Uzbekistan*

The current-voltage characteristics of a thin-film solar cell pCdTe - i - nCdS with a transition i-layer of the interface from an i-$CdTe_{1-x}S_x$ solid solution with a nanostructure are investigated as a function of temperature. It is shown that an increase in the efficiency of the output parameters of the solar cell pCdTe - i - nCdS. To simulate the pCdTe - i - nCdS solar cell with a transition i-layer of the interface, some parameters (thickness, band gap, electron and hole mobility) were changed for simulating the pCdTe - i - nCdS thin-film solar cell.

STUDIES OF THE PRODUCTION OF ZINC OXIDE BY PRECIPITATION IN THE LABORATORY

Sh.Tavashov[1*], B.Farmanov[1], A.Dadakhodjayev[2]
[1]*Karshi Engineering-Economic Institute, Uzbekistan,*
[2]*Tashkent State Technical University named after Islam Karimov, Uzbekistan*

The results of studies on the production of zinc ions by precipitation from a solution of zinc nitric acid with an 18% solution of sodium carbonate are presented. The influence of technological factors on the degree of deposition of zinc ions is investigated and the optimal parameters of the process are established. The solution of zinc nitric acid contains 42,83 %. The maximum degree of precipitation of zinc ions is observed in the pH of the medium (7,0-7,6), the temperature is 65-70°C. At the same time, increasing the duration of the process from 45 to 60 minutes increases the degree of precipitation of zinc ions from 99,34 % to 99,78 %.

X-ray investigation of high pressure material of system Al-TiN

O.V. Ignatenko*, A. I. Alkhimenok, A. L. Zhaludkevich, V.S. Goncharov, V. V. Tkachenko, V.A. Komar, N.A. Shempel
SSPA «Scientific-Practical Materials Research Centre of NAS of Belarus», 220072, Belarus, Minsk, st. P. Brovki, 19

The influence of high pressure on the formation of the material of the Al-TiN system was investigated (pressure 1-5 GPa, temperature 298-1773 K, synthesis time 1-5 minutes). X-ray diffraction data indicate that no significant changes have occurred. New compounds and solid solutions are not formed. The position of the peaks within the measurement error. The intensity of the peaks is also within the measurement error, corrected for the formation of a denser texture of the sample. With an increase in temperature and holding time, a decrease in pressure, there is a decrease in the peaks of the peaks of aluminum. Most likely amorphization of the aluminum structure.

Figures show the effect of high pressure on the formation processes of a sample of the Al-TiN system obtained under a high pressure of 5 GPa and at different temperatures with different holding times. X-ray diffraction data indicate that no significant changes have occurred. New compounds and solid solutions are not formed. The position of the peaks within the measurement error. The intensity of the peaks is also within the measurement error, corrected for the formation of a denser texture of the sample.

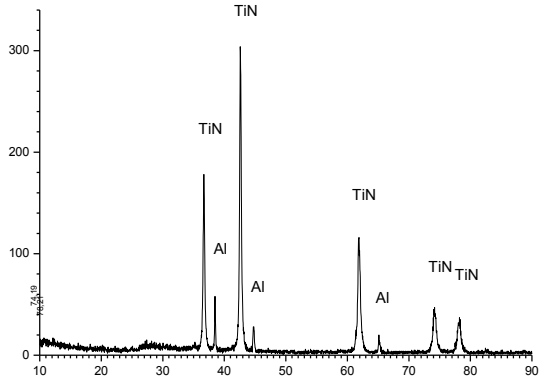

Figure 1. X-ray diffraction spectrum of a sample of the Al-TiN system obtained under a high pressure of 5 GPa and at a temperature of 298 K with a holding time of 1 minute

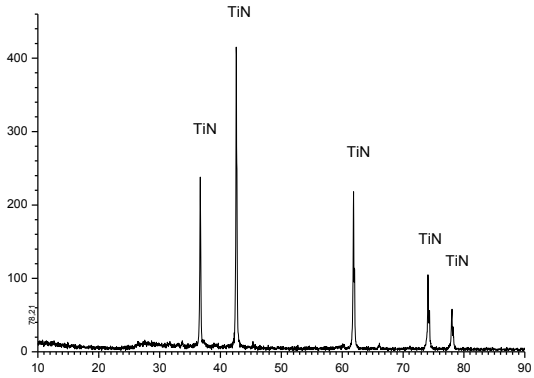

Figure 2. X-ray diffraction spectrum of a sample of the Al-TiN system obtained under a high pressure of 1 GPa and at a temperature of 1773 K with a holding time of 1 minute

1. The effect of high pressure on the formation of the material of the Al-TiN system was studied (modes: pressure 5 GPa, temperature 298 K, synthesis time 1 minute; pressure 5 GPa, temperature 773 K, synthesis time 1 minute; pressure 5 GPa, temperature 1273 K, synthesis time 1 minute; pressure 4 GPa, temperature 1773 K, synthesis time 1 minute; pressure 3 GPa, temperature 1773 K, synthesis time 1 minute; pressure 2 GPa, temperature 1773 K, synthesis time 1 minute; pressure 1 GPa, temperature 1773 K, synthesis time 1 minute; pressure 5 GPa, temperature 1773 K, synthesis time 2 minutes; pressure 5 GPa, temperature 1773 K, synthesis time 3 minutes; pressure 5 GPa, temperature 1773 K, synthesis time 4 minutes; pressure 5 GPa, temperature 1773 K, synthesis time 5 minutes.

2. X-ray diffraction data indicate that no significant changes have occurred. New compounds and solid solutions are not formed. The position of the peaks within the

measurement error. The intensity of the peaks is also within the measurement error, corrected for the formation of a denser texture of the sample.

3. With an increase in temperature and holding time, a decrease in pressure, there is a decrease in the peaks of the peaks of aluminum. Most likely amorphization of the aluminum structure.

Formation of coatings on the surface of the AZ31 magnesium alloy by plasma electrolytic oxidation using boron nitride microparticles

A.L. Zhaludkevich[1]*, M. Serdechnova[2], C. Blawert[2], S.A. Karpushenkov[1], O.V. Ignatenko[1]
[1]*SSPA «Scientific-Practical Materials Research Centre of NAS of Belarus», 220072, Belarus, Minsk, st. P. Brovki, 19, zheludkevich27@gmail.com*
[2]*Helmholtz-Zentrum Hereon, 21502 Geesthacht, Germany, Max-Planck-Straße, 1*

Thin oxide films (up to 100 microns) in a phosphate electrolyte with the addition of micro particls of hexagonal boron nitride on the surface of the AZ31 magnesium alloy were obtained by plasma electric oxidation (PEO). Since boron nitride exhibits dielectric properties and is chemically inert enough, it is logical to assume that boron nitride particles are included in the structure of the PEO coatings by an inert mechanism, and not by a reactive one, as is typical for oxide particles. The hNB particles are included in the coating quite evenly and retain their shape (Figure 1, a), which means that they do not enter into any reactions and do not change the phase composition.

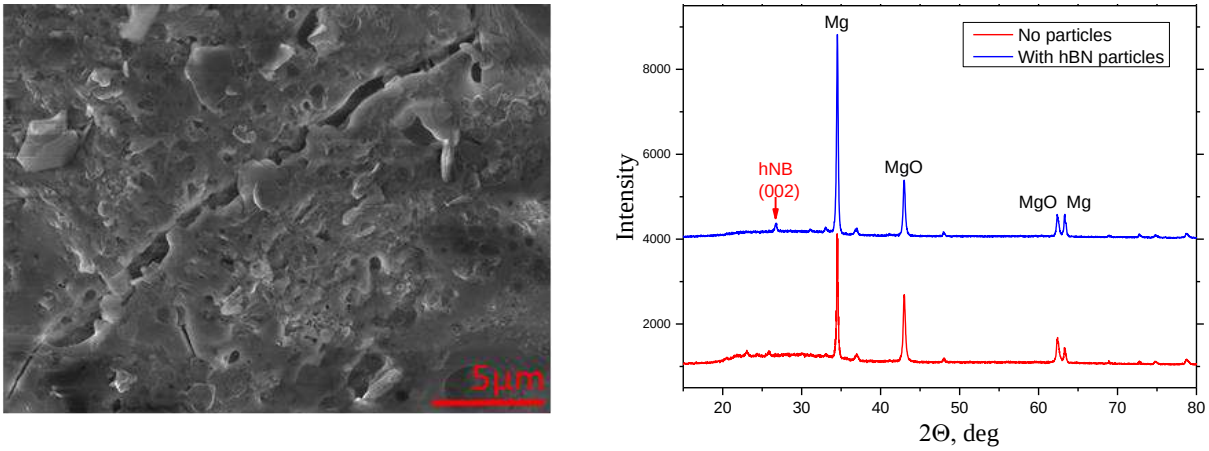

(a) (b)

Figure 1. Surface morphology PEO coatings with added hNB (a) and XRD patterns of obtained PEO coatings with micro particles hNB (b)

It was found by X-ray analysis that PEO coatings are composed of a phase of magnesium oxide MgO, peaks 43°, 63°, 75°, 79° (Figure 1, b). The spectra show pronounced peaks of magnesium (34.5°, 48°, 64°, 69° and 73°). In PEO coatings obtained in an electrolyte with the addition of hNB particles, a characteristic peak appears at 26.7° which corresponds to hNB. With an increase in the oxidation time, the thickness of the coating also increases and, accordingly, the content of the hNB phase.

Acknowledgment
This work was supported by REA in frame of Horizon2020-MSCA/RISE-2018, Nr. 823942 (FUNCOAT project: «Development and design of novelmultiFUNctional PEO COATings»). The reported study was funded by BRFFR (grant No. F21RM-040). The study was partly supported by the European Union's Horizon 2020 research and innovation programme under the Marie Skłodowska-Curie grant agreement No. 778070.

Investigation of the influence of varying the chemical composition of the container on the phase composition of the materials obtained by the method of high pressures and temperatures

A. L. Zhaludkevich[1]*, S.F. Parshutich[1], V.S. Goncharov[1], , A.V. Pysk[1], V.A. Komar[1], N.A. Shempel[1], Yu.V. Aleksiayenak[2], K. N. Vergel[2], O.V. Ignatenko[1]
[1]*SSPA «Scientific-Practical Materials Research Centre of NAS of Belarus», 220072, Belarus, Minsk, st. P. Brovki, 19*
[2]*Joint Institute for Nuclear Research, Russian Federation, Dubna, str. Joliot Curie, 6*

Phase formation under high pressure in Cu – S system has been studied at 1 – 5 GPa and 1000 °C. It was revealed that under high-pressure and high-temperature conditions (after 3 GPa), at the stoichiometric ratio of the elemental constituents copper disulfide is formed. The results of the determination of the impurity composition in the formation of copper disulphide with a pyrite structure obtained at high pressures are reported. Neutron activation analysis made it possible to determine Na, Mg, Al, Si, Cl, Ca, V, Mn, Cu, Sr, and I in the elements of high-pressure cells over a wide range of concentrations. It is shown that the use of a tantalum screen allows almost completely screening the resulting compound (CuS_2) from the impurities existing in the cell elements.

Anomalous Growth of Cobald Sferical Particles During the Electrorlytic Deposition of CoNiP Coatings

M.I. Panasyuk[1]*, T.I. Zubar[1,2] , T.I. Usovich[1], V.A. Fedkin[1], A.N. Kotelnikova[1], O.D. Kanafiev[1], A.V. Trukhanov[1,2,3].

*[1] SSPA "Scientific and practical materials research centre of NAS of Belarus", 220072, Minsk, P. Brovki str., 19, Belarus, maria.panasiuk.99@gmail.com**
[2] South Ural State University, 454080, Chelyabinsk, Lenin Prospect, 76, Russia
[3] National University of Science and Technology MISiS, 119049, Moscow, Leninsky Prospekt, 4, Russia

Three dimensional cobalt nanostructures are successfully synthesized by an electrochemical method without any template and surfactants. The dependence of the growth of cobalt particles on the surface of the CoNiP alloy on the deposition time was studied (Figure 1). The composition of the surface of the samples was determined. Three characteristic points were revealed on the surface of the samples, which radically differ in composition. The growth mechanisms behind the formation of such structures were discussed.

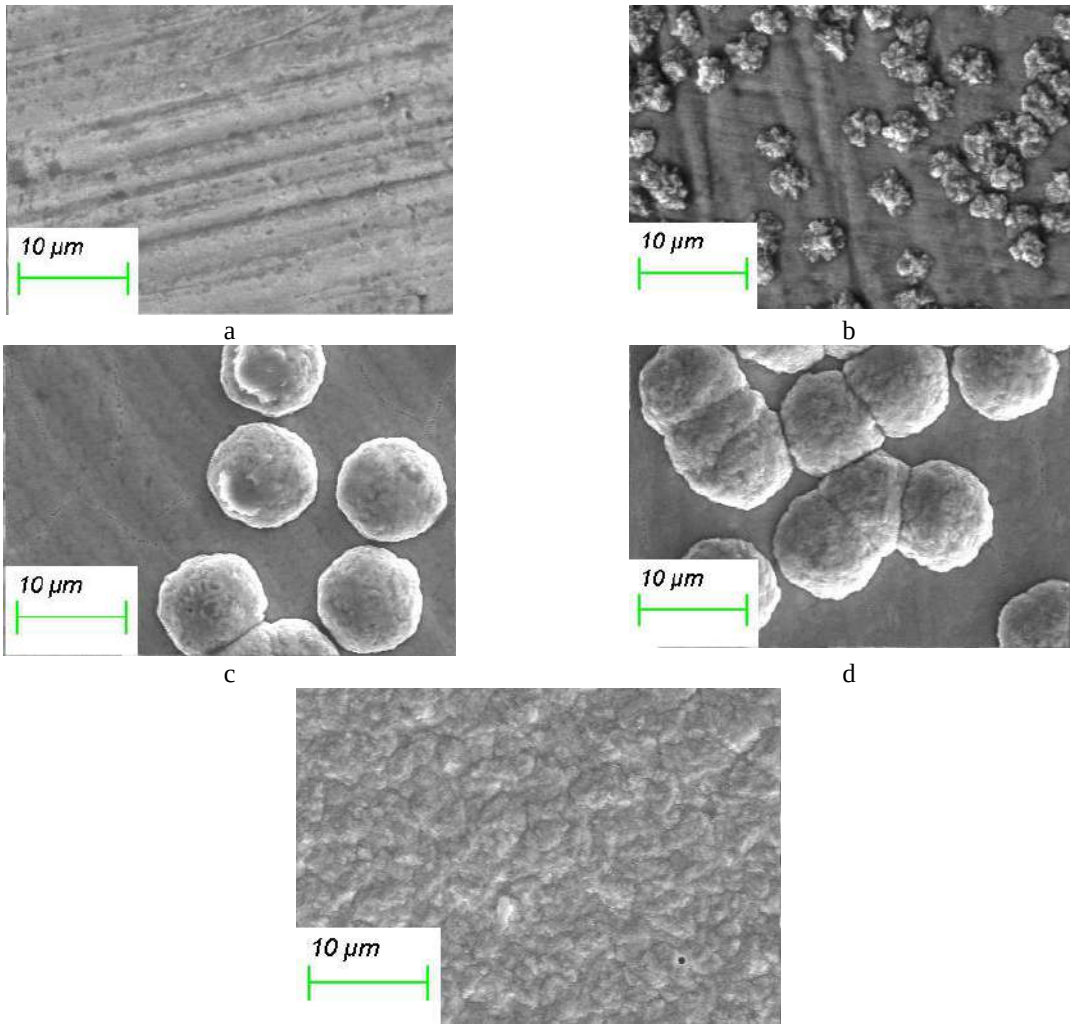

a - CoNiP1; b - CoNiP10; c - CoNiP20; d - CoNiP30; e - CoNiP60
Figure 1. Surface microstructure examined by SEM

Defect transformation in irradiated p-type silicon under thermal annealing at intermediate temperatures

L. F. Makarenko[1]*, S. B. Lastovskii[2], V.E. Gusakov[2], T. Ceponis[3], E. Gaubas[3], J. Pavlov[3], V. V. Kozlovskii[4], Y. Gurimskaya[5], M. Moll[5]
[1]*Belarusian State University, Independence Ave. 4, 220030 Minsk, Belarus,*
[2]*Scientific-Practical Materials Research Centre of NAS, P. Browka str. 17, Minsk, Belarus,*
[3]*Institute of Photonics and Nanotechnology, Sauletekio Ave. 3, LT-10257 Vilnius, Lithuania*
[4]*Peter the Great St. Petersburg State Polytechnic University, 195251 St. Petersburg, Russia,*
[5]*CERN, CH-1211 Geneva 23 Switzerland*

Annealing kinetics of interstitial boron-interstitial oxygen (B_iO_i) and interstitial boron-substitutional boron (B_iB_s) defects at temperatures 160-400 °C have been studied. Diodes made of epitaxial and Czochralski-grown silicon differ in boron and carbon concentrations have been used. A preliminary irradiation with 0.9 and 6 MeV electrons was performed before annealing. Radiation-induced defects were monitored using DLTS and C-V measurements.

It has been found that the annealing results in the formation of several new traps and the additional growth of a DLTS peak related to the interstitial carbon-interstitial oxygen (C_iO_i) complex. One of the traps formed under the annealing has an energy level of E_v+0.28 eV (H028) and was identified according to Ref. 1 as complex of interstitial boron-substitutional carbon (B_iC_s).

Analysis of the annealing features shows that in order to get a consistent interpretation of the obtained experimental data one has to take into account the following defect reactions

$$B_iO_i \Leftrightarrow B_i + O_i, \quad (1)$$

$$B_i + B_s \rightarrow B_iB_s, \quad (2)$$

$$B_i + C_s \rightarrow B_iC_s, \quad (3)$$

$$B_i + C_s \rightarrow B_s + C_i, \quad (4)$$

Reaction (2) describes the main channel of interstitial boron capture in low resistivity epitaxial diodes. The formation of B_iB_s complexes hinders a carrier concentration recovery after B_iO_i disappearance.

An essential component in our considerations is reaction (4) which allows to explain the growth of the C_iO_i concentration during the annealing process and to get the correct dependence of B_iC_s concentration on carbon and boron content. The study of this dependence enabled us to determine the ratio between capture radii of interstitial boron by substitutional boron and carbon.

An ab initio analysis of the formation and stability of the C_s + B_i defect has been performed. It shows that a split B-C configuration is the most stable configuration of the defect.

It is supposed to use the carbon-by-boron replacement reaction in order to activate implanted boron at low temperatures.

References

[1] L.C. Kimerling, M.T. Asom, J.L. Benton, P.J. Drevinsky, C.E. Caefer. Materials Science Forum 38, 141 (1989).

SIMPLE METHOD FOR DEVICE FABRICATION PROCESS OF INORGANIC CESIUM LEAD TRIIODIDE ($CsPbI_3$) PEROVSKITE SOLAR CELLS

Saparbaev Aziz*, Nurumbetova Lobar, Boynazarov Ilkhom
Institute of Ion-Plasma and Laser Technologies of Uzbekistan Academy of Uzbekistan

Recently, solar cells based on inorganic cesium lead triiodide ($CsPbI_3$) perovskite materials have been receiving considerable attention. However, the quality and thickness of perovskite films are still unsatisfactory due to the limited solubility of the precursor materials. In order to upgrade the efficiency of the inorganic perovskite cells, various techniques have been developed to uniformly coat the perovskite film, for example, heating, gas flow, vacuum, anti-solvent, one step coating, two step coating methods, chemical additives such as acid additives and surface modification.

In this work, synthesized inorganic cesium lead triiodide perovskite cells and employed simple coating process with fabrication of high-quality perovskite films without anti-solvent solution in air condition. To prepare the $CsPbI_3$ precursor solution, CsI and PbI_2 were dissolved in DMF with 1:1 M ratio (0.3 M) and stirred for 24 hours at room temperature in air condition, then, 66 µL of HI acid was added into 1 mL precursor solution before 1 hour of preparing perovskite films (Figure1). ITO-coated glass substrates were cleaned by ultrasonication in acetone, deionized (DI) water and isopropyl alcohol (IPA) for 10 minutes each, after then dried by high pure nitrogen gas. Subsequently, the substrates were treated with oxygen plasma for 8 minutes. Afterwards, 40 nm PEDOT:PSS was spin-coated on the substrates, and then, baked in an oven at 160 °C for 20 minutes under air conditions. Then, a simple once more-coating process (4000 rpm, 10 s) was employed for fabrication of high-quality perovskite films in air condition.

The absorption spectra exhibit that the $CsPbI_3$ film is the yellow phase before annealing, and it becomes black phase after thermal annealing. The bandgap E_g of the yellow phase $CsPbI_3$ perovskite was measured to be 2.81 eV and molecular structure is orthorhombic form with an absorption spectra peak in ultraviolet wavelength[1] and device parameters are very poor (PCE is 0.09%)[2]. After annealing the absorption area was increased and the bandgap decreased to 1.72 eV.

The perovskite films were prepared by spin-coating the precursor solution on the substrates at 4000 rpm speed. In order to improve the film quality and thicknesses, quick drip coating process was repeated once more. The defects like pinholes can be effectively eliminated without antisolvent engineering, by the second coating method with further growth of the grain sizes, thus, greatly suppressing the charge recombination in these perovskite films. The substrates were subsequently heated at 100 °C temperature for 10 minutes on a hot plate under air conditions. The color of the perovskite films changed from transparent yellow phase to black phase. [3].

For concluding, the method is effective or not, absorption coefficient and surface morphology of the solar cells is of great importance. In this work show that simple methods can effectively improve optical properties and device performance. Results demonstrate that pinholes of the films can be effectively eliminated with the once more re-grown grain sizes. Their charge recombination can be greatly inhibited as well. Consequently, efficient inverted all inorganic $CsPbI_3$ perovskite solar cells exhibited good PCE of 12 % with all improved device parameters.

References <optional>

[1] Steele JA, Jin H, Dovgaliuk I, et al. Thermal unequilibrium of strained black $CsPbI_3$ thin films. Science: 2019, 365 (6454): 679-684.

[2] Choi H, Jeong J, Kim H-B, et al. Cesium-doped methylammonium lead iodide perovskite light absorber for hybrid solar cells. Nano Energy: 2014, 7: 80-85.
[3] Ahmad W, Khan J, Niu G, et al. Inorganic $CsPbI_3$ perovskite-based solar cells: A choice for a tandem device. Solar RRL: 2017, 1 (7): 1700048

Photoluminescence of defective chalcopyrite $ZnGa_2S_4$ and $ZnGa_2Se_4:Nd^{3+}$

S.Q. Asadullayeva* A.H. Bayramov, N.A. Ismayilova
Institute of Physics, Azerbaijan National Academy of Sciences, Az-1143, Baku, Azerbaijan

Compounds belonging to the triple class with the general formula MB_2S_4 differ in significant optical properties defective chalcopyrite $ZnGa_2S_4$, which we are currently studying, is a promising material for solar photovoltaic and other optoelectronic applications. [1-3] The inclusion of certain lanthanides in this type of sulfides significantly affects their optical properties. Thus, when activating them with different ions, interesting emission spectra are observed, which can be interpreted in terms of the local states of these activator ions. For many of these emission spectra, logical interpretations are made in terms of the symmetry and numerical coordination of the cation nodes[4, 5].

Zn (99.99%), Ga (99.99%) and S (99.99%) elements with high purity were used to synthesize the $ZnGa_2S_4$ compound. First, a high vacuum is created. The synthesis is carried out in quartz ampoules. The oven temperature is gradually increased from low temperature to 1250 C. The substance is stored at this temperature for 6 hours. The bulb is then cooled to 500 C and annealed at this temperature for 24 hours. An impurity of the rare earth element Nd (2%) was introduced during the synthesis. PL emission and excitation spectra were measured using PL/PLE/ Raman spectrometer (Tokyo Instruments, Inc.). PL from the sample was dispersed through a grating (150g mm^{-1}) monochromator MS 5704 I (SOL Instruments, Inc.) and detected by CCD multiplier DU 491A-1.7 (Tokyo Instruments, Inc.). About 532nm wavelength of laser beam was used as excitation source for PL emission. Figure shows the photoluminescence spectra of undoped (1-line), neodymium_activated $ZnGa_2S_4$ at 300K(2-line) and 10K (3-line) . As can be seen, $ZnGa_2S_4$:Nd is observed at the same wavelength as the luminescence maximum of the $ZnGa_2S_4$ crystal. $ZnGa_2S_4$:Nd The narrow peak observed at 596nm in the $ZnGa_2S_4$:Nd crystal is due to the $^2G_{5/2} \rightarrow {}^4I_{9/2}$ transition of Nd^{+3}[6]. The fact that the value of the full width at half maximum in the visible region is less than 13nm suggests that this crystal has a laser effect . Figure The PL spectra of $ZnGa_2S_4$ (1-line) and $ZnGa_2S_4$:Nd crystals at different temperatures : 2-300K ; 3 -10K;

Reference
[1] S.G. Asadullayeva, Z.A. Jahangirli, T.G. Naghiyev, D.A. Mammadov, Phys. Status Solidi B 258 (8)(2021)
[2] O. Tagiyev, S. Asadullayeva, G. Eyyubov, U. Gasimov, K. Tagiyev, J. Mod.
Phys.B 3 (2012) 827–830
[3] J. Xiao-Shu, Y. Ying-Ce, Y. Shi-Min, M. Shu, N. Zhen-Guo, L. Jiu-Qing, Chin.
Phys. B 19 (2010) 107104-1–107104-8
[4] Masako Matsumura Yuta' and William B. White *J. Electrochem. Soc.*, Vol. 139, No. 8, p.2347, 1992
[5] Claudia Wickleder, Shuang Zhang and Hartmut Haeuseler Z. Kristallogr. 220 (2005) 277–280
[6] N.N. Sirota, S.N. Chizhevskaya. Physics and Physics chemical analysis, Moscow: Gosstroy, (1957) 185.

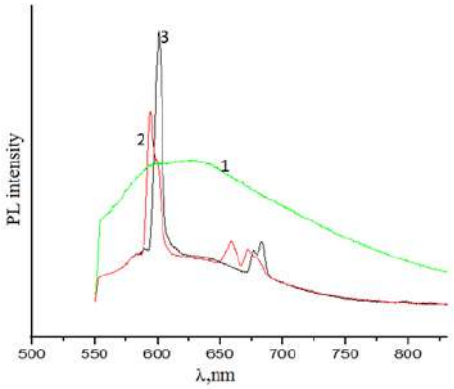

Ab-initio simulations magnetic properties of $ZnGa_2S_4$

N.A. Ismayilova*, S.Q. Asadullayeva
Institute of Physics, Azerbaijan National Academy of Sciences Az-1143 Baku, Azerbaijan
Az-1143 Baku, Azerbaijan

DFT [1] calculation was performed for calculation magnetic properties of $ZnGa_2S_4$ doped Mn atoms. We use supercells contained 28, 56 and 112 atoms. Calculation carried out using Spin Generalized Gradient Approximation (SGGA) [2] by the Atomistix Tool Kit program software (ATK, http://quantumwise.com/) [3]. The electron-ion interactions were taken into account through pseudopotentials of the SG15 [4]. The Becke Lee-Yang-Parr (BLYP) exchange-correlation functional and double zeta polarized basis sets were used in our calculations. The kinetic cut-off energy was 150 Ry. Our optimized lattice parameters a=5.27Å, c=10.44 Å, c/a=1.97 is in good agreement with both experimental and theoretical results [5, 6].

From the free energy difference between FM and AFM states, $\Delta E = E_{FM} - E_{AFM}$, we can estimate which state is more energetically favorable. Negative ΔE means that FM state is lower in energy than the AFM state, indicating that the FM state is more favorable. How we can see from comporision DOS for pure and doped with Mn supercell, that the spin up and spin down of Mn d-electron density of state do not cover each other. Which mean that Mn atoms induce magnetic properties.

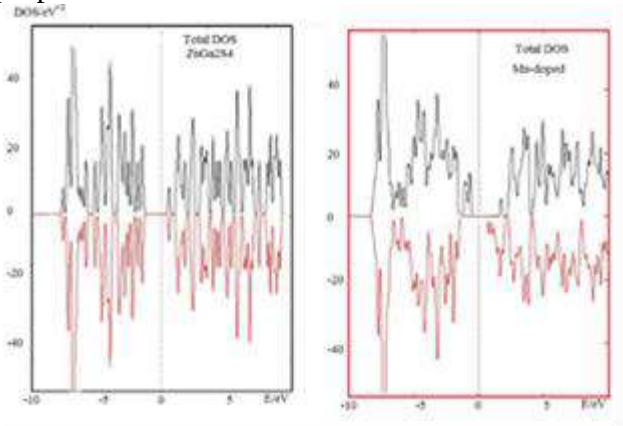

Figure Calculated total DOS for pure and Mn doped $ZnGa_2S_4$ compound

Reference

[1] P. Hohenberg and W. Khon, Phys. Rev. B 136 864 (1964).
https://doi.org/10.1103/PhysRev.136.B864
[2] J. Perdew, K. Burk, and Y. Wang, Phys. Rev. B 54 16533 (1996).
https://doi.org/10.1103/PhysRevB.54.16533
[3] http://quantumwise.com/.
[4] Martin S., François G. Comput. Phys. Commun. 196 36-44 (2015).
https://doi.org/10.1016/j.cpc.2015.05.011
[5] M. Cannas, L. Garbato, A. G. Lehmann, N. Lampis, and F. Ledda, Cryst. Res. Technol. 33 417 (1998).
[6] G. B. Carpenter, P. Wu, Y-M. Gao, and A. Wold, Mat. Res. Bull., 24 1077-1082 (1989).

Ab-initio simulations electronic band structure of $TlGaSe_2$ under pressure

TG Mammadov[1], SH Jabarov[2], NA Ismayilova[3]
[1]*Institute of Physics, Azerbaijan National Academy of Sciences Az-1143 Baku,*
[2]*Azerbaijan State University of Economics, Baku, AZ-1063, Azerbaijan*

At ambient conditions, the layered semiconductor $TlGaSe_2$ crystallizes in a monoclinic system with basecentered lattice and space group C2/c. $TlGaSe_2$ is indirect-gap semiconductor where direct transition is located very close to indirect [1, 2]. According the results of studying of neutron diffraction [3] and Raman spectra [4] under hidrostatic pressure at the pressure P ~ 0.9 GPa $TlGaSe_2$ undergoes to the first-order structural phase transition without a change in symmetry.

We have studied the band structure of $TlGaSe_2$ under pressure in the range of 0 GPa to 4 GPa. Ab initio calculations of electronic properties were carried out on the basis of DFT and dynamic characteristics by implementing the density functional perturbation theory DFPT [5, 6] using the pseudopotential method based on plane waves implemented in the ABINIT code [7].

Our calculation results show that with increasing pressure in all calculated pressure range both the value of indirect E_{id} and direct E_d band gaps were decreased and intersection between them is not observed. At P ~ 0.9 GPa their values becomes almost equal. In the vicinity of P ~ 0.9 GPa, the widths of the E_d and the E_{id} are undergoing a small jamping (ΔE_d ~ -0.12eV and ΔE_{id} ~ -0.08eV) wich is typical to the first-order phase transition. Thus, in the whole investigated pressure range the $TlGaSe_2$ remains an indirect-gap semiconductor. The values of the pressure coefficients of E_{id} and E_d are determined in both phases and comparison with the results of experimental studies carried out.

Reference

[1] N. M. Gasanly, J. of Kor. Phys. Soc. 57(1), 164 (2010).
[2] N. A. Ismayilova, S. H. Jabarov, Optoelectronics And Advanced Materials – Rapid Communications, Vol. 11, No. 5-6, 2017, p. 353 - 356
[3] S. H. Jabarov, T. G. Mammadov, A. I. Mammadov V. B. Aliyeva, J. Synch. Investig. 9, 35–40 (2015).
[4] S.H. Jabarov , V.B. Aliyeva, T.G. Mammadov, A.I. Mammadov, S.E. Kichanov, L.S. Dubrovinsky, Materials Science-Poland, 36(2), 2018, pp. 203-208
[5] P. Gianozzi, S. de Gironcoli, P. Pavone, S. Baroni. Phys. Rev. B43, 7231 (1991)
[6] X. Gonze. Phys. Rev. B 55, 10337 (1997).
[7] X. Gonze, J.M. Beuken, R. Caracas, F. Detraux, M. Fuchs. G.M. Rignanese, L. Sindic, M. Verstraete, G. Zerah, F. Jallet.Comput. Mater. Sci. 25, 478 (2002).

A Novel Tea Factory Waste supported Cu catalyst as a high performance supercapacitor electrode

S. Özarslan[1], Gunel T. Imanova[2]*, M. R. Atelge[3], M. Kaya[4], S. Ünalan[5]
[1]*Department of Mechanical Engineering, Erciyes University, Turkey*
[2*]*Department of Physical, Mathematical and Technical Sciences, Institute of Radiation Problems, Azerbaijan National Academy of Sciences, AZ 1143-Baku, Azerbaijan*
[3]*Department of Mechanical Engineering, Siirt University, Turkey*
[4]*Department of Chemical Engineering, Siirt University, Turkey*
[5]*Department of Mechanical Engineering, Erciyes University, Turkey*

In current study, TFW catalyst treated with acetic acid loaded with copper (Cu) was produced using tea factory waste (TFW). Subsequently, the TFW catalyst was used in H_2 production via methanolysis of $NaBH_4$. The highest active catalyst was determined according to four parameters which are metal types, metal fractions, burning temperatures and burning periods. As a result, TFW treated with 30% Cu loaded acetic acid was burned at 300^{o}C burning temperature for 60 minutes and the most active catalyst was synthesized. The hydrogen generation rate (HGR) of the catalyst was investigated by experimenting with different catalyst amounts, different $NaBH_4$ percentages and different temperature values.

Influence of metal concentrations on H_2 generation: Figure 1 shows H_2 recovery from $NaBH_4$ of 10, 20, 30, 40 and 50% by weight Cu supported tea factory waste catalyst with acetic acid. The highest yield was recorded with a catalyst containing 30% Cu. The reaction time was 4 min and it gave the shortest reaction. Hydrogen generation yields were recorded as 3059.3, 2603.7, 3687.6, 2758.8 and 1982 mL (min.g)$^{-1}$, respectively. In the next tests, 30% of Cu was used found that 30% metal percentage gave the shortest completion time in their studies using CuB metal catalyst with zinc chloride modified Chlorella vulgaris microalgae support material [1].

Today, when energy and its storage are so important, energy production from waste that has no economic value and the use of these wastes in energy storage is very interesting. In the first stage of this study, an active and cost-effective catalyst to be used in the production of hydrogen in the methanolysis of $NaBH_4$ from tea factory waste was synthesized. The most efficient catalyst was determined by investigating the effects of different metal types, metal ratios, burning temperatures and burning times. By using different methods and materials, the efficiency of the supercapacitor can be increased. The use of the produced catalyst in the generation of efficient energy such as hydrogen and the production of supercapacitor, which is an efficient energy storage, made our work versatile and innovative. This bifunctional material has been named 'cap-cat' [2-3] .

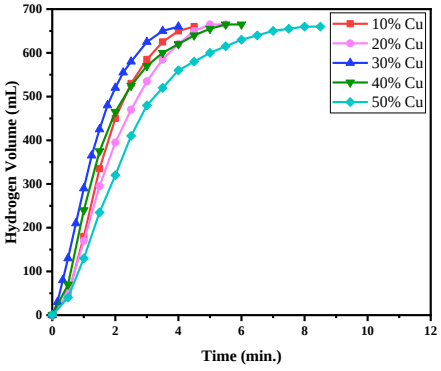

Fig. 1. The change of hydrogen volume of the media including various metal amounts as a function of time (Reaction Condition: $NaBH_4$=2.5%, Catalyst=0.1-gram, Temperature = 30 ^{o}C, Volume of methanol = 10 mL)

References

[1] C. Saka, M. Kaya, M. Bekiroğullari, Int. J. Hydrog. Energy. **45**(3), (2020),1959-1968.
[2] M. Bolat, C. Yavuz, M. Kaya, J. Mater. Sci.: Mater. Electron. (2021), 1-15.
[3] I.I. G. Inal, M. Akdemir, M. Kaya, Int. J. Hydrog. Energy, (2021), 5-16.

Synthesis of Ce:YIG nanopowder by gel combustion

M. N. Smirnova*, G. E. Nikiforova, M. A. Kop'eva1 and V. A. Ketsko
Kurnakov Institute of General and Inorganic Chemistry of the Russian Academy of Sciences, 119991, 31 Leninsky Prospect, Moscow, Russia

.

At last years there has been an active search new functional materials for new generation magneto-optical devices. In terms of the combination of such characteristics as optical transparency and magneto-optical effect, one of the possible candidates for these purposes is cerium ferro-garnet ($Ce_3Fe_5O_{12}$). However, $Ce_3Fe_5O_{12}$ doesn't exist in the form of single crystals or ceramics due to the large ionic radius of Ce^{3+} (1.14 Å). In this regard, the possibility obtaining homogeneous cerium-substituted ferro-garnets with the maximum possible content of Ce^{3+}, for example, by replacing some of the Y^{3+} ions in $Y_3Fe_5O_{12}$ with Ce^{3+}.

This work presents the results the synthesis and study a solid solution of cerium-substituted yttrium iron garnet, aimed at achieving the maximum possible substitution of Y^{3+} for Ce^{3+}. The replacement of Fe^{3+} ions by Ga^{3+} in the 1:1 ratio and using vacuum annealing of the precursor obtained by the method gel combustion made possible to increase the cerium content in the garnet structure to 16.7% relative to yttrium without the formation of CeO_2 impurities.

Particular attention was paid to the creation of oxygen-deficient conditions for heat treatment of the samples to reduce the probability the oxidation of Ce^{3+} cations to Ce^{4+}. In this regard, after the synthesis the preliminary annealing of the samples immediately was carried out in a vacuum. The cations ratio in the sample with the maximum cerium content was confirmed by X-ray fluorescence analysis and energy-dispersive X-ray spectroscopy. Both methods showed that the composition of the studied sample is close to the theoretical one within the experimental error.

According the SEM data, it was shown that the $Y_{2.5}Ce_{0.5}(Fe_{0.5}Ga_{0.5})_5O_{12}$ sample after annealing in vacuum has a developed surface and a monodisperse porous structure, which provides the possibility of its industrial and technical use. Thus, low-temperature heat treatment of the samples under vacuum conditions prevents the oxidation of Ce^{3+} to Ce^{4+} and minimizes the probability formation CeO_2. The results obtained in this work can be used in the future develop effective approaches to the synthesis of functional Ce-containing materials and to improve their properties.

The ratio of cations in the sample with the maximum cerium content was confirmed by X-ray fluorescence analysis and energy-dispersive X-ray spectroscopy. Both methods showed that the composition of the studied sample is close to the theoretical one within the experimental error. According to the SEM data, it was shown that the sample $Y_{2.5}Ce_{0.5}(Fe_{0.5}Ga_{0.5})_5O_{12}$ after annealing in vacuum has a developed surface and a monodisperse porous structure, which provides the possibility of its industrial and technical use.

Thus, low-temperature heat treatment of the samples under vacuum conditions prevents the oxidation of Ce^{3+} to Ce^{4+} and minimizes the probability formation CeO_2. The results obtained in this work can be used in the future to develop effective approaches to the synthesis of functional Ce-containing materials and to improve their properties.

Acknowledgements
This synthesis and study of the samples was supported by the Russian Foundation for Basic Research (project No. 19-08-00643).

References:

[1] M. Smirnova [et al.] Nanosystems: physics, chemistry, mathematics, 2021, 12 (2), P. 210–217.

Effect of Nd doping on the phase composition, morphology, and magnetic properties of $SrFe_{12}O_{19}$ produced by mechanochemical process

Ashraf M. Semaida[1,2]*
[1]*National University of Science and Technology MISiS, Moscow, 119049, Russian Federation*
[2] *Physics Department, Faculty of Science, Damanhour University, Damanhour, 22516, Egypt*

The high energy ball milling (HEBM) process has been used to synthesize M-type hexagonal $Sr_{1-x}Nd_xFe_{12}O_{19}$ (x = 0.1, 0.2 and 0.3). The effect of heat treatment in the air on the microstructure, morphology, and magnetic properties was studied. X-ray powder diffraction (XRD), scanning electron microscopy (SEM), thermogravimetric analysis/differential scanning calorimetry, and vibrating sample magnetometry have been used to characterize the M-type hexagonal nanocomposites. In the case of 0.2 Nd substitution, XRD showed the presence of $SrFe_{12}O_{19}$ (SFO) phase and a small amount of α-Fe_2O_3 phase in the sample annealed at 1150 ^oC for 2 h. A slight increase in lattice parameters "a" and "c" values of the SFO phase was detected, implying that Nd ions were situated in the crystal position of the SFO structure. The growth of the average crystallite size <D> of $Sr_{1-x}Nd_xFe_{12}O_{19}$ after heat treatment was due to the crystal grains' boundary movement. SEM micrographs showed all appropriate elements (Sr, Fe, Nd, and O) of the synthesized nanocomposites were uniformly distributed. Magnetic characterization indicated that all samples exhibited hard ferromagnetic behavior at room temperature. It was found that the magnetic properties of these nanocomposite magnets are strongly influenced by the annealing temperature and the ratio of Nd substitutions. The coercivity (H_c) of the nanocomposites was increased with increasing the Nd substitution. As the annealing temperature increased, the saturation magnetization (M_s) increased until it reached the maximum value for $Sr_{0.8}Nd_{0.2}Fe_{12}O_{19}$ annealed at 1150 °C. A three-dimensional finite element model was presented to study the magnetization reversal of $Sr_{1-x}Nd_xFe_{12}O_{19}$ nanocomposite materials. The impacts of volume fraction, width of the grain boundary (GB) on the coercivity were investigated by the Object-Oriented Micromagnetic Framework (OOMMF). Synthesized $Sr_{1-x}Nd_xFe_{12}O_{19}$ nanocomposite and the HEBM process can be regarded as a candidate technique for preparing hard magnetic nanomaterial for applications such as permanent magnets.

Acknowledgment
The work was carried out with financial support from the Ministry of Education and Science of the Russian Federation in the framework of the Increase Competitiveness Program of MISiS. The researcher A.M. Semaida is funded by a full scholarship from the Ministry of Higher Education of the Arab Republic of Egypt.

Shielding features of heavy metal based glasses for protection against gamma rays in several applications

M.I.Sayyed[1,2]*
[1]*Department of physics, Faculty of Science, Isra University, Amman – Jordan*
[2]*Department of Nuclear Medicine Research, Institute for Research and Medical Consultations (IRMC), Imam Abdulrahman bin Faisal University (IAU), P.O. Box 1982, Dammam, 31441, Saudi Arabia, e-mail:dr.mabualssayed@gmail.com*

Recently, ionizing radiations are commonly utilized in our daily life. However, these radiation can be harmful to people who are exposed to it because of the high energy from the photons. To protect people from the hazardous of the ionizing radiations radiation, protective shielding materials that can absorb incoming photons are used. Practically, there are different kinds of radiation protection such as lead, alloys, ceramics, composite materials and glasses. Glasses are presently used in medical, nuclear and other fields. Heavy metal based glasses have interesting shielding performance and other superior physical and chemical properties. Also, they have high density, high effective atomic number, high radiation protection efficient and low half value layer. Recent studies showed that one of the possible way to improve the radiation shielding features of the glasses is to incorporate heavy metal oxides. These heavy metal oxides have a considerable influence on the density of the glasses and accordingly on the attenuation features of the glasses. In the last decades, the radiation attenuation features of some heavy metal based glasses have been investigated, however there is still great interest in studying the this kind of glass system as radiation protection materials.

Adsorbents and Catalysts Based on Mesoporous Metal Oxides

Andrei Ivanets *, Vladimir Prozorovich, Tatyana Kouznetsova
Institute of General and Inorganic Chemistry of National Academy of Sciences of Belarus, st. Surganova 9/1, 220072 Minsk, Belarus

The development of nanotechnology has a significant impact on science and technology. Heavy metal ions, organic dyes, pharmasutically active compounds, radionuclides are thwe major pollutants of aqutic systems. The use of green and environmentally friendly technologies based on nanomaterials is widely used to solve the problem of water purification from toxic pollutants. This is primarily due to the creation of nanostructured hybrid (organomineral) membranes, catalysts for *Advanced Oxidation Processes* and effective nanoscale adsorbents [1]. The current report is aimed to the preparation of adsorbents and catalysts based on mesoporous metal oxides for environmental pollution recovery and wastewater treatment.

The first part devoted to manganese oxides with layerd and tunnel structure, which were used as a selective adsorbents for strontium radioniclides removal from modeling liquid radioactive wastes. High exchange capacity, stability in alkaline media allow to consider manganese oxides with a layered and channel structure as a promising materials for the removal of radioactive metal ions from aqueous media. Manganese oxides have a structure of octahedral molecular sieves (OMS) with tunnels 2×2 or 3×3, which is formed from octahedra MnO_6. The dimensions of the tunnels of OMS 2 (cryptomelane with ions K^+) and OMS-1 (type todorokite with ions Ca^{2+} or Mg^{2+}) depend on the cations located inside and around of 0.46 and 0.70 nm respectively The relationship between the conditions of preparation, physical-chemical and sorption-selective properties of manganese oxides will allow to define general regularities and approaches to the directed synthesis of highly selective sorbents of strontium radionuclides. [2].

The second part descrided the results of carrying out of magnesium ferrites as Fenton-like catalysts and nanostructured adsorbent of heavy metal ions and organic dyes. The results of the study of the regularities of synthesis and the study of the physico-chemical properties of adsorbents and catalysts based on nanostructured ferrites were presented. The relationship in the series “synthesis – structure – properties” for individual and lanthanide-doped magnesium ferrites, as well as for composites with graphitic carbone nitride, has been established. The mechanism and the features of the behavior of the obtained materials in the processes of adsorption of metal ions and organic dyes were studied. The results of the study of the catalytic properties of ferrites in *Advanced Oxidation Processes* on the example of heterogeneous Fenton-like catalysts for the destruction of various organic pollutants were presented. The main factors determining the effectiveness of adsorbents and catalysts based on ferrites in water treatment processes were established [3].

The presented results are important for understanding the adsorption-desorption processes, catalytic and regeneration mechanism, and for real application for wastewater treatment. The prospects of mesoporous metal oxides can serve as an effective material for adsorption and catalytic treatment of multi-component aqueous solutions containing heavy metal ions, radionuclides, and toxic organic pollutants.

References

[1] R. Li [et al.] Nanoscale 7 (2015) 17167.
[2] A. Ivanets [et al.] Environmental Nanotechnology, Monitoring & Management 6 (2016) 261-269.
[3] A. Ivanets [et al.] Chemical Engineering Journal 411 (2021) 128523.

FUNCTIONAL MATERIALS & APPLICATIONS

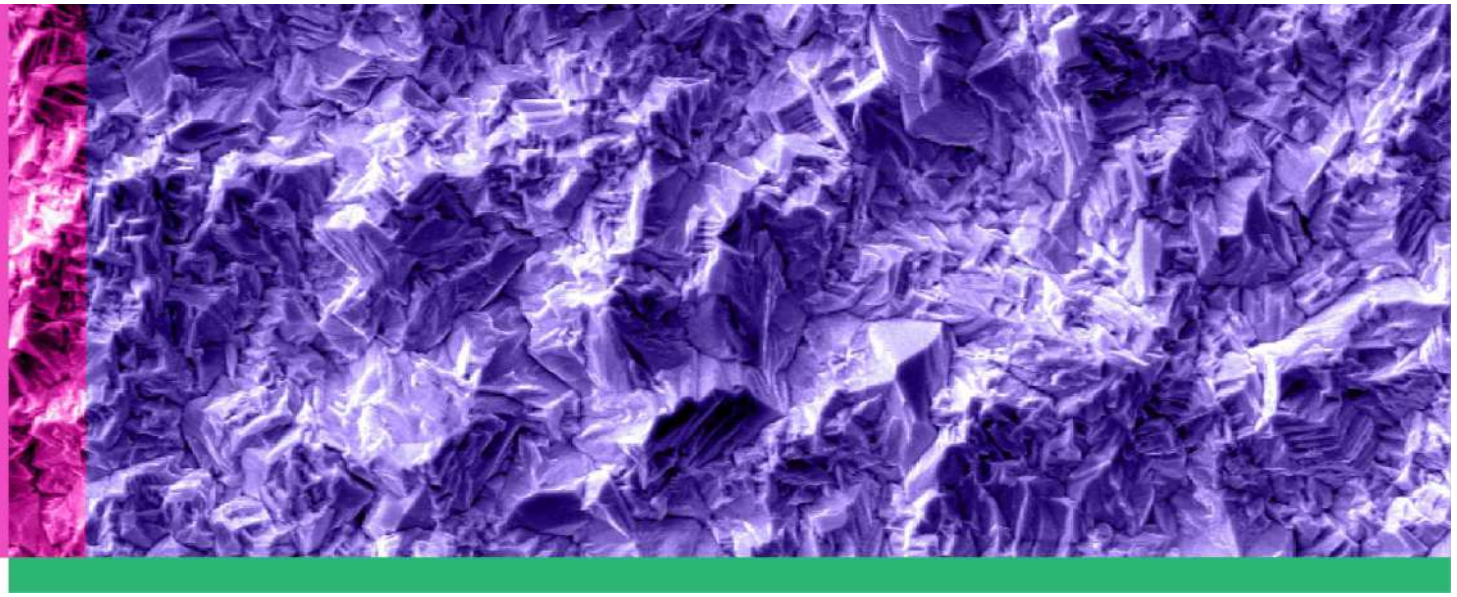

Influence of the microstructure of Ni-Fe-based coatings on the efficiency of magnetostatic shielding

O.D. Kanafyev[1*] ,V.A. Fedzkin[1], A.N. Kotelnikova[1], M.I. Panasyuk[1], T.I. Zubar[1]
[1] *SSPA "Scientific and practical materials research centre of NAS of Belarus", 220072, Minsk, P. Brovki str., 19, Belarus*
** corresponding author e-mail: olegkan96@mail.ru*

The rapid development of high-precision instruments opens up many possibilities for exploring and improving the world around us. At the same time there is a problem of protection of sensitive elements of these devices from permanent magnetic fields, electromagnetic radiation and electromagnetic pulse. A passive method of electromagnetic protection are shields obtained by various methods, including the method of electrolytic deposition. The technology and synthesis conditions determine the microstructure of the material, which in turn affects the mechanical and functional properties. The most common shields are films based on Ni and Fe alloys. The influence of the surface microstructure on the mechanical properties of Ni-Fe thin films, will determine the method of synthesis of shields with optimal mechanical characteristics[1-2]. In this work the influence of microstructure on the shielding efficiency of permalloy shields was investigated. For this purpose, Ni-Fe shield coatings were obtained in the mode of constant and pulsed electrodeposition, the pulse duration was 1, 0.1 and 0.01 s. The obtained shields had a composition of 50 wt.% Fe + 50 wt.% Ni with slight changes not exceeding a few percent, which were caused by changes in the kinetics of the redox reaction. The microstructure of the obtained samples was studied by SEM and AFM.

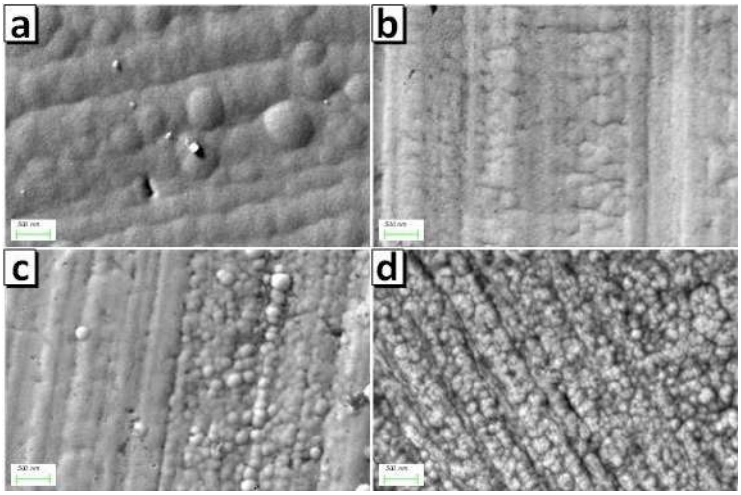

Figure 1. Surface microstructure of FeNi shields investigated using SEM: (a) P_0, (b) P_1, (c) $P_{0.1}$, and (d) $P_{0.01}$

All coatings had a pronounced grain structure and showed a decrease in the average grain size from 0.5 μm for the stationary P_0 mode to 100 nm for the pulsed $P_{0.01}$ mode. Along with the decrease in grain size, the size of the domain examined by MFM also decreased. It is shown that the samples with grain size of 0.3-0.6 μm have disordered domain structure, which allows achieving higher values of maximum shielding efficiency (SE_{max} = 29 dB for P_0 shield), but they are characterized by a narrow operating range. Samples with grain size less than 200 nm have an ordered two-domain magnetic structure with possible partial transition to the superparamagnetic state in areas with grain size less than 100 nm. Such characteristics as ordered magnetic structure, small domain size and coexistence of ferromagnetic and superparamagnetic regions, although reducing the maximum efficiency value from 29 to 25.5 dB, but significantly extend the operating range of the shields from 24.5 to 33 E. As a result, a correlation between the grain and domain structure and the efficiency of magnetostatic shielding was found.

References

[1] Panagopoulos, D. J. [et al.], *Sci. Total Environ.* 2019, *667*, pp. 255–262.
[2] Zhang, Q. [et al.], *Adv. Funct. Mater.* 2018, *28*, 1703801.

Erbium 1.53 μm and up-conversion luminescence from sol-gel derived structures

N.V. Gaponenko[1]*, L.V. Sudnik[2], P.A. Vityaz[2], A.V. Mudryi[3], A.R. Luchanok[2], M.V. Stepikhova[4], A.N. Yablonskiy[4], B.A. Andreev[4], Yu.V. Radyush[3], V.D. Zhivulko[3], E.I. Lashkovskaya[1], Yu. D. Karnilava[1], M.V. Rudenko[1], K.V. Shustsikava[1], A.N. Petlitskii[5], D.V. Zhigulin[5], N.M. Kazuchits[6], M.S. Rusetsky[6]

[1] *Belarusian State University of Informatics and Radioelectronics, P. Browki 6, 220013 Minsk, Belarus, nik@nano.bsuir.edu.by**

[2] *State Scientific Institution «Powder Metallurgy Institute named after academician O. V. Roman», Platonova str., 41, 220005, Minsk, Belarus*

[3] *Scientific-Practical Materials Research Centre of National Academy of Sciences of Belarus, P. Browki 19, 220072 Minsk, Belarus*

[4] *Institute for Physics of Microstructures Russian Academy of Sciences, 607680 Nizhny Novgorod, Russia*

[5] *Joint Stock Company "Integral" 121 A, Kazintsa Str., 220108, Minsk, Belarus*

[6] *Belarusian State University, 4 Nezavisimosti Avenue, 220030, Minsk, Belarus*

The review of fabrication methods and luminescence properties of optically anisotropic structures doped with trivalent lanthanides, in particular, porous anodic alumina, synthetic opals, porous silicon or sol-gel derived microcavities is given. Erbium 1.53 μm luminescence is reported from xerogel films generated on porous silicon and porous anodic alumina. Photo- and cathodoluminescence in the visible range is observed from barium titanate xerogel powders and targets, fabricated from xerogels using the explosive pressing method. The powders and targets demonstrate upconversion luminescence at excitation wavelength 980 nm with the bands at 650, 520 - 560 and 820 nm, corresponding to transitions $^4F_{9/2} \rightarrow {}^4I_{15/2}$, $^2H_{11/2} \rightarrow {}^4I_{15/2}$, $^4S_{3/2} \rightarrow {}^4I_{15/2}$, $^4I_{9/2} \rightarrow {}^4I_{15/2}$ of trivalent erbium. The targets demonstrate also cathodoluminescence at the temperatures 300 and 77 K with the most intensive bands at 650, 520 and 538 nm. Finally, erbium 1.53 μm and up-conversion luminescence from barium titanate fims is reported.

The work was carried out under support of the collaborative grant of the Belarusian Republican Foundation for Fundamental Research (BRFFR Kh20R-388) and Russian Foundation for Basic Research (RFBR 20-52-00039 Bel_a).

Structure and magnetic properties of $FeCo@SiO_2$ nanoparticles obtained by the coprecipitation method for targeted drug delivery

U. Gumiennik[1,2,*], J. Fedotova[1], S. Vorobyova[3] and M. Mašláň[4]
[1] *Institute for Nuclear Problems of Belarusian State University, Babrujskaja Str. 11, 220006 Minsk, Belarus* *uladzislaw.gumiennik@gmail.com
[2] *Department of Solid State Physics, Faculty of Physics and Applied Computer Science, AGH University of Science and Technology, Mickiewicza Av. 30, 30-059 Kraków, Poland*
[3] *Research Institute for Physical Chemical Problems of Belarusian State University, Lieninhradskaja Str. 14, 220006 Minsk, Belarus*
[4] *Department of Experimental Physics, Faculty of Science, Palacký University, 17. Listopadu Str. 1192/12, 779 00 Olomouc, Czech Republic*

In this work, we investigate structure and magnetic properties of nanoparticles (NPs) containing Fe_xCo_{1-x} ($25 \le x \le 75$, wt.%) core inside mesoporous SiO_2 shell sintered with different molar ratios of FeCo and SiO_2 by two-stage procedure including FeCo coprecipitation and SiO_2 TEOS hydrolysis.

Biocompatible FeCo-SiO_2 NPs generally possessing high magnetic moment [1] are considered as promising agents for drug delivery inside blood vessels under external magnetic field [2]. Core-shell NPs are characterized with scanning electron microscopy (SEM), transmission electron microscopy (TEM), ^{57}Fe Mössbauer spectroscopy (at T_{room} and 5 K) and vibrating sample magnetometry (VSM) at T between 5-300 K and magnetic fields up to 9 T.

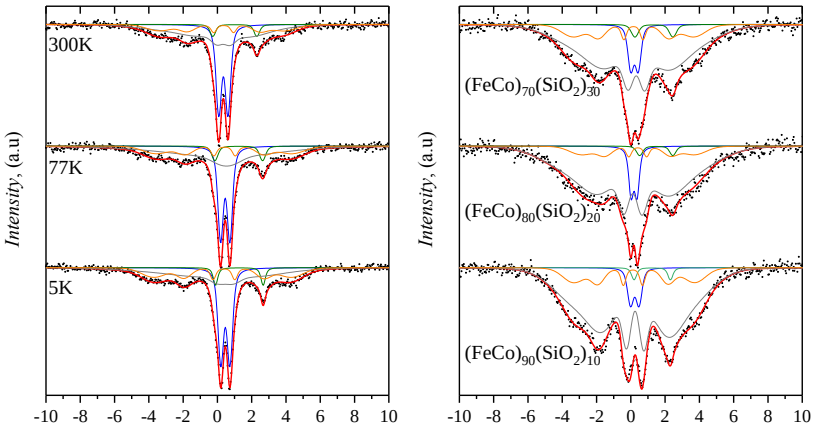

Figure 1 – Mössbauer spectra of FeCo nanoparticles: left – temperature evolution of FeCo NPs spectra without mesoporous SiO_2 shell, right – NPs spectra with different SiO_2 contribution

Temperature evolution of Mössbauer spectra as well as magnetization loops and FC-ZFC curves evidently reveal that NPs with medium diameter around 100 nm containing oxidized FeCo cores form magnetically–interacting aggregates. By analyzing the values of hyperfine parameters extracted from Mössbauer spectra one may conclude that they do not show vivid variation tendencies with the Fe:Co ration while the formation of SiO_2 shells promotes aggregation of FeCo cores at the expense of separate NPs. Values of saturation magnetization and coercive force at T_{room} up to 65 emu/g and 300 Oe, correspondingly, evidence some surface oxidation of FeCo cores. The results of VSM and Mössbauer spectroscopy reveal less pronounced oxidation of FeCo cores with the increase of SiO_2 contribution which enhances.

This work was supported financially by the BRFFR-VAST scientific project Ph21V-008 «Nanoparticles "CoFe core-shell mesoporous SiO_2" for targeted drug delivery: study of loading capacity and modeling of transport in an external magnetic field». Uladzislaw E. Gumiennik acknowledges the financial support of the Belarus National Scholarship Programme of the World Federation of Scientists. The authors are also grateful to Artjom Konakov for synthesizing of samples, Tomáš Ingr for SEM studies, and Ondřej Malina for magnetic studies.

References

[1] J. Liu, D. Su, K. Wu, and J.-P. Wang Journal of Nanoparticles Research 22 (2020) 66.
[2] C. Bárcena, A.K. Sra, and J. Gao, Nanoscale Magnetic Materials and Applications (2009) 591-626.

Crystalline structure and magnetic properties of the GaSb-Fe_3Ga_4 composite

I. Ch. Mamedov[1], D.G. Arasly[1], R.N. Ragimov[1], A.A. Khalilova[1], P.Yu. Lapotko[2], A.I. Galyas[2], V.S. Goncharov[2], A.M. Zhivulko[2], T.C. Mazanik[2], K.I. Yanushkevich[2]
[1]*Institute of Physics of the National Academy of Sciences of Azerbaijan; Az-1143, Baku, G.Javid Ave. 33*
[2]*State Scientific and Production Association "Scientific - Practical Center Materials Research Centre of the National Academy of Sciences of Belarus" 220072, st. P. Brovki 19, Minsk, Belarus*

A magnetic multicomponent semiconductor composite material GaSb-Fe_3Ga_4 has been synthesized. The elemental composition of the matrix and metal inclusions in the interfacial zone has been determined. It was found that at the temperature of liquid nitrogen, the specific magnetization of the composite has a value of $\sigma \approx 1.5$ $A \cdot m^2 \cdot kg^{-1}$ and an average magnetic moment $\mu \approx 0{,}17$ μV. It was revealed that the magnetic characteristics of the composite are resistant to thermal loads up to 750 K and external magnetic fields up to 14 Tesla.

SYNTHESIS AND MICROWAVE ABSORPTION PROPERTIES OF SUBSTITUTED BARIUM FERRITES

D. Ivashenko[1*], Y. Haiduk[1], G. Melnikova[2], D. Bychanok[3], V. Pankov[1]
[1] *Faculty of Chemistry, Belarusian State University, 14, Leningradskaya Str., 220030, Minsk, Belarus*
[2]*A.V. Luikov Heat and Mass Transfer Institute of NAS of Belarus, 15, Brovki Str., 220072, Minsk, Belarus*
[2]*Research Institute for Nuclear Problems, Belarusian State University, 11 Bobruiskaya Str., 220030, Minsk, Belarus*

In this work, barium hexaferrites substituted with aluminum with the M-type structure were obtained using the method of sol-gel synthesis and the method of spray drying followed by annealing.

When spray drying a suspension of particles in the process of removing the solvent from a liquid droplet, spherical agglomerates with a diameter of about 1–2 μm are formed. Using the sol-gel method, ferrite particles were obtained in the form of plates with a diameter of the order of 1-2 microns. The resulting products were annealed at a temperature of 900 ℃ before investigations.

Measurements of the amplitude of the reflected signal from the studied samples of radio-absorbing materials were carried out in the frequency range of 1-12 GHz by the coaxial method using a Mikran R4M vector network analyzer.

Figure 1 shows the frequency dependences of the complex permittivity and permeability of $BaAl_2Fe_{10}O_{19}$ samples obtained by sol-gel synthesis and spray drying in the frequency range 1-12 GHz. Shows that the samples under study have similar electromagnetic characteristics in the given frequency range. The frequency dependence of the magnetic permeability μ indicates weak magnetic properties (from 1.2 at 1 GHz to 1.1 at 12 GHz) of the samples in the investigated frequency range. From the frequency dependence of the permittivity ε, it is noticeable that the samples under study exceed the permittivity of a dispersion medium (paraffin wax has a dielectric constant of about 2), which has a real part close to 3, has a relatively small imaginary part and has a low dispersion. It is worth noting that in work [6], ferrite of the same composition was obtained, but having a significantly higher dielectric constant (6.5 vs 3.0 at 1.0 GHz). These results may relate to matrix effects arising from sample preparation when measured with a vector network analyzer.

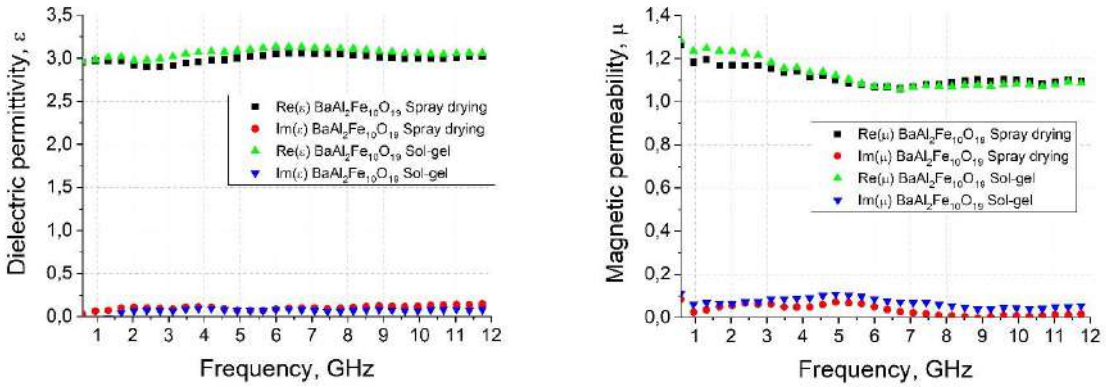

Figure 1. Comparison of the frequency dependence of the dielectric and magnetic permeability for $BaAl_2Fe_{10}O_{19}$, obtained by the methods of sol-gel synthesis and spray drying

Prospects for the use of thermochemical treatment with subsequent deposition of DLC coatings on tool steels

A.V. Kovalchuk
Belarusian National Technical University,
220013, 65, Nezavisimosty ave., Minsk, Belarus

Comprehensive study of structure and mechanical properties of the surface of tool carbon steel with metalloid-containing diffusion layer obtained by thermochemical treatment, and subsequent deposition of Diamond Like Carbon (DLC) coatings were investigated with support by Belarus National Scholarship Programme of World Federation of Scientists. It was found that the preliminary hardening of the steel substrate as a result of boriding allows us to significantly increase the properties of the surface with DLC coating. The fact of an increase in the nanohardness, microhardness, the elastic modulus and wear resistance of coated borided steel surface compared to the DLC coating on utreated steel without diffusion layer have been established.

Multilayer structure of nitride layer obtained by saturation with thermal cycling on tool steel

A.V. Kovalchuk, N.A. Vereshchak
Belarusian National Technical University,
220013, 65, Nezavisimosty ave., Minsk, Belarus

Regularities of the formation of a structure with a periodic distribution of nitride phases in a thermodiffusion nitrided layer, formed as a result of nitriding on tool alloy steel after the saturation at the 690...910 K with a frequency of heat cycles during processing up to 6 times have been established. The optimal parameters of the nitriding regime have been established, which make it possible to accelerate the formation of the diffusion layer by 15-20 % and to obtain a composite structure of the nitride layer with alternating layers of high-nitrogen and low-nitrogen phases as well as nitrogenous ferrite.

Problems and prospects of micro- and nanocrystalline silicon

N.V. Latukhina[1], V.S. Pavelyev[1], V.I. Chepurnov[1], D.A. Shishkina[1]
[1] *Samara National Research University 34, Moskovskoe shosse, Samara 443086, Russia, natalat@yandex.ru*

Silicon continues to be the most common electronics material due to its ubiquity and well-established technology for the production of semiconductor-quality crystals. The development of technology has led to the creation of new modifications of silicon with unique qualities - micro- and nanocrystalline silicon. When any characteristic quantities of matter are transferred to a nanoscale scale due to the manifestation of the quantum-dimensional effect, its fundamental properties radically change. The electronic structure of silicon changes, it has new electrical and optical properties, so that the scope of its application is even more expanded.

The most extensive class of nanocrystalline silicon is porous silicon[1]. It is a kindofcrystal sponge andis formed when many pores are etched ina single siliconcrystal, the walls of which are systems of nanocrystals of various shapes and sizes.Depending on the size, shape, number of pores, their mutual arrangement, the properties of the material vary widely. With an ordered pore arrangement, porous silicon can be a photonic crystal,which is the basis of many nanophotonics devices. In optoelectronics, porous silicon is used in both photosensitive devices and luminescent ones. The extensive chemically active free surface and high sensitivity of pores to filling with various substances makes porous silicon a promising material for various sensors. Due to the low toxicity of porous silicon, materials based on it have good prospects for various medical applications:substrates for the growth of various biological tissues, vectors for targeted delivery of drug substances, biosensors, biochips, etc.

One of the significant problems of porous silicon is the instability of itsparameters, caused by the presence of residues of reagents in the pores. However, this problem is effectively solved by the use of various stabilizing coatings. A promising method of stabilizing the surface of porous silicon is its carbonization by endotaxy. In this method, a layer of silicon carbide is formed by a chemical reaction of carbon with surface silicon atoms. The resulting heterostructure of silicon carbide on silicon has high performance characteristics of a layer of silicon carbide with the convenience of silicon technology. With endotaxy of porous silicon, there is no problem of matching the crystal lattices of the silicon substrate and the resulting layer of silicon carbide existing in the technology of manufacturing these heterostructures.

Microcrystalline silicon is formed during the structuring of silicon at the micron level and is used in terahertz optoelectronics for the manufacture of diffraction optical elements, axons, lenses, mirrors.

It can be concluded that thanks to the development of technology and the creation of new modifications of silicon,it continues to be the main material of electronics, conquering more and more new areas of application.

Reference

[1] O. Bisi et al. / Surface Science Reports 38 (2000) 1–126

The structural and magnetic properties of SMC materials based on high-purity iron powders in the frequency range of oscillations up to 100 kHz

Govor G.A.[1], Vecher A.K.[1], Demidenko O.F.[1], Larin A.O.[1*]
[1]*SSPA "Scientific-Practical Materials Research Centre of NAS of Belarus", 220072, Belarus, Minsk, 19 P. Brovki st, larin@physics.by**

In a wide range of temperatures and magnetic fields, a study of soft magnetic composite (SMC) materials based on ABC100.30 iron powder with an insulating coating on phosphorus oxides in a frequency range of up to 100 kHz was carried out.

Soft magnetic composites (SMC) based on iron powder have increasingly received intensive research interests because of the potential using for the SMC within many engineering fields covering electrical equipment, high-power transformers and modern communication. Compared with traditional silicon steel material, the SMC have remarkable advantages such as high magnetic inductions, high frequency properties, decreased core losses, three-dimensional isotropic magnetic properties [1–3], low magnetocrystalline anisotropy constant and flexible design [4]. In this work, we investigated the structural and magnetic properties of SMC materials based on high-purity iron powders ABC100.30 with nanoscale insulating coatings based on phosphorus oxide.

It is shown that, under normal conditions, the composite material, due to the presence of interparticle conduction channels, forms the electron density on the Fermi surface, which is characteristic of the metallic state. In this case, the specific resistivity of the SMC material is orders of magnitude higher than for the metallic state.

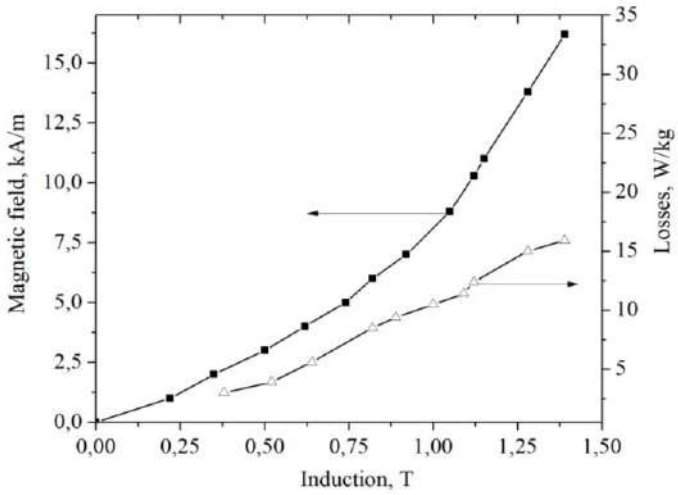

Figure 1 – Magnetization and loss curves at a frequency of 1 kHz SMC based on ABC100.30 in magnetic fields up to 15 kA/m.

With a decrease in temperature, it occurs as a result of thermal compression of metal particles with an exponential decrease in the number of interparticle conduction channels. As a result, the magnetic state can be characterized as superparamagnetic, in which only interparticle magnetic interaction is retained.

The study of magnetization reversal losses in the frequency range up to 100 kHz (Fig.1) has shown that they can be used in various energy conversion devices due to the high saturation induction and low losses.

Acknowledgement: This work was financial supported by Belarusian Republican Foundation for Basic Research as part of the projects BRFFR No. T21ET-007.

References:

[1] J.M. Silveyra, E. Ferrara, D.L. Huber, T.C. Monson, Soft magnetic materials for a sustainable and electrified world, Science 362 (2018) 195–203.
[2] J. Füzer, M. Strečková, S. Dobák, Ľ. Ďáková, P. Kollár, M. Fáberová, R. Bureš, Y. Osadchuk, P. Kurek, M. Vojtko, Innovative ferrite nanofibres reinforced soft magnetic composite with enhanced electrical resistivity, J. Alloys Compd. 753 (2018) 219–227
[3] B. Meng, et al. Low-loss and high-induction Fe-based soft magnetic composites coated with agnetic insulating layers Journal of Magnetism and Magnetic Materials 492 (2019) 165651 2019
[4] S. Wu, A. Sun, F. Zhai, J. Wang, Q. Zhang, W. Xu, P. Logan, A.A. Volinsky, Annealing effects on magnetic properties of silicone-coated iron-based soft magnetic composites, J. Magn. Magn. Mater. 324 (2012) 818–822.

Features of growing Tm^{3+}:$KY(WO_4)_2$ single crystals and their optical properties

S.A. Guretskii[1*], E.L. Trukhanova[1], A.V. Kravtsov[1], N.V. Gusakova[2], K.N. Gorbachenya[2], V.E. Kisel[2], A.S. Yasukevich[2], R. Lisiecki[3], A. Lukowiak[3], D.V. Karpinsky[1], S. Ozcelik[4] and N.V. Kuleshov[2]*

[1] *Scientific and Practical Materials Research Center NAS Belarus, P.Brovki st., 19, Minsk, Belarus*

[2]*Center for Optical Materials and Technologies, Belarusian National Technical University, Nezavisimosty Ave., 65, Minsk, Belarus*

[3]*Institute of Low Temperature and Structure Research, PAS, Okolna, 2, 50-422, Wroclaw, Poland*

[4]*Photonics Application & Research Center, Gazi University, Ankara, Turkey*

The factors influencing the crystallization processes of Tm doped $KY(WO_4)_2$ single crystals in order to optimize the crystallization mode and improve the quality of the crystals are studied. The laser spectroscopic properties of the Tm^{3+}:$KY(WO_4)_2$ crystals, the absorption and luminescence spectra, and the luminescence decay kinetics are analyzed.

References:

[1] M. Gaponenko, N. Kuleshov, and T. Sudmeyer, Opt. Express. 22 (2014) 11578-11582.
[2] M.S. Gaponenko, A.A. Onushchenko, V.E. Kisel, A.M. Malyarevich, K.V. Yumashev, N.V. Kuleshov, Laser. Phys. Lett. 9 (2012) 291-294.
[3] A.A. Lagatsky, S. Calvez, J.A. Gupta, V.E. Kisel, N.V. Kuleshov, C.T.A. Brown, M.D. Dawson, W. Sibbett, Opt. Exp. 19 (2011) 9995-10000.
[4] X. Mateos, R. Solé, Jna. Gavaldà, M. Aguiló, J. Massons, F. Díaz, Opt. Mater. 28 (2006) 423-431.
[5] A.S. Kumaran, S.M. Babu, S. Ganesamoorthy, I. Bhaumik, A.K. Karnal, J. Cryst. Growth. 292(2) (2006) 368-372.
[6] A.E. Troshin, V.E. Kisel, A.S. Yasukevich, N.V. Kuleshov, A.A. Pavlyuk, E.B. Dunina, A.A. Kornienko, Appl. Phys. B 86 (2007) 287-292.
[7] N.V. Gusakova, M.P. Demesh, A.S. Yasukevich, A.A. Pavlyuk, N.V. Kuleshov, J. Belarusian State University. Physics. 1 (2021) 33–40.
[8] A.S. Yasukevich, V.G. Shcherbitsky, V.E. Kisel, A.V. Mandrik, N.V. Kuleshov, ASSP Top. Meet. (2004) 426.

Magnetic properties of solid solutions $Bi_{1-x}Ba_xFe_{1-y}Ti_yO_{3-d}$ across the morphotropic phase boundary

M.V. Silibin[1,2], D.V. Zhaludkevich[3], S.I. Latushka[3], A.V.Sysa[1,2], V.V. Sikolenko[4], D.V. Karpinsky[3]

[1]*National Research University of Electronic Technology "MIET", 124498 Zelenograd, Moscow, Russia*

[2]*Scientific-Manufacturing Complex "Technological Centre", 124498 Zelenograd, Moscow, Russia*

[3]*Scientific-Practical Materials Research Centre of NAS of Belarus, 220072 Minsk, Belarus*

[4]*REC "Functional nanomaterials", Immanuel Kant Baltic University, 236041 Kaliningrad, Russia*

The present study is focused on a correlation between the magnetic properties, crystal structure and structural parameters of the compounds $Bi_{1-x}Ba_xFe_{1-x}Ti_xO_3$ across the rhombohedral - cubic phase transition. A relation between the type of lattice distortion, structural parameters and magnetic properties is discussed for the ceramics $(1-x)BiFeO_3 - (x)BaTiO_3$ with $x < 0.40$ depending on the dopant content and temperature.

The results of diffraction measurements of the compounds $Bi_{1-x}Ba_xFe_{1-x}Ti_xO_3$ ($x \leq 0.40$) indicate that an increase in the dopant concentration leads to a gradual reduction of the rhombohedral distortions (Fig. 1). The structure of the compounds with $x = 0.25 - 0.33$ can be refined assuming a coexistence of the rhombohedral and cubic phases; further increase in the dopant content leads to the phase transition to the single phase cubic structure. Analysis of the isothermal dependences of the magnetization as well as neutron diffraction measurements points at the G-type antiferromagnetic structure which is stable in the compounds with $0.15 \leq x \leq 0.4$ in the wide temperature range in spite of the chemical dilution by nonmagnetic Ti ions. The obtained results imply that magnetic properties of the polar phase are strongly dependent on the structural distortions involving the oxygen octahedra tilting which mainly determines the modification of remanent magnetization. The absence of a direct correlation between the type of lattice system and the existence of remanent magnetization observed for the co-doped compounds testifies an inapplicability of the related model used to describe the magnetic properties of $BiFeO_3$ compounds doped with rare-earth ions to those co-substituted by Ba and Ti ions.

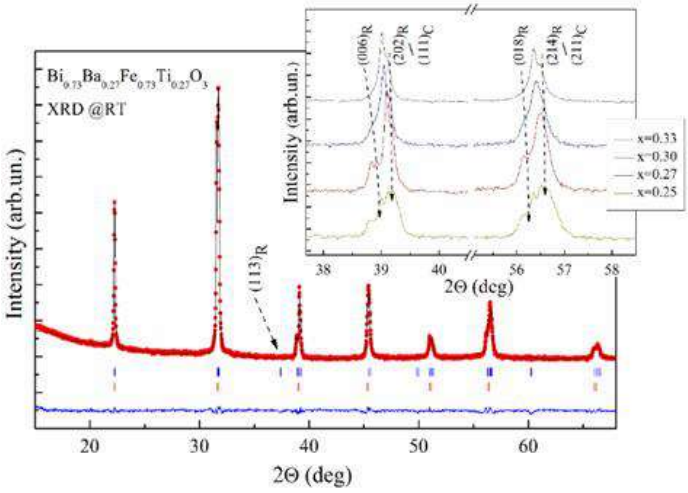

Figure 1. X-ray diffraction patterns of $Bi_{1-x}Ba_xFe_{1-x}Ti_xO_3$ compounds.

Acknowledgement

The authors M.V.S. and D.V.K. acknowledge RFBR (projects # 20-58-00030) and BRFFR (project # F20R-123).

Sintered porous materials for advanced nanosatellites propulsion

E. Chubenko[1], S. Redko[1], A. Dolgiy[1], V. Bondarenko[1,*], V. Mazyuk[2] and M. Krakow[3]
[1]*Belarusian State University of Informatics and Radioelectronics, P.Provka str. 6 220013 Minsk, Belarus*
[2] *The State Scientific Institution "Powder Metallurgy Institute", Platonova str. 41 220013, Minsk, Belarus*
[3] *Belarusian National Technical University, Nezavisimosti ave. 65 220013, Minsk, Belarus*

Fabrication techniques for Ni/Cu capillary insertions for FEEP microthruster emitters were developed. The slit emitter based on planar quartz substrates and the point emitter based on a quartz tube were filled with a Ni/Cu composite proved to be compatible with both EMIM:BF_4 and EMIM:IC ionic liquids used as a propellant. The EMIM:IC showed better results with a 3 – 5 times higher infiltration rate. According to the simulation of the propellant flow inside the capillary system alternation of polarization of the emitter-extractor system was found to be necessary for a normal operation. The frequency and duration of polarity steps determined by the porosity of the insertion, the mass of ions and the electrical potential difference. Obtained results will be used for FEEP microthruster systems of both linear and point configurations that is under development.

Effect of proton radiation on optical and mechanical properties of TiAlN coating

I. Parkhomenko[*1], L. Vlasukova[1], S. Konstantinov[2], V. Zaikov[1], F.Komarov[2]
[1]*Belarusian State University, Kurchatova Str., 5, 220108, Minsk, Belarus, parkhomenko@bsu.by*
[2]*A.N. Sevchenko Research Institute of Applied Physics Problems, Kurchatova Str, 7, 220108, Minsk, Belarus*

Titanium aluminum nitride (TiAlN) coating is promising material for application in space. During the operation such coatings are exposed to the energetic particles flux. We present the effect of protons on mechanical and optical properties of TiAlN coating deposited by reactive magnetron sputtering after proton irradiation.

TiAlN coating with thikness 2 μm was deposited on the 12X18H10T steel substrate by the reactive magnetron sputtering technique. The samples of (2×2 cm^2) were cut and irradiated with 500 keV protons (H^+ ions). The fluences of implanted ions were $1\cdot10^{16}$, $5\cdot10^{16}$, $1\cdot10^{17}$ and $2\cdot10^{17}$ cm^{-2}. To prevent annihilation of radiative defects via sample heating during irradiation the ion current did not exceed 1-3 μA/cm^2. Mechanical properties of the coatings were studied from nanoindentation data using the Oliver–Pharr method. Reflectance measurements were performed using a LAMBDA-1050 UV-VIS spectrophotometer in the range of 190–2500 nm. Universal Reflectance Accessory was used to measure the specular reflectance at 8° incident angle. Diffuse reflectance spectra were registerd using implemented 150 mm integrating sphere. Using diffuse reflectance spectra, the band gap energy has been determined by using Kubelka−Munk function.

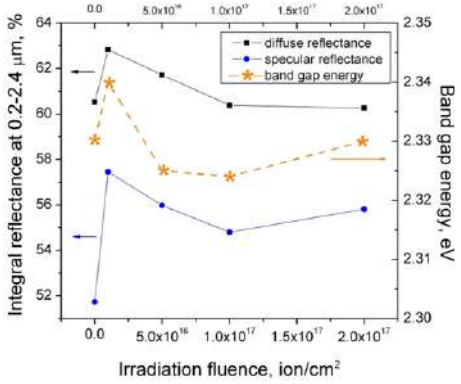

Intergral reflectance of TiAlN coating at spectral range of 190 – 2500 nm versus the fluence of 500 keV H^+ ions

The irradiation with small fluence ($1\cdot10^{16}$ – $5\cdot10^{16}$ cm^{-2}) results in improvement of mechanical properties (increase of nanohardness and Yong's modulus), while futher increase of proton fluence ($1\cdot10^{17}$ – $2\cdot10^{17}$ cm^{-2}) lead to decrease of these mechanical characterisics. Proton irradiation with the smallest fluence $1\cdot10^{16}$ ion/cm^2 results in increase of specular on average by 6 % and diffuse reflection on average only by 2.5 % in full investigated spectral range. In other words, specular reflection increases while scattered light decreases. It suggests the coating surface is becoming smoother. Band gap energy is also increase from 2.33 to 2.34 eV that can indicate weak improvement of crystal quality of TiAlN coating. Further increase of fluence to $5\cdot10^{16}$ ion/cm^2 results in decrease of specular and diffuse reflectance (by 1.5 %) as well as band gap below its initial value. An increase of fluence to $1\cdot10^{17}$ ion/cm^2 maintains the decreasing trend of reflectance and E_g. It can indicates some change in the textural orientation of crystalline planes, which also imply an increase in the film roughness. The proton irradiation with the maximum fluence of $2\cdot10^{17}$ ion/cm^2 results in slight decrease of diffuse reflectance and in increase, to a greater extent, in specular reflectance and energy band gap. It suggests the coating surface is becoming smoother again, and the size of crystallites of grains is decreasing that implies band structure modification.

Thus the improvement of mechanical properties after proton irradiation with fluences of $2\div5\cdot10^{16}$ ion/cm^2 can be explained by decrease of coating roughness, that implicitly confirmed by decrease of the scattering component of coating reflectance. The weak degradation of mechanical characterisits after irradiation with maximum fluence of $2\cdot10^{17}$ cm^{-2} can not be explained by blistering effect because of specular reflectance does not decrease. Probably, it can be attributed to radiative defects or degradation of steel substrate.

Light-emitting compositions on the base of SiO_2 and SiN_x films on Si:Electroluminescence and its degradation

I. Romanov[1], L. Vlasukova[1*], F. Komarov[2], I. Parkhomenko[1], N. Kovalchuk[3]
[1]*Belarusian State University, 4 Nezavisimosti Ave., 220030, Minsk, Belarus*
[2]*A.N. Sevchenko Institute of Applied Physical Problems of Belarusian State University, Kurchatov Ave. 7, 220108, Minsk, Belarus*
[3]*Joint Stock Company "Integral" – «INTEGRAL» Holding Managing Company, 121A Kazintsa Street, 220108, Minsk, Belarus*

The creation of the Si-based light-emitting device is an important and necessary step in the development of silicon photonics. Over the past 30 years, various approaches have been applied to improve the emission properties of thin amorphous silicon oxide and nitride films. The commonly used method to analyse light-emitting properties of such films is photoluminescence. However, from the point of view of the future technological application of such structures, electroluminescence (EL) is the most important technique to study light-emitting centers. The EL method provides information about the relationship between the electric and luminescent properties of dielectric layers, the structure of dielectric films and the charge carrier transport. In this work, electroluminescence was excited in the 'electrolyte-dielectric-semiconductor' (EDS) system. Electrolyte as a contact makes it possible to realize a higher breakdown voltage than with standard solid-state transparent contacts (indium tin oxide , ZnO:Al, SiC or polysilicon thin films). In addition, the electrolyte is high-transparent in the spectral range of emission of discussed structures (350–700 nm).

We studied the origin of the observed EL bands, and the effect of the electric field on the electroluminescence and conductivity of SiO_2/Si and $SiN_{1.2}$/SiO_2/Si structures. The analysis of EL degradation can determine the best structure for future device design.

The SiO_2(dry oxidation)/Si sample exhibited the intense EL band at 1.9 eV attributed to silanol groups (Si–OH) in SiO_2. An intensity of this band decreases by a factor of 2.8 after passing a charge of 270 mC/cm^2 through the sample. Passing a charge of 300 mC/cm^2 and 500 mC/cm^2 resulted in self-healing breakdowns and irreversible breakdown of dielectric films, respectively.

The EL intensity of the $SiN_{1.3}$/Si structure was below the sensitivity threshold of the registration system.

The $SiN_{1.2}$/SiO_2/Si sample exhibits EL bands with maxima at 1.9 eV, 2.3 eV, and 2.7 eV. The band at 1.9 eV is related to a dissociation and subsequent recombination of silanol groups (Si–OH). The band at 2.3 eV is attributed to intracenter transitions involving three-coordinated silicon atoms in SiO_2 layers. The band at 2.7 eV is probably due to the radiative relaxation of excited two-coordinated silicon atoms located in the silicon oxynitride layer which formed at the oxide-nitride interfaces.

Analysis of the EL spectra and the U(Q) kinetics of the $SiN_{1.2}$/SiO_2/Si sample reveals the stable intensity of the EL bands at 2.3 and 2.7 eV and the absence of self-healing breakdown. It indicates the protective properties of silicon nitride film. Thus, the silicon nitride layer deposited on top of the SiO_2 layer protects the underlying layer from field degradation and premature breakdown.

Features of the formation of thin films of functional coatings deposited on silicon by ion-beam sputtering of Mo, Cr, W.

S. Baraishuk[1*], V. Dolgiy[1], A. Shevchenok[1], M. Wiertel[2], M. Budzynski[2], A. Turavets[3]and O. Mikhalkovich[3]
[1] *Belarusian State Agrarian Technical University, 99, Nesavisimosti av., Minsk, 220023, Belarus*
[2] *Institute of Physics, University n.a. M. Curie-Sklodowska, 20-031, Lublin, Poland*
[3] *Belarusian State Pedagogical University, 18, Sovetskaja st., Minsk, 220050 Belarus*

A metallic (Mo, Cr, W) coating was deposited on single-crystal silicon (111) Si wafers with the assistance of ions of the deposited metal (Mo+, Cr+, W+) at accelerating voltages of 5 kV – 15 kV. For this, a resonant ion source of a vacuum electric arc plasma was used, which simultaneously generates both a neutral flux of atoms and a flux of ions of the deposited metal. The used type of ion source with electrodes made of the material of the applied coating (molybdenum, chromium, tungsten) allows one to simultaneously obtain controlled fluxes of metal ions and neutral atoms of the deposited metal. The ratio of the density of the ion flux to the density of the neutral flux was in the experiments from 0.01 to 0.1, which corresponded to the conditions for the growth of the coating on the substrate. The pressure in the vacuum chamber during the deposition of coatings was ~ 10^{-2} Pa, and the rate of deposition of coatings in different experiments was ~0.12 ÷ 0.54 nm/min.

The layer-by-layer elemental analysis of the initial (111)Si samples modified by ion-assisted deposition of a metal coating was studied using the Rutherford backscattering (RBS) method of helium ions with E_0 = 1.5 MeV at scattering, inlet and outlet angles of 110°, 0°, 70°, respectively, and computer simulation of the experimental ROP spectra with the RUMP program. The energy resolution of the analyzing system was 15 keV, which provided a depth resolution of ~ 15 nm.

The topography of the coating surface was studied by scanning electron probe microscopy (EDX Oxford Instruments AZtecEnergy-Advanced) and atomic force microscopy (NT 206 (Microtestmachines Co., Belarus).

As a result of studies carried out by the Rutherford backscattering method, it was found that the composition of coatings obtained on silicon wafers includes atoms of the deposited metal, technological impurities of carbon and oxygen from the vacuum chamber, as well as silicon as a result of counter diffusion from the substrate into the coating. With a decrease in the accelerating voltage for assisting ions from 15 kV to 5 kV, the coating thickness increases from 30-45 nm to 90-120 nm, which is explained by the different intensity of the coating sputtering processes. are deposited at different energies of auxiliary ions, and the activation of migration processes during coating. It should be noted that the deposition of coatings with ions on the prepared metal/Si structures contributes to the production of thicker films containing metal silicide phases.

Along with the formation of silicides, carbides, and oxides during ionic deposition of coatings, amorphization of the surface layer of the silicon substrate is observed.

The possibility of controlling the wettability, and hence the free surface energy of the surface, by applying metal-containing coatings on silicon is shown. The roughness of the surface during the ion formation of metal/Si systems remains low, which indicates the quality of the surface of the modified silicon wafers of the systems under study that meets the high requirements for microelectronic products similar to the previously investigated Mo/glass structures.

This work was prepared with the financial support of the Ministry of Education of the Republic of Belarus (No. GR 20211250 and 20211394).

The temperature dependencies on physical properties of $(TlGaSe_2)_{1-x}(TlInS_2)_x$ crystals

V. Hurtavy*, T. Shoukavaya, and V. Chumak
Scientific-Practical Materials Research Centre of National Academy of Sciences of Belarus, Brovki str. 19, Minsk, Belarus

The effect of composition and temperature on the dielectric constant and electrical conductivity of single crystals of $(TlGaSe_2)_{1-x}(TlInS_2)_x$ solid solutions has been studied. The existence of a continuous serie of solid solutions in the $Tl(GaSe_2)_{1-x}(InS_2)_x$ system was confirmed. It is shown that with an temperature growth, the dielectric constant and conductivity increase, and with a concentration x increase, they change according to a linear law, while the conductivity decreases and the dielectric constant increases.

Spark plasma sintering of a mechanochemically obtained solid solution of aluminum in copper

T. Grigoreva[1]*, S. Kovaleva[2], D. Dudina[1,3,4], S. Petrova[5], S. Vosmerikov[1], E. Devyatkina[1], I. Batraev[3], A. Ukhina[1], P. Vitiaz[2], and N. Lyakhov[1,6]
[1]*Institute of Solid State Chemistry and Mechanochemistry of SB RAS, 18 Kutateladze str., Novosibirsk, 630128 Russia, e-mail: grig@solid.nsc.ru**
[2]*Joint Institute of Mechanical Engineering of NASB, 12 Akademicheskaya str., 220072,Minsk, Republic of Belarus*
[3]*Lavrentiev Institute of Hydrodynamics of SB RAS, 15 Akad. Lavrentiev ave., Novosibirsk, 630090 Russia*
[4]*Novosibirsk State Technical University, 20 K. Marks ave., Novosibirsk, 630073 Russia*
[5]*Institute of Metallurgy of UrB RAS, 101 Amundsen str., Ekaterinburg, 620016 Russia*
[6]*Novosibirsk State University, 1 Pirogov str., Novosibirsk, 630090 Russia*

A new approach to the production of monophase aluminum bronzes is proposed: mechanochemical synthesis of a solid solution of aluminum in copper with its subsequent consolidation by electric spark sintering.

The mechanochemically synthesized solid solution of aluminum in copper and the product of its consolidation by spark plasma sintering were studied using X-ray diffraction analysis, optical and electron microscopy. It is shown that the product of mechanochemical synthesis is a mixture of two phases: 90 wt.% Cu(Al) solid solution and 10 wt.% Cu_9Al_4. The lattice parameter of Cu(Al) is 0.3655±0.0001 nm, the level of microstrainges is 1.04±0.08%. The average size of crystallites is 35-40 nm. Particles have a lamellar shape, their dimensions are 10-50 μm in the plane and 2-10 μm in thickness.

After sintering the system becomes single-phase, the lattice parameter of the solid solution increases from 0.3655 to 0.3669 nm, the average crystallite size increases from 35-40 to 80-90 nm. The residual porosity of the sintered alloy is ~0.5 %, the hardness is 290 ± 30 *HV*.

The work was carried out with the financial support of RFBR (project No. 20-53-00037) and BRFBR (project No. T 20R-037).

Mechanochemical modification of copper with aluminum oxide

T. Grigoreva[1*], T. Talako[2], A. Letsko[3], S. Tsybulya[4], A. Ancharov[1,5], E. Devyatkina[1], S. Vosmerikov[1], P. Vitiaz[6], and N. Lyakhov[1, 4]
[1]*Institute of Solid State Chemistry and Mechanochemistry of SB RAS, 18 Kutateladze str., Novosibirsk, 630128 Russia, e-mail: grig@solid.nsc.ru**
[2]*Department of Physical and Technical Sciences of NASB, 66 Nezavisimosti Ave., Minsk, 220072, Belarus*
[3]*Powder Metallurgy Institute, 41 Platonov str., Minsk, 220005 Belarus*
[4]*Novosibirsk State University, 1 Pirogov str., Novosibirsk, 630090 Russia*
[5]*Budker Institute of Nuclear Physics of SB RAS, 11 Akad. Lavrentiev ave., Novosibirsk, 630090 Russia*
[6]*Joint Institute of Mechanical Engineering of NASB, 12 Akademicheskaya str., 220072,Minsk, Belarus*

Hardening of plastic metals, such as copper, aluminum, silver, platinum and others, is an urgent task. Traditionally, copper is modified with ceramic additives, but the poor wettability of ceramic particles with liquid metals does not allow for their uniform distribution in melts.

In this paper, an approach to the modification of copper by aluminum oxide during the mechanochemical reduction of copper oxide is proposed.

The products of mechanochemical reduction of copper oxide by aluminum and a solid solution of aluminum in copper have been studied by X-ray diffraction analysis, IR-spectroscopy and electron microscopy. It is shown that the mechanochemical reduction of copper oxide by aluminum with a sharp increase in temperature occurs in the activator, yielding the formation of α-Al_2O_3. Since the reaction of copper oxide reduction is highly exothermic, a decrease in the synthesis temperature is possible when the same compounds that are formed during the reaction, for example, copper, are introduced into the reaction mixture as a diluent. To increase the copper content while maintaining the stoichiometric ratio of copper and aluminum oxide, a mechanochemically obtained solid solution of aluminum in copper containing 20% aluminum was used as a reduction agent: $CuO + Cu(Al) \rightarrow Al_2O_3 + Cu$. The mechanochemical reduction of copper oxide with a solid solution of aluminum in copper leads to the formation of Cu/Al_2O_3 nanocomposites after 2 min of mechanical activation at the selected modes. This composite material can be effectively admixed into the molten copper.

The work was carried out with the financial support of RFBR (project No. 20-53-00037) and BRFBR (project No. T 20R-037).

Mechanochemical preparation of iron and nickel aluminides modified with aluminum oxide

T. Grigoreva[1]*, T. Kiseleva[2], T. Talako[3], A. Letsko[4], E. Devyatkina[1], S. Vosmerikov[1], D. Sangaa[5], P. Vitiaz[6], and N. Lyakhov[1]
[1]*Institute of Solid State Chemistry and Mechanochemistry of SB RAS, 18 Kutateladze str., Novosibirsk, 630128 Russia, e-mail: grig@solid.nsc.ru**
[2]*Lomonosov Moscow State University, Faculty of Physics, 1-2 Leninskiye Gory, GSP-1, Moscow, 119991 Russia*
[3]*Department of Physical and Technical Sciences of NASB, 66 Nezavisimosti Ave., Minsk, 220072, Belarus*
[4]*Powder Metallurgy Institute, 41 Platonov str., Minsk, 220005 Belarus*
[5]*Institute of Physics and Technology of Mongolian Academy of Sciences, Ulaanbaatar, 13330 Mongolia*
[6]*Joint Institute of Mechanical Engineering of NASB, 12 Akademicheskaya str., 220072,Minsk, Belarus*

Nickel and iron aluminides are characterized by high melting points, low density, heat resistance, and high resistance to thermal shock. Their strength practically does not degrade up to temperatures of 600-900 °C. At higher temperatures, the mechanical properties of aluminides worsen. To reduce their high-temperature creep, highly dispersed ceramic additives are introduced into them.

For the dispersed hardening of nickel and iron aluminides used at high temperatures, highly dispersed ceramic additives are traditionally introduced. However, there are serious technological difficulties in the uniform distribution of additives in the metal matrix due to their poor wettability by metals. The solution to this problem becomes possible if, during the mechanochemical synthesis of nickel and iron aluminides, a stable ceramic phase is simultaneously formed, for example, aluminum oxide, which will immediately be located in the matrix of the resulting intermetallic.

It is known that chemical reactions of reduction of nickel and iron oxides by aluminum are highly exothermic, which makes it possible to dilute reaction mixtures with metals and ceramic additives.

In order to create the composites $NiAl/Al_2O_3$ and $FeAl/Al_2O_3$ the processes of mechanochemical interaction in NiO − Al and Fe_2O_3 − Al systems with stoichiometric ratios of nickel and iron oxides to aluminum and with an excess of aluminum were investigated.

IR spectroscopic and X-ray study of the products of mechanochemical reduction of nickel oxide by aluminum in stoichiometric mixture showed that after 40 c of MA, nickel oxide is partially reduced to metallic nickel, while α-Al_2O_3 and complex oxide $NiAl_{26}O_{40}$ are formed. The phase composition does not change practically during further activation for 4 min. With a twofold excess of aluminum in the mixture the nickel oxide is reduced and NiAl and α-Al_2O_3 are formed. The crystallite size of the NiAl phase is ~ 7 nm.

IR spectroscopic and X-ray study of the products of mechanical activation of the stoichiometric mixture Fe_2O_3 + 2Al showed that MA for 120 s leads to the reduction of iron oxide by aluminum and the formation of about 21 wt % of spinel $FeAl_2O_4$. The Mossbauer spectra of such a mixture demonstrate the formation of a solid solution α-Fe(Al) and spinel. According to the Mössbauer spectroscopy data, with a twofold excess of aluminum in the mixture, mainly the intermetallic phase FeAl is formed, as well as small amounts of Fe_2Al_5, $FeAl_2$ and a solid solution of aluminum in iron α-Fe(Al).

The work was carried out with the financial support of RFBR (project No. 19-52-44003 Монг_т).

Electrical conductivity of nanocrystalline nonstoichiometric tin dioxide films near the metal-insulator transition

V. Dorosinets*, V.K. Ksenevich, D.V. Adamchuk
Belarusian State University, Nezavisimosti av. 4, 220030 Minsk, Republic of Belarus

The temperature dependence of conductivity $\sigma(T)$ of nonstoichiometric tin dioxide films were studied in the temperature range 4-300 K. The films were fabricated by reactive DC magnetron sputtering with following 2-stage temperature annealing. Samples are characterized by high electron concentration (more than 10^{20} cm^{-3}) and a high degree of disorder. Several methods used to distinguish between metallic or insulating types of conductivity were employed to interpret experimental $\sigma(T)$ dependences. These methods give opposite conclusions. Model of polaron transport in metallic systems with strong lattice disorder stimulating dynamic process of electron-phonon coupling was proposed for our samples in order to settle the discrepancies.

UV photodetectors based on nanostructured ZnO thin films

E.B. Chubenko* and V.P. Bondarenko
Belarusian State University of Informatics and Radioelectronics, P.Provka str. 6 220013 Minsk, Belarus

In this work, the design and fabrication technology of ZnO ultraviolet (UV) photodetectors have been developed. Obtained devices are based on silicon substrates covered with ZnO seed sublayer deposited by atomic layer deposition. This allowed to obtain continuous nanostructured ZnO thin films on the substrate surface by the hydrothermal deposition method. Obtained films have low resistivity of 0.73 Ω×cm. Fabricated ZnO UV photodetectors demonstrated good photoresponse in the range of 300 – 390 nm and signal decay time of 10 – 15 ms. Obtained devices can be used as discrete or integrated UV photodetectors.

Synthesis and crystal structure of composites based on bismuth ferrite

D.V. Zhaludkevich[1], K.N. Nekludov[2], A.V. Sysa[2], M.V. Silibin[2], D.V. Karpinsky[1]
[1] *Scientific-Practical Materials Research Centre of NAS of Belarus, 220072 Minsk, Belarus*
[2] *National Research University of Electronic Technology "MIET", 124498 Zelenograd, Moscow, Russia*

Crystal structure of the solid solutions (1-y)$BiFeO_3$ – (y)$Ba_{1-x}Sr_xTiO_3$ ($0 \le y \le 0.3$; $0 \le x \le 1$) prepared by modified sol-gel technique have been studied using X-ray diffraction and scanning electron microscopy methods. The compounds (1-y)$BiFeO_3$ – (y)$Ba_{1-x}Sr_xTiO_3$ with $y \sim 0.3$ are characterized by a metastable structural state described by a pseudocubic structure. Chemical substitution of barium ions for strontium ions leads to a decrease in the structural symmetry observed as an increase of rhombohedral distortion accompanied by decrease in the unit cell volume. Concentration driven evolution of the structural state and structural parameters are studied using the X-ray diffraction and electron microscopy data.

Membranes of porous anodic aluminum oxide as passive luminance enhancers in LCDs

S. Gaponenko[1], S. Pryslopsky[1], V. Yakovtseva[2]*, S. Volchek[2]
[1]*B.I. Stepanov Institute of Physics of the National Academy of Sciences of Belarus, Minsk, 220072, Belarus*
[2]*Belarusian State University of Informatics and Radioelectronics (BSUIR), 6 P.Brovka, Minsk BY-220013, Belarus; yakovtseva@yahoo.com**

Visible range materials are of a great optoelectronic interest. The transmission band of alumina ranges from 0.25 to 4 μm. Therefore, free alumina films can be used for optical devices operating in different spectral ranges. Nanostructured (porous) alumina films can be easily obtained by the anodic etching of aluminum. Unique optical properties of nanoporous anodic alumina have been discovered: a high transmission along pores with simultaneous high reflection from cut-edges [1], an optical birefringence [2], etc.

This work presents a basic experimental procedure for the production of anodic alumina membranes transparent in the visible spectrum and promising as passive broadband light amplifiers. The 100 mm thick aluminum foils were anodized from the front side of the sample. The pore diameter and spacing were dictated by parameters of the anodization process, specifically by the electrolyte composition and the anodization voltage. The alumina film thickness was defined by the anodization time and the anodization current density. Then the rest of aluminum foil was etched to get free-standing films of porous alumina. We found that the additional removal of alumina bottoms in pores can be reasonable to get hollow cylindrical pores throughout the sample.

The light brightness enhancement with the anodic alumina membranes because of anisotropic light scattering by spatially arranged nanometer-sized pores was observed by the naked eye. To get more detail on the light transfer by the anodic alumina oxide film, the light intensity from a flat white light emitting diode panel was examined. The porous anodic alumina film was placed between LEDs and a detector at a variable LED/film distance and the light intensity I_{PAA} was measured by the detector and compared with the light intensity registered without the alumina film. The 20% intensity enhancement was detected at the 100 mm distance between the sample and the LED panel as shown in Fig. 1.

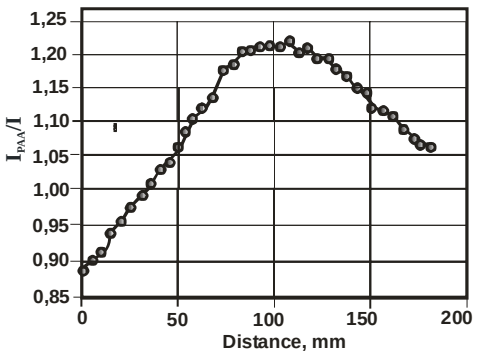

Figure 1. The ratio of light intensities with and without the alumina film between the LED panel and the detector depending on the distance between the film and the LED panel

Nanoporous anodic alumina membranes produced demonstrated a 5-fold higher transparency of the porous anodic alumina as compared to the reference commercial Kimoto film at the normal incidence ($\alpha = 0$) and more than 2-fold enhancement for $\alpha = 20^{\circ}$. The overall enhancement in the light transfer efficiency occurs in the range $-40^{\circ}<\alpha<+40^{\circ}$ whereas beyond this range the opaque Kimoto film gives higher intensities. The results obtained show that anodic alumina films can be purposefully used in LCD to control a light propagation.

Acknowledgement

This work has been partially supported by grants 4.1.5 of the Belarus State Program for the Scientific Research "Material science, new materials and technologies" and 3.6 of the Belarus State Program for the Scientific Research " Photonics and electronics for innovation".

References

[1] A. Lutich, M. Danailov, S. Volchek, V. Yakovtseva etc. Applied Physics B – Lasers and Optics, 84 (2006) 327.
[2] A. Lutich, L. Carbone, S. Volchek, V. Yakovtseva etc. Phys. Status Solidi, 5 (2009) 151.

Alumina structures with integrated conductive thick-layer metallization for microwave elements

D. Shimanovich[1]*, D. Tishkevich[2], A. Trukhanov[2]
[1]*Belarusian State University of Informatics and Radioelectronics, 220013, Minsk, 6 P.Brovki str., Belarus, e-mail: ShDL@tut.by**
[2]*Scientific-Practical Materials Research Centre of National Academy of Sciences of Belarus, 220072, Minsk, 19 P.Brovki str., Belarus*

An increasing of the functional complexity of microwave devices with a simultaneous increasing of the requirements for their electrophysical parameters, reliability and manufacturability require new approaches to the selection of load-bearing bases and conductive switching structures that perform the function of microstrip microwave lines.

The analysis of the alumina technology capabilities and performed studies [1,2] showed that using the combined processes of photoresist masking, two-sided through thickness anodizing and chemical etching of the original aluminum plates, it is possible to simultaneously form load-bearing bases and systems of aluminum interconnections. These interconnections will be built inside the dielectric body of the plates made of free anodic alumina with one-sided or two-sided exits to the surface of the contact pads, which can be used in a passive element base of microwave systems. The related scientific area is very relevant if take into account that the use of vacuum deposition or electrochemical deposition of metal films is excluded, and the thickness of the integrated built-in conductive elements and the depth of their occurrence in the dielectric bulk can be varied.

The essence of the developed technology for the manufacture of two-sided through Al_2O_3 plates which perform the function of supporting dielectric bases and at the same are an interelement dielectric medium for integrate built-in metallization is as follows. At first, the photoresist masks for conductors and contact pads were applied in two stages for a previously pretreated and polished Al plates with a thickness of 150-200 μm according to the multi-temperature hardening scheme (T = 120 ^{o}C and T = 180 ^{o}C respectively). Then, the open free places of Al were anodized to the required thickness in 7% oxalic acid ($H_2C_2O_4$) in a galvanostatic regime at a current density of 25-35 mA/cm^2. Then, the grown Al_2O_3 was removed by selective chemical etching in a CrO_3 : H_3PO_4 : H_2O solution at a temperature of 85 ^{o}C in order to form a microrelief. The second stage of anodizing was carried out in the same electrolyte. After that weakly hardened photoresist masks were removed from the formed built-in conductors and two-sided through thickness anodizing was performed on the entire open free surface of the bases. Since the thickness of Al in the places corresponding to the future zones of interelement separation is smaller they were fully anodized until the intergrowing Al_2O_3 layers closed to each other. In other areas the anodization was stopped with the formation of conductors embedded inside the alumina. Moreover, the microrelief size thickness was made so, that the same thickness of Al conductors was formed inside the Al_2O_3 plates. Thus, integrated built-in conductive elements with a Al thickness of 5-100 μm and different depths of their occurrence in the volume of Al_2O_3 plates were obtained (Figure 1).

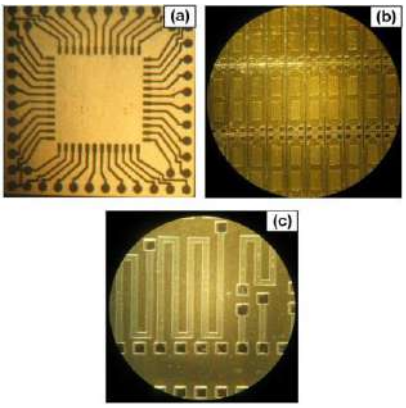

Figure 1. Images of alumina structures with integrated conductive elements: chip holder (a); meanders (b); switching elements (c)

References

[1] D.L. Shimanovich [et al.] Fundamentalnye problemy radioelektronnogo priborostroeniya 13 (2013) 182-185.
[2] D.L. Shimanovich [et al.] Doklady BGUIR 3 (2019) 5-11.

Young's modulus of free anodic aluminum oxide films

S. Biran[1*], D. Korotkevich[1], A. Korotkevich [1], K. Garifov[1], A. Dashkevich
[1]*BSUIR, Belarus, Minsk, 6 P.Brovki str., 220013, biran@bsuir.by**

Anodic aluminum oxide are used for the production of MEMS. Electrical and mechanical components are combined in MEMS devices. The functional characteristics of these devices are determined by the mechanical properties of the materials on the basis of which they are made. o design devices with specified characteristics, it is necessary to know exactly the properties of materials in order to obtain the best sensitivity and accuracy of measurements. In this paper, we show the measurement method and calculate the Young's modulus of free anodic aluminum oxide films.

The method for studying Young's modulus of free aluminum oxide films includes measuring the deflection of the samples depending on the applied mechanical load. Bending deformation occurs when a force perpendicular to its axis is applied to the film, which is freely lying on the supports. The deflection of the samples, depending on the applied mechanical load, was messured by using microinterferometer and special equipment printed on a 3D printer. The free aluminum oxide film is placed on a special device. A mechanical load is applied to the center of the sample, which can be changed. The deflection value is used to calculate the Young's modulus.

The free aluminum oxide film were used as samples for studying Young's modulus. ere obtained in an electrolyte based on oxalic acid in a galvanostatic mode. The film structures were free rectangular anodic alumina films 1 to 5 mm wide. By varying the anodizing time, samples with different thicknesses of aluminum oxide were obtained. The results of measuring the dependence of the deflection on the applied mechanical load are shown in Figure 1.

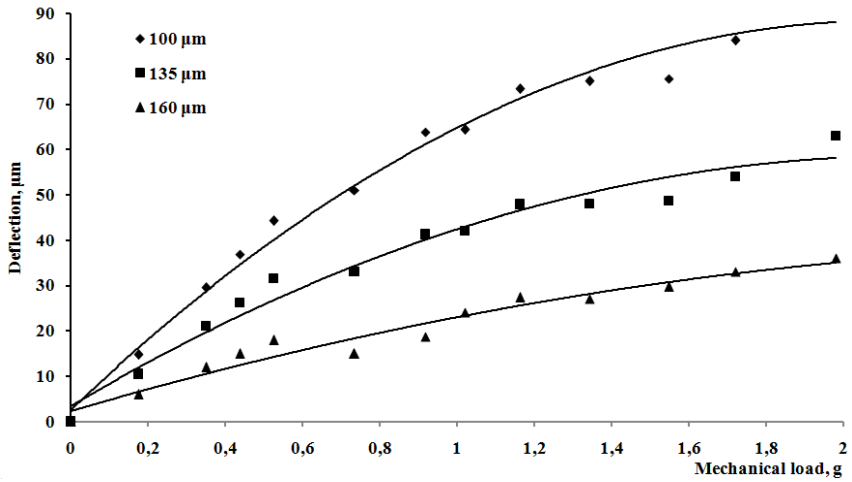

Figure 2. Deflection value vs. mechanical load

As a result of calculation the Young's modulus of free anodic aluminum oxide films obtained by anodizing in a solution based on oxalic acid, it was found to be in the range from 20 to 40 GPa.

Cyclic thermal desorption as a mechanism for identifying conductivity in condensed films

V.K.Dolgiy[1*], S.M.Baraishuk[1], A.V.Misevich[2], A.E.Pochtenny
[1]*Belarusian State Agrarian Technical University, 220023 Minsk, Independence Avenue 99, Belarus*
[2]*Belarusian State Technological University, 220006 Minsk, Sverdlova Street 13a, Belarus*

The technique to study the conductivity of condensed films by cyclic thermal desorption of gaseous impurities is described. The examples of identification of the conduction mechanism in thin film fluorosubstituted copper phthalocyanine and titanium dioxide are considered based on the method of cyclic thermal desorption. It was found that the cyclic thermal desorption method is applicable for the identification of the conduction mechanism in the film with a hopping conductivity and band conductivity. It is shown that in the films of fluorosubstituted copper phthalocyanine is realized the hopping conduction mechanism. The conductivities can be carried out either by its intrinsic states or by oxygen impurity states depending on the concentration of adsorbed oxygen; impurity levels being above intrinsic levels on the energy scale. The numerical values of the localization radius of intrinsic and extrinsic states and the concentration of centers of localization in the original materials have been defined. In the films of titanium dioxide produced by a sol-gel process the band conduction mechanism is implemented. These films are extrinsic semiconductors, in which the adsorbed oxygen is a shallow impurity.

Synthesis of composite materials based on macroporous silicon and graphitic carbon nitride

V.P. Grebnev* and E.B. Chubenko
Belarusian State University of Informatics and Radioelectronics, P.Provka str. 6 220013 Minsk, Belarus

In this work, the pyrolytic synthesis of a composite material based on graphitic carbon nitride (*g*-C_3N_4), zinc oxide (ZnO) and zinc sulfide (ZnS) deposited on macroporous silicon from thiourea and zinc acetate mixture at 500 – 600 °C is investigated. SEM and EDX analysis revealed the conform filling of the pore structure with *g*-C_3N_4/ZnO/ZnS composite and formation of continuous composite film on the top of the porous silicon layer. Photoluminescence of the samples is controlled by the synthesis temperature. Its maximum position changes in the range 565 – 515 nm. Obtained composite materials are prominent to photocatalytic and optoelectronic applications.

Study of diffraction phenomena on TGS crystals with impurity periodic distribution

V. N. Shut[1], S. E. Mozzharov[1], I. F. Kashevich[2*]
[1]*Institute of Technical Acoustics, National Academy of Sciences of Belarus, Vitebsk, 210027 Belarus*
[2]*Vitebsk State University, Vitebsk, 210032 Belarus*

The diffraction of light by the periodic impurity structure of triglycine sulfate crystals is investigated. The results obtained on the observation of Bragg and Nath-Raman diffraction are interpreted on the basis of the theory of light diffraction by ultrasonic waves.

Carbon based $LaCoO_3$ composites for thermoelectric applications

Nithya Davis[1], Ihar Razanau[2], Uladzimir Novikau[2], Anuradha M. Ashok[1]*
[1]*Functional Materials Laboratory, PSG Institute of Advanced Studies, Coimbatore – 641004, India.*
[2]*Laboratory of physical-chemical technologies, Scientific-Practical Materials Research Centre of NAS of Belarus, Minsk, Belarus.*

$LaCoO_3$ as a mid-high temperature thermoelectric material has attracted wider attention owing to their large room temperature Seebeck coefficient and superior electrical conductivity values. Making composites of carbon with oxide ceramics has been gaining wider attention in recent years. In this work, composites of $LaCoO_3$ with different carbon phases has been studied for thermoelectric performance. This work has attained a significant enhancement in electrical conductivity from a value of ~96 S/cm for pure LCO to ~5300 S/cm for multi-layer graphene-LCO composite and ~900 S/cm for CNF-LCO composite at 750K.

Redox-Active Organic Additives for Increasing the Energy Density of Supercapacitors

U. Novikau[1], I. Razanau[1*], S. Filipovich[1], and V. Lomonosov[1]
[1]*Scientific-Practical Materials Research Centre of NAS of Belarus, 19 Brovki Str., 220072 Minsk, Belarus, razanau@physics.by**

One of the possible ways to improve the energy density of supercapacitors without compromising much on their power density is using surface Faradaic reactions. In such cases, due to the fast kinetics, the charging-discharging curves look similar to EDL supercapacitors, but the energy storage mechanism involves charge transfer through the electrode-electrolyte interface. The current report is dedicated to studying peculiarities of redox-active hydroquinone (HQ) additive influence on the operation of supercapacitor cells. It undergoes a reversible $2e^-$ $2H^+$ quinone-hydroquinone reduction-oxidation reaction.

The study has shown that the electrochemical modification of activated carbon electrodes with hydroquinone increases the specific capacitance of the electrode material in acid-based aqueous electrolyte up to 35% when cycling to 1 V. The cell's energy density increases by approximately 17%. The modified electrode material is characterized by a pseudocapacitive behavior below 0.5 V in symmetrical supercapacitor cells. The mechanism of the modification involves gradual hydroquinone immobilization on the surface of activated carbon electrodes during cycling.

Acknowledgment. The work was financially supported by the BRFFR grant F20PTI-002.

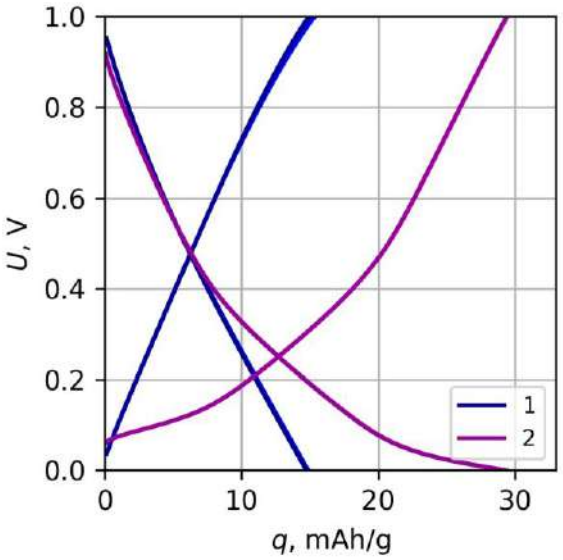

Galvanostatic charging-discharging curves of the supercapacitor cell with pristine (1) and hydroquinone-modified (2) activated carbon electrodes

Modification of Lead-Acid Battery Electrodes with Graphene-Like Carbon

U. Novikau[1], S. Filipovich[1], I. Razanau[1*], H. Daletskaya[1], V. Lomonosov[1]
[1]*Scientific-Practical Materials Research Centre of NAS of Belarus, 19 Brovki Str., 220072 Minsk, Belarus, razanau@physics.by**

Carbon nanomaterials are perspective additives to the negative electrode paste of lead-acid batteries. Their application improves charge acceptance and operation under high-rate partial state-of-charge (HRPSoC) conditions. We synthesize graphene-like carbon (GLC) material using an original high-productivity nonoxidative method of graphite exfoliation. This work aimed to study the effect of graphene-like carbon additive to the negative electrode paste on the performance of lead-acid battery cells.

The GLC synthesis is a two-stage process. In the first stage, the intercalation compound of sodium ammoniate in natural graphite is prepared by soaking natural graphite in the solution of metallic sodium in liquid ammonia. In the second stage, the graphite intercalation compound is exfoliated through flame pyrolysis. The GLC powder synthesized is characterized by a high structural perfection of graphene layers and a low degree of oxidation.

Experimental cells were produced using positive electrodes from a commercially available lead-acid battery and negative electrodes prepared in the laboratory with varying amounts of GLC as an additive. It is shown that the addition of GLC to the negative electrode paste of lead-acid battery cells allows increasing their lifetime under the deep discharge cycling conditions by up to 70% and under the high rate partial state of charge cycling conditions by approximately three times. The cells with 0.25% content of the additive demonstrated the best performance.

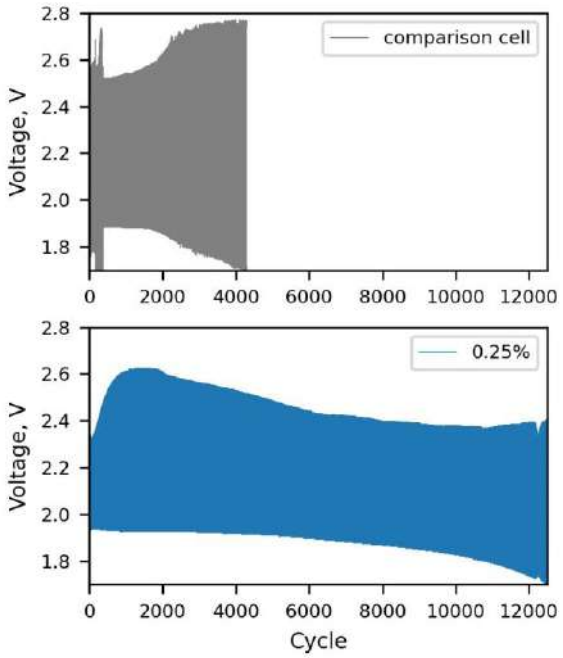

High-rate partial state-of-charge (HRPSoC) cycling of a commercially available lead-acid battery cell and analogous cell with negative electrode produced with 0.25% graphene-like carbon additive

Morphology and structure of mechanically activated functional particles

Y.Auchynnikau
Yanka Kupala State University of Grodno

Investigations of the structure and charge activity of mechanically activated nanosized particles, which can be wear inhibitors in metal-polymer tribosystems, have been carried out. The charge activity of nanocomposite particles based on silicates, metal oxides and composite particles based on them has been studied. The rheological characteristics of nanocomposite materials based on thermoplastic polymers have been investigated. It is shown that mechanical activation increases the charge activity of dispersed particles of inorganic nature, which makes this type of energy impact promising for obtaining nanoscale and nanophase modifiers of polymer matrices.

Effect of thermobaric treatment on the generation and annealing of a radiation defect V^- in synthetic diamonds of type Ia+Ib

A. Konovalova[1*], O. Ignatenko[1], I. Azarko[2], D. Kuznetsov[1], S. Lastovsky[1]
[1] *SSPA "Scientific-Practical Materials Research Centre of NAS of Belarus", 19 P. Brovki str, Minsk, Belarus 220072*
[2] *Faculty of Physics, BSU, Independence Ave. 4, Minsk, Belarus 220050*

The effect of fast thermobaric annealing on the formation of negatively charged vacancies in synthetic diamonds of type Ia+b is investigated. According to EPR spectroscopy data, HPHT annealing makes it possible to increase the number of V^- defects by several times upon subsequent irradiation of diamonds with fast electrons.

Electrophysical properties of $BaFe_{12}O_{19}$:Ti in the high frequency range at low temperatures

Denis Klygach [1,2]*, Maksim Vakhitov [1,2], and Alex Trukhanov [3]
[1] *School of Electronic Engineering and Computer Science South Ural State University Chelyabinsk, Russian Federation*
[2] *Ural Federal University Yekaterinburg, Russian Federation*
[3] *Scientific and practical materials research centre of NAS of Belarus, Minsk, Belarus*

The paper describes a method for measuring electrodynamic parameters in the frequency range from 10 MHz to 18 GHz at temperatures up to -180 ˚C. The measurement results are given for an empty transmission line and the line filled with the test material. Frequency dependences of the S-parameters depending on the sample temperature are shown.

Layer-by-layer coated metal-organic frameworks for water vapor sorption applications

T. Shutava[1]* and V. Pankov[2]
[1]*Institute of Chemistry of New Materials, National Academy of Scienses of Belarus, F.Skaryna St. 36, Minsk 220141, Belarus, shutova@ichnm.by*
[2]*Belarusian State University, Nezavisimosti Av. 4, Minsk 220030, Belarus*

Metal-organic frameworks (MOFs) due to their 3D mesoporous structure and high specific surface area, can be used as sorbents for technologies based on water vapor sorption/desorption cycle (heating/cooling, atmospheric water harvesting etc.). For practical use, MOFs are molded with binders into tablets or pelettes [1-3]. With emphasis on two dicarboxylic acid-based MOFs, Al fumarate (Al-Fum) and Zr fumarate (Zr-Fum), it has been shown that the modification of MOF particles with a single polyelectrolyte (PE) layer or layer-by-layer (LbL) shell improves sorption characteristics of several composites, namely increases water uptake in selected regions of relative vapor pressure (p/p_0), shifts the inflection point, and accelerates saturation and dehumidification.

Among other MOFs, Al-Fum and Zr-Fum were synthesized as described elsewhere [2-3]. LbL shells consisting of 0.5-3.0 polyelectrolyte bilayers were obtained around MOF particles using the sonication-assisted LbL assembly technique [4-5].

MOFs with an average diameter less than 700 nm tend to aggregate through the polymer shell to varying degree. Using Al-Fum and Zr-Fum as examples, the fact that most MOFs coated with PE or LbL shell retain their phase, crystallinity, and high specific surface comparable to that of the pristine powders is confirmed. The divergences for some samples are related to the specificity of PE interaction with MOF surface (clogging template's pores by small M_w or less/more hydrophilic PE) and additional porosity brought in by polyelectrolyte shell material.

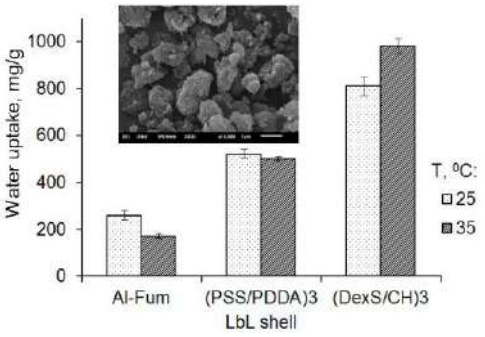

Figure. Water uptake by Al-Fum with a LbL shell (measured by QCM). Insert: SEM of Al-Fum/$(PSS/CH)_3$. PSS – polystyrene sulfonate, PDDA – polydiallyldimethyl ammonium chloride, DexS – dextran sulfate, CH – chitosan

The majority of MOF/PE and MOF/LbL powders are characterized by a moderate increase of water vapor uptake in arid atmosphere ($p/p_0<0.3$). For the MOF/LbL, a decline of up to 40 % in water uptake in humid range is more typical than for MOF/PE. At $p/p_0=0.9$, most composites resume high water capacity comparable or higher than that of corresponding pristine powder. As that for many MOFs, the process of water vapor sorption/desorption by a Al-Fum/LbL and Zr-Fum/LbL composite is cyclical and can be repeated several times. As measured by quartz crystal microbalance (QCM), the effective water uptake of Al-Fum/LbL powders can be increased by 2-3 folds as compared with the pristine MOF (Figure). The enhanced water uptake by LbL coated powders is apparently caused by the changes introduced by a polyelectrolyte shell at the particle-gas interface to the conditions of water vapor condensation. Another advantage of hydrophilic LbL shell coating on MOFs is the acceleration of moisture uptake and loss.

References

[1] N. Tannert,C.Jansen, S.Nießing and C. Janiak, Dalton Trans. 48 (2019) 2967-2976.
[2] E. Leung, U. Müller, N. Trukhan, H. Mattenheimer, G. Cox, and S. Blei, US 2012/0082864 A1.
[3] G. Zahn, H. A. Schulze, J. Lippke, S. König, U. Sazama, M. Fröba, and P. Behrens, Microporous Mesoporous Mater. 203 (2015) 186–194.

[4] Y. Lvov, P. Pattekari, and T. Shutava, Multilayer Thin Films: Sequential Assembly of Nanocomposite Materials, Wiley-VCH (2012) 151-170.
[5] T.G. Shutava, V.V. Pankov, Colloids Surf. A. 539 (2018) 69-79

Growth of PEO coatings on zinc alloy in aluminate-phosphate electrolyte

C. Blawert[1], S.A. Karpushenkov[2]*, M. Serdechnova[1], L.S. Karpushenkava[2], M.L. Zheludkevich[1,3]*
[1]*Magnesium Innovation Center, Helmholtz-Zentrum Geesthacht, Max-Plank-Straße 1, 21502 Geesthacht, Germany*
[2]*Belarusian State University, Faculty of Chemistry, 4, Nezavisimosti avenue, 220030, Minsk, Belarus*
[3]*Institute for Materials Science, Faculty of Engineering, University of Kiel, Kaiserstraße 2, 24143 Kiel, Germany*

This work presents data on the growth of coatings on a zinc alloy under conditions of plasma electrolytic oxidation in an aluminate-phosphate electrolyte. The coatings are consist of ZnO and $ZnAl_2O_4$ and have a sponge-like structure with internal porous. At lower discharge energies, ZnO predominates during the formation of the coating, and with an increase in the discharge energy, the reactive formation of $ZnAl_2O_4$ occurs. The composite coatings, which consisted of ZnO and higher amounts of $ZnAl_2O_4$ can be promising for transport, biomedical, or environmental applications.

Metal-organic framework/ magnetite composites for water vapor sorption applications

T. G. Shutava[1], V. V. Pankov [2] and A. S. Tsimanenkava[2]*
[1]*Institute of Chemistry of New Materials, National Academy of Sciences of Belarus, F.Skaryny St., 36, 220141 Minsk, Belarus*
[2] *Belarusian State University, Nezavisimosti av. 4, 220030 Minsk, Belarus, e-mail: alinatimon16@gmail.com**

This study is devoted to the development of composite materials consisting of metal–organic frameworks and magnetite nanoparticles with potential applications for water vapor sorption.

Aluminum fumarate (Al-Fum) was synthesized according to [1]. The obtained powder has a good water uptake (about 0.62 g/g), a hydrodynamic diameter of about 340 nm and a ζ-potential of +20±1 mV. Two types of Al-Fum-based composites were obtained. The microparticles consisting of the metal-organic framework coated with a (polydiallyldimethylammonium chloride/magnetite)$_6$ shell (Al-Fum/PSS/(PDDA/Fe_3O_4)$_6$) were obtained by the layer-by-layer assembly method [2]. The composite in which magnetite nanoparticles are surrounded by a matrix of porous material (Fe_3O_4/Al-Fum) was obtained by admixing them to one of reagents at the early stages of the synthesis. SEM microphotographs of the composites show that the particles have an irregular shape and size up to 200 nm. The FTIR spectra of the samples have bands characteristic of Al-Fum and magnetite (Fig.). For Fe_3O_4/Al-Fum and Al-Fum/PSS/(PDDA/Fe_3O_4)$_6$, the water uptake is about 0.57±0.03 and 0.27±0.02 g/g, respectively. The obtained results on sorption of water vapor by composites are in good agreement with the mass fractions of magnetite in the composites obtained by spectrophotometric assay for total iron with o-phenanthroline. Al-Fum/PSS/(PDDA/Fe_3O_4)$_6$ and Fe_3O_4/Al-Fum have 58.2±1.7 and 9.4±0.3% of magnetite, respectively. The mass fraction of magnetite in the Fe_3O_4/Al-Fum composite also agrees well with the amount of the magnetic phase which, according to magnetization measurements, corresponds to 10 wt.%.

The Curie point for the both composites is about 741 K, which is lower than the temperature reported in literature for bulk magnetite material (858 K) [3]. The magnetite particles in the composites retain their original dispersion and exhibit superparamagnetic properties.

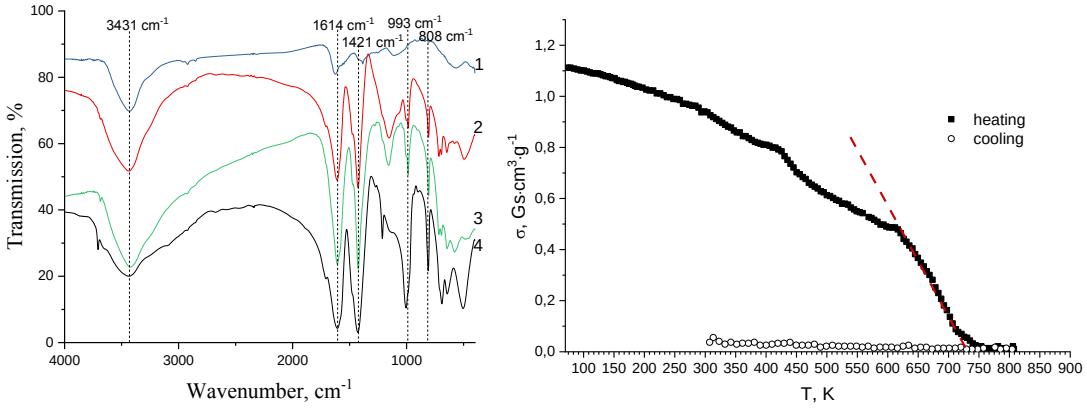

Figure. *a*) FTIR spectra: 1 - Fe_3O_4, 2 - Al-Fum, 3 – Fe_3O_4/ Al-Fum, 4 – Al-Fum/PSS/(PDDA/Fe_3O_4)$_6$. b) The dependence of specific saturation magnetization of Fe_3O_4/ Al-Fum on temperature

References

[1] US patent 2012/0082864 A1
[2] T.G. Shutava and V.V. Pankov, Colloids Surf. A. 539 (2018) 69-79
[3] D. Levy, R. Giustetto, A. Hoser. Phys. Chem. Miner. 39, №2 (2011), 169–176.

Polarized Mossbauer spectroscopy study of $MgFe_2O_4$ particle's with heat generation ability synthesized for hyperthermia

Kiseleva T.Yu.[1], Zholudev S.I.[1,2] , Lazareva E.V.[1] , Ivanenko I.P.[1] Chumakov A.I.[3], Uyanga E. [4], Sangaa D.[4]
[1]*Moscow M.V.Lomonosov State University, Physics Faculty, Moscow 119192, Russia*
[2]*Technological Institute of superhard and novel carbon material, Moscow, Russia*
[3]*ESRF-The European Synchrotron, CS40220 38043 Grenoble Cedex 9, France*
[4]*Institute of Physics and Technology, MAS, Ulaanbaatar 13330, Mongolia*

Magnesium ferrite ($MgFe_2O_4$) particles have the favorable magnetic properties and biological compatibility among a number of industrial important ferrite compositions. $MgFe_2O_4$ particles of micrometer-range sizes are reported to exhibit greater magnetic heating than other ferrites do and too much attractive for hyperthermia applications both by themselves and as component of the composites. To reveal particle's size and magnetic structure peculiarity influence on the magnetic and magnetocaloric properties of fine magnesium ferrite particles synthesized for biomedical purposes, such particles were obtained by different techniques: sol-gels, reverse co-precipitation, and ceramics solid reaction methods. Synthesised particles demonstrate different heat generation performance in AC magnetic field of clinically achieved parameters. The influence of particle's dimension, purity and magnetic structure was characterized by Mössbauer spectroscopy using polarized synchrotron radiation. Mössbauer spectra obtained at 300 K and 4 K below Neel's temperature and in applied magnetic field allowed to account the effects of low dimensionality, spin disordering to obtain the exact value of inversion degree. Obtained result let to explain the magnetocaloric functional behavior of the synthesised particles.

Acknowledgement.
The authors thank Moscow University Program of Development for supporting equipment renewal. We acknowledge the European Synchrotron Radiation Facility for provision of synchrotron radiation resources at the beamline ID18. The authors thank partial supporting RFBR project №19-44003.

Numerical and experimental study of $Ba_2TiSi_2O_8$ ceramics for microwave engineering applications

Roterdan Fernandes Abreu[1,7*], Felipe Rodrigues da Silva[4], Diego da Mota Colares[1,7], Tallison Oliveira Abreu[2,7], Samuel Oliveira Saturno[1,7], João Paulo Costa do Nascimento[3], Francisco Alekson Chaves Nobrega[2,7], Anupama Ghosh[5], Juscelino Chaves Sales[6], Daniel Xavier Gouveia[3], Ronaldo Santos da Silva[8] and Antônio Sérgio Bezerra Sombra[7]

[1] *Telecommunication Engineering Department, Federal University of Ceará (UFC), Fortaleza, Ceará, Brazil.*

[2]*Department of Organic and Inorganic Chemistry, Science Center, Federal University of Ceará (UFC), Brazil.*

[3]*Federal Institute of Education, Science and Technology of Ceará, PPGET, Fortaleza, Ceará, Brazil.*

[4]*Federal Institute of Education, Science and Technology of Ceará, Maracanaú, Brasil.*

[5]*LaMFA - Advanced Functional Materials Laboratory, Central Analítica, Physics Department, Federal University of Ceará - UFC, Fortaleza, Brazil.*

[6]*State University of Vale do Acaraú, Center for Exact Sciences and Technology, Department of Civil Engineering.*

[7] *Telecommunication and Materials Science and Engineering of Laboratory (LOCEM) Federal University of Ceará (UFC), Physics Department , Fortaleza, Ceará, Brazil.*

[8] *Group Functional Nanomaterials, Physics Department, Federal University of Sergipe, 49100-000 Sao Cristóvão, SE, Brazil*

This work presents the dielectric properties of $Ba_2TiSi_2O_8$ in the Microwave (MW) region. X-ray diffraction analysis showed that the material was obtained as a single-phase without the presence of spurious phases. Numerical simulation using HFSS presented the operation of the $Ba_2TiSi_2O_8$ as a Dielectric Resonator Antenna (DRA) with return loss (S_{11}) below -10 dB, a realised gain of 6.739 dBi, a bandwidth of 452.96 MHz, and a radiation efficiency 100%. These results demonstrate that evaluated ceramic would be an interesting candidate in microwave devices in the C-band.

Interconnection between structure, thermoelectric and electric properties of doped ZnO-based ceramic materials

A.K. Fedotov[1], L.A. Bliznyuk[2], A. Pashkevich[1,3], A. Kharchenka[1],
E.N. Poddenezhny[4], T.P. Petrochenko[2], V.V. Fedotova[2]
[1]*Institute for Nuclear Problems of Belarusian State University, Bobruiskaya str. 19, 220006, Minsk,, Belarus*
[2]*National Scientific-Practical Center for Naterial Science, P. Brovks str. 19, 220066, Munsk, Belarus*
[3]*Belarusian State University, Nezavisimosti av. 4, 220030, Minsk,, Belarus*
[4]*Sukhoi State Technical University of Gomel, Octyabrya av. 48, 246029, Gomel, Belarus*

Nowadays, great attention is paid to the search for new wide-gap oxides as thermoelectric materials, as well as to studying correlation between their structural and electrical properties. However, as to ZnO-based ceramics, the influence of doping on this interconnection are not fully understood. The aim of this work is to study influence of doping with Fe, Co and Al on the properties of ZnO-based ceramics to agree their thermoelectric and electric properties tuning their chemical/phase composition, grain sizes, porosity and other morphological characteristics of samples.

To prepare ceramic samples, we used powder mixtures of doping metal oxides MO and ZnO with their different mass relations, where MO = Fe_xO_y, CoO, and Al_2O_3. After uniaxial pressing of powder mixtures at 300 K we prepared tablets by either one-step (for 3 hours at 800 ^oC) or/and two-step (for 2 hours annealing at 1200 ^oC at the second stage) synthesis, accordingly. The initial powders were either commercial with micrometer-sized particles or nanosized grains prepared by thermo-chemical combustion process.

We revealed the following peculiarities of the ZnO–based ceramics behavior. The grain sizes were some tenths of micrometers after one-step technology and decreased to nanosized after two-step synthesis (independently on initial powders). Doping with cobalt and iron was accompanied by the preservation of the wurtzite crystal structure in the majority of ZnO ceramics bulk; however, the iron solubility did not exceed 0.8 at.%, while the cobalt and aluminum solubility reached 3-5 at.%. Undissolved Fe and Al atoms formed secondary phases ($ZnFe_2O_4$ and $ZnAl_2O_4$, respectively) inside of wurtzite. At the same time, doping with Co did not result in the formation of extra phases. The presence of $ZnFe_2O_4$ led to an increase in the Seebeck coefficient S(300 K) from 300–400 μV / K for ZnO to 1000 μV / K for two-stage $ZnO_{90}(Fe_xO_y)_{10}$ (in Wt.%) ceramics. In binary ceramics doped with iron, in the presence of the $ZnFe_2O_4$ phase, the dependence of the S(300 K) on the average electron concentration n had the form of an inverted parabola, reaching a maximum (800 μV / K) at $n \approx 1 \cdot 10^{21}$ cm^{-3}. Doping with all impurities, except aluminum, leaded to an increase in electrical resistivity. Doping with aluminum (up to 3-5 at.%) and increasing the $ZnFe_2O_4$ phase content due to extra iron reduces the resistivity, leading to an increase in the power factor in doped ceramics.

Magnetroelectric properties of hybrid multiferroics

N.N. Poddubnaya*, V.M. Laletin
Institute of Technical Acoustics of National Academy of Sciences of Belarus, 210009 Vitebsk, Ave. Generala Lyudnikova, 13, Belarus

Magnetoelectric structures with 2/3-0/2 connectivity type were obtained for the first time [1]. Piezoelectric materials based on lead zirconate-titanate (phase 3) with different concentrations of nickel ferrite additives (phase 0) were used as a bulk composite with 3-0 connectivity type. Electrochemically deposited nickel was used as phase 2. The linear magnetoelectric coefficient and magnetoelectric sensitivity were experimentally investigated.

Influence of electric properties of inclusions on permeability spectra and microwave absorption in magnetic polymer composites based on spinel ferrites

R. Shakirzyanov[1,*], V. Kostishin[1], I. Isaev[1], A. Kayumova[1], B. Skibo[1], D. Salogub[1]
[1]*National University of Science and technology "MISIS", Leninsky Prospect, 4, 119049, Moscow, Russia, halfraf@mail.ru**

Polymer functional composites are of great interest to scientists because of opportunity for overcoming limitation of traditional single phase materials. Last decades a lot of studies were dedicated to investigation of microwave absorption properties of polymer composites containing dielectric, magnetic and conductive micro- and nanoparticles. These researches are in demand because of growing problems with electromagnetic interference and electromagnetic pollution. Composites based on iron oxides (ferrites) are very suitable for above-mentioned issues due to possibility to vary magnetic and dielectric properties through modification of composition and structure [1-4]. In this report dynamic magnetic and dielectric properties in the wide frequency range of spinel ferrite based polymer composites are investigated. Conventional microsized powders of Ni-Zn and Mn-Zn ferrites branches 2000NN and 2000NM, respectively, were used as magnetic phases. Commercial PVA, P(VDF-TFE), were used as matrix and binder. Additionally, some composites were made by introduction of small volume fraction of graphite and carbonyl iron. Obtained results indicate that electric properties of magnetic and non-magnetic inclusions can significantly affect on the shape and frequency position of the permeability dispersion. For example, permebility spectra of polymer composites with Mn-Zn ferrites addition shows significant frequency shift of dispersion region with growth of magnetic particles concentration. Composites with Ni-Zn ferrite do not exhibit such properties. The possible explanation of this effect is connected with influence of eddy current in composites with relatively high conductivity above the electric percolacion threshold concentration.

Obtained samples of composites show good microwave absorption characteristics with lowest reflection losses ~ -30-40 dB and bandwidth on -10 dB about 2 GHz in the frequency range of 2-7 GHz (Fig. 1).

Acknowledgement This study was supported by the Russian Science Foundation, agreement no. 19-19-00694 of May 6, 2019.

References

[1] A. Author, B. Author, and C. Author, Journal Title Abbreviation Volume (Year) Pages.
[1] D. Kumar, A. Moharana, A. Kumar, Mater. Today Chem. 17 (2020) art. no. 100346.
[2] P. Thakur, D. Chahar, S. Taneja, N. Bhalla, A. Thakur, Ceram. Inter. 46 (2020) 15740-15763.
[3] S. Narang, K. Pubby, J. Magn. Magn. Mater. 519 (2021) 167163.
[4] A. Houbi, Z. A. Aldashevich, Y. Atassi, Z. Bagasharova Telmanovna, M. Saule, K. Kubanych, J. Magn. Magn. Mater. 529 (2021) 167839.

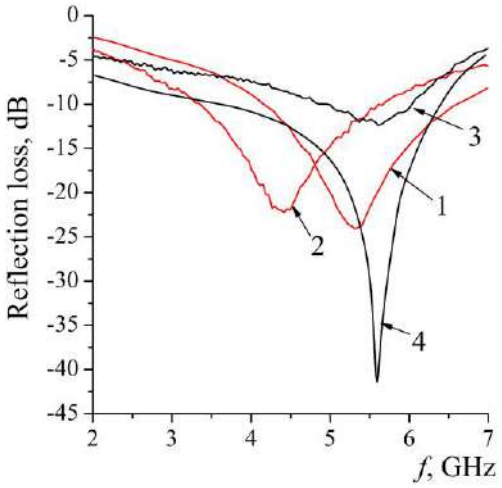

Fig. 1 – Reflection loss spectra for composites with composition: 1 – P(VDF-TFE)(80%)/Mn-Zn ferrite(20%); 2 – PVA (60%)/Mn-Zn ferrite(40%); 3 – PVA(20%)/Ni-Zn ferrite(80%); 4 – P(VDF-TFE) (20%)/Ni-Zn ferrite(80%)

Effect of pressure on surface morphology n-Si <Ni>

Sh.B. Utamuradova[1], Sh.Kh. Daliev[1], F.A. Saparov [1*], and A.R. Turaev [1]
[1]*Institute of Semiconductor Physics and Microelectronics at the National University of Uzbekistan, Tashkent, 100057, Republic of Uzbekistan*

The influence of pressure on the electrical characteristics of n-Cu <Ni> has been studied. The dependence of the parameters of defect centers on the size of the uniform compression has been established.

The effect of Cr on phase composition and microstructure of Mo_2NiB_2-Ni alloyed with carbon

T.N. Vershinina[1]*, M.B. Ivanov[2]
[1] *Joint Institute for Nuclear Research, 6 Joliot-Curie St, Dubna, Russian Federation, vershinina@nf.jinr.ru**
[2] *S7 R&D Center, 5 Vostochnaya St, M4 Technopark, Gorki Leninskiye, Russian Federation*

Materials based on ternary borides Mo_2NiB_2 are very promising as tungsten-free hard alloys. Comparative analysis of the effect of chromium on the structure and phase composition of cermets of the Mo_2NiB_2-Mo system doped with carbon was carried out on the following materials: *Cermet 1* - 67.6Mo-5.9B-24.9Ni-1.6C, *Cermet 2* - 52.7Mo-6B-25.3Ni-1.7C-14.3Cr (wt.%).

Analysis of the phase composition showed that in the chromium-free state (Figures 1a-b) the precipitation of three phases is observed: boride Mo2NiB2 with an orthorhombic crystal lattice (grey areas), Mo2C carbide (light areas), and a solid solution based on the FCC lattice of nickel (dark area). The introduction of chromium into the composition of the material leads to the fact that in addition to the above-mentioned phases tetragonal boride (Mo, Cr, Ni)3B2 and a solid solution based on the BCC chromium lattice are also formed.

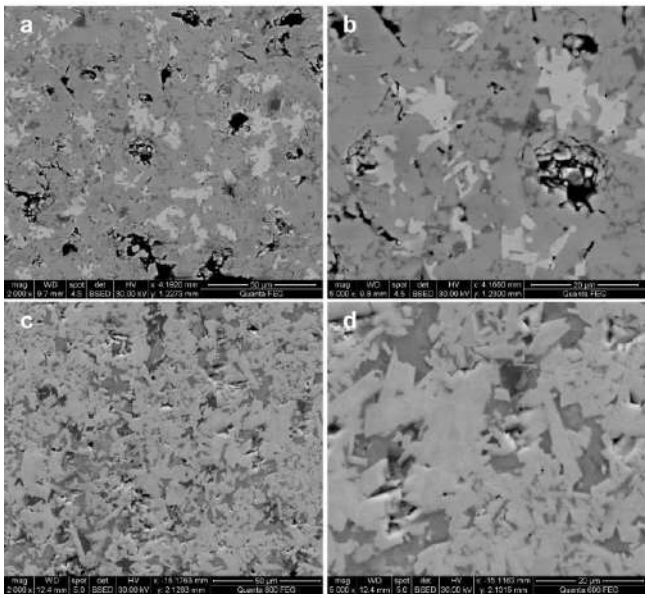

Figure 1. Microstructure of cermets: a, b – cermet 1; c, d – cermet 2

The particles of Mo_2C carbide have a sharp-edge shape in Cermet 1 (Figure 1b). Their sizes are comparable to those of borides. Thin layers of nickel binder are observed between the carbides. Both the shape and the presence of a binder indicated that the carbide particles were precipitated from the liquid during the heating of the sample. That is this took place at the same time as the particles of ternary boride were precipitated. So the liquid was not enough at the stage of shrinkage of the sample and the result was a high porosity of the sintered material.

When doped with chromium, the temperature of liquid formation decreases from 1320 to 1280 °C and a significant decrease in the porosity of cermet is observed. So, the volume fraction of the liquid phase and its ability to wet the borides was sufficient to fill almost all pores, including large ones. Taking into account the morphology of Mo_2C particles (Mo_2C carbide with irregular shape filled large spaces), it can be assumed that they crystallized from a liquid that had previously completely wetted the surrounding borides. Therefore, it can be concluded that the decomposition according to the reaction $L \rightarrow FCC + BCC + Mo_2C$ occurred already during the cooling of the sintered samples.

Thus, alloying with chromium provided a high volume fraction of the liquid during sintering. Also, the simultaneous introduction of chromium and carbon into the composition could lead to a decrease in the solid/liquid surface energy γ_{SL} of the liquid filling large pores. These two factors contributed to the good wettability of borides with a liquid and, as a consequence, the formation of low porosity in cermets.

Influence of geometry to the self heating effect in 2D MoS2 based MOSFET

A.E. Atamuratov[1], X. Sh. Saparov[1] , T. A. Atamuratov[1], A. Yusupov[2] , F. Schwierz[3] .
[1]*Urgench State University, Urgench, Kh.Olimjan str.,14, Urgench, Uzbekistan, atabek.atamuratov@yahoo.com*
[2]*Tashkent University of Information Technologies, A.Temur str., 108, Tashkent, Uzbekistan*
[3]*Technical University of Ilmenau3, Ehrenbergstraße 29, 98693 Ilmenau, Germany*

One of the main trends of today's semiconductor electronics is decreasing the size of MOSFETs in digital logic circuits down to the nanometer scale. According to one of suggestions, decreasing to nanometer scale is possible by designing of MOSFET on the basis of two-dimensional transition metal dichalcogenides (TMD).

However, one of disadvantages of such devices can be circumstance that the top as well as the bottom of the transistor channel has borders with oxide layers. Upper oxide layer is gate oxide layer and bottom oxide layer is back oxide layer. Because of low heat conductivity of the oxides, this condition can lead to decreasing the heat flow from the channel, during flow of current, in comparison with bulk MOSFET that results in self-heating effect, which influence to characteristics of the transistor. Therefore it is interesting and important to consider self-heating effect in MOSFET based on two dimensional DTM.

Two-dimensional MoS_2 is most prominent representative of the TMDs and popular as the channel in 2D MOSFETs. Therefore in this work the self-heating effect (SHE) is simulated in for a MoS_2 MOSFET. The influence of the degree of covering the channel by the gate oxide (on the top) to SHE and the dependence of SHE on the thickness of back-oxide of the transistor is investigated. For the numerical device simulations, the advanced Sentaurus TCAD tool is used. The temperature and his distribution in the channel depend on the heat dissipation rate through interfaces and contacts with channel and therefore depend on materials contacted with channel. Degree of covering the top surface of the channel by gate oxide considerably influence to the temperature of the channel.

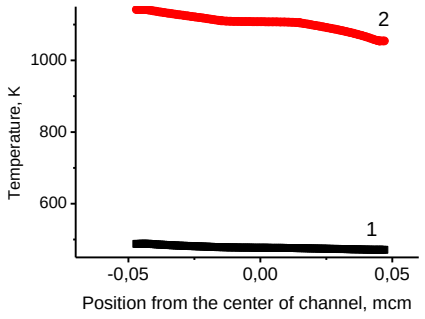

Fig.1.T*emperature distribution along the channel center at full (curve 1) and partly (curve 2) covered channel top by gate oxide* Al_2O_3.

Temperature distribution along the channel center in the case of full covering the channel top and in case of covering only channel part under the gate by gate oxide is shown in Figure 1. It is seen, at only partly covered the channel top by aluminum oxide the temperature of the channel is considerably higher than at partly covererd channel top. It is connected with relatively less thermo conductivity of air, which cover the part of channel top not covered by aluminum oxide.

The influence of back oxide thickness T_{box} to the temperature in the center of channel of 2D MoS_2 based MOSFET also was considered (Fig 2). The increasing temperature with increasing the T_{box} is caused by increasing the distance between channel and contact to back oxide, which promotes heat dissipation from the channel.

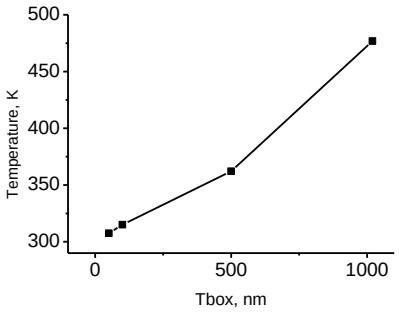

Fig.2. T*he dependence of temperature in the center of channel on the thickness* T_{box}. *of back oxide.*

Capacitance method for estimation lateral distributions of hot carriers injected in the gate oxide of nanometer MOSFET

A.E. Atamuratov[1*] , Z.A. Atamuratova[1] , A. Yusupov[2]
[1]*Urgench State University, Urgench, Kh.Olimjan str.,14, Urgench, Uzbekistan, atabek.atamuratov@yahoo.com*
[2]*Tashkent University of Information Technologies, A.Temur str., 108, Tashkent, Uzbekistan*

It is known, under long time electrical stress in MOSFET it can take place degradtion connected with injection and trapping hot carriers in gate oxide as well as at oxide-semiconductor interface. Oxide trapped charge as well as interface trapped charge leads to undesirable changing of characteristics and transistor parameters.Therefore one of important problems of MOSFET electronics is research of lateral distribution of the injected charge along the channel and development the optimal tools for defining this distributions. In this work by simulation it is considered the opportunity to use lateral capacitance method to estimation lateral (along channel) distribution of injected and trapped hot carriers in gate oxide layer of nanosized planar MOSFET. The essence of the method consist of influence of oxide trapped charge to C-V dependence of source-base and drain-base lateral transitions of MOSFET. Certainly, the oxide trapped charge influence to the distribution of space charge near source-base and drain-base transitions and consequently this should be reflected in capacitance of this transitions.

3D simulation was carried out with using TCAD Sentaurus. C-V dependences were simulated by using small AC signal method. Used model was calibrated by the experimental dependence of threshold voltage changes on the drain voltage at defined distribution of oxide trapped charge presented on the literature. At simulation the planar MOSFET with polysilicon gate with length and width 47 nm were considered. SiO_2 gate oxide has 4.46 nm thickness. Doping level of silicon base by arsenic is 10^{17} cm^{-3} , source and drain areas was doped by boron up to concentration 10^{19} cm^{-3}. Distribution of oxide trapped charge corresponding to HCI stress, which was used at calibration the simulation model, is considered (Fig. 1, distr 5). Besides it, for comparison, the distributions which resulted from displacement of HCI stress distribution along the channel in direction to source is considered (Fig 1, distr 1-distr 4). the simulation results show that maximal capacitances of lateral transitions source-base C_{sbmax} sbmax and drain-base C_{dbmax} dependences on position of the oxide trapped charge distribution maximum is different.While the ratio C_{sbmax} /C_{dbmax} dependence on the position of the maximum is monotonic (Fig 2). This dependence allow to estimate oxide trapped charge distribution along the channel by measuring the ratio C_{sbmax} /C_{dbmax}.

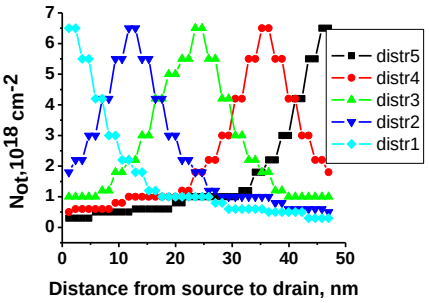

Fig.1 Different considered cases of oxide trapped charge distributions along the channel from source to drain

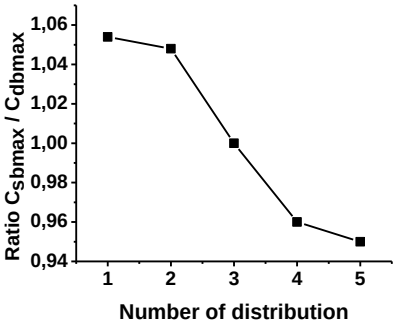

Fig.2 C_{sbmax}/C_{dbmax} ratio depndence on number of oxide trapped charge distribution

Optical properties of Ni-MOF metal-organic framework structures

A.K. Vetcher[1], K.P. Buskis[1], O.F. Demidenko[1,*], V.F. Gremenok[1], Q. Chen[2], and Y. Li[2]
[1] *SSPA "Scientific-Practical Materials Research Centre of NAS of Belarus", Minsk, 19 P. Brovki st 220072, Belarus, e-mail for the corresponding author: orion_minsk@tut.by*
[2] *Beijing institute of technology, 5 South Zhongguancun Street, Haidian District, Beijing, 100081, China*

MOF represent a new class of porous materials. Due to the huge variability in the choice of initial components, they are characterized by a huge variety of possible structures, which allows researchers to create structures with the necessary properties. For the synthesis of these structures, both traditional methods (using a solvent) and non-traditional ones are used.

As a result of the synthesis, one -, two - and three-dimensional structures with different pore sizes can be obtained, the size of which can be varied by selecting organic ligands, or linkers. In the future, these structures will find their application in a variety of fields [1-3]. The aim of this work is obtain the samples of metal-organic framework Ni-MOF structures and to study treir morphology chemical composition and optical properties.

Samples of metal-organic framework Ni-MOF structures have been obtained. As a result of MOF material processing in a special vacuum chamber, heating to 150°C and mixing the introduced components for 30 minutes, a complex chemical compound with inclusions of iron particles with a particle diameter of 3-5 microns is formed on the substrate surface. The embedded particles act as crystallization centers and, in general, a material with ferromagnetic properties is formed. The morphology and chemical composition of the obtained Ni-MOF materials with ferromagnetic properties were studied by scanning electron microscopy (SEM) and energy dispersive X-ray spectroscopy (EDS). Transmission spectra were obtained in the range 200 − 2500 nm, as well as Raman spectra for Ni-MOF materials with ferromagnetic properties at room temperature. Powders consist of particles ranging in size from 10 to 50 microns, and the content of ferromagnetic metal reaches 99.16%. No extraneous impurity phases are observed, which indicates the successful formation of Ni-MOF material. Studies of the optical properties of Ni-MOF materials with ferromagnetic properties have shown that such materials have an absorption rate of more than 85%, which is important for creating efficient solar cells. There are five distinct peaks of Raman scattering in the range 600 − 1650 cm^{-1} (Figure 1), which are due to the main crystal structure of Ni-MOF materials. The different ratio of the intensities of the strongest lines indicates a different content of carboxyl groups in the samples.

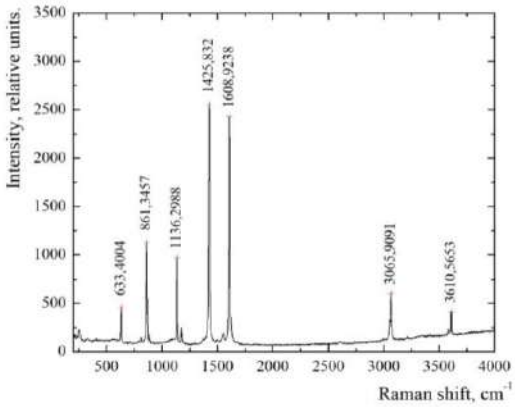

Figure 1 - Raman spectrum of Ni-MOF

Acknowledgement
This work was financial supported by Belarusian Republican Foundation for Basic Research as part of the projects BRFFR No. T20PTI-013 «Development of functional materials based on metal-organic framework structures (MOF) for perovskite solar cells».

References

[1] Li J.-R., Luppler R. J., and Zhou H.-C., Chemical Society Reviews 38 (2009) 1477.
[2] Li J.-R., Sculley J., and Zhou H.-C., Chem. Rev. 112 (2012) 869.
[3] Sumida K., Horike S., Kaye S. S., Herm Z. R., Queen W. L., Brown C. M., Grandjean F., Long G. J., Dailly A., and Long J. R., Chem. Sci. 1 (2010) 184.

Study of electromagnetic properties of corrosion resistant based on iron composites

A.K. Vetcher[1,*], O. Demidenko[1], V. Constantin[2], A.M. Popescu[2]
[1] *SSPA "Scientific-Practical Materials Research Centre of NAS of Belarus", Minsk, 19 P. Brovki st 220072, Belarus, e-mail for the corresponding author: vetcher@physics.by*
[2] *"Ilie Murgulescu" Institute of Physical Chemistry, Romanian Academy, 202 Splaiul Independentei, Bucharest, 060021, Romania*

Currently, the world is actively developing the production of electric vehicles, such as electric cars, electric buses, electric scooters, etc. Many advanced technologies are used to improve the performance of electric machines, but there still remain problems requiring comprehensive research. The use of soft magnetic materials based on iron powders will make it possible to replace electrical steel and significantly improve the parameters of electrical products [1-3]. Low-quality materials are the reason for frequent repair or replacement of worn parts. Therefore, a clear understanding of the corrosion resistance, mechanical, physical properties of the obtained composite materials, as well as knowledge of the specifics of their processing and operation is the key to significant savings.

The aim of this work is obtain based on water-atomized iron powder ASC100.29 composites by boron layers deposition on iron particles using an optimized technique and to study a corrosion resistance of its structure and electromagnetic properties.

The water-atomized iron powder ASC100.29, produced by Höganäs AB Sweden, was selected as the object of study. Purity of ASC100.29 powder is 99.5%. The chemical composition (wt.%) of the powder is: Fe:99.5, Mn:0.008, Si:0.04, C:0.08, P:0.01. Composite was received by applying an insulating boron layer B_2O_5 to the surface of the iron particles, and subsequent pressing under a pressure of 7-8 $t \cdot cm^{-2}$. Corrosion tests on composite were carried out in 3.5% NaCl solution at a temperature 25ºC. Crystal structure, specific magnetization and hysteresis loops of received composites was studied. It was established, that studied materials keeps it ferromagnetic properties after corrosion, but specific magnetization value decreses in 11% (Fig.1) at liquid nitrogen temperature. A phase transition Curie temperature before and after corrosive influence nearly 940 K. It was revealed, that main α-Fe phase remains with unit cell parameter 0.2866(4) ±0.0003 nm, but is observed the presence of a certain amount of iron oxides on the surface of the samples.

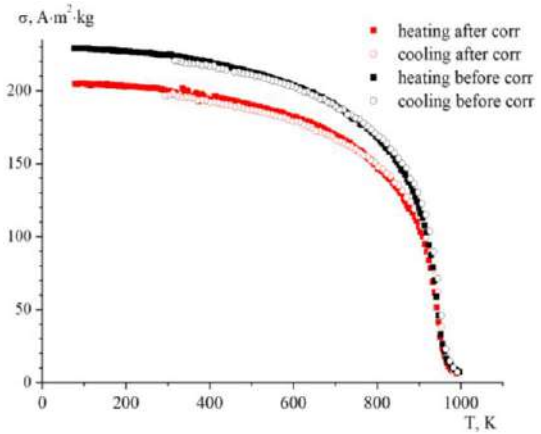

Figure 1 - Temperature dependences of specific magnetization for composite based on iron powder with boron layer B_2O_5 capsulation before and after corrosion action

Acknowledgement
This work was financial supported by Belarusian Republican Foundation for Basic Research as part of the projects BRFFR No. T20RA-004 «Corrosion resistance of new composite materials based on encapsulated iron powders for the electrical industry». Authors equally contributed to this work.

References

[1] Janta T., and Kordecki A., PM soft magnetic composition versus electrical sheets. Soft magnetic material workshop, Euro PM Japan, (2000)
[2] Tulchinskii L.N., and Panasiuk A.A., Powder Metall. 7-8 (1995) P.53 (in Russian)
[3] Gheiratmand T., Madaah Hosseini H.R., and Seyed Reihani S.M., J. of Mag. and Mag. Mat., 429 (2017) P.241.

Ferromagnetism of weakly substituted ferrite Bi(Ln)FeO_3: Ln – La, Nd, Gd

V.Sobol[1], K.Yanushkevich[2], B.Korzun[3], O.Mazurenko[4]
[1]*M.Tank Belarusian State Pedagogical University, Minsk, Belarus.*
[2] *SSPA "Scientific-Practical Materials Reseach Centre of NAS of Belarus", Minsk, Belarus*
[3] *The City University of New York, Borough of Manhattan Community College, U.S.A.*
[3]*The Belarusian Republican Foundation for Fundamental Research, Minsk, Belarus*

Multiferroic ceramic samples of $Gd_xBi_{1-x}FeO_3$, $Nd_xBi_{1-x}FeO_3$, $La_xBi_{1-x}FeO_3$, (x = 0 – 0.2) have been prepared by solid state reaction method. Some ferromagnetic order of pure $BiFeO_3$ was observed for these polycrystalline samples with an enhanced magnetization (M) and coercivity (H_C) for all the doped samples. Paramagnetic order of doped samples was observed in high magnetic fields (of the order of 10^6 A/m), at substitution of Bi by ions of Gd. This order correlates with paramagnetic ordering of free Gd ions in lattice of bismuth ferrite. At substitution of Bi by ions of Nd paramagnetic ordering in high magnetic fields was observed too, but to describe it is necessary to insert in Brilluen function expression a half mean of full quantum number of three-charged Nd-ion.

Bismuth films with different microstructure features for radiation shielding applications

D. Tishkevich[1*], D. Vasin[1], S. Grabchikov[1], A. Bondaruk[1,2], T. Zubar[1] and A. Trukhanov[1]
[1]*SSPA "Scientific and Practical Materials Research Centre of NAS of Belarus", 220072 Minsk, P. Brovki str. 19, Belarus,* [*]*dashachushkova@gmail.com*
[2]*Belarusian State Technological University, 220006 Minsk, Sverdlova str. 13A, Belarus*

Bismuth is a promising materials for radiation shielding applications. The problem of dense films obtaining is a key factor that needs improvement. In this regard two electrodeposition regimes (galvanostatic and pulse) were proposed for the formation of Bi films with microstructural characteriastics and density values meeting the requirements for radiation shielding materials. Scanning electron microscopy, X-ray energy dispersive analysis and Archimedes' principle were used for the Bi samples characterization. The optimal electrodeposition conditions in galvanostatic and pulse regimes were suggested for the Bi films formation with the best microstructure parameters and relative density.

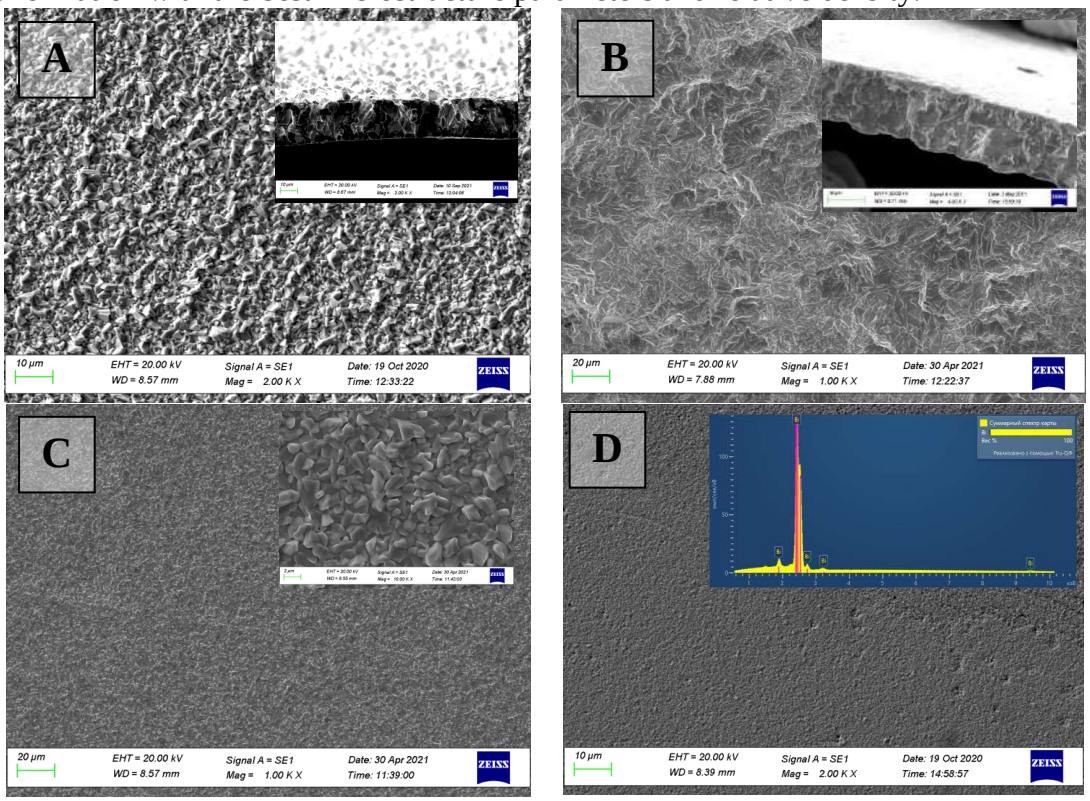

Figure 1. SEM images of the Bi films with the 20±2 µm thickness obtained in the following conditions: A – galvanostatic regime, current density (D_c) 15 mA/cm^2, B – long pulse regime, D_c=15 mA/cm^2, pulse duration (P) 1 s; C – medium pulse regime, D_c=15 mA/cm^2, P=20 ms; D – short pulse regime, D_c=15 mA/cm^2, P=20 µs. Inserts – SEM cross-section images of the Bi films (A and B), inlarge SEM image of the Bi films surface (C), EDX spectra of the Bi film

It has been shown that Bi films obtained in galvanostatic regime have a grains with granular sharp shape (Fig. 1 A). The relative density increases from 96.8 to 98.6% with the D_c rising from 10 to 25 mA/cm^2. It has been demonstrated that in pulse regime with a decrease in the pulse duration from 1 s to 20 µs, a significant change in the average grain size and microstructure of the films is observed. Thus, during electrodeposition with a pulse duration of 1 s Bi films with an average grain size of 0.4-2 µm are obtained. The average grain size becomes 300-700 nm when the pulse value decreases to a 20 µs. From the practical point of view the most optimal conditions for obtaining dense films as follows: galvanostatic regime – D_c=15 mA/cm^2 when Bi films with a grain size of 4-7 µm and a relative density of 97.9% are formed; pulse regime – D_c=15 mA/cm^2 and short pulse with duration of 20 µs when the Bi films with a grain size of 300-700 nm and relative density of 99.1% are formed.

THE ROLE OF THE ELASTIC-STRESSED STATE IN THE INTERFACE MAGNETOELECTRIC EFFECT IN LAYERED FERROMAGNETIC / FERROELECTRIC STRUCTURES

S. Sharko*[1], A. Serokurova[1], N. Novitskii[1], A. Stognij[1], N. Poddubnaya[2]
[1] *Scietific Practical Materials Research Centre of National Academy of Sciences, P. Brovki str., 19, 220072 Minsk, Belarus*
[2] *Institute of Technical Acoustics, ave. General Lyudnikova, 13, 210023, Vitebsk, Belarus*

The magnetoelectric (ME) effect [1] in the layered ferromagnet / ferroelectric structures is of great scientific and technical interest and consists in polarization of the sample in an external magnetic field (direct effect), or in its magnetization in an electric field (converse effect). The ME effect can find various applications in non-volatile converters, for example, in magnetic field sensors.

In the layered composite structures with thin (~1-2 μm) cobalt, nickel and permendur layers on substrates of ferroelectric ceramics of 400 μm based on lead zirconate titanate the elastic strains of the interface regions make a more noticeable contribution to the magnetoelectric effect than the magnetostriction of the ferromagnetic layer. These structures were obtained by the ion-beam sputtering – deposition with preliminary ion-beam planarization of the substrate surface.

A comparative analysis of the ME and elastic properties of layered structures was carried out. The ME effect at the maximum is the greatest for structures with cobalt and the least of all for structures with a permendur (Fig. 1).

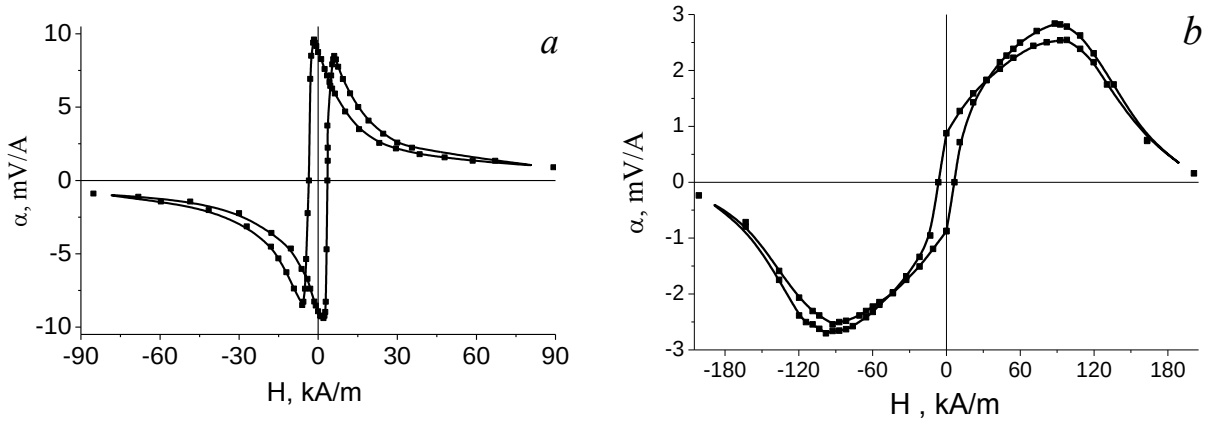

Figure 1. Low-frequency ME voltage coefficient of Co (2 μm) /PZT (400 μm) (*a*), and Pdr (2 μm) /PZT (400 μm) heterostructures (*b*). Pdr is permendur

It is shown that the elastic stresses of the region near the interface make a more noticeable contribution to the magnetoelectric properties in comparison with the magnetostriction of the ferromagnetic layer. These structures can be used as working elements of magnetoelectric sensors, which do not require standby power supply.

References:

[1] C.-W. Nan, M. I. Bichurin, S. Dong, D. Viehland and G. Srinivasan, J. Appl. Phys., 103 (2008) 031101-1-35.

Crystal and magnetic phase transitions in $BiMnO_3$-based ceramics

D.V. Karpinsky[1*], S.I. Latushka[1], D.V. Zhaludkevich[1], M.V. Silibin[2,3], V. Sikolenko[4,5]
[1] *Scientific-Practical Materials Research Centre of NAS of Belarus, 220072 Minsk, Belarus, karpinsky@physics.by**
[2] *National Research University of Electronic Technology "MIET", 124498 Zelenograd, Moscow*
[3] *Scientific-Manufacturing Complex "Technological Centre", 124498 Zelenograd, Moscow, Russia*
[5] *Joint Institute for Nuclear Research, 141980 Dubna, Russia;*
[6] *Karlsruhe Institute of Technology, 76131 Karlsruhe, Germany*

The crystal structure of ceramic compounds $BiMnO_{3+\delta}$ was studied by synchrotron and neutron diffraction, magnetometry and differential scanning calorimetry depending on oxygen excess and temperature. The presence of two phase transitions was established, from a monoclinic structure to an orthorhombic structure with an increase in the excess of oxygen. Phase transitions occur with a change in the orbital order with its gradual violation, which leads to changes in the magnetic structure with violation of the long-range magnetic order.

Analysis of the laboratory and synchrotron X-ray diffraction patterns of the compounds $BiMnO_{3+\delta}$ confirms the changes of crystal structures from the monoclinic structure (*C2/c*) to another monoclinic ($P2_1/c$) and then to the orthorhombic structure (*Pnma*) with nominal increase in the oxygen content (Fig. 1). The mentioned sequence of the structural transformations is accompanied by a gradual decrease in the unit cell volume, while the crystal symmetry of the compounds changes non-monotonously. Along with the information about the structural transformation, the diffraction measurements have also provided detailed information about the structural parameters, ionic coordinates and occupations. The occupation values calculated for the bismuth and manganese ions confirm nearly equal amount of the cations vacancies of about 3% and 5% for the compounds with nominal oxygen excess $\delta = 0.08$ and 0.14 which correspond to their chemical formulas. Further decrease in the cation/anion ratio specific to the $BiMnO_{3.08}$ sample leads to a stabilization of the monoclinic structure having lower symmetry, viz. $P2_1/c$ (SG #14) as compared to the stoichiometric compound - *C2/c* (SG #15), while further decrease in the cations content leads to a stabilization of the non-polar orthorhombic structure *Pnma* (SG #62).

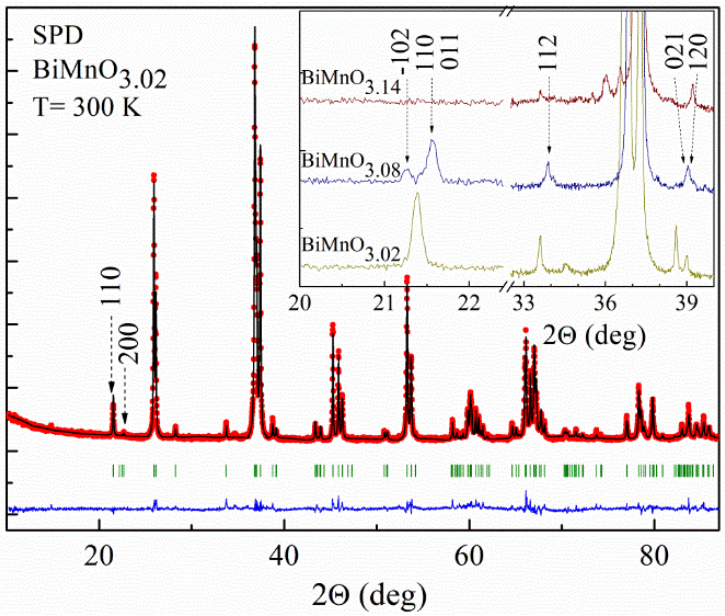

Figure 1. SPD pattern of the compound $BiMnO_{3.02}$ refined using the space group *C2/c*. Inset shows the reflections specific for the compounds $BiMnO_{3+\delta}$ (δ=0.02, 0.08, 0.14).

Functional composites based on hexaferrites for 5G-technologies

M.A. Darwish[1,2], A.I. Afifi [3,4], A.S. Abd El-Hameed [4,5], H.F. Abosheiasha [6], A.M.A. Henaish [2,7], D.I. Tishkevich[1,8], T.I. Zubar[8], E.L. Trukhanova[1,8] and A.V. Trukhanov[1,8*]
[1]*NUST MISiS, 119049, 4, Leninsky ave., Moscow, Russia*
[2]*Physics Department,Tanta University, 31527, Tanta, Egypt*
[3]*Egypt-Japan University of Science and Technology, Alexandria 21934, Egypt.*
[4]*Electronics Research Institute, Giza 12622, Egypt.*
[5]*Tohoku University, Sendai, Miyagi, 980-8576 Japan.*
[6]*Engineering Physics and Mathematics Department, Tanta University, Tanta 31511, Egypt.*
[7]*NANOTECH Center, Ural Federal University, Ekaterinburg 620002, Russia.*
[8]*SSPA "Scientific and Practical Materials Research Center of NASB", 220072, 19 P. Brovki St., Minsk Belarus,*

Speedy progress in information technology (IT) and significant growth in the use of electronic and electrical appliances have created specific types of electronic environmental pollution such as electromagnetic radiations, electronic noise, radiofrequency interference, electromagnetic interference, etc. Electromagnetic waves, such as radiofrequency waves and microwaves, are being radiated all the time around us. These unwanted electromagnetic waves, which are created from the electronic components (devices), may interfere and couple with the neighboring electronic components. According our previous stydies we observed some perspectives for hexaferrite-based composites for 5G applications [1]. Composited based on hexagonal ferrites and PVDF were prepared by the termal pressing. The ratio between phases was varied (PVDF from 5 till 20 %). Initial characterization of the composites was done by XRD and VSM. The persopectives for antenna application (5G) was estimated based on electrodynamic characteristics at 2.45 GHz. The studied samples may be promising candidates for an EMI suppressor. The shielding efficiency due to the reflection of 10% PVDF composite is -32 dB. Such kinds of composites can be working as an EMI suppressor by controlling the magnetic properties limits according to the VSM results without giving attention to the conductivity values. The prepared composites can be easily manipulated into flexible shapes to solve the main drawbacks of ferrites. Our antenna design can provide high performance, gain up to 5.2 dB, radiation efficiency up to 80% and a uniform radiation pattern over a wide frequency band. The PVDF/HF composites are promising materials for future gigahertz antenna applications due to their excellent electrical characteristics and low cost.

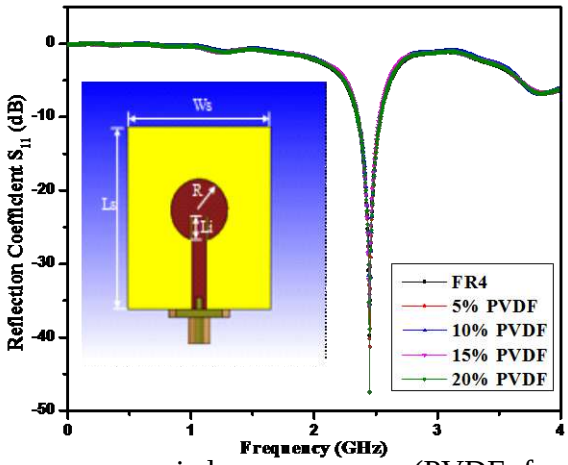

Acknowledgement
The work was support by the Russian Science Foundation (Agreement No. 19-72-10071 from 06 Aug. 2019).

References

[1] M.A. Darwish et all Can hexaferrite composites be used as a new artificial material for Antenna applications? Ceramics International 47(2), (2021) 2615-2623

Experimental and analytical study of the electromagnetic shielding effectiveness of materials promising for ensuring electromagnetic safety of electric transport users

S.S Grabchikov*, E.A.Grabchikova, T.I. Zubar, O.D. Kanafyev, A.V. Trukhanov
SSPA "Scientific and practical materials research centre of NAS of Belarus", 220072, Minsk, P. Brovki str., 19, Belarus

In this work, the shielding properties of structures with different numbers of layers in low-frequency magnetic fields were investigated. Samples were synthesized via electrodeposition with different numbers of $Ni_{80}Fe_{20}$ and Cu layers (1, 4, 10). It was found that multilayer $Ni_{80}Fe_{20}$/Cu shields have a higher shielding efficiency of low-frequency electromagnetic fields than shields based on single-layer materials of equivalent thickness.

Restructured Graphite as a Novel Carbon Material and its Applications

U. Novikau[1*], K. Sergeev[1], I. Razanau[1], V. Lomonosov[1], and V. Kazachenko[2]
[1]*Scientific-Practical Materials Research Centre of NAS of Belarus, 19 Brovki Str., 220072 Minsk, Belarus, phaust@list.ru**
[2]*Science and Technology Park of BNTU "Polytechnic," 37/1 Surganova Str., 220013 Minsk, Belarus*

Our report describes a novel type of bulk graphite-based binder-free material synthesized under relatively mild conditions or, as we call it, restructured graphite. The synthesis of the restructured graphite is based on the low-temperature intercalation of alkali metal ammines into natural graphite from alkali metal solutions in liquid ammonia. After the intercalate synthesis, it is subjected to hot forming under temperatures of up to 900 ℃. Depending on the material mass-to-volume ratio during the hot forming stage, the bulk restructured graphite samples range from lightweight foams to high-density solids.

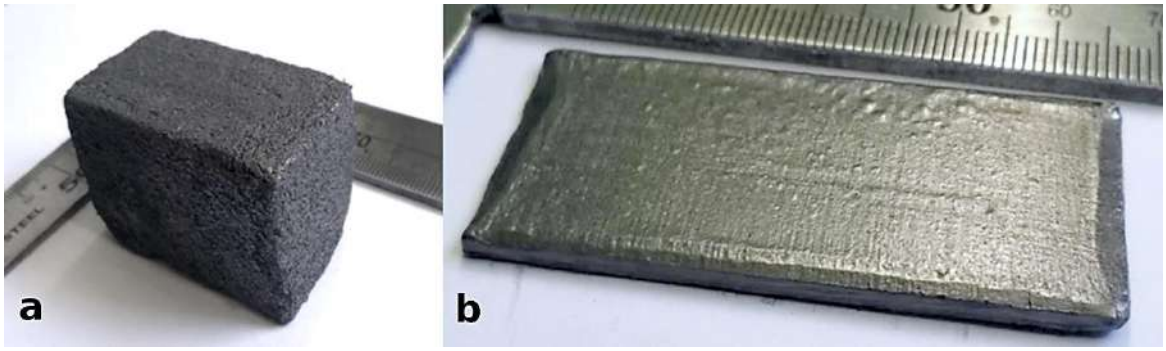

Photographs of the samples of restructured graphite: a — low-density sample, b — high-density sample

The mass density of restructured graphite reaches the value of 2.08 g/cm^3 that is 92% of the theoretical one for graphite monocrystals. The in-plane thermal conductivity of the high-density restructured graphite reaches the value of 455 W/(m·K). For comparison, the thermal conductivity of copper is around 400 W/(m·K), the thermal conductivity of commercial POCO polycrystalline graphite is around 80 W/(m·K). Such high mass density values and in-plane thermal conductivity are the results of strong material structure anisotropy.

The synthesis method developed allows producing various composites of restructured graphite with metals or ceramics and doping the material with additional elements such as boron. Restructured graphite has a wide range of potential application areas, including heat dissipation engineering, vacuum-plasma carbon coating deposition, electric metallurgy, electric energy storage.

Comparative studies of electrophysical properties of soft magnetic composite on base of ABC100.30 iron powder and Fenotron 553H material

G.A. Govor[1,*], A.K. Vetcher[1], A.O. Larin[1], O.F. Demidenko[1] and I.I. Vegera[2]
[1] *SSPA "Scientific-Practical Materials Research Centre of NAS of Belarus", Minsk, 19 P. Brovki st 220072, Belarus, e-mail for the corresponding author: govor@physics.by*
[2] *Physical-technical Institute of the National Academy of Sciences of Belarus, Minsk, 10 Kuprevicha str. 220141 Belarus*

The development and production of magnetic materials with low energy losses during magnetization reversal is one of the urgent problems of the industry today. Despite the fact that research and development of such materials have been going on since the beginning of the last century, the study of the mechanism of magnetization – magnetization reversal and improvement of the quality of these materials is still topical [1–5]. This is due to the fact that magnetic materials are widely used in various electrical devices (generators, motors, measuring devices, inductors, etc.).

To develop and create a new generation of highly efficient electrical products, it is necessary to use a completely new class of soft magnetic materials with improved characteristics [6]. Such materials must meet a whole range of requirements: high values of saturation induction, low electromagnetic losses, required mechanical strength, thermal stability and resistance to sudden heat changes, good machinability by cutting, turning, milling, and low cost. To reduce the weight and size characteristics of the device (inductor) must be able to operate at high frequencies up to 250 kHz. Only composite materials based on metal powders with insulating coatings meet these requirements. This paper presents comparative studies of the widely used material Ferrotron 559H and a special soft magnetic material based on ABC100.30 iron powder.

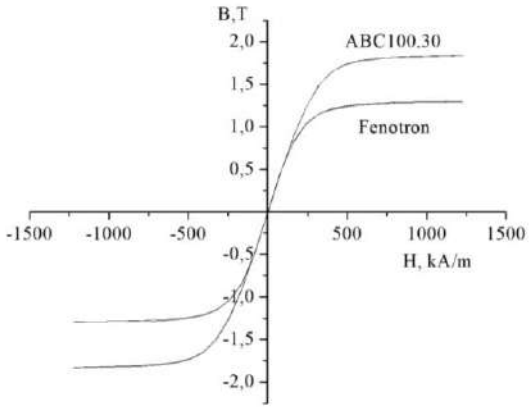

Figure 1 - Magnetization curves of Fenotron 553H and SMC material based on ABC100.30 iron powder in strong magnetic fields

Studies have shown that composite soft magnetic materials based on ABC100.30 iron powder with special coatings can be effectively used in the production of magnetic cores of various configurations in inductors intended for surface treatment of parts with external electromagnetic field. Heat treatment of internal holes, flat and figured surfaces with inductors with magnetic cores made of composite soft magnetic materials has shown that on the surface of parts it is possible to form a hardened layer uniform in depth with high hardness.

Acknowledgement
This work was financial supported by Belarusian Republican Foundation for Basic Research as part of the projects BRFFR No. T21ET-007.

References

[1] Shokrollahi H., and Janghorban K., J. Mater. Process. Technol. 189 (2007) P. 1–12.
[2] Gilberta I.P., Moorthya V., Bulla S.J., Evansa J.T., and Jackb A.G., J. MMM. 242/245 (2002) P. 232–234.
[3] Snelling E.C., and Mendham, NJ : PSMA. (2005) 385 p.
[4] Birčáková Z., Füzer J., Kollár P., Streckova M., Szabó J., Bureš R., and Fáberová M., J. of Mag. and Mag. Mater. 485 (2019). P. 1–7.

[5] Hongting P., Fengjing J., Yongxing W., and Biao Y., Colloids and Surfaces A: Physicochemical and Engineering Aspects. 361 № 1–3 (2010) P. 62–65.
[6] Vetcher A., Yanushkevich K., Material science «Nonequilibrium phase transformations» : Proceedings of V International scientific conference, Varna (2019). P.27–29.

Synthesis and crystal structure of Sc-doped $LuFeO_3$ ceramics

A.L. Zhaludkevich[1]*, A.P. Turygin[2], D.O. Alikin[2], A. Pakalniškis[3], D.V. Karpinsky[1]
[1] *SSPA «Scientific-Practical Materials Research Centre of NAS of Belarus», 220072, Belarus, Minsk, st. P. Brovki, 19, zhaludkevich@physics.by*
[2] *Ural Federal University named after the First President of Russia B. N. Yeltsin, 620002, Russia, Ekaterinburg, st. Mira 19*
[3] *Institute of Chemistry, Vilnius University, Naugarduko 24, LT-03225 Vilnius, Lithuania*

For the preparation of samples $Lu_{1-x}Sc_xFeO_3$ an ethylene glycol assisted sol-gel synthesis procedure was used. Firstly, diffraction experiments were performed for $LuFeO_3$ compound. From the given it was observed that amorphous phase was obtained after sintering the obtained xerogells at up to 650 °C. However, the further increase in temperature to 800 °C lead to a formation of a typical orthoferrite phase with orthorhombic symmetry and a space group *Pnma*. The additional increase in temperature up to 950 and 1100 °C led to a narrowing in diffraction peaks and increase in their intensity. This is most likely caused by the increased crystallinity and crystallite size. A slightly different case was discovered for the $ScFeO_3$ samples. Even at the initial temperature of 650 °C an appearance of multiple diffraction peaks was observed indicating a formation of crystalline phase. This phase was most likely consistent of the $ScFeO_3$ compound with bixbyite type structure, with cubic symmetry and a space group *I-a*3 and an unidentified impurity phase.

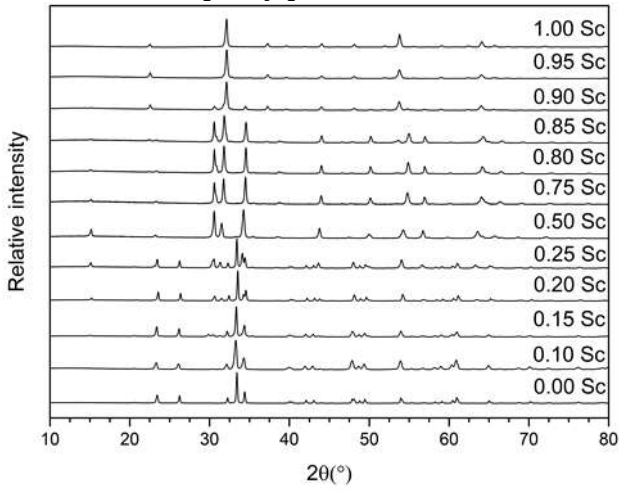

Figure 1. XRD patterns of $Lu_{1-x}Sc_xFeO_3$ ($0 \le x \le 1$) prepared by sol-gel method.

This phase mixture was consistent up to 950 °C, however the specific peak intensity for bixbyite structure shows an increase in intensity relatively to the impurity phase. At 1100 °C a single phase cubic bixbyite structure was obtained, but even in this case quite high intensity background was obtained, indicating a residual amorphous component and the need for even higher sintering temperature. Furthermore, it is worthy to note that the bixbyite structure is no longer considered a perovskite, since in the structure the Sc and Fe ions are distributed randomly, due to their relatively similar ionic radii. The XRD data confirm a formation of solid solutions across the entire doping range. Introduction of scandium ions up to 0.5 leads to a gradual increase in volume fraction of the hexagonal phase. Meanwhile the reflections attributed to the orthorhombic phase become less intensive. A single phase hexagonal structure was observed for the compound doped with 0.75 of Sc.

Acknowledgement
The authors acknowledge RFBR (projects # 20-52-04011) and BRFFR (project # T21RM-040).

Electrodeposition of NiFe Alloys at Direct, Pulse and Pulse-Reverse Current Modes

A.N. Kotelnikova[1]*, T.I. Zubar[1,2], T.V. Vershinina[4], T.I. Usovich[1], M.I. Panasyuk[1], V.A. Fedkin[1], O.D. Kanafiev[1], A.V. Trukhanov[1,2,3]

[1] *SSPA "Scientific and practical materials research centre of NAS of Belarus", 220072, Minsk, P. Brovki str., 19, Belarus, anna.kotelnikova.98@mail.ru **
[2] *South Ural State University, 454080, Chelyabinsk, Lenin Prospect, 76, Russia*
[3] *National University of Science and Technology MISiS, 119049, Moscow, Leninsky Prospekt, 4, Russia*
[4] *Joint Institute for Nuclear Research, 141980 Dubna, Joliot-Curie St, 6, Russia,*

The effect of current modes on composition, crystal structure and microstructure was investigated in this work. For this purpose, NiFe coatings were obtained using stationary, pulsed and pulse-reversed electrodeposition. The coatings composition, crystal structure and surface microstructure were studied. It has been shown that coatings obtained in direct current have less concentration of Fe (36.4%) then coatings obtained in pulse current (42.15%). And the sample obtained in pulse-reversed mode have the Fe concentration of 27.5%. It has been shown that all the samples have a Ni face-centered cubic lattice (Figure 1). DC and PC coatings have a smooth surface, while a PRC coating have a volumetric "cauliflower" structure (Figure 2).

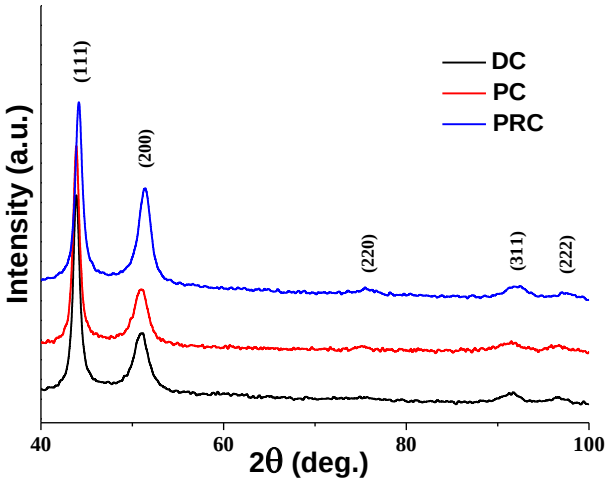

Figure 1. X-ray diffraction data of NiFe coatings

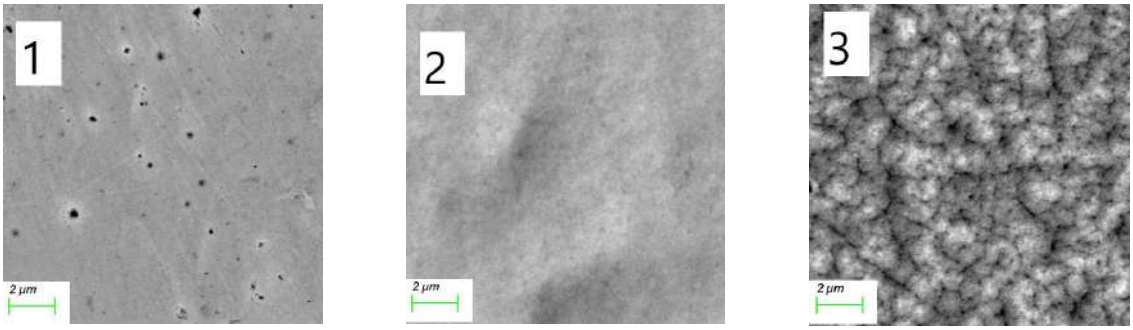

Figure 2. Microstructure of the surface of NiFe coatings, investigated using SEM: 1-DC, 2-PC, 3-PRC

Influence of Fe-Ni Films Microstructure on Magnetoresistive Effect

V. Fedkin[1] , A. Kotelnikova[1] , T. Zubar[1] ,O. Kanafyev[1], A. Trukhanov[1]
[1]*Scientific and Practical Materials Research Center of the National Academy of Sciences of Belarus, Minsk, Republic of Belarus*

Currently, many researchers are showing interest in materials that be used as a magnetic transducer. One of these materials is Fe-Ni. This material is widely used to create magnetic field sensors, as well as magnetic recording devices, etc.

The purpose of this article was to study the influence of the microstructure of Fe-Ni films on the magnetoresistive effect at different directions of the magnetic field.

The results show that with a perpendicular orientation of the magnetic induction vector relative to the flowing current, an increase in electrical resistance is observed. The increase in resistance occurs due to the influence of the magnetic field on the trajectory of charged particles, which leads to a decrease in their free path, which, in turn, increases the electrical resistance of the film.

Electric Properties of Black Phosphorus Single Crystals

[1]A.K. Fedotov, [1]A. Kharchanka, [1]J. Fedotova, [2]V. Slabuho, [3]M. Bushinski, [2]I. Svito
[1]*Institute for Nuclear Problems of Belarusian State University,*
Bobruiskaya str. 19, 220006, Minsk,, Belarus
[2]*Belarusian State University, Nezavisimosti av. 4, 220030, Minsk,, Belarus*
[3] *National Scientific-Practical Center for Naterial Science,*
P. Brovks str. 19, 220066, Munsk, Belarus

A large number of results are known from the literature on the study of the temperature dependences of electrical conductivity or resistivity, Hall constant and magnetoresistance in bulk crystals of black phosphorus (b-P) in a wide range of temperatures T and magnetic fields with induction B, as well as at different pressures [1-3]. Nevertheless, an analysis of the literature shows that a number of questions regarding the observed behavior of the electrical properties of b-P single crystals have not been fully clarified until now. So, in this work, we have studied the temperature dependences of electrical properties in several perfect b-P single crystals from the same set of growth manufactured by 2D Semiconductors (USA). The investigated single crystals (b-P) were grown in a high-pressure setup with six diamond anvils at a pressure of ~ 1 GPa, a temperature of 800 °C, and a synthesis time of 12 hours. The crystals were certified by the manufacturer with X-ray diffraction analysis and Raman spectroscopy.

Standard measurements of the temperature dependences of electrical conductivity $\sigma(T)$ (or resistivity $\rho(T,B)$), Hall constant $R_H(T,B)$, and relative magnetoresistance $MR = 100\%\cdot[\rho(T,B) - \rho(T,0)]/\rho(T,0)$ depending on the temperature T and the magnetic field with induction B were carried out. The electric current during measurements was directed along the crystallographic axes *a* or c. The magnetic induction vector was always directed along the b axis, i.e. normally to the plane *ac*.

Our measurements of temperature and magnetic field dependences of carrier transport properties (resistivity, Hall constant, magnetoresistance, concentrations and mobilities of electrons) in single crystals of b-P at $2<T<300$ K and $B\leq 8$ T have found their highly anisotropic behaviour, i.e. their dependences on orientation of electric current vector relative to direction of crystallographic axes *a* and *c*. Temperature dependences of conductivity show semiconducting behavior at all temperatures along *c*-axis and only below 250 K along *a*-axis, passing in the last case to metallic one at $T>250$ K. The MR values are negative below 25 K in magnetic fields $B < 4$-5 T. Above 25 K MR becomes positive at all fields with squared-like field dependence at low fields and linear one for $B > 5$ T. Behaviour of $\mu(T)$ curves follows a power-like character of the type $\mu(T) = AT^{\pm\kappa}$, when negative values of the exponent κ are usually assigned to scattering by phonons, and positive – to scattering by ionized impurities. Note also that the maximal values of the electron mobilities for the I||*a* orientation is about 6 times higher than for the I||*c* orientation.

References:

[1] Inamuddin Boddula R., Asiri A. M. (Eds.), Black Phosphorus. Engineering Materials. (2020).
[2] Yuichi Akahama, Masashi Miyakawa, Takashi Taniguchi, Asami Sano-Furukawa, Shinichi Machida, and Takanori Hattori. J. Chem. Phys. 153 (2020) 014704.
[3] Yanli Zhang, Jiahong Wang, Qian Liu, Shuang Gu, Zhengbo Sun, Paul K. Chu, and Xuefeng Yu. APL Materials 8 (2020) 120903

THE EFFECT OF TERBIUM AND ERBIUM RARE EARTH IMPURITIES ON THE ELECTRIC TRANSPORT PROPERTIES OF $TlInS_2$ LAYERED SEMICONDUCTOR

Serdar Gören [1], Cihan Kaya [1], V.B. Aliyeva [2*], T.G.Mammadov [2], MirHasan Yu. Seyidov[1]
[1] *Department of Physics, Gebze Technical University, Gebze 41400, Kocaeli, Turkey*
[2] *Institute of Physics, Azerbaijan Academy of Sciences, AZ-143 Baku, Azerbaycan*

The TSC spectra of $TlInS_2$ samples with 0.1 % Tb and Er dopants were obtained for the first time. Four distinct peaks were observed in ~ 80 – 300 K region. Various fitting procedures are used to obtain the parameters of impurity centers corresponding to TSC peaks. These parameters were compared to PICTS technique. Our results show the TSC spectra of $TlInS_2$ layered semiconductor doped by 0.1 % Tb and Er impurities are very similar to those observed for the same samples by PICTS method. Main trap peaks existing in TSC spectra of $TlInS_2$ originated from Tb and Er dopants were identified.

Mangetoelectric effect in $(Ba,Ca)(Ti,Zr)O_3$-$Co(Ni)Fe_2O_4$ multiferroic composites

V. V. Shvartsman[1*], M. Naveed Ul-Haq[2], D. Lewin[1], and D. C. Lupascu[1]
[1]*Institute for Materials Science, University of Duisburg-Essen, Universitätsstrasse 15, 45141 Essen, Germany, vladimir.shvartsman@uni-due.de*
[2]*Department of Physics, COMSATS University Islamabad, Department of Physics, Park Road, Chak Shahzad, Islamabad, Pakistan*

Multiferroic materials with the coexistence of ferroelectric and magnetic order have attracted considerable attention due to a number of promising applications, including highly sensitive magnetic field sensors or devices for harvesting the energy of electromagnetic fields [1]. The most attractive property of multiferroics is the magnetoelectric effect, that is, the control of polarization by a magnetic field or magnetization by an electric field. The magnetoelectric effect in single-phase multiferroics is small for applications. On the other hand, multiferroics can be obtained "artificially" by combining ferromagnetic and ferroelectric materials [2]. In such composite multiferroics, the application of a magnetic field induces magnetostriction of the ferromagnetic component, which leads to mechanical stress at the interface. In turn, this mechanical stress causes a change in the polarization of the ferroelectric component due to the direct piezoelectric effect. Thus, the magnetoelectric effect in multiferroic composites is mechanically mediated.

We report on the study of the magnetoelectric effect in bulk multiferroics composites consisting of a ferroelectric based on barium titanate and a ferrimagnetic spinel based on cobalt/ nickel ferrites [3-8]. The magnetoelectric effect has been studied both at the macroscopic and nanoscale. The dependences of the magnetoelectric coefficient on the magnetic field, temperature, microstructure of the samples and the relative content of the magnetic phase are discussed. It is shown that the decisive factor for the dynamic magnetoelectric effect is not the magnitude of magnetostriction, but its derivative with respect to the magnetic field, as well as the magnetic susceptibility of the ferrimagnet. The temperature dependences of the magnetoelectric effect exhibit a maximum near the polymorphic phase transition between two ferroelectric states with different crystal structures. Scanning probe microscopy was used to study the dependence of the local piezoelectric coefficient on the magnetic field [8]. Microscopic measurements made it possible to estimate the change in the magnetoelectric effect depending on the distance from the interface between the magnetic and ferroelectric phases.

References

[1] H. Palneedi et al., Actuators 5 (2016) 9.
[2] C.-W. Nan et al., J. Appl. Phys. 103 (2008) 031101.
[3] M. Naveed-Ul-Haq et al., Sci. Reports 6 (2016) 32164.
[4] M. Naveed-Ul-Haq et al., J. Mater Sci. 52 (2017) 13402.
[5] M. Naveed-Ul-Haq et al., Acta Mater. 144 (2018) 305.
[6] M. Naveed-Ul-Haq et al., Nanoscale, 10 (2018) 20618.
[7] M. Naveed-Ul-Haq et al., J. Mater. Sci. 56 (2021) 14678.
[8] H. Trivedi et al., npj Compt. Mater. 4, (2018) 28.

Magnetocaloric properties of Mn(Fe)As(P) in cyclic magnetic fields

A. Aliev[1*], L. Khanov[1], A. Gadzhiev[1], A. Gamzatov[1], K. Yanushkevich[2], G. Govor[2]
[1]*1Amirkhanov Institute of Physics, Daghestan Federal Research Centre, Russian Academy of Sciences, 367003 Makhachkala, Russia, lowtemp@mail.ru**
[2]*Scientific-Practical Materials Research Centre of the National Academy of Sciences, 220072 Minsk, Belarus*

Magnetocaloric properties of the materials under single and repeated application of the cyclic magnetic fields can exhibit significantly different behavior. For practical applications materials with time-stable and no frequency dependence, magnetocaloric properties are required.

In this report, we present results of studying the magnetocaloric properties in Mn(Fe)As(P) compounds in cyclic magnetic fields with frequencies up to 30 Hz with an amplitude of 1.2 T and in high magnetic fields up to 8 T at 0.2 Hz. The dependency of the MCE on the frequency of cyclic magnetic field and the effect of prolonged action of cyclic magnetic fields on magnetocaloric properties of the materials are studied in detail. Based on the field dependences of the adiabatic temperature change and magnetostriction results the lattice and magnetic contributions to the total magnetocaloric effect are estimated. It was also found that the effect of degradation of the magnetocaloric properties as a decrease in the MCE value under the action of a cyclic magnetic field is observed. An explanation of the observed behavior of the MCE in cyclic magnetic fields is given in the report. The degradation of the MCE and its frequency dependency impose restrictions on the use of this material in magnetic cooling technology.

The research was supported by a grant of the RFBR-BRFBR (Project No. 20-52-00047).

Role of defects in polarization switching of undoped and La - doped $TlInS_2$ ferroelectric – semiconductors

Vafa B. Aliyeva [1], T. G. Mammadov [1], Faik A. Mikailzade [2], Mehman M. Shirinov[1], and MirHasan Yu. Seyidov [2*]
[1]*Institute of Physics ANAS, Baku, AZ-1143, Azerbaijan,* [2]*Department of Physics, Gebze Technical University, Gebze, Kocaeli, 41400, Turkey smirhasan@gtu.edu.tr*

Present study reports the role of as - grown defects and La dopant in the polarization (P - E) switching phenomenon of undoped and La - doped $TlInS_2$ layered crystals. It is well known that the presence of defect dipoles strongly influences the properties of ferroelectric materials such as spontanious polarization, dielectric hysteresis loop, aging and conductivity. For instance, the effect of rare - earth dopants, such as La metal, are expected to have a major impact on properties and performance of on $TlInS_2$ ferroelectric – semiconductor compounds. Moreover, the ordering of charged defects in dc electric fields could induce imprint, namely, novel ferroelectric behavior in the crystalline structure of materials due to the formation of nanodomains around of charged defects. The attribute of these novel ferroelectric behaviors are narrow single loops, double hysteresis loops and even triple dielectric hysteresis loops.

$TlInS_2$ is the semiconductor with an optical band gap of ~ 2.3 eV at room temperature and the ferroelectric at temperatures below ~ 200 K. At room temperature $TlInS_2$ belongs to the monoclinic system having space group of C_{2h}^6. The $TlInS_2$ single crystal always contains a few native deep level defects which can significantly affect its all physical characteristics [1 - 3]. Two phase transitions occur in $TlInS_2$: from the paraphase to an incommensurate phase at ~ 216 K and from the incommensurate phase to the ferroelectric phase at the Curie temperature T_c ~ 200 K. The lattice structure of $TlInS_2$ consists of alternating two - dimensional layers parallel to the (001) plane with each successive layer turned through a right angle with respect to the preceding layer. The fundamental structural unit of a layer is the In_4S_{10} polyhedron representing a combination of four elementaryInS_4 tetrahedra linked together by bridging S atoms. The combination of the In_4S_{10} polyhedra into a layer resultsin trigonal prismatic voids where Tl atoms are located.

$TlInS_2$ single crystals were grown by using the modified Bridgman method. The starting elements Tl, In and S of 5 N purity were located in conical quartz ampoules. The ampoules were charged with quantities of Tl, In and S in the ratio corresponding to the stoichiometry. The charged ampoules werethen evacuated to a pressure of 10^{-5} Torr and sealed. The doping was performed by adding the corresponding weighted portion of lanthanum to the cell with the preliminarily synthesized $TlInS_2$ compound. The EDX analysis demonstrated that the doped $TlInS_2$ sample is enrichedby the lanthanum impurity with a content of ~ 0.37 at %. High - purity silver paste was coated on two opposite faces of the sample as electrodes. The polarization -electric field P - E hysteresis loops were measured using a modified Sawyer - Tower circuit at temperatures below T_c.

It has been revealed that, without any poling procedure, pure $TlInS_2$ exhibits normal single hysteresis loops at $T < T_c$. After poling the shape of hysteresis loops was strongly affected by corresponding charged deep level defects. As a result, an additional defect polarization state from space charges accumulated on the intrinsic deep level defects has been revealed in pure $TlInS_2$ at the temperatures below T_c. Besides, unusual multiple hysteresis loops were observed in La doped $TlInS_2$ below ~ 200 K after application of different external perturbations (electric field, exposition and memory effect). The slim single, double and even triple polarization – electric field ($P – E$) hysteresis loops were observed. This could be explained by the long - range interactions among activted La ions and ferroelectric domains. Double and triple hysteresis loops are an exceptional phenomenon in ferroelectrics which are often

observed in antiferroelectric and ferrielectric materials. Therefore research on the feasible formation of double P - E loops in $TlInS_2$ single crystal layered ferroelectrics and their relation to defect dipoles is of great scientific and technological significance.

References

[1] A. P. Odrinsky, T. G. Mammadov, M. Yu. Seyidov, V. B. Aliyeva, Physics of the Solid State, v.56, N 8, pp. 1605 - 1609 (2014)
[2] M. Yu.Seyidov, A. P. Odrinsy, R. A. Suleymanov, E. Acar, T. G. Mammadov, V. B. Aliyeva, Physics of the Solid State, v.56, N 10, pp. 2028 - 2034 (2014)
[3] M. Yu. Seyidov, R. A. Suleymanov, E. Acar, A .P. Odrinsky, T. G. Mammadov, A. I. Nadjafov, V. B. Aliyeva, Low Temperature Physics, v. 40, N 9, pp. 830 - 836 (2014)

Development of pure and strontium substituted $LaFeO_3$ single crystals by optical floating zone technique

N. Sivakumar[1]*, R. Jayavel[2], G. Anbalagan[3] S. Ganesamoorthy[4]
[1]*Sri Sai Ram Engineering College, West Tambaram, Chennai 600 044.*
[2]*Crystal Growth Centre, Anna University, Chennai 600 025.*
[3]*Department of Nuclear Physics, University of Madras, Guindy Campus, Chennai 600 025.*
[4]*Materials Science Group, IGCAR, Kalpakkam 603 102.*

Single crystals pure and strontium substituted $LaFeO_3$ are grown by optical floating-zone technique. Crystals are subjected to powder X-ray diffraction and Rietveld refinement analysis. There is no significant structural changes are observed. However, the small shift in the Sr substituted X-ray spectrum explains the lanthanide contraction nature. The crystalline perfection of the grown materials is analyzed through Laue pattern. Dielectric studies are carried out on both the samples in the temperature range from 300 to 900 K for the frequency range from 2.5 kHz to 125 kHz. Grown crystals show their Neel temperature at 742 K. The Sr substituted $LaFeO_3$ crystal show improved dielectric constant. Colossal dielectric behavior, electrical and thermal conductivities are analyzed through dielectric studies for an efficient high temperature dielectric applications.

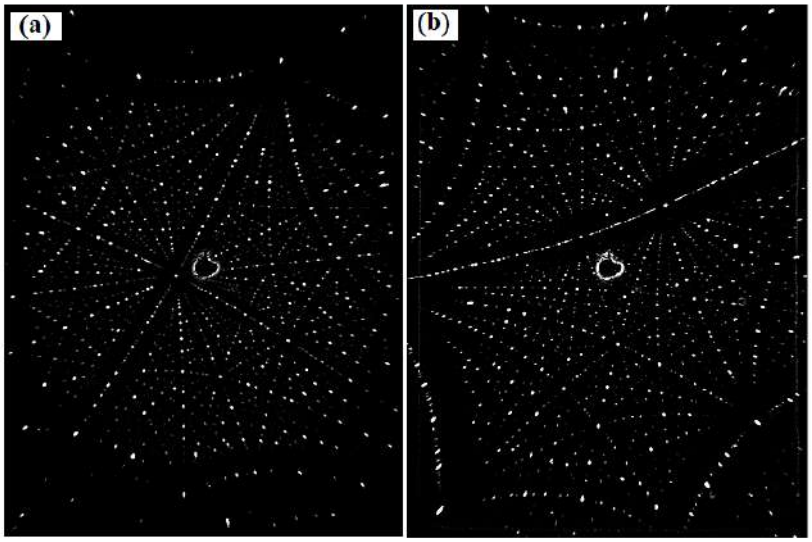

Laue pattern for (a) $LaFeO_3$ and (b) $LaSrFeO_3$ single crystal

High Performance One-Body Core/Shell Nanoarray Supercapacitor

Fangya Qi[1], Zhipeng Sun[1,*]
[1]*School of Materials and Energy, Guangdong University of Technology, Guangzhou, 510006, Guangdong,, zpsunxj@gdut.edu.cn**

An integrated electrode of core-shell coaxially structured $NiCo_2S_4$@TiO_2 nanorod arrays/carbon cloth ($NiCo_2S_4$@TiO_2@CC) have been fabricated, via a two-step hydrothermal method. Comprehensive structural and compositional analyses are performed to understand the effects of the $NiCo_2S_4$ shell on the TiO_2 core. Such core-shell arrays structure can significantly provide abundant electroactive sites for redox reactions, convenient ion transport paths, and favorable structure stability. The $NiCo_2S_4$@TiO_2@CC electrode represents a splendid specific capacitance (650 F g^{-1} at 1 A g^{-1}) and enhanced cycling stability (capacitance retention of 97% over 10000 cycles at 5 A g^{-1}). Additionally, the assembled $NiCo_2S_4$@TiO_2@CC //CNT@CC solid-state asymmetric supercapacitors exhibit a maximal energy density of 0.6 mWh cm^{-3} at 32.4 W cm^{-3}, and topping cycling stability (85% capacitance retention after 5000 cycles at 5 mA cm^{-2}). The results demonstrate that the well-designed $NiCo_2S_4$@TiO_2@CC presented in this work are applicable for the development of electrode materials in energy storage devices.

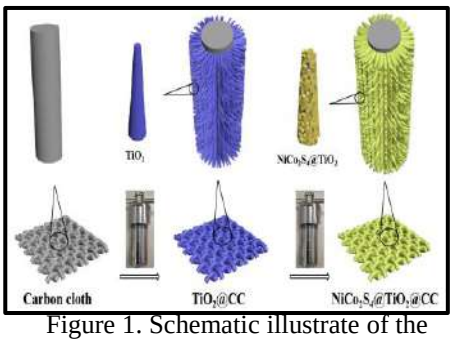

Figure 1. Schematic illustrate of the fabrication processes for flexible $NiCo_2S_4$@TiO_2@CC.

Reference

[1] Z.P. Sun [et al.] Journal of Colloid and Interface Science 601 (2021) 669–677
[2] Z.P. Sun [et al.] Nanotechnology 32 (2021) 295705 (9pp)
[3] Z.P. Sun [et al.] Journal of Colloid and Interface Science 587 (2021) 302–31

Photocatalytic reduction of CO2 over TiO2 nanowires catalyst

S. Dubkov[1]*, A. Tarasov[1], A. Savitskiy[1,4], A. Dudin[2], O. Shtyka[3], R. Ciesielski[3], A. Kedziora[3], J. Rogowski[3], T. Maniecki[1], R. Ryazanov[4] and D. Gromov[1]
[1]*National Research University of Electronic Technology, 124498 Moscow, Russia, *sv.dubkov@gmail.com*
[2]*Institute of Nanotechnology of Microelectronics of the Russian Academy of Sciences, 115487Moscow, Russia*
[3]*Lodz University of Technology, 90-924 Lodz, Poland*
[4]*Scientific-Manufacturing Complex "Technological Centre", Moscow, Russia*

The photocatalytic conversion of carbon dioxide into valueadded chemicals is recognized as a promising approach to address both energy and environmental issues. The photocatalytic reduction of carbon dioxide can be performed on various kinds of material, including inorganic semiconductors, carbon-based semiconductors, metal complexes, supermolecules, and their derivatives. Among various photocatalysts, TiO_2 is one of the most well-known and widely used materials due to its high oxidative efficiency, high chemical stability, nontoxicity and low-cost. The main aim of the work was to study the photocatalytic activity of TiO_2 nanowires samples under continuous flow conditions.

TiO_2 nanowires were synthesized using the hydrothermal method in an autoclave. The resulting nanowires were heat treated at 500, 700 and 900 ^oC for 4 hours in an air atmosphere. In the course of the experiments, studies of the specific surface area, diffuse reflectance spectra of the nanothread samples were carried out. The phase composition of photocatalysts was studied with a PANalytical X'Pert Pro MPD diffractometer. The surface morphology of the investigated samples was studied by HITACHI scanning electron microscope. At the final stage of research the photocatalytic activity of the obtained samples was investigated.

Photocatalytic studies have shown that the activity of titanium oxide nanowires depends on the temperature of their heat treatment. The studied samples showed high activity at the beginning of the process. The main photocatalytic products were methane and methanol. It was found that with an increase in the heat treatment temperature, the activity of the photocatalytic activity of the samples decreases, which can be explained by a change in the ratio of the rutile: anatase phases.

Acknowledgement
This research was funded by the Russian Science Foundation (Project No. 19-19-00595).

Application of solution combustion synthesis in ceramic membrane preparation

M.M. Hundzilovich, Yu.G. Pavliukevich
Belarusian State Technological University, 220006, Belarus, Minsk,13a, Sverdlova str., mikalai.hundzilovich@gmail.com

Currently, porous ceramic membranes are widely used for filtration processes in a lot of industries such as chemical and petrochemical, pharmaceutical, food and beverage, metal processing and other. Ceramic membranes have a number of advantages over polymer and metal membranes: high mechanical strength, permeability, chemical and heat resistance.

Corundum ceramic membranes are the most common in modern industry due to their availability and high physicochemical properties. However, corundum ceramics are expensive due to the high sintering temperatures during their production. The solution to this issue is the use of additives that intensify the sintering process and energy-efficient methods for membrane preparation, which allow the additive to be evenly distributed in the volume of the material.

Solution combustion synthesis (SCS) is one of the most promising energy-efficient methods for producing ultrafine ceramic particles which have modified by additives structure. SCS is a method based on thermally initiated exothermic combustion reactions of components in systems containing an oxidizing agent (metal nitrate) and an organic reducing agent (water-soluble linear and cyclic organic amines, amino acids).

The research study the formation process regularities of the porous permeable structure of corundum ceramics obtained by the SHS method, in relation to their physicochemical properties, additive amount, sintering parameters, phase composition and operational characteristics. Efficiency of MnO_2, Fe_2O_3, ZnO and CuO as additives intensifying the corundum ceramics sintering process were investigated.

The reaction mixture preparation: the solution containing metal nitrates and an organic reducing agent was evaporated then it was subjected to heat treatment which provides interaction in the metal nitrate – carbamide system accompanied by the formation of a self-igniting gas mixture and the release of a large amount of heat. The initiation of an exothermic reactions occurred at temperatures of 350–500 °C. Temperatures of the reaction area were reached up to 1600 °C due to exothermic process. The size of the formed during the process highly porous ceramic particles was from 20 nm to 300 μm.

The results of the X-ray diffraction analysis of the synthesized materials allowed establishing predominant phase of corundum α-Al_2O_3, as well as aluminates $ZnAl_2O_4$, $FeAl_2O_4$, $MnAl_2O_4$, $Cu_2Al_2O_4$, CuO in the investigated systems.

Dual-layer ceramic membranes were prepared by doctor's blade method on the surface of the macroporous corundum ceramic substrate followed by sintering at 1200–1350 °C. The ceramic membranes have the porous permeable structure with advanced network of open channel-forming slit-shaped pores. The thickness of the membrane layer is 30–60 μm, the open porosity of the membrane layer is 35–42 % (fig.1). The penetration of membrane layer particles into the pores of the substrate is 5–10 μm. The average equivalent pore diameter is 1–4 μm.

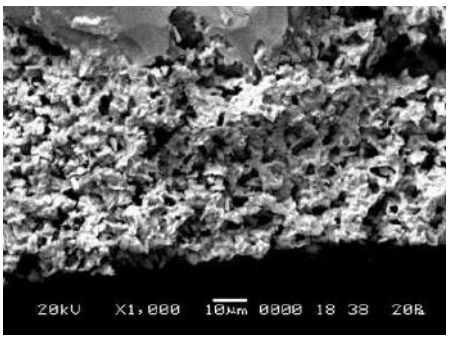

Figure 1 – Structure of the microfiltration layer of the dual-layer ceramic membrane

The developed dual-layer microfiltration ceramic membranes have the following characteristic: coefficient of linear thermal expansion is $(6–8)\cdot10^{-6}$ K^{-1}, compressive

mechanical strength – 19.46–21.76 MPa, acid resistance – 98.19–99.51 %, water permeability coefficient – $(1{,}312–1{,}614)\cdot10^{-14}$ m^2.

Crystal structure and electromechanical properties in Fe-doped $BiMnO_3$

S.I. Latushka[1*], A.L. Zhaludkevich[1], A.N. Chobot[1], V.V. Sikolenko[2], G.M. Chobot[3], T.V. Latushka[4], D.V. Karpinsky[1]
[1] *Scientific-Practical Materials Research Centre of NAS of Belarus, 220072 Minsk, Belarus, *e-mail address: latushkasi@gmail.com*
[2] *Joint Institute for Nuclear Research, 141980 Dubna, Russia*
[3] *Belarusian State Agrarian Technical University 220023 Minsk, Belarus*
[4] *Belarusian State Medical University, 220116 Minsk, Belarus*

Recently, manganites and ferrites have been of great importance for the initial community [1, 2]. Of greatest interest are compounds in the vicinity of the phase boundary and characterized by a metastable structural state. According to the structural data obtained for solid solutions $BiMn_{1-x}Fe_xO_3$ by X-ray diffraction, compounds with a concentration of x = 0.1 - 0.3 are characterized by a two-phase structural state (the compositions are characterized by the coexistence of monoclinic and orthorhombic phases). The structure of the $BiMn_{1-x}Fe_xO_3$ composition with x = 0.2 is characterized by a dominant orthorhombic phase with a characteristic antipolar displacement of bismuth and manganese ions (space group Pbam), as well as the presence of an insignificant (~ 10-15 %) part of the monoclinic phase.

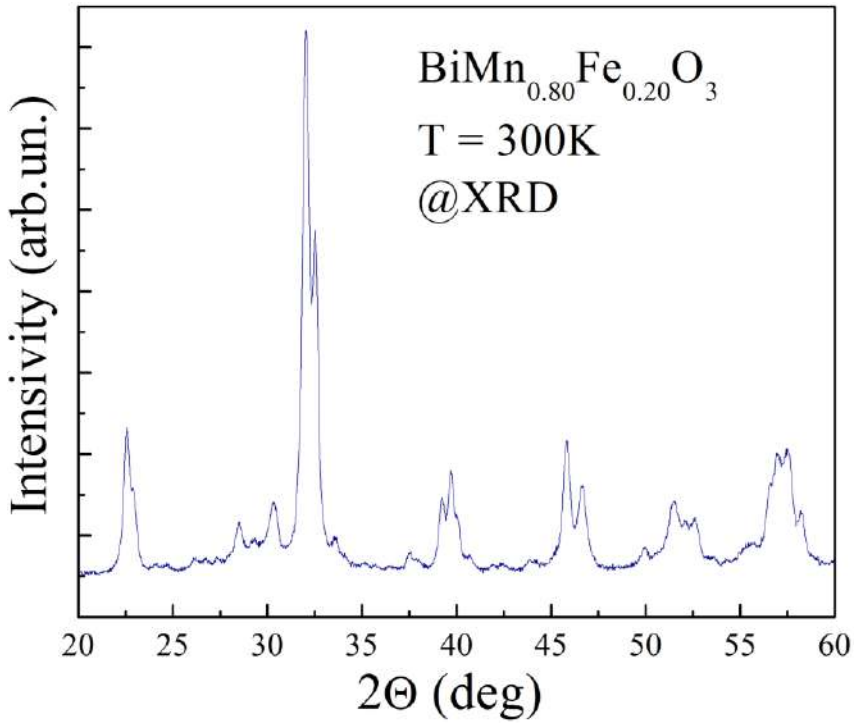

Figure 1. Room-temperature XRD patterns obtained for the compounds $BiMn_{0.80}Fe_{0.20}O_3$

The data obtained by the method of piezoelectric force microscopy (PFM) for ceramic compounds $BiMn_{0.80}Fe_{0.20}O_3$ showed the presence of a domain structure with different orientations of dipole moments, which is consistent with the available X-ray data.

Acknowledgement
This work was supported by BRFFR (projects # T20P-121), RFBR (projects # 20-52-00023).

References
[1] R. Masrour, A. Jabar et al. Solid State Commun, 268 (2017) 64–69.
[2] R. Masrour, A. Jabar et al. J. Magn. Magn. Mater, 401 (2016) 91–95.

Synthesis, characterization and corrosion behaviour of CoCuFeMnNi high entropy alloy

A.M.Popescu[1*], M.Burada[2] , V.Constantin[1], I.Constantin[1], M.T.Olaru[2], F.Branzoi[1], D.Mitrica[2], C.Donath[1], E.I.Neacsu[1], J.Calderon Moreno[1], I.Atkinson[1]
[1] *"Ilie Murgulescu" Institute of Physical Chemistry-IPC,202 Splaiul Independentei, Bucharest, Romania; popescuamj@yahoo.com*
[2] *National R&D Institute for Nonferrous and Rare Metals – IMNR, 102 Biruinţei Blvd., Pantelimon, Ilfov County, Romania*

Alloy coatings are widely prepared on the surface of tools and machines. High-entropy alloys are potential replacements of nickel-, iron-, and cobalt-base alloys in machining due to their excellent strength and toughness. In this work CoCrFeMnNi high entropy alloy thin films were produced on copper substrate by potentiostatic electrodeposition in an electrolyte based on a DMF (dimethyformamide) - AN (acetonitrile) organic compound. The following flow chart present the work line:

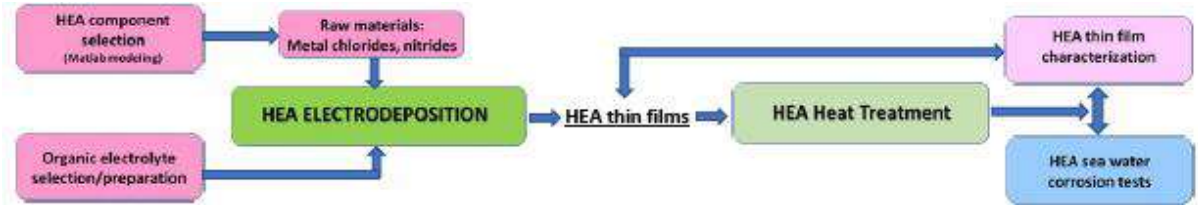

The potentiodynamic electrodeposition conditions were: electrolyte wa formed of DMF-AN (4:1 in volume) and 0.5mol/l $LiClO_4$,, which contains 0.01 mol/l of $Co(NO_3)_2$, $CrCl_2$, $FeCl_2$, $MnCl_2$ and $NiCl_2$; T=298K, anode-cathode distance 2.0 cm, sweep 1000-2500 mV, t=1h. Microstructure structure was studied by X-ray diffraction and scanning electron microscopy. The XRD patterns indicated that the as-deposited thin films were amorphous. SEM analysis revealed that the film consists of compact and cauliflower particles with holes. The Tafel plots indicated that the present HEA alloy has a good corrosion resistance in artificial sea water, better than Cu substrate.

.

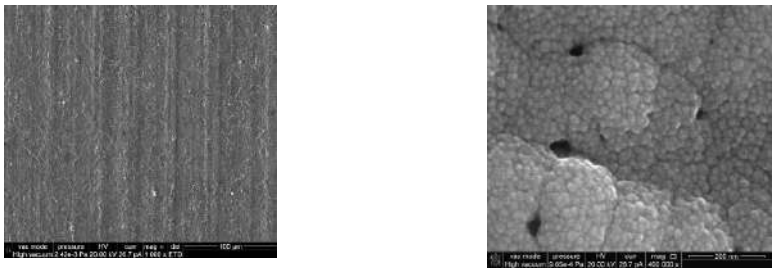

Fig.1 SEM images at magnification x1000 and x400.000

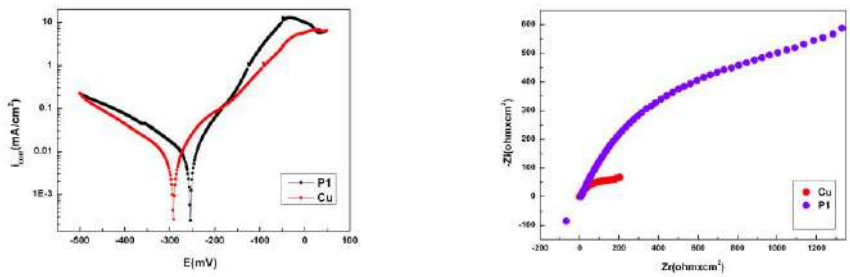

Fig.2 Tafel and Niquist plots of P1 and Cu substrate

Acknowledgement
This work was supported by „Ministerul Cercetării şi Inovării: PN-III-P2-2.1-PED-2019-2022"

Structure and magentic properties of Monel-400 influenced by the corrosion in black seawater

V.Constantin[1] ,A.M.Popescu[1], K.Yanushkevich[2*],O.Demidenko[2], E.I.Neacsu[1], C.Donath[1], A.Galyas[2], A.Zyvulka[2]
[1] *"Ilie Murgulescu" Institute of Physical Chemistry of the Romanian Academy, Laboratory of Electrochemistry and Corrosion, 202 Splaiul Independentei, Bucharest, Romania*
[2] *Scientific Practical Materials Research Centre of NAS Belarus, Laboratory of Physics of Magnetic Materials 19 P. Brovki Str.,Minsk, Belarus ; * k.yanushkevitch@yandex.by*

Monel is a group of nickel alloys, primarily composed of nickel (up to 67%) and copper, with small amounts of iron, manganese, carbon, and silicon. The alloy Monel 400 is used: marine fixtures, pumps, valves and piping systems for sea water applications. The long term corrosion processes of special steels Monel 400 in black seawater at 298K has been investigated by mass loss method. The corresponding corrosion parameters were calculated. Micrographic images before and after corrosion were obtained. The influence of the corrosion process on the crystal structure and specific magnetization of the studied steels was carried out by using X-ray diffraction and respectivelly ponderomotive methods.

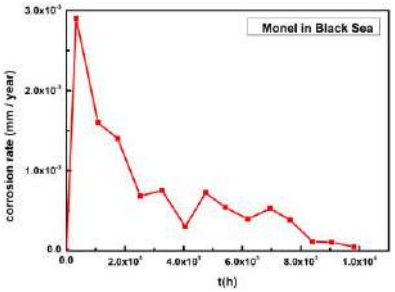

Fig.1-Long term corrosion in black seawater

Gravimetric data within 409 days (Fig.1) showed that the corrosion rate has a big sharp increase and then decreases up to $5.01 \cdot 10^{-5}$ mm/year, which means a very good corrosion resistance of Monel 400 in black seawater.

The XRD data confirm this good result, as no changes were found on the crystal structure of Monel before and after corrosion in black seawater.

Table 1- Crystal parameters

Sample Monel	a, (nm)	average size of crystallites , d (nm)	dislocations density, $\delta\ 10^{-3}$ (nm^{-2})
before corrosion	0.3566	20.71	2.33
corroded in Black Sea	0.3564	21.32	2.20

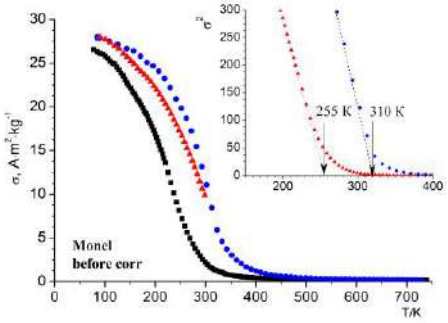

Fig.2 Magnetis of Monel-400 before corrosion

The same behaviour was observed on the magnetic properties of Monel before (Fig,2) and after corrosion in black seawater (Table 2), proving that black seawater has no effect on the magnetic properties.

Table 2- Magnetic parameters

Sample Monel	σ77 (A·m2·kg-1)	TC, (K)
before corrosion	26.5	255
corroded in Black Sea	26	265

Magnetic properties of layered cobaltite Sr0.78Tb0.22CoO3-δ

N. Tereshko, M. Bushinsky, R. Lanovsky*, O. Mantytskaya,V. Fedotova, A. Nikitsin and A. Chobot
[1] *Scientific-Practical Materials Research Centre NAS of Belarus, 220072 P. Brovki str. 19, Minsk, Belarus, rommelfiz1@gmail.com**

A comprehensive study of crystal and magnetic structure, magnetic and magnetotransport properties of layered perovskite $Sr_{0.78}Tb_{0.22}CoO_{3-\square}$ has been carried out. The main contribution to the diffraction spectrum of neutron diffraction patterns can be well described by the space group I4/mmm with the superstructure $2a_p$ x $2a_p$ x $4a_p$ (a_p is the parameter of the primitive cell). The oxygen content calculated from the neutron diffraction data analysis is 2.65.

This composition is a layered perovskite with an antiferromagnetic G-type structure and a Neel temperature of ~ 370 K with different magnetic moments in anion-deficient ($CoO_{4.5}$) and oxygen-stoichiometric layers (CoO_6). The magnetic moment at T = 50 K in $CoO_{4.5}$ layers is 2.4 μ_B / Co, while in CoO_6 layers it is lower - 1.6 μ_B / Co. According to [16], cobalt ions in the CoO_6 layers are in the IS state, and orbital ordering occurs in the CoO_6 layers due to the Jahn – Teller activity of Co^{3+} in the IS state. However, in CoO_6 layers, superexchange interactions are strong and antiferromagnetic, which is typical for Co^{3+} ions in the HS state. The high point T_N = 370 K is also characteristic of the HS state of Co^{3+} ions. Therefore, we can conclude that in the CoO_6 layers, Co^{3+} ions are in both the HS and LS states. Co^{3+} ions in HS are Jahn - Teller inactive and orbital ordering in CoO_6 layers is impossible. In $CoO_{4.5}$ layers, some Co^{3+} ions are located in CoO_6 pyramids, articulated at the base, which creates a distinguished axis along which, during magnetic ordering, ordering of e_g Co^{3+} orbitals in the HS state is possible. Apparently, this situation is realized in $Sr_{0.78}Tb_{0.22}CoO_{2.65}$ and leads to a doubling of the unit cell along the a axis, as was observed in $Sr_{3.12}Er_{0.88}Co_4O_{10.5}$ [14].

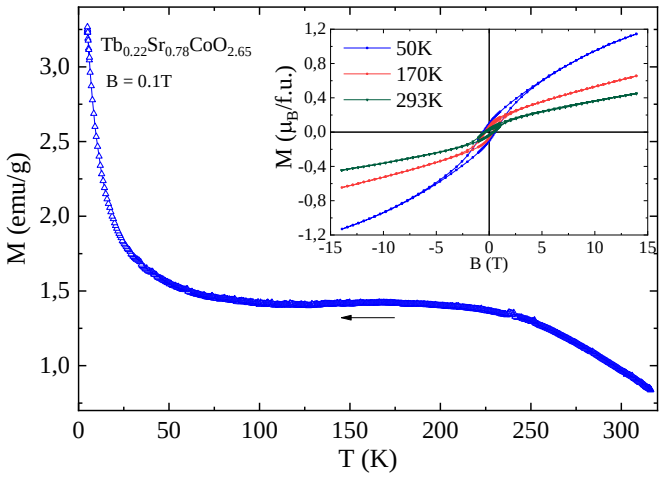

Fig 1 Temperature and field (inset) dependences of the magnetization of $Sr_{0.78}Tb_{0.22}CoO_{2.65}$.

It is assumed that the ferromagnetic component arises due to the orbital ordering in the Co^{3+} ions in the HS state in the anion-deficient layers and the presence of ferromagnetic exchange bonds in the anion-deficient $CoO_{4.5}$ layers between the pyramids joined at the base.

New ferroelectric lead-free oxide materials on the base of modified KNN and NBT perovskites

E.D. Politova[1*], G.M. Kaleva[1], N.V. Sadovskaya[2], A.V. Mosunov[3], S. Yu. Stefanovich[3], D.A. Kiselev[4], T.S. Ilina[4] , V.V. Shvartsman[5]
[1]*Semenov Institute of Chemical Physics RAS, Kosygina, 4, Moscow 119991 Russia*
politova@nifhi.ru
[2] *FSRC «Crystallography and Photonics» RAS, Leninskii pr. 59, Moscow 119333 Russia*
[3] *Lomonosov Moscow State University, Leninskie gory 1, Moscow 119992 Russia*
[4] *National University of Science & Technology "MISiS", Leninskii pr. 4, Moscow 119991 Russia*
[5] *Institute for Materials Science Duisburg-Essen, University of Duisburg-Essen, Universitatsstrasse 15, Essen 45141 Germany*

Though Pb-based perovskite materials are widely used in different branches of industry, environmental problems caused by toxic elements stimulated intensive studies of lead-free oxide materials in order to replace toxic Pb-based ones. Ferroelectrics with perovskite structure on the base of $BaTiO_3$ (BT), $(K_{0.5}Na_{0.5})NbO_3$ (KNN) and relaxor $(Na_{0.5}Bi_{0.5})TiO_3$ (NBT) are being among the most popular objects studied. They are promising for development of new lead-free capacitor, piezoelectric, electrocaloric and other materials.

We studied influence of cation modification of compositions on structure, microstructure, and functional properties of compositions close to the Morphotropic Phase Boundary in the KNN-BT and NBT-BT systems additionally modified with donor (La^{3+}), and acceptor (Li^+, Ag^+, K^+, Mn^{3+}, Ni^{3+}, and Fe^{3+}) cations and with overstoichiometric additives ZnO, SiO_2, CuO [1-3].

Ceramic samples were prepared using the two-step solid-state reaction and sol-gel methods. Their properties were characterized and studied by the X-ray Diffraction, Scanning Electron Microscopy, Second Harmonic Generation, Dielectric Spectroscopy, and Piezorespone Force Microscopy methods. The observed unit cell parameters and size of grains changed in modified compositions correlating with ionic radii of substituting cations.

Ferroelectric phase transitions were observed in the range of ~ 400 – 700 K. Phase transitions in NBT-based ceramics revealed typical relaxor behavior related to the presence of polar nanoregions in a nonpolar matrix. At temperatures > 700 K effects of dielectric relaxation caused by formation of oxygen vacancies due to deficiency in the A-sites and/or presence of cations with mixed valency in the B-sites of perovskite lattice were observed in some acceptor doped compositions.

Local PFM hysteresis loops observed for KNN- and NBT-based samples indicated to ferroelectric polarization switching at nanoscale. In KNN-based samples high effective d_{33} piezoelectric coefficient values correlated with dielectric permittivity at the room temperature were observed. The results obtained confirmed prospects of new lead-free materials development on the base of the KNN- and NBT-perovskites.

Acknowledgement
The work was supported by the RFBR and DFG (Project 21-53-12005).

References
[1] E.D. Politova, D.A. Strebkov, A.V. Mosunov et al., Inorganic Materials, 2020, vol. 56, pp. 91-96.
[2] E.D. Politova, G.M. Kaleva, A.V. Mosunov et al., Ferroelectrics, 2021, vol. 575, pp. 158–166.
[3] E.D. Politova, G.M. Kaleva, D.A. Bel'kova et al., Inorganic Materials, 2021, vol. 57, No. 9, pp. 942–949.

Compare of dielectric relaxation of gamma irradiated and non-irradiated $TlInS_2$< 5%C >crystals

O.A.Samedov[1], O.Z.Alekperov[2], Kh.B.Orujova[1], N.M.Mehtiyev[1,3], A.I.Nadjafov[1,2]
[1]*Institute of Radiation Problems, Azerbaijan National Academy of Sciences, AZ1143, B.Vahabzade 9, Baku, Azerbaijan*
[2]*Instituteof Physics of Azerbaijan National Academy of Sciences, AZ1143, H.Javid 131, Baku, Azerbaijan*
[3]*Azerbaijan State Oil and Industry University, Azadliq pr. 16/21, Baku, Azerbaijan*

We show observations of anomalies in temperature dependence of permittivity, and tangent in $TlInS_2$ crystals at temperatures higher than 300K (in the form of paraelectric phase). Mechanism of conductivity has been determined for unirradiated and irradiated crystals of $TlInS_2$ (electrons and, at high temperature, ions). Polarization type have been discovered as electronic and ion- relaxation [1-2]. This work aims to determine regularities governing $TlInS_2$ <5% C> impedance spectra at temperature range of 120-500 K in the frequency range 25-10^6 Hz. It is important to note that, over the past few years investigation irradiation effects on the materials are very important [3]. In this situation, it is interesting to study irradiation effects on the layered $TlInS_2$ compounds.

Monocrystalline $TlInS_2$<5%C> investigated at higher than room temperatures using impedance spectroscopy. It has been found out that nature of conductivity is predominantly ionic in the $TlInS_2$<5%C> crystals at temperatures higher than 400K. It was established that Tl^+ ions were responsible for ion conductivity. It is shown that curves of active and reactive impedance decreasing due to the frequency and radiation dose are increased. (Fig.1.)

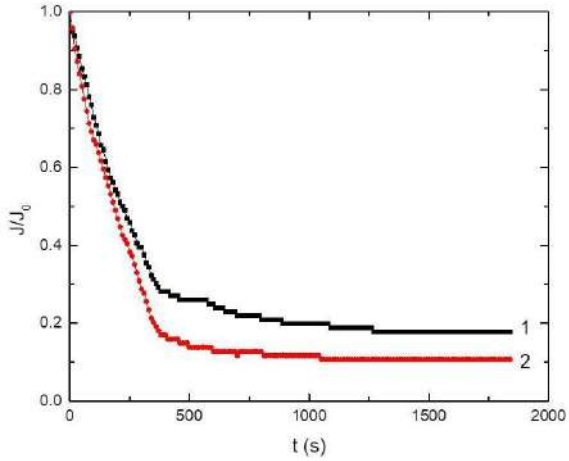

Fig.1. Dependences of reduced electrical conductivity from time $\sigma(t)/\sigma_0(t = 0)$ for $TlInS_2$<5% C> crystals (1- non-irradiation; 2 -20Mrad).

References

[1] S. F. Samadov, O. A. Samedov, O. Z. Alekperov,M. Kulikz, A. I. Najafov, N. M. Mehdiyev and E. M. Huseynov. Dielectric and electrical properties of near-surface layers of TlInS2 crystals under the proton irradiation.International Journal of Modern Physics B Vol. 33, No. 27 (2019) 1950320 (7 pages),
[2] O.A. Samedov, O.Z. Alekperov, A.I. Nadjafov, S.F. Samedov, M.M. Guliyev, X.Z. Fatalizadeh, N.T. Mosumli, N.I. Huseynov.DIELECTRIC AND ELECTRICAL RELAXATION IN TlInS2 CRYSTALS. Journal of Radiation Research, vol.2, №1, 2015, Baku.
[3] RM Sardarly, OA Samedov, AI Nadzhafov, IS Sadykhov "The influence of cation impurities on phase transitions in the TlInS2 compound" Physics of the Solid State 45 (6), 1137-1140, 2003

Influence of the impurities on the wear resistance of synthetic diamond single crystals

G.A. Gusakov*, G.V. Sharonov
A.N. Sevchenko Research Institute of Applied Physical Problems, Belarusian State University, Kurchatov str., 7, Minsk 220045, Belarus, gga68@rambler.ru

Recently, there has been a steady increase in the use of single-crystal diamond tools for ultra-precise processing of products from modern structural composite materials, ceramics, non-ferrous metals and alloys [1,2]. For a long time, predominantly high-quality natural diamonds were used for the manufacture of single-crystal diamond tools. However, the decline in the production of natural diamonds and the development of technologies for the synthesis of large diamond single crystals raised the question of replacing natural crystals with their synthetic analogue [1,3]. Nevertheless, despite the obvious importance of the issue, the data on the effect of impurities on the mechanical characteristics of diamond single crystals are not numerous and the problem of criteria for the selection of synthetic crystals for the manufacture of high-quality diamond tools remains unsolved.

In this work, we investigated synthetic diamond crystals grown by the temperature gradient method in the Ni-Fe-C system using high-pressure apparatus of the "split sphere" type. The impurity composition of diamonds was investigated by the method of light absorption in the infrared and visible spectral ranges. According to IR spectroscopy data, the investigated crystals contained nitrogen impurities mainly in the form of a C-defect (a single atom in a substitutional position). For some crystals, the presence of A defects (a pair of atoms in neighbor lattice sites) was also recorded. The total concentration of nitrogen impurities ranged from 160 to 200 ppm. In the visible range of the spectrum, bands systems at 658 nm and 732 nm associated with a nickel impurity are recorded. The 658 nm system corresponds to a negatively charged nickel ion in the substitution position, and the 732 nm system corresponds to a complex containing nickel and nitrogen atoms and vacancies.

For the study of wear resistance 4 crystals with different contents of nickel impurity were selected. The absorption spectra in the visible range of the selected diamond crystals are shown in Figure 1. Differences in the integral absorption intensity in the bands of nickel-containing defects reached 7 times (samples 1 and 4).

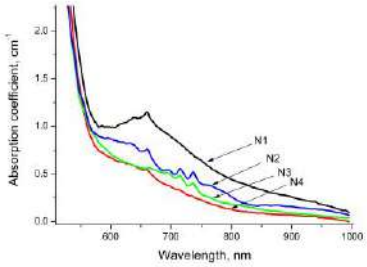

Figure 1. The absorption spectra of the synthetic diamond crystals with different contents of nickel impurity

The study of the wear rate of synthetic diamonds was carried out by flat grinding on a 6A2 type diamond wheel with a grain size of 80/100 nm. The grinding speed was 21 m/s, the load on the processed crystal was 10 N, and the surface area to be ground was about 3 mm^2. The processing was carried out in the (100) plane in the direction deviated by 15 degrees from the <110> axis. The wear rate Q was defined as the weight loss of the crystal per unit time. Experimental values of Q were 3,6; 3,7; 5,6 and $6,4x10^{-4}$ ct/min for samples 1, 2, 3 and 4, respectively. Comparing the obtained results with the impurity composition of the studied samples (Fig. 1), it can be concluded that the wear rate of synthetic diamond crystals is inversely proportional to the content of nickel impurities in them. This conclusion runs counter to the well-established concept that the presence of impurities reduces the wear resistance of a diamond [1-3]. Therefore, the observed effect requires a more detailed study.

References

[1] K. Obata, SEI Technical Review, 82 (2016) P. 82-88
[2] E. Brinksmeier et. al., Precision Engineering, 49 (2017) P. 293-304
[3] J. Wang et. al., Int. J. Adv. Manuf. Technol., 113 (2021) P. 3027–3055

Anisotropy of paramagnetic structures in industrial photoresist films implanted with iron ions (E = 40 keV)

A. Oleshkevich, T. Lapchuk, and N. Lapchuk
Department of Physics of Semiconductors and Nanoelectronics, Faculty of Physics, Belarusian State University, Nezavisimosti Ave., 220030 Minsk, Belarus,
e-mail: lapchuk@bsu.by

In the experiment, we used a FP-9120 positive photoresist based on phenol-formaldehyde resins. As a substrate, we used KDB-10 monocrystalline silicon wafers with the (111) orientation. The thickness of the photoresist film is 1.8 microns. The films were irradiated with iron ions with an energy of 40 keV and doses of $2.5 \times 10^{16} - 1 \times 10^{17}$ cm^{-2}. EPR spectra were recorded on a RadioPan SE / X-2543 spectrometer with an H102 resonator in the X-band. The polarizing magnetic field was modulated with a frequency of 100 kHz and an amplitude of 0.01 mT.

Purpose of the work: to establish the features of the effect on the structural and paramagnetic properties of the photoresist films of the implantation of iron ions with an energy of 40 keV, depending on the radiation dose No EPR signal was observed in the initial samples. Beginning with a dose of 5×10^{16} cm^{-2}, anisotropic EPR signals with g-factor values in the range 1.03 - 1.86 and line widths from 225 to 444 Oe, varying depending on the implantation dose, were recorded in the photoresist films (Fig.1 a, b). The change in ohmic losses in the resonator when the studied samples of the photoresist are introduced into it is controlled indirectly by the change in the amplitude of the reference ruby sample (Al_2O_3:Cr^{3+}) glued to the wall of the resonator. Thus, when rotated 90 degrees in the magnetic field of the photoresist samples implanted with iron ions, the nonresonant losses introduced by them increase by a factor of 2.1, which can be used to create variable resistors in the microwave range.

A sharp change in the values of the g-factor, line width, and resonance field of the reference sample (Fig. 1c) with a change in the orientation of the photoresist films implanted with iron ions in the magnetic field was found. This may indicate the onset of the formation of iron clusters with different degrees of magnetization in the films. It is shown that the EPR method is a sensitive technique for diagnosing the efficiency of changes in the magnetic and conductive properties of low-dimensional layers in modified polymer matrices.

The values of the parameters of the EPR spectra indicate the predominant contribution of the orbital angular momentum of the electron spins, which indicates the internal magnetism of the film structures doped with iron ions, which are not magnetic in the initial state.

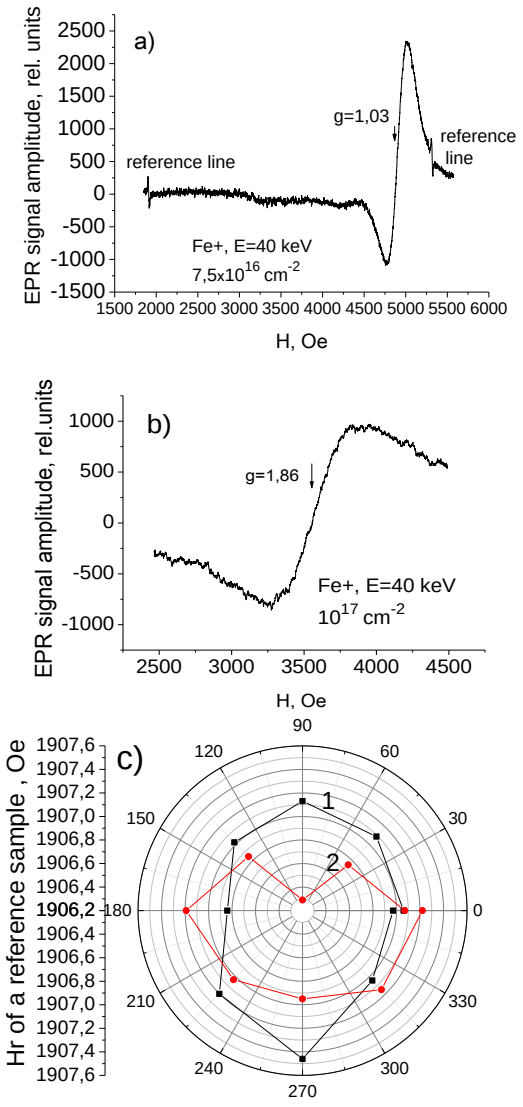

Fig. 1. EPR spectra of photoresist films irradiated with iron ions: a) 7.5x10^{16} cm^{-2}; b) 10^{17} cm^{-2}; c) anisotropy of the resonant field of the EPR line of the reference sample during rotation of the photoresist film in a magnetic field: 1) 7,5x10^{16} cm^{-2}; 2) 10^{17} cm^{-2}

Electrotransport characteristics of $Sr_2FeMoO_{6-\delta}$ ceramics with structurally inhomogeneous grain surfaces

N. Kalanda[1]*, S. Demyanov [1], M. Yarmolich[1], A. Petrov[1] and N. Sobolev[2]
[1]*Scientific-Practical Materials Research Centre of the NAS of Belarus, 220072 Minsk, Belarus, kalanda@physics.by*
[2]*i3N, Departamento de Física, Universidade de Aveiro, 3810-193, Aveiro, Portugal*

One of the most important properties for the use of $Sr_2FeMoO_{6-\delta}$ as sensors and functional elements of nanoelectronics are the properties of electron charge transport in these materials. Therefore, an urgent task is to study the features of the mechanisms of charge transport in such structures.

The measurement of the temperature dependence of resistance and the dependence of resistance on the magnetic field are one of the most common and reliable methods for studying various materials in order to establish the mechanisms of charge transport that determine the conductivity of various systems.

Two series of samples were prepared for the investigations of the electric charge transfer mechanisms: an unannealed series (SFMO – I), annealed at T = 700 K and p(O_2) = 10 Pa for t = 3 h (SFMO – II). The temperature dependence of the SFMO-I resistivity exhibits metallic behavior at temperatures above 36 K and a slight increase in the resistivity at T ≤ 36 K. The SFMO-II sample with magnetic induction B = 0 and T = 300 K has a higher resistivity ρ = 0.692 Ohm· cm than the SFMO-I sample, decreasing with a decrease in temperature to T_{mII} = 133 K, followed by its growth with a further decrease in temperature to 4.2 K (Fig.). It should be pointed out that the minimum ρ_{min} (T) in the SFMO – I, which is not subject to oxidative annealing and does not have island growth of the $SrMoO_4$ dielectric phase on the grain surface, appears at a lower temperature than that in the SFMO – II.

Thus, we have shown that the conductivity at temperatures $T < T_{min}$ decreases with decreasing temperature, which indicates the presence of weak localization. The foregoing indicates that, in a structurally inhomogeneous state, when studying the conduction mechanisms of a magnet, one should take into account the processes of weak localization caused by the quantum interference of conduction electrons.

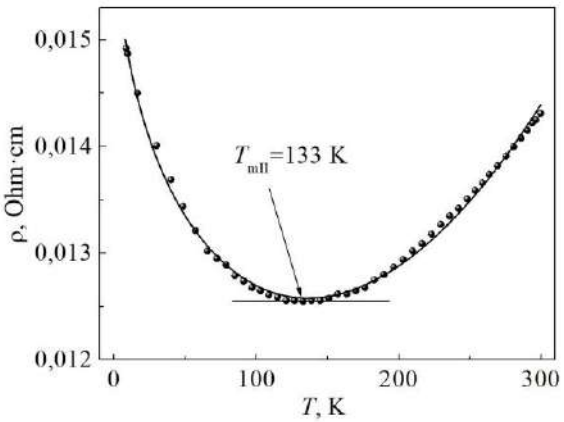

Temperature dependence of the resistivity for the SFMO–II sample

In addition, it should be taken into account that in the disordered magnet $Sr_2FeMoO_{6-\delta}$ in the low-temperature region, the probability of electron-electron interaction increases due to diffusion rather than ballistic motion of electrons with multiple elastic scattering by structural inhomogeneities.

Acknowledgement
The work was supported by the European project H2020–MSCA–RISE –2017 –778308 – SPINMULTIFILM

Magnetic states in $Sr_2FeMoO_{6-\delta}$ nanoscale powder

N. Kalanda[1], S. Demyanov [1], M. Yarmolich[1]*, A. Petrov[1] and N. Sobolev[2]
[1]*Scientific-Practical Materials Research Centre of the NAS of Belarus, 220072 Minsk, Belarus, jarmolich@physics.by*
[2]*i3N, Departamento de Física, Universidade de Aveiro, 3810-193 Aveiro, Portugal*

The nanosized semimetallic ferrimagnetics $Sr_2FeMoO_{6-\delta}$ with an ordered double perovskite structure belong to the most promising materials for spintronics. Particular interest in them is due to the presence of significant magnetoresistance (~ 38%) in relatively weak magnetic fields (1T at T = 50 K), high values of the Curie temperature (400–450 K), and almost 100% degree of spin polarization.

As a result of using the citrate-gel synthesis technique, it was possible to obtain the $Sr_2FeMoO_{6-\delta}$ single-phase compound with the crystal lattice parameters $\boldsymbol{a}$=$\boldsymbol{b}$=5.5629Å, $\boldsymbol{c}$=7.8936 Å, $\boldsymbol{V}$=244.2742 Å^3 and with P=88 % [1].

From the temperature dependences of the magnetization performed in the ZFC/FC modes, it was found that when a magnetic field with a magnetic induction B = 0.01 T is turned on at T = 4.2 K, followed by their heating, a sharp increase in the magnetization of the powder to T_B occurs on the ZFC dependences (fig). In this case, the T_B temperature is a critical point, delimiting areas with different magnetic states. With a further increase in temperature, a smooth decrease of M is observed, and at T_H (irreversibility temperature) the curves of the ZFC and FC dependences converge. The average blocking temperature of superparamagnetic particles is T_B = 20 K, and the irreversibility temperature at which the maximum size ferrimagnetic particles are thawed is T_H = 164 K. This circumstance indicates the magnetic two-phase state of the $Sr_2FeMoO_{6-\delta}$ nanopowder with the presence of a mixture of superparamagnetic and ferrimagnetic particles.

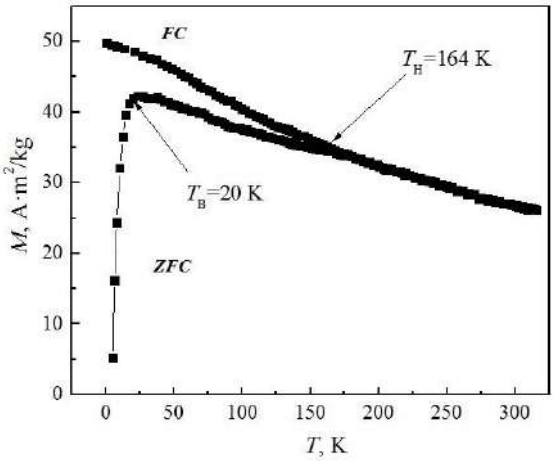

Temperature dependence of the magnetization of $Sr_2FeMoO_{6-\delta}$ nanopowder synthesized under combined conditions in a field of 0.01 T

Based on the results of Mössbauer spectroscopy and magnetic measurements, it was established that the nanosized $Sr_2FeMoO_{6-\delta}$ powder is in a magnetically inhomogeneous state, consisting of superparamagnetic and ferrimagnetic phases. The ferrimagnetic component of magnetization is characterized by higher values of magnetization in comparison with the superparamagnetic component, and a smooth increase is noted for this component, which reaches saturation with decreasing temperature. It is shown that there is no exchange magnetic interaction between superparamagnetic grains in the superparamagnetic phase, which made it possible, being based on the Néel-Brown model, to estimate the critical sizes of nanoparticles in the single-domain state.

Acknowledgement
The work was supported by the European project H2020–MSCA–RISE–2017 –778308 – SPINMULTIFILM, and the BRFFR project No. F12U-003.

References

[1] M.Yarmolich, N. Kalanda, S.Demyanov, H. Terryn, J. Ustarroz, M.Silibin, G.Gorokh, Beilstein J. Nanotechnol. 7 (2016) 1202–1207.

Identification of low concentrations of aromatic nitrocompounds by the SERS method using Ni@Au nanotubes

A. Shumskaya[1]*, T. Zhidko[1], E. Kulesh[2], I. Korolkov[3,4], M. Zdorovets[3,4], Yu. Matveenko[1], N. Galinovsky[1], V. Petushok[1], Zh.Ihnatovich[1], A. Rogachev[1,2]
[1]*Institute of Chemistry of New Materials, 220141 Minsk, st. F. Skaryna 36, Belarus, lunka7@mail.ru**
[2]*F. Skorina Gomel State University, 246019 Gomel, st. Sovetskaya 104, Belarus*
[3]*Gumilyov Eurasian National University, 010000 Nur-Sultan, st. Satpaeva 11, Kazakhstan*
[4]*The Institute of Nuclear Physics, Almaty, Kazakhstan*

A promising method for detecting of low concentrations of substances is surface-enhanced Raman spectroscopy (SERS). The morphology, composition, and surface structure of the substrates are determine the signal amplification. One of the directions in SERS is the use of nanostructures (NSs) "magnetic core-plasmonic metal shell". The combination of a magnetic core and gold covering makes it possible to realize the unique features of SERS and additionally concentrate the analyte by using of magnetic field. The aim of this work is to develop magneto-optical 1D NSs by template synthesis using plasmon metals and to demonstrate the efficiency of their application for signal amplification in SERS.

The synthesis of nickel nanotubes was carried out according to the procedure described in [1]. SEM images show the formation of gold particles on the surface of Ni NTs - needles. Due to the covering, the size of the NTs increased to 480 ± 20 nm. The results of EDA mapping showed that the atomic content of Au and Ni in the structure is 22% and 78%, respectively.

Polynitro compounds are usually yellow crystalline substances. The most important property of nitro compounds is their ability to reduce with the formation of aromatic amines, which are used for the production of a very large group of organic dyes, medicinal compounds, plastics and also explosives. It is important not only to determine the presence of such compounds in low concentrations, but also to accurately differentiate them.

Synthesised Ni@Au was used as magneto-operated SERS substrates to detect low concentrations of aromatic polynitro compounds: 3-nitroaniline, 2-methyl-4-nitroaniline, 2,4,6-trinitro-1,3-benzenediol. The possibility of operating of Ni@Au NTs by magnetic field could help us to concentrate of analite, as well as accumulate it near NTs aglometations. The enhancement of the Raman spectrum was estimated for solutions with a concentration of 10^{-1}-10^{-6} M in acetone. The measurements were carried out on an amplifying substrate consisting of a silicon wafer with deposited Ni@Au NTs. A drop of 10 μL solution was dropped onto a previously prepared substrate and dried in air. Raman spectra were recorded using a Senterra Raman microscope (Bruker) with 532 nm lazer. The analites, when dried, is adsorbed around the NTs, which contributes to its concentration and more accurate detection. Peaks characteristic of aromatic ring are present in the spectra for all concentrations of the analites. The enhanced spectra are characterized by a shift of the peaks. In addition, the spectra contain peaks of O-H and methyl bonds are present for spectra with concentrations of 10^{-1}-10^{-4} M for corresponding analites. Also, the peack shifts were estimatied for isomers. When using Ni@Au core-shell magnetic NTs synthesized by the two-step method as SERS substrates, it is possible to accurately set aromatic polynitro compounds up to a concentration of 10^{-4} M and differentiate them by present of all peaks and their shift (“fingerprints” of the substance). This method could be used to identify potentially dangerous compounds in lower concentrations.

References

[1] Kozlovskiy A. L., D. I. Shlimas, A. E. Shumskaya, E. Y. Kaniukov, M. V. Zdorovets, and K. K. Kadyrzhanov. Influence of electrodeposition parameters on structural and morphological features of Ni nanotubes. *Phys. Met. Metallogr.*, 2017, vol. 118 (2), https://doi.org/ 10.1134/S0031918X17020065.

Study of the influence of substrate roughness on the composition and structure of permalloy films

T.I. Usovich[1,2*], T.I. Zubar[1], A.N. Kotelnikova[1], M.I. Panasyuk[1], V.A. Fed'kin[1], O.D. Kanafiev[1], A.V. Trukhanov[1]
[1]*SSPA "Scientific and Practical Materials Research Centre of NAS of Belarus", 220072 Minsk, P.Brovki str. 19, Belarus, *tanya_usovich@gmail.com*
[2]*Belarusian State Technological University, 220006 Minsk, Sverdlova str. 13A, Belarus*

Permalloy is an alloy consisting of iron and nickel. Permalloy has abnormal deposition. This anomaly manifests itself as a composition gradient in the films. Therefore, we studied the effect of substrate roughness on the composition and structure of permalloy films in this work. For this, copper substrates are prepared in three ways (mechanical polishing, etching using ammonium persulfate and hydrochloric acid). Permalloy films were deposited on the Cu substrates in a stationary electrodeposition mode. The deposition time was 1, 3, 10 and 25 minutes. Short description of samples presented in table 1. The composition of the films and the roughness of the substrates were investigated. According to the results of the study, sample Polish-1 (Ra = 22 nm) contains Fe = 38.8 at. %, sample Etch-1 (Ra = 83 nm) - Fe = 39.5 at. %, sample Initial-1 (Ra = 66 nm) - Fe = 43.4 at.%. However, the iron content becomes equal for all sample (45.6-45.9 at. %) with a deposition time of 25 minutes (Figure 1).

Table 1. Short description of samples

Short name	Substrate preparation	Substrate toughness, nm	Deposition time, min
Polish-1	Mechanical polishing, HCl etching (5 s)	22	1
Polish -3			3
Polish -10			10
Polish -25			25
Initial-1	HCl etching (60 s)	66	1
Initial-3			3
Initial -10			10
Initial -25			25
Etch-1	(NH4)2SO8 ammonium persulfate etching (60 s)	83	1
Etch-3			3
Etch-10			10
Etch-25			25

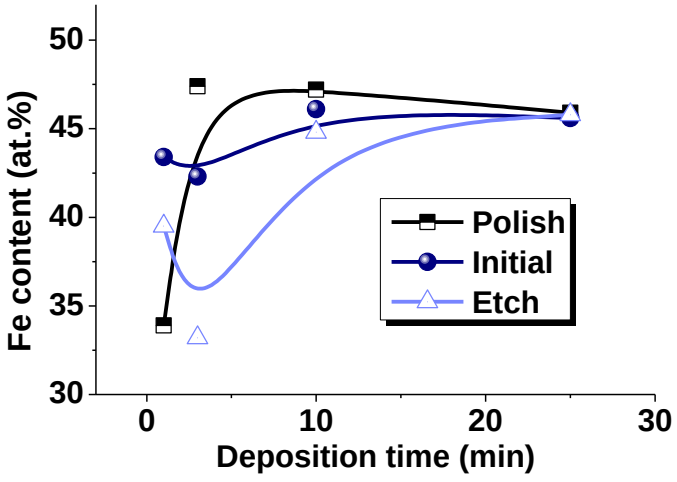

Figure 1. Iron content in permalloy films obtained different deposition time

Plasma-electrolytic method for synthesizing black wear-resistant anticorrosion coatings on AA2024 aluminum alloy

Tran Van Tuan[1]*, Z.V.Khabibullina[1], and A.G. Rakoch[1]
[1] *National University of Science and Technology 'MISiS', Leninskiy prospekt 4, 119049 Moscow, Russia, tuan.tranvan@edu.misis.ru*

Plasma electrolytic oxidation (PEO) is a widely used method for producing wear-resistance and anticorrosion oxide-ceramic coatings on the surface of aluminum alloys [1-3]. In this work, visually black coatings with high functional properties have been successfully obtained on AA2024 alloy by PEO method in an alkaline-silicate aqueous solution with the addition of $CoOOH \cdot H_2O$.

The results of color analysis by CIE (Commission Internationale d'Eclairage) method are presented in Table 1, where the L* value indicates color lightness, while the a* and b* values indicate red-green and yellow-blue components of a color, respectively. L*, a* and b* parameters are low, indicating that the colors of the synthesized PEO coating can be classified as black [3]. Moreover, the thicker coatings (~48, 82 μm) have more blue tone than the thin one (~17 μm). Black color with blue tone of the coatings may be caused by the formation of Co-containing compounds (CoO, Co_3O4, Co_2SiO_4) during PEO treatments.

Table 1. CIE L*a*b* color coordinate values of the PEO coatings

Average coating thickness, μm	L*	a*	b*
17	30.3±0.6	0.16 ± 0.02	-0.30 ± 0.03
48	29.6±0.6	-0.07 ± 0.01	-1.92 ± 0.07
82	28.4±0.5	-0.10 ± 0.02	-1.83 ± 0.06

Additionally, the PEO treatment also significantly improved the wear resistance of AA2024 alloy. According to the results of the pin-on-disk wear test with the applied load of 5 H, the coatings increased the wear resistance of the alloy by more than 6 times.

Figure 1 displays potentiodynamic polarization curves of uncoated and black PEO coated samples in 0.5 wt.% NaCl solution. As shown in Figure 1, the anodic and cathodic current densities of AA2024 alloy after PEO treatment decreased significantly. Moreover, it can be seen that these values are lowest for the sample with the thinnest (~17 μm) black PEO coating. Higher anticorrosion ability of this coating compared to the thicker ones (~48, 82 μm) may be due to the closure of most of its vertical pores with compounds containing Co. As a result, the quantity of through-pores in the thinnest coating is much lower, leading to its higher anticorrosion properties.

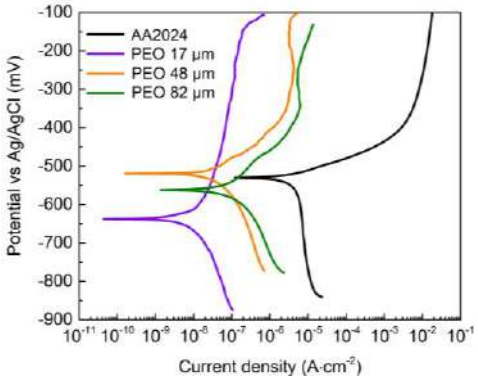

Figure 1. Potentiodynamic polarization curves of uncoated AA2024 and black PEO coated sample in 0.5 wt.% NaCl solution.

References

[1] A. G. Rakoch, A. A. Gladkova, and A.V. Dub, Plasma-Electrolytic Treatment of Aluminum and Titanium Alloys. MISiS Publishing House (2017) 160.
[2] I. V. Suminov, A. V. Jepelfeld, V. B. Ludin, B. L. Krit, A. M. Borisov, Microarc Oxidation: Theory, Technonogy, Equipment. Ecomet (2005) 368.
[3] P. Gupta, F. Fang, S. Rubanov, T. Loho, A. Koo, N. Swift, H. Fiedler, J. Leveneur, P.P. Murmu, A. Markwitz, and J. Kennedy, Surf. Coat. Technol. 358 (2019) 386.

Catalytic active PET-membranes modified with titanium dioxide

O. Alisienok [1], A. Lavitskaya[1], A. Shumskaya[2*], E. Kaniukov[2], T. Zhidko[2], L. Khoroshko[3], A. Kozlovskiy[4,5], M. Zdorovets[4,5], D. Voroshkevich[3]
[1]*Belarusian State Technological University, 220006 Minsk, 13a Sverdlova str, Belarus*
[2]*Institute of Chemistry of New Materials, 220141 Minsk, 36 F. Skaryna str, Belarus, lunka7@mail.ru**
[4] *Belarusian State University, 220030 Minsk, 4 Nezavisimosti Ave, Belarus*
[4]*Gumilyov Eurasian National University, 010000 Nur-Sultan, 11 Satpaeva str, Kazakhstan*
[5]*The Institute of Nuclear Physics, 050032 Almaty, 1 Ibragimova str, Kazakhstan*

Titanium dioxide (TiO_2, titania) based structures are widely used as sorbents and catalizators. TiO_2 phorocatalisators can be activated UV and visible light and decompose a large number of organic compounds to CO_2 and H_2O. For water and air purification titania can be used in the powder form or as the film composites on substrates, which contributes to expansion of such photocatalysts application field.

In this work track membranes (PET TM) modified with titania obtained by sol-gel technology were designed. Systems "PET TM + TiO_2" morphology, structural characteristics and photocatalytic activity was investigated.

PET films with a thickness of 12 microns (Hostaphan®, Mitsubishi Polyester Film, Germany) were irradiated on cyclotron DC-60 with Kr ions with an energy of 1.75 MeV/nucleon and fluence 10^{-7} cm^{-2} and then etched in NaOH solution at 85 °C to obtain pores with diameters about 500±15 nm. Titania hydrosols were prepared by a two-step method: at the first stage, hydrated titanium dioxide was precipitated from titanium tetrachloride solutions; at the second stage, the resulting hydrated titanium dioxide precipitate was peptized using monobasic inorganic acids. For the production of systems "PET TM + TiO_2" TM were immersed in a sol with TiO_2 concentration of 0.5 wt.% for 60 seconds, then washed in distilled water. Three layers of TiO_2 were formed and then PET TM with deposited TiO_2 was annealed at 120 ° C for 15 min on air. The photocatalytic activity of the systems was studied by the degree of decomposition of the model pollutant Rhodamine B in an aqueous solution (2.5 mg/L) under the UV irradiation (365 nm) within 4 hours. The change in the concentration of the analite in the solution was determined from the optical absorption spectra in the wavelength range of 400–800 nm.

According SEM-images, a uniform coating is formed on the polymer membrane surface, consisting of TiO_2 nanoparticles with sizes up to 50 nm. TiO_2 anatase with tetragonal crystal structure with the space group I41/amd(141) in the systems "PET TM + TiO_2" was found by the X-ray diffraction analysis in amount of 23 %.

Relative decrease in concentration of the Rhodamine B in solution (C/C_0), estimated from the ratio of the peak absorption intensity in the irradiated solution to the peak absorption intensity in the initial solution (at 553 nm), was 31 %.

The fundamental possibility of forming a photocatalytic pattern of active coatings on TM by the sol-gel method was indicated. The systems are promising for the creation of a active functional material and can be used, for example, for packaging of food products or sterile medical plasters with an antibacterial and self-cleaning surface. The photocatalytic process provides a unique opportunity to oxidize organic compounds and allows to count on broad prospects for using photocatalysis in practice. The important advantage of the designed systems "PET TM + TiO_2" is that the catalyst can be reused.

Monophasic phosphor powders obtained by sol-gel method

L. Khoroshko[1,2]*, A. Baglov[1,2]
[1]*Belarusian State University of Informatics and Radioelectronics, 6 P. Browka str., Minsk 220013, Republic of Belarus, L_Khoroshko@bsuir.by**
[2]*Belarusian State University, 4 Nezalezhnasci ave., Minsk 220030, Republic of Belarus*

Sol-gel technology is interesting for synthesis of the wide range of compounds due to the possibility fine control of doping pure phosphors of a given phase composition to obtaining predictable luminescent properties. Materials with a garnet and perovskite structure doped with lanthanides are of interest in laser technology, photonics, and optoelectronics and can be manufactured by the sol-gel method. This work presents some results on the synthesis and structure study of monophasic powders doped with lanthanides obtained by the sol-gel method.

Powders of garnets $Y_3Al_5O_{12}$ and perovskite $BaTiO_3$ with lanthanides were obtained by multistage heat treatment of sols. For the preparation of sols, Pechini-type methods and citrate synthesis are chosen. In the first case, polyhydric alcohols were introduced into the composition of the sol to form the polymer framework of the sol; in the second case, the framework of the sol is formed directly with the participation of the cations of the final compound. Pechini methods make it possible to obtain a guaranteed monophasic composition of the finished powder with a minimum grain size (up to 5–10 nm), while in citrate synthesis reduced carbon residues in the final product.

According to X-ray diffraction analysis results, xerogels crystallize in the $Y_3Al_5O_{12}$ phase with $Ia\bar{3}d$ space group from garnet sols, and in the $BaTiO_3$ phase with P4mm space group from perovskite sols. Incorporating of different dopants (Er and Yb) in sols not affect to crystalline structure of garnet powders. The size of the coherent scattering region calculated by the Debye-Scherrer method is about 50 nm for garnets and 40 nm for perovskites. Studies of the reasons for the broadening of peaks in the diffractograms of phosphor powders show that the main reason is the tendency to form different sizes crystallites for yttrium-aluminum garnets, while for perovskite powders the crystal lattice parameters distortion is high, presumably, due to the displacement of oxygen atoms during the transition from the cubic to the tetragonal phase as a result of a stepwise increase in the annealing temperature.

Dispersion of prepared monophasic powders in film-forming sols or polymer matrix will make it possible to obtain combined coatings with specified luminescent properties, and the choice of the sol composition will allow to control the temperature of coating synthesis. A coating from a suspension can be used as a filler in substrates with a complex predetermined relief formed by the use of photolithography. Erbium-doped composite coatings can be interesting for creating additional up-conversion layers in silicon solar elements and increasing their efficiency by converting part of the infrared radiation into visible range. Other lanthanides with ultraviolet-activated irradiation, such Eu and Tb, may be used as additional luminescent coatings for imparting new optical properties or to the creation of luminescence techniques on finishing products of electronics and photonics.

The authors are grateful to Dr. S. Zlotsky (Belarusian State University) for the X-ray diffraction analysis of the phosphor powders.

Magnetic phase transitions in multiferroic perovskite solid solutions based on $BiFeO_3$

E. Čižmár[1,*], S. Vorobiov[1], J.P.V. Cardoso[2], V.V. Shvartsman[3], D.D. Khalyavin[4], E.L. Fertman[5], A.V. Fedorchenko[5], A.V. Pushkarev[6], Y.V. Radyush[6], N.M. Olekhnovich[6], R. Tarasenko[1], A. Feher[1], J.M. Vieira[2], A.N. Salak[2]

[1]*Institute of Physics, Faculty of Science, P.J. Šafárik University, Park Angelinum 9, Košice 041 54, Slovakia, erik.cizmar@upjs.sk**
[2]*Department of Materials and Ceramics Engineering/CICECO-Aveiro Institute of Materials, University of Aveiro, Aveiro 3810-193, Portugal*
[3]*Institute for Materials Science and CENIDE-Center for Nanointegration Duisburg-Essen, University of Duisburg-Essen, Essen 45141, Germany*
[4]*ISIS Facility, Rutherford Appleton Laboratory, Chilton, Didcot, Oxfordshire OX11 0QX, UK*
[5]*B. Verkin Institute for Low Temperature Physics and Engineering of the National Academy of Sciences of Ukraine, Nauky 47, Kharkiv 61103, Ukraine*
[6]*Scientific-Practical Materials Research Centre of the National Academy of Sciences of Belarus, P. Brovka 19, Minsk 220072, Belarus*

Lead-free materials with piezo properties comparable to those observed in lead zirconate-titanate at the morphotropic phase boundary are of current application interest. Most of the reported single-phase perovskite $BiFe_{1-y}B^{3+}{}_yO_3$ compositions with $y>0.1$ can be prepared only using the high-pressure synthesis technique. These high-pressure stabilized perovskites demonstrate a series of structural transitions with increasing y. In addition, the annealing of the as-prepared metastable perovskites may result in irreversible transformations into new perovskite phases with unique combinations of ferroic orders [1]. Particularly, in the $0.1 \leq y < 0.3$ range of the $BiFe_{1-y}Sc_yO_3$ solid solution system, the anomalies associated with possible transitions between three different antiferromagnetic (AFM) structures (collinear, canted, and cycloidal spin arrangements) were observed below Néel temperature (T_N) [2]. Therefore, the Fe-rich compositional range of the $BiFe_{1-y}[Zn_{0.5}Ti_{0.5}]_yO_3$ system is also of particular interest.

This work reports on structural and magnetic studies of $BiFe_{1-y}[Zn_{0.5}Ti_{0.5}]_yO_3$ in the compositional range with y=0.05-0.25. The $T_N(y)$ evolution obtained from magnetic measurements was compared with that reported for compositions of the $BiFe_{1-y}B^{3+}{}_yO_3$ family with B^{3+}= Co, Mn, Cr, and Sc. It showed the same general trend, independent of both the type (magnetic or non-magnetic) and the size of substituting ion. The study of the temperature-dependent magnetic moment revealed similarities to $BiFe_{1-y}Sc_yO_3$, but possible transformation between different AFM structures was observed only for $y \geq 0.2$. In addition, the short- and long-range structural distortions due to substitution or mechanical strain in $BiFeO_3$ may induce uncompensated induced ferromagnetic moment because of the suppression of cycloidal order or appearance of spin-canting. The evidence of the spin-canting is pronounced in all $BiFe_{1-y}[Zn_{0.5}Ti_{0.5}]_yO_3$ samples by a jump in magnetization close to a zero magnetic field, and the magnetization loops have a much higher coercive field in comparison to those observed in $BiFe_{1-y}Sc_yO_3$, up to 4.63 kOe found in the annealed $BiFe_{0.85}[Zn_{0.5}Ti_{0.5}]_{0.15}O_3$ at 300 K. We also discuss the possible role of the high-pressure synthesis in the onset of ferromagnetic contribution in magnetization below T_N.

The authors acknowledge the financial support of the bilateral Slovakia-Belarus project APVV-SK-BY-RD-19-0008 / T20SLKG-001.

[1] D.D. Khalyavin, et al., ChemComm. 55 (2019) 4683-4686.
[2] E.L. Fertman, et al., Crystals 10 (2020) 00950.

Crystal and magnetic structure of half-Heusler compounds $MnNi_{0.9}M_{0.1}Sb$ (M = Ti, V, Cr, Fe, Co)

A.V. Rutkauskas[1]*, G.S. Rimsky [2], I.Yu. Zel[1], N.M. Belozeroval[1], D. P. Kozlenko and S.E. Kichanov[1]

[1] *Joint Institute for Nuclear Research, 141980, 6, Joliot-Curie St., Dubna, Moscow Region, Russia, ranton@nf.jine.ru**

[2] *SSPA «Scientific-Practical Materials Research Centre of NAS of Belarus», 220072, Belarus, 19, P. Brovki st., Minsk, Belarus*

Half-Heisler magnetic intermetallic compounds of transition metals exhibit interesting physical properties such as magnetoresistance, ferromagnetic and antiferromagnetic magnetic states, and superconductivity. It is observed the shape memory effect and superelasticity with opportunity to control there phenomena by means magnetic field. It makes these compounds promising materials to apply for creation permanent magnets, elements of electronic devices and cooling technology.

To understand the formation of magnetic states in doped half-Heusler compounds based on MnNiSb it is necessary to correctly separate the contribution to the magnetic properties from the sublattices of nickel and manganese ions and to identify the relationship between the structural and magnetic properties of these materials.

In our work we present the results of investigation the crystal and magnetic structure of half-Heusler intemetallic compounds $MnNi_{0.9}M_{0.1}Sb$ (M = Ti, V, Cr, Fe, Co) by means of neutron diffraction under normal conditions. Partial substitution of another transition element for nickel leads to a decrease in the magnetic moment of the Mn ions. Also MnNiSb, $MnNi_{0.9}Cr_{0.1}Sb$ and $MnNi_{0.9}Fe_{0.1}Sb$ compounds have been studied in the temperature range from 13 to 300 K. It has been found that the initial cubic structure $F\bar{4}3m$ and ferromagnetic phase remain in the investigated temperature range. New reflections corresponds to the antiferromagnetic phase have not been found.

This work have been supported by the Russian Foundation for Basic Research, project no. 20-52-04003 Bel_mol_a (Belarusian Foundation for Basic Research, project no. T21RM-029).

Preparation of solid solutions of titanates $Sr_{1-x}Ln_xTiO_3$

A. Nikitsin[*1], M. Bushinsky[1], R. Lanovsky[1], S. Pastushonok[2] and Yu. Orlov[3]
[1] *Scientific-Practical Materials Research Centre NAS of Belarus, 220072 P. Brovki str. 19, Minsk, Belarus, shyrik_n@physics.by*[*]
[2]*Military Academy of the Republic of Belarus, Minsk, Independence av. 220*
[3]*Kirensky Institute of Physics, Krasnoyarsk Scientific Center, Siberian Branch, Russian Academy of Sciences, Russia, Krasnoyarsk*

Recently the problems of environment energy pollution and waste-heat utilization have become increasingly acute. Thermoelectric energy converters can transform the low-potential heat energy into useful electricity, thus providing a solution for waste-heat utilization [1]. The implementation of an advanced thermoelectric converter requires n- and p-type-conductivity materials.

Promising n-type-conductivity thermoelectric materials are strontium titanate-based compounds [2]. The parent composition $SrTiO_3$ is a virtual ferroelectric, which is a typical ABO_3 cubic perovskite (sp.gr: Pm3m) with a lattice parameter of a = 3.904 Å [3]. The properties of the $SrTiO_3$ compound depend, to a great extent, on doping with different elements and on synthesis techniques, which cause various microstructure modulations. To improve the thermoelectric properties of strontium titanate, stoichiometric substitution in the A and B sites and the creation of a certain degree of nonstoichiometry in these sites were used.

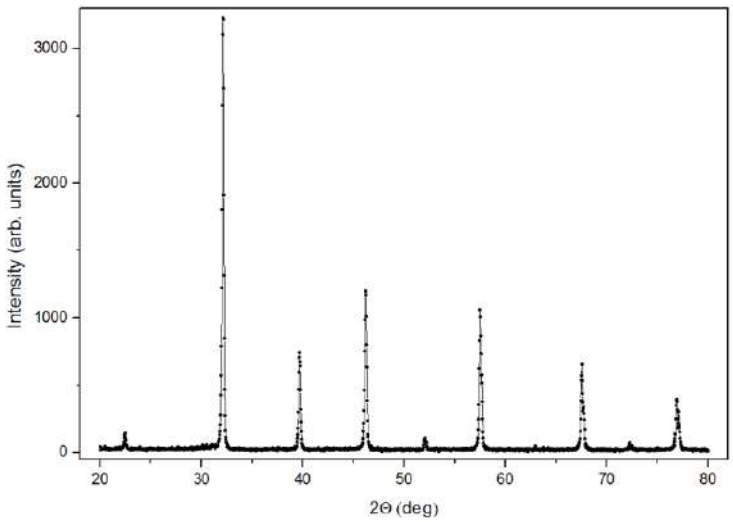

Fig 1 X-ray diffraction spectrum of the composition $Sr_{0.9}La_{0.1}TiO_3$ at room temperature.

Polycrystalline samples with compositions $Sr_{1-x}Ln_xTiO_3$ (Ln: La, Eu; x: 0.05, 0.1) have been prepared from oxides La_2O_3, previously dried at 1000 °C in air, Eu_2O_3 and TiO_2 as well as carbonate $SrCO_3$ of purity of not less than 99.9%, mixed in stoichiometric ratio using a planetary ball mill RETSCH PM-100. Preliminary annealing has been performed at 1000 °C. The $Sr_{1-x}Ln_xTiO_3$ samples were synthesized at T = 1300 °C for 10 h in air. All the samples have been cooled at a rate 100 °C = h. X-ray diffraction analysis was performed using diffractometer DRON-3 M (Fig.1).

X-ray diffraction structural studies performed at room temperature have shown that all the compositions $Sr_{1-x}Ln_xTiO_3$ (Ln: La, Eu; x: 0.05, 0.1) can be refined in perovskite structure with cubic symmetry (sp. gr: Pm3m).

References

[1] Y.H. Lin, J. Lan, C. Nan, Oxide Thermoelectric Materials, Wiley-VCH, (2019).
[2] A.V. Kovalevsky, A.A. Yaremchenko, S. Populoh, P. Thiel, D.P. Fagg, A. Weidenkaff, J. R. Frade, Towards a high thermoelectric performance in rare-earth substituted SrTiO3: effects provided by stronglyreducing sintering conditions, Phys. Chem. 16, 26946-26954 (2014).
[3] K. Koumoto, Y. Wang, R. Zhang, A. Kosuga, R. Funahashi, Oxide thermoelectric materials: a nanostructuring approach, Annual review of materials research. 40, 363-394 (2010).

The Rietveld method and XRD POWDIX 600 - a powerful package for X-ray diffraction analysis for industry and research

S.N. Magonov
CJSC «LINEV ADANI», Department of Scientific Instruments, Selitsky Str., Minsk 220075, Belarus

Profile refinement by the Rietveld method is one of the most used analytical methods in conducting quantitative phase analysis of a wide range of materials, be it crystalline multiphase systems or samples containing an amorphous fraction. As a result of this proliferation, many academic and private laboratories are conducting quantitative phase analysis using the Rietveld method as a service to third parties.

The POWDIX 600 diffractometer was used to measure the intensity and diffraction angles of X-ray radiation in order to obtain qualitative and quantitative characteristics of polycrystalline substances in the form of powders (cement and geological samples) with analytical processing in the ALMAZ software using the Rietveld method [1].

The device implements a vertical θ-θ optical Bragg-Brentano scheme.

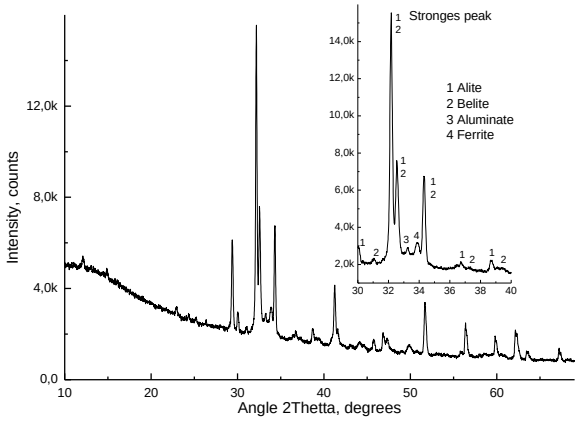

Figure 1 – Observed X-ray diffractrion pattern of portland cement.

A cement sample (portland cement) provided by RUE “Belorusskiy Cementny Zavod” was taken as an initial sample to enable analysis on a POWDIX 600 X-ray diffractometer [2]. The resulting diffraction pattern is shown in Figure 1.

After carrying out a quantitative analysis using the ALMAZ program by the Rietveld profile refinement method results of the cement sample was (Table 1):

Table 1. – Quantative X-ray diffraction analysis of portland cement

Phase Name/Formula	**ICDD Ref**	**Portland cement, weight %**
Tricalcium Silicate (Alite, C3S); Ca_3SiO_5	42-0551	69
Dicalcium Silicate (Belite, C2S); Ca_2SiO_4	33-0302	15
Tricalcium Aluminate (C3A); $Ca_3Al_2O_6$	38-1429	2
Brownmillerite (C4AF); $Ca_2(Al, Fe)_2O_5$	30-0226	14

The profile calculation in the software used data cards from the commercial PDF-2 database.

The value of the quality of fit was:

$$\chi^2 = 4{,}27\ \%;\ R_{wp} = 13{,}31\%$$

The results obtained on the use of an X-ray diffractometer POWDIX 600 with analytical processing in the ALMAZ software using profile refinement by the Rietveld method [3] indicate the possibility of fast and high-quality control of the quality of products in industry, in particular in cement industry. The capabilities of the instrument with software are also suitable for use in research laboratories.

References

[1] D. S. Young, B. S. Sachais and L. C. Jefferies, "The Rietveld method", Citeseer, 1993.
[2] XRD PowDiX diffractometer (2021). Available at: https://lab.adanisystems.com/products/product-line/xrd-powdix-diffractometer-/ (accessed 21 september 2021).
[3] N. Lundgaard , E.S. Jons, "Quantitative Rietveld XRD Analysis", World Cem, 2003, 34:59-63.

Physical properties of polycrystalline cobaltites $Ln_{1-x}Sr_xCoO_{3-y}$ (Ln is a rare earth ion)

O. Mantytskaya[1*], V. Dudnikov[2], Yu. Orlov[2], M. Bushinsky[1], N. Tereshko[1], R. Lanovsky[1], A. Nikitsin[1] and A. Chobot[1]
[1]*Scientific-Practical Materials Research Centre NAS of Belarus, 220072 P. Brovki str. 19, Minsk, Belarus, mantytskaja@physics.by**
[2]*Kirensky Institute of Physics, SB RAS, 660036 Akademgorodok 50/38, Krasnoyarsk, Russia*

The structural, magnetic, electrical transport and dilatation properties of the polycrystalline cobaltite samples $Ln_{1-x}Sr_xCoO_{3-y}$ (Ln is a rare earth ion) have been investigated.

It was found that single-phase samples of polycrystalline cobalt oxides with the same oxygen nonstoichiometric index $Ln_{0.2}Sr_{0.8}CoO_{2.63}$ (Ln = Sm, Gd, Dy) are characterized by a tetragonal unit cell (the space group I4/mmm). The structure of the studied perovskites is similar to the structure of double strontium cobaltates with rare earth ions [1]. In the temperature range above room temperature all the studied compositions are characterized by the presence of a sharp maximum which slightly shifts to the region of lower temperatures with a decrease in the ionic radius of the rare-earth ion (Fig.1). In the intermediate temperature range a maximum is also observed, which is strongly smeared in temperature and shifts to higher temperatures with a decrease in the ionic radius of the rare earth ion (Fig.1). The maximum near 350 K in the temperature dependences of the magnetic susceptibility correlates with anomalies in the temperature dependences of the coefficient of thermal expansion, heat capacity, and electrical resistivity (Fig.2,3), indicating a strong relationship between the structural, magnetic, and electronic degrees of freedom in these materials.

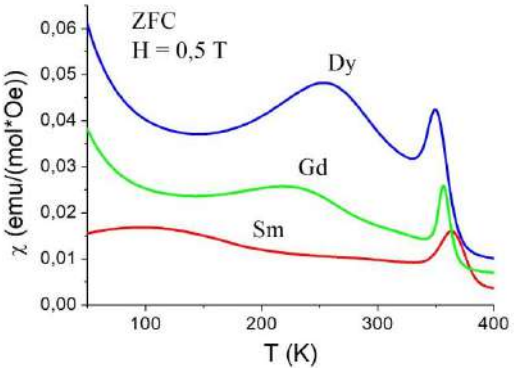

Figure 1 - Temperature dependences of the molar magnetic susceptibility of the $Ln_{0.2}Sr_{0.8}CoO_{2.63}$ samples

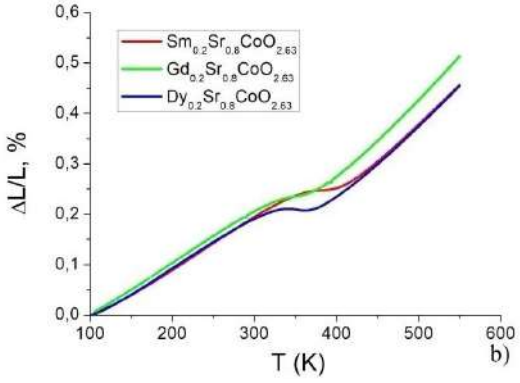

Figure 2 - Temperature dependences of the coefficient of deformation ΔL/L

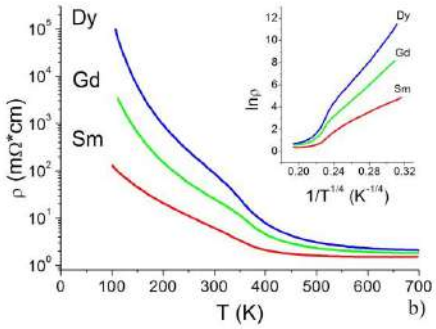

Figure 3 - Temperature dependences of the electrical resistivity of $Ln_{0.2}Sr_{0.8}CoO_{2.63}$ samples

Acknowledgement. The authors would like to acknowledge the financial support from the State Scientific Research Programme "Condensed matter physics and creation of new functional materials and technologies for their production", project 1.2.2.

References

[1] M. James [et al.] J. Solid State Chem.177 (2004) 1886-1895.

Preparation and properties of piezoceramics on the basis of lead zirconate-titanate

A. Letko[1], V. Kasko[1]
[1] *Scientific-Practical Materials Research Centre of National Academy of Sciences of Belarus, Belarus, Minsk, Brovki 17, e-mail letko@physics.by*

Despite the existing significant achievements in the field of research of piezoceramic materials, progress in improving the physical properties of these materials has decreased in recent years.The capacities for an improvement of physical properties of piezoelectric ceramic materials by means of the change of the chemical composition are practically exhausted. Nowadays, the problem of the search for new methods of enhancement of the structural and morphological perfection of existing materials comes to the fore.

Piezoelectric ceramic material is obtained by a two-stage technology: synthesis of lead zirconate-titanate powders with additions of cadmium oxide, bismuth and manganese and sintering. The solid solutions of the $Pb_{0,98}(Zr_{0,53}Ti_{0,47})O_3$ - $Cd_{0,02}(Bi_{2/3}Mn_{1/3})O_3$ system obtained during the synthesis were ground for 10-60 minutes in a "Sand" ball mill. Sintering of tablets obtained from mechanically activated powders was carried out at T = 1200-1240^{0}C for 2 hours.

The crystal structure and electrophysical properties of ceramics obtained from mechanically activated powders of lead zirconate-titanate have been investigated.

We revealed the following peculiarities of the PZT–based ceramics behavior. All the obtained ceramic samples of the $Pb_{0,98}(Zr_{0,53}Ti_{0,47})O_3$ - $Cd_{0,02}(Bi_{2/3}Mn_{1/3})O_3$ composition were single phase, containing only the tetragonal one. After sintering, the granular structure of the ceramics was inhomogeneous, the average grain size reached 3 μm, while the density of the samples varied from 98% to 99% of the theoretical density. With an increase in the mechanical activation time, the coarsening of grains occurs, the sizes of which vary from 4 to 6 μm. An increase in the time of mechanical activation leads to an increase in the dielectric constant of the ceramics and a decrease in dielectric losses (Figure 1).

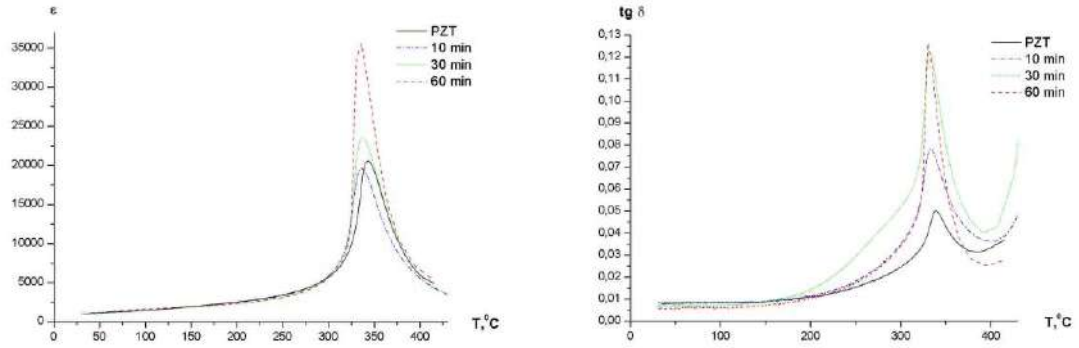

Figure 1 Temperature dependence of the dielectric constant ε and the dielectric loss tangent tgδ of the samples for different activation times at the frequency of 1 kHz

It was found that mechanical activation of the synthesized powders $Pb_{0,98}(Zr_{0,53}Ti_{0,47})O_3$ - $Cd_{0,02}(Bi_{2/3}Mn_{1/3})O_3$ improves the electrophysical characteristics of ceramics.

Compositional ordering and magnetic phase transitions in multiferroic (1-*x*)$BiFeO_3$–*x*$AFe_{1/2}B_{1/2}O_3$-(*A*-Pb, Sr; *B*-Nb,Sb) solid solutions

I.P. Raevski[1], S.P. Kubrin[1], A.V. Pushkarev[2], N.M. Olekhnovich[2,*], Yu.V. Radyush[2], V.V. Titov[1], S.I. Raevskaya[1], M.A. Evstigneeva[1], I.G. Sheptun[1] and M.A. Malitskaya[1]
[1]*Physics Research Institute and Faculty of Physics, Southern Federal University, Stachki Ave.,194, Rostov-on-Don, Russia, igorraevsky@gmail.com*
[2]*Scientific-Practical Materials Research Centre of NAS of Belarus, P. Brovki St., 19, Minsk, 220072, Belarus, olekhnov@physics.by**

Compositional dependences of magnetic phase transition temperature T_M for $BiFeO_3$(BFO) -based perovskite solid solutions with the highly-ordered complex perovskites $PbFe_{1/2}Sb_{1/2}O_3$ (PFS) and $SrFe_{1/2}Sb_{1/2}O_3$ (SFS) and their disordered counterparts $PbFe_{1/2}Nb_{1/2}O_3$ (PFN) and $SrFe_{1/2}Nb_{1/2}O_3$ (SFN) were studied using Mössbauer spectroscopy. Ceramic samples of BFO-PFS and BFO-SFS were obtained using high-pressure synthesis at 4-6 GPa and those of BFO-PFN and BFO-SFN by usual synthesis at atmospheric pressure. Neither XRD nor Mössbauer studies detected the presence of the long-range ordering in the compositions studied except BFO-PFS and BFO-SFS compositions with x=0.9 and 1. Figure 1 shows the measured $T_M(x)$ dependences for BFO-xPFS and BFO-xSFS solid solution systems. For BFO-PFN system the results of Mössbauer studies nicely match the data of the magnetization measurements [1] shown by the dotted red line. For this system experimental T_M values are somewhat lower than those calculated for the case of the disordered distribution of Fe^{3+} and non-magnetic B^{5+} ions in the lattice [1]. This difference is usually ascribed to the short-range ordering not detectable by the XRD. In contrast to this $T_M(x)$ dependence for BFO-PFS compositions nicely follows the theoretical one calculated for the case of the full ordering of Fe^{3+} and non-magnetic B^{5+} ions [1].

$T_M(x)$ dependences for both BFO-SFS and BFO-SFN systems show an abrupt drop in the x=0.6-0.8 compositional range, i.e. in the vicinity of the percolation threshold for Bi ions in the *A* - sublattice. The results obtained seem to be an experimental evidence of the magnetic superexchange between Fe^{3+} ions in $BiFeO_3$ via the empty 6p states of Bi ions theoretically predicted by De Sousa et al. [2]. In accord with these results no abrupt changes in T_M are observed in the BFO-PFN system (Fig.1), as similar superexchange between Fe^{3+} ions via the empty 6p states of Pb ions was discovered earlier in PFN-based solid solutions [3].

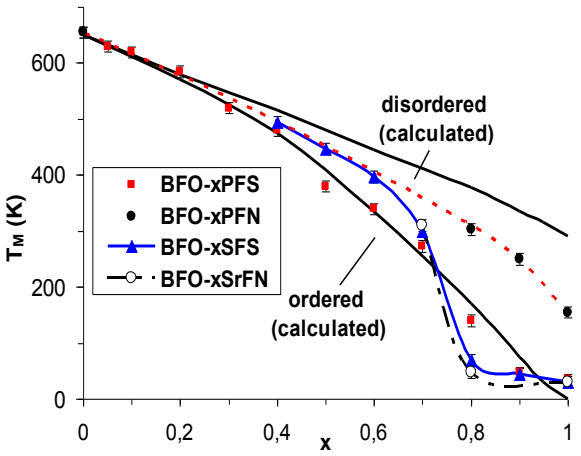

Figure 1. T_M vs x dependence for (1-x)$BiFeO_3$-$xAFe_{1/2}B_{1/2}O_3$ (*A*-Pb, Sr; *B*-Nb,Sb) solid solutions

Acknowledgement: This study was funded by the Russian Foundation for Basic Research (Grants 20-52-00045, 20-52-00045 Bel_a) and Belarusian Republican Foundation for Fundamental Researches (Grant T20R-169).

References

[1] G. A. Smolenskii and V. M. Yudin, Sov. Phys.-Solid St. 6 (1965) 2936-2942.
[2] R. De Sousa, M. Allen, and M. Cazayous, Phys. Rev. Lett. 110 (2013), 267202.
[3] I.P. Raevski, S.P. Kubrin, S.I. Raevskaya, et al., Phys. Rev. B 80 (2009) 024108.

Oxyselenides RE_2O_2Se (RE=Y, La, Gd): synthesis, optical properties and applications

V. Malyutina-Bronskaya[1]*, V. Zalesski[1], and M. Tarasenko[2]
[1]*SSPA of Optics, Optoelectronics and Laser Technology, Belarus, Nezavisimosti Ave. 68, Minsk, 220072, Belarus, malyutina@oelt.basnet.by **
[2] *Nikolaev Institute of Inorganic Chemistry. SB RAS, prosp. Akad. Lavrentieva, 3, Novosibirsk 630090, Russia*

The Rare Earth (RE) oxyselenides: RE_2O_2Se , where RE = Y, La, Gd, doped with green light emitted RE-ions are the promising candidates for their use as scintillators, since they exhibit luminescence characteristic of doped ions upon excitation by ionizing radiation. In order to efficiently use these new scintillating materials, it is necessary to optimize the activator ion concentration for each host—activator pair because, in different hosts, ions can be distributed in different manners over the bulk of the material.

In this work we have prepared doped rare earth oxyselenides and have studied the their optical properties. At the first stage to prepare the doped oxides of RE, the aqua solutions of nitrite salts with the required concentration of Tb were precipitated by oxalic acid and then were calcined in a furnace in air. Further transformation of doped oxides to oxyselenides was performed according to the technique described in [1].

It is known that optical properties, in particular luminescence, strongly depend on the size of the particles under investigation. Therefore, in nanoparticles the number of surface atoms is comparable to those in the bulk of the volume and surface phenomena significantly affect the radiation. In the powders of these materials, the average particle size was estimated to be 10 to 100 μm. Thus, optical properties of doped rare earth oxyselenides were investigated for micron-sized particles.

The figure shows photoluminescence spectra of the Y_2O_2Se:xTb, x=1,3,4,5,10 mol%, samples. The main peaks of the photoluminescence spectrum of the Tb^{3+} ion in the Y_2O_2Se matrix correspond to the characteristic transitions: $^3D_4 \rightarrow {}^7F_6$, (491 nm), $^3D_4 \rightarrow {}^7F_5$ (545 nm), $^3D_4 \rightarrow {}^7F_4$ (588 nm), $^3D_4 \rightarrow {}^7F_3$ (622 nm), $^3D_4 \rightarrow {}^7F_2$ (654 nm), $^3D_4 \rightarrow {}^7F_1$ (672 nm), $^3D_4 \rightarrow {}^7F_0$ (682 nm). For phosphores containing Tb^{3+} ions, the optimal concentration of the activator ion is 3 mol %, above which concentration quenching of photoluminescence occurs. Photoluminescence spectrum in the Y_2O_2Se matrix, as well as Tb doped solid solutions, demonstrates the emission peaks 956 nm and 984 nm. These peaks may be attributed to phonon emission from excitation Y-Se pairs in the matrix.

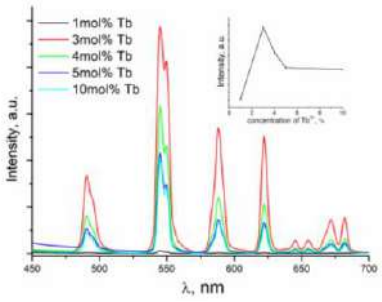

Photoluminescence spectra (λ_{ex}= 375 nm): Y_2O_2Se:Tb at 300K. (Inset) The dependence of the emission intensity on the Tb^{3+} concentration at 545 nm ($^3D_4 \rightarrow {}^7F_5$ transition)

The quenching contentration and photoluminescence properties of other doped RE_2O_2Se , where RE = Y, La, Gd were also investigated. The photoluminescence spectrum of oxyselenides is in good agreement with the sensitivity spectra of silicon photomultipliers and avalanche photodiodes, which makes these materials suitable for use as scintillators in detectors of ionizing radiation.

Acknowledgement
This work was supported by the RFBR(Grant No. 20-53-00036 Bel_a) and BRFBR (Grant No. Ф20Р-256)

References

[1] M.S.Tarasenko, et al., Materials Today Communications, 21 (2019) p. 10.

Magnetocaloric effect in polycrystalline Mn_5Si_3

A. Mashirov[1], I. Musabirov[2], T. Tkachenka[3], A. Kuznetsov[1], V. Shavrov[1], and V. Mitsiuk[4]*
[1]*Kotelnikov Institute of Radioengineering and Electronics, Russian Academy of Sciences, 125009, Russia, Moscow, 11-7 Mokhovaya st.*
[2]*Institute for Metals Superplasticity Problems, Russian Academy of Sciences, 450001, Russia, Ufa, 39, Stepana Khalturina st.*
[3]*BSATU, 220023, Belarus, Minsk, 99 Nezavisimosti Avenue*
[4]*Scientific-Practical Materials Research Centre of NAS of Belarus, 220072, Belarus, Minsk, 19 P. Brovki st., mitsiuk@physics.by*

The interest of researchers in magnetics with phase transitions and with a magnetocaloric effect in the cryogenic temperature range is associated with the possibility of their application in cryocoolers [1]. The single-crystal Mn_5Si_3 sample demonstrates a strong inverse magnetocaloric effect upon the metamagnetic transition at T_{N1}= 65 K [2]. We have investigated the magnetic and magnetocaloric properties of a polycrystalline Mn_5Si_3 sample, which is easier to manufacture. A polycrystalline sample of the nominal composition Mn_5Si_3 was prepared by argon-arc melting with three remelts. The sample sealed in a vacuum quartz ampoule was annealed for 50 hours at a temperature of 1273 K, after which it was quenched in water at room temperature. Measurements of the isofield magnetization of the sample showed that a metamagnetic transition with temperature hysteresis is observed in the temperature range from 5 K to 70 K. With an increase in the magnetic field from 1 T to 10 T, the characteristic temperatures of this metamagnetic transition shift to low temperatures with a coefficient of 4.9 K/T (Fig. 1 left). A sample of the Mn_5Si_3 alloy at a temperature of 50 K demonstrates a sharp change in magnetization of about 20 emu/g in the range of the applied magnetic field from 5.5 T to 6.5 T (Fig. 1 right). In this region, an inverse magnetocaloric effect can be observed at cryogenic temperatures.

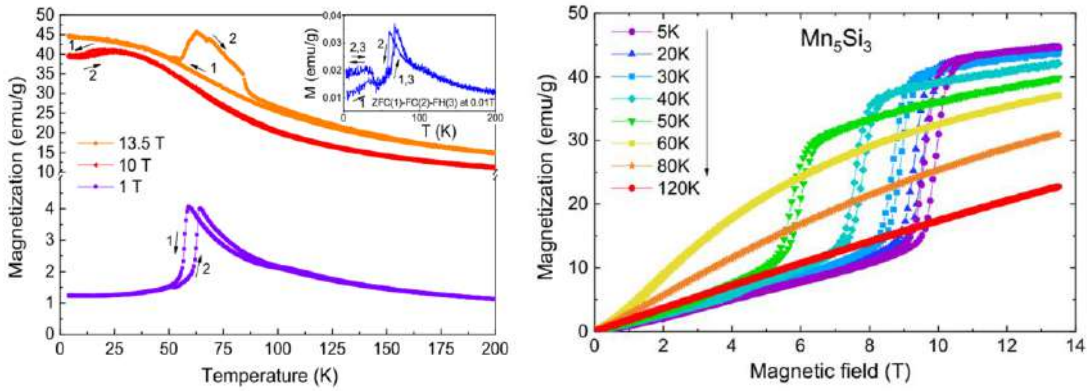

Fig. 1.Left graph: isofield magnetization of the Mn_5Si_3 sample versus temperature in magnetic fields. The inset shows the view isofield magnetization at magnetic field 0.01 T. Right graph: measured isothermal magnetization of Mn_5Si_3 in a magnetic field to 13.5 T.

The reported study was funded by BRFBR and RFBR, project number T20R-204 and 20-58-00059, respectively.

References

[1] I. Park and S. Jeong, Cryogenics 88, (2007) 106.
[2] R. F. Luccas et al., J. Magn. Magn.Mater.489, (2019) 165451.

Features of the phase formation of high-pressure solid solutions $Bi_{1-y}La_y(Mg_{1-x}Zn_x)_{0.5}Ti_{0.5}O_3$

N.M. Olekhnovich[1], E. Čižmár[2], A. Feher[2], Y.V. Radyush[1]*, A.V. Pushkarev[1], A.N. Salak[3], E. L. Fertman[4]

[1] *Scientific-Practical Materials Research Centre of NASB, 220072, P. Brovka str, 19, Minsk, Belarus, radyush@physics.by**

[2] *Institute of Physics, Faculty of Sciences, P. J. Šafárik University, 041 54, Košice Slovakia*

[3] *Department of Materials and Ceramics Engineering and CICECO – Aveiro Institute of Materials, University of Aveiro, 3810-193, Aveiro, Portugal*

[4] *B.Verkin Institute for Low Temperature Physics and Engineering of NAS of Ukraine, 47 Nauky Ave., Kharkiv, 61103, Ukraine*

Experimental

For the synthesis of solid solutions of the system $Bi_{1-y}La_y(Mg_{1-x}Zn_x)_{0.5}Ti_{0.5}O_3$, we used Bi_2O_3, La_2O_3 and a pre-synthesized precursor $Mg_{1-x}Zn_xTiO_3$. The ceramics of the $Bi_{1-y}La_y(Mg_{1-x}Zn_x)_{0.5}Ti_{0.5}O_3$ were synthesized at high-pressure under the following conditions: pressure – 4-6 GPa, temperature – 1450-1550 °C, synthesis time – 1-3 min. Details of the high-pressure synthesis are similar to those described [1]. XRD measurements were performed using a DRON-3 diffractometer (Cu*K*α radiation, graphite monochromator) with an exposition of about 2 s per 0.04° step.

Results and Discussion

It was found from the comparative analysis of the XRD patterns that the perovskite phase is the main crystalline phase in the samples under study. The relative intensities and the splitting types of the fundamental reflections suggested that, in the range of $0 \le x \le 0.75$, the perovskite phase is the orthorhombic *Pnnm*, similar to that observed in BMT [2], while the perovskite phase in the range of $x>0.75$ is the tetragonal *P*4*mm*, the same as that reported for BZT [3]. In the solution with $y=0.75$, both phases coexist forming a morphotropic phase boundary (MPB) [4].

The addition of La ions to the *A*-sublattice of high-pressure perovskite shifts the MPB region towards $x>0.75$. As can be seen from the figure, for the composition with $x=0.85$ after synthesis at high pressure, the composition with $y=0$ has orthorhombic *Pnnm* symmetry, the crystal lattice symmetry of the composition with $y=0.1$ is tetragonal *P*4*mm*, and in the X-ray diffraction spectrum of the composition with $y=0.05$, you can see lines related to both orthorhombic and tetragonal modifications of perovskite. This composition lies in the field of MPB.

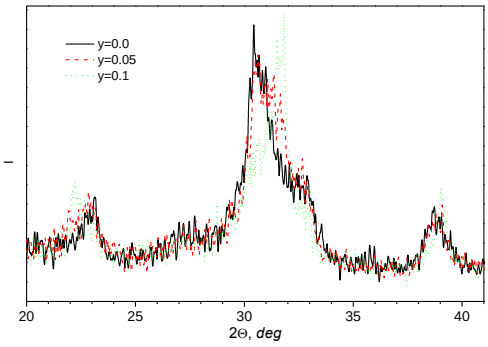

A representative range of the XRD patterns of $Bi_{1-y}La_yMg_{0.15}Zn_{0.85}TiO_3$ synthesized at 6 GPa and 1450 ºC

Acknowledgement: The authors acknowledge financial support of the bilateral Slovakia-Belarus project through grants APVV-SK-BY-RD-19-0008 and T20SLKG-001, respectively.

References

[1] A.V. Pushkarev, N.M. Olekhnovich, Yu.V.Radyush, Inorg. Mater. 47 (2011) 1116-1119.

[2] D.D. Khalyavin, A.N. Salak, N.P. Vyshatko, A.L.-B. Lopes, N.M. Olekhnovich, A.V. Pushkarev, I.I. Maroz, Y.V. Radyush, Chem. Mater. 18. (2006) 5104–5110.

[3] M.R. Suchomel, A.M. Fogg, M. Allix, H. Niu, J.B. Claridge, M.J. Rosseinsky, Chem. Mater. 18 (2006) 4987-4989.

[4] A.N. Salak, V.V. Shvartsman, J.P. Cardoso, A.V. Pushkarev, Yu.V. Radyush, N.M. Olekhnovich, D.D. Khalyavin, J. M. Vieira, E. Čižmár, A. Feher, J. Phys. Chem. Solids. 161 (2022) 110392(1-5).

Ion implantation technology for the synthesis and modification of gallium oxide

D. Korolev[1]*, A. Nikolskaya[1], T. Mullagaliev[1], A. Nezhdanov[1], A. Belov[1], A. Mikhaylov[1], R. Kryukov[1], M. Kumar[2], A. Almaev[3] and D. Tetelbaum[1]
[1]*Lobachevsky State University of Nizhny Novgorod, 23/3 Gagarina pr., Nizhny Novgorod, 603022, Russia, dmkorolev@phys.unn.ru**
[2]*Indian Institute of Technology Jodhpur, NH-65 Nagaur Road Karwad, Jodhpur, 342037, India*
[3] *Tomsk State University, 36 Lenin Avenue, Tomsk, 634050, Russia*

Currently, gallium oxide is gaining popularity due to its unique properties, such as a large band gap, and, consequently, high breakdown voltages and sensitivity in the UV spectral region, which provide the use of this material for promising power devices, solar-blind photodetectors and sensors. However, a number of unresolved problems limit its practical application. Ion implantation is a promising method for modifying the properties of materials. Along with the unique capabilities of a controlled change in the defect-impurity composition, the application of this method allows the ion-beam synthesis of nanoinclusions in solid matrices. In this work the application of the ion implantation method for gallium oxide based materials is demonstrated.

The problem of doping of gallium oxide is currently one of the most technologically important. The available variants for solving this problem, which consist in doping during the growth of single crystals and thin Ga_2O_3 films, face the difficulty of creating layers with a sufficiently high concentration and controlled content of impurity atoms. In this work, we used the implantation of silicon ions into bulk β-Ga_2O_3 samples, as well as magnetron films on sapphire substrates. Changes in the structure depending on the irradiation dose, as well as its recovery upon subsequent thermal annealing, were investigated. For the bulk β-Ga_2O_3 samples, the difference in the effect of ion implantation on the structure and properties of samples with different orientations is demonstrated, and the possibility of ion doping of semi-insulating (Fe-doped) samples is shown.

As one of the fundamentally new methods for obtaining high-quality structures with controlled parameters, for the first time in this work it is proposed to use ion-beam synthesis of Ga_2O_3 nanocrystals in dielectric matrices. To implement this approach, the implantation of Ga^+ and O^+ ions into SiO_2 and Al_2O_3 films on silicon substrates followed by high-temperature annealing is used. The results of studying the structure and composition of the synthesized samples are presented. For individual combinations of implantation regimes and oxide matrices, composite layers with Ga_2O_3 nanocrystals were obtained. Such structures demonstrated record characteristics in terms of photosensitivity.

The obtained results demonstrate the promise of using the ion implantation technique for the synthesis and modification of the properties of gallium oxide based nanomaterials for the creation of a new generation of electronic and optoelectronic devices.

Acknowledgement
The study of the effect of ion irradiation on bulk-Ga_2O_3 was carried out with the support of the RFBR grant № 19-57-80011; Study of the formation of Ga_2O_3 nanoinclusions was supported by a grant from the Russian Science Foundation № 21-79-10233, https://rscf.ru/en/project/21-79-10233/.

Increasing the breakdown voltage of double-sided alumina bases with vias for power multichip modules

D. Shimanovich[1]*, D. Tishkevich[2]
[1]*Belarusian State University of Informatics and Radioelectronics, 220013, Minsk, 6 P.Brovki str., Belarus, e-mail: ShDL@tut.by**
[2]*Scientific-Practical Materials Research Centre of National Academy of Sciences of Belarus, 220072, Minsk, 19 P.Brovki str., Belarus*

The aim of the presented research is developing of the methods and techniques using optimized technological regimes to improve the electrical insulation strength of anodic Al_2O_3 in vias of double-sided alumina bases for potential use in power multichip modules [1-3].

Preliminary experimental studies of fabricated alumina bases with vias matrices showed that in the process of electrochemical anodization at the junction of horizontal and vertical surfaces in vias, microcracks inevitably appeared due to anodizing fronts competing in different directions, restructuring of the porous structure and arising mechanical stresses, even if on the continuous surface of alumina bases, microcracks were completely absent.

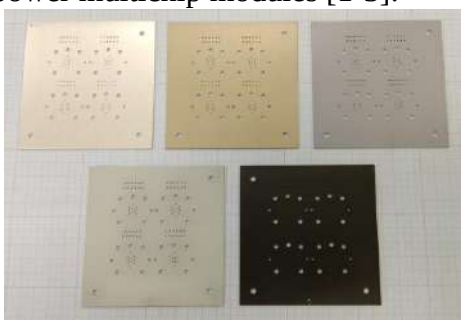

Figure 1. Photo of various double-sided alumina bases with vias

It was shown that the dielectric strength of anodic Al_2O_3 in vias increased by minimizing the number of microcracks due to vias have chamfers (at an angle of up to 45°), a smooth profile at the inputs with satisfactory roughness parameters were formed on the initial samples of aluminum bases by machining and due to the smoothing of microcracks during reanodization. Various methods and techniques were developed and investigated consisting the compositions of single- and multicomponent electrolytes and the electrochemical conditions of multistage anodizing for the beneficial (in terms of increasing the breakdown voltages in vias) structural rearrangement of anodic Al_2O_3 and the formation of multilayer elastic and flexible coatings with minimization of the number of microcracks and internal mechanical stresses. It was found that to ensure the high breakdown voltages, it is necessary to prime (fill the pores) of anodic Al_2O_3 and heal defective microcracks in vias with organosilicon varnish in an ultrasonic bath at a frequency of ~20-40 kHz at a maximum power of ~0,5 kW and temperature ~30 °C during 20 min. Moreover, this technological technique should be carried out in two cycles. Then after filling the excess varnish in the vias should be blowed out with compressed air and after removed from the surface with a squeegee and treated with a toluene solution, after which a multistage heat treatment procedure is carried out with a maximum temperature of 280 °C.

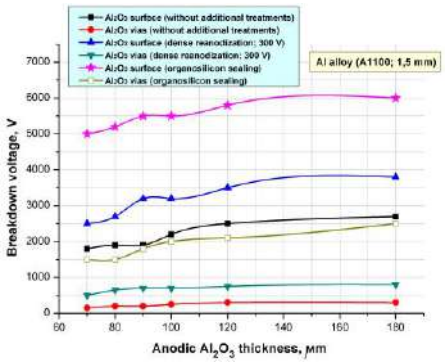

Figure 2. Comparative analysis of technological methods influence on the breakdown voltage

Thus, it was shown that after using of the appropriate technological methods the breakdown voltages of the obtained test samples (Figure 1) were up to ~6 kV on working surfaces without holes and up to ~2,5 kV in vias (Figure 2).

References

[1] D.L. Shimanovich [et al.] Doklady BGUIR 3 (2019) 5-11.
[2] D.L. Shimanovich [et al.] Fundamentalnye problemy radioelektronnogo priborostroeniya 14 (2014) 170-173.
[3] V.A. Sokol [et al.] Doklady BGUIR 8 (2012) 44-49.

Effects of synthesis methods and surface modification on nanoporous alumina coatings wettability

D. Shimanovich[1]*, D. Tishkevich[2], A. Vorobjova[1], A. Trukhanov[2]
[1]*Belarusian State University of Informatics and Radioelectronics, 220013, Minsk, 6 P.Brovki str., Belarus, e-mail: ShDL@tut.by**
[2]*Scientific-Practical Materials Research Centre of National Academy of Sciences of Belarus, 220072, Minsk, 19 P.Brovki str., Belarus*

In recent years coatings with special wettability such as hydrophobic (superhydrophobic) or hydrophilic (superhydrophilic) have attracted considerable interest due to their practical application – from self-cleaning surfaces to microfluidic and drip technologies.

Electrochemical anodizaion is one of the most effective methods of surface treatment and the formation of a nanostructured Al_2O_3 surface matrix. Structural and topological parameters of Al_2O_3 matrix significantly affect the functional characteristics and quality of coatings. Materials with low or high surface energy are usually combined with surface structuring with hierarchical topography on the nano- or micrometer scale for the hydrophobic or hydrophilic coatings synthesis. Therefore, due to the possibility of controlling the pore size and regulating the chemical composition of the surface the porous anodic alumina structures represent a great potential for obtaining surfaces with special wettability [1,2]. Alumina itself has a certain tendency to be wetted with water and therefore is a moderately hydrophilic with a contact angle in the tage of 45-60°. However, in combination with its specific surface structure and surface chemistry high hydrophilicity or hydrophobicity can be achieved.

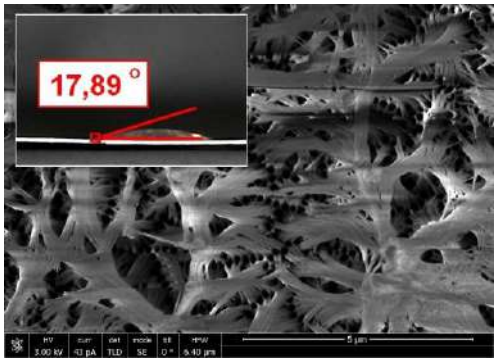

Figure 1. SEM image of a modified porous alumina coating and associated low contact angle

Based on experimental data the effect of technological regimes of an aluminum electrochemical anodizing and pores chemical modification on morphological parameters of nanoporous Al_2O_3 and on the contact angle of alumina structures in order to increase the hydrophilic properties of the final modified coatings was studied. Two- and three-step anodization methods were carried out in a 4% H_3PO_4 at 18-20 °C under various galvanostatic modes at each stage (current densities of 15, 20 and 25 mA/cm^2) during 60-240 min for the synthesis of various types of Al_2O_3 structures. The methods based on increasing the electrolyte temperature to 30-35 °C at the final anodization stage or post-anodizing chemical etching of Al_2O_3 in a 5% H_3PO_4 solution at 40 °C for various times from 7 to 25 min were used for the chemical modification of the alumina porous structure combined with pore expansion. It was shown that it is possible to obtain high hydrophilic parameters with a contact angle value up to 17-20° using high values of current density, anodizing time, and electrolyte temperature by adjusting the electrochemical conditions. It was found that the obtained Al_2O_3 coatings with a thickness of 5-12 μm have a disordered branched porous structure with a pore diameter from 120 to 180 nm. The average pores diameter increased up to 210 nm with significant thinning and destruction of the pore walls after expansion of the pores using chemical etching (Figure 1). It is seen that this type of Al_2O_3 structure provides direct experimental evidence for the theory of three-dimensional capillaries regarding superhydrophilicity.

References

[1] D.L. Shimanovich [et al.] Beilstein Journal of Nanotechnology 9 (2018) 1423-1436.
[2] R. Redon [et al.] Journal of Colloid and Interface Science 287 (2005) 664-670.

EFFECT OF THE DURATION OF HEAT TREATMENT IN GLYCERIN ON THE PROPERTIES OF TITANIUM OXIDE NANOTUBES

M.F. Kamaleev*, D.A. Krupanova, I.M. Gavrilin, A.A. Dronov, S.A. Gavrilov
National Research University of Electronic Technology, Moscow, Russia
**+7-977-876-12-66, kamaleev.maks@gmail.com*

Currently, hydrogen attracts a lot of attention as an environmentally friendly fuel. Its reserves are limitless and in the future can replace traditional energy resources, reducing their share in consumption. However, all existing industrial methods of producing hydrogen fuel (steam conversion of methane, water electrolysis, coal gasification) are environmentally unsafe due to the large amount of emissions into the environment. A more environmentally friendly method of producing hydrogen is the photoelectrochemical splitting of water into molecular hydrogen and oxygen under the action of sunlight. As a suitable semiconductor material for the photocatalyst, TiO_2 nanotubes (TNT) with high chemical inertia, low cost and a developed surface area are used. However, the limiting factors for their large-scale application are the insufficient absorption of TNT solar energy due to the large band gap width, as well as the high rate of recombination of electron-hole pairs on crystal lattice defects.

In this paper, an original method was proposed for modifying TNT obtained in a fluorinated electrolyte by heat treatment in glycerin.

The results of the photocurrent measurement showed that with an increase in the modification time of the structure, there is an increase in photoactivity in both the visible and UV spectral regions. Measuring the width of the optical band gap demonstrates a shift to the visible region of the spectrum. Measurements of photocatalytic activity show an increase in hydrogen generation by modified samples compared to unmodified ones.

The results of this work can be used for further research in the field of increasing the photocatalytic efficiency of materials based on TNT.

Acknowledgments:

The study was carried out with the financial support of the Russian Foundation for Basic Research within the framework of the scientific project No18-29-23038 MK and the state assignment for 2020-2022 of the Agreement FSMR-2020-0018.

Synthesis and magnetic properties of Fe, Ni, Co-doped tin oxide films

V. Ksenevich*, V. Dorosinets, and D. Adamchuk
Belarusian State University, Nezavisimosti av. 4, 220030 Minsk, Republic of Belarus,
**corresponding author e-mail: ksenevich@bsu.by*

Metal oxide semiconductors doped by ferromagnetic metals have attracted essential interest amoung scientists during last decades due to possibility of applications of their magnetic and electric properties for spintronic devices fabrication [1]. Tin dioxide films doped with ferromagnetic ions are considered as a promising candidate for spintronic applications [2].

We propose method for fabrication of tin oxide films codoped by magnetic metals (Fe, Ni, Co). Reactive DC magnetron sputtering of tin target with nickel–cobalt ferrous alloy inserts in argon-oxygen plasma (with oxygen content within range 0–8 vol. %) onto glass substrates with subsequent 2-stage thermal oxidation of the synthesized layers in air (isothermal annealing at 200 °C during 2 hours followed by high temperature annealing at the temperatures within range 300–450 °C during 1 hour). X-ray diffraction (XRD) analysis and Raman scattering was used to control phase composition and crystalline structure of the synthesized films. Magnetization measurements were done using vibrating magnetometer installed in the closed-cycle Helium refrigerator CFHF Cryogenics Ltd. in the temperature range of 2–300 K and in magnetic field up to 8 T.

XRD analysis and Raman scattering of the synthesized films shown that doped by ferromagnetic metals tin oxide films are characterized by more disordered crystalline structure in comparison with undoped tin oxide films fabricated using the same technological procedure [3]. Broad lines inherent to SnO_2, SnO crystalline structure and to nonstoichiometric phases Sn_2O_3 и Sn_3O_4 were detected on the XRD patterns for samples synthesized in argon plasma and in argon-oxygen plasma (with 2 vol. % of oxygen content). Amorhous tin oxide films doped with Fe, Ni, Co were fabricated at the oxygen content ≥4 vol. % in argon-oxygen plasma.

Magnetization measurements were made both for undoped and doped with Fe, Ni, Co tin oxide films. It was found that magnetization behavior of doped by ferromagnetic metals samples is paramagnetic in the whole investigated temperature range (2–300 K). In contrast for undoped $SnO_{2-\delta}$ paramagnetism only at low temperatures (within range 2–4 K) at low magnetic fields ≤2T was observed due to existence of oxygen vacancies in the samples. At the higher temperatures $SnO_{2-\delta}$ films were diamagnetic. The further investigations will be focused on the optimization of the technological parameters of the synthesis procedure of doped by ferromagnetic metals tin oxide films in order to fabricate samples characterized by high-temperature ferromagnetism.

Acknowledgement

The work was supported by Belarusian National Research Programs “Convergence-2025” (grant No. 3.02.1.4), “Materials science, new materials and technologies” (grant No. 2.14.3) and by Program of EU H2020-MSCA-RISE-2015 (grant No. 871284 SSHARE)

References

[1] K. Nomura, Croat. Chem. Acta 88 (2015) 579–590.
[2] K. Gopinadhan, S.C. Kashyap, D.K. Pandya, and S. Chaudhary, Journ. Appl. Phys. 102 (2007) 113513.
[3] D.V. Adamchuck, and V.K. Ksenevich, Dev. Meth. Meas. 10 (2019) 138–150.

Synthesis and characterization of titanium oxo-carbo-nitrides for photocatalytic applications

V. Shatsila[1,2]*, U. Novikau[1], U. Lamanosau[1], I. Razanau[1], W. Maniukiewicz[2], A. Kiędziora[2], R. Ciesielski[2]

[1] *Scientific and Prcatical Centre of NAS of Belarus for Material Science, 19 Brouki str., Minsk 220072, Belarus; *viktar.shatsila@dokt.p.lodz.pl*

[2] *Lodz University of Technology, 116 Żeromskiego str., 90-924 Łódź, Poland*

Catalysts that allow for carbon dioxide (CO_2) conversion into value-added products have been a subject of numerous research attempts. Heterogeneous photocatalysts used in such processes are of semiconductor nature at most. The most common photocatalyst material is titania (TiO_2). While it offers lots of advantages over other types of materials, it also has a few significant flaws limiting its applicability, such as large band gap (E_g = 3,2 eV), that restricts its activity to UV range only, as well as high extent of electron-hole recombination, which reduces catalytic activity overall.

It is known that titanium (III) oxide (Ti_2O_3) is a semiconductor with an exceptionally low band gap ($E_g \approx 0{,}09$ eV), although it's inactive as a photocatalyst. It has been reported that TiO_2-based catalyst activity relies on presence of Ti^{3+} content in the material, thus its stabilization is a subject of great interest.

We report a technique to fabricate mixed titanium-based oxy-carbo-nitride materials based on titanium (IV) chloride ammonolysis with subsequent precipitate calcination. The composition of obtained titanium oxy-carbo-nitrides was found to be adjustable by varying post-precipitation heat treatment conditions. The increase in calcination temperature to shifting towards TiN/TiC formation. The obtained compounds are multi-phase, with target product being concentrated in the crystallic phase.

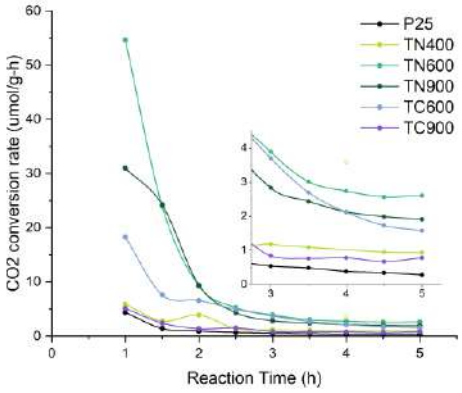

The photocatalytic activity of samples under UV irradiation as a function of reaction time on-stream (inset: scaled up portion)

The synthesized samples were found to exhibit significantly improved activity under UV light in photocatalytic process of CO_2 reduction, compared to commercially-available TiO_2 (Degussa P25). The photocatalytic activity depends on both TiO_2 and TiN/TiC content.

Optical properties of Er doped Zinc Oxide thin films for optoelectronic devices

E. P. Zaretskaya *[1], V.F. Gremenok [1], O. M. Borodavchenko.[1]
[1]*State Scientific and Production Association «Scientific-Practical Materials Research Centre of the National Academy of Sciences of Belarus», 220072, Minsk, P. Brovka str., 19, Belarus, phone: + 375 173532145, e-mail:ezaret@ifttp.bas-net.by**

Er-doped zinc oxide (ZnO:Er) is a very promising optoelectronic material due to its optical transparency ≥95% and to the Er intra-4f shell transition with a photoemission at a wavelength of 1.54 μm, which lies in the minimum loss region of silica-based optical fibres.

In this study ZnO:Er films were prepared by DC magnetron sputtering of Zn and $ErCl_3$ compounds in oxygen atmosphere and then were annealed at different temperatures. X-ray analysys showed that doped films exhibit the hexagonal wurtzite crystal structure with a preferential orientation along [002] direction without any secondary phase.

Photoluminescence (PL) and photoluminescence excitation (PLE) measurements were carried out as a function of annealing temperature and deposition conditions. It was found that with an increase in the annealing temperature in the range 400 - 900 ºC, an increase in the luminescence intensity was observed in the spectral range of 1.5 - 3.0 eV. Fig. 1 shows the PL and PLE spectra of Er-doped ZnO thin films for different annealing temperature.

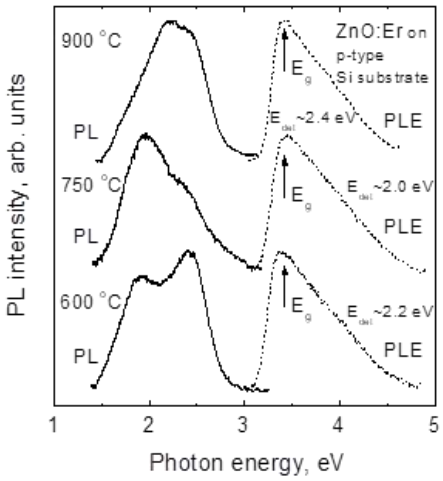

PL and PLE spectra of ZnO:Er thin films for different annealing temperature.

Fig. 1 shows that the peak intensity and energy position of deep-level emission varies with annealing temperatures. In particular, ZnO:Er films annealed at 900 ºC shows only one broad PL band related with the formation of defects induced by a Er atom incorporation in ZnO lattice. The rate of formation point defects is low for ZnO:Er films annealed at low temperature ~ 600 ºC. More defects responsible for the radiative transitions introduce into the films for the temperature higher than 600 ºC. In addition to thermal treatment doping by Er atoms plays an important role in the mechanism responsible for the deep-level luminescence as well. It is notable that the yellow emission decreases with increasing annealing temperature for ZnO:Er thin films. One cause is most likely due to formation Er VO bonds in ZnO:Er films. Another possibility of the variation in intensity of yellow band at ~ 1.94 eV can be ascribed to additional formation of interstitial oxygen. The probability of the electron charge transfer from localized impurity states to the conductive states is increased due to potential fluctuation of Er impurities in ZnO films. It is assumed that both probable mechanisms are responsible for the increasing of green emission. The PLE spectra of ZnO:Er thin films also contains broad band with maximum at 3.40 ± 0.05 eV which is correspond to the band gap energy of ZnO.

The most interesting experimental fact is a more efficient excitation of radiation in the region of 1.54 mm, caused by Er3 + ions, through the 3.2 eV band as compared with band-to-band optical transition in PLE spectra of ZnO:Er thin films. An increase in the intensity of PLE band at 3.2 eV with increasing annealing temperature results from higer concentration of structural Er – O defects and the formation of impurity energy band with shallow levels.

Acknowledgements

This work has been supported by the Belarusian Republican Foundation for Fundamental Research (Grant № T20UK-022).

Improving the properties of a semiconductor material of indium gallium zinc oxide (IGZO) obtained from a solution

B. Kazarkin, A. Stsiapanau, Y. Mukha and A. Smirnov
Belarusian State University of Informatics and Radioelectronics, Brovki str. 6, Minsk 220013, Belarus; e-mail: kazarkin_boris@mail.ru

It should be noted that the annealing process is very important for obtaining semiconductor layers with good electrical characteristics from solutions using centrifugation or injection printing. The composition of the atmosphere upon annealing after deposition of a solution of a semiconductor material can significantly affect the morphology and structure of the obtained active TFT layer, and, consequently, the electrophysical characteristics of device structures. In this work, we investigated the electrical characteristics of IGZO test structures, the active layer of which was formed on silicon substrates from a solution, followed by two-stage annealing in a nitrogen and / or air atmosphere.

To produce test structures with IGZO thin layer films had been used next ratio of solution: Ga:Zn:In = 10:63:27. After spin coating solution on Si wafer with 100nm SiO_2 layer different 2-step types of annealing had been used (Table 1). Photolithography was performed after annealing.

Table 1 Different 2-step annealing processes for IGZO test structures.

Sample	**1st annealing**	**2nd annealing**
A/A	10 min 180°C in air	1 hour 380°C in air
N/A	10 min 180°C in nitrogen	1 hour 380°C in air
A/N	10 min 180°C in air	1 hour 380°C in nitrogen
N/N	10 min 180°C in nitrogen	1 hour 380°C in nitrogen

Fig. 1 shows Vgs-Ids (Vds=5V) characteristics of IGZO test structure after A/A, N/A, A/N, N/N annealing processes. (a) and (b) are shown summary Vgs-Ids (Vds=5V) characteristics with logarithmic and linear scales respectively. Current on IGZO test structure after N/N annealing bigger more than 3 times than current on IGZO test structure after A/A annealing.

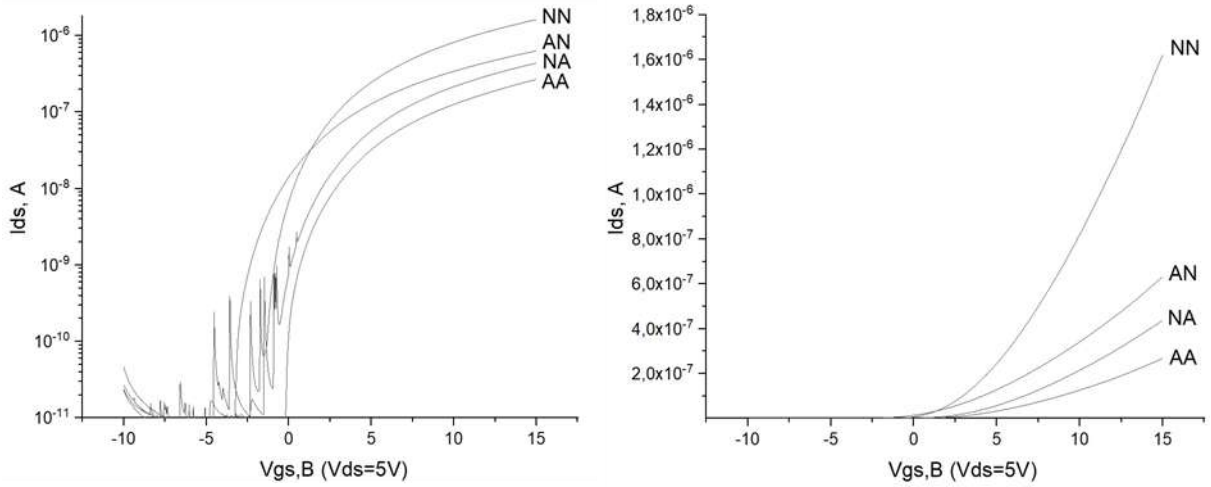

Figure 1 - Characteristics of Vgs-Ids (Vds = 5 V) of the InGaZnO test structures after annealing processes A/A, N/A, A/N, N/N with logarithmic (a) and linear (b) scales, respectively.

References

[1] Wangying Xu [et al.], Applied Surface Science 455 (2018) 554–560.
[2] Kwan-Soo Kim [et al.], Materials Science and Engineering 178 (2013) 811–815.

Magnetic Field Sensing with Bidomain $LiNbO_3$-Based Magnetoelectric Composite

A. Turutin[1,2,*], J. Vidal[3], I. Kubasov[1], A. Kislyuk, M. Malinkovich[1], Y. Parkhomenko[1] and N. Sobolev[1,2]
[1] *National University of Science and Technology MISiS, 119049 Moscow, Russia, e-mail for the corresponding author* aturutin92@gmail.com*
[2] *Department of Physics and i3N, University of Aveiro, 3810-193 Aveiro, Portugal*
[2] *Department of Physics and CICECO, University of Aveiro, 3810-193 Aveiro, Portugal*

Composite multiferroics are materials in which electric polarization of the material is possible under the action of an external magnetic field and vice versa, a change in the magnetization of the structure when an electric field is applied. Such properties have a high practical potential for application in science and technology. Based on these materials, it is possible to manufacture a number of devices with unique properties, such as, for example, random access magnetoelectric (ME) memory, ME sensors of magnetic fields, current, magnetic nanoparticles, micromechanical ME antennas, voltage-adjustable microwave filters, resonators and phase shifters. Therefore, the search for new materials of composite multiferroics and the study of the ME effect in them is a priority and urgent task in the search and creation of new electronic devices. One of the most promising and close to practical implementation directions is the creation of highly sensitive sensors of ultra-weak magnetic fields on the basis of composite multiferroics. The absence of the need to cool such sensors is a significant technical advantage over superconducting quantum interferometers currently used for these purposes.

We have developed a laminate composite based on bidomain $LiNbO_3$ (b-LN) / metglas. b-LN / metglas composites can detect low magnetic fields at room temperature with a record value of sensitivity to the magnetic field as low as 92 $fT/Hz^{1/2}$ at a frequency of ca. 7 kHz. Furthermore, ME tuning-fork-shaped composite structure based on a b-LN / metglas has shown a sensitivity down to 3 pT under real-life conditions at a low resonance frequency of ca. 300 Hz.

Importantly, the lead-free nature of LN meets the demands of the RoHS directive which assumes the restriction of the use of certain hazardous substances in electrical and electronic equipment. Thus, applications based on LN can substitute commonly used PZT ceramics. The b-LN crystals demonstrated excellent properties in the application of magnetoelectric magnetic sensors, vibration sensors, energy harvesters, actuators, position and magnetic field sensors.

Memristive properties of charged domain walls in chemically reduced lithium niobate crystals

I. V. Kubasov[1]*, A. M. Kislyuk[1], T. S. Ilina[1], A. S. Shportenko[1], D. A. Kiselev[1], A. V. Turutin[1], A. A. Temirov[1], M. D. Malinkovich[1], and Y. N. Parkhomenko[1,2]
[1] *National University of Science and Technology MISiS, Leninskiy prospect, 4, Moscow, 119049, Russia, kubasov.ilya@gmail.com**
[2] *JSC "Giredmet", 2 Elektrodnaya Str., Moscow, 111524, Russia*

Among many materials considered for use in domain-wall nanoelectronics, lithium niobate ($LiNbO_3$, LN) is one of the most technological and physically stable. The domain walls in LN are usually characterized by an inclination angle θ between the spontaneous polarization vector $\mathbf{P_s}$ and the domain boundary. There exist many methods to form domain walls in LN single crystals. Most of them utilize an external electric field causing formation of domains divided by inclined partially charged domain boundaries that form an angle $0<\theta<90°$ with the polar axis. Compared with many other reports where inclined domain walls are investigated, this study is focused on flat and almost completely charged domain walls (CDWs) of large area in undoped bidomain LN crystals heat-treated in reducing ambient.

Bidomain head-to-head and tail-to-tail ferroelectric structures were engineered in two undoped congruent z-cut LN single-crystal wafers by diffusion annealing in Li_2O-deficient and Li_2O-rich atmosphere at 1140 °C, respectively. Then, the samples were reduced for 1 hour at 1030 °C in nitrogen of 6N purity.

The samples were investigated by piezoresponse force microscopy (PFM) and c-AFM with registration of I-V curves and thermal dependencies using scanning probe microscope MFP 3D Stand Alone (Asylum Research). It was revealed that the electrical conductivity of head-to-head CDWs in the reduced LN (RLN) is accessible without super-bandgap photoexcitation, shows memristive behavior and can be tuned by external voltage while tail-to-tail CDWs are insulating. The activation energy of polaron mobility as well as electron localization energy was estimated based on I-V curve measurements. The data obtained for the head-to-head CDWs in bidomain crystals shows comparative or even higher local conductivity relatively to inclined CDWs in $LiNbO_3$:Mg as well as ion-sliced single-crystal LN films. Moreover, domain walls in bidomain crystals are highly reproducible, almost flat and possess maximum interface charge density which is promising for future mass production of CDW-based nano-electronic devices operating at the intersection of electronics, optics and mechanics.

The study was performed with financial support from the Ministry of Education and Science of the Russian Federation for the support in the frameworks of the Increase Competitiveness Program of NUST «MISiS» (Project No. K2-2020-033) and the State Assignment (basic research, Project No. 0718-2020-0031)

Electrophysical Properties, Morphology and Memristive Behavior of Completely Charged Domain Walls in Reduced Bidomain Lithium Niobate

A.M. Kislyuk[1]*, I.V. Kubasov[1], T.S. Ilina[1], A.V. Turutin[1], D.A. Kiselev[1], A. S. Shportenko[1], A.A. Temirov[1], M.D. Malinkovich[1], Yu.N. Parkhomenko[1]
[1]*National University of Science and Technology MISiS, 119049, Moscow, Russia, akislyuk94@gmail.com**

The influence of a charged domain wall (CDW) on the formation of the induced domain structures in congruent x-cut lithium niobate crystals ($LiNbO_3$, LN) was studied. By diffusion annealing in air ambient near Curie temperature, as well as infrared annealing in oxygen-free ambient bi- and multidomain ferroelectric structures containing CDWs head-to-head and tail-to-tail were formed. By Kelvin probe mode of atomic force microscopy (AFM) surface potential near the CDWs was investigated. We studied surface needle-shaped induced microdomains which were formed in a vicinity of the domain boundary and far from it by applying of voltage to the cantilever being in a contact with the surface of the sample. Dependence of morphology of the induced domain structure on the crystal's electric conductivity was demonstrated. Screening effect of charged head-to-head domain wall on a shape and size of the domain, that was induced near the boundary was shown. We described partition of the single needle-shaped domains formed by AFM cantilever to several microdomains having a shape of several beams based in a common nucleation point. We found an influence of the CDW on the topography of the samples, which consisted in the appearance of a long groove corresponding to the domain boundary after the reducing annealing.

It was revealed that the electrical conductivity of head-to-head CDWs in the reduced LN is accessible without super-bandgap photoexcitation, shows memristive behavior and can be tuned by external voltage while tail-to-tail CDWs are insulating. The activation energy of polaron mobility as well as electron localization energy was estimated based on I-V curve measurements. The data obtained for the head-to-head CDWs in bidomain crystals shows comparative or even higher local conductivity relatively to inclined CDWs in LiNbO3:Mg as well as ion-sliced single-crystal LN films. Moreover, domain walls in bidomain crystals are highly reproducible, almost flat and possess maximum interface charge density which is promising for future mass production of CDW-based nano-electronic devices operating at the intersection of electronics, optics and mechanics.

Acknowledgement
The reported study was funded by RFBR, project number 20-32-90141.

Composite fibers based on ordered carbon nanotubes and polyvinyl alcohol

N. I. Savchina-Imbro, S. A. Filatov, G. S. Akhremkova
A.V. Luikov Heat and Mass Transfer Institute of NAS of Belarus,
15 P. Brovka Str.,Minsk, 220072, Belarus; e-mail: <savchina.nata@mail.ru>

Carbon nanotubes which possess record mechanical characteristics, are considered by many researchers as an efficient means of increasing the strength characteristics of composite polymeric materials [1]. Such a combination of the properties and shape of a product in conjunction with modern technologies of development and fabrication of polymers ensure the creation of new structural materials. As fillers of polymers, the carbon nanotubes (CNT) are capable of: increasing the electrical conductivity, thermal stability, ignition temperature; improving the mechanical characteristics; changing the structure of a polymer, increasing the degree of its crystallicity; increasing the vitrification temperature; imparting composites with particular functional properties (the ability of removing static charges, scattering and absorbing radio emission, increasing electroluminescence, etc.). Microfibers with carbon nanotubes are promising for the creation of unique materials and products with respect to the strength and functional possibilities: lightweight important parts of flying vehicles, mechanical facilities, and special-purpose suits. Conceivably cloths capable of operating under very severe conditions can be created. Fibers and cloths with carbon nanotubes are promising for producing practice hall equipment [2]. The use of carbon nanotubes to impart antistatic and conducting properties to polymers is today a commercial practice finding application in such branches as electronics and the automotive industry.

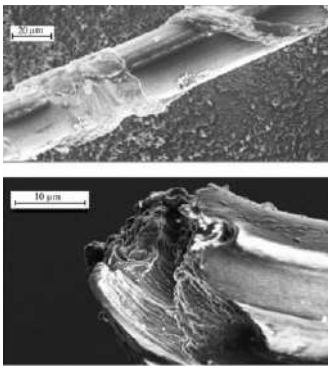

Figure 1. SEM-Images of the surface (a) and of the cleavage (b) of a PVA-CNT fiber

The aim of the present work is to obtain and investigate the properties of polyvinyl alcohol (PVA)–carbon nanotube composite fibers. Materials, Production Technique, and Experimental Investigation of Fibers. The object of investigation was PVA–CNT fibers obtained on a laboratory setup whose basic diagram is given in [3]. In fabrication of composite fibers, carbon nanotubes produced by the following companies were used as fillers: Thomas Swan (Elicarb) - singlewall carbon nanotubes (SWNT), Arkema and Nanocyl - multiwall carbon nanotubes (MWNT), and Nanocyl — double-wall carbon nanotubes (DWNT).

The presented technique of obtaining PVA–CNT fibers (Figure1) is relatively simple to implement and allows one to produce a composite fiber with carbon nanotubes orientated predominantly along the fiber axis. It has been established that the addition of carbon nanotubes to polyvinyl alcohol promotes the improvement of their mechanical and electrical characteristics: the Young modulus and electrical conductivity increase. It is shown that the washing of composite fibers with water exerts a different effect on their properties. On the whole, their electrical conductivity increases and the Young modulus decreases.

References

[1] A. V. Eletskii, Carbon nanomaterials, Usp. Fiz. Nauk, 167, 9 (1997) 25–41.
[2] E.G. Rakov, Fibers with carbon nanotubes, Ryn. Legk. Prom., 48 (2007) 10–19.
[3] B. Vigolo, et.al., Science, 290, 1, (2000) 2569–2573.

Structure and optical properties of chemical deposited double-phase films in system CdS - PbS

I.V. Vaganova[1,2]*, L.N. Maskaeva[1,2], V.F. Markov[1,2], V.I. Voronin[3] , O.A. Lipina[4] and E.V. Mostovshchikova[3]

[1] *Ural Federal University, 19 Mira Str., 620002 Yekaterinburg, Russia, irina_vaganova@inbox.ru*

[2] *Ural Institute of State Fire Service of EMERCOM of Russia, 22 Mira Str., 620062 Yekaterinburg, Russia*

[3] *M.N. Miheev Institute of Metal Physics of Ural Branch of Russian Academy of Sciences, 18 S. Kovalevskaya Str., 620108 Yekaterinburg, Russia*

[4] *Institute of Solid State Chemistry of the Ural Branch of the Russian Academy of Sciences, 91 Pervomaiskaya Str., 620990 Yekaterinburg, Russia*

The possibility of forming double-phase films in system CdS-PbS using chemical bath deposition from aqueous media with adding various cadmium salts (acetate $Cd(CH_3COO)_2$, nitrate $Cd(NO_3)_2$, and sulfate $CdSO_4$) has been demonstrated. The crystal structure were studied by the X-ray diffraction. Figure 1 shows the fragment of XRD pattern with reflection (111) of cubic phase $Cd_{0.07}Pb_{0.93}S$ and hexagonal CdS.

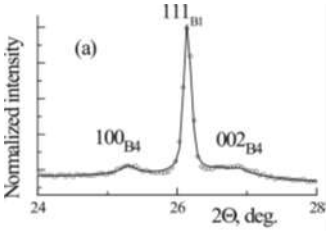

Fig.1 Fragment of XRD pattern of CdPbS

According to the change in the lattice period determined from minimizing the XRD patterns, the following estimates of the compositions of the synthesized solid solutions were made: $Cd_{0.067}Pb_{0.933}S$ ($Cd(CH_3COO)_2$), $Cd_{0.071}Pb_{0.929}S$ ($Cd(NO_3)_2$), $Cd_{0.076}Pb_{0.924}S$ ($CdSO_4$). In the series from cadmium acetate to cadmium sulfate, a decrease in the size of the coherent scattering regions of the $Cd_xPb_{1-x}S$ solid solution from ~ 1000 nm to 312 nm was found, and in the ($Cd_{1-d}S$) phase from 33.0 to 7.5 nm.

The calculated value of microstrains Δd/d in the mentioned sequence of films increases from 16.1×10^{-4} to 28.5×10^{-4} and 27.8×10^{-4}, respectively. The revealed differences are the result of the influence of the nucleophilicity of the anionic component of cadmium salts on the kinetics of thiourea decomposition.

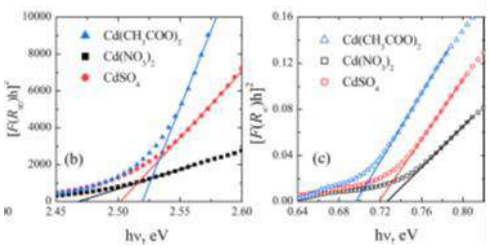

Fig.2 Results of graphical determination of the band gap of two-phase $Cd_xPb_{1-x}S/Cd_{1-d}S$ compositions deposited from the bath containing $Cd(NO_3)_2$, $CdSO_4$, $Cd(CH_3COO)_2$

The Kubelka-Munk function was calculated from the diffuse reflectance data and the dependences $[F(R_\infty)h\nu]^2 = f(h\nu)$ are plotted in Fig. 2. In the case of the direct allowed transitions, the extrapolation of the linear sections of the curves to the abscissa axis made it possible to determine the value of the band gap E_g. It is seen, that for all the films deposited in the presence of the cadmium salt it is possible to find two values of E_g, which vary in the ranges of 2.47–2.52 eV and 0.69–0.73 eV indicating the two-phase composition of the films. In this case, the higher E_g values belong to the band gap of the $Cd_xPb_{1-x}S$ solid solutions located on the sublayer of the amorphous phase of cadmium sulfide. Thus, the complex studies carried out have confirmed the chemical synthesis of the two-phase $Cd_xPb_{1-x}S/Cd_{1-d}S$ films, which differ in their composition depending on the cadmium salts used, as well as in their semiconducting properties. In the future, this gives an opportunity in one technological stage to form the compositions and heterostructures that can be used in the creation of the solar radiation converters.

Enhancing the electrical properties of $Bi_4Ti_3O_{12}$ matrix

V. L. Bessa[1,2*], M. A. S. Silva[1], and A. S. B. Sombra[1,2]
[1] *LOCEM -Telecommunication and Materials Science and Engineering of Laboratory, Physics Department, Federal University of Ceará, P.O. Box 6030, Fortaleza, Ceará 60455-760, Brazil*
[2] *Telecommunication Engineering Department, Federal University of Ceará, P.O. Box 6007, Fortaleza, Ceará 60755-640, Brazil*

In this work, the electrical and dielectric properties of $Bi_4Ti_3O_{12}$ (BiT) in the microwave (MW) range were analysed. BiT has many applications in telecommunication systems and MW circuits. In this work, it was synthesized by the solid-state reaction method (800 ºC for 4 h) and the ceramic pellets were sintered at 900 ºC for 4 h. X-ray diffraction was used for structural characterization of this phase. The dielectric properties in the MW range were measured using the Hakki–Coleman method, and the thermal stability was measured using the Silva–Fernandes–Sombra (SFS) technique. In the microwave range, the temperature coefficient of the resonant frequency (τ_f) is around -439 ppm/ºC (for 2.5GHz). In this range of frequencies, the matrix is not stable enough to be used as an element in a circuit, considering that the temperature coefficient is not close to 0 ppm/ºC. However, the permittivity found for BiT in the microwave range of 30.39 and a loss tangent of 3.6 10^{-2}, with a material resonant frequency of 4.63 GHz and Q_0 = 27.88 enable this material to be applied in satellite and antenna communication systems. The experimental and simulated S11 spectrum for the antenna are -26.79 dB and -31.75 dB, respectively, showing that the resonator cylinder is working as an antenna. The parameter as bandwidth, where values experimental, and simulated are, respectively, 185.33 MHz and 182.54 MHz, representing 7.35% of experimental BW. The gain was 2.17 dBi and the 32.12% efficiency needs to be improved for BiT to function effectively as an antenna Smith's experimental and simulated chart shows good agreement and that the impedance matching was around 50 Ω. It also shows that the simulated antenna is reactive, that is, purely inductive. In Radiation diagram of sample BiT, we noticed symmetry in the lobes, indicating a typical diagram of a cylindrical DRA.

References

[1] L. Wang, W. Ma, Y. Fang, Y. Zhang, M. Jia, R. Li, Y. Huang,
Procedia Environ. Sci. 18, 547 (2013)
[2] HAKKI, B. W.; COLEMAN, P. D. IEEE Transactions on Microwave Theory and Techniques, v. 8, n. 4, p. 402–410, jul. 1960.
[3] M.A.S. Silva, T.S.M. Fernandes, A.S.B. Sombra, J. Appl. Phys. 112, 074106 (2012).

Anomalous low-temperature behaviour of As_xS_{100-x} glassy system

P. Baloh[1]*, V. Tkáč[1], M. Orendáč[1], K. Paulovičová[2], V. Mitsa[3], R. Holomb[3,4], M. Veres[4], and A. Feher[1]
[1]*P. J. Šafárik University, Park Angelinum 9, Košice 040 01, Slovakia, pavlo.baloh@student.upjs.sk**
[2]*Institute of Experimental Physics SAS, Watsonova 47, Košice 040 01, Slovakia*
[3]*Uzhhorod National University, Voloshin Str. 54, Uzhhorod 88 000, Ukraine*
[4]*Wigner Research Centre for Physics, Konkoly-Thege Miklós Str. 29-33, Budapest 1121, Hungary*

It is known that low-temperature (LT) thermal properties of noncrystalline solids do not follow the Debye prediction, unlike their crystalline counterparts. Instead of constant contribution (Debye contribution) usually observed in the reduced specific heat C_p/T^3 of crystalline solids, the broad maximum (boson peak) is found for glassy materials. Such behaviour of noncrystalline solids along with some other universal LT properties (*e.g.*, plateau in thermal conductivity) became famous in literature as "anomalous" behaviour.

This work is focused on the experimental study of LT specific heat and low-frequency (LF) Raman spectra of As_xS_{100-x} (x = 20, 28.6, 40, 45 and 50) glasses.

A deeper insight into the unique vibrational properties of the above-mentioned samples can be obtained by a detailed analysis of rigid and soft vibrations of different nanoclusters. The microscopic origin of LF modes could be explained using the vibrations of small As-S nanoclusters, namely: closed and opened 12-membered rings and branched structures based on the $AsS_{3/2}$ pyramids. The results of DFT calculations of Raman spectra of As-S rings and chains at very low wavenumbers indicate that the very low-frequency vibrations can arise due to variations of nanocluster connections with the host network structural matrix [1,2].

There exist three elastic phases in As_xS_{100-x} glassy system: flexible ("floppy") at x < 22.5 %, intermediate in the 22.5 % < x < 29.5 % range and stress-rigid at x > 29.5 % [3]. Theoretical considerations predict that the quasi-localized modes are most apparent in the stress-rigid systems [4]. Stoichiometric glass (g) g-As_2S_3 (g-$As_{40}S_{60}$) with stress-rigid structure showed an anomaly in C_p/T^3 at 5.3 K that originates from LF vibrations of "defective" clusters. These clusters, containing free ends at their edges, are only partially connected to the stress-rigid matrix of glass [1]. In contrast, the degree of freedom in covalent bindings of sulfur-rich As_x-S_{100-x} compositions is lower.

The C_p/T^3 maximum observed for stoichiometric g-As_2S_3 and associated with the relatively stress-rigid structure of the glassy matrix is compared with those measured for compositions belonging to intermediate and flexible structures. The role of soft and rigid vibrations of As-S nanoclusters as well as their interconnections on compositional dependence of C_p/T^3 maximum of As_xS_{100-x} glasses is discussed.

Acknowledgement
This work has been supported by projects APVV-18-0197 and APVV-SK-BY-RD-19-0008.

References

[1] R. Holomb, V. Tkáč, V. Mitsa, and M. Veres, Phys. Stat. Sol. B 257 (2020) 1900525.
[2] R. Holomb, P. Ihnatolia, O. Mitsa, V. Mitsa, L. Himics, M. Veres, Appl. Nanosci. 9 (2019) 975.
[3] P. Chen, C. Holbrook, P. Boolchand, D. G. Georgiev, K. A. Jackson, M. Micoulaut, Phys. Rev. B 78 (2008) 224208.
[4] E. Lerner and E. Bouchbinder, Phys. Rev. E 97 (2018) 032140.

Correlation of the chemical composition and structural characteristics in the partially substituted spinel ferrites

D. Sherstyuk[1*], D. Zherebtsov[1], S. Gudkova[1], N. Perov[2], Yu. Alekhina[2], K. Astapovich[3], D. Vinnik[1], A. Trukhanov[1,3]
[1]*South Ural State University, Chelyabinsk, Russia, sherstiukd@susu.ru**
[2]*Lomonosov Moscow State University, Moscow, Russia*
[3]*SSPA "Scientific and Practical Materials Research Centre of NAS of Belarus", Minsk, Belarus*

Samples of nickel-zinc-cobalt ferrite with the general formula $Ni_{0.3}Zn_{0.7-x}Co_xFe_2O_4$ (x=0-0.7) were prepared by solid-phase synthesis. The sintering process was carried out at a temperature of 1150 °C for 5 hours.

$$0{,}3NiO+(0{,}7–x)ZnO+xCoO+Fe_2O_3 \rightarrow Ni_{0,3}Zn_{0,7–x}Co_xFe_2O_4$$

As a result of the study on a SEM Jeol JSM 7001F equipped with an Oxford INCA X-max 80 the actual sample formulas were calculated. The elemental composition of the synthesized samples is in good agreement with the initial charge of the samples. The data about phase composition and lattice parameters were investigate on powder X-ray diffractometer Rigaku Ultima IV. X-ray phase analysis showed that all prepared samples are monophasic and have a spinel structure.

One of the important parameters of ceramic materials, which affect the properties of the final product, is also determined - this is porosity. The apparent density ρ was investigated with an AccuPyc 1340 helium pycnometer, Micromeritics. X-ray density was calculated using the formula: $\rho_X = 8M / Na^3$, where M is the molecular weight, N is Avogadro's constant, and an is the crystal lattice parameter. The porosity value is the ratio: $P = (1– (\rho / \rho_X)) \cdot 100\%$ (Fig. 1).

The measurements of magnetic properties were carried out using a vibrating sample magnetometer Lakeshore 7400 series in the magnetic field range of ±16 kOe at room temperature (see fig. 2).

As a result, the following conclusions were obtained: established the optimal physicochemical synthesis conditions for the formation of monophase samples of spinel ferrites; the saturation magnetization increases to 81.1 emu/g and then decreases, the maximum is observed in the sample $Ni_{0.3}Zn_{0.3}Co_{0.4}Fe_2O_4$. Remanent magnetization and coercivity increases with the cobalt concentration.

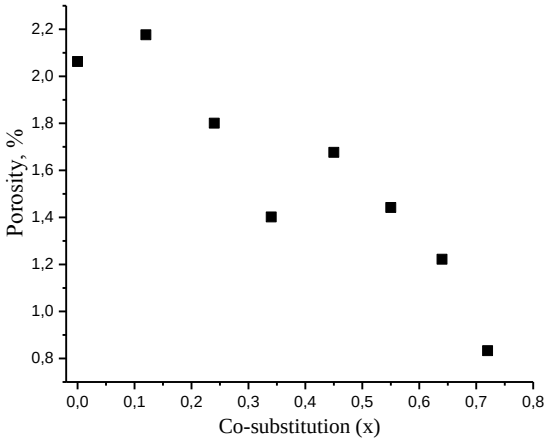

Dependence of structural characteristic (porosity) of the Co-substitution

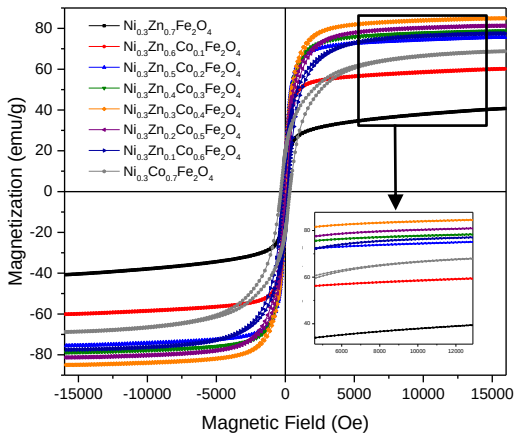

Hysteresis loops of the $Ni_{0.3}Zn_{0.7–x}Co_xFe_2O_4$ system

Acknowledgement
This work was supported by the RFBR (project No 20-38-70057) and President's grants for young doctors of science (MD-5612.2021.4).

Measuring the electrical conductivity of noncompactable powders

D.E. Zhivulin[1]
[1]*Sout Ural State University, 454080, Russian Federation, Chelyabinsk, Lenin avenue, 76, zhivulin-74@mail.ru*

The study of electrical conductivity is one of the most important tasks of modern solid state physics. An analysis of the temperature dependences of resistance makes it possible to judge the electronic structure of the samples under study. Classical methods for electrical resistance measuring demand in dense sample. Samples are often unsuitable for making monolithic samples of standard geometry from them. The reason could be the disordered porous macrostructure of the samples, or the morphology of the samples as noncompactable powders like many of carbon materials. One of the options for solving the problem is to prepare a sample for measurement in the form of a powder of a certain fraction.

To measure the temperature dependences of the resistance of powdered samples, a vacuum cell was designed (Figure 1). The sample for measurement is placed between two copper electrodes inside a quartz glass tube. One electrode rests against the bottom of the quartz test tube, the other electrode is pressed by the spring-loaded ceramic rod. The spring, which loading the sample, is located in the zone, which is not subject to heating, and due to this, it does not change its elastic properties when the sample is heated. Outside the vacuum tube is heated by a resistance oven. A thermocouple is located in the immediate vicinity of the sample. Wires are connected to the cell electrodes through vacuum current leads located in the cover of the measuring cell. The hermetically sealed cell design allows measurements in a vacuum or inert gas.

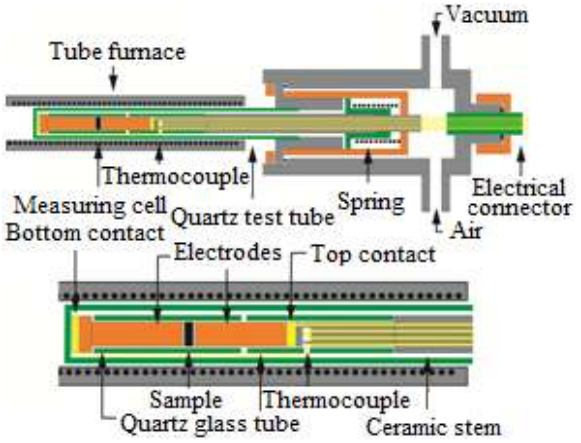

Fig. 1 Measuring cell layout

Figure 2 shows the temperature dependences of the resistance of carbon powder doped with nitrogen. To control the convergence of the measurement results, two heating - cooling cycles were performed. During the first heating, moisture is removed from the sample and therefore the resistivity for the first heating differs significantly from the set of next measurements. The subsequent measurements show good reproducibility.

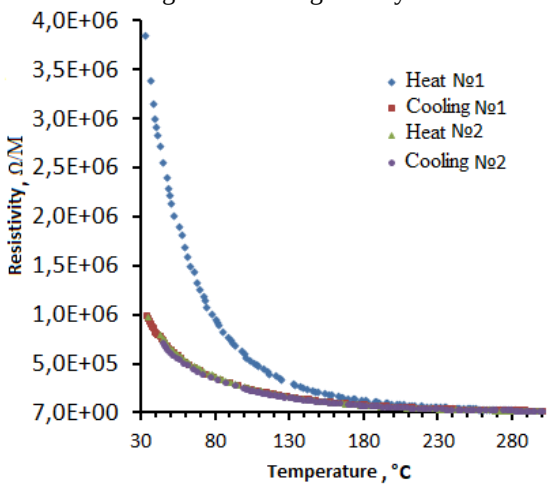

Fig. 2 Temperature dependence of the resistance of a carbon material doped with nitrogen

This method of measuring the temperature dependences of resistance can be used in the study of powdered samples, from which it is impossible to prepare dense samples of standard geometry. This cell has been successfully used to study the temperature dependence of the resistance of carbon-nitrogen materials and determine their band gap.

Study of a hybrid organic-inorganic system for X-ray detection

K. Pudzs*, I. Pudza, N. Strautnieks, A. Tokmakov and A. Kuzmin
Institute of Solid State Physics, University of Latvia, 8 Kengaraga street, LV-1063, Riga, Latvia.
** Kaspars.Pudzs@cfi.lu.lv*

The development of X-ray radiation detectors is an active field of modern research due to their wide range of possible applications in modern medicine, security control and scientific research. Currently used semiconductor crystal X-ray detectors have several negative properties such as a limited size, high operating voltages, poor X-ray absorption capacity and no plasticity and flexibility. These problems can be solved by developing new types of hybrid X-ray detectors consisting of high-Z nanoparticles arranged in an organic matrix.

In this study, we developed and tested hybrid organic-inorganic thin-film systems operating by converting incident X-ray photons into the current. Hybrid systems were formed from tungstate nanoparticles of various metals (cadmium, zinc, nickel, strontium, calcium, cobalt) and various organic compounds - poly(3-hexylthiophene-2,5-diyl) or P3HT, Phenyl-C61-butyric acid methylester or PCBM (fullerene), Poly(9-vinylcarbazole) or PVK and poly(3,4-ethylenedioxythiophene) polystyrene sulfonate or PEDOT:PSS.

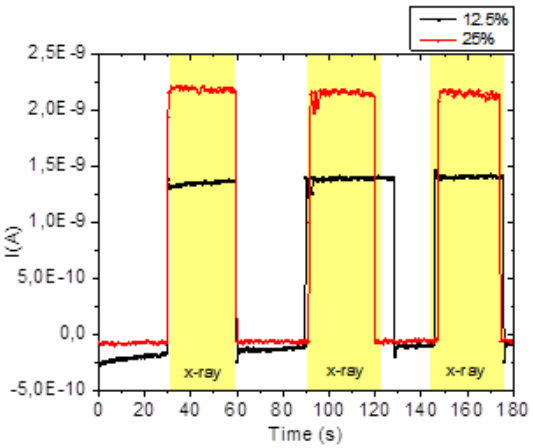

X-ray generated photocurrent of hybrid systems $CaWO_4$+P3HT/PCBM with 12.5 and 25 wt% $CaWO_4$ nanoparticles.

Thin-film samples were fabricated from a solution by the blade casting method. Scanning electron microscopy was used to characterize the nanoparticles and their distribution in an organic matrix. The X-ray detection capability and sensitivity of hybrid systems were determined using radiation from an X-ray tube with a tungsten anode. Current-voltage characteristics and X-ray current curves were obtained during the operation, and the sensitivity of the obtained systems was calculated. The obtained results are compared with the state-of-the-art data available in the literature.

The financial support provided by the Latvian Council of Science project No. lzp-2019/1-0071 is greatly acknowledged.

STUDY OF THE SYNTHESIS OF CERAMIC MATERIALS BASED ON BARIUM HEXAFERRITE, SUBSTITUTED WITH ALUMINUM, WITH A VIEW TO IMPROVING THE PHYSICOCHEMICAL PROPERTIES

Bogatyreva K.A, Zhivulin V.E., Vinnik D.A., Pavlova K.P.
South Ural State University, Chelyabinsk, Lenin ave. 76, Russia bogatyreva2000@bk.ru

The purpose of this study is to study the possibility of synthesizing ferrite with a magnetoplumbite structure, in which iron atoms are partially replaced by aluminum atoms for the possibility of further modification of the properties. A sample of ceramic material $BaFe_{10}Al_2O_{19}$ was obtained by solid-phase synthesis at a temperature of 1380 ° C. The initial components for preparing the samples were powders of Fe_2O_3 (72.7 wt%), Al_2O_3 (9.3 wt%), and $BaCO_3$ (18.9 wt%). The resulting sample was placed on a platinum sheet in a high-temperature electric furnace and sintered at a temperature of 1380 ° C for 5 hours.

X-ray phase analysis and electron microscopy were used as research methods. The obtained sample was examined on an Optima IV powder diffractometer of the Rigaku model (Cu radiation). The morphological features of the surface (Figure 1 a, b) were studied using a JEOL scanning electron microscope, model JSM7001F, equipped with an INCAX-max 80 X-ray energy dispersive spectrometer (Oxford Instruments). X-ray diffraction patterns were recorded in the 2θ angle range from 5 to 90 degrees. with a step of 0.02 deg. and a shooting speed of 5 deg / min (Figure 2).

a) 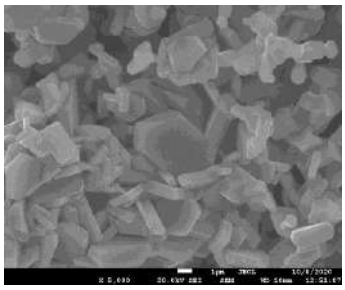 b) 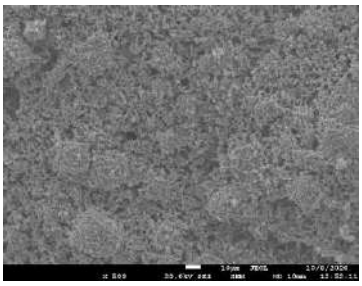

Figure 1: a) Structure of barium hexaferrite $BaFe_{10}Al_2O_{19}$, magnification x5000; b). Surface morphology of barium hexaferrite $BaFe_{10}Al_2O_{19}$, magnification x500

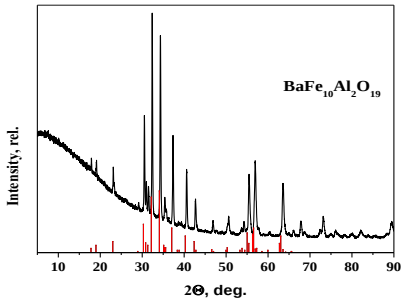

Figure 2: Diffraction pattern of the $BaFe_{10}Al_2O_{19}$ sample

A sample of ceramic material $BaFe_{10}Al_2O_{19}$ was obtained by solid-phase synthesis at a temperature of 1380 ° C. Based on the data obtained, it can be concluded that the temperature of 1380 ° C is optimal for obtaining the synthesis of the sample. Comparing the literature data [1] with the obtained X-ray diffraction pattern, we can conclude that the sample is monophasic. Obtaining monophase samples of barium hexaferrite substituted with aluminum will allow further research aimed at modifying the base matrix. Varying the chemical composition of the samples will allow obtaining materials with customizable physical and chemical properties that meet operational requirements.

Acknowledgement

The reported study was funded by RFBR (project number 20-38-70057). Additionally, the project was supported President's grants for young doctors of science (MD-5612.2021.4).

References

[1] X. Obradors, A. Collomb, *Journal of Solid State Chemistry*, 1985, 171-181

Changes of chemical states of Ni, Zn, and W ions in $NiWO_4$ upon doping with $ZnWO_4$: an x-ray photoelectron spectroscopy study

G. Bakradze[1]*, and A. Kuzmin[1]
[1]*Institute of Solid State Physics, University of Latvia, Kengaraga 8, LV-1063, Latvia,*
**georgijs.bakradze@cfi.lu.lv*

X-ray photoemission spectroscopy (XPS) was used to monitor the chemical states of Ni, Zn, and W in microcrystalline $NiWO_4$ upon its doping with isomorphous $ZnWO_4$. It was found that the recorded spectra of the Ni 2p, Zn 2p, and W 4f photoelectron lines and Ni $L_2M_{23}M_{45}$, Zn $L_3M_{45}M_{45}$, and W $N_4N_{67}N_7$ Auger-transition lines show pronounced changes with increasing Zn concentration. The positions of resolved photoelectron and Auger-transition lines were combined to construct so-called chemical-state plots for metal ions in solid solutions. With increasing Zn concentration, the Auger-parameter values increase for Ni and decrease for W; thus, evidencing a decrease and increase of the electronic polarizability around core-ionized Ni and W ions, respectively. At the same time, the character of Zn-O bonds and the local structure around Zn ions do not change. It was concluded that the dilution of $NiWO_4$ with Zn ions is accompanied with an increase of the Ni-O bond ionicity and an increases of the W-O bond covalency. These changes are attributed to the charge redistribution among $[NiO_6]$ and $[WO_6]$ structural units. We show that a careful in-depth analysis of XPS data obtained using a laboratory-based XPS facility can give chemically sensitive, qualitative information on the changes in the first coordination spheres of each metal ion. This information is otherwise only accessible by synchrotron-based techniques (such as x-ray absorption spectroscopy).

Acknowledgement

G.B. acknowledges the financial support provided by the State Education Development Agency for project No.
1.1.1.2/VIAA/3/19/444 (agreement No. 1.1.1.2/16/I/001) realized at the Institute of Solid State Physics, University of Latvia.

Study of the efficiency of shielding gamma radiation by telluride glasses

A. Kozlovskiy[1,2]*
[1]*The Institute of Nuclear Physics, Almaty 050032, Kazakhstan, kozlovskiy.a@inp.kz*
[2] *L.N. Gumilyov Eurasian National University, Nur-Sultan, 010008, Kazakhstan*

In recent years, one of the promising protective materials with fairly good transparency are amorphous-like glasses or ceramics based on TeO_2, WO_3, SiO_2, Bi_2O_3, Sm_2O_3, Nb_2O_5, MoO, NaO, CeO_2, etc. [1-3]. The interest of researchers in these structures is due to their unique combination of structural, optical, strength properties, as well as their high density, comparable to that of lead. Of great interest among all combinations of these oxides are structures based on TeO_2, WO_3, and Bi_2O_3, which have not only good strength and optical characteristics, but also high shielding characteristic.

This work is devoted to the study of the effect of doping glass based on TeO_2-WO_3 with Bi_2O_3, as well as the assessment of their strength, optical and radiation shielding characteristics. A distinctive feature of this work from previous similar studies is the acquisition of real experimental data on the gamma radiation shielding characteristic. It should be noted that in view of the low availability of gamma radiation sources, most of the studies known to date are limited to theoretical data of radiation shielding characteristics based on calculations of the Monte Carlo model and MCNP5, WINXCOM program codes. Despite the high value of these works, real experimental data of shielding characteristics for real practical application and introduction of glasses into industry are required, which makes such works relevant today. The influence of Bi_2O_3 doping on the radiation shielding characteristics of the synthesized glasses was determined by determining the transmitted intensity through 10 mm thick glass from Co^{57}, Cs^{137}, Na^{22} gamma quanta sources with energies of 130, 660, and 1270 keV, respectively. The use of these source types makes it possible to assess radiation shielding efficiency in gamma-quantum energy range from 0.1 to 1.3 MeV, which are the most common in use.

During the experiments conducted, it was found that doping Bi_2O_3 at X above 0.15 leads to a significant increase in strength by more than 30 %, which indicates an increase in glass resistance to external effects. Analysis of optical characteristics showed that the addition of Bi_2O_3 to the glass composition leads to a slight decrease in transmission in the visible light region, as well as an increase in band gap from 3.32 eV to 3.78-3.81 eV. According to the obtained radiation shielding characteristics data, TWBO-4 and TWBO-5 samples, for which a decrease in gamma quanta intensity is observed, have the highest radiation shielding efficiency, which varies from 50 % (for gamma quanta with an energy of 1270 keV) to 75 % and 96 % (for gamma quanta with energies of 660 keV and 130 keV), respectively. The radiation shielding efficiency greater than 50 % for TWBO-4 and TWBO-5 samples in the case of shielding of gamma quanta with an energy of 1270 keV is due to the presence of additional electron traps and absorption bands leading to additional absorption of the formed electron-positron pairs.

References

[1] A. Temir, et al. Solid State Sciences 115 (2021): 106604.
[2] A.L. Kozlovskiy, and M. V. Zdorovets. Materials Chemistry and Physics (2021): 124444.
[3] A. Temir, et al. Optical Materials 115 (2021): 111037.

Investigation of the effect of swelling in lithium-containing ceramics

B. Abyshev[1], K.Sh. Zhumadilov[1], A. Kozlovskiy[1,2]*
[1] *L.N. Gumilyov Eurasian National University, Nur-Sultan, 010008, Kazakhstan*
[2]*The Institute of Nuclear Physics, Almaty 050032, Kazakhstan, kozlovskiy.a@inp.kz*

At present, one of the promising research areas in the field of nuclear structural materials science is the study of the swelling processes of structural materials as a result of the radiation defect accumulation. The interest in this research topic is due to the need to obtain new data on radiation resistance and further evolution of defects in the structure of the near-surface layer, which can have a significant negative effect on mechanical, strength and heat-conducting properties. Lithium-containing ceramics such as Li_2ZrO_3, Li_2AlO_3, Li_2TiO_3 are promising materials for thermonuclear power engineering and new generation reactors. These ceramics have high mechanical properties, good degradation resistance, and conductive properties. Special interest in them on the part of researchers engaged in nuclear materials for thermonuclear energy is due to the high multiplication factor and release of tritium as a result of nuclear reactions under the influence of thermal neutrons $^6Li + n \rightarrow {}^4He + T + 4{,}8$ MeV. However, despite all the prospects of these materials for use as blanket materials, a number of questions remain that are associated with the influence of structural parameters and the structural ordering degree on the resistance to the accumulation of radiation defects arising both as a result of irradiation and in the process of nuclear reactions during the accumulation of helium. in the structure.

The aim of this work is to study the stability of Li_2ZrO_3 ceramic obtained using solid-phase synthesis method combined with thermal annealing at temperatures of 600-1100°C to the radiation damage accumulation and subsequent swelling as a result of helium bubble formation. Radiation damage processes were simulated by irradiation with 40 keV He^{2+} ions and 10^{15}-10^{18} ion/cm^2 doses. The choice of these irradiation conditions is due to the possibility of modeling the effect of helium swelling as a result of helium implantation with concentration of 0.1-5 at % into the structure of the near-surface layer with thickness of 100-200 nm.

As a result of the studies carried out, it was found that selected ceramics have a high degree of resistance to helium swelling processes, while the amorphization processes of the near-surface layer are associated with the helium accumulation and subsequent swelling processes.

Influence of heat treatment on photovoltaic properties of CdS/$Cd_xPb_{1-x}S$ solar cell grown by CBD method

M. Lysanova[1], V. Rogozin[1*], V. Markov[1,2] and I. Selyanin[1]
[1]*Physical and Colloidal Chemistry Department. Ural Federal University Named After the First President of Russia B.N. Yeltsin. Mira St., 19. Yekaterinburg, 620002. Sverdlovsk Region. Russia. E-mail: rogozin0904@gmail.com*
[2]*Ural State Fire Service Institute of Emergency Ministry of Russia. Mira St., 22. Yekaterinburg, 620022. Sverdlovsk Region. Russia.*

Solid solutions of lead-cadmium sulfide have many applications due to their unique photoelectric properties. Our study shows an example of obtaining a solar cell based on a heterostructure with a p-n junction, where cadmium sulfide CdS is used as the n-layer, and the p-layer is a solid solution of substitution of lead-cadmium sulfide $Cd_xPb_{1-x}S$.

The study was carried out in order to find out the effect of preliminary heat treatment on the properties of a solar cell with the FTO/CdS/$Cd_xPb_{1-x}S$. structure. Slides were used as a substrate, on which a layer of FTO (Fluorine-doped Tin Oxide) with a thickness of ~ 430 nm was applied by ultrasonic spray pyrolysis. Cadmium sulfide was deposited on top of the FTO layer by the hydrochemical bath deposition (CBD) method according to the technology described in [1]. Then, according to a similar procedure [2], a layer of lead sulfide was deposited with the content of Cd^{2+} ions in the mixture up to a concentration of 0.01 mol/L. The deposited films evenly cover the substrate and have good adhesion. The layer thicknesses were determined by electron microscopy and amounted to 400 nm and 492 nm for CdS and $Cd_xPb_{1-x}S$, respectively.

Films of cadmium sulfide were additionally subjected to temperature treatment in an air atmosphere at temperatures from 250 °C to 450 °C.

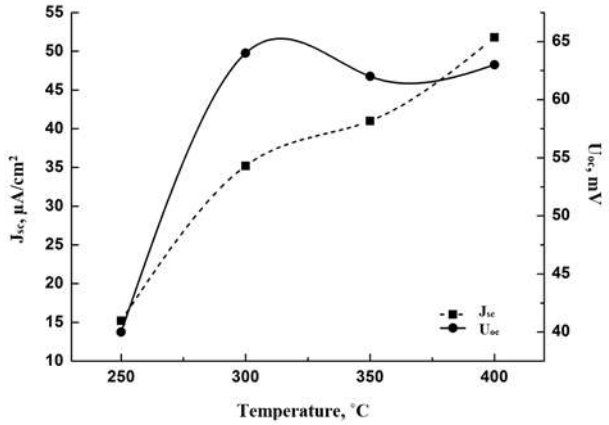

Fig. 1. Dependence of J_{sc} and U_{oc} of the FTO/CdS/$Cd_xPb_{1-x}S$ solar cell on the temperature of preliminary heat treatment.

Photoelectric properties were studied using a Keithley 2450 source-meter (Calibrator-multimeter) under illumination of 100 mW/cm^2 with a xenon lamp. The important parameters characterizing the efficiency of the solar cell are the short-circuit current J_{sc} and the open-circuit voltage U_{oc}. With an increase in the annealing temperature of the cadmium sulfide layer for the FTO/CdS/$Cd_xPb_{1-x}S$ system, there is a threefold increase in the parameter J_{sc} (Fig. 1). This effect can be explained by the fact that during the heat treatment the residues of the reaction mixture and other impurities are removed from the intergranular space of the cadmium sulfide film and the additional formation of oxide phases, as evidenced by the appearance of an orange-red tint in all samples upon exposure to temperature. Also, according to literature data, it is known about the polymorphic transition of cadmium sulfide from the sphalerite structure to wurtzite at ~300 ° C, which can also affect the properties of photoactive layers.

The results of the study show that the preliminary temperature treatment contributes to an increase in the photoelectric characteristics of solar cells of the FTO/CdS/$Cd_xPb_{1-x}S$ structure.

References

[1] N.Forostyanaya, A. Polepishina, V. Markov and L. Maskaeva, Chimica Techno Acta Volume 1. No. 3. (2014) Pages 98-103.
[2] L. Maskaeva, A. Kutyavina, V. Markov, I. Vaganova and V. Voronin, Journal of General Chemistry Volume 88 №. 2 (2018) Pages 295-304.

Electrophysical properties of single crystals of ferrite with a magnetoplumbite structure

N.A. Cherkasova[1], V.E. Zhivulin[1]* and Vinnik D.A.[1]
[1]*South Ural State University (National Research University), 454080, Lenin ave.76, Chelyabinsk, Russia, zhivulinve@mail.ru**

Hexagonal ferrites with a magnetoplumbite structure ($MeFe_{12}O_{19}$ where Me = Sr, Ba, Pb) are promising functional materials for use in high-frequency electronics. Varying the chemical composition of ferrite by replacing some of the iron atoms with atoms of other elements such as Ti, Al, Mn leads to a strong change in the magnetic and electrophysical properties of the material. The degree of change in physical properties is proportional to the concentration of the doping element. This makes it possible to obtain materials whose properties can be controlled.

This work is devoted to the study of the temperature dependence of the resistance of a single crystal of barium hexaferrite with the composition $BaFe_{10.7}Ti_{1.3}O_{19}$.

The studied single crystal was obtained by the method of spontaneous crystallization from solution. As the initial components for the preparation of the charge were used: iron oxide (Fe_2O_3), titanium oxide (TiO_2), barium carbonate ($BaCO_3$). Sodium oxide (Na_2O) in a form of sodium carbonate was used as a solvent. In work [1], the optimal concentration 26.6 molar % of the solvent for growing single crystals of barium hexaferrite was determined.

The temperature dependence of the resistance was measured using a digital multimeter in a two-wire circuit. Two copper cylinders were used as conductive electrodes, providing a constant clamping force to the sample.

The obtained single crystals have a natural faceting in the form of flattened hexagons. The presence of faces allows to visually determine the crystallographic planes. The direction along the hexagonal crystal is the easy magnetization axis (*c* axis).

The temperature dependence of the resistance was measured along the *c* axis (easy magnetization axis). Figure 1 shows the logarithm of the resistance as a function of reciprocal temperature, the curve has two linear sections. The beginning of the inflection of the curve occurs at a temperature of 245 °C and, in our opinion, this is due to the transition from a magnetic state to a nonmagnetic one (Curie temperature). The activation energies were calculated from the linear sections of the dependence, which are E1 = 0.41 eV and E2 = 2.85 eV.

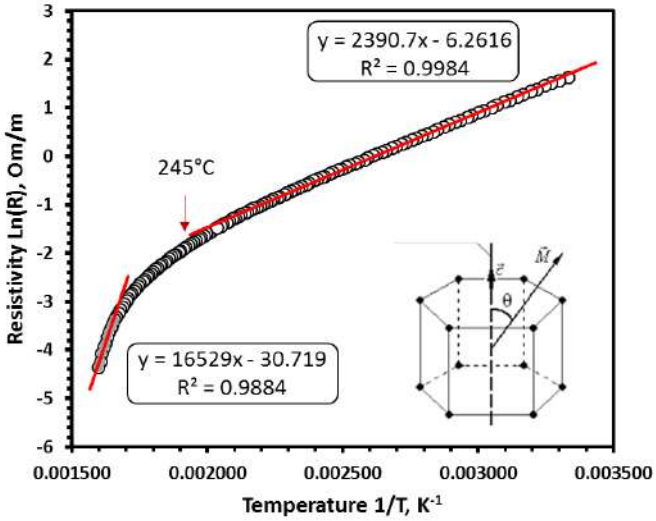

Fig. 1. Temperature dependence of the logarithm of resistance for a $BaFe_{10.7}Ti_{1.3}O_{19}$ single crystal

References

[1] R.J. Gambino, F. Leonard, Journal of the American Ceramic Society Volume 44(5) (1961) Pages 221-224.
The reported study was funded by RFBR (project number 20-38-70057).

Impact of Al^{3+} ions on the magnetic properties of barium hexaferrite

I.A. Solizoda[1*], V.E. Zhivulin[1], S.V. Taskaev[1,2,3] and D.A. Vinnic[1]
[1]*Sout Ural State University, 454080, Russian Federation, Chelyabinsk, Lenin Avenue, 76*
[2]*Chelyabinsk State University, 454001, Russian Federation, Chelyabinsk, 129 Bratiev Kashirinykh St.*
[3]*National University of Science and Technology "MISIS", 119049, Russian Federation, Moscow, Lenin Avenue, 4*

The purpose of this work is to study the magnetic properties of aluminum-substituted M-type barium hexaferrite, with the general formula **$BaFe_{12-x}Al_xO_{19}$ ($BaM:Al_x$)**, where **x** varies from **0** to **5**, synthesized by the solid-phase synthesis method.

Formulas of synthesized samples (Fig.1) were calculated from the data of energy dispersion spectroscopy using the Oxford INCA X-max 80 EDX analyzer installed on the SEM Jeol JSM 7001F electron microscope. The Curie temperatures of the samples (Fig.2) were measured using differential scanning calorimetry STA 449 F1 Jupiter NETZCH.

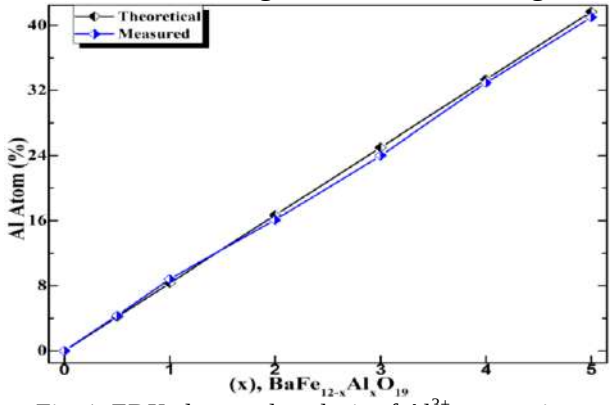

Fig. 1. EDX elemental analysis of Al^{3+} content in $BaM:Al_x$ samples

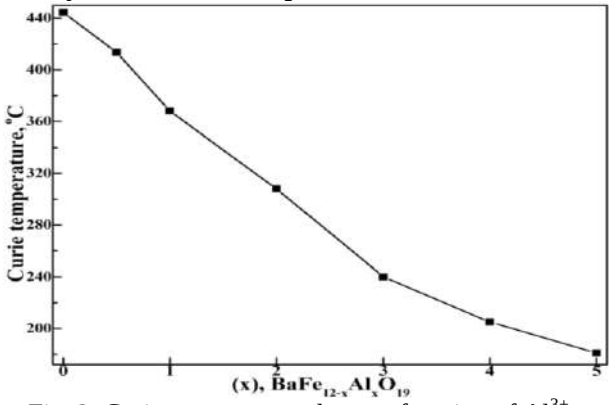

Fig. 2. Curie temperature plot as a function of Al^{3+} content for $BaM:Al_x$ samples

The magnetic properties of the samples (Fig. 3-4) were measured at room temperature using a Versa Lab Quantum Design magnetometer. An increase in the concentration of Al^{3+} in this system leads to a decrease in the Curie temperature (Tc), magnetization saturation (Ms) and an increase in the value of the coercive force (Hc).

The monotonic decrease in Tc and Ms with an increase in the concentration of Al^{3+} is associated with the statistical distribution of Al^{3+} ions in the structure of barium hexaferrite.

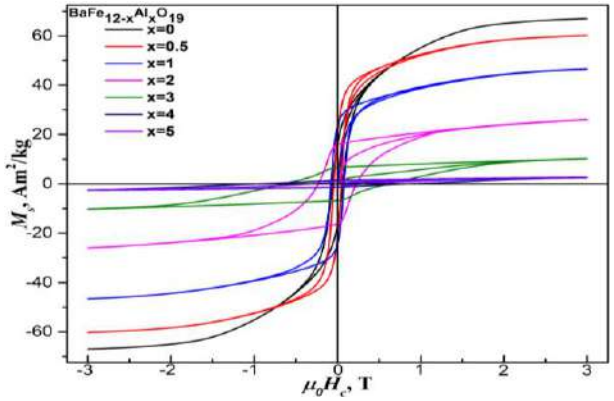

Fig. 3. Hysteresis loops for $BaM:Al_x$ samples

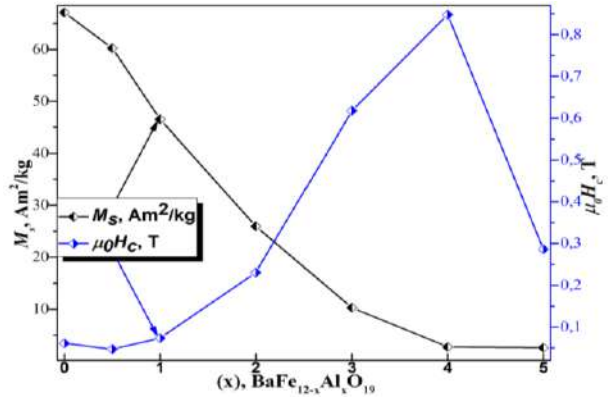

Fig. 4. Concentration dependence of the Ms and Hc for the $BaM:Al_x$ samples

The reported study was funded by RFBR (project number 20-38-70057). Additionally, the project wassupported President's grants for young doctors of science (MD-5612.2021.4).

Investigation of the electrophysical properties of titanium-substituted barium hexaferrite in the high-frequency range

A.Yu. Starikov[1]*, D.S. Klygach[1], M.G. Vakhitov[1], V.E. Zhivulin[1] and D.A. Vinnik[1]
[1] *South Ural State University, 454080, 76, Leninn Ave., Chelyabinsk, Russia, starikov-andrey@mail.ru**

The aim of the presented work is to study the electrophysical properties of the obtained by solid synthesis reaction titanium substituted barium hexaferrite.

The use of the material obtained in this way will largely depend on its properties, which are due to the introduction of certain elements. Many articles describe the electromagnetic properties, the dependence of the dielectric and magnetic permeability on frequency, and the magnetic properties of hexafferite using various dopants [1-3]. A significant increase in the dielectric and magnetic permeability and their nonlinear dependence on frequency is explained by the fact that when ions of another material are introduced into the crystal, ionic polarization increases. This, in turn, leads to an increase in dielectric and magnetic permeability.

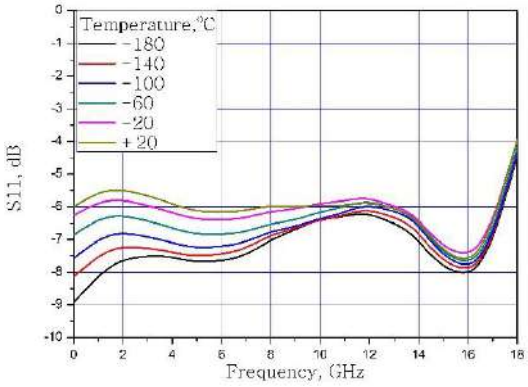

Fig. 1. Frequency dependence of the S11 measuring line with $BaFe_{11.75}Ti_{0.25}O_{19}$ at different temperatures

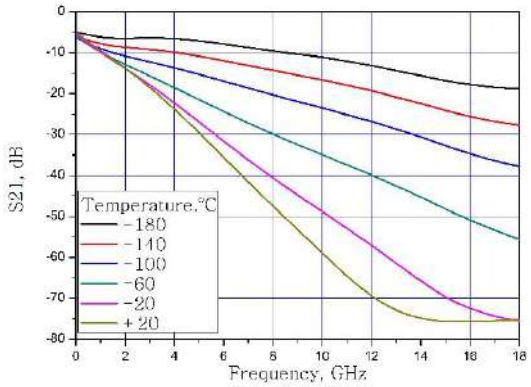

Fig. 2. Frequency dependence of the S21 measuring line with $BaFe_{11.75}Ti_{0.25}O_{19}$ at different temperatures

The main effect on the dielectric constant is the incorporation of the titanium ion in the frequency range 2 - 18 GHz. In this frequency range, the main contribution to polarization is made by dipole polarization. Since the dipole moment of the Ti^{+4} and O^{-2} pair is 2.5 times greater than for Fe^{+3} and O^{-2}. The introduction of titanium significantly changes the dielectric constant of the material in the frequency range 2 - 18 GHz. For comparison, if we consider barium hexaferrite with aluminum Al in the same frequency range, then at low frequencies the introduction of aluminum has no effect. Since the dipole moment for the pair Al^{+3} and O^{-2} is practically equal to the dipole moment of Fe^{+3} and O^{-2}.

Acknowledgement

The reported study was funded by RFBR (project number 20-38-70057). Additionally, the project was supported President's grants for young doctors of science (MD-5612.2021.4).

References

[1] S.-E. Lee, H.-J. Kim, J.-H.. Lee, K.-S. Oh, H.T. Hahn and J.-W. Choi, Mater. Lett. 187 (2017) 94-97.
[2] S. Pignard, H. Vincent, E. Flavin and F. Boust, J. Magn. Magn. Mater. 260 (2003) 437-446.
[3] S.S.S. Afghahi, M. Jafarian, and C.A. Stergiou, J. Magn. Magn. Mater. 419 (2016) 386-393.

Influence of the Mn, Ti- doped of Barium Hexaferrite on lattice parameters and Curie Temperatureuence

K. Pavlova[1]*, A. Starikov[1], and D. Vinnik[1]
[1]South Ural State University, 76, Lenin Ave., Chelyabinsk 454080, Russia.
*pavlovakp@susu.ru

Mn, Ti substituted samples of barium hexaferrite were obtained. In the course of the study, the technology of obtaining the investigated material by solid-phase synthesis was developed.

Pure powders of iron Fe_2O_3, titanium TiO_2, manganese Mn_2O_3, and barium carbonate oxides $BaCO_3$ were used to obtain substituted barium hexaferrite. The obtained tablets were placed in a high-temperature electric furnace and sintered for 5 hours at temperatures $BaFe_{12}O_{19}$, $BaFe_{11}Ti_1O_{19}$, $BaFe_{10.9}Ti_1Mn_{0.1}O_{19}$, of 1400 °C, the $BaFe_{11.9}Mn_{0.1}O_{19}$ sample was sintered at a temperature of 1300°C. Because of the sintering operation, four ceramic samples with different chemical compositions were obtained.

Figure 1 shows the X-ray diffraction curves of the studied samples. The vertical lines indicate the literary data [1]. The coincidence of the positions and intensities of the reflexes given in the literature and on the experimental spectra indicates that the structure of the obtained samples coincides with the structure of barium hexaferrite.

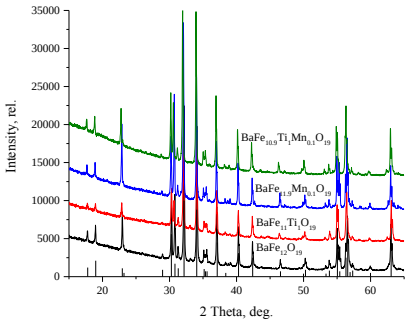

Figure 1. X-ray diffraction patterns of the obtained samples.

Table 1. The lattice parameters and Curie tempherature

№	Formula	Tc, [℃]	*a, [Å]*	*c, [Å]*	*V, [Å^3]*
1	$BaFe_{12}O_{19}$	450	5,8934(4)	23,2031(11)	698,01(9)
2	$BaFe_{10,98}Ti_{1,02}O_{19}$	320	5,8869(3)	23,2768(11)	698,59(7)
3	$BaFe_{11,85}Mn_{0,15}O_{19}$	447	5.8896(3)	23.2015(8)	696.97(6)
4	$BaFe_{10,96}Mn_{0,1}Ti_1O_{19}$	322	5,89217±0.00012	5,89217±0.00012	23,2949±0.0006
	$BaFe_{12}O_{19}$[1,2]	457	*a= 5,8930 Å; c= 23,1940 Å, V= 697,5 Å^3*		

Table 1 shows the calculation of the crystal lattice parameters based on the data‘s powder rengenograms and the Curie temperatures of the obtained samples are indicated, which was obtained from scanning differential calorimetry data with using the heating rate data of the furnace. The Curie temperature for the initial barium hexaferrite is noticed in the literature [2].Table shows that when iron atoms are replaced by titanium and manganese atoms, the crystal lattice is distorted. The distortion of the crystal lattice is associated with the substitution of Fe^{3+} iron atoms having an effective ionic radius (0.63 Å) for Mn^{3+} (065 Å) and Ti^{4+} (0.42 Å, at CN= 4) atoms. Based on experimental data, it can be assumed that the closer the substituted element is in its electronic configuration to iron atoms, the smaller the deviations from the linear nature of the relationship between the size of the crystal lattice and the concentration of impurity atoms, accordingly, the smaller the difference in the value of the Curie temperature.

Acknowledgement
This work was supported by the RFBR (project No 20-38-70057) and President’s grants for young doctors of science (MD-5612.2021.4).

References

[1] W.D. Townes, J.H. Fang, A.J. Perrotta, The crystal structure and refinement of ferromagnetic barium ferrite, $BaFe_{12}O_{19}$, Zeitschrift für Kristallographie. 125 (1967) 437-449.
[2] S.A. Gudkova, D.A. Vinnik, V.E. Zhivulin et. al. Synthesis, Structure and Properties of Barium and Barium Lead Hexaferrite, J. Magn. Magn. Mater. 470 (2019) 101-104.

New strategies for producing of film structures based on Si_xGe_{1-x}

I. Gavrilin[1,3]*, N. Grevtsov[2], A. Dronov[1,4], E. Chubenko[2], V. Bondarenko[2] and S. Gavrilov[1]
[1] *National Research University of Electronic Technology (MIET), Shokin Square, Zelenograd, 124498, Russia , gavrilin.ilya@gmail.com**
[2] *Belarusian State University of Informatics and Radioelectronics, P. Brovki str. 6, Minsk 220013, Belarus*
[3]*Frumkin Institute of Physical Chemistry and Electrochemistry Russian Academy of Sciences, 31, bld.4, Leninsky prospect, Moscow, 119071, Russia*
[4]*Faculty of Physics, M.V. Lomonosov Moscow State University, Leninskie Gory, Moscow 119991,Russia*

Film structures based on Si_xGe_{1-x} are widely used in high-temperature thermoelectric converters, which have high stability and high efficiency in the temperature range 800-1100 °C, which provides a wide range of their application. For example, such materials use for the utilization of heat removed during various high-temperature processes [1]. Also Si_xGe_{1-x} films are used in optoelectronic devices [2].

However, in view of the high cost of crystalline Ge and its gaseous precursors, compounds with a low Ge concentration, which do not have a combination of electrophysical and physicochemical parameters that are optimal for thermoelectric conversion, are usually used to obtain Si_xGe_{1-x} alloys. The scientific novelty of the research consists in the application of a new approach to the formation of film Si_xGe_{1-x} structures. The technology are based on the recently established possibility of producing Ge by its electrochemical reduction on metal particles with lowmelting point from solutions containing germanium oxide [3]. The technology under development includes electrochemical processes for the formation of porous silicon, the deposition of metals with low melting point and Ge, which, after high-temperature processing, allow the synthesis of film structures based on Si_xGe_{1-x} solid solutions with the required composition. The morphology and composition of the samples are investigated by scanning electron microscopy, Raman spectroscopy and X-ray diffraction.

This method will provide the ability to obtain film structures of silicon-germanium, but it will be more technologically advanced at lower cost compared to existing methods for producing thin-film Si_xGe_{1-x} structures.

Acknowledgement
This research was financially supported by the Russian Science Foundation (Project no. 20-19-00720).

References

[1] A. Usenko, D. Moskovskikh, M. Gorshenkov, A. Voronin, A. Stepashkin, S. Kaloshkin, D. Arkhipov, V. Khovaylo, “Enhanced thermoelectric figure of merit of p -type Si 0.8 Ge 0.2 nanostructured spark plasma sintered alloys with embedded SiO 2 nanoinclusions,” Scripta Materialia, 127 (2017), 63–67.
[2] C. Kriso, F. Triozon, C. Delerue, L. Schneider, F. Abbate, E. Nolot, D. Rideau, Y.-M. Niquet, G. Mugny, C. Tavernier, Solid-State Electronics, 129 (2017), 93–96.
[3] I. Gavrilin, D. Gromov, A. Dronov, S. Dubkov, R. Volkov, A. Trifonov, N. Borgardt, S. Gavrilov, Semiconductors 51 (2017) 1067-1071.

Influence of the synthesis conditions and surface modification of nanoporous alumina on the contact angle

A. Bondaruk[1,2]*, T. Klimovich[3], D. Shimanovich[4], A. Vorobjova[4] A. Truhanov[1] and D.Tishkevich[1]

[1]*SSPA "Scientific and Practical Materials Research Centre of NAS of Belarus", 220072 Minsk, P.Brovki str. 19, Belarus, *bondaruk625@gmail.com*

[2]*Belarusian State Technological University, 220006 Minsk, Sverdlova str. 13A, Belarus*

[3]*Belarusian National Technical Uniiversity, 220013Minsk, Nezavisimosti ave. 65, Belarus*

[4]*Belarusian State University of Informatics and Radioelectronics, 220013 Minsk, P.Brovki str. 6, Belarus*

Porous alumina films have a number of unique properties: nanosized an ordering porous structure, a small dispersion of pores' diameter, high mechanical strength etc. The presence of nanopores is one of the main reasons for the possibility of wettability properties variation on the porous alumina (PA) surface. The PA films wettability has an importance for the using in the functional composites obtaining, corrosion resistance and for biological transport.

The experimental samples were formed from Al foil (99.994%) with 100 μm thickness. After preliminary treatment the PA samples were two-step anodized in 4% $H_2C_2O_4$ at 40, 50, 60 V. The contact angle was measured using the dispensed drop technique. Scanning electron microscope (SEM) CarlZiess EVO10 was used for the PA surface investigations.The surface modification of the PA films was carried out by etching in 10% NaOH solution at a 35-40 ^oC temperature with 15-60 sec duration.

Figure 1 shows SEM images of the PA films surface. It is seen that with an increase of the anodizing voltage from 40 to 60 V the average pore diameter (d) rises from 50 to 85 nm respectively.

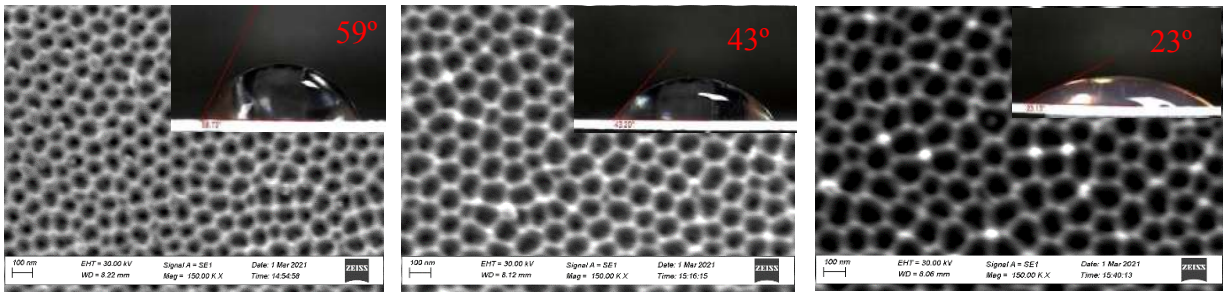

A **b** **C**

Figure 1 – SEM images of PA samples surface obtained at 40 V (a), 50 V (b), 60 V (c) anodizing voltage and the values of corresponding contact angle

It has been shown that with an increase in the pore diameter in the range of 50-85 nm the wettability of the PA surface grows up due to the capillary effect. However, the surface modification via chemical etching in 10% NaOH solution leads to the more intensive process of porous structure destruction due to uncontrolled etching of an ordered pores walls. At the same time, this process affects to the contact angle which changes from 48 to 31° for the samples obtained at 50 V.

Thus, it has been found that variation using both the synthesis conditions and surface modification of the PA films it is possible to obtain a microstructure with controllable wettability, which is promising for electronics, optoelectronics, magnetism studying, biomaterials using etc.

References

[1] A. Vorobjova, D. Tishkevich et al.The influence of the synthesis conditions on the magnetic behaviour of the densely packed arrays of Ni nanowires in porous anodic alumina membranes// RSC Advances. – 2021. – 11:3952.

Physical Investigations on Cu_2ZnSnS_4 Monograin Solar Cells

K. T. Ramakrishna Reddy[1*], P. Padma Priyanka[1], P. Babu[1], M. A. Gapanovich[2]
[1]*Solar Photovoltaic Laboratory, Department of Physics, Sri Venkateswara University, Tirupati, 517502, India. *e-mail: ktrkreddy1@gmail.com*
[2]*Laboratory of Photoelectrolysis, Institute of Problems in Chemical Physics, Russian Academy of Sciences, Chernogolovka, 142432, Russia.*

Currently, solar cells made using earth abundant and low-toxic materials are attracting much attention. Cu_2ZnSnS_4 (CZTS) is one such material that possesses suitable properties for solar cell development [1,2]. Monograin solar cells have many advantages compared to thin film solar cells. The fabrication of CZTS-based monograin solar cell and its performance is presented. CZTS monograin powder was prepared using its constituent binary using simple chemical precipitation method. The monograin powders were prepared with three different Zn/Sn ratios, in the range, 0.90 – 1.12 with a constant Cu/(Zn+Sn) ratio of 0.8.

The synthesized monograin powders were subjected to chemical treatment using NH_4OH and HCl to prepare phase pure CZTS monograins by removing secondary phases. The X-ray diffraction data and Raman analysis of as-grown powders showed Cu_xS and SnO_2 phases in addition to CZTS phase while the chemically treated samples indicated only CZTS phase without any impurity phases. CZTS-based monograin solar cells were developed using chemical bath deposited CdS as the buffer on CZTS grains in epoxy film. DC sputtered Al-doped ZnO was coated as the window layer. The initial results on CZTS/CdS/AZO devices showed a conversion efficiency of 2.8 %.

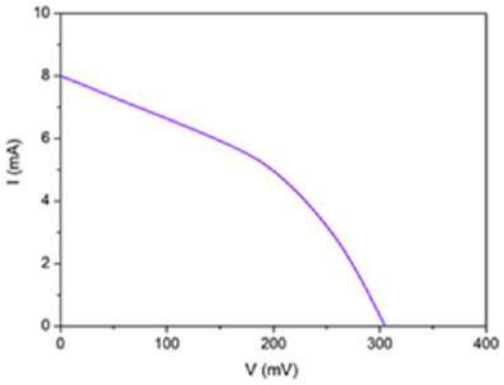

Figure: Current - voltage characteristics of CZTS/CdS/AZO monograin solar cell.

Acknowledgements
The authors wish to acknowledge the financial support from the Ministry of Science and Technology, Governemnt of India and Ministry of Education and Science, Russia Federation via Indo-Russian Joint Research Project.

References
[1] K. Ito, T. Nakazawa, Jpn. J. Appl. Phys. 27, 1988, pp. 2094-2097.
[2] E. Mellikov, J. Hiie, M. Altosaar, SPIE Proceedings. 222, 1994, pp. 177-185.

Vibrational properties of Cu_3SeTe by Raman spectroscopy

S. Ibrahimova
Institute of Physics ANAS, H. Javid, 131, AZ-1143, fizik-3@mail.ru

Copper-chalcogen (Se, S, Te) systems occupy an important place among semiconductor compounds. The reason for the interest in these materials is the significant physical and chemical properties observed in them. Copper chalcogenides exhibit superconductivity at very low temperatures ($T \leq 5.6$ K), semiconducting or metallic conductivity at intermediate temperatures, and ionic conductivity above $T = 350$ K. Another interesting feature of these systemic compounds is that they have several structural phase transitions that occur depending on temperature. As we have already mentioned, copper-chalcogen systems have been repeatedly used in detail by different authors. Among these studies, works on the Cu-Te system attract more attention. The above studies are mainly devoted to the construction of phase diagrams of these systems, the study of the physicochemical and thermodynamic properties of crystals of compounds and solid solutions formed in the system, as well as the influence of the chalcogen-Cu ratios on the phase formation process in the system.

In this work, a compound containing Cu_3SeTe at the same concentrations of Se and Te halogen atoms was synthesized, its crystal structure was investigated by X-ray diffraction, and atomic dynamics was investigated by Raman spectroscopy.

Vibrational properties of the samples were studied by Raman spectroscopy method. The experiments were carried out on the Nanofinder 30 Raman spectrometer at room temperature. Nd:YAG laser with a wavelength $\lambda = 532$ nm and a maximum power of 10 mW was used as an excitation source. The obtained spectra were analyzed by the Gaussian function.

During the analysis of the spectrum, it was determined that 6 Raman modes are observed in the frequency range $\nu = 0 – 800$ cm^{-1}: $\nu_1 = 41.56$ cm^{-1}, $\nu_2 = 91.47$ cm^{-1}, $\nu_3 = 119.83$ cm^{-1}, $\nu_4 = 139.51$ cm^{-1}, $\nu_5 = 208.18$ cm^{-1} and $\nu_6 = 266.41$ cm^{-1}. It is known from studies of Raman spectroscopy that the frequencies of bonds formed by heavy ions fall into the range of low frequencies. In the high-frequency region, the frequencies of bonds formed by atoms of light elements such as oxygen and hydrogen are observed. When studying a composite material based on the composition Cu_3Se_2, it was determined that the vibrations observed at a frequency $\nu = 259$ cm^{-1} correspond to Cu-Se bonds. For the CuSe content in the study of the $CuS_{1-x}Se_x$ system: $\nu_1 = 17$ cm^{-1}, $\nu_2 = 43$ cm^{-1}, $\nu_3 = 45$ cm^{-1}, $\nu_4 = 192$ cm^{-1}, $\nu_5 = 206$ cm^{-1} and $\nu_6 = 263$ cm^{-1} the vibration mode was observed. It was shown that the vibrational mode $\nu_6 = 263$ cm^{-1}, which has a higher frequency, corresponds to the frequencies of chalcogen Se-Se bonds. These modes were observed in thin Cu_3Se_2 thin films at $\nu_1 = 195.5$ cm^{-1} and $\nu_2 = 259.2$ cm^{-1}.

During the theoretical calculation of the vibrational modes of the Cu_3Te_2 compound, it was determined that a large number of Raman and IQ modes can be observed in this compound. In the frequency range $\nu = 50$-180 cm^{-1}, 12 optical modes can be observed. Modes $\nu_1 = 131.3$ cm^{-1} and $\nu_2 = 179.2$ cm^{-1} can be shown, which correspond to the modes observed in the compound of Cu_3SeTe. Experimental Raman modes of the $Cu_{2-x}Te$ system were observed at frequencies: $\nu_1 = 68$ cm^{-1}, $\nu_2 = 77$ cm^{-1}, $\nu_3 = 116$ cm^{-1}, $\nu_4 = 138$ cm^{-1}.

Comparing the values of the combination modes obtained experimentally for the Cu_3SeTe compound with the values of the combination modes obtained for the Cu-Se and Cu-Te systems, we see that $\nu_1 = 41.56$ cm^{-1}, $\nu_5 = 208.18$ cm^{-1} and $\nu_6 = 266.41$ cm^{-1} modes corresponds to Cu-Se and Cu-Se bonds. $\nu_2 = 91.47$ cm^{-1}, $\nu_3 = 119.83$ cm^{-1}, $\nu_4 = 139.51$ cm^{-1} Raman modes correspond to Cu-Te and Te-Te bonds.

Roughness Parameters of Cu_2SnS_3Thin Films Using Atomic Force Microscopy

C. Sumalatha[a], G. Phaneendra Reddy[a], K.T. Ramakrishna Reddy[a]*, M.S. Tivanov[b], V.Gremenok[c]
[a]*Department of Physics, Sri Venkateswara University, Tirupati - 517 502, India.*
[b]*Faculty of Physics, Belarusian State University, Minsk, Belarus.*
[c]*Scientific-Practical Materials Research Centre, National Academy of Sciences of Belarus, Minsk, Belarus.*

Surface roughness evaluation is very important for many fundamental problems such as friction, contact deformation, heat and electric conduction, tightness of contact joints and potential accuracy. Particularly in solar photovoltaic cells, surface roughness plays a crucial role in light scattering, minimizing the device efficiency. For this reason surface roughness has been the subject of experimental and theoretical investigations. In the current study, CTS films were prepared by using two-stage process, via sulfurization of DC magnetron sputtered Cu/Sn/Cu stacked layers at various sulfurization times ranging from 60 min to150 min at a constant sulfirization ttemperature of 450 ^{o}C. A detailed investigatyion of the surface properties in relation to sulfurization time was carried out using Atomoc Force Microscopy (AFM).The grain size, height parameters like root mean square roughness (S_q) and average roughness (S_a) were also calculated. Further, the shape parameters such as skewness (S_{sk}) and Kurtosis (S_{ku}) of the prepared films with sulfurization time was made in order to optimize the sufurization time to synthesize CTS layers for the deveopment of thin fim heterounction solar cells.

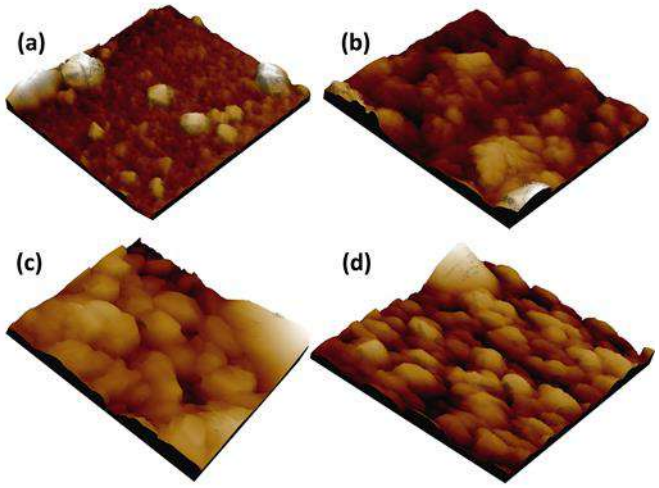

Figure. 1. AFM imges of sulfurized CTS films grown at sulfurization time of (a) 60 min, (b) 90 min, (c) 120 min, (d) 150 min.

Referances

[1] H. Dahman, L. El Mir, Cu2SnS3 thin films deposited by spin coating route: a promise candidate for low cost, safe and flexible solar cells, J. Mater. Sci. Mater. Electron. 26 (2015) 6032–6039. http://dx.doi.org/10.1007/s10854-015-3180-3.
[2] A. Boukhachem, M. Mokhtari, N. Benameur, A. Ziouche, M. Martlnez, P. Petkova, M. Ghamnia, A. Cobo, M. Zergoug, M. Amlouk, Structural optical magnetic properties of Co doped α-MoO3 sprayed thin films, Sens. Actuators A Phys. 253 (2017) 198–209, http://dx.doi.org/10.1016/j.sna.2016.11.032.
[3] E.S. Gadelmawla, M.M. Koura, T.M.A. Maksoud, I.M. Elewa, H.H. Soliman, Roughness parameters, J. Mater. Process. Technol. 123 (2002) 133–145, http://dx. doi.org/10.1016/S0924-0136(02)00060-2.

Electron structure and density of states' calculations of GeS crystal from first-principle

A. Dashdemirov
Azerbaijan State Pedagogical University, U. Hajibeyli, 68, AZ-1000,
dashdamirovarzu@gmail.com

From first principles, the phonon spectrum and phonon density of states of the layered ε-GaSe semiconductor are investigated in the linear response approximation based on the density functional theory. In the present work, the electronic structure and the density of states were studied for the GeS compound using the density functional theory method.

The article presents the results of calculations from first principles within the framework of the density functional theory of the electronic spectrum of a GeS crystal. The electronic structure of the crystal was studied using the Quantum Wise - Atomistix Tool Kit using MGGA approximation. Electron-ion interactions were taken into account through the FHI pseudopotential (Fritz Haber Institute).

Germanium monosulfide belongs to the class of semiconductors $A^{V}B^{VI}$ with p-type conductivity and is characterized by the orthorhombic crystal structure D^{16}_{2h} (Pnma). GeS has a layered crystal structure, where atomic layers are bound only by van der Waals forces. In this regard, there are no unfilled electronic levels on the surface of a GeS single crystal, due to which the material surface is characterized by high chemical stability. The number of electrons considered as valence electrons was 6 for Ge [Ar] $3\boldsymbol{d}^{10}4\boldsymbol{s}^{2}4\boldsymbol{p}^{2}$ и 6 for S [Ne] $3\boldsymbol{s}^{2}3\boldsymbol{p}^{4}$. The primitive and supercell were optimized with force and stress tolerances of 0.0001 eV/Å and 0.0001 eV/Å^3, respectively.

The calculated band structure of the GeS crystal is shown in fig. 1. It can be seen from the figure that the bottom of the conduction band is located at the symmetric point of the Brillouin zone Γ, and the top of the valence band is located between the symmetric points Γ and Z. This fact shows that the fundamental absorption edge of the crystal is formed by indirect transitions. The bandgap is 1.52 eV. This ensures the accuracy of further calculations such as optical transitions. It should be noted that in more than one theoretical work, the calculated width of the bandgap does not coincide with the experimental results as closely as in our work.

From the calculated partial densities of states of the crystal, it was found that the bottom of the conduction band is mainly formed from 3***p***- states of Ge with a small mixture of 3***p***- states of S atoms. There is an overlap between the 3***p***- S and 3***s***- Ge states in the energy range from – 0.65 to – 4.42 eV. Energy bands in the range – 2.3 - – 4.5 eV mainly take their origin from the 3***p***- states of Ge atoms. The 3***p***- states of S atoms contribute to the formation of the energy range (– 14 - –16) eV. The 3***s***- states of Ge atoms are partially involved in the formation of these bands.

It was found that GeS compounds have semiconducting properties with a bandgap of 1.96 eV. The main contribution of the bands in the vicinity of the Fermi level is from the - 3***p*** and 3***s*** states of the S and Ge atoms, respectively. The highest amplitude, about 2.3 eV ($\varepsilon_{\perp}$), is mainly associated with interband optical transitions between states S(***p***) + Ge(***s***) → Ge(***p***) + S(***s***).

The study of phase transitions in a system $Tm_XMn_{1-X}Se$ by means of ultrasonic experiments

O. Romanova[1*], S. Aplesnin [1,2], M. Sitnikov[2], A. Kharkov[2], L. Udod[1,2] and A. Galyas[3]
[1]*Kirensky Institute of Physics, Federal Research Center KSC SB RAS,660036 Krasnoyarsk, Russia, rob@iph.krasn.ru**
[2] *Reshetnev Siberian State University of Science and Technology,660014 Krasnoyarsk, Russia*
[3] *Scientific-Practical Materials Research Center NAS of Belarus, 220072 Minsk, Belarus*

It is known that in compounds doped with rare-earth elements (thulium, ytterbium and et all) along with a smooth change of the lattice parameters (lanthanoid compression), there is an anomalous interatomic distance [1]. This is explained by the fact that rare-earth metal ions are in two- valence states (or close to it). The corresponding ion has a larger ionic radius, which is reflected in an increase of the unit cell parameter, lattice deformation found in the measurement of structural, thermal and optical properties.

The work aims is to determine the structural and electronic phase transitions in manganese chalcogenides by elements of thulium with variable valence depending from temperature and concentration.

The $Tm_XMn_{1-X}Se$ samples were synthesized by the solid-state reaction in a stepwise mode. X-ray powder diffraction patterns of the compounds were detected at room temperature on a DRON-3. The ultrasound damping in the $Tm_XMn_{1-X}Se$ ($0.05 \le X \le 0.2$) compounds was measured on the tablets with two piezoelectric sensors, one being an ultrasound generator and the other, a sonic signal sensor, which was glued with a silver paste to the tablet planes. The ultrasound passage time was $\tau = 10^{-6}$ s at a frequency of 5 MHz; the sample thickness was 0.4 cm. The ultrasound damping coefficient was calculated by the formula: $\alpha = \ln (U_0/U)/d$, where U and U_0 are the voltage amplitudes detected by the ultrasound generator and sonic signal sensor and d is the thickness of the sample.

The X-ray diffraction analysis shows that the synthesized $Tm_XMn_{1-X}Se$ ($0.05 \le X \le 0.2$) samples have a NaCl-type cubic lattice typical of MnSe.

In the region of structural and magnetic (T_N=134K) phase transitions characteristic of monoselenide manganese, the ultrasound damping coefficient (α) is maximum and is associated with fluctuations in the density of the material. MnSe manifests a structural phase transition from a cubic phase to NiAs structure in 248 K < T < 266 K temperatures range, and below this temperature the phases coexistence in the sample is observed. For X = 0.05 and 0.1, a maximum was found on the dependence $\alpha(T)$ at 450K, which disappears with increasing concentration. The high-temperature maximum is associated with the dynamic Jahn-Teller effect as a result of a change in the lattice volume. The inclusion of ultrasound leads to an asymmetry of the I - V characteristic for X = 0.05 and 0.1 at T>300K. The dependence of current on voltage is nonlinear and there is no I - V characteristic hysteresis. With an increase in the substitution concentration up to X = 0.2, the asymmetry of the current-voltage characteristics disappears. The $Tm_XMn_{1-X}Se$ system has a critical temperature associated with a change in the sign of the electrical sound.

Acknowledgement
The reported study was funded by RFBR according to the research project №20-52-00005 Bel_a. The reported study was funded by BRFBR according to the research project № T20P-052.

References
[1] O. Romanova, L. Udod, O. Demidenko, IOP Conference Series: Materials Science and Engineering 918 (2020) 012001.

Impedance and Hall effect in $Tm_XMn_{1-X}Se$

O. Romanova[1*], S. Aplesnin [1,2], L. Udod[1,2], K. Yanushkevich[3] and A. Zhivulko[3]
[1]*Kirensky Institute of Physics, Federal Research Center KSC SB RAS,660036 Krasnoyarsk, Russia, rob@iph.krasn.ru**
[2] *Reshetnev Siberian State University of Science and Technology,660014 Krasnoyarsk, Russia*
[3] *Scientific-Practical Materials Research Center NAS of Belarus, 220072 Minsk, Belarus*

Manganese chalcogenides and solid solutions synthesized on their basis are promising materials for studying the magnetoresistive effect, magnetoimpedance, and thermoelectric power [1]. These materials find wide application in rapidly developed spintronics and microelectronics [2]. Doping of chalcogenide systems with rare-earth elements (gadolinium, cerium, samarium, etc.) leads to the formation of an orbitally disordered state with orbital polarons, which induced magnetotransport effects in the absence of static deformations of the lattice [3].

The aim of the research is to investigate the effect of variable valence elements (Tm) in manganese selenide (MnSe) on kinetic properties.

The $Tm_XMn_{1-X}Se$ samples were synthesized by the solid-state reaction in a stepwise mode. The X-ray diffraction (XRD) study was carried out at 300 K on a DRON-3 X-ray diffractometer (CuK_α radiation) before and after the measurements. According to the XRD data, the synthesized samples with substitution concentrations up to X = 0.2 have a face-centered cubic (FCC) structure of the NaCl type similar to manganese monoselenide.

The kinetic properties of the $Tm_XMn_{1-X}Se$ ($0.025 \le X \le 0.2$) system have been investigated in the temperature range of 80–500 K in magnetic fields of up to 12 kOe and at frequencies of ω = 300-10^5Hz.

The majority carrier type, density, and mobility have been determined from the Hall-effect measurement data. A change in the type of the charge carriers from n - type to p-type depending on the temperature was found. For $X \le 0.05$ a sign change in the magnetic transition region, and for $X \ge 0.1$ at the structural transition was found. We use the relation $R_X = 1/ne$ to estimate the carrier density, which was found to be $n = 10^{16}$–10^{20} cm^{-3}. The mobility of majority carriers mobility has a wide maximum in the range of room temperatures.

Impedance spectroscopy provides important information on conductivity in doped semiconductors. The relaxation time for X=0.05 and X=0.2 was determined from the frequency dependence of the active and reactive resistances, which are described in the Debye model. The imaginary part of the impedance for X= 0.1 is described well by the function Im Z =1/ωC with the capacitance decreasing upon heating. The maximum magnetoimpedance in the low-frequency region at the two concentrations was observed. Magnetoimpedance was found in the region where holes are the main charge carriers and the mobility has maximum values. The analysis of the impedance spectrum in the approximation of equivalent circuits.

Acknowledgement
The reported study was funded by RFBR according to the research project №20-52-00005 Bel_a. The reported study was funded by BRFBR according to the research project № T20P-052

References

[1] S.S. Aplesnin, O.B. Romanova, V.V. Korolev, M.N. Sitnikov, K.I. Yanushkevich, J. Appl. Phys. 121 (2017) 075701.
[2] G.K. Ahluwalia, *Applications of Chalcogenides: S, Se, and Te* (Springer International Publishing, Switzerland, 2017)
[3] S. S. Aplesnin, O. B. Romanova, O. F. Demidenko, and K. I. Yanushkevich, *Magnetic Phase Transitions and Kinetic Properties of 3d-Metal Chalcogenides* (Sib. Gos. Aerokosm. Univ., Krasnoyarsk, 2017) [in Russian].

Magneto-electrical properties of iron-substituted bismuth pyrostannate $Bi_2(Sn_{0.8}Fe_{0.2})_2O_7$

L. Udod[1,2,*], S. Aplesnin[1,2], M.Sitnikov[2], O. Romanova[1], A Galyas[3]
[1]*Kirensky Institute of Physics, Federal Research Center KSC SB RAS, Krasnoyarsk, Russia*
[2]*Reshetnev Siberian State University of Science and Technology, Krasnoyarsk, Russia*
[3]*Scientific Practical Materials Research Center, National Academy of Science of Belarus, Minsk, Belarus*
**e-mail: luba@iph.krasn.ru*

Substitution of iron for tin in the $Bi_2Sn_2O_7$ compound causes the magnetic ordering and, due to the interaction between the magnetic and ferroelectric subsystems, one can expect the manifestation of the magnetoelectric effect. The heterovalent substitution of tin ions for 3d elements in $Bi_2Sn_2O_7$ changes the temperature of the $\alpha \rightarrow \beta$ transition. Iron-substituted bismuth pyrostannate $Bi_2(Sn_{1-x}Fe_x)_2O_7$ (x = 0.2) undergoes a low-temperature shift-type transition at 140 K related to the change in the Bi–O–Fe bond lengths. Iron ions in the pyrochlore crystal structure occupy two nonequivalent octahedral positions and are in the high-spin state. The antiferromagnetic exchange exists between the spins of iron ions and the paramagnetic Curie temperature sharply increases with increasing concentration of iron ions.

The aim of this study is to establish magnetoelectric interaction in bismuth pyrostannate $Bi_2(Sn_{0.8}Fe_{0.2})_2O_7$.

The magnetoelectric interaction of polycristal $Bi_2(Sn_{0.8}Fe_{0.2})_2O_7$ was established from the induced electric polarization in magnetic fields of up to 13 kOe. A monotonic magnetic-field dependence of the polarization was found at the temperatures range of 80-300 K. The magnetoelectric interaction is caused by the spin-orbit interaction with a linear field dependence and the electron-lattice interaction with a quadratic field dependence. At low temperatures (down to 120 K), the induced polarization is an even function of the magnetic field. In the region of the structural transition (140–160 K), the polarization changes its sign at the magnetic field inversion, which points out the existence of the linear magnetoelectric effect. Further heating of the sample to room temperature leads to the predominance of the quadratic magnetoelectric effect. The magnetic-field-induced electric polarization decreases upon heating. The magnetoelectric effect in $Bi_2(Sn_{1-x}Fe_x)_2O_7$, x=0.2 is associated with electric polarization due to the relativistic mechanism and as a results of the electron density redistribution in the intercrystalline domain walls under the spin-orbit interaction in the magnetic field.

Compaund of $Bi_2(Sn_{0.8}Fe_{0.2})_2O_7$ was synthesized in form of thin films. The study of polycristal and film $Bi_2(Sn_{0.8}Fe_{0.2})_2O_7$ impedance was carried out on an AM-3028 component analyzer in the frequency range of 1-1000 kHz and temperatures of 100-600 K. The normalized part of the impedance of polycrystalline $Bi_2(Sn_{1-x}Fe_x)_2O_7$, x = 0.2, has a minimum at Tmin = 310 K. The value of minimum decreases by two orders of magnitude with increasing frequency. The decrease of impedance in the range of 260-310 K is due to the inductive resistance. Heating up to 400K leads to an increase of impedance and increase of capacitance. This is due to polymorphic transitions and crystalline domains in which current carriers are localized. The decrease of impedance above 460 K is due to an increase in capacitance as a result of relaxation conductivity. Nonlinear decreasing of impedance of $Bi_2(Sn_{0.8}Fe_{0.2})_2O_7$ film up to 335 K, a sharp rise and a sharp decline in the region of 340 K is observed. The character of the $Re(Z)/Re(Z_{T=80K})$ curve of the film shows a shift in the boundaries of structural phase transitions.

The reported study was funded by Russian Foundation for Basic Research project № 20-52-00005 Bel_a.

Improvement in the performances of high-temperature superconductors

Yassine Slimani
Department of Biophysics, Institute for Research and Medical Consultations (IRMC), Imam Abdulrahman Bin Faisal University, P.O. Box 1982, 31441 Dammam, Saudi Arabia.
yaslimani@iau.edu.sa; slimaniyassine18@gmail.com

Abstract

The discovery of high-temperature superconductors (HTS) opened the way to practical applications. Since then, researchers worldwide have sought to further improved their properties especially their capacities to transport high amount of current with minimum loss of energy. Different approaches including doping, additions, preparation methods, etc. were adopted to achieve these goals.

The inclusion of nanomaterials having a size matching with the coherence length of superconducting material could be a useful and practical way in increasing the critical superconducting transition temperature and critical current density (J_c). The type, amount, and shape of nanomaterials have a great impact on the performances of HTS.

We have performed numerous research to improve vortex-pinning capabilities and hence boost J_c through controlled inclusion of diverse kinds of nanomaterials varying from semiconductors, insulators, and metals with one-dimensional, two-dimensional, and three-dimensional nanostructured materials.

This talk will offer an overview on how these nanomaterials influence on the structure, morphology, microstructure, electrical and magnetic performances of HTS. Role of generated defects, vortex pinning mechanisms, diagram phase will be presented.

Memristor effect in films of bismuth ferrite garnet

S. Aplesnin[1,2*] M.Sitnikov[2] and F.V. Zelenov[2]
[1]*Kirensky Institute of Physics, Federal Research Center KSC SB RAS, Krasnoyarsk, Russia*
[2]*Reshetnev Siberian State University of Science and Technology, Krasnoyarsk, Russia*
**e-mail: apl@iph.krasn.ru*

Study of materials for spintronic [1] and memristor [2] devices are interesting for both fundamental research and application. In recent years, along with conventional storage devices, much attention has been paid to the resistive memory, which combines the advantages of fast random-access memory and nonvolatility of programmable memory. The resistance of a memristor depends on the charge passed through it. Most memristors are based on metal–insulator–metal tunnel structures with the oxygen nonstoichiometry [3].

Another mechanism can be related to the coexistence of ferroelectric and semiconductor properties. Changing the polarization direction, one can control the carrier transport. These properties can be observed in multiferroics with the magnetoelectric coupling. The magnetoelectric coupling was observed in the bismuth ferrite garnet $Nd_1Bi_2Fe_5O_{12}/Nd_2Bi_1Fe_4Ga_1O_{12}$ epitaxial films on the glass substrate and the $Nd_{0.5}Bi_{2.5}Fe_5O_{12}$ epitaxial films on the single-crystal gadolinium gallium garnet substrate [4]. The electric polarization of the films of bismuth ferrite garnet is caused by the displacement of bismuth ions as a result of elastic stresses from the side of the substrate. The linear response of the ME susceptibility is explained in the model with spin-orbit interaction, the quadratic ME effect is associated with the exchange-striction mechanism.

In the ferroelectric region, the I – V hysteresis was found, which is due to the conduction current and the polarization current. Conduction is ohmic, electrical polarization exhibits hysteresis. Above the temperature of the disappearance of the electric polarization in the vicinity of the Curie temperature, the critical voltage is found at which the I – V is nonlinear. A bistable current state is found, which depends on the external magnetic field. This dependence is due to the induced magnetoelectric interaction. The I – V hysteresis and electric polarization in a polycrystalline film disappear at a lower temperature than in a single crystal film.

The negative magnetoresistance on alternating current is found. A decrease in the impedance components in the film depending on the magnetic field is explained by the interaction of ferroelectric domains with magnetic domain walls. Upon approaching the resonance frequency of domain wall, the absorption of electromagnetic radiation increases. The ferroelectric walls interact with magnetic domain walls and a part of the energy of vibrations of the ferroelectric walls passes into the magnetic system. With an increase in the magnetic field, the density of magnetic domain walls decreases, which weakens the absorption of electromagnetic radiation.

Acknowledgement
The research was funded by RSF, Krasnoyarsk Territory and Krasnoyarsk Regional Fund of Science, project number 22-22-20004**.**

References

[1] A. Avsar, H. Ochoa, F. Guinea, B. Özyilmaz, B.J. Van Wees, I.J. Vera-Marun, Rev. Mod. Phys. 92, 021003 (2020)
[2] D.B. Strukov, G.S. Snider, D.R. Stewart, R.S. Williams, Nature 453, 80 (2008)
[3] J.J. Yang, D.B. Strukov, D.R. Stewart, Nat. Nanotechnol. 8, 13 (2013)
[4] S.S. Aplesnin, A.N. Masyugin, M.N. Sitnikov, T. Ishibashi, JETP Lett. 110, 223 (2019)

Low temperature Raman spectroscopy of Cu_2ZnSnS_4 and $Cu_2ZnSnSe_4$ compounds

V.F. Gremenok[1,2]*, A.V. Stanchik[1], Kobylatski A.V.[1], M.S. Tivanov[3], V.V. Khoroshko[2]
[1]*State Scientific and Production Association "Scientific-Practical Materials Research Centre of the National Academy of Sciences of Belarus", 220072, Minsk, P. Brovka Str. 19, Republic of Belarus, e-mail: gremenok@physics.by*
[2]*Belarusian State University of Informatics and Radioelecrtonics, 220013, Minsk, P. Brovka str., 6, Republic of Belarus*
[3]*Belarusian State University, 220030, Minsk, 4 Nezavisimosti Avenue, Republic of Belarus*

Earth abundant quaternary semiconductors Cu_2ZnSnS_4 (CZTS) and $Cu_2ZnSnSe_4$ (CZTSe) have been intensively studied because of their desired optoelectronical properties for photovoltaic (PV) applications. The best solar cell efficiency has reached values of 12.6% for alloyed kesterite (CZTSSe) photovoltaic devices [1]. In order to achieve an increase in the efficiency, problems involving material require for an accurate control of the microstructure of the kesterite absorbers. Raman spectroscopy has big potential in the analysis of crystal structure. This work presents the temperature dependence of the Raman peaks position for Cu_2ZnSnS_4 and $Cu_2ZnSnSe_4$ compounds in the temperature range of 24–290 K.

Single crystals of CZTS and CZTSe were grown by chemical vapor transport using iodine as a transport agent [2]. Raman spectra were obtained using confocal Raman spectrometer Nanofinder HE and were excited with a solid laser emitting at a wavelength of 532 nm.

Raman spectra of Cu_2ZnSnS_4 and $Cu_2ZnSnSe_4$ compounds in the range of 50–400 cm^{-1} are shown in Fig. 1. The peak positions at room temperature matche well with previously published results for kesterite phase of CZTS and CZTSe [3]. A decrease in the frequency and intensity of modes is observed with an increase in temperature. An increase in linewidth/damping is also observed with increase in temperature.

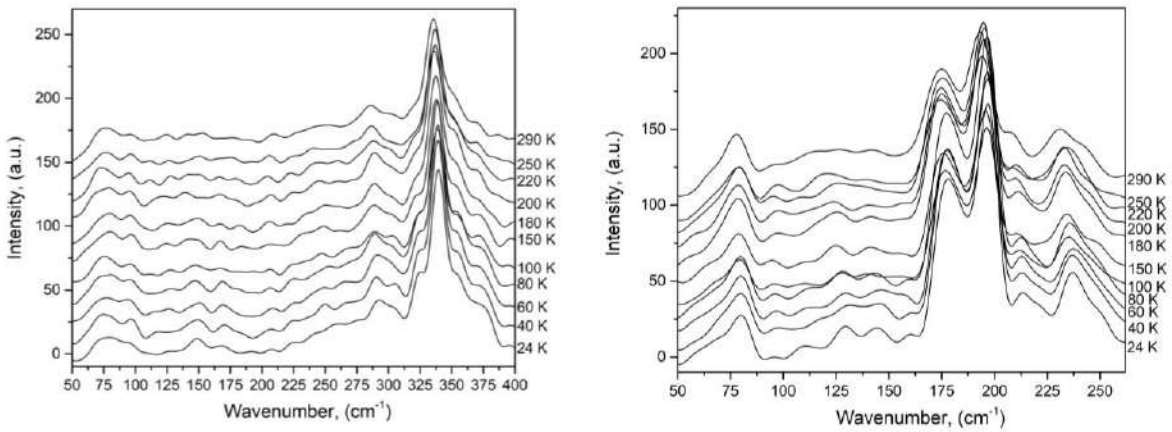

a) b)

Raman spectra for CZTS (a) and CZTSe (b) compounds recorded in the temperature range of 24–290 K

The analysis of Raman data showed that the phonon damping process is the main factor responsible for the observed frequency shift as well as for the linewidth variation.

References

[1] M.A. Green, E.D. Dunlop, J. Hohl-Ebinger, M. Yoshita, N. Kopidakis, X. Hao, Progress in Photovoltaics: Research and Applications 28 (2020)629-638.
[2] V. G. Hurtavy, A. U. Sheleg, Proceedings of the National Academy of Sciences of Belarus. Physics and Mathematics Series 4 (2014) 87-91.
[3] M. Dimitrievska, H. Xie, A. Fairbrother, X. Fontané, G. Gurieva, E. Saucedo, Al. Pérez-Rodríguez, S. Schorr and V. Izquierdo-Roca, Appl. Phys. Lett. 105 (2014) 031913.

Mössbauer study of $Bi_{1-x}Nd_xFe_{1-y}Cr_yO_3$ solid solutions fabricated by a high-pressure synthesis

S.P. Kubrin[1],A.V. Pushkarev[2,*], N.M. Olekhnovich[2], Yu.V. Radyush[2], S.I. Raevskaya[1], V.V. Titov[1], M.A. Malitskaya[1], I.P. Raevski[1]

[1] *Physics Research Institute and Faculty of Physics, Southern Federal University, 344090, Rostov-on-Don, Russia*

[2] *Scientific-Practical Materials Research Centre of NASB, 220072, P. Brovka str, 19, Minsk, Belarus, pushk@physics.by**

Mössbauer spectra of $Bi_{1-x}Nd_xFe_{0.5}Cr_{0.5}O_3$ (x=0, 0.2, 0.4, 0.6, 0.8) and $Bi_{1-x}Nd_xFe_{0.75}Cr_{0.25}O_3$ (x=0.05, 0.1, 0.2,..., 0.9) solid solutions fabricated by a high-pressure synthesis were measured in the magnetic and paramagnetic phases. The spectra of $Bi_{1-x}Nd_xFe_{0.5}Cr_{0.5}O_3$ consist of 4 sextets while spectra of $Bi_{1-x}Nd_xFe_{0.75}Cr_{0.25}O_3$ consist of six sextets. Each sextet corresponds to the Fe^{3+} ions with different number of Cr^{3+} ions in their local environment. According to binominal distribution calculation there are 7 possible Fe^{3+} local configurations for the $Bi_{1-x}Nd_xFe_{0.5}Cr_{0.5}O_3$ and 6 for the $Bi_{1-x}Nd_xFe_{0.75}Cr_{0.25}O_3$. The area and number of sextets in the measured spectra differ from the calculated probabilities of Fe^{3+} local configurations. This indicates that Fe^{3+} and Cr^{3+} ions are distributed non-randomly in the B-sublattice and the partial B-cation ordering (clustering) takes place in the samples. It should be noted that Mössbauer spectrum of $BiFe_{0.5}Cr_{0.5}O_3$ consists of 6 sextets. Therefore, the Nd^{3+} ions stimulate the local B-cation ordering. In paramagnetic phase all the spectra contain only doublets. The quadrupole splitting values of compositions with x>0.1 are about 0.2 mm/s. The quadrupole splitting values of $BiFe_{0.5}Cr_{0.5}O_3$ and $Bi_{0.95}Nd_{0.05}Fe_{0.75}Cr_{0.75}O_3$ samples are about 0.44 mm/s which are close to the values obtained for $BiFeO_3$.

The temperature dependencies of paramagnetic line intensity (*Im)* for $Bi_{1-x}Nd_xFe_{0.5}Cr_{0.5}O_3$ and $Bi_{1-x}Nd_xFe_{0.75}Cr_{0.25}O_3$ were measured using the temperature scanning technique. The *Im*(*T*) dependencies of $Bi_{1-x}Nd_xFe_{0.5}Cr_{0.5}O_3$ compositions have two anomalies. The low-temperature anomalies are observed at ~240 K and seem to correspond to the Neel temperature. The high-temperature anomalies are observed at ~250 K and above. Their temperatures increase with the growth of Nd content. The high-temperature anomalies can be attributed to the magnetic coupling of "$Bi_{1-x}Nd_xFeO_3$" and "$Bi_{1-x}Nd_xCrO_3$" clusters. The Im(T) curves for $Bi_{1-x}Nd_xFe_{0.75}Cr_{0.25}O_3$ compositions have only one anomaly at ~470 K independent of Nd^{3+} concentration. The absence of the *Im*(*T*) anomaly due to coupling of "$Bi_{1-x}Nd_xFeO_3$" and "$Bi_{1-x}Nd_xCrO_3$" clusters may be caused by the much smaller amount of the latter clusters as compared to $Bi_{1-x}Nd_xFe_{0.5}Cr_{0.5}O_3$ and/or by the closeness of the temperatures of these anomalies.

Acknowledgement

This study was partially supported by RFBR (project 20-52-00045 Bel_a) and by the BRFFR (project T20R-169).

The $Cu_2NiSn(S,Se)_4$ thin films for new generation solar cells

A. Stanchik[1*], M. Gapanovich[2], V. Rakitin[2], A. Kobylatski[1]
[1]*State Scientific and Production Association «Scientific-Practical Materials Research Centre of the National Academy of Sciences of Belarus», 220072 Belarus, Minsk, P. Brovki str., 19, e-mail: stanchik@physics.by*
[2]*Institute of Problems of Chemical Physics of Russian Academy of Sciences, 142432 Russian Federation, Chernogolovka, Ac. Semenov av. 1*

Kesterite $Cu_2ZnSn(S,Se)_4$ (CZT(S,Se)) is a promising material as a light-absorbing layer for thin-film solar cells due to low-toxic, inexpensive, and abundant elements, as well as suitable optical and photoelectric properties. However, at present, the efficiency of solar cells based on them does not exceed 13%, which is lower than the theoretically possible (~30%). One of the probable reasons for a low efficiency is antistructural defects Zn_{Cu} and Cu_{Zn} in the kesterite lattice formed due to the closeness of the atomic radii of Cu and Zn. Which lead to a significant decrease in the lifetime of photogenerated current carriers. These fundamental problems can be overcome by replacing the Zn atoms in the CZT(S,Se) structure with elements with an atomic radius other than Zn and Cu (for example, Mg, Ba, Cd, Co, Mn, Fe, and Ni). Among all possible elements, Ni has the advantage of abundant elements in nature and low-toxicity. Therefore, compounds of the Cu-Ni-Sn-(S,Se) ($Cu_2NiSn(S,Se)_4$ or CNT(S,Se)) type is promising absorber material for inexpensive and effective thin film solar cells.

In 2014, CNTS films were obtained from a suspension of nanoparticles with a wurtzite structure for the first time by the hot injection method [1]. In 2016 it was reported about CNTS films obtained by the method of one-stage electrodeposition on ITO substrates [2]. The CNTS films had a stannite-type structure and an E_g of 1.61 eV. In [3], CNTS films were obtained on glass substrates by the Spray Sandwich method and were characterized by *p*-type conductivity, had a high absorption coefficient (~10^4 cm^{-1}) in the visible region, and E_g equal to 1.23 eV. It was found that CNTS films deposited for 20 min of sputtering have an amorphous structure, while films deposited for 40 and 60 min are polycrystalline. It was found in [4] that a change in the thickness and elemental composition of CNTS films obtained by direct immersion in a solution of various substrates (SLG, glass/Mo, FTO) affects their morphology and optoelectronic properties. In [5], CNTS thin films with a cubic structure were obtained on glass substrates by direct deposition from molecular ink followed by annealing at 160 °C in air. The band gap of the films was ~1.6 eV, the electrical conductivity was 1.7×10^{-3} Ohm/cm, and the hole mobility was 2.3×10^{-3} $cm^2/V \cdot s$. In 2020, CNTS films were obtained by centrifugation followed by annealing at 300 °C in an N atmosphere for 1 hour without a sulfurization step [6].

In 2016, for the first time, a solar cells based on CNTS films with an efficiency of 0.09% was reported [7]. In 2018, using a modular solar cells simulator (SCAPS, 1.5AM), an efficiency of 17.06% was obtained [8]. Thus, it can be seen from the results presented above that at present there are no detailed data on the synthesis conditions and their effect on the formation of CNTS films, and for CNTSe they are completely absent.

Acknowledgement. This work was supported by the Belarusian Republican Foundation for Basic Research (Project No. T21PM-033) and the Russian Foundation for Basic Research (Grant No. 20-58-04005).

References

[1]. Kamble A. et al. Materials Letters. 2014. V. 137. P. 440–443.
[2]. Yang C.L. et al. Materials Letters. 2016. V. 166. P. 101–104.
[3]. Dridi S., Bitri N., Abaab M. Materials Letters. 2017. V. 204. P. 61–64.
[4]. Mokurala K. et al. Journal of Alloys and Compounds. 2017. V. 725. P. 510–518.
[5]. Jariwala A. et al. Materials Letters. 2018. V. 215. P. 118–120.

[6]. Aitelhaj D. et al. Materials Science in Semiconductor Processing. 2020. V. 107. P. 104811.
[7]. Rondiya S. et al. Chem. Mater. 2017. V. 29. P. 3133–3142.
[8]. Khattak Y.H. et al. Optik. 2018. V. 171. P. 453–462.

Engineering electronic properties of electrodeposited Bi films

A.S. Fedotov[1], D. Tishkevich[2], R. Kirichenkov[1] and D. Vasin[2]
[1]*Computer Modelling Department of Physics Faculty, Belarusian State University, Minsk 220030, Belarus*
[2] *Laboratory of Magnetic Films Physics, SSPA "Scientific and Practical Materials Research Centre of National Academy of Sciences of Belarus", Minsk 220072, Belarus*

Bi is a semimetal which combines high electrical conductivity, reasonable thermoelectric parameters, resistance to strong ionizing radiation and lowest toxicity among pure heavy elements. Bi attracts attention of reserachers in applied sciences and in fundamental physics as well due to a wide spectrum of applications and unusual electronic structure [1].

Single crystals of Bi are expensive to synthesize so there is a demand for cheaper techniques of high-quality sample fabrications. Electrochemical deposition method provides dense polycrystalline samples and combines low costs with high deposition rate (up to 200 μm/h) [1].

We study the influence of cathode current on the electrical properties of resulting Bi deposits fabricated using the novel perchlorate electrolyte. We consider three DC cathode current regimes for current densities j = 20 mA/cm^2, 15 mA/cm^2, 10 mA/cm^2 and one pulse regime with density j = 10 mA/cm^2, pulse duration and pause equal to 1s.

It was found that resistivity of all samples (given in Figure 1) lies in a range (1 – 1,6)·10^{-6} Ohm·m which is of the same order of magnitude as the resistivity of single-crystals. Relative magnetoresistance at 2 K reaches about 10^2 under 8 T field which is about the two orders of magnitude lower than magnetoresistance of single-crystals which indicates suppression of electron mean free path due to scattering on the grain boundaries.

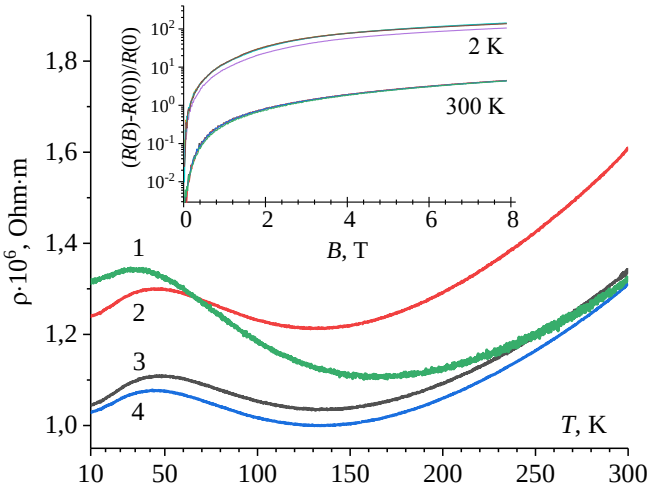

Figure 1. Resistivity temperature dependence for Bi samples: 1 – DC regime, j = 10 mA/cm^2, 2 – DC regime, j = 15 mA/cm^2, 3 – DC regime, j = 20 mA/cm^2, 4 – pulse regime, j = 10 mA/cm^2 Inset: relative magnetoresistance dependence on magnetic field at temperature T = 2 K and T = 300 K

The effect of pulse regime usage instead of DC (1 and 4 in Fig.) is in weakened temperature dependence of resistivity. During electrical measurements of pulse-deposited samples we observe higher noise of electric signal than for any of DC-deposited samples. Moreover, real thickness of pulse-deposited samples is about 30 μm while for DC-deposited samples thickness is about 25 μm. We suggest that pulse-deposited sample has more micropores which acts as capacities and define noisy behaviour of resistivity signal during measurements.

QMSA [1] method has shown that the non-monotonous temperature dependences of resistivity are result of competition between concentration and mobility temperature dependences of two charge carrier types. This opens wide possibilities for engeineering the temperature dependencies of Bi resistivity through change of deposition conditions and Bi grain size.

References

[1] Fedotov, A. [et al.] Electrodeposition conditions-dependent crystal structure, morphology and electronic properties of Bi films. J. Alloys Compd. 887 (2021), 161451.

IR SPECTROSCOPIC STUDY OF ZIRCONIUM SAMPLES IN AN H_2O_2 MEDIUM

Teymur N. Agayev, Gunel T. Imanova[1*],Imran Ali[2]
[1]*Department of Physical, Mathematical and Technical Sciences, Institute of Radiation Problems, Azerbaijan National Academy of Sciences, AZ 1143 - Baku, Azerbaijan*
[2]*Department of Chemistry, Jamia Millia Islamia (Central University), New Delhi-110025, India*

The method of reflection-adsorption IR spectroscopy was used to study the radiation-oxidation of untreated and preliminary radiation-oxidatively treated zirconium samples in an H_2O_2 medium in contact with water at T=300K. It was revealed that the formed protective oxide layer also hinders the introduction of oxygen atoms into the bulk and the exit of new metal atoms to the surface, as a result of which the metal-oxide interface is completely screened and the thickness of this layer changes insignificantly.Figure 1 shows the IR reflectance spectra of pure and radiation-oxidatively treated zirconium samples. Three regions of the absorption band are distinguished in the spectra:

- the region of stretching vibrations of surface states ν-4000-2800 cm^{-1} (Fig. 1, a)
- the area of deformation vibrations ν-1700-1300 cm^{-1} (Fig. 1, b);

During the radiation-oxidative treatment of zirconium in contact with H_2O_2, numerous homogeneous and heterogeneous processes occur. OH, O_2, H and H_2 are formed as final products. Thus, the increase in temperature to T=300K is accompanied by the complete and partial decomposition of molecular water, H-bonded OH-groups and the formation of isolated OH-groups. This leads to a decrease in the intensity of H-bonded OH-groups, and an increase in isolated hydroxyl groups. The decomposition products of H_2O_2 during radiolysis in the Zr-H_2O_2 system can be identified using IR spectroscopy. Since, during the radiation-oxidative treatment of Zr in the presence of H_2O_2, radiolysis products are found in the range of OH stretching vibrations of ν-4000-2800 cm^{-1}, the decomposition of H_2O_2 in the Zr-H_2O_2 system in this region is accompanied by the formation of an absorption band with maxima at ν-3780 , 3450 and 3240 cm^{-1} (Fig. 1, a), and in the range of bending vibrations ν-1700-1200 cm^{-1} is accompanied by the formation of an absorption band with maxima at 1630, 1540, 1520, and 1505 cm^{-1} (Fig. 1., b). The absorption bands at 3240 and 1630 cm^{-1} refer to H_2O molecules, and the absorption bands at 1540-1505 cm^{-1} are associated with the formation of O_2^- radical ions. The location of the bands and the shape of the vibrational-rotational spectrum (strong Q-branch at 1520 cm^{-1} accompanied by weak P and R branches at 1540 and 1505 cm^{-1}) indicate physical adsorption of molecular oxygen.

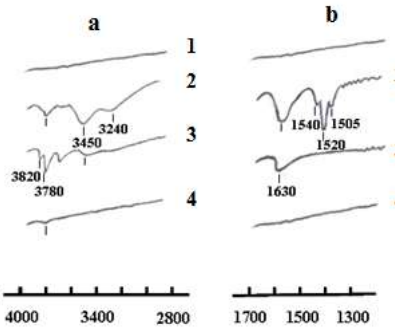

Fig. 1. IR reflection spectra of a clean surface of metallic Zr (curve 1) and heterosystem Zr-H_2O_2 (curves 2-4) depending on the contact time under the action of γ-irradiation D = 0.45 Gy/s,
τ= 11 (2), 110 (3) and 220 (4) hours.

A further increase in the time of radiation-oxidative treatment τ to 110 hours or the absorbed radiation dose to D=800 kGy leads to the complete decomposition of intermediate surface-active particles and the formation of a continuous protective oxide film on the surface.

Manganese-substituted magnetite $Mn_{0.3}Fe_{2.7}O_4$ for magnetorheological materials

Yu. Haiduk[1*], E. Korobko[2], L. Radkevich[2], D. Kotsikau[1], A. Usenka[1], V. Pankov[1]
[1]*Belarusian State University, Belarus, 220030, Minsk, Niezaleznasci Av., 4*
[2]*A. V. Luikov Heat and Mass Transfer Institute of The National Academy of Scientis of Belarus, 220072, Belarus, Minsk, Brovki str., 15*

A series of powders of Mn-substituted magnetite $Mn_xFe_{3-x}O_4$ (x = 0.1 – 0.6) with cubic spinel lattice were synthesised by chemical co-precipitation in aqueous solutions of inorganic salts. The samples were studied using powder X-ray diffraction, scanning electron microscopy, IR spectroscopy, and magnetometery. The highest shear stress value was observed for a magnetorheological suspension based on the $Mn_{0.3}Fe_{2.7}O_4$ powder that was obtaineded by annealing the precipitated precursor under argon flow at 740 °C for 8 h.

Investigation of the properties of TiC nanocompounds by FTIR

Raisa Hakhiyeva
Institute of Radiation Problems, Azerbaijan, Baku, 9 B.Vahabzade str.,Baku,Azerbaijan, AZ1143

Infrared spectra of Nano TiC particles were obtained at room temperature in the range 400-4000 sm^{-1} of the wavelength (space frequency) by Varian 640 FT-IR device. For experiment used powdered nano TiC particles consisting of 40-60 nm particles . Note that TiC nanoparticles have a density of 0.08 g / sm^3. The major purpose of the IR analysis is to observe the spatial oscillations in the TiC nanoparticles. According to the analysis of the spectra, it was determined that in the range of space frequency 400 - 4000 sm^{-1} the sample has four sharp peaks (Fig.) . The first peak data corresponding to the value of the wave number 650 sm^{-1} is related on the Ti-C bond. The peak observed at 650 sm^{-1} clearly characterizes the vibration between Ti and C atoms. TiC nanoparticles also have a very large specific surface area (SSA) and so sensitive to the environment. As a result, a peak corresponding to the value of the wave number 1550 sm^{-1} was observed. This peak determines the C-O bonds on the surface of TiC nanoparticles.

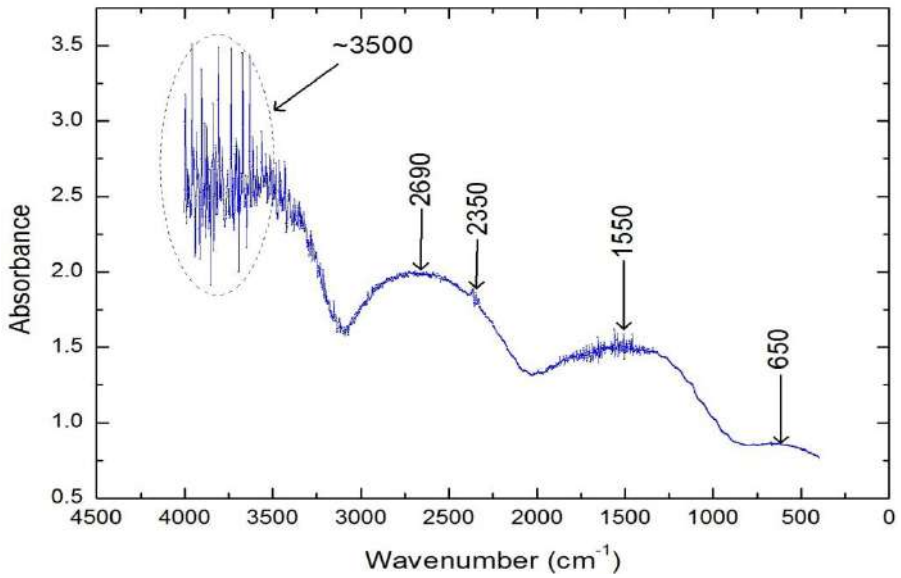

Fig. FTIR spectra of TiC nanoparticles

The peaks observed at 2350 sm^{-1} and 2690 sm^{-1} of the wave number are probably due to the Ti-OH or Ti-O bonds formed by the interaction of Ti atoms on the surface with water molecules or oxygen in the environment. However, in some approaches, the peaks around the value of the wave number 2500 sm^{-1} are explained by defects that occur for various reasons in such combinations. Because of the adsorption ability of nano TiC particles, -OH groups are visible at ~ 3500 sm^{-1}.

Structural and Magneto-thermal Properties of Fe-Ga Alloy

V. Vijayanarayanan[1], Himalay Basumatary[2], M. Manivel Raja[2], V. Aravindan[1], and M. Mahendran[1*]
[1]*Smart Materials Laboratory, Department of Physics, Thiagarajar College of Engineering, Madurai – 625015, India.*
[2]*Defence Metallurgical Research Laboratory, Kanchanbagh, Hyderabad – 500058, India*

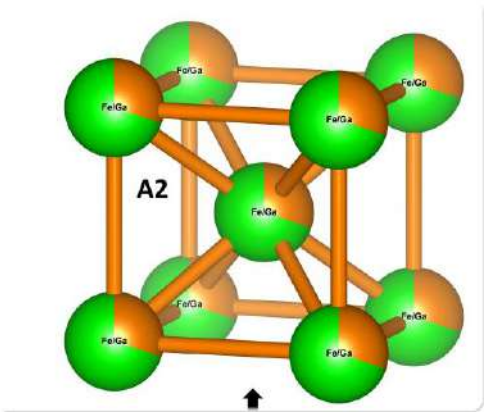

A2 Phase Crystal Structure

In recent years, Fe-Ga alloys, which are among the most important functional magnetic materials, have found their way into sonar systems and sensors such as displacement and force sensors, as well as acoustic, tactile, and torque sensors. It has already been demonstrated that the addition of Ga significantly increases the magnetostriction of bcc Fe. Magnetostriction in Fe–Ga alloys can be tenfold that of bcc Fe at room temperature. Additionally, the low cost, high ductility, high mechanical strength, and ability to withstand high imposed stress levels have attracted considerable attention to these alloys. Alloys containing Fe 73 at. percent exhibit the $D0_3$ structure after casting, and the first-order $L1_2$ to $D0_{19}$ transition occurs. Additionally, it was discovered for the first time that the phase transition between two ordered phases involves disordered states. When temperature transformation processes, most notably cooling from A2 to high temperature phase, occur, the phase diagrams of Fe-Ga alloys undergo structural ordering and disordering changes. A faster cooling rate indicates that the room temperature alloys are a mixture of A2, $L1_2$, and $D0_3$ phases. The results of the X-Ray Diffraction study confirm that the alloy has a Body Centered Cubic structure and that the A2 phase is present in it. In addition, an optical microscopy study has confirmed the presence of equiaxed grains of only one phase (A2). In addition, differential scanning calorimetry confirms the presence of the A2 and $D0_3$ phases, which were previously suspected. In order to determine the saturation and remanent magnetization, a vibrating sample magnetometer was employed.

.

Acknowledgement
All the authors would like to thank DMRL Hyderabad for supporting this research.

References
[1] V. Vijayanarayanan, Manickam Mahendran *et al*, In *AIP Conference Proceedings*, 2265, (2020) 030544. .https://doi.org/10.1063/5.0017123
[2] Basumatary, Himalay, *et al*, *Journal of Magnetism and Magnetic Materials* 384, (2015) 58-63. https://doi.org/10.1016/j.jmmm.2015.02.021

Dielectric properties of xMgFe$_2$O$_4$/(1-x)UHMWPE composite functional materials via its structure and composition

T.Yu. Kiseleva[1], E.V. Yakuta[1*], T.F. Grigoreva[2], I.A. Malyshkina[1], M.V. Ilyin[1], I.P. Ivanenko[1], E.T. Devyatkina[2], S.V. Vosmerikov[2], E. Uyanga[3], D. Sangaa[3]
[1]*Moscow M.V.Lomonosov State University, Faculty of Physics, Leninskie Gory, Moscow, 119991, Russia, e-mail: kipr@polly.phys.msu.ru*
[2]*Institute of solid state chemistry and mechanochemistry, SB RAS, Kutateladze str., 18, Novosibirsk, 630128, Russia*
[3]*Mongolian Academy of Sciences Institute of science and technology, Peace avenue 54B, Ulaanbaatar 13330, Mongolia*

We investigate composite materials synthesized by hot pressing from mechanoprecursors based on ultra-high molecular weight polyethylene (UHMWPE) and magnesium ferrite particles of different dispersion and concentration. Structural characteristics have been studied by scanning electron microscopy, X-ray diffraction. Dielectric properties were analysed testing frequency dependance of dielectric permeability, losses and conductivity. The effect of the size and concentration of ferrite particles on the composite dielectric properties have been established.

We considered two types of specimens which are labeled ***F*-MS** and ***F*-MSA.** X-ray phase analysis of the corresponding composites structure showed the absence of new phase formation in all composite compositions. The diffraction pattern contains only broadened structural maxima of UHMWPE and ferrite particles according their mutual concentration. An analysis of the line profile of composites via concentration for ***F*-MS** and ***F*-MSA** fillers indicates a decrease in grain sizes as for particles as for UHWMPE relatively to initial state. The grain size of the ferrite phase decreases relatively to initial state as much as more the concentration of particles in composite because of grinding in the mode of interaction between plastic and enriched brittle components. UHMWPE changes its degree of ctystallinity.

The measured frequency dependence of the real permittivity (ε′) and the loss tangent (tanδ) for the composites demonstrated different behavior both on the particle size and concentration. The presence of ferrite particles in synthesized composites reduces the UHMWPE dielectric constant and increases the value of losess. For specimens with 15, 30%, 50% ***F*-MS**, a constant value of the dielectric coefficient is observed in the entire frequency range up to 10^7 Hz. In samples with ***F*-MSA**, a constant value is observed for 15, 30%, but the higher concentration leads to relaxation behavior characteristic of pure micron-sized ferrites when ε′ decrease with increasing frequency in the range from 1 kHz to 1 MHz. At a certain frequency, characteristic of a particular composition, this decrease slows down and becomes constant. A model description of this behavior of the permeability for ferrites is carried out on the basis of the migration model and spatial charge polarization. The maximum at a low field frequency is characteristic of a change in the polarization mechanism.

All dielectric materials have two types of losses. One is a conduction loss, representing the flow of actual charges through the dielectric material. The other loss is due to the movement or rotation of atoms in an alternating field. Tanδ for 15, 30% is practically independent of the particle size, however, at a high concentration of particles, its value increases 10 times at a large and perfect particle size. From several known models determined possible behavior of the composite final permittivity uses assumption of particles regular shapes and monodispersity.

By varying the volume percentage of fillers in the matrix one can minimizing unwanted contributions to the dielectric constant and dielectric loss under designing the magnetically active light composite.

Acknowledgement
This work was supported by the RFBR joint project N19-52-44003.

THEORY & MODELING IN MATERIAL SCIENCE

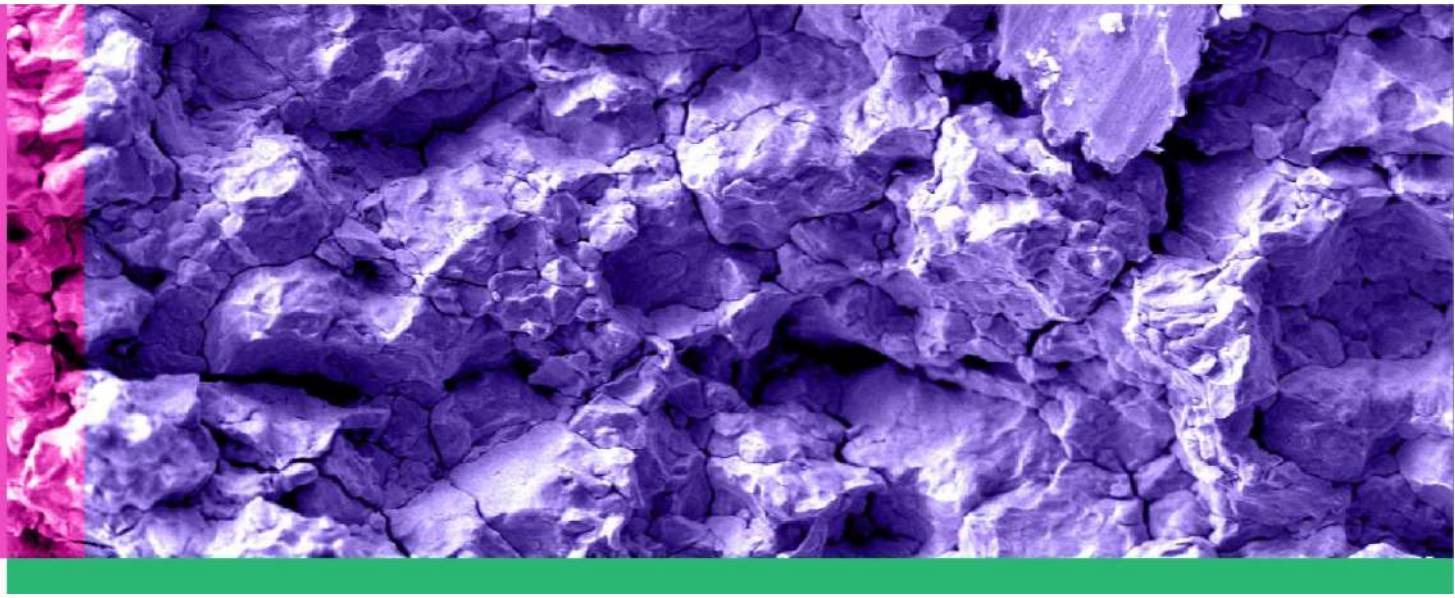

Empirical tight binding method with sp3s* orbital basis for computation of the electronic states of nanostructures

Petr Klenovský[1,2]*
[1] *Masaryk University, Kotlářská 267/2, 61137 Brno, Czech Republic*
[2] *Czech Metrology Institute, Okružní 31, 63800 Brno, Czech Republic*
klenovsky@physics.muni.cz

In this talk I will present my recent results of the development of the empirical tight binding method (ETB) and its use for computations of bandstructure of materials and electronic states of nanostructures. A comparison to the results obtained using envelope function **k·p** approximation will be also given.

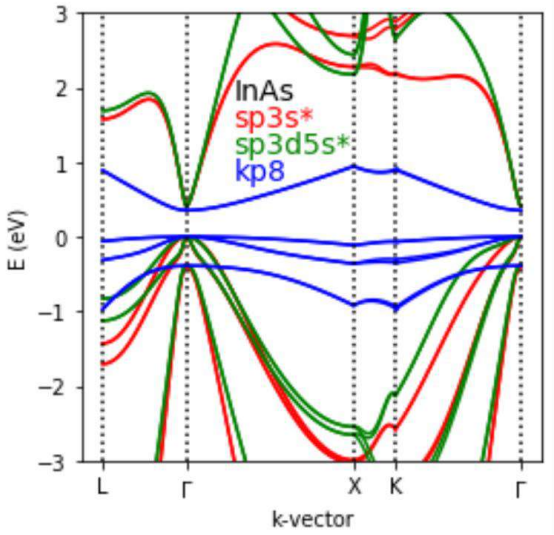

Similar to **k·p** approximation, ETB was developed in the past for full-Brillouin zone description of bulk electronic structure. In ETB, the Schrödinger equation is solved, similarly as for **k·p**, and ETB wavefunctions are also envelopes, yet in a basis of atomic orbitals or crystal Bloch waves. Generally, the larger number of basis atomic orbitals is used, the larger part of **k**-space is reproduced by ETB correctly. The usually used bases are sp3s*[1] and sp3d5s*[2].

In the model used, spin-orbit interaction, piezoelectricity and strain are also considered. While piezoelectricity or external electric fields are accounted for in ETB in the same way as in the **k·p** model, the elastic strain is calculated at the atomistic level using the molecular dynamics simulator LAMMPS and nonlinear Stillinger-Webber potentials of the valence-force-field (VFF) model. The resulting deviations from the ideal structure are realized in the ETB model by the direction cosines in the Slater-Koster formulas (angle change) and Harrison's power law (distance change). It will be shown, that for the calculations of the highest occupied and lowest unoccupied states of the InAs QDs at the gamma point both for ETB with sp3s* basis per atom and **k·p** model provide accurate results.

References

[1] Vogl, P., Hjalmarson, H. P. and Dow, J. D. A Semi-empirical tight-binding theory of the electronic structure of semiconductors. Journal of Physics and Chemistry of Solids 44, 365–378 (1983).
[2] Jancu, J.-M., Scholz, R., Beltram, F. and Bassani, F. Empirical sp3d5s* tight-binding calculation for cubic semiconductors: General method and material parameter. Physical Review B 57, 6493 (1998).

Ab initio modeling of the narrow-gap semiconductor $TlInTe_2$

M. M. Asadov[1,*], S. N. Mustafaeva[2], S. S. Guseinova[3], V. F. Lukichev[3], K. I. Yanushkevich[4]
[1]*Nagiev Institute of Catalysis and Inorganic Chemistry, Azerbaijan National Academy of Sciences, Baku, Azerbaijan*
[2]*Institute of Physics, Azerbaijan National Academy of Sciences, Baku, Azerbaijan*
[3]*K.A. Valiev Physicotechnological Institute, Russian Academy of Sciences, Moscow, Russia*
[4]*Scientific-practical center on material science of the NAS of Belarus, Minsk, Belarus*

The local environment of atoms in a $TlInTe_2$ crystal with a chain structure is studied by the density functional theory (DFT) method. DFT calculations of electronic properties were carried out both for a primitive $TlInTe_2$ cell (16 atoms per unit cell) and for a supercell consisting of 32 atoms. DFT calculations of the band structure (the band gap E_g = 1.21 eV), crystal lattice parameters with a tetragonal system of the $TlInTe_2$ compound with a neutral indium vacancy, vacancy formation energy, indium chemical potential and standard enthalpy of formation of $TlInTe_2$ have been performed. The mechanism of conduction in the direction of the chains (c-axis of the crystal) in the $TlInTe_2$ compound has been established. From experimental data in the temperature range T = 148–420 K, the band gap E_g = 0.94 eV and the activation energy of impurity conductivity E_t = 0.1 eV (at 210–300 K) were estimated.

Biological activity of cortisone-fullerenol agents in the therapy of oncological diseases. DFT symulation.

E.A. Dikusar[1], A.L. Pushkarchuk[1], T.V. Bezyazychnaya[1], E.A. Akishina[1,*], V.I. Potkin[1,], A.G. Soldatov[2], S. A. Kuten[3], S.G. Stepin[4], A.P. Nizovtsev[5], S.Ya. Kilin[5], L.F. Babichev[6]
[1]*Institute of Physical-Organic Chemistry, NASB, 13, Surganova Str., 220072, Minsk, Belarus, che.semenovaea@mail.ru*
[2]*The Scientific and Practical Materials Research Center, NASB, 19, P.Brovka Str., 220072, Minsk, Belarus*
[3]*Institute for Nuclear Problems, BSU, 11, Bobruiskaia Str., 220030, Minsk, Belarus*
[4]*Vitebsk State Order of Peoples' Friendship Medical University, 27, Phrunze Ave., 210023, Vitebsk, Belarus*
[5]*B.I. Stepanov Institute for Physics, NASB, 68, Nezavisimosti Ave., 220072, Minsk, Belarus*
[6]*Joint Institute for Power and Nuclear Research – «Sosny», NASB, 99, Acad. Krasina Str., 220109, Minsk, Belarus*

Fullerene derivatives are potential antitumor agents due to their ability to induce cell death under certain conditions. The risks of intoxication and radioactive contamination can be eliminated by introduction of radioactive isotopes into strong fullerene cage. To increase the effectiveness of these drugs, it is promising to introduce structural fragments of known dosage forms, for example, steroid hormones, into their molecules. Cortisone belongs to the glucocorticoid hormones of the adrenal cortex.

The aim of this work is the quantum chemical modeling of the electronic structure and the analysis of the thermodynamic stability of the new cortisone-fullerenol agents for the tumor neoplasms treatment. The need for preliminary studies of modeling such objects is due to the very high labor intensity, cost and complexity of their practical production.

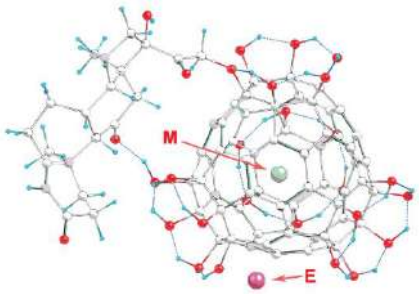

E and M are absent **1**; E = He, M is absent **3**; E is absent, M = He **4**; E = M = He **5**; E = Rn, M is absent **7**; E is absent, M = Rn **8**; E = M = Rn **9**; E = Na, M = Cl **12**; E = Cl, M = Na **13**; E = K, M = Br **14**; E = Br, M = K **15**

Figure 1 - Model of the structure of cortisone-fullerenol clusters 3−5, 7−9, 12-15

As the endohedral components of inclusion in the inner spheres of cortisone-fullerenol clusters He, ^{222}Rn and NaCl, KBr were chosen. The choice of these objects of inclusion is due to the fact that the ^{222}Rn radionuclide are convenient sources of therapeutic ionizing α-radiation, and He is a convenient inert model object of comparison. The introduction of one of the ions from NaCl, KBr into the internal cavities of fullerenol leads to a significant increase in the polarity of the resulting endohedral cluster systems, which is a determining factor facilitating their penetration through cell membranes. Quantum-chemical modeling of the process of building a cluster based on cortisone and symmetric fullerenol $C_{60}(OH)_{24}$ has been carried out. Total system energies (*E*, a.u.), energies HOMO (eV) and LUMO (eV) and dipole moments (*D*, Debye) of compounds were calculated in vacuum and in aqueous medium From the data of quantum chemical calculations it follows that the interaction energy ($\Delta E_{Int.}$) of clusters (**3−5, 7−9, 12-15**), obtained by the formula

$$\Delta E_{Int.(\mathbf{3-5,\ 7-9,\ 12-15})} = E_{(\mathbf{3-5,\ 7-9,\ 12-15})} - [E_{(\mathbf{1})} + E_{(\mathbf{2,\ 6,\ 10,\ 11})}]$$

shows their stability and a decrease or increase in the total energy of the system with a hypothetical «dissolution» of 1 or 2 gram-atoms of He **2** or Rn **6**, or 1 gram-mole of E_1E_2 salt (NaCl or KBr) **10**, **11** in 1 gram-mole of cortisone-fullerenol **1**.

Conclusions. From the obtained data on the stability of clusters investigated by the method of quantum chemical DFT simulation, we can draw conclusions about the possibility of their practical obtaining.

Jump diffusion of the lattice fluid on the two-level lattice

Ya. G. Groda* and R. N. Lasovsky
*BSTU, 13a, Sverdlova str., 220006, Minsk, Belarus, yar.groda@gmail.com**

Mass transfer, and the associated charge transfer, through diffusion plays an important role in many physical, chemical and biological processes. The lattice gas or lattice fluid model is one of the simplest models suitable for describing this process.

In this report, we present the results of a study diffusion properties of the lattice fluide with interaction of nearest neighbours on the two-level lattice. In particular, the influence of the type of the interparticle interaction on the jump diffusion coefficient of the system is investigated.

The diffusion properties of the model are investigated by simulating the diffusion process using the Monte Carlo method.

In addition, an analytical expresion for evaluating the jump diffusion coefficient is proposed. Using this relationship, the jump diffusion coefficient can be determined based on information on the equilibrium properties of the model.

In Fig. 1 the dependences versus the concentration of the jump diffusion coefficients of the lattice fluid with the interaction of the nearest neighbors on the two-level lattice are represented.

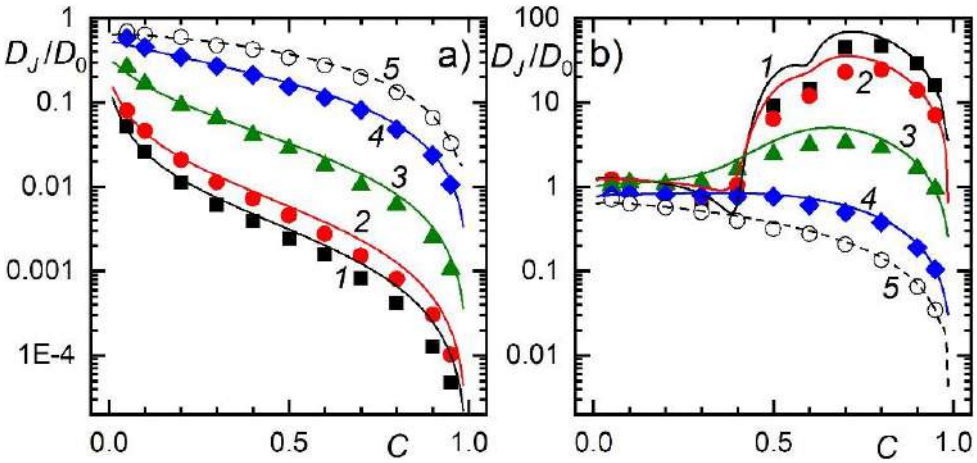

Figure 1. The jump diffusion coefficient versus concentration of the lattice fluid with the attraction (a) and repulsion (b) of the nearest neighbors on the two-level lattice. The dots represent the MC simulation data, lines – the results of analytical calculation. T/T_c = 1.05 (*1*), 1.2 (*2*); 2.0 (*3*); 6.0 (*4*) and 10^3 (*5*)

The comparison of the results of simulation and analytical calculations showed that the proposed expression for the jump diffusion coefficient give it possible to correctly estimate the transport properties of the model both at attracted between particles and at repulsed between them. Equilibrium values of concentration, chemical potential and probability function can be determined with the sufficient degree of accuracy within the framework of the diagram approximation.

In general, it can be noted that the diffusion properties of the system with attraction are similar to the properties of similar one-level models. At the same time, systems with repulsive interaction exhibit the set of features caused by the macroscopic ordering of the system. These features are most pronounced when the concentration of particles is equal to 2/5. They are manifested in the sharp decrease in the mobility of particles caused both by the peculiarities of their distribution over lattice sites and by the nature of interparticle interactions.

Acknowledgement

The project is co-financed by the Polish National Agency for Academic Exchange within “Solidarity with scientists Initiative” and European Union’s Horizon-2020 research and innovation program under the Marie Sklodowska-Curie grant agreement No 734276.

Biological Activity of Fullerenol - Cisplatin Conjugate as Agent of Antitumor Therapy: DFT Simulation

A. Pushkarchuk[1], T. Bezyazychnaya[1], V. Potkin[1], E. Dikusar[1], A. Soldatov[1,2], S. Kilin[3], A. Nizovtsev[3], S. Kuten[4], V. Pushkarchuk[5], Dominik Ludewig Michels[6], D. Lyakhov[6], V. Kulchitsky[7]

[1] *Institute of Physical and Organic Chemistry, NASB, 13 Surganova str., 220072 Minsk, Belarus, alexp51@bk.ru*
[2] *The Scientific and Practical Materials Research Center, NASB, 19 P.Brovka Str., 220072 Minsk, Belarus*
[3] *B.I. Stepanov Institute for Physics, NASB, Nezavisimosti Ave. 68, 220072 Minsk, Belarus*
[4] *Institute for Nuclear Problems, BSU, 11 Bobruiskaia Str., 220030 Minsk, Belarus, kuten@inp.bsu.by*
[5] *Belarusian State University of Informatics and Radioelectronics, 6 P.Brovka Str., 220013 Minsk, Belarus,*
[6] *Computer, Electrical and Mathematical Science and Engineering Division, 4700 King Abdullah University of Science and Technology, Thuwal 23955-6900, Saudi Arabia*
[7] *Institute for physiology, NASB, 13 Surganova str., 220072 Minsk, Belarus,*

In the era of increasing the effectiveness of treatment methods and drugs used in modern neuro-oncology, the targeted delivery of diagnostic and medicinal substances to the tumor is of great importance. The aim of the work is to study optimal and rational approaches to the creation of nanocontainers for targeted drug delivery.

Here we present the results of DFT simulation of the atomic and electronic structure of water-soluble conjugate of cisplatin (Cis) and nanocarbon structure, such as fullerenol ($C_{60}OH_{24}$), as well as the results of studying the possible mechanisms of the biological activity of these complexes. We studied the structural and electronic characteristics, as well as possible mechanisms for the formation of the conjugates of the cytotoxic drug cisplatin (cis-$[Pt(NH_3)_2Cl_2]$) and fullerenol. The investigated complex consisting of $C_{60}OH_{24}$+ Cis is shown in Figure 1.

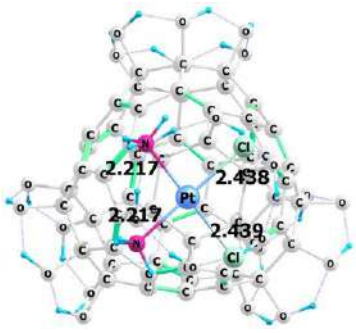

Fig.1 $C_{60}(OH)_{24}$ + Cis complex after calculation by the DFT method in water. Distances are given in Å

Isolated molecules in vacuum and with consideration to aqueous medium, which simulates situation in living cells where studied. Polarizable continuum model (PCM) was used for solvent phase calculations. The calculations were performed using the DFT/CAM-B3LYP/pvdz/LanL2DZ(Pt) level of theory. The Gaussian 16 software was used.

Thus, using DFT simulation we estimated the atomic and electronic characteristics of C60(OH)24 + Cis conjugates. These conjugates form stable, non-covalently bound complexes. This is established that fullerenol is not only a carrier of cisplatin, but also is able to directly participate in the processes of influencing the tumor.

First principles study of magnetic configurations in $YFeO_3$ multiferroic

A. Baglov[1,2*], L. Khoroshko[1,2]
[1]*Belarusian State University of Informatics and Radioelectronics, 6 P. Browka str., Minsk 220013, Republic of Belarus, baglov@bsuir.by**
[2]*Belarusian State University, 4 Nezalezhnasci ave., Minsk 220030, Republic of Belarus*

Multiferroics are materials that combine magnetic and electrical ordering. Usually, it is the materials which exhibiting both ferromagnetic and ferroelectric properties. The last few years of research on multiferroics and (nano) structures based on them are motivated by the possibility of creating on their basis new energy-efficient information processing devices based on the principles of straintronics – a new direction in the physics of condensed matter using methods of deformation engineering and physical effects induced mechanical deformations in solids, for the implementation of a new generation of devices for information, sensor and energy-saving technologies. In this work, we have studied the structural properties and found the ground state of the multiferroic $YFeO_3$ with a perovskite structure in various magnetic configurations by the ab-initio methods.

The study of structural and electronic properties was carried out in the *OpenMX* package, which implements the density functional theory in combination with the pseudopotential theory. The basis of pseudo-atomic orbitals was constructed using two optimized basis functions for each valence electron with one additional polarization optimized basis function to more accurately take into account the chemical bond in the crystal. The unit cell of $YFeO_3$ perovskite has an orthorhombic system and includes four formula units. Taking into account the symmetry, 4 iron ions can create 4 magnetic configurations: ferromagnetic (FM) and three antiferromagnetic – A-type (A-AFM), C-type (C-AFM) and G-type (G-AFM).

Taking into account that calculations by the generalized gradient approximation usually overestimate the interatomic distances and the unit cell parameters, we can conclude that the properties of the lattice are in good agreement with the experimental data for all calculated magnetic configurations. We observe an increase in the unit cell volume from 1.1% (FM) to 2.6% (C-AFM) for all configurations. Abnormal behavior observed for FM configuration is working out in the parameter *b* of lattice decreasing in comparison with the experimental data. This can be explained by the numerical simulation peculiarity, namely, the process of structural relaxation included a change in the positions of ions moving in the O_x axis direction, didn't compensate for the forces in the O_y axis direction.

Comparison of the obtained results with the scarce experimental data in the literature for this compound shows the applicability of the method of the generalized gradient approximation. Type of the ground magnetic state of the studied system was established from the calculation of the total energy of the magnetic configuration: it's the G-type antiferromagnetic state (G-AFM). Taking its total energy as zero, the energy for other magnetic configurations per formula unit is: 0.09 eV for C-AFM; 0.18 eV for A-AFM; 0.23 eV for FM. Thus, antiferromagnetic configurations lie under the ferromagnetic state and are separated by approximately the same energy value 90 meV. Considering that different directions of unit cell deformation correspond to different magnetic configurations, the use of the multiferroic $YFeO_3$ is promising in the composition of straintronic structures.

The authors are grateful for partial financial support of the research by the grant M20MV-022 BRFFR.

Sensing single molecules at diamond surface with the NV centers: Quantum chemistry simulation of simple test systems

V. Pushkarchuk[1], A. Pushkarchuk[2], S.Kilin[3], A.Nizovtsev[3], S.Kuten[4], D. Michels[5], D.Lyakhov[5], F.Jelezko[6]
[1] *Belarusian State University of Informatics and Radioelectronics, Belarus*
**e-mail:* *pushkarchuk@bsuir.by*
[2]*Institute of Physical and Organic Chemistry, Nat. Acad. Sci., 220072 Minsk, Belarus.*
[3]*Institute of Physics, Nat. Acad. Sci., 220072 Minsk, Belarus*
[4] *Institute for Nuclear Problems, Belarusian State University, 220006 Minsk, Belarus.*
[5]*Computer, Electrical and Mathematical Science and Engineering Division, 4700 King Abdullah University of Science and Technology, Thuwal 23955-6900, Saudi Arabia.*
[6] *Institute for Quantum Optics, Ulm University, 89069 Ulm, Germany*

In the last decade there was rapid development of quntum magnetic sensing technology based on the nitrogen-vacancy (NV) color centers in diamond (see, e.g. [1] for recent review). Magnetometer based on single NV center can to detect distinguish (by their chemical shifts) inequivalent nulear spins of molecules located at diamond surface [3], using single-spin nuclear magnetic resonance (NMR). In this respect, finding out of the high-resolution NMR parameters is essential.

The theoretical analysis of this latest experiment [2], on the registration of chemical shifts for various nuclear spins in the ethyl formate (EF) molecule, is the subject of this article. We have calculated values of Anisotropic Spin Dipole Couplings (ASDC) of conjugates consisting of a "surface" clusters hosting the NV center in central part of nanodiamond ($ND[NV]^{-1}$)(111), simulating the (111) surface of diamond, by functionalizing this surface, the COOH-groups and the EF, which is non-covalently bound to this surface are located.

The calculations were carried out for 2 conjugates. Fig. 1 shows the results of DFT calculation of the atomic structure of $C_{66}[NV]^{-}H_{72}$(111)6COOH–EF and $C_{68}[NV]^{-}H_{83}$(1DB111)1COOH–EF conjugates after their full geometry optimization.

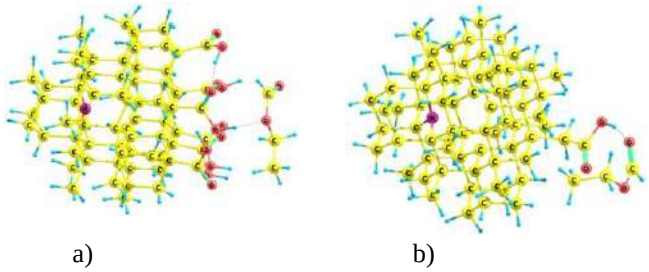

a) b)

Fig.1 Conjugates after full geometry optimizatiom
a) C66[NV]-H72(111)6COOH–EF,
b) C68[NV]-H83(1DB 111)1COOH–EF. Hydrogen atoms are not labeled, dotted lines indicate hydrogen bonds

Conjugates under study form stable, non-covalently bound complexes. The ASDCs for these conjugates showed that, the value of Couplings indicates the formation of three groups of H atoms obtained in NMR experiments. It has been shown that DFT calculations of the studied structures make it possible to interpret the corresponding NMR results and also be predictive and used in planning the corresponding experiments.

Acknowledgement
The work was carried out within the framework of the State Research Programs ”Convergence 2025”. All Gaussian 16 package computation were performed on KAUST’s Ibex HPC. The authors thank the KAUST Supercomputing Core Lab team for assistance with execution tasks on Skylake nodes..

References

[1] Barry J.F. et al. Sensitivity optimization for NV-diamond magnetometry. Rev. Mod. Phys. 92 (2020) 015004.
[2] Glenn D.R. et al. High-resolution magnetic resonance spectroscopy using a solid-state spin sensor. Nature. 555 (2018) 351.

Ab initio study of intrinsic point defects in bulk and monolayer MoS_2: formation and diffusion

V. Gusakov[1*], J. Gusakova[2], and B. K. Tay[2]
[1] *Scientific-Practical Materials Research Center of NAS of Belarus, 19 P. Brovki, 220072 Minsk, Belarus** gusakov@*ifttp.bas-net.by*
[2] *Novitas Center, Nanyang Technological University, 50 Nanyang Avenue, 639798 Singapore, Singapore*

Semiconducting transition metal dichalcogenides (TMDs) represent a class of layered materials. TMD monolayers such as MoS_2, $MoSe_2$, WS_2, and WSe_2 are direct band gap semiconductors (with an optical band gap of 1–2 eV). Owing to a nonzero band gap, rich physics, and promising applications in electronic and optoelectronic devices, transition metal dichalcogenides have attracted much attention.

We for the first time have calculated the formation energy of a split Frenkel pair in 3D and 2D MoS_2 without using the chemical potential, which makes it possible to determine the thermodynamically equilibrium concentrations of vacancies and interstitial atoms. All calculations have been performed using a crystal supercell method. Quantum Espresso implementation of the DFT was used for the computation of the structure and electronic properties of bulk and monolayer MoS_2.

Table presents the calculated energy of formation of the split Frenkel pair $E_{form}[V+I]$ in MoS_2. We note that the energy of formation of the split Frenkel pair in bulk material is greater than in a MoS_2 monolayer. Knowing the formation energy of the split Frenkel pair, we can directly determine the thermal equilibrium concentration of intrinsic defects. We can also express the formation energy of a vacancy and an interstitial atom as a function of the chemical potential μ_S. So for a sulfur atom we have $E_V(S) = 5.59 + \mu_S[eV]$, $E_I(S) = -2{,}11 - \mu_S[eV]$.

Table. The energy of formation (E_{form}) of the split Frenkel pair (V + I), vacancy (V), interstitial (I) atom, of sulfur and molybdenum in bulk and monolayer MoS_2. The diffusion barrier (ΔE) of a single chalcogen vacancy (V_{S1}) in bulk and monolayer MoS_2. All energy values are in eV.

MoS_2		$E_{form}[V+I]$ (PZ LDA / PBEGGA)	$E_{form}[V]$	$E_{form}[I]$	$\Delta E(V)$ (PZ LDA)	$D_0(V)$ cm^2s^{-1}	$\Delta E(I)$ (PBE)	$D_0(I)$ cm^2s^{-1}
L1	S	3.95 / 3.53	3.5	0.45	2.3	$2.9\cdot10^{-3}$	1.63	$6.8\cdot10^{-4}$
	Mo	12.1	11.7	0.4	3.23	$3.3\cdot10^{-3}$	1.1	$1.2\cdot10^{-3}$
bulk	S	6.56 / 6.77	3.5	3.06	2.3	$2.9\cdot10^{-3}$	≤0.08	-
	Mo	12.6	11.7	0.9	3.23	$3.3\cdot10^{-3}$	0.45	-

We performed also a complete calculation of the diffusion coefficient (the pre-exponential factor and activation barrier) of intrinsic defects in different charge states. The calculated diffusion barrier of the single sulfur vacancy in both monolayer and bulk MoS_2 equals to 2.3 eV.

Acknowledgment
Vasilii Gusakov thanks the support from the BRFFR project No F20MC-002.

Ab initio study of 2D $MoS_{2(1-x)}Se_{2x}$ alloy: structure and electronic properties

V. Gusakov[1*], J. Gusakova[2], and B. K. Tay[2]
[1] *Scientific-Practical Materials Research Center of NAS of Belarus, 19 P. Brovki, 220072 Minsk, Belarus** gusakov@ifttp.bas-net.by
[2] *Novitas Center, Nanyang Technological University, 50 Nanyang Avenue, 639798 Singapore, Singapore*

Semiconducting transition metal dichalcogenides (TMDs) represent a class of layered materials with a nonzero band gap, which exploration started decades ago and continues until present. Transition metal dichalcogenides have attracted much attention owing to their rich physics and promising applications in electronic and optoelectronic devices [2]. TMD monolayers such as MoS_2, $MoSe_2$, WS_2, WSe_2 are direct band gap semiconductors (with optical band gap of 1-2 eV). The crystal-phase engineering of TMDs is critically important to form new structures phase-based TMD, showing tunable physicochemical properties.

We present calculation fundamental band gap of $MoS_{2(1-x)}Se_{2x}$ alloy.The effects of relative positions of Se atoms in a real monolayer alloy $MoS_{1.5}Se_{0.5}$ have been studied. It is demonstrated that the distribution of Se atoms between top and bottom chalcogen planes is most energetically favorable. For a more probable distribution of Se atoms in $MoS_{2(1-x)}Se_{2x}$, monolayer is a direct band semiconductor with the fundamental band gap equal 2.35 eV ($MoS_{1.5}Se_{0.5}$). We have also evaluated the optical band gap of alloy at 77 K (1.86 eV) and room temperature (1.80 eV), which is in good agreement with the experimentally measured band gap of 1.79 eV.

Table present calculated (GVJ-2e) fundamental band gap of $MoS_{2(1-x)}Se_{2x}$ alloy. The average value of the fundamental band gap lies between experimental values of 2.40 eV, 2.5 eV for MoS_2, and 2.18 eV for $MoSe_2$ and corresponds to about 30 % shift from experimental band gap of monolayer MoS_2 towards $MoSe_2$. Comparison of the effective masses of electrons (holes) in the alloy with the effective masses of electrons in MoS_2 and $MoSe_2$ monolayers reveals that electrons (holes) become slightly heavier in the alloy.

Table. Fundamental band gap of a single-layer $MoS_{2(1-x)}Se_{2x}$ (GVJ-2e QP); exciton binding energy ($E_{exc.binding}$); Optical band gap at low (GVJ-2e PL LT) and room temperature (GVJ-2e PL RT); temperature shift of the band gap ($\Delta E_g^{T,\ alloy}$). All values are in eV.

1L	x	GVJ-2e QP	$E_{exc.binding}$	GVJ-2e PL LT	$\Delta E_g^{T,alloy}$	GVJ-2e PL RT
MoS_2	0	2.39	0.501	1.89	0.0475	1.84
$MoS_{1.75}Se_{0.25}$	0.125	2.37	0.4965	1.87	0.0516	1.82
$MoS_{1.5}Se_{0.5}$	0.25	2.35	0.492	1.86	0.0557	1.80
$MoS_{1.25}Se_{0.75}$	0.375	2.28	0.4875	1.79	0.0598	1.73
MoS_1Se_1	0.50	2.27	0.483	1.78	0.0639	1.72
$MoS_{0.75}Se_{1.25}$	0.625	2.24	0.4785	1.76	0.0679	1.69
$MoS_{0.5}Se_{1.5}$	0.75	2.23	0.474	1.76	0.0720	1.68
$MoS_{0.25}Se_{1.75}$	0.875	2.12	0.4695	1.65	0.0761	1.58
$MoSe_2$	1	2.12	0.465	1.65	0.0802	1.57

Acknowledgment
V. Gusakov thanks the support from the BRFFR project No F20MC-002.

Ab initio study of Exchange Interactions In the Nanoscale Magnetic Systems Based on $CrGeX_3$ (X=S, Se, Te)

M. Baranava*, V. Stempitsky
R&D Department, Belarusian State University of Informatics and Radioelectronics, Minsk, Republic of Belarus

In this work, to analyze the spin-dependent properties in 2D vdW structures ($CrGeX_3$, where X = S, Se, Te), the exchange interaction integrals were calculated for Cr atoms located at a distance of up to 8 Å. To calculate the exchange interaction integrals (Jn, where n = 1, 2, 3 the order of the atom in accordance with the distance), 2 × 2 × 1 supercells were created. The orientations of the magnetic moment (spin) were set for each Cr atom in such a way as to form 4 magnetic configurations. One of which had a ferromagnetic order (FM), the other three were antiferromagnetic (AFM). Structural optimizations were performed for all configurations. The structural parameters such as the angles between the two nearest metal atoms through the chalcogen atom ($\alpha_{M\text{-}A\text{-}M}$) and the distance between the Cr atom and the chalcogen (Table 1) of the investigated atomic systems have been calculated. All structures under study are ferromagnets. However, the value of the exchange interaction integral for $CrGeS_3$ is so small that the formation of a stable ferromagnetic order in such structures is hardly possible. The strongest ferromagnet is $CrGeTe_3$. In this case, almost all the contribution to the exchange interaction is made by J_1. At the same time, in this structure, the largest distance between the magnetic atoms is observed. If the exchange interaction in this class of materials were direct (direct overlap of the atomic orbitals of the transition elements), then the value of the exchange interaction integral would decrease with increasing distance. Here we observe an inverse relationship, which is evidence in favor of an indirect exchange interaction. The Cr-X-Cr angles (about 90 degrees) and the Cr-X distance also contribute to the hybridization of the unfilled transition metal *d*-orbital and the chalcogen *p*-orbital. Thus, it can be assumed that the exchange interaction between metals occurs through the mechanisms of superexchange.

Analysis of the magnetization distribution (M) showed that the entire magnetic moment is localized on the Cr atom. It is equals 3.13-3.42 μ_B , which corresponds to its stoichiometry (Cr^{3+}). In this case, the electrons uncompensated in spin are localized on the *d*-orbital. Thus, hybridization of the *p*-orbitals of the chalcogen and the *d*-orbital of the transition metal occurs. Such hybridization helps to carry out exchange interaction by the mechanism of superexchange.

Previously, we have already simulated the ground magnetic state in 2D vdW structures ($CrGeX_3$, where X = S, Se, Te) [1]. There, we found that $CrGeSe_3$ and $CrGeS_3$ are antiferromagnets and did not calculate the exchange interaction integral for them. In this work, we found that all three compounds are ferromagnets. The difference between the works lies in the additional parameter of the exchange-correlative energy in the quantum-mechanical simulation and larger numbers of k-points in the calculation. Also, in our earlier study, we took into account only the exchange interaction to the second most distant magnetic atom. Here we looked at up to the third neighboring magnetic atom, which makes a small contribution. However, we believe that the differences in results are not significant. For example, for $CrGeS_3$, the value of the exchange interaction integral is so small that it cannot be considered a ferromagnet. For $CrGeSe_3$, the differences are more significant, but they are still small in order to consider this material a strong ferromagnet. The exchange interaction integral for $CrGeTe_3$ does not differ much (-2.35 meV in this work, -2.40 meV in early studies [1]. Thus, the results in terms of quality characteristics do not contradict each other.

References

[1] M. S. Baranava, P. A. Praskurava, Doklady BGUIR 18(7) (2020) 87-95.

An optomechanical system with a bistable effective mechanical potential

A.P. Saiko[1*], G.A. Rusetsky[1], S.A. Markevich[1], R. Fedaruk[2]
[1] *Scientific-Practical Material Research Centre, Belarus National Academy of Sciences, 19 P. Brovka str., Minsk 220072 Belarus*
[2] *Institute of Physics, University of Szczecin, 15 Wielkopolska str., 70-451, Szczecin, Poland*

A nano-optomechanical system, in which the coupling between a photon field and a mechanical resonator is described by interacting terms, linear, quadratic, and cubic in mechanical displacements, is studied. It is shown that under the conditions of the adiabatic elimination of the cavity field, the dynamics of the mechanical resonator is determined by some effective, generally bistable, potential. The shape of this potential depends on the power of the photon pumping field, pumping detuning from the cavity resonance, the parameters of nonlinear interactions and the decay rate of the cavity field.

The behaviour of multiple signals of single-pulse echo dependence on the excitation conditions in magnetically ordered materials with Ising interaction

V.M. Kolesenko, G.A. Rusetsky
Scientific-Practical Material Research Centre, Belarus National Academy of Sciences, 19 P. Brovka str., Minsk 220072 Belarus

We analyze the behaviour of the primary and multiple single-pulse echos in magnetically ordered materials. Such signals are formed upon excitation of a two-component nuclear system by a rf pulse. We found that the spin-spin interaction within nuclear subsystems leads to nonmonotonic primary single-pulse echo amplitude dependence on rf pulse detuning from resonance. We also show that the spin-spin interaction between the subsystems decreases the amplitude of the single-pulse echos.

First-principles investigation of dynamic and mechanical stabilities of 2D monoelement materials

D. Hvazdouski*, V. Stempitsky
Belarusian State University of Informatics and Radioelectronic, 6 P. Brovki Street, office 119, Minsk 220013, Republic of Belarus
** e-mail: gvozdovsky@bsuir.by*

An important task is to determine the stability of two-dimensional materials using a numerical experiment, in particular, using *ab initio* methods. A numerical experiment is much cheaper than a physical one. In the course of a numerical experiment, it is possible to simulate conditions that cannot be created in the laboratory and, therefore, to investigate the material over a wide range of characteristics. Real materials must be simultaneously satisfy thermodynamic, mechanical, dynamic and thermal stability.

We have estimated stability of 2D monoelement materials (C_2, Si_2, Ge_2, Sn_2, Pb_2, P_2, As_2, Sb_2 and Bi_2) by *ab initio* calculations. The structural and mechanical properties calculations of 2D materials were performed using the VASP software package.

To calculate the elasticity constants, the $E_s(\varepsilon)$ function was investigated in the deformation range of $-1.5\% \leq \varepsilon \leq 1.5\%$ with a step of 0.5%. The elasticity constants C_{ij} were obtained by fitting a second-order polynomial of the total energy change function of the system depending on the applied deformation. Post-processing of the calculated data was carried out the VASPKIT code [1]. The mechanical properties of 2D monoelement materials calculated using *ab initio* methods and presented in Table 1. Results of stiffness tensors, Young's modulus and Poisson's ratios calculations show that all studied 2D monoelement materials are mechanically stable.

Table 1. Mechanical properties of 2D monoelement materials

Parameter		2D monoelement material								
		C_2	**Si_2**	**Ge_2**	**Sn_2**	**Pb_2**	**P_2**	**As_2**	**Sb_2**	**Bi_2**
This wok	**C_{11}, N/m**	343.07	69.28	49.78	27.04	15.62	77.73	52.91	32.89	25.04
	C_{12}, N/m	78.82	22.19	17.69	10.99	5.65	8.73	9.57	5.74	6.27
	ν	0.23	0.32	0.35	0.41	0.36	0.11	0.18	0.17	0.25
	Y, N/m	324.96	62.17	43.49	22.57	13.58	76.75	51.16	31.89	23.47
Ref. [2]	**C_{11}, N/m**	345.65	66.62	48.87	28.56	–	77.37	52.51	32.61	24.49
	C_{12}, N/m	70.61	21.51	16.22	11.41	–	7.95	8.50	6.23	6.05

Dynamic stability investigated by calculating the phonon dispersion of the materials using the finite displacement method. We have utilized 5×5×1 supercell for the 2D structures and the atomic displacement distance of 0.01 Å. Phonon dispersion has been evaluated in the Phonopy program [3]. Only Pb_2 have imaginary modes in the phonon dispersion curves and therefore it is dynamic unstable structure at low temperature.

It is necessary to carry out additional calculations based on molecular dynamics for a more accurate analysis of the stability of materials.

Acknowledgement

This work was supported by the grant 3.02.3 of Belarusian National Scientific Research Program "Convergence-2025" and the grant of The Belarusian Republican Foundation for Fundamental Research for young scientists "Science M - 2021" (contract № F21M-122). Computing cluster of BSUIR was used for computer modeling.

References

[1] V. Wang, N. Xu, J. C. Liu et al., Comp. Phys. Commun. 267 (2021) 108033.
[2] M. N. Gjerding, A. Taghizadeh, A. Rasmussen et al., 2D Materials 8 (2021) 044002.
[3] A. Togo and I. Tanaka, Scr. Mater. 108 (2015) 1-5.

Nonlinear reflection of femtosecond pulses from a thin layer of a resonant medium

G.A. Rusetsky[1], V.M. Kolesenko[1], and D.A. Klezovich[2]*
[1]*SSPA "ScientificPractical Material Research Centre of NAS of Belarus", 19 Brovki, Minsk, Belarus*
[2] *Belarusian State University, Faculty of Physics, Department of Laser Physics and Spectroscopy, 5 Bobruiskaya str., Minsk, Belarus*

The reflection spectrum of few-cycle pulse from a thin layer of dense resonant two-level medium was numerically and analytically studied. The fundamental difference in the reflection spectra as an area function of the rectangular pulse and a pulse in the form of a hyperbolic secant is demonstrated. It was shown that there are regions of pulse area where the position of the spectral lines in the reflection spectrum is practically constant.

Numerical simulation of thermomechanical action of ultrashort laser pulses on metals

S. Lipski[1], I. Timoshchenko[1], Y. Levy[2], O. Fedotova[3], O. Romanov[1*],
[1] *Belarusian State University, 220030, 4 Nezavisimosti Avenue, Minsk, Belarus*
[2] *HiLASE Centre, Institute of Physics ASCR, 25241 Dolni Brezany, Czech Republic*
[3] *Scientific and Practical Materials Research Center of the National Academy of Sciences of Belarus, 220072,*
15 P.Brovki, Minsk, Belarus

Physical, mathematical and numerical models of laser-induced excitation of acoustic pulses in metals have been developed to study the regularities of propagation of acoustic signals excited by ultrashort laser pulses of various spatial structures. The space-time structure of temperature fields and pressure waves excited in metals is simulated numerically, depending on the duration of laser pulses and the thermophysical characteristics of materials.

Computation of the Dielectric Permittivity of Powder Compositions

Denis Klygach [1,2]*, Maksim Vakhitov [1,2], and Alex Trukhanov [3]
[1] *School of Electronic Engineering and Computer Science South Ural State University Chelyabinsk, Russian Federation*
[2] *Ural Federal University Yekaterinburg, Russian Federation*
[3] *Scientific and practical materials research centre of NAS of Belarus, Minsk, Belarus*

The paper presents a mathematical model for calculating the dielectric permittivity of a two-component mixture of powder materials. Measurements of electrodynamic parameters of powder materials are described and experimental and calculated frequency dependences are given. Comparison of calculated and experimental values for a two-component mixture with different volumetric concentration ratios is performed.

Geometrodynamics of the first-order phase transition in the generalized cosmological models and interface layers

H.V. Grushevskaya[1] and N.G. Krylova[1,2]*
[1]*Belarusian state university, 220030 Nezavisimosti Ave. 4, Minsk, Belarus*
[2]*Belarusian state agrarian technical university, 220023 Nezavisimosti Ave. 99, Minsk, Belarus*

The geometrodynamical model of the first-order phase transition in the generalized cosmological models and interface layers has been studied. The Euler-Lagrange equation system for the phase transition in the configuration space has been solved numerically. It has been shown that the production of the “true vacuum” phase nuclei with sizes much more than a critical one occurs at supersaturation of the system under the condition of rapid compression/expansion and is accompanied by appearing of the additional local minimum in the potential. It has been found that the “true vacuum” state and the metastable state is characterized by the Jacobi stability.

Dimension-dependent phenomenological model of excitonic electric dipole in InGaAs quantum dots

P. Steindl[1,2], P. Klenovský[1,3]*
[1]*Department of Condensed Matter Physics, Faculty of Science, Masaryk University, Kotlářská 267/2, 61137 Brno, Czech Republic*
[2] *Huygens-Kamerlingh Onnes Laboratory, Leiden University, P.O. Box 9504, 2300 RA Leiden, Netherlands*
[3] *Czech Metrology Institute, Okružní 31, 63800 Brno, Czech Republic*

Permanent electric dipole p is a key property for effective control of semiconductor quantum-dot-based sources of quantum light. For its prediction, complex geometry-dependent quantum simulations are necessary. Here, we use $\boldsymbol{k}\cdot\boldsymbol{p}$ simulations to derive a simple geometry-dependent analytical model of p.

Efficiency of the shielding of radio-electronic devices from space radiation exposure

H. Yakushevich[1]*, S. Lastovskii[1], G. Protopopov[2]**, Y. Bogatyrev[1], S. Grabchikov[1], N. Vasilenkov[3], A. Koziukov[2]

[1] *Scientific-Practical Materials Research Centre of NAS of Belarus, 19, P. Brovka Str., 220072, Minsk, Belarus, yakushevich@ifttp.bas-net.by*

[2] *Branch of JSC United Rocket Space Corporation – Institute of Space Device Engineering, 53, Aviamotornaya Str., 111250, Moscow, g.a.protopopov@mail.ru*

[3] *JSC «TESTPRIBOR», 7a, Planernaya Str., 125480, Moscow, Russia*

Simulation of radiation shield efficiency for electronic component by metallic packages with W-Cu composites was carried out with taking spacecraft shielding into account.

Absorbed doses were calculated inside of silicon die 10 × 10 × 0.1 mm. The silicon die was placed in a typical metallic package with outside dimension 20 × 20 × 2 mm. Thickness of all package's walls is 0.1 mm. The typical package is made of kovar with density 8.4 g/cm^3 and composition following: Ni – 29%, Fe – 53%, Co – 18%.

The local radiation shield (LRS) is W-Cu composite plates surrounding the typical metallic package. We consider three types of LRS with effective thickness d_{WCu} – 0.5 g/cm^2, 1.0 g/cm^2, 1.65 g/cm^2. Density of W-Cu composite is equal to 16.5 g/cm^3. Composition of elements is follow: W – 85%, Cu – 15%. Spacecraft shielding is considered as an aluminum sphere with constant inner radius R = 30 mm, investigated packages are placed in the center of the sphere. We consider six sphere thickness d_{Al}: 0.01, 0.1, 0.5, 1.0, 2.0 and 3.0 g/cm^2. The calculation geometry is shown in Fig.1*a*.

The calculations were carried out for three typical orbits: medium Earth orbit (MEO) H = 4000 km with inclination 60º; low Earth orbit (LEO) H = 700 km with inclination 98º; high-elliptic orbit (HEO) H_A = 40000 km, H_P = 600 km with inclination 63º and perigee angle ω = 90º. Electron and proton differential spectra at these orbits for 15 years are shown in Fig.1*b*.

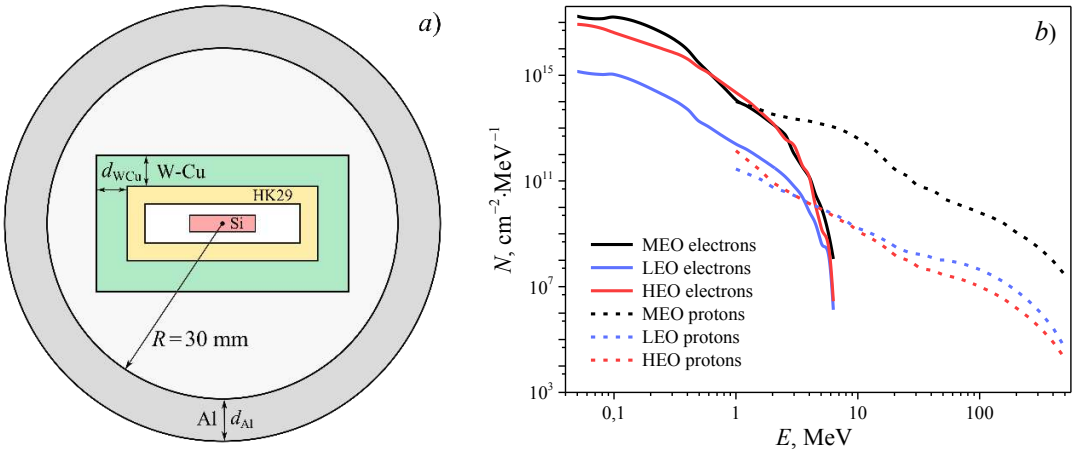

Figure 1. Geometrical model (*a*) and differential spectra for 15 years (*b*)

Calculation of radiation shield efficiency of W-Cu composite LRS for electron (K_e) and proton (K_p) exposure was carried out using Geant4 toolkit. It has been shown that LRS efficiency depends on aluminum spherical shielding thickness and the orbit type. With increasing of d_{Al} K_e values as well as K_p values are decreasing monotonously for all three orbits. But LRS efficiency for electrons is much greater than one for protons for all d_{Al} values.

The greatest attenuation coefficients for electron and proton exposure are achieved for aluminum sphere thickness < 2 g/cm^2 and < 1 g/cm^2, correspondingly. The efficiency of LRS with thickness of 1.65 g/cm^2 and aluminum sphere thickness of 0.01 g/cm^2 depends on the orbit type and is equal to K_e = 4750–9180 for electrons and K_p = 8–58 for protons.

Exploration of Structural, Electronic, Magnetic, and Thermoelectric Properties of CoRuVAl Heusler Alloy

V. Aravindan[1], A. K. Rajarajan[2], V. Vijayanarayanan[1] and M. Mahendran[1,*]
[1]*Smart Materials Laboratory, Department of Physics, Thiagarajar College of Engineering, Madurai – 625 015, India*
[2] *Solid State Physics Division, Bhabha Atomic Research Centre, Mumbai – 400 085, India*

Using density functional theory and Boltzmann transport theory, We have computed physical and thermoelectric transport properties of CoRuVAl quaternary Heusler alloy. The presence of metallic overlap in up spin and semiconductor band gap in down spin confirms half-metallic nature. We implemented Hubbard potential (U_{eff}) to generalized gradient approximation for all calculations. This alloy has a total magnetic moment (M_T) of 0.99 μ_B which follows the Slater-Pauling rule of $M_T = Z_T - 24$. The calculated thermoelectric coefficients of the present alloy are enhanced due to the semiconductor band gap in the spin down channel.

On the law of dispersion of an electromagnetic wave in a medium with a double type of anisotropy

V.Sobol[1*], K.Yanushkevich[2], B.Korzun[3]
[1]*M.Tank Belarusian State Pedagogical University, Minsk, Belarus.*
[2] *SSPA "Scientific-Practical Materials Reseach Centre of NAS of Belarus", Minsk, Belarus*
[3] *The City University of New York, Borough of Manhattan Community College, U.S.A.*

Dispersion relations are considered for a one particular case of propagation of an electromagnetic wave being linearly polarized with respect to the electric induction vector after its incidence into the optical medium described by the tensors of the dielectric and magnetic permeability. For a wave being transverse in electric induction and wave vector, the relations between the angles of incidence and refraction are obtained in general form, which in the limiting case of spherical tensors are transformed to the well-known Snell law. One particular case of anisotropy is presented with reduction of the dielectric tensor to the principal axes and with the analysis of the corresponding form of section of wave normal surface. Here the tensor, characterized only by a one pair of nonzero off-diagonal components of the so-called Hall type.

Effects of hydrogen on trap neutralization in $BaSi_2$ with iterstitial silicon atoms

D.B. Migas[1,2]*
[1] *Belarusian State University of Informatics and Radioelectronics, P. Browki 6, 220013 Minsk, Belarus*
[2] *National Research Nuclear University MEPhI (Moscow Engineering Physics Institute), Kashirskoe shosse 31, 115409 Moscow, Russia*

By means of *ab initio* calculations we show that a Si interstitial atom in semiconducting $BaSi_2$ can provide trap states. At least two H atoms are necessary to eliminate these traps, while one or three H atoms, on the contrary, promote the appearance of the traps. Thus, the H incorporation in $BaSi_2$ films during growth, which is used to neutralize traps due to Si vacancies, requires a careful adjustment of treatment time in hydrogen RF plasma for $BaSi_2$ where Si interstitial atoms are the main point defects.

Counter-rotating effects in coherent dynamics of Raman transitions

A.P. Saiko[1]*, S.A. Markevich[1], R. Fedaruk[2]
[1]*Scientific-Practical Material Research Centre, Belarus National Academy of Sciences, 19 P.Brovka str., Minsk 220072 Belarus*
[2]*Institute of Physics, University of Szczecin, 15 Wielkopolska str., 70-451, Szczecin, Poland*

We study Rabi oscillations of the first and second-order Raman transition realized on dressed states of a qubit excited by an amplitude-modulated microwave field. It is shown that for properly chosen parameters of the modulation field and qubit, the Rabi oscillations in the rotating wave approximation vanish due to destructive interference of multiple photon processes. In this case the Rabi oscillation results exclusively from the Bloch–Siegert effect and is directly observed in the time-resolved coherent dynamics as the Bloch–Siegert oscillation. Correspondingly, in Fourier spectra of the coherent response, triplets are transformed into doublets with the splitting between the lines equal to twice the Bloch–Siegert shift. We demonstrate these features by calculations of the qubit's evolution in the conditions of experiments with a NV center in diamond, where Raman transitions were observed.

Exchange energy calculation in the system of donors and embedded quantum dots

E.A. Levchuk*, L.F. Makrenko
Belarusian State University,4 Nezavisimosti Avenue, Minsk 220030, Belarus,
*liauchuk.alena@gmail.com**

The possibility of realizing the solid-state elements of quantum information devices has attracted a lot of attention due to long coherence times, promise to scalability and compatibility with existing semiconductor technologies. In order to control spin-qubit operations for several quantum computing proposals, it is necessary to manipulate spin and exchange interaction between electrons bound to a pair of donors or quantum dots (QDs). In this work, we study the effect of geometrical and material parameters on the value of exchange interaction of the near-surface system of two donors and two embedded quantum dots (QDs). We also consider manipulation of the exchange interaction with external electric field of disk-shaped gate.

We consider three-dimensional problem for the stationary Schrödinger equation for two electrons bound to donors pair or pair of spherical quantum dots with piecewise constant confining potential. To solve the problem, Hartree-Forck method has been used.

The proposed algorithm includes variational method with gassian trial functions for the Schrödinger equations and finite element method (FEM) for self-consistent field calculations. The combination of used variational basis and numerical method allows to perform calcualtions for different quantum dot types, which has been demonstrated on the system of embedded quantum dots. The algorithm allows to perform calculations more efficiently as compared with pure analytical methods (Heitler-London, etc.) and increase accuracy with growing variational basis and FEM accuracy. At the same time the method has less computational cost as compared with direct diagonalization method.

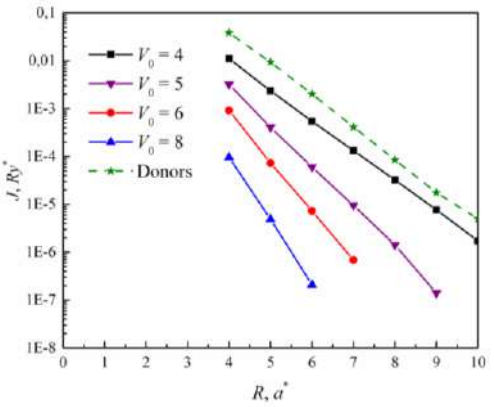

Exchange energy in the system of double embedded spherical quantum dots depending on the distance between dots R for different QDs depths V_0, QDs radius $r_0 = 1$. Dashed line corresponds to exchange energy of two-donor system

On the basis of the calculation results, we have obtained analytical formula for the dependence of the exchange energy on the distance between the dots, as well as it has been found for a pair of donors [1]. This dependence can be expressed in terms of ground state energy of individual quantum dots.

We have shown that gate potential does not have sufficient effect on exchange interaction in two-donor system, as exchange energy varies in the range of only one order before electron relocation to the gate occurs. This means that quantum computing applications require other electric field configurations or additional control tool to manipulate exchange interaction.

We have found that for deep quantum dot pairs (as well as for donor pairs [1]) the dependence of exhcange coupling on the gate potential is approximately exponential. However, for shallow quantum dots with small values of QD depth, exchange energy demostrates faster growth with increasing gate potential.

Based on the calculation results, optimal system configurations can be proposed for more efficient exchange energy control.

References

[1] A. Fang, Phys. Rev. B 66, 155331 (2002).

Theoretical study of the optical properties of the crystal systems doped by the elements with an unfilled f-shell

L.A. Fomicheva[1*], A.A. Kornienko[2], E.B. Dunina[2]
[1] *Belarusian State University of Informatics and Radioelectronics, 220013, P. Brovki st., 6, Minsk, Belarus, famichova@mail.ru**
[2] *Vitebsk State Technological University, 210035, Moskovskiy avenue, 72, Vitebsk, Belarus*

The theory of crystal field is used to describe the experimental data on the Stark splitting of elements with an unfilled f-shell. The lanthanides and actinides have a similar electronic structure. The similarity of electron transitions and optical spectra of 4f- and 5f-elements allows to create the unified theoretical models to describe their spectroscopic properties.

At the moment there exist different ways of describing crystal systems activated by f-elements. But as far as none of the theories produces a full coincidence between theory and experiment, the works generating new theories are of great current interest.

We have designed a mathematical model [1,2] that allows to obtain the optical properties of the crystal systems doped by the elements with an unfilled f-shell on the basis of the experimental data on the Stark structure. This theory considers the anomalously strong influence of configurations with opposite parity and configurations with charge transfer. Then the Hamiltonian of the crystal field is as follows:

$$H_{cf} = \sum_{k,q}\left\{ B_q^k + \left(\frac{\Delta_d^2}{\Delta_d - E_J} + \frac{\Delta_d^2}{\Delta_d - E_{J'}} \right) \tilde{G}_q^k(d) + \sum_i \left(\frac{\Delta_{ci}^2}{\Delta_{ci} - E_J} + \frac{\Delta_{ci}^2}{\Delta_{ci} - E_{J'}} \right) \tilde{G}_q^k(c) \right\} C_q^k$$

Where Δ_d is the energy of an excited configuration with opposite parity; Δ_{ci} is the energy of a charge-transfer configuration.

The calculations within the suggested model result in the notable improvement of coincidence between theory and experiment. Furthermore, we can obtain the parameters of the odd-symmetry crystal field and the covalence parameters, which can be used to estimate the intensity values of f-f transfers.

References

[1] E.B. Dunina, A.A. Kornienko, L.A. Fomicheva. CEJP. 6 (2008) 407-414.
[2] L. Fomicheva, E. Dunina, A. Kornienko. Universal Journal of Physics and Application. 7 (2013) 98-104.

Simulation of the process of sublimation of the anodic resistive coating of DLC GEM detectors of the NICA accelerator under the temperature action of the plasma channel of a spark discharge

I. Zur[1,2*], E. Shmanay[1], G. Remnev[3] and J. Fedotova[1]
[1]*Institute for Nuclear Problems of Belarusian State University, st. Bobruiskaya* 11, *Minsk* 220006, *Belarus, zur.ilya01@gmail.com*
[2]*Department of energy physics of Belarusian State University, st. Bobruiskaya* 5, *Minsk*
[3]*Tomsk Polytechnic University*, 4a *Usov Street, Tomsk, Russian Federation*

Progress in modern physics of elementary particles is largely due to the level of experimental capabilities of detectors. One of the main problems of gas-discharge detectors is the development of self-sustaining gas discharges. The purpose of this research is to study the effect of a cathodic spark gas discharge with a duration of $1 \cdot 10^{-3}$ s in an $Ar_{90}(CO_2)_{10}$ gas medium on the structure of the surface of a diamond-like coating (DLC) of a flat anode.

The study of the breakdown resistance of DLC was carried out on a setup consisting of a Marx generator with an output power of 0.8 MW, electrodes, and a dielectric base for the sample. Samples of two types were used: 1 - DLC_{pi} (polyimide substrate) with a thickness of 200 nm and 2 - DLC_{Si} (silicon substrate) with a thickness of 166 nm.

For DLC_{pi} samples, a sliding gas discharge was observed, with flask-like damage on the surface (Figure 1a). It was found, that the sublimation of the DLC layer is caused by the radiant heating of the surface by the plasma channel. For DLC_{Si} samples, a through-breakdown of the coating was obtained when the plasma channel closed the electrodes through the DLC layer and the substrate. In this case, the sublimation of the coating is caused by self-heating due to the flow of current (Figure 1b).

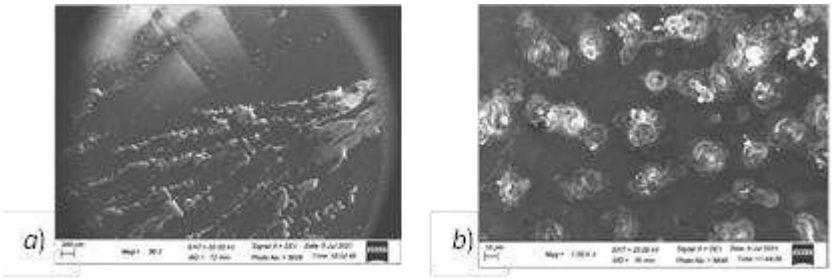

Figure 1 – Images of scanning electron microscopy after the breakdown on samples DLC_{pi} (a) and DLC_{Si} (b)

To simulate the DLC sublimation process under the temperature effect of a plasma channel using the Comsol Multiphysics package. The non-stationary problem of heat transfer is solved taking into account radiant heat transfer and phase transition (sublimation) for both types of breakdown - the sliding one and the through one.

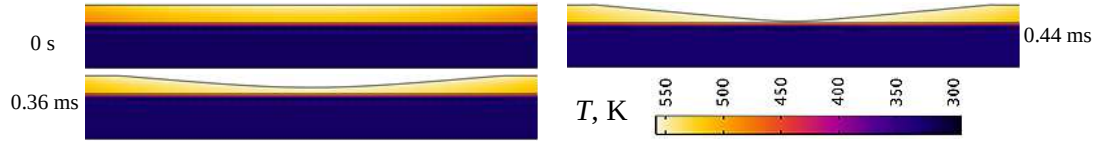

Figure 2 – Temperature map images in the DLC layer during sublimation

Thus, the process of destruction of the DLC coating under the influence of cold plasma in various modes has been investigated, and a numerical experiment has been carried out, which makes it possible to predict the degree of damage to the coating from the parameters of the plasma channel. The authors of the article would like to thank the Joint Institute for Nuclear

Research for financial support. The work was performed under contract №08626319/201142470-74.

Emergence of biaxial polarization in lone pair substituted $HoMnO_3$: A DFT study

Sathya Sheela S.[1]*, N. Basakaran[2]
[1]*RV Institute of Technology and Managemnet, Chaithanya Layout, 8th Phase, J. P. Nagar, Bengaluru, Karnataka-560076, India, spicysathu@gmail.com**
[2]*National Institute of Technology, Tiruchiraplalli, India*

Multiferroic materials are materials that exhibit at least two ferroic order parameters in the same phase. $HoMnO_3$ is one such compound which exhibits multiferroic behavior in both the hexagonal and the orthorhombic phase. In the orthorhombic phase, it exhibits Type II multiferroicity, which entails that the electric polarization of this material is low but it exhibits a good coupling between the electric and the magnetic order parameters. Electric polarization in orthorhombic $HoMnO_3$ is induced in the E-type antiferromagnetic state.

We carry out first principle density functional theory studies to analyze the effect of lone pair substitution on the A-site of orthorhombic $HoMnO_3$. Our objective is to induce a Type I multiferroicity in a Type II multiferroic and to study the magnetic, electric and structural effects of this new compound.

Using first principles method we report the most stable ground state structure of $Ho_{0.5}As_{0.5}MnO_3$ and analyze the structure and bonding of the new compound using charge density and ELF plots. We also report the emergence of biaxial polarization due to the symmetry breaking in this new compound and relate it to the structural effects. Thus $Ho_{0.5}As_{0.5}MnO_3$ is expected to demonstrate promise as a multiferroic with enhanced properties as compared to its parent compound.

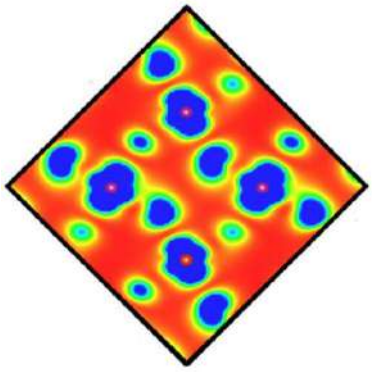

Partial density of states of Mn e_g orbitals

Dynamic stimulation of superconductivity in superconductor/2D-crystal systems

V.N. Kushnir[1,2]*, S.L. Prischepa[1], and I.V. Komissarov[1]
[1]*Belarusian State University of Informatics and Radioelectronics, P. Browka 6, 220013 Minsk, Belarus, vnkushnir@gmail.com**
[2] *Belarusian State University, Nezalezhnasci av. 4, 220030 Minsk Belarus*

In this paper, we propose a method for the critical temperature tuning of the superconducting thin film (Nb) by modifying its phonon spectrum by a layer of graphene (G) in contact with a film. Due to the oxidation of the film surface, we have an effective superconducting structure Nb/I/G (I – insulator) with a weak bond between Nb and G. It is known [1] that in a layer of graphene with a thickness of a few atomic layers, on a top of I-layer, out-of-plane acoustic (ZA) waves are induced. Moreover, it turns out, that the spectrum of ZA-waves substantially overlaps with the phonon spectrum of Niobium. As a result of a weak interaction of Nb and G "hybridization" of the phonon spectrum of the structure Nb/I/G occurs. This is reflected in (*i*) an increase in the density of the phonon states and (*ii*) "softening" of the phonon spectrum of Niobium [2]. Consequently, the effective electron-phonon coupling constant, which is expressed through the structural function of the Eliashberg's theory [3], increases. As a result, the critical temperature of the Nb film also increases. We emphasize that for a number of superconducting materials, including Niobium, the structural function in the main frequency range (i.e., contributing to superconductivity) is proportional to the phonon spectral density. This means that the critical temperature of the film can be changed in a controlled way, affecting the phonon spectrum. Finally, we note that the described effect is similar to the effect of ultrasonic stimulation of superconductivity; the difference is that in the considered case the wave source (G) is in a thermodynamic equilibrium state with a superconducting film.

References

[1] L. Chen and S. Kumar, J. Appl. Phys. 112 (2012) 043501.
[2] W.L. McMillan, Phys. Rev. 167 (1968) 331–344.
[3] G.M. Eliashberg, Zh. Eksp. Teor. Fiz. 38 (1960) 966–976 [Sov. Phys. JETP 11 (1960) 696–702].

Electric conductivity in lattice models with SALR-potential

R. Lasovsky* and Ya. Groda
*BSTU, 13a, Sverdlova str., 220006, Minsk, Belarus, lasovskyr@gmail.com**

One of the challenges facing humanity is the production of energy in an economically beneficial and environmentally friendly way. Traditional methods of power generation in thermal, nuclear and hydroelectric power plants are fraught with serious environmental problems. Electrochemical devices for energy storage and conversion include chemical batteries, accumulators, fuel cells, supercapacitors, etc. Currently, liquid solutions of ionic salts or polymer ion-exchange membranes are actively used in electrochemical systems, which is associated with the danger of leaks and ignition. The transition to electrochemical cells with solid electrolytes will increase the strength, durability, environmental friendliness and safety of energy sources, expand the range of operating temperatures.

In this report, we present the results of a study the conductivity in a lattice system with short-range attraction and long-range electrostatic repulsion between mobile particles. Moreover, lattice model of a ceramic ionic conductor containing a grain and an intergranular boundary is considered. The boundary is described by a layer with segregated immobile ions.

The simulation of the described system using the Monte-Carlo kinetic method was performed. The Coulomb energy was determined by the Ewald summation for systems with a slab geometry. The dependences of the particles number passing through the boundary, which is proportional to the electric current, on the reciprocal temperature are determined. These dependences are typical for solid electrolytes. It was noted that an increase in the concentration of mobile ions, as well as an increase in the resistance of the grain boundary, leads to an increase in the activation energy, i.e. to reduce the lability of ions.

The project is co-financed by the European Union’s Horizon-2020 research and innovation program under the Marie Sklodowska-Curie grant agreement No 734276 and the Polish National Agency for Academic Exchange within ”Solidarity with scientists Initiative”.

Quantum chemistry simulation of Nanodiamond and Graphene Quantum Dot during the formation of hybrid GQD/ND structure

T. Khlopina[1], A. Pushkarchuk [1,2], A. Paddubskaya[1], K. Batrakov[1], S. Kuten[1], Dominik Ludewig Michels[3], D. Lyakhov[3], P. Kuzhir [4]
[1]*Institute for Nuclear Problems of Belarusian State University, Bobruiskaya Str. 11 Minsk 220006, Belarus tantanhlopina@gmail.com*
[2]*Institute of Physical and Organic Chemistry, NASB, 13, Surganova Str., 220072, Minsk, Belarus*
[3]*Computer, Electrical and Mathematical Science and Engineering Division, 4700 King Abdullah University of Science and Technology, Thuwal 23955-6900, Saudi Arabia*
[4]*Institute of Photonics, University of Eastern Finland, P.O.Box 111 JOENSUU FI-80101, Finland*

The main drawback of existing THz components is their restricted tunability, which is the must for future and emerging THz devices. That is why graphene, which optical and electromagnetic properties are easily and smoothly adjustable in a controllable way by chemical doping, mechanical deformations, and biasing, is one of the best material base for THz detectors, such as photodetectors and bolometers.

Along with conventional ways to tune the graphene electromagnetic response, the influence of substrate used for graphene handling and processing has to be taken into account. In this communication, we will discuss the influence of (111) and (100) diamond substrates on the electronic band structure as well as optical properties of graphene.

We have studied the equilibrium morphology, electronic structure and Raman spectra, of the interface between a Nanodiamond (ND) and Graphene Quantum Dot (GQD) during the formation graphene monolayer and the diamond C(111) and C(100) surfaces (GQD/ND) using quantum chemical density functional theory (DFT) simulation in the cluster approximation. DFT-D/B3LYP/cc-pvdz level of theory with full geometry optimization implemented in Gaussian-16 package have been used.

We found that for (111) surface the optimum epitaxial interface morphology contains a wavy graphene structure that is covalently bonded to the substrate. In turn, the formation of a Van der Waals bonds between graphene and the substrate was shown for the (100) surface. Further, the electronic structure and density of states (DOS) was calculated for the nanoflakes and cluster under study. An estimate was made of the localization of the occupied molecular orbital and the lower unoccupied molecular orbital (HOMO and LUMO, respectively) (Fig.1).

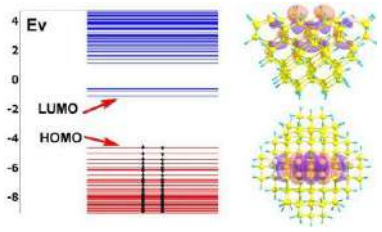

a) b)

Fig.1 Electronic structure of (100) surface of nanodiamond simulated by cluster C96H78 (a), localization of HOMO for cluster C96H78 (two points of view) (b)

The main tendencies in the tuning of electronic structure and Raman spectra of diamond and graphene during the formation of hybrid GQD/ND structures are analyzed. The influence of the diamond substrate on the THz electromagnetic constituents for the doped graphene due to its interaction with the diamonds surfaces are discussed and compared with the experimental data collected for graphene transferred to monocrystalline diamond.

Estimation of the percolation threshold for mixed site-bonds problems using polynomial mappings

A.S. Fedotov and Y.Tsitavets
Computer Modelling Department of Physics Faculty, Belarusian State University, Minsk 220030, Belarus, e-mail:<fedotov.alehandro@gmail.com>

Many properties of composite materials such as electrical conduction, dielectric response and others are closely related to the geometrical arrangement of the constitutive phases. Percolation theory, whose objective is to characterize the connectivity properties in random geometries and to explore them with respect to physical processes, thus provides a natural frame for the theoretical description of random composites.

In recent years, great progress has been made in the field of numerical methods of percolation theory; however, analytical descriptions for many important cases still remain open. In particular, mixed problems, in which both nodes and bonds can be removed from the lattice, are resource-demanding for numerical experiments and require at least rough methods of analytical estimates.

In this work we propose applying the generalized renormalization group method to obtain the position of the percolation threshold for a mixed problem. The work considers mixed percolation problems on square and cubic lattices. Polynomial mappings were constructed for the relationship between the probability p_{n+1} of a renormalized cell conductance at n+1 iteration and p_n at the n-th iteration. The percolation threshold was calculated as the position of the real-space fixed points of the mentioned polynomial mapping.

The estimates were verified using a numerical method based on the construction of regular graphs of the corresponding lattices for different probabilities (Figure) of filling with conducting nodes and connections.

Two direct modelling approach for mixed percolation studies were developed and tested on square and cubic lattices. Time complexity of both algorithms increases no faster than $O(V^{1.04})$, which means good scalability. New analytical estimation approach was developed for mixed percolation problem on the basis of fixed-points analysis of polynomial maps. It was established that there is an imaginary fixed point, which limits the percolation threshold from below and real fixed point, which limits the percolation threshold from above.

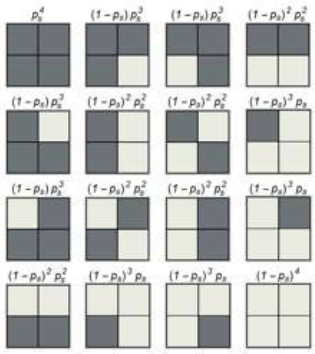

Figure. Probabilities of different configurations of 2x2 cell

References

[1] Gould, H., Tobochnik, J., Christian, W., 2007. An introduction to computer simulation methods: applications to physical systems, 3rd ed. ed. Pearson Addison Wesley, San Francisco.

Global reactivity analysis from quantum parameters on 2,6-bis((E)-2-(furan-2-yl)vinyl)-4-(4,6,8-trimethylazulen-1-yl)pyridine structure

Alina-Alexandra Vasile [1], Gabriela Stanciu [2], Eleonora-Mihaela Ungureanu [1] and Amalia Stefaniu [3*]
[1]*Politehnica" University of Bucharest, Gheorghe Polizu 1-7, 011061, Sector 1, Bucharest, Romania*
[2]*Department of Chemistry and Chemical Engineering, Ovidius University of Constanta, 124 Mamaia Blvd, 900527, Constanta, Romania*
[3]*National Institute for Chemical - Pharmaceutical Research and Development (ICCF), 112 Vitan av., 031299 Bucharest, Romania*
Corresponding author: astefaniu@gmail.com

The structure of 2,6-bis((E)-2-(furan-2-yl)vinyl)-4-(4,6,8-trimethylazulen-1-yl)pyridine was submitted to predictive calculations using Density Functional Theory (DFT) with B3LYP algorithm [1] and 6-31+G (d, p) basis set [2] for the equilibrium geometry, at the lowest energy level. Quantum reactivity parameters such as ionization potential, electron affinity, electronegativity, chemical potential and electrophilicity index were obtained from calculated energies values of the Highest Occupied Molecular Orbital (HOMO) and of the Lowest Unoccupied Molecular Orbital (LUMO), according to the Koopmans's theorem [3]. Furthermore, starting from frontier molecular orbitals, the oxidation and reduction potentials are predicted using the empirical equations of Bredas et al. [4, 5] in an attempt to correlate the computed molecular descriptors to electrochemical properties.

References

[1] C. Lee, W. Yang, R. G. Parr, Phys. Rev. B.37 (1988) 785 -778.
[2] Y. Shao, L. F. Molnar, Y. Jung, et al., Phys. Chem. Chem. Phys. 8 (2006) 3172 – 3191.
[3] T. Koopmans, Physica 1 (1934) 104–113.
[4] J. L. Bredas, R. Silbey, D. S. Boudreux, R. R. Chance, J. Am. Chem. Soc. 105 (1983) 6555–6559.
[5] L. Leonat, G. Sbârcea, I. V. Brânzoi, U.P.B. Sci. Bull. B 75 (2013) 111–118.

QUANTUM STATES IN A CYLINDRICAL QUANTUM HOLE AND A BARRIER

Yu.I. Bokhan
Belorussian State Academy of Communication, Vitebsk branch,
Ilinsky, 45, 210001, Vitebsk, Belarus, yuibokhan@gmail.com

The modern level of development nanotechnology allows buildings of electronic devices, such as resonance-tunnel diodes (RTD) [1]. Building RTD is routine bases on the production technology of heteroframes which is developed enough. During too time the technology of building carbon наноструктур, such as fullerenes, carbon nanotube, etc. [2] is not less widely applied. In such frames probably building of quantum holes and barriers with cylindrical symmetry (a Fig. 1.). Such frames can be used as RTD by placement on an axis of a tube of various ions.

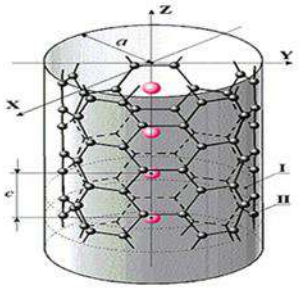

Fig. 1. Alloyed by metal (color balls) carbon nanotube in cylindrical potential energy barrier. [2].

The Quantum mechanics problem about a cylindrical hole or a barrier is known and solved for a long time. Its decision defines levels of energy and own functions of a particle of mass in cylindrical potential trough of radius. The particle can be in potential trough or out of it $\rho \geq a$ and, hence, wave function at should be sewed with wave function in a hole. The decision of this equation $\phi(\rho) = CJ_m\left(\sqrt{\frac{2ME}{\hbar^2}}\rho\right)$ – function of Bessel's. Generally, the spectrum of states in a cylindrical quantum hole is defined from an interrelation:

$$\frac{\mathbf{k}J'_m(ka)}{J_m(ka)} = \frac{\chi K'_m(\chi a)}{K_m(\chi a)} \qquad (1)$$

were $\mathbf{k^2}$ = [2M (U_0 - $|E|$)/h^2] = $2MU_0/h^2 - \chi^2$, $J_m(x)$ – function of Bessel's, $K_m(x)$ – modified function of Bessel's of 2nd sort, U_0 – Barrier height. From a boundary condition $J_m\left(\sqrt{\frac{2ME}{\hbar^2}}a\right) = 0$ the power spectrum of a particle (λ_{km} - roots of function of Bessel's) is received:

$$E_{km} = \frac{\hbar^2\lambda_{km}^2}{2Ma^2}, \qquad (2).$$

As it is known, roots of functions of Bessel's have property of intermittency [3], i.e. their sizes depending on value of an index can be located is close to each other. For an example we will result first three roots of functions of Bessel's of the whole index n = 0, 1, 2 and 3 [3].

Roots	$J_0(x)= 0$	$J_1(x)= 0$	$J_2(x)= 0$	$J_3(x)= 0$
1	2.405	3.832	5.136	6.380
2	5.520	7.016	8.417	9.761
3	8.654	10.173	11.620	13.015

Key feature of such system is possibility, at the expense of introduction of the conforming atoms or ions in carbon nanotube, to create reverberators states with certain frequencies of

transferring. Besides, degeneration presence on orbital number m gives the chance to create additional states action of a choronomic magnetic field that will allow to carry out smooth rearrangement of a spectrum and selectivity of a choice of a frequency range.

References

[1] Elesin V.F. JETP, Vol. 89, No 2, (1999) p. 377-391.
[2] Diychkov P.N. Nature, №11, (2000), p.23-30 (in Russian).
[3] Watson G. A treatise on the theory of Bessel functions. Published by University Press in Cambridge (1966**)** . 816 p.

Structural and electronic properties of bulk triclinic Rhenium Disulfide

A.V. Baglov[1,2*], D.M. Malakhau[1], and L.S. Khoroshko[1,2]
[1]*Belarusian State University, 4 Nezalezhnasci ave., Minsk 220030, Republic of Belarus, baglov@bsu.by**
[2]*Belarusian State University of Informatics and Radioelectronics, 6 P. Browka str., Minsk 220013, Republic of Belarus*

Rhenium disulfide (ReS_2) is a layered semiconducting transition metal dichalcogenide (TMDC) with an optical bandgap around 1.4 eV in bulk crystals [1]. The most famous layered TMDCs – Mo and W dichalcogenides – have generated significant interest direct-gap semiconductors in the monolayer limit for electronic, piezotronic, and optoelectronic applications. In contrast the ReS_2 is studied in general experimentally and a lot less than other TMDCs. Traditionally, correct reproduction of structural properties of layered TMDCs within the first principles methods needs comparing obtained results with experimental data due to van der Waals interaction between layers. In this work we study structural and electronic properties of bulk ReS_2 within first principles methods and compare our predicted results with the experiment.

Our first principles calculations within the local density approximation (LDA) and the Ceperley – Alder parameterization as implemented in the *OpenMX* code were performed [2-4]. We were used pseudopotentials with the following valence states configuration: Re – 5s, 5p, 5d, and 6s states; S – 3s and 3p states. We selected the basis sets pseudoatomic orbital functions similar to classical DZP basis set. The integration over the 4×5×5 regular Γ-centered k-points mesh for self consistent field calculation were performed. Structure optimization was stopped when the atomic forces and the stress tensor each component have become less than 0.01 eV/Å. Density of states calculation over the 5×6×6 regular Γ-centered k-points mesh by the tethrahedron method were perfomed.

After structure relaxation, we found next lattice parameters (in brackets given differences with experimental data from [5]): a = 6.4217 Å (+0.07%), b = 6.4695 Å (-0.62%), c = 6.4077 Å (-0.82%), α = 121.47° (-0.30%), β = 88.17° (-0.24%), γ = 106.43° (-0.04%). Traditionally, the LDA gives underestimated lattice parameters for all directions except for the plane in which the van der Waals (vdW) interaction act. Very close results between calculation and experiment in this direction allow recommend the LDA method as a simple way for calculation structural parameters in ReS_2 and other Re dichalcogenides. Cell parameter in this direction approximately twofold less than in MoS_2 and WS_2, which indicates a minor role vdW interaction, that can allow using the generalized gradient approximation (GGA) for calculation different properties (ionization potential, equipotential surface etc.) with better accuracy than LDA. Our calculation predicts semiconducting behavior with a band gap 1.24 eV, that close to experimental results. Our calculations show that the valence band includes rhenium d-states and sulfur p-states, in conductance band sulfur p-states playing a minor role.

Thus, in this work we studied structural and electronic properties of rhenium disulphide, calculated within the local density approximation. Shown that using the approximation good describe lattice parameters and angles comparing experimental data. In our calculation the band gap underestimated only 10%. This result allows recommend the LDA method for studying structural and electronic properties in first approximation with good accuracy, that can be useful for describing other rhenium dichalcogenides.

References

[1] C.H. Ho, C.E. Huang, Journal of Alloys and Compounds 383 (2004) 74-79.
[2] T. Ozaki, Phys. Rev. B 67 (2003) 155108-1–155108-5.
[3] T. Ozaki, H. Kino, Phys. Rev. B 69 (2004) 195113-1–195113-19.

[4] T. Ozaki, H. Kino, Phys. Rev. B 72 (2005) 045121-1–045121-8.
[5] H.H. Murray, S.P. Kelty, R.R. Chianelli, C.S. Day, Inorganic Chemistry 33 (1994) 4418-4420.

DFT study on the interaction of methanol with magnesium orthosilicate under gas phase condition

B. Karthikeyan[1,*], R. Vettumperumal[2], and K. Sakthiraj[3]
[1]*Department of Physics, Mepco Schlenk Engineering College, Sivakasi 626 005 India*
[2]*Department of Physics, Fodhdhoo School, Fodhdhoo, Noonu Atoll 04120 Republic of Maldives*
[3]*Department of Physics, Kamaraj College of Engineering and Technology, Madurai 625 701 India*
[*]*Corresponding author: karthi.madhubalan@gmail.com; karthikeyanb@mepcoeng.ac.in*

Laboratory catalytic reactions of methanol over heated crystalline magnesium orthosilicate (forsterite) lead to the formation of gas-phase olefinic and polycyclic aromatic hydrocarbon (PAH) molecules, and are of potential importance in astrophysical environments including hot molecular cores, protoplanetary disks and shocks (Li et al 2018). It is therefore very much essential for an astrochemist to understand such kind of interaction. The present paper describes the interaction of methanol (CH_3OH) with magnesium orthosilicate (Mg_2SiO_4). The gas-phase optimized geometries of methanol (M), forstertite (F), and methanol−forsterite (MF) mixed cluster have been calculated using the Density Functional Theory (DFT) with B3LYP method in conjunction with 6311G basis set. The bond lengths, vibrational parameters related to infrared (IR) spectrum, and thermo-chemical parameters like thermal energy, thermal correction to enthalpy (ΔH) and Gibbs free energy (ΔG), specific heat capacity (C_v) and entropy (S) were derived for M, F, and MF cluster. The results obtained in the present study were also compared with already reported values for better understanding.

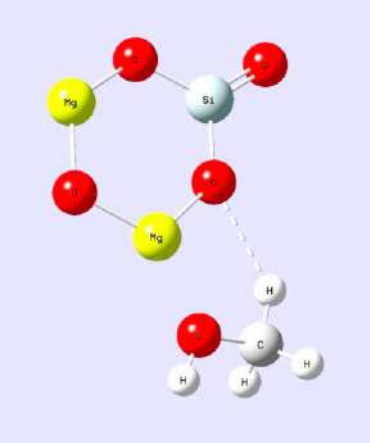

References

[1] Q. Li , W. Dai , B.S. Liu , P.J. Sarre , M.H. Xie , A.S-C. Cheung , Catalytic conversion of methanol to larger organic molecules over crystalline forsterite: laboratory study and astrophysical implications, Molecular Astrophysics (2018), doi: https://doi.org/10.1016/j.molap.2018.09.002

Laser-Driven Convection in Molten Metal: Numerical Experiment

S. Sharyna[1], I. Timoshchenko[1*], Y. Levy[2], O. Romanov[1]
[1]*Belarusian State University, 220030, 4 Nezavisimosti Avenue, Minsk, Belarus, timoshchenkoia@bsu.by**
[2]*HiLASE Centre, Institute of Physics ASCR, 25241 Dolni Brezany, Czech Republic*

The processes of melting and subsequent solidification of material are an integral part of laser technology. These technologies include welding, surface engineering, sintering of powder materials, making holes, processing and cutting metal materials. The interaction of a laser with a material can be used to impart new properties to it, to structure material surface as well by formation of so-called laser-induced periodic surface structures (LIPSS) [1].

In this work, we made the first steps to construct a hydrodynamic-like mathematical model of LIPSS formation based on a numerical solution of the two-dimensional problem of thermal convection and melting with a heat source in the form of CW laser radiation and microsecond laser pulse incident on the sample surface. The motion of the melt is described by the Navier–Stokes equations in the Boussinesq approximation

$$\nabla \cdot \mathbf{u} = 0,$$

$$\rho \frac{\partial \mathbf{u}}{\partial t} + \rho(\mathbf{u}\cdot\nabla)\mathbf{u} = -\nabla p + \mu \Delta \mathbf{u} - \beta \mathbf{g}(T - T^*),$$

and the Stefan problem is formulated in a generalized form for the melting/crystallization processes [2]

$$\left(\rho c + L\delta(T - T^*)\right)\frac{\partial T}{\partial t} = \nabla \cdot (k \nabla T) + S(x, y, t)$$

Here $\mathbf{u}$, p, μ, β are melt velocity, pressure, viscosity, and expansion coefficient respectively, S is a heat source term, L is the enthalpy of phase transition, T^* is a melting temperature. Heat capacity c, density ρ, and heat conductivity k are considered as piecewise functions of temperature

$$c, \rho, k = \begin{cases} c_l, \rho_l, k_l, & T(x, y) > T^*; \\ c_s, \rho_s, k_s, & T(x, y) < T^*. \end{cases}$$

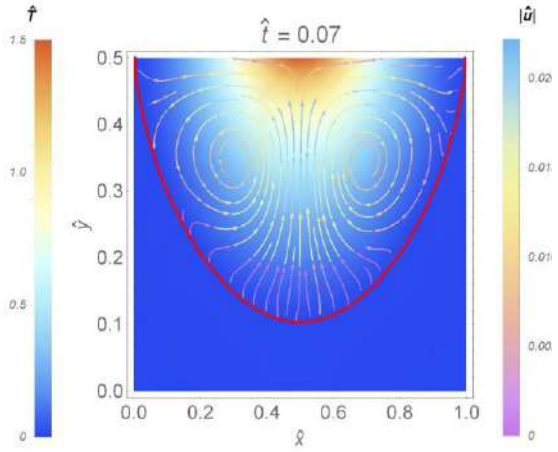

Motion of iron melt and temperature distribution under gaussian beam irradiation in dimensionless variables. Red line depicts the melting front.

The numerical method is based on locally one-dimensional schemes for velocity, pressure, and temperature. Equations are reduced to difference analogs by the finite volume method on staggered grids [3].

Calculations of the motion of the melt under irradiation of the iron surface with Gaussian laser pulses were performed (see figure). The influence of laser beam parameters on melting front propagation is studied.

Acknowlengement

Part of this work was performed in the frame of the ATLANTIC project. The project has received funding from the European Union's Horizon 2020 research and innovation programm under the Marie Skłodowska-Curie grant agreement No 823897.

References

[1] I. Gnilitskyi, T.J.Y. Derrien, Y. Levy [et. al], Scientific Reports 7 (2017) 1–11.
[2] A.A. Samarskii, P.N. Vabishchevich. Computational Heat Transfer: Mathematical Modelling. Wiley (1996).
[3] H. Versteeg, W. Malalasekra. An Introduction to Computational Fluid Dynamics. The Finite Volume Method. Prentice Hall (2007).

Promising materials for THz and second harmonic generation by femtosecond laser pulses

O. Fedotova[1*], A. Husakou[2], R. Rusetski[1], O. Khasanov[1],
A. Fedotov[3], T.Smirnova[4], U. Sapaev[5], P. Klenovsky[6,7], and I. Babushkin[8,9,2]
[1]*SPMRC of NASB, P. Brouki 19, Minsk 220072, Belarus, <eowynknight@gmail.com>*
[2]*Max Born Institute, Max Born Str. 2a, 12489 Berlin, Germany*
[3]*Belarusian State University, Nezalezhnasci Ave. 2, Minsk 220030, Belarus*
[4]*ISEI BSU, Dauhabrodskaya str. 23, Minsk, Belarus*
[5]*TSTU, st. University 2, Olmazar district, 100095 Tashkent, Uzbekistan*
[6] *Masaryk University, Kotlářská 267/2, 61137 Brno, Czech Republic*
[7] *Czech Metrology Institute, Okružní 31, 63800 Brno, Czech Republic*
[8] *IQO, Leibnitz Hannover University, Welfengarten 1, 30167 Hannover, Germany*
[9]*Cluster of Excellence PhoenixD, Welfengarten 1, 30167 Hannover, Germany*

Nanocomposites (NC) are promising media for the goal of creation of compact intense THz- source [1] as well as for frequency convertor to higher harmonics (HH) due to their large nonlinearities bringing wide set of the opportunities. Large values of permanent dipole moment (PDM) are revealed in nanostructures (~10^2 - 10^3 Debye), such as semiconductor quantum dots (QDs) of ZnO, ZnS, CdSe what is comparable with values of transition dipole moments between the exciton states. As well, the additional transitions between exciton states allowed due to PDM may play a significant role in the nanoparticle response, in particular for the generation of new frequencies in the THz range.

In the work presented we optimize the conditions of THz and second harmonic (SH) generation in NC consisted of QD inclusions (ZnO) in transparent dielectric matrix (SiO_2 or KDP host). Pumping pulse carrier frequency is resonant to the frequency transition between lower excitonic states. Theoretical models allowing study coupled resonant and non-resonant mechanisms of frequency down and up conversion in nanocomposite have been developed. Simulations of the pulse propagation were performed on the base of self-consisted system for the density matrix (Bloch) equations describing multilevel excitonic transitions and the unidirectional propagation equation, accounting for chromatic dispersion, second- and third-order optical nonlinearities of both host and inclusions, photoionization of inclusions, plasma dynamics (in case of higher pulse input power) and its influence on the dielectric function of the inclusions. Numerical simulations were performed using a SOLPIC software developed in the frame of RISE-ATLANTIC project. As an analysis shows, for the case of PDM smaller than 10 Debay and moderate input intensity (less than 0.07 TW/cm^2) the output efficiency of THz may reach 0.23% after 50 mkm of propagation of two 15-fs pulses at central circular frequencies (FWHM) of 2.26 fs^{-1} and 2.40 fs^{-1}, what may be explained by significant exciton resonance contribution. With increase of the input intensity up to 1 TW/cm^2 and PDM up to 100 Debay for pulse propagating over distances 50 mkm in NC it is established that the THz part of the spectrum is increased with the propagation distance. The THz efficiency at the same propagation length is by 2-3 order of magnitude more for the case with lagrer PDM. It has been found for SH possible conversion efficiency for such materials may reach up to 65-70%. The few approaches to the real level structure computation have been proposed.

Acknowledgement.
This study was supported by H2020-MSCA-RISE- ATLANTIC project (2019-2023), GA 823897

References

[1] S. B. Bodrov, A. N. Stepanov, and M. I. Bakunov, "Generalized analysis of terahertz generation by tilted-pulse-front excitation in a LiNbO3 prism," Opt. Express 27, (2019) 2396-2410

Ultrafast excitation of electrons in crystals: insights from non-equilibrium band structure calculations

Thibault J.-Y. Derrien[1]*
Institute of Physics AS CR, HiLASE Centre, Za Radnici 828, 25241 Dolni Brezany, Czech Republic.

Last decade, understanding of transient excitation of electrons in solids has brought important developments for several classes of materials, at the level of both fundamentals and applications. While laser-excitation of dielectrics induces measurable ultrafast currents in the PHz regime [1], employing few-cycle laser pulses with controlled carrier envelope phase enables a coherent control of the electron dynamics with reduced crystal damage probability [2,3]. Notably, the possibility of transiently closing the band-gap of solids during their irradiation by linearly polarized ultrashort laser pulses was evidenced and attributed to the light-induced Zener tunneling [3,4].

The corresponding ultrafast modification of the band structure induced by laser dressing of electronic states can be measured experimentally [5,6] and analyzed theoretically using the Floquet formalism [7,8]. Despite its simplicity and limitations, it is applicable to several classes of materials [5,6,8] and enables to study the effects of light coupling with electrons in solids for a wide range of experimental conditions [9].

In this work, after preparing the electronic band structures of two metals (Au and Mo), a semiconductor (Si) and a dielectric (α-SiO_2) using the density functional theory (DFT), the effects of dressing by a polarized laser light on the corresponding electronic band structures were investigated using the Floquet formalism [9]. While a selective excitation of the electrons can be achieved via a choice of laser wavelength and field strength [9], the Floquet simulations illustrate how the change in crystal orientation [10-13] affects the electron dynamics in solids.

Overall, the proposed approach outlines promising ways for selecting materials and laser parameters, via a computer-aided manner, broadening perspectives in ultrafast photonics [5].

Acknowledgment.
The research of T.J.-Y.D. is financed by the European Regional Development Fund and the state budget of the Czech Republic (project HiLASE CoE: No. CZ.02.1.01/0.0/0.0/15_006/0000674). T.J.-Y.D. also acknowledges funding from the European Commission research and innovation programme under the Marie Sklodowska-Curie grant agreement No 823897. This work was supported by the Ministry of Education, Youth and Sports of the Czech Republic through the e-INFRA CZ (ID:90140). Access to storage facilities owned by parties and projects contributing to the National Grid Infrastructure MetaCentrum provided under the programme "Projects of Large Research, Development, and Innovations Infrastructures" (CESNET LM2015042)

References

[1] Schiffrin, A. et al. Nature, **2012**, *493*, 70-74.
[2] Schultze, M. et al. Nature, **2012**, *493*, 75-78.
[3] Kwon, O. et al. Scientific Reports, **2016**, *6*, 21272.
[4] Keldysh, L. Sov. Phys. JETP, **1965**, *20*, 1307-1314.
[5] Wang, Y. H. et al. Science, **2013**, *342*, 453.
[6] Reutzel, M. et al. Nature Communications, **2020**, *11*, 2230.
[7] Higuchi, T. et al.Phys. Rev. Lett., **2014**, *113*, 213901.
[8] De Giovannini, U. et al. Nano Letters, **2016**, *16*, 7993-7998.
[9] **Derrien, T. J.-Y.**; Tancogne-Dejean, N.; Zhukov, V.; Appel, H.; Rubio, A. & Bulgakova, N. M. arXiv preprint arXiv:2104.0897, **2021**, Submitted
[10] Tancogne-Dejean, N. et al. Phys. Rev. Lett., **2017**, *118*, 087403.
[11] Kozák, M. et al. Physical Review B, **2019**, *99*, 104305.
[12] Apostolova, T. et al. Applied Surface Science, **2020**, *519*, 146087.
[13] Florian, C. et al. Materials, **2021**, *14*, 1651.

Spectral ellipsometry of nickel oxide thin films

I.V. Ivashkevich
Mogilev State A. Kuleshov University, Kosmonavtov street 1, Mogilev, 212022, Republic of Belarus; e-mail: iivashkevich@yandex.by

Because of its unique optical and electrical properties, as well as its good chemical stability, nickel oxide (NiO) has recently become the most promising material for photovoltaic solar cells, primarily as transparent conducting electrodes. Therefore, it is necessary to work out the technological regimes for obtaining NiO thin films with optimal characteristics for their application in photovoltaics. The most suitable method to study the optical and electrical properties of such films is the spectral ellipsometry method due to its informativeness and as a non-destructive method.

A series of samples of nickel oxide films deposited on silicon and glass substrates by HF magnetron sputtering at different modes of obtaining was provided for study (BSUIR, Minsk).

The spectra of polarization parameters $tg\Psi(\lambda)$ and $cos\Delta(\lambda)$ of investigated films were measured on spectral ellipsometer ES-2.

Analysis of the obtained solutions of direct and inverse problems of spectral ellipsometry has shown:

- the dispersion dependences of the refractive index $n(\lambda)$ and the absorption index $k(\lambda)$ of nickel oxide films on silicon and glass substrates are satisfactorily described by the Selmeyer formula for films with a thickness $d > 100$ nm;
- films deposited on silicon substrates have the most optimal properties for photovoltaic cell applications;
- addition of pure nickel target during the formation of nickel oxide films by HF magnetron sputtering produces nickel oxide films of non-stoichiometric composition (NiO_x, $x < 1$); calculated refractive index spectrum of such films (Fig., spectrum 2) is much lower than analogous spectrum $n(\lambda)$ (Fig., spectrum 1) of stoichiometric NiO film, while transparency of NiO_x film is much higher in the area $\lambda > 500$ nm;
- an increase in the substrate temperature leads to a significant decrease in the absorption index of nickel oxide films deposited on glass substrates.

The results of the study can be used to correct the conditions of deposition of nickel oxide films on silicon and glass substrates by HF magnetron sputtering with optimal conditions for use in photovoltaics.

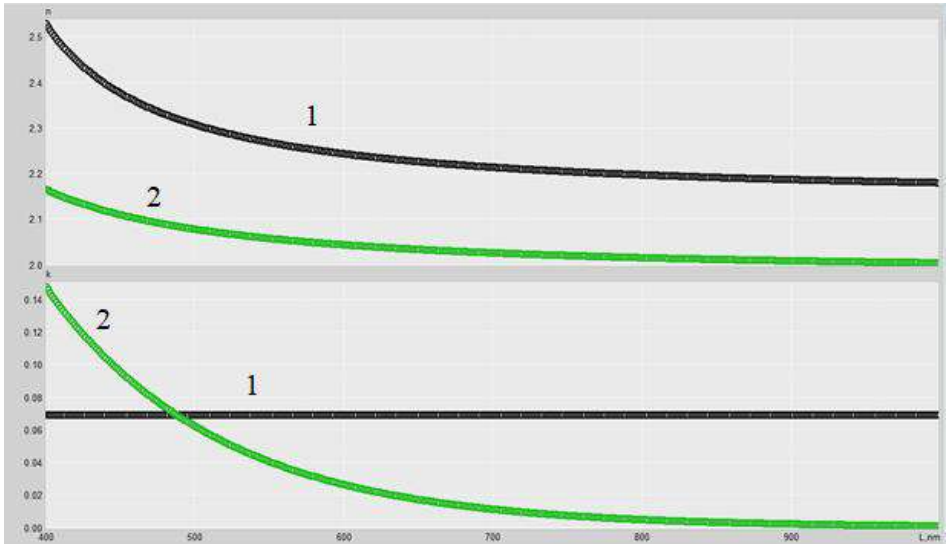

Figure – Calculated optical functions $n(\lambda)$, $k(\lambda)$ of NiO_x films on silicon substrates

Energy structure of oxygen and silicon DX-centers in AlN

I.A. Aleksandrov*, K.S. Zhuravlev
Rzhanov Institute of Semiconductor Physics SB RAS, 630090, pr. Lavrentieva 13, Novosibirsk, Russia
**e-mail: aleksandrov@isp.nsc.ru*

Group-III nitrides are promising for creation of various electronic and optoelectronic devices, such as light-emitting diodes and laser diodes of the ultraviolet and visible range, high-frequency transistors, photodetectors, and single-photon sources. To improve the quality of materials, it is necessary to know the atomic and energy structure of native point defects and impurity centers. The study of defects in AlN is of fundamental importance and is in demand for various applications of this material. Optical methods, such as photoluminescence spectroscopy, are effective instruments for investigation of energy structure of defects. Luminescence bands with donor-acceptor nature are often observed in experiments. For identification of these bands it is necessary to calculate energy structure of donors and acceptors taking into account lattice relaxations. Oxygen and silicon are most common donor impurities in AlN preferably forming substitutional O_N and Si_{Al} defects. These defects exhibit the properties of DX-centers, for which the addition of a second electron to a neutral defect leads to strong relaxation of the lattice with the formation of a deep level. In this work we have studied energy structure of oxygen and silicon DX-centers in AlN. Hybrid-functional calculations with HSE exchange-correlation functional shows that oxygen and silicon donors in single positive charge state have symmetric atomic configurations with impurity atom positions close to bulk AlN lattice sites, while in the neutral charge state the energy minimum configurations have lower symmetry with impurity atom shifted from the lattice site [1]. Along with the energy minimum configurations we have found metastable states for the neutral oxygen and silicon donors with impurity atoms positions closer to the bulk lattice sites. Configuration diagrams of O_N and Si_{Al} defects have been calculated for transitions between neutral and single positive charges state and between single negative and neutral charge states. The energy-minimum configurations in the neutral charge states of the silicon and oxygen donors have relatively large Franck-Condon shifts of about one and a half eV for optical transitions to the single positive charge state.

References

[1] I.A. Aleksandrov, K.S. Zhuravlev, Journal of Physics: Condensed Matter, 32 (2020) 435501.

Synthesis of multicomponent perovskites ($Cr_{0.2}$, $Mn_{0.2}$, $Fe_{0.2}$, $Co_{0.2}$, $Ni_{0.2}$) XO_3

A. Punda[1*],V. Zhivulin[1], D. Zherebtsov[1], S. Gudkova[1],D. Vinnik[1], A. Trukhanov[1,2]
[1]*South Ural State University, Chelyabinsk, Russia, sherstiukd@susu.ru**
[2]*SSPA "Scientific and Practical Materials Research Centre of NAS of Belarus", Minsk, Belarus*

La-, Nd- and La/Nd-based polysubstituted high-entropy oxides (HEOs) were produced by solid-state reactions. Composition of the B-site was fixed for all samples (Cr0.2Mn0.2Fe0.2Co0.2Ni0.2) with varying of A-site cation (La, Nd and La0.5Nd0.5). Nominal chemical composition of the HEOs correlates well with initial calculated stoichiometry. All produced samples are single phase with perovskite-like structure.

Average particle size is critically dependent on chemical composition. Minimal average particle size (~400 nm) was observed for the La-based sample and maximal average particle size (5.8 μm) was observed for the Nd-based sample. The values of the configurational entropy of mixing for each sample were calculated. The chemical composition of the obtained samples was studied by a JEOL JSM 7001F scanning microscope equipped with an energy-dispersive X-ray fluorescence analyzer INCA X-max 80 (Oxford Instruments). The structure was studied on a Rigaku Ultima IV powder diffractometer by X-ray phase analysis. The results of electron microscopic investigation showed that the studied samples contained a large number of cubic crystals, which composition had the perovskite structure.

Acknowledgement
This work was supported by the RFBR (project No 20-38-70057) and President's grants for young doctors of science (MD-5612.2021.4).

Hall and bend resistance of a phosphorene Hall bar

L. P. Miranda[1,2*], S. P. Milovanovic[2], R. N. Costa Filho[1] and F. M. Peeters[2]
[1]*Departamento de Física, Universidade Federal do Ceará, Campus do Pici, 60455-760 Fortaleza, Cear\á, Brazil, lucasmiranda@fisica.ufc.br**
[2]*Department of Physics, University of Antwerp, Groenenborgerlaan 171, B-2020 Antwerp, Belgium*

The continuous downscaling of electronic devices made the scientists focus their attention on two-dimensional (2D) materials due to their nanoscale thickness and their intriguing properties. Among these materials, black phosphorus, which is the most stable phosphorus crystal at room temperature and pressure, has drawn a lot of attention recently due to its unique electronic properties making it a suitable candidate for next generation of field effects transistor. To better understand its characteristics we theoretically analyzed the electrical transport properties of a phosphorene Hall bar in the presence of a magnetic field and vacancy defects. The presence of axial and non axial terminals (present on a four terminal Hall bar), allowed us to study different transport properties of phosphorene material. To study this device a tight-binding model in combination with the Landauer-Büttiker formalism is used to calculate the energy spectrum, the lead-to-lead transmissions, and the Hall and bend resistances of the system. Depending on the terminal orientation (armchair or zigzag) it will has semi-conductor or metallic properties. These properties can be seen due appearance of a negative bend resistance for characterizing a ballistic regime. Further, we also analysed single and double vacancies defects on phosphorene Hall bar and its effects on the magneto resistance. The vacancies are implemented by removing a random atom from the phosphorene unit cell and it can be categorized based on the sublattice symmetry. The effects on the resistance are most noticeable for vacancy types with broken sublattice symmetry, which are mainly seeing due the lack of Landau-levels, present for the pristine system. The analyses presented clearly indicates the much richer transport features present in phosphorene than in graphene.

TOWARDS DESCRIPTION OF MECHANICAL DAMAGE OF THIN MOLYBDENUM FILM UPON PULSED LASER IRRADIATION

K. Hlinomaz[1,2*], A. S. Fedotov[3], I. Timoshchenko[3], A. Kozlovski[3], Y. Levy[1], T. J.-Y. Derrien[1], V. P. Zhukov[4], O. G. Romanov[3], N. M. Bulgakova[1]
[1]*HiLASE Centre, Institute of Physics of the Czech Academy of Sciences, Za Radnicí 828, 25241 Dolní Břežany, Czech Republic, * hlinomazk@fzu.cz*
[2]*Czech Technical University in Prague, Faculty of Nuclear Sciences and Physical Engineering, Břehová 7, 115 19 Praha 1, Czech Republic*
[3]*Belarusian State University, 4 Nezavisimosti Ave., Minsk 220030, Belarus*
[4]*Institute of Computational Technologies SB RAS, Novosibirsk, Russia*

Upon femtosecond laser pulse irradiation the experimental damage threshold of Mo thin films [1] can be well described by associating the damage with melting of the material [2,3]. For film thicknesses from ~20 nm up to bulk, a 1D description based on the two-temperature model (TTM) along with constant optical properties was sufficient to reach agreement with available experimental results in the ultraviolet regime.

For infrared irradiation, a Mo film exhibits strong changes of absorptivity as function of time and laser wavelength [4]. While electronic response of the solid may lead to a decrease of the reflectivity at high fluence, its optical response should also be affected by the expansion/compression of the lattice, as was shown for other metals [5]. A comprehensive description of the optical, thermal and mechanical effects is thus desirable for Mo.

In this work, as a first step, we study the role of stress as a damage mechanism for a thin molybdenum film deposited on a glass substrate and irradiated by an ultrashort laser pulse using two different models: an hydrodynamic model and a thermo-elastic model. Coupled with a two-temperature model (TTM) and an equation of state, the hydrodynamical description enables us to compute the pressure and density of the solid as function of laser irradiation parameters. A Lagrangian approach [6] was adopted to easily determine the laser-induced motion of the free surface. The thermoelastic model, relatively simpler to implement, is based on the two temperature energy balance equations supplemented by an equation tracking the lattice displacement induced by the thermal stress [7] but without accounting for the deformation of the material.

This work provides insights on the damage mechanisms of laser-irradiated thin metallic films, a step of importance for improving the control of thin film modification by pulsed laser light.

References

[1] S.-S. Wellershoff, J. Hohlfeld, J. Güdde, and E. Matthias, Appl. Phys. A 69 (1999) S99-S107.
[2] K. Hlinomaz, Y. Levy, T. J.-Y. Derrien, and N. M. Bulgakova, Modern Machinery (MM) Science Journal, Dec. 2019, (2019) 3585-3593.
[3] K. Hlinomaz, Y. Levy, T. J.-Y. Derrien, and N. M. Bulgakova, Modeling thermal response of Mo thin films upon single femtosecond laser irradiation: dynamics of film melting and substrate softening, in preparation.
[4] S. Rapp, M. Kaiser, M. Schmidt, and H. P. Huber, Opt. Express 24 (2016) 17572-17592.
[5] J. Winter, S. Rapp, M. Schmidt, and H. P. Huber, Appl. Surf. Sci. 417 (2017) 2-15.
[6] O. G. Romanov, G. I. Zheltov and G. S. Romanov, Bull. Russ. Acad. Sci.: Phys. 75 (2011) 1589-1591.
[7] M. V. Shugaev, and N. M. Bulgakova, Appl. Phys. A 101 (2010) 103–109.

Acknowledgement.
This work was performed in the frame of the project ATLANTIC. The project has received funding from the European Union's Horizon 2020 research and innovation programme under the Marie Sklodowska-Curie Actions (2019-2023) under grant agreement No 823897.

Analytical solutions of elastic contact problems for inhomogeneous coatings with complex structure

S.M. Aizikovich[1]*, S.S. Volkov[1], A.S. Vasiliev[1]
[1]*Don State Technical University, Rostov-on-Don, Russia, saizikovich@gmail.com**

Tribological characteristics of a coating mostly depend on its elastic properties. For inhomogeneous coatings, distribution of elastic properties by depth is essential characteristic. Use of coatings ensures reduction of pressure on structures and decrease of wear rate. Most applicable mathematical theory for modeling contact behavior of coatings is the theory of elasticity, together with methods and approaches being developed in its framework. Most of existing solution methods for contact problems can be used only in limited ranges of physical and geometrical parameters of such problems. When modelling mechanical behavior of a real coating, it is important to account for real distribution of elastic moduli (Young's modulus, Poisson's ratio) in the coating material. Generally, Wide-known solution methods are applicable for some particular cases of coating inhomogeneity.

In this report, we demonstrate application of the bilateral asymptotic method for solution of dual integral equations arising from for solution static contact problems of elasticity theory for bodies with inhomogeneous (functionally graded) coatings. By this method, it became possible to obtain analytical form of solution of contact problems for thin (thick) functionally graded or layered, soft or hard inhomogeneous coatings in a wide range of problem parameters.

The bilateral asymptotic method of solution of dual integral equations allows to construct an high-accuracy approximate analytic solution to contact problems for inhomogeneous coatings. Contact stresses distribution on the surface of a coating obtained in such a way can be used for more accurate investigation of stress-strain state also in the depth of the coating. Obtained stress-strain state allows estimation of strength characteristics of the coating, areas of stresses concentration, and areas where fracture or delamination of the coating can happen most likely.

The study was supported by the Government of the Russian Federation (grant 14.Z50.31.0046).

Surface states in cubic Mg_2Si and Ca_2Si thin films

A. Alekseev[1,*], A. B. Filonov[1], D. B. Migas[1,2], N. G. Galkin[3], and N. V. Skorodumova[4,5]
[1]*Belarusian State University of Informatics and Radioelectronics, P. Browka 6, 220013 Minsk, Belarus, *e-mail: lucky.alexey94@gmail.com*
[2] *National Research Nuclear University MEPhI (Moscow Engineering Physics Institute), Kashirskoe shosse 31, 115409 Moscow, Russia*
[3] *Laboratory of Optics and Electrophysics, Institute of Automation and Control Processes, Far Eastern Branch of Russian Academy of Sciences, Radio Str. 5, 690041, Vladivostok, Russia*
[4] *Multiscale Materials Modelling, Department of Materials and Engineering, Royal Institute of Technology (KTH), SE-10044 Stockholm, Sweden*
[5] *Department of Physics and Astronomy, Uppsala University, Box 516, SE-75121 Uppsala, Sweden*

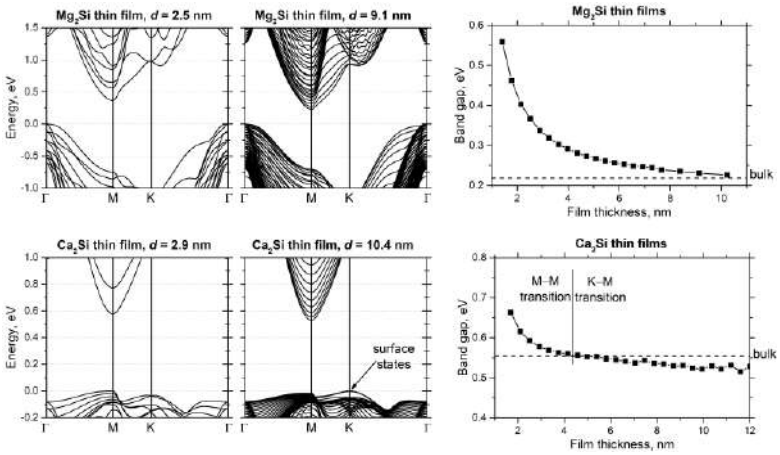

Band structures of Mg_2Si and Ca_2Si thin films with particular film thickness (d) and the dependencies of their band-gap values on *d*.

By means of *ab initio* calculations (the projector augmented-wave method within the generalized gradient approximation) we investigate the role of surface states in electronic properties of thin films of semiconducting cubic Mg_2Si and Ca_2Si slabs with two equal surfaces and with thicknesses starting from 17 nm down to the monolayer 2D structure. It is found that the (111)-oriented Mg_2Si and Ca_2Si slabs display the lowest surface energies (37.1 and 31.0 meV/Å^2 respectively) among the (110) and (211) other ones. The performed structural optimization has revealed pronounced changes in Mg – Si and Ca – Si interatomic distances in the surface region with recpect to the ones in the corresponding bulks as well as in the in-plane lattice parameters especially for thinner slabs. However, the calculated band structures of both $Mg_2Si(111)$ and $Ca_2Si(111)$ slabs possess almost the same dispersion of the bands close to the gap region (Figure) regardless of the slab thickness. We also trace how the band gap of $Mg_2Si(111)$ and $Ca_2Si(111)$ slabs changes with respect to the slab thickness under the influence of the quantum confinement effects (Figure) and indicate that the simple effective mass approximation is not fully suitable to predict correct changes. In addition, we have found the band gap to be sensitive to structural variations in the interatomic distances and in-plane lattice parameters.

SIMULATION OF HIGH ENERGY NEON PATHS IN SHIELDS BASED ON W-CU COMPOSITE

D.S. Vasin[1], S.S. Grabchikov[1], E.A. Grabchikova[1], S.B. Lastovsky[1], D.I. Tishkevich[1], and A.S. Yakushevich[1,2]*
[1] *SSPA "Scientific-Practical Materials Research Centre of NAS of Belarus", 220072, Belarus, Minsk, 19 P. Brovki st., d.s.vasin@outlook.com*

The active development of astronautics leads to the development of radiation protection materials. This study demonstrates the results of investigation of the W-Cu comosite shielding efficiency. It is proposed to use shields based on $W_{85}Cu_{15}$ composite material with a density value of 16.3 g/cm^3 obtained using solid-phase synthesis. OMERE 5.31 software was used in order to determine the energy of heavy charged particles in outer space [1]. The spectrum was analyzed using the Ne ions maximum energy. The analysis of the results was prepared as input data for the calculation in a SRIM-2013 program [2]. In the SRIM-2013 program was used for the preliminary modeling for the full-scale experiment. The experimantal and simulation results were compared. The modeling results of the cosmic radiation spectra showed that the main value of the high-energy Ne ions lies in the range of 1 GeV.

The simulation results indicate a small (<10%) discrepancy between the experimental results and the calculated values. Figure 1 shows that the value of the relative error in the position of the Bragg peak is within 5% in the case of simulation and experiment. The Bragg peak for high-energy Ne ions in the W-Cu shield is located at a 580 μm depth. Thus it allows to use such materials as radiation protective shields against Ne ions with energy above 1 GeV. Also it was showed that the used detection method for the shielding efficiency estimating is suitable for resistance of electronic equipment evaluation in active mode. Therefore, proposed calculation method can be considered as effective one for further experiments planning.

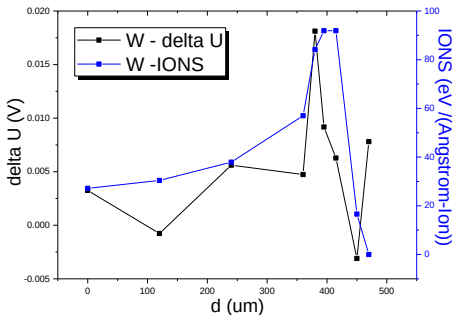

Figure 1 – Results of theoretical and experimental study of linear energy losses of the high-energy Ne ions lies in the range of 1 GeV

References

[1] Our Radiation Software. Available at: https://www.trad.fr/en/space/omere-software/. (accessed 1 September 2021).
[2] Interactions of ions with matte. Available at: http://www.srim.org. (accessed 1 September 2021).

Conical Optical Singularities in Gyrotropic Crystals and Metamaterials

V. S. Merkulov
Scientific-Practical Materials Research Centre of NAS of Belarus
19 P.Brovki str. 220072 Minsk, merkul@physics.by

The closed lines of intersection of refraction surfaces corresponding to cones of optical axes occur in transparent gyrotropic crystals under several conditions [1]. It was shown [2] that dichroism leads to splitting of cones of the optical axes into cones of singular optical axes, between which a "gap" with equal velocities of proper waves is formed. A singular cone separates the regions of equal velocities and equal absorption coefficients of proper waves. In this study various types of irreducible singular optical cones are established for gyrotropic crystals of arbitrary symmetry.

Only seven types of singular points can exist on the stereographic projection of the cone under definite relations between the gyration and absorption tensor components. There are: nodal point A_1; isolated point A_1^*; cusp A_2; tangency point A_3; isolated tangency point A_3^*; beak A_4 (or second order cusp) and triple point D_4.

The possible bifurcations for the available set of singular points:

- node A_1 can split into two branches;
- isolated point A_1^* can be transformed into an oval or disappear;
- cusp A_2 can be transformed into a node or can split into isolated point and a branch;
- tangency point A_3 can be transformed to cusp A_2 or can split to two coupled nodes A_1;
- isolated tangency point A_3^* can be transformed into cusp A_2 or can split into two isolated points A_1;
- beak A_4 can be transformed into tangency point A_3 or can split to isolated tangency point A_3^* and a branch, to coupled cusp A_2 and node A_1, or to cusp A_2 and isolated point A_1^*;
- triple point D_4 can be transformed into tangency point A_3 and a branch.

Splittings of singular points are described exactly by the decay of the corresponding Dynkin diagrams [3].

There are 8 irreducible curves containing single beak A_4, triple point D_4, and combinations $A^*_1A^*_3$, A_1A_3, $2A_2$, $A^*_1\tilde{A}_3$, $2\tilde{A}_1\tilde{A}_2$, $\tilde{A}_1\tilde{A}_3$ (where "~" indicates the open shape of the curve). Sequential bifurcations of that main singular cones result in different 49 types of singular optical cones [4].

The available data on real gyrotropic crystals under presence of dichroism indicate limited potential for the realization of various topological configurations of singular cones. But as for photonic metamaterials, which has intensely developed in recent years, the artificial construction of materials with preset refractive indices and relations between the gyration and absorption tensor components at a given wavelength is possible in principle. The results show that crystal optics can serve as a convenient object for studying various polarization singularities and topological effects (in particular, conical ones).

References

[1] V. I. Al'shits, V. N. Lyubimov. J. Exp. Theor. Phys. 106 (2008) 744-751.
[2] V. S. Merkulov. JETP Lett. 99 (2014) 382-385.
[3] V. I. Arnol'd. Sov. Phys. Usp. 26 (1983) 1025-1058.
[4] V. S. Merkulov. J. Exp. Theor. Phys. 120 (2015) 182-190.

NANOMATERIALS & NANOTECHNOLOGIES

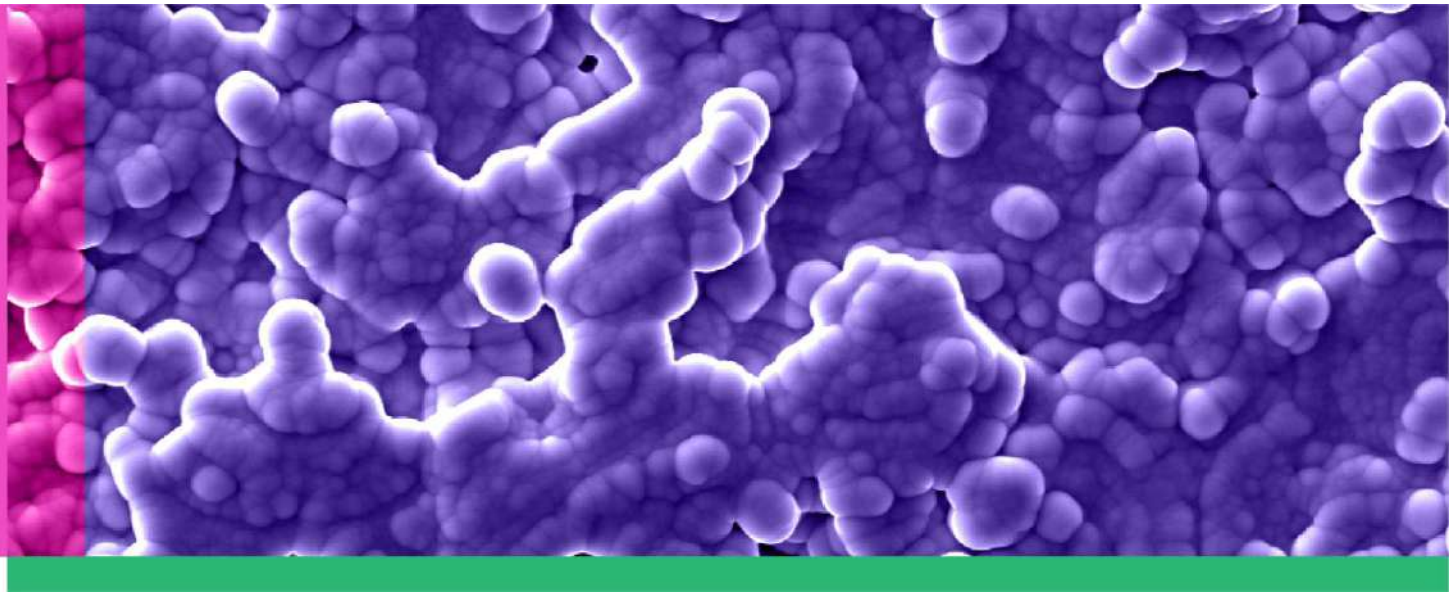

The relaxor behaviour of the $BiFeO_3$-$BaTiO_3$ solid solutions

D. Alikin[1,2,*], A Abramov[1], D. Karpinsky[3], D. Zheludkevich[3], A. Kholkin[1,2]
[1]*School of Natural Sciences and Mathematics, Ural Federal University, 51 Lenina Av., 620000, Ekaterinburg, Russia, denis.alikin@urfu.ru*
[2]*Department of Physics & CICECO – Aveiro Institute of Materials, University of Aveiro, Campus Universitario, 3810-193, Aveiro, Portugal*
[3]*Scientific-Practical Materials Research Centre of NAS of Belarus, 19 P. Brovki str., 220072, Minsk, Belarus*

The bismuth ferrite ($BiFeO_3$, BFO) is one of the important ferroelectric materials with enormously large polarization and high Curie point, which is attractive in energy storage applications [1]. The other important requirement of the materials for the energy storage applications is large recoverable energy storage density, which assumes a decrease of the remnant polarization [1]. The last can be achieved either by formation of the antiferroelectric or relaxor composition using doping or formation of the solid solution with other perovskites. In this work we studied $xBiFeO_3$-$(1-x)BaTiO_3$ (BFO-BTO) solid solutions at the Bi-rich side. BFO-BTO exhibits the relaxor state in the x = 0.2-0.3 range of dopant concentration. The position of the dielectric maximum revealing transition from the non-ergodic-to-ergodic relaxor state is controlled by the temperature and dopant concentration. In the macro-scale measurements, the ferroelectric-to-relaxor transition is accompanied by the "slimming" of the ferroelectric polarization loop and change of the piezoelectric response from the linear bi-polar, piezoelectric, to the non-linear unipolar, electrostrictive. The ceramics produced using sol-gel pathway and conventional solid-phase sintering reveal a similar trend of the polar phase reduction [2,3], which, thereby, approve that the material's grain size and defect state aren't the major factors of the polar phase compactification. On the other hand, the complementary measurements with backscattered scanning electron microscopy revealed a clear spatial correlation of the relaxor phase and Ba-rich phase distribution, which, thus, apparently approves the classical Isupov model of compositionally driven formation of the relaxor phase.

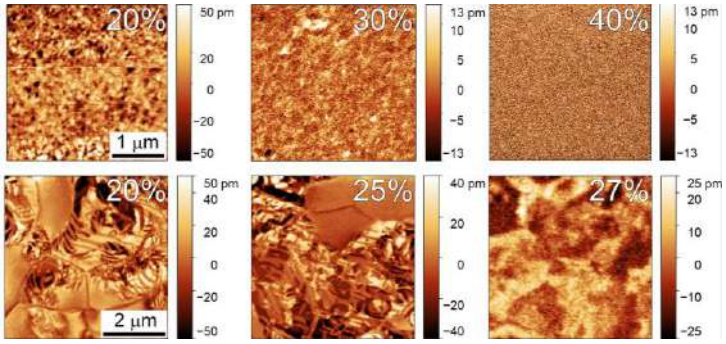

Figure 1. Compactification of the polar state with an increase of the BTO concentration in ceramics produced using sol-gel (top row) and solid-phase (bottom row) sintering.

Acknowledgement

The reported study was funded by RFBR (grant No. 19-52- 04015) and BRFFR (grant No. F19RM-008). The work has been done in frame of the project TransFerr. This project has received funding from the European Union's Horizon 2020 research and innovation programme under the Marie Sklodowska-Curie grant agreement No. 778070. This work was developed within the scope of the project CICECO-Aveiro Institute of Materials, UIDB/50011/2020 & UIDP/50011/2020, financed by national funds through the FCT/MEC and when appropriate co-financed by FEDER under the PT2020 Partnership Agreement.

References

[1] Q. Hu et al. Nano Energy 67 (2020) 104264.

[2] D. V. Karpinsky et al. Nanomaterials 10 (2020) 801.
[3] A. Pakalniškis et al. J. Alloys Compd. 830 (2020) 154632.
[4] V. V. Kirillov and V.A. Isupov, Ferroelectrics 5, 3 (1973).

Photoluminescence of CaF_2/Si/Si(111) nanostructures and effect of hydrogen plasma treatment

A.V. Mudryi[1*], V.D. Zhivulko[1], O.M. Borodavchenko[1], V.A. Zinovyev[2], A.V. Kacyuba[2], A.Y. Krupin[4], Zh.V. Smagina[2], A.F. Zinovyeva[2,3], A.V. Dvurechenskii[2,3]
[1]*Scientific Practical Materials Research Centre of National Academy of Sciences, P. Brovki str., 19, 220072 Minsk, Belarus*
[2]*Rzhanov Institute of Semiconductor Physics, SB RAS, 630090 Novosibirsk, Russia*
[3]*Novosibirsk State University,63090 Novosibirsk, Russia*
[4]*Novosibirsk State Technical University, 630073 Novosibirsk, Russia*

Effects of a remote radio-frequency hydrogen plasma treatment on photoluminescence (PL) properties of crystalline Si and CaF_2/Si/Si(111) nanostructures have been studied. It was found that the PL band at ~ 1.08 eV from crystalline Si caused by interband transition with the participation of optical phonons strongly decreases in intensity due to the deposition of CaF_2 nanolayers.This effect is due to the formation of structural defects at the interface, which are nonradiative recombination centers. Hydrogen plasma irradiation of CaF_2/Si/Si(111) nanostructures was found to result in the enhancement of photoluminescence intensity of crystalline Si. The broad PL bands observed in the below-band-gap region may be related to defects caused by hydrogen plasma treatment.

Structural, Electromagnetic and Magnetic properties of YIG Nanoferrites prepared by Citrate Precursor Method

Shilpa Taneja[1*], Preeti Thakur[1], Atul Thakur[2]
[1]*Department of Physics, Amity School of Applied Sciences, Amity University Haryana, Gurugram, India-122413*
[2]*Centre for Nanotechnology, Amity University Haryana, Gurugram, India-122413*

Yttrium iron garnet (YIG) nanoferrite sample was synthesized by citrate precursor method. The effect of sintering was examined by heating the sample at 1150 °C. The YIG sample was then characterized using X-ray diffraction and scanning electron microscopy. XRD data was used to calculate lattice parameter, crystallite size and density, values which revealed that YIG nanoferrites display a single phase cubic spinel structures. Average crystallite size was found to be 22 nm. Static and dynamic electromagnetic properties were measured by evaluating initial permeability 1.17 and permittivity 10.2 of YIG sample. Magnetic behavior is demonstrated indicates specific saturation magnetization value 25.35 emu/g. Thus, YIG sintered at 1150 °C can be used for wide-ranging frequency applications.

Application of zinc oxide nanoparticles on the carbon nanotubes surface

A. Soldatov[1]*, V. Filippov[2], O. Pavlenko[3], E. Dikusar[4], A. Pushkarchuk[4]
[1] *State Association "Scientific-practical Materials Research Center of the NASB", Minsk, Belarus, andreisoldatov@mail.ru*
[2] *Belarusian State University of Informatics and Radioelectronics, Minsk, Belarus*
[3] *Taras Shevchenko National University of Kyiv, Ukraine*
[4] *Institute of Physical Organic Chemistry, NASB, Minsk, Belarus*

One of the application for the ZnO nanoparticles is a basic material for gas sensors (see for example [1]). The main goal of this investigation is to define a possibility of the formation the ZnO nanoparticles on the carbon nanotube (CNT) surface. Nanoparticles of ZnO, used as an adsorption material for gas sensors, were deposited on the CNT surface by magnetron sputtering. The general view of the formed material is shown in Figure 1.

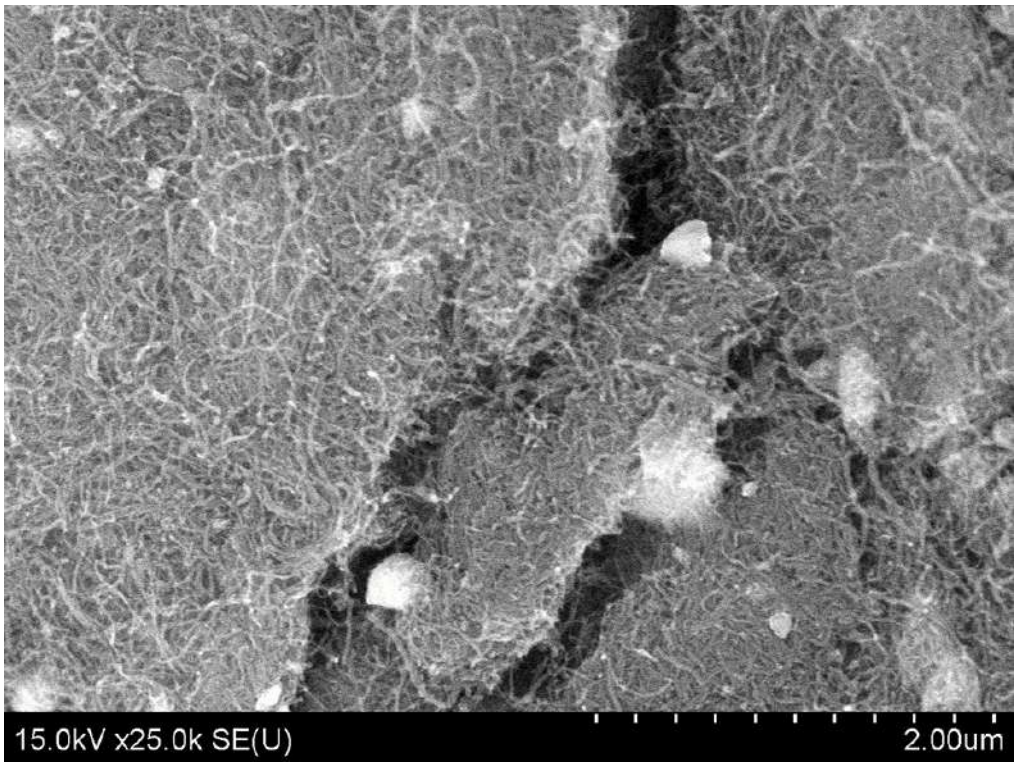

Figure 1. ZnO nanoparticles on the CNT surface.

As can be seen in Figure 1, a significant number of formed nanoparticles with this method of applying ZnO are prone to the formation of submicron crystals, which reduces the surface area of the sensitive material and ultimately reduces the detection limit of a potential sensor device.

The developed method allows applying zinc oxide nanoparticles to the CNT surface, creating a high surface area of the sensitive material per unit volume of the sensor device.

Acknowledgement

The work was carried out within the framework of the State Research Programs "Convergence 2025» and "Materials science, new materials and technologies".

References

[1] Xin Chan, and Shunpu Li, Sensors 2020 (20), 562-567

Quaternary chalcogenide/carbon composites for energy applications

D. Sivagami, Kallol Mohanta, B. Geetha Priyadarshini*
Department of Physics, Nanotech Research Innovation and Incubation Center, PSG Institute of Advanced Studies, Peelamedu, Coimbatore, Tamil Nadu, India-641004

Quaternary chalcogenides (Cu_2ZnSnS_4, Cu_2CoSnS_4,) is a low-cost good absorber and serves as an excellent hole-transporting layer for high efficiency quantum dot solar cells (QDSC). They have a direct transition band gap (1.0-1.65 eV) and a high absorption coefficient (>10^4 cm^{-1}) with superior stability, ease of fabrication, and elemental abundance, it can also be considered as an alternative to conventional organic based hole-transport layer (HTL). Further improvement in the performance of QDSC involves making use of carbon quantum dots (CQDs) which is efficient and enable fast charge carrier separation and subsequently transport charges to the electrodes, making them promising for QDSC. One-dimensional quaternary chalcogenides exhibit charge carrier mobilities much higher than QDs but their light absorption is not freely tunable. Therefore, hybrid materials of nanoparticles sensitized with carbon nanostructures (Carbon dots, graphene, reduced graphene) are very promising for application in optoelectronic devices like solar cells. Herein, quaternary chalcogenides-carbon nanocomposite were successfully synthesized using a simple and cost-effective hydrothermal route. The phase and structural analysis of nanocomposites were characterized by XRD and Raman Spectroscopy. The morphological and micro structural analysis of quaternary chalcogenides nanoparticles and quaternary chalcogenides-carbon nanocomposites were done by Scanning electron microscopy and High resolution TEM. The optical properties of quaternary chalcogenides-carbon nanocomposites were determined by using UV-Visible spectroscopy and photoluminscence spectroscopy. The prepared QDs have the potential to enhance solar cell performance at short photon wavelengths (UV-range). The photo response behavior demonstrates that chalcogenides-carbon nanocomposites have a potential application for use as the absorber layer in solar cells. The obtained quaternary chalcogenides-CQDs can utilize photo-generated carriers to produce higher photocurrents is certainly advantage for further improvement in photon conversion efficienies.

Correlation of the wettability properties and synthesis conditions of the porous anodic alumina

D. Tishkevich[1], A. Vorobjova[2*], A. Bondaruk[1,3], D. Shimanovich[2], T. Zubar[1] and A. Trukhanov[1]

[1]*SSPA "Scientific and Practical Materials Research Centre of NAS of Belarus", 220072 Minsk, P. Brovki str. 19, Belarus*

[2]*Belarusian State University of Informatics and Radioelectronics, 220013 Minsk, P. Brovki str. 6, Belarus,*vorobjova@bsuir.by*

[3]*Belarusian State Technological University, 220006 Minsk, Sverdlova str. 13A, Belarus*

Porous anodic alumina (PAA) is attracted the scientists attention due to its unique ordered honeycomb cell structure which allows the formation of many new multifunctional films and micro- and nanoelements by the template-assistant method [1]. Recently PAA have been intensively studied for use in medical and biotechnological development: bio-filtration for the separation of proteins and organic molecules; in drug delivery systems; biosensor devices etc. Anodization of Al results a nanoporous multichannel structure of alumina with pore size range from 10 to 150 nm and density of about 1×10^{10} pores cm^{-2}. This technique is easier than lithographic methods. In this case, it is desirable to modify the PAA surface in order to obtain a well-wetted surface and pore walls.

Samples of the PAA membranes were prepared via two-step anodization of 99.9994 Al foil in 4% $C_2H_2O_4$ aqueous solution at 40, 50, 60 V [2]. Figure 1 are shown the contact angle images and SEM views of outer surface of as-fabricated samples.

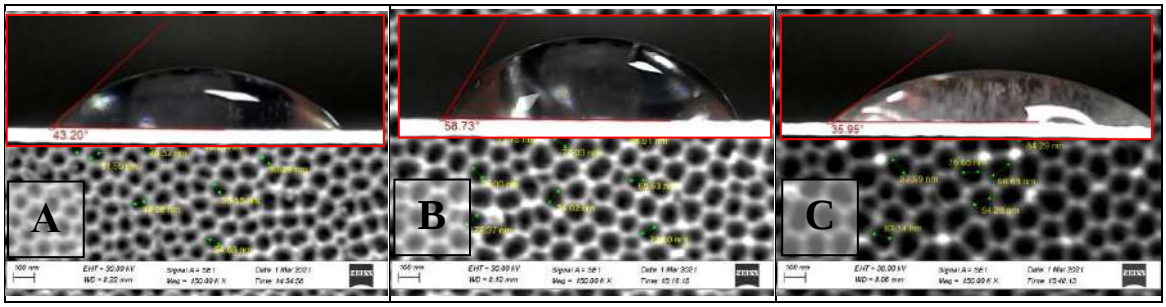

Figure 1. Contact angle as a function of surface topology for as-fabricated samples at 40V (A), 50V (B) and 60V (C) and corresponding SEM images of outer surfaces

An outer surface of PAA were chemically modified using 5% H_3PO_4 at a temperature of (35±2)°C for 5-20 min. As a result PAA membranes with an ordered structure of 8 μm thickness with 50-85 nm pore diameter has been obtained. The PAA morphology were examined using scanning electron microscopy (SEM) Carl Ziess EVO10. The wettability properties were determined by measuring the contact angle using the "recumbent drop" method [3].

The surface chemistry of the PAA samples was not specially modified in order to investigate only the effect of own PAA surface morphology on the wettability properties. It was shown that the contact angle depends not only on the pore diameter and anodization voltage but also on the etching time of the barrier layer, that is, it changes during the fabrication process. It was found that with etching duration increasing the pore diameter and contact angle firstly linear rises then this growth more noticeable. These results indicate that it is possible to select the optimal PAA fabrication condition (anodizing voltage, etching duration) depending on the future application of the PAA membranes.

References

[1] W. Lee [et al.] Chem. Rev. 114 (2014) 7487-7556.
[2] D.I. Tishkevich [et al.] Nanomater. 11 (2021) 1775.
[3] B.D. Summ. Chemistry. Moscow, 1976.

STRUCTURAL FORMATION AND ELEMENTAL COMPOSITION OF NICKEL AND COBALT IMPURITY ACCUMULATION IN SILICON

E.Kh.Berkinov*, R.M. Turmanova, D.Kh. Nurmirzayeva, N.A.Turgunov
Research Institute of Semiconductor Physics and Microelectronics at the National University of Uzbekistan, Tashkent, Uzbekistan
***Corresponding author e-mail: elmurod_8883@umail.uz*

The paper considers the effect of diffusion parameters on the structural formation and chemical composition of impurity accumulations of cobalt and nickel in silicon. The morphological parameters of impurity accumulations were determined by the method of electron probe microscopy. It was revealed that at high values of the cooling rate of the samples, in their volume different geometric shaped single-layer impurity clusters are formed. In the volumes of impurity accumulations of nickel and cobalt in silicon, the presence of atoms of technological impurities, such as Fe, Cu, Cr, Al, and others, was found.

Structural reorganization of graphite nitrate cointercalation compounds in liquid media on the base of XRD and NMR 1H spectroscopy data

E. Raksha[1], A. Voitash[1*], Yu. Berestneva[2], G. Volkova[3], A. Davydova[1], A. Eresko[1], and M. Savoskin[1]

[1]*L.M. Litvinenko Institute of Physical Organic and Coal Chemistry, R. Luxemburg Street 70, Donetsk 83114, Ukraine, anna.voytash@gmail.com*

[2]*Federal Scientific Centre of Agroecology, Complex Melioration and Protective Afforestation of the Russian Academy of Sciences, Universitetskij pr. 97, Volgograd 400006, Russian Federation*

[3]*Donetsk Institute for Physics and Engineering named after A.A. Galkin, R. Luxemburg Street 72, Donetsk 83114, Ukraine*

Graphite nitrate cointercalation compounds (GNCCs) with acetic acid, ethyl acetate and ethyl formate were obtained. Structural reorganization of the GNCCs in liquid medium has been demonstrated by the XRD and NMR ^{1}H spectroscopy. A partial release as well as exchange of the intercalants were observed for studied GNCCs in ethyl formate and ethyl alcohol media.

GNCCs (binary with acetic acid and triple with acetic acid and ethyl formate) were prepared as described in [1] using a natural flake graphite GT-1 (Zavalie Graphite Works, Kirovograd region, Ukraine) as a starting material. The GNCCs samples were stirred with a solvent (ethyl formate, 95 % wt. ethanol, or 10 % solution of ethyl formate in CH_2Cl_2).

GNCCs behavior in ethanol, ethyl formate and ethyl formate solution in CH_2Cl_2 was studied by NMR ^{1}H spectroscopy. The intercalant partial release in a solution (up to 5% by weight of the sample) was observed as a result of the GNCCs treatment by the ethyl alcohol and ethyl formate. According to NMR ^{1}H spectroscopy data treatment of as-prepared sample of graphite nitrate, cointercalated with acetic acid, by the 10% solution of ethyl formate in CH_2Cl_2, leads to acetic acid partial release in a solution and ethyl formate concentration reduction therein. The amount of released acetic acid in a solution for 120 hours was 0,035 g per 1 g of the sample, and the ethyl formate concentration in CH_2Cl_2 solution has decreased by 36 % during this time.

Structural characteristics of the obtained compounds (identity period I_C and height of the layer filled with intercalant d_i) were determined from X-ray patterns of GNCCs samples. As a result of the binary GNCC treatment by pure ethyl formate for 120 hours its structural reorganization was observed apart from the release of acetic acid. Transition from the stage II to higher IV stage of intercalation was observed, also the reflexes corresponding to the lower stage II were still present. Moreover, treatment of the binary GNCC in ethyl formate leads to the formation of the ternary cointercalation compound, which is basically a compound of β-type. As a result of the binary GNCC structural reorganization in ethyl formate the filled interplanar distance corresponding to the IV intercalation stage decreases while d_i corresponding to the II intercalation stage increases. After treatment of the graphite nitrate, cointercalated with ethyl formate and ethyl acetate, by ethyl alcohol for 120 hs similar results were observed. Structural reorganization of the ternary GNCC in ethyl alcohol medium is characterized by decrease of the filled interplanar distance corresponding to IV intercalation stage, increase of the d_i value for the II stage of intercalation and transition of the GNCC into a β-type cointercalation compound. These results indicate occurrence of very strong interactions in intercalant layers.

References

[1] A.A. Davydova, E.V. Raksha, V.A. Glazunova, O.N. Oskolkova, V.V. Gnatovskaya, P.V. Sukhov, V.V. Burkhovetskij, G.K. Volkova, Yu.V. Berestneva, and M.V. Savoskin Russ. J. Inorg. Chem. 66 (2021), 324–331.

Structure and properties of a-C coatings deposited from pulsed carbon plasma flows separated by various methods

D. G. Piliptsou*, A.V. Rogachev, A.S. Pobiyaha, A.S. Rudenkov
Francisk Skorina Gomel State University, 104, Sovetskaya str., 246019, Gomel, Belarus,
**corresponding author e-mail: pdg_mail.ru*

The formation of carbon-based coatings using a vacuum cathode-arc discharge is an effective method for producing hard coatings. However, a significant disadvantage typical of pulsed deposition methods is the presence of macroparticles in the plasma flow, the deposition of which on the surface reduces the phase and morphological homogeneity of the coating. Therefore, the top priority is to develop methods for reducing the macro-droplet component in the flow of carbon plasma.

This work aims to determine the peculiar features of forming the structure and optical properties of coatings deposited from a pulsed flow of carbon plasma using various designs of separating devices.

The coatings were deposited in a vacuum chamber at a residual pressure of 3.7×10^{-3} Pa on pre-cleaned polished substrates (silicon and quartz) at a discharge voltage of 350 V and a pulse repetition rate of 3 Hz. The separation was carried out using a solenoid (length is 380 mm, number of turns is 16, diameter is 130 mm, flow rotation angle is 90°). The solenoid was included in the evaporator's anode part and created a magnetic field when a discharge current pulse passes through it. The field changes the trajectory of the ion component of the flow. Meanwhile, the trajectory of the macroparticles is not subject to changes. A separator was also used, consisting of a screen separating a part of the plasma flow with the propagation direction along the source axis, which subsequently passes through the magnetic field created by permanent magnets and rotates through an angle close to 90°.

Atomic force microscopy showed that macroparticles are most effectively removed when the solenoid is used as a filter, which allows depositing coatings with roughness RMS=1.51 nm. The high rate of ion supply to the substrate surface predominantly determines the lateral growth of the coating; when using a magnetic separation system based on permanent magnets, the deposition rate is lower compared to the solenoid, and the RMS roughness is higher with the grain size D of 8.5 nm. There are also single particles on the surface, which is apparently due to the pulse mode of the separator. The maximum roughness values RMS=4.47 nm were specified for the a-C coatings deposited without flow separation. The Raman spectroscopy showed that using the solenoid located inside the vacuum chamber as a separator leads to the formation of a-C coatings with a minimum size of Csp^2 clusters and a maximum content of carbon atoms with sp^3-hybridized bonds. This determines an increase in the refractive index up to 2.71 and the width of the band gap Eg up to 2.63 eV. Using UV-Vis spectroscopy, an increase in the optical transparency of the coatings deposited under the flow separation conditions was found. Using a separator of this design leads to a decrease in the surface roughness, and the formation of the isotropic structure with more stable values of n, Eg.

PHOTOLUMINESCENCE IN THIN FILMS OF $Cu(In,Ga)(S,Se)_2$ SOLID SOLUTIONS AT PULSE LASER EXCITATION

O. Borodavchenko*, V. Zhivulko, A. Mudryi, A. Hatsak
Scietific Practical Materials Research Centre of National Academy of Sciences,
P. Brovki str., 19, 220072 Minsk, Belarus

The photoluminescence spectra of thin nanocrystalline films of $Cu(In_{1-x}Ga_x)(S_ySe_{1-y})_2$ (CIGSSe) direct-band gap semiconductors were investigated at nanosecond pulsed laser excitation in the range of excitation power density 0.1 – 40 kW/cm^2 and temperature at ~ 10 K. It was found that with increasing intensity of the exciting emission the photoluminescence bands shift toward higher energies and their full width at half maximum intensity (FWHM) decreases. Possible mechanism of the influence of excitation laser intensity on the spectral positions and FWHM of stimulated emission of CIGSSe thin films are discussed.

PHOTOLUMINESCENCE OF THIN FILMS $Cu(In,Ga)(S,Se)_2$ SOLID SOLUTIONS IRRADIATED BY ELECTRONS

O. Borodavchenko*, V. Zhivulko, A. Hatsak
Scietific Practical Materials Research Centre of National Academy of Sciences,
P. Brovki str., 19, 220072 Minsk, Belarus

Effects of 4 MeV electron irradiation on luminescence properties of $Cu(In,Ga)(S,Se)_2$ thin films have been investigated. Before irradiation the photoluminescence spectra reveal some of wide bands relating to band-to-band and band-to-defects optical transitions at 1.07 eV and at 0.8 eV, respectively. The irradiation of thin films by electrons reduces the intensity of the broad band at 1.07 eV and also enhances the intensity of the broad band at 0.8 eV, suggesting a rise in concentration of defects due to electron irradiation. A possible nature of defects and process of radiative recombination are discussed.

Impedance Spectroscopy of FeCo Alloy Nanoparticles in Alumina and PZT

A.V. Larkin[1*], A.K. Fedotov[2], T.N. Koltunowicz[3], and P. Zhukowski[3]
[1]*Belarusian State University, Nezavisimosti av. 4, 220030, Minsk, Belarus, larkinav@bsu.by**
[2]*Institute for Nuclear Problems of Belarusian State University, Bobruyskaya 11, 220006, Minsk, Belarus*
[3]*Lublin University of Technology, Nadbystrzycka 38a, 20-618 Lublin, Poland*

The paper substantiates the extended use of impedance spectroscopy in the analysis of electrical transport in composite nanogranular metal-dielectric films of the $(Fe_{0.45}Co_{0.45}Zr_{0.10})_x(Al_2O_3)_{1-x}$ and $(Fe_{0.45}Co_{0.45}Zr_{0.10})_x(PZT)_{1-x}$ types based on taking into account the chemical and phase composition, as well as the morphological features of the samples (the type of nanoparticles and dielectric matrices, the metal / dielectric phase ratio x, the presence of intrinsic oxides around the metal "core", etc.) [1, 2].

The dependences of total impedance $Z(f,T)$ on frequency and temperature in the films with the relative content of FeCoZr alloy in the range $0.3 < x < 0.8$ are studied. The samples were prepared by ion-beam sputtering of composite targets in a pure Ar medium or in an $Ar+O_2$ gas mixture, followed by annealing in air at temperatures of 398 — 873 K.

The study of the $Z(f,T)$ dependences have shown that in the case of the films deposited in $Ar+O_2$ gas mixture and (or) after subsequent annealing in air, the FeCoZr granules were coated with their own Fe and Co oxides. In this case, the samples were characterized by two critical values of x: the threshold of "shells" touching x_{c1} and the threshold of a continuous conducting cluster formation x_{c2}.

The analysis of the $Z(f,T)$ dependences based on the hopping conductivity model [3] showed that the lifetime of electrons on FeCoZr nanoparticles increases from 0.1 to 400 μs, and the value of the hopping barrier decreases from 300 to 1 meV with the increase of concentration in the region $x < x_{c1}$. In this case, there is a positive phase shift between the applied voltage and current (the current lags behind the voltage), called negative capacitance effect (NCE) [4].

Based on the $Z(f)$ dependences, the equivalent circuits (EC) of the samples were carried out, which made it possible to estimate the temperature/frequency dependences of the EC elements (R, C, L) and compare them with the formed phases giving contributions to $Z(f)$ due to NCE. As a result, the average electron hopping lengths between metal clusters (through dielectric matrices) or "shells" of intrinsic oxides (FeO, Fe_3O_4, Fe_2O_3, CoO), formed around nanoparticles during synthesis and (or) annealing of films, were calculated

It is shown that the NCE is always accompanied by the presence of two peaks on the $Z(f)$ curves (Figure 1), which corresponds to an EC with two resonant RCL-circuits and an additional resistance.

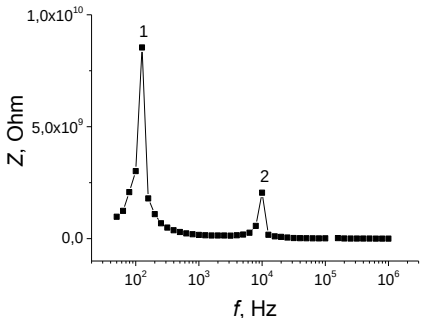

Figure 1. Dependence of the total impedance of the film $(Fe_{0.45}Co_{0.45}Zr_{0.10})_{0.31}(Al_2O_3)_{0.69}$ at T = 80 K deposited in Ar gas and annealed at T_{an} = 623 K

References

[1] J.Fedotova, J.Kasiuk, J.Przewoznik, Cz.Kapusta, I.Svito, Yu.Kalinin, A.Sitnikov, Journal of Alloys and Compounds 509, 41 (2011) 9869-9875.
[2] Kasiuk J.V., Fedotova J.A., Marszalek M., Karczmarska A., Mitura-Nowak M., Kalinin Yu.E., and Sitnikov A.V., Physics of the Solid State 54 (2012) 178-184.
[3] P. Zukowski, T.N. Koltunowicz, O. Boiko, V. Bondariev, K. Czarnacka, J.A. Fedotova, A.K. Fedotov, I.A. Svito, Vacuum 120 (2015) 37-43.
[4] P. Zhukowski, T.N. Koltunowicz, P. Wegierek, J.A. Fedotova, A.K. Fedotov and A.V. Larkin, Acta Physica Polonica A 120 (2012) 43-45.

Growth mechanism of silver nanostructures in a limited volume

D.V. Yakimchuk[1*], V.V. Prigodich[1], S.A. Khubezhov[2,3],S.E. Demyanov[1], V. Sivakov[4]
[1]*Scientific-Practical Materials Research Center NAS of Belarus, 19 St. P.Brovka 220072 Minsk, Belarus*
[2]*School of Physics and Engineering, ITMO University, 191002 St. Petersburg, Russian Federation,*
[3]*Research Laboratory of Functional Nanomaterials Technology, 2 St. Shevchenko 347922 Taganrog, Russian Federation,*
[4]*Leibniz Institute of Photonic Technology, 9 St. Albert-Einstein-Straße 07745 Jena, Germany*

The formation of nanostructures using template synthesis is a popular way due to the simplicity of this technique and the possibility of varying the geometric parameters of the structures by changing the template formation parameters. Additionally, we will single out the ion-track SiO_2/Si templates , since the technology of their preparation is well-known [1], and previously were successfully implements by our tema by the creation of broad spectrum of nanostructures. In particular, we have shown that silver nanostructures with different morphologies can be formed in the pores of the SiO_2/Si template by the galvanic displacement method: crystallites, dendrites, "sunflower-like" nanostructures, as well as their intermediate configurations [2]. The present work is devoted to a detailed study of the influence of the geometric parameters of the template pores on the morphology of silver nanostructures. It was found that the morphology of silver is determined by the lower (*d*) and upper (*D*) pore diameters. It was observed that during the chemical deposition, diffusion-limited processes arise in the pores, which are depending on the pore size and proceed according to different scenarios. The obtained results in frame of these studies allowed us to identify scenarios of chemical processes occurring in different ranges of *D*. The presented figure shows a schematical representation of the morphology of the silver deposits depending on the pore size *D* (all other conditions being equal for the synthesis).

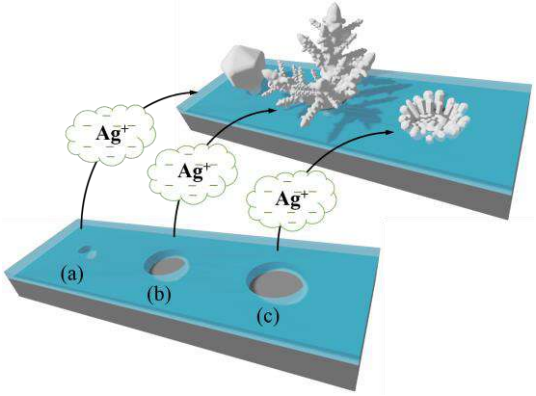

Schematic representation of the obtained silver nanostructures with different morphologies in templates with different pore diameters D: (a) up to 400 nm - crystal, (b) 700-800 nm - dendrite, (c) 800-1000 nm - "sunflower-like" structure.

Acknowledgement: the authors acknowledge the support of the work in frames of H2020 - MSCA - RISE2017 - 778308 - SPINMULTIFILM Project, Belarusian Foundation for Basic Research [project number Ф21PM-054] and supported by the Ministry of Science and Higher Education of the Russian Federation; the state task in the field of scientific activity No. 0852-2020-0015.

References

[1] D. Yakimchuk, E. Kaniukov, S. Lepeshov, V. Bundyukova, S. Demyanov, G. Arzumanyan, N. Doroshkevich, K. Mamatkulov, A. Bochmann, M. Presselt, O. Stranik, S. Khubezhov, A. Krasnok, A. Alù, and V. Sivakov. Journal of Applied Physics. Vol. 126. (2019) P. 233105.
[2] D. Yakimchuk, E. Kaniukov, V. Bundyukova, L. Osminkina, S. Teichert, S. Demyanov, and V. Sivakov. MRS communications. Vol. 8 (1). (2018) P. 95-99.

Structure and electrophysical properties of thermal control nanostructured coatings TiAlN, TiAlCN

S.V. Konstantinov[1*], F.F. Komarov[1], V.A. Zaykov[2], and I.V. Chyzhou[2]
[1]*A.N. Sevchenko Institute of Applied Physics Problems of Belarusian State University, Belarus, 220045 Minsk, Kurchatov Str 7, svkonstantinov@bsu.by, komarovF@bsu.by*
[2] *Belarusian State University, Belarus, 220030, Minsk, 4 Nezavisimosti Avenue*

Nanostructured TiAlN and TiAlCN coatings were formed by reactive magnetron sputtering in various technological modes. The surface resistance was measured using a four-probe method, and the dependence of electrical conductivity on temperature (15 K – 375 K) in the frequency range 50 Hz – 5 MHz was determined on a specialized device. The investigated coatings are highly conductive and are characterized by low values of surface resistance (1.07–20.82 Ohm/□). This important characteristic avoids the accumulation of static charge on the surface of space systems. At the same time, according to the results of studies of the dependence of the TiAlCN coatings electrical conductivity on temperature and frequency, an increase in electrical conductivity with increasing temperature was established, which indicates the manifestation of their semiconducting properties.

The physical properties of $Ag_xCu_{2-x}ZnSnS_4$ nanocrystallic thin films

Yu. Radyush, V. Hurtavy*, T. Shoukavaya
Scientific-Practical Materials Research Centre of National Academy of Sciences of Belarus, Brovki str. 19, Minsk, Belarus

The synthesis methods of $Ag_xCu_{2-x}ZnSnS_4$ solid solutions are optimized taking into account their significant dissociation during melting. Polycrystalline samples $Ag_xCu_{2-x}ZnSnS_4$ were synthesized by the one-temperature method from elementary components.

The preparation of thin films from a colloidal solution of nanoparticles has been developed.

The effect of the composition on the structural characteristics of thin nanocrystalline films $Ag_xCu_{2-x}ZnSnS_4$ has been studied by X-ray diffraction. It is shown that the unit cell parameters increase with an increase in the concentration of silver ions.

Features of electrochemical formation of metal and semiconductor nanowires in anodic alumina matrices with variable pores

G.G. Gorokh*, A.A. Lozovenko, M.V. Kasatkin, M.M. Iji, V.S. Fedosenko
Belarusian State University of Informatics and Radioelectronics, P.Brovki Str. 6, Minsk 220013, Belarus

Due to the fact that quantum laws operate at the nanoscale, any change in the composition or geometry of a nanoobject can lead to fundamental change in the physical and chemical properties of the entire structure. This necessitates the creation of more complex structures (nanotubes and nanowires with different diameters at different heights, with branching, etc.). In comparison with other methods, electrochemical template synthesis of nanostructures in porous matrices with complex nanopore geometry is distinguished by relative simplicity of operations and low cost.

This work presents the series of laboratory experiments in which the technology of creating anodic aluminum (AA) oxide matrices with alternating pore diameters has been developed. Such a matrix consists of several layers of adjustable depth with specific pore diameters along the entire height of these layers and was used as template for electrochemical deposition of metal and semiconductor nanowires. Each layer formed in potentiostatic mode, so pore diameter and other morphological parameters depends on applied voltage. Between each layer there were thin transition zones, where pore diameters smoothly changed. It was found, that on the transitions from the smaller pores to the larger one, part of pores was sealed. Presumably, competition for the charge passing through them leads to the preferential sealing, rather than the unification of most of the pores. This is a significant problem for filling such a structure with metal by the electrochemical deposition, since the pores sealed even on one side are not electrically connected either with the contact or with the electrolyte and, as a result, are not filled. Investigation of features electrochemical deposition of metals and semiconductors into such matrices were carried out on AA consist of four layers of anodic oxide, 10 μm each, formed on an aluminum foil with alternating voltages of 120 V (malonic acid 0.4 M) and 50 V (oxalic acid 0.3 M), with a deposited copper layer. The electrochemical deposition of Cu into test sample was carried out from the solution of 0.5 M $CuSO_4$, 0.1 M H_2SO_4 at an anodic current density of about 2 mA/cm^2 to determine principal possibility of deposition into metrices. REM images demonstrated significant filling of Cu pores along the entire height.

Electrochemical deposition of a semiconductor compound InSb was carried out from a solution containing 0.1 M $SbCl_3$, 0.15 M $InCl_3$, 0.36 M citric acid, 0.17 M potassium citrate and 0.1 g of surfactant. The filling of the pores with indium antimonide from the bottom of the matrix to the surface has som features, so the cations, when moving through the branched pores, encounter difficulties in overcoming each transition between the branching pores, not all are uniformly filled. However, InSb is capable of overcoming transitions and branching in accordance with the pore configuration during deposition. On the kinetics of InSb deposition, synchronous fluctuations of the voltage and current density values were observed, which can be associated with a change in the working area during the transition between the layers.

Techniques for the formation of nano-porous membranes from anodic alumina with alternating pore sizes have been developed and investigated, and were adapted for the deposition of metals and semiconductors. Manufactured membranes were tested in the electrochemical deposition of copper and indium antimonide. Electron microscopic studies of the formed nanosystems have been carried out and a pore filling mechanism has been proposed. The current-voltage characteristics of arrays of nanowires with a variable diameter

are investigated. The data obtained make it possible to determine the technological parameters in order to reproduce and controllably obtain arrays of nanowires with variable morphology.

Synthesis of matrix nanostructures from oxides and sulfides of transition metals

G.G. Gorokh*, V.S. Fedosenko, A.A. Lozovenko, M.M. Iji
[1]*Belarusian State University of Informatics and RadioelectronicsBelarus, 220013, Minsk, P.Brovki str., 6, e-mail: gorokh@bsuir.by*

In modern photovoltaic, sensor and thermoelectric devices, multicomponent metal oxides and sulfides of transition metal metal oxides are widely used [1], while the the apply of combined oxide and sulfide layers can significantly increase their functional properties [2,3].

In this work, we propose an original technology for the formation of multicomponent composites based on oxides and sulfides.

To create a template with TiO_2 island nanostructures, a two-layer Ti/Al thin-film system (Ti – 200 nm, Al – 1 μm), deposited on a silicon substrate, was used. Anodizing of two-layer Ti/Al composition was carried out in 0.4 M H_3PO_4 in a combined mode: first, the layer of porous anodic alumina (PAA) was formed at a constant current density of 6 A/cm^2; when the anodizing front reached the titanium sublayer, the voltage was stabilized at 120 V. During this period, the formation of the PAA matrix was completed, and through its pores, local oxidation of the titanium sublayer and the formation of TiO_2 nanoislands, accompanied by a sharp drop in the current, began. The anodizing process was stopped after the anodic current decreased to 60 μA/cm^2. Then, the formed PAA was etched away in a 50% H_3PO_4 solution at 50°C. As a result, a structure remained on the silicon wafer, which was the titanium layer with the nanostructured film of TiO_2 nanoislands.The process of layer-by-layer deposition of bismuth oxide on island nanostructures of titanium oxide, as in the case of ionic deposition on PAA matrices [3], included surface preparation, consisting in boiling the initial workpiece in distilled water for 30 minutes at a temperature of 100°C. An aqueous solution of 0.1 M $Bi(NO_3)\times5H_2O$ was used as a cationic solution. Heated distilled water was used as an anionic solution. Composite multioxide films were obtained by ionic layer-by-layer cyclic deposition by sequential processing of the initial samples in cationic and anionic solutions for 30 s. at temperature of 30°C. One deposition cycle included treatment in cationic and anionic solutions with intermediate washings in distilled water for 5 s. to remove ions weakly bound to the surface. The total of 150 cycles were carried out.

The CdS compound was obtained by preparing two intermediate solutions and mixing them. First, the 2 g of ammonia was added to 1 g of $CdSO_4$ and gradually mixed until a homogeneous mass was obtained. Then, the 1 g of thiourea was dissolved in the 10 ml of distilled water. The resulting compositions were mixed in 1:2 ratio. The resulting mass was placed in a water bath and intensively stirred at temperature of 30°C for 5-10 minutes until complete dissolution and obtaining the homogeneous solution. Then the resulting solution was applied to heated substrate with the nanostructured TiO_2 film with 2 ml dispenser and centrifuged at 1000 rpm for 30 s. The resulting film was dried in a SNOL 3.2/1100 muffle furnace under air at 70°C for 30 min. and 150°C for 60 min.

A film of bismuth oxide with a thickness of about 400 nm is a cluster of grains in the form of plates. The grain length was about 250 nm, and the width was up to 40 nm. The CdS film is a granular formation with a grain size of about 20 nm, the film thickness is about 3 microns, and the total thickness of titanium and its oxide is about 265 nm.

Thus, the electrochemical and chemical methods allows to form nanostructured multicomponent oxides consisted of two or three metal components. The formed multicomponent films have great potential to applicate in high-sensitivity gas sensors, photovoltaic and thermoelectric devices.

References

[1] Y. Deng, Semiconducting Metal Oxides for Gas Sensing. Springer Nature Singapore Pte Ltd. 2019, 253 pp.

[2] M. Punginsang, et al., Materials Science in Semiconductor Processing. 90 (2019) 263–275.
[3] G. Gorokh, et al., Physica Status Solidi (b). 257 3 (2020) 1900283-1900291.

Mechanochemical reduction of simple and complex oxides of tungsten and molybdenum

T.A. Udalova[1,2]*, C.V. Vosmerikov[1], E.T. Devyatkina[1], T.F. Grigoreva[1], N.Z. Lyakhov[1]
[1]*Institute of Solid State Chemistry and Mechanochemistry of Siberian Branch of Russian Academy of Sciences,630128 Novosibirsk, Russia*
[2]*Novosibirsk State Technical University, K. Marx ave 20, Novosibirsk 630073, Russia*

Highly dispersed metal powders are in demand in various industries. There are many methods for their preparation, among which the most technologically simple and efficient is mechanochemical synthesis in high-energy systems. The products of the mechanochemical redox reaction, the $Me/(Me_{act})_xO_y$ composites, are a mixture of powders of highly dispersed particles of active metal oxide $(Me_{act})_xO_y$ and reduced elements. Magnesium oxide, having a high melting point, prevents the sintering of mechanical activation products and upon interaction of the Me/MgO composites with solutions of hydrochloric or sulfuric acids, MgO transforms into readily soluble compounds. The stages of the process of mechanochemical reduction of oxides WO_3 and MoO_3 with magnesium were studied by X-ray phase analysis and electron microscopy. It was show that magnesium tungstate and magnesium molybdate are formed as intermediates.

Sintering is a traditional solid-phase method for the synthesis of $MgWO_4$ ($MgMoO_4$) [6-9], but its disadvantages are the high synthesis temperature (~ 1173 K) and duration (from 10 to 24 hours). It is of interest to study the possibility of obtaining $MgWO_4$ and $MgMoO_4$ by mechanochemical activation of a mixture of tungsten (molybdenum) and magnesium oxides, as well as the use of magnesium wolframite (molybdate) for their mechanochemical reduction with magnesium in the synthesis of fine powders of tungsten and molybdenum. The reactions of formation of magnesium wolframite (MgWO4) and molybdate (MgMoO4) from tungsten (molybdenum) oxides with magnesium oxide are exothermic:

$$MgO + WO_3 = MgWO_4;\ \Delta_rH^o_{298} = -71.1\ kJ \quad (1)$$

$$MgO + MoO_3 \rightarrow MgMoO_4;\ \Delta_rH_{298} = -54.05 kJ \quad (2)$$

X-ray phase studies of the mechanochemical interaction of magnesium oxide and tungsten (molybdenum) oxides showed that when an activation time of 8 (12) minutes is reached, magnesium wolframite (molybdate) is formed only $MgWO_4$ ($MgMoO_4$) reflections are recorded on the diffractogram. In addition, this mechanochemically synthesized magnesium wolframite (molybdate) was used as a precursor for the mechanochemical synthesis of highly dispersed tungsten (molybdenum). X-ray diffraction of samples of mechanochemical reduction of $MgWO_4$ ($MgMoO_4$) obtained with different stoichiometric compositions and modes of mechanical activation showed that at a ratio of $MgWO_4$ ($MgMoO_4$) : Mg = 1: 3.1 the speed of rotation of bubbles around a common axis, the reduction is completed by 8 min with the formation of a W(Mo)/MgO composite. Sequential treatment of the mechanochemical composite W(Mo)/MgO with 1M H_2SO_4 solution, distilled water and acetone ensures effective separation of tungsten (molybdenum) powder from magnesium oxide. Scanning electron microscopy showed that the tungsten (molybdenum) powder is finely dispersed and consists of primary particles of 50–100 μm in size, aggregated into secondary particles of 2–4 μm in size. The stability of W(Mo)/MgO mechanochemical composites are maintained for several months.

Acknowledgement
The work was carried out as part of the state task of ISSC SC RAS (project regional №. 121032500062-4) and as thematic plan TP-HHT-1_21.

Few-layer graphenes from thermally expanded graphite intercalated compound

E. Raksha[1*], O. Oskolkova[1], P. Sukhov[1], A. Davydova[1], V. Gnatovskaya[1], V. Glazunova[2], G. Volkova[2], V. Burkhovetskij[2], and M. Savoskin[1]
[1]*L.M. Litvinenko Institute of Physical Organic and Coal Chemistry, 70 R. Luxemburg Street, Donetsk 83114, Ukraine, elenaraksha411@gmail.com**
[2]*Donetsk Institute for Physics and Engineering named after A.A. Galkin, 72 R. Luxemburg Street, Donetsk 83114, Ukraine*

This paper presents the results of complex investigations of structural features of tripe graphite nitrate cointercalation compound (GNCC) with acetic acid and acetonitrile. Stability of the GNCC as well as effect of the additional cointercalant in the GNCC structure on its structural and expansion properties are discussed. GNCC was used as a source for termally expanded graphite (TEG) which can be considered as perspective precursor for graphene and related structures. Morphology of the carbon nanoparticles formed from corresponded TEGs by liquid phase exfoliation in *tert*-butanol assisted with sonication is discussed.

Triple cointercalate was obtained by the introduction of two organic intercalants (acetic acid and acetonitrile) into graphite nitrate. The overall scheme of the process involves graphite nitrate synthesis as a first stage followed by cointercalation with two organic compounds (Fig. 1). Structural changes in graphite matrix resulted from its interaction with nitric acid and subsequent treatment with organic cointercalants have been studied by powder XRD method. It should be noted that formation of studied triple GNCC is accompanied by an activation of the intercalated structure as compared with graphite nitrate. Discussed cointercalate (both stage II and stage IV intercalation compounds) is characterized by higher values of identity period. TEG samples obtained from triple GNCCs were used as a source of carbon nanoparticles. GNCCs samples were undergoing thermal shock at 900 °C. The surface morphology of the flake graphite, GNCC, and expanded graphite samples was investigated by scanning electron microscopy method. Destruction of the TEG cellular structure during sonication in liquid phase may result in generation of single as well as few-layer graphenes and related structures due to exfoliation.

Step-by-step scheme of the carbon nanoparticles obtaining starting from graphite is presented in fig. 1. Dispersions of carbon nanoparticles were obtained by corresponded TEGs liquid phase exfoliation assisted with sonication in *tert*-butanol.

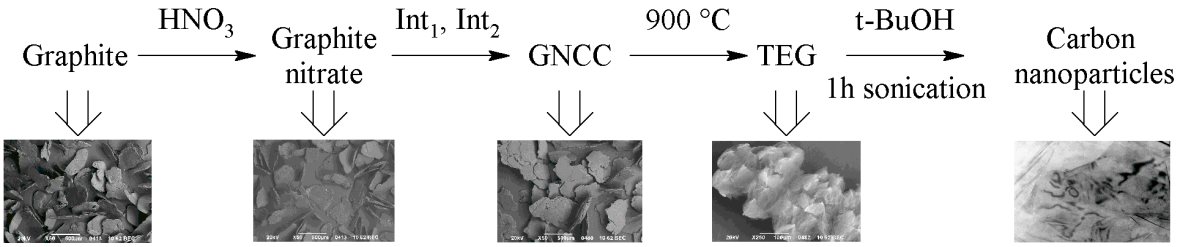

Fig. 1. Step-by-step scheme of the carbon nanoparticles obtaining (with representative SEM-images of initial graphite, intermediate graphite nitrate, GNCC with acetic acid and acetonitrile, TEG, and representative TEM-image of the final few-layer graphene particle)

The microstructure of prepared nanoparticles was estimated by transmission electron microscopy. The SAED patterns of resulted graphenes displayed six-fold symmetry consistent with the typical hexagonal crystalline structure. Planar sizes of the few-layer graphene particles reached several tens of μm, the thickness varied within 2 - 10 atomic layers.

Effect of carbon nanotubes on electromagnetic response of epoxy composites filled with Ga^{3+} substituted M-type barium hexaferrites

O. Yakovenko[1]*, L. Matzui[1], L. Vovchenko[1], V. Oliynyk[1], V. Zagorodnii[1], A. Trukhanov[2] and S. Trukhanov[2]
[1]*Taras Shevchenko National University of Kyiv, 01601, Ukraine, Kyiv, Volodymyrska Str. 64/13, *alenka-ya@ukr.net*
[2]*Scientific Practical Materials Research Centre of NAS of Belarus, 220072, Belarus, Minsk, P. Brovki str., 19*

Microwave properties of epoxy composites filled with 30 wt.% of $BaFe_{12-x}Ga_xO_{19}$ ($0.1 < x < 1.2$) and with 1 wt.% of multiwall carbon nanotubes (CNT) were investigated in the frequency range 36-55 GHz. A sufficient increase of microwave shielding efficiency was found for ternary 1wt.%CNT/30wt.% $BaFe_{12-x}Ga_xO_{19}$/epoxy composites compared with binary 1%CNT/epoxy and 30wt.% $BaFe_{12-x}Ga_xO_{19}$/epoxy due to complementary contributions of dielectric and magnetic losses. Thus the adding only 1wt.% of CNT along with 30 wt.% of barium hexaferrite into epoxy resin increases the frequency range where electromagnetic radiation is intensely attenuated. A correlation between cation Ga^{3+} concentration in $BaFe_{12-x}Ga_xO_{19}$ filler and amplitude–frequency characteristics of natural ferromagnetic resonance (NFMR) in 1wt.%CNT/30wt.% $BaFe_{12-x}Ga_xO_{19}$/epoxy composites was determined. The higher values of resonance frequency f_{res} (51.8-52.4 GHz) and weaker dependence of f_{res} on Ga^{3+} concentration were observed compared with pressed polycrystalline $BaFe_{12-x}Ga_xO_{19}$ (f_{res} =49.6-50.4 GHz).

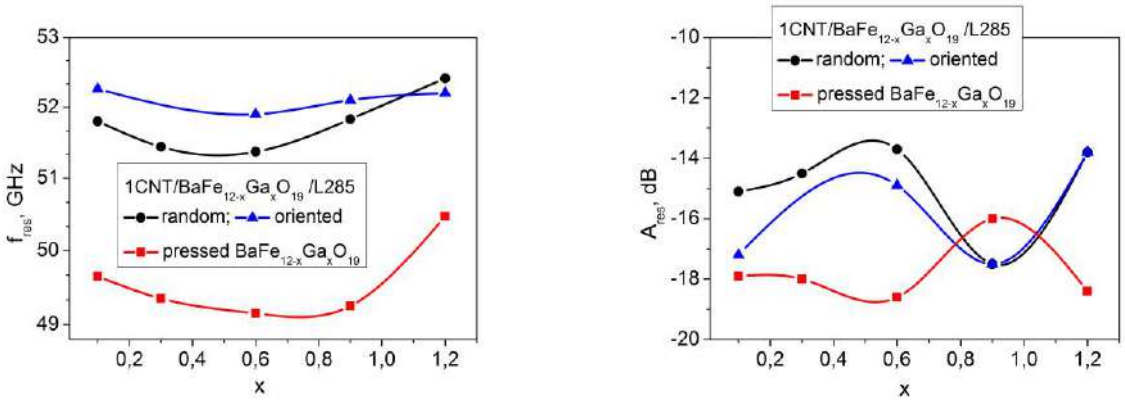

a) b)

Figure 1. Concentration dependences of resonance NFMR frequency f_{res} for epoxy composites with 1% CNT/$BaFe_{12-x}Ga_xO_{19}$(random and oriented filler distribution) and initial pressed sample $BaFe_{12-x}Ga_xO_{19}$

The increase of NFMR amplitude on applied magnetic field for both random and aligned 1wt.%CNT/30wt.% $BaFe_{12-x}Ga_xO_{19}$/epoxy composites was found. The frequency of NFMR was approximately constant in the range of applied magnetic field H=0-5 kOe for random 1wt.%CNT/30wt.% $BaFe_{12-x}Ga_xO_{19}$/epoxy composite and slightly increased for aligned 1wt.%CNT/30wt.% $BaFe_{12-x}Ga_xO_{19}$/epoxy composite.

Synthesis of fibrous magnesium aluminate spinel by biomimetic method, and their characteristics

T.M. Ulyanova[1*], P.A. Vitiaz[2], L.V. Ovseenko[1], N.P. Krutko[1], L.V. Kulbitskaya[1]
[1] *Institute of General and Inorganic Chemistry of NAS of Belarus, 9/1, Surganov str., Minsk, 220072, Belarus, ulya@igic.bas-net.by*
[2] *Presidium of NAS of Belarus, Independence Ave. 66, 220072, Republic of Belarus, Minsk*

The process of synthesis of nanostructured spinel $MgAl_2O_4$ and solid solution based on them by biomimetic method was studied. In the process of spinel reactive layers preparation aluminum and magnesium chlorides aqua solutions, and hydrated cellulose needle felt as precursors were used. The composition and structure of intermediate and finish products forming during heat treatment had been investigated. X-ray method suggested that magnesia, spinel and intermediate composites exist in samples annealed at the 450 ^oC. It has been found that the initial size of spinel was 10-15 nm, and MgO – near 100 nm, alumina was as amorphous phase. Correlation between structure, particle size of spinel, and their properties was discussed. Initial particle size of spinel less this parameter of magnesia in 5-6 times. When magnesia content in active nanostructured layer has been increased the pore diameter was grown, and specific surface was reduced at the annealed samples. The optimum temperature of thermal treatment spinel active layers is 750^oC , when content of $MgAl_2O_4$ consisted of more 90 wt.%.

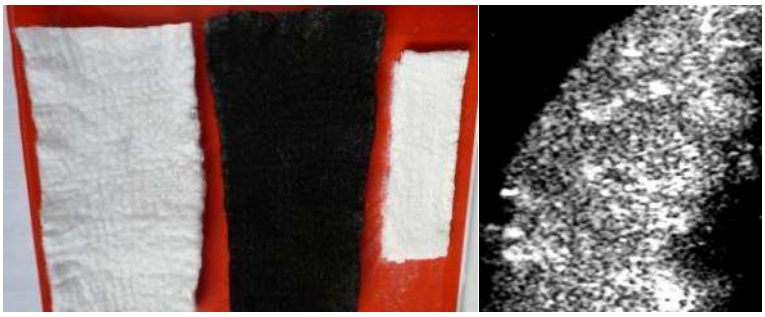

A B C D

Fig. 1 The sample of impregnated hydrated cellulose (needl felt) – A, it is after 500^oC- B, it is after 750^oC (fibrous alumina-magnesia spinel) – C, nanostructure of spinel fiber (TEM x 70000) - D

Investigation showed that the spinel formation reaction proceeds through the formation of intermediate compounds - layered oxides-hydroxides of magnesium-aluminum, followed by their dissociation in the temperature range of 450- 750^oC.

An important factor is the sintering process of active particles, accompanied by overgrowth of micro-, nanopores and the formation of large pores, as well as branched channels in the material. The variety of physical and chemical interactions forms new structures that determine the physical-chemical properties of active nanostructural materials. An important factor is the sintering process of active particles, accompanied by overgrowth of micro-, nanopores and the formation of large pores, as well as branched channels in the material. The variety of physical and chemical interactions forms new structures that determine the physical-chemical properties of active nanostructured materials.

Hydrothermal synthesis and optical properties of ZnO nanorods

K. Yanushkevich*, E. Chubenko, V. Bondarenko
R&D Laboratory 4.3 BSUIR, P. Brovka st. 6, Minsk, Belarus
*corresponding author e-mail: *k.yanushkevich@bsuir.by*

ZnO nanorods films were synthesized on silicon substrates with ZnO buffer layer via hydrothermal method from aqueous alkaline solutions and their optical properties were studied. The solution, which contains zinc nitrate and sodium hydroxide, was transferred into a glass autoclave at 80 ^{o}C for 30 minutes. The surface morphology of films was studied by scanning electron microscopy (SEM). The investigation confirmed that the obtained films have a nanorods array structure with a rods length of 1.15 um and a diameter of 56 nm. Optical properties were determined by photoluminescence (PL) spectroscopy and PL spectra contains from a strong yellow (600 nm) and small near UV (375 nm) emission bands.

Statistical-variational calculation of structural and thermodynamic characteristics of system «crystalline nanoparticle – homogeneous gaseous enviponment»

E. Farafontova* and I. Narkevich
Belarusian State Technological University,13a Sverdlov Str., Minsk, 220006, Belarus, e-mail: varj71@mail.ru

In this study we used the procedure developed before for system of statistical equations solution, and formula, determining structural and thermodynamic characteristics of inhomogeneous molecular systems. These equations were derived within two-level statistical approach [1], based on Bogolubov – Born – Green – Kirkwood – Ivon correlation function method (BBGKI), Rott condition correlative function method [2] and thermodynamic density functionals method. The two-level statistical method takes into account the inhomogeneous distribution of the microcells filling numbers for Rott conditional distribution method. The shape and size of the cells change near the boundaries of the nanoparticle with the surrounding (gaseous environment). Thus, there is a spatial relaxation of the crystal lattice at the boundary.

When implementing the main idea of the two-level statistical method, the description of equilibrium properties of the system is carried out using the potentials of average forces [3], which are functionals of the density field.

The used closed system of integral equations for the potentials of average forces and additional algebraic relations establishes connection between microscopic system parameters of interacting particles (atoms or molecules) and macroscopic characteristics of crystalline nanoparticles in the state of equilibrium with gaseous environment. When solving this system, the radial density profile in the interphase region is approximated using a function containing three parameters and a hyperbolic tangent. One of the parameters is found from the condition of equilibrium of a liquid or gaseous medium with investigated crystalline spherical nanoparticle, and the other two are variation parameters while solving the variational problem of finding the minimum of the large thermodynamic potential of a heterogeneous system.

The system of transformed integral and algebraic equations for a heterogeneous system is solved by the iterative-variational method. As a result we calculated medium force potentials, unary and binary distribution functions, radial field of displacements of lattice sites at the nanoparticle boundary, root-mean-square deviations of particles from the nodes of the deformed lattice, functionals of entropy, internal energy, free energy, and large thermodynamic potential of a nanoparticle and the surrounding gaseous environment. As a consequence of this, the equilibrium density field in the interphase region of the system «crystalline nanoparticle – homogeneous gaseous enviponment» was determined at a temperature below the triple point ($\theta = 0{,}6$).

[1] I. Narkevich, Two-level statistical method for describing heterogeneous systems. Symbiosis of methods of correlative functions and thermodynamic functionals of density. Norderstedt, LAP LAMBERT Academic Publishing RU Publ. (2019) 114.
[2] L. Rott, Statistical Theory of Molecular Systems. Moscow: Nauka Press (1979) 280.
[3] I. Narkevich, E. Farafontova, and K. Unuchek, Actual problems of solid state physics: proceedings of the VIII Intern. scientific Conf., 24–28 september 2018, Minsk, 2 (2018) 149–151.

Structure and optical properties of nanocomposite Langmuir–Blodgett films of poly(methyl methacrylate) with SiO_2 nanoparticles

D. V. Sapsaliou[1*], G. B. Melnikova[1,2], T. N. Tolstaya[2], S. A. Chizhik[2]
[1]*Belarusian State Pedagogical University named after Maxim Tank, Sovetskaya street, 18, 220050, Minsk, Belarus*
[2]*A.V. Luikov Heat and Mass Transfer Institute of National Academy of Sciences of Belarus, P. Brovki street, 15, 220072, Minsk, Belarus*
*corresponding author e-mail: dsapsalev@list.ru

Conditions of the formation of thin polymer Langmuir–Blodgett films based on poly(methyl methacrylate) and composite coatings with silicon dioxide nanoparticles on glass and silicon substrates were optimized. Structural and morphological characteristics of the formed coatings were studied by atomic force microscopy. Presented experimental data proved that the introduction of silicon dioxide nanoparticles into the structure of the poly(methyl methacrylate) matrix leads to a change in the structure of the films and affects their optical properties.

Effect of boron on the properties of nanocomposites based on impact diamond sintered by HPHT method

P.A. Vityaz[1], V.S. Urbanovich[2], N.V. Shipilo[2]*, S.V. Grigoriev[3], V.P. Afanasyev[4]

[1] *Presidium of the NAS of Belarus 220072, Independence Ave. 66, Минск, Belarus*
[2] *SSPA "Scientific-Practical Materials Research Centre of NAS of Belarus", 220072, Minsk, Brovki 19, Belarus*
[3] *Belarussian National Technical University, 220013, Minsk, Independence Ave. 65, Belarus*
[4] *Institute of Geology and Mineralogy of Siberian Department of RAS, 630090, Novosibirsk, Acad. Koptyug ave., 90, Russia*
*corresponding author e-mail: shipilo@physics.by

The work is devoted to the study of the effect of the amorphous boron addition on the sintering ability of impacted diamond powders and the study of the physicomechanical and performance properties of nanocomposites obtained under the conditions of HPHT. It is known [1] that amorphous boron promotes the transformation of graphite into diamond by conversion sintering. The effectiveness of using boron in the sintering of impact diamond powders has not been previously studied. The samples were sintered at the pressure of 7 GPa and different temperatures, controlled by changing the heating current power in the range of 0.6–1.6 kW and during 30 s. A dense non-porous material was obtained in a narrow sintering temperature range (1.3 - 1.35 kW) with a maximum density of 3.515 g/cm^3 (fig. 1). The activation of the densification was due to the Headwall effect during the transformation of lonsdaleite into diamond. The catalytic activity of the amorphous boron addition in the process of transformation of lonsdaleite and graphite into cubic diamond was revealed during sintering of impacted diamond powders. An increase in the parameter a of the elementary cell of diamond has been established, which may indicate the formation of a solid solution of boron in diamond. The resistance to abrasive wear of samples is 5 times higher than that of samples without boron additive (fig. 2). The sintered nanocomposite has a complex microstructure, which is represented by large nanostructured diamond grains in a polycrystalline diamond matrix.

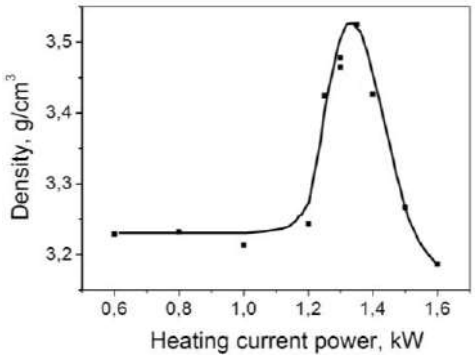

Figure 1. Dependence of the density of a composite based on impact diamonds with the addition of amorphous boron on the heating current power

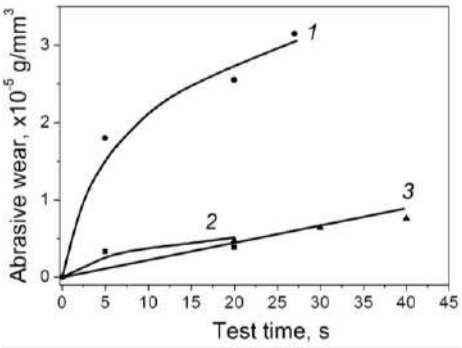

Figure 2. Dependences of the abrasive wear of samples sintered without boron additive (1) with boron additive (2, 3) at heating current powers, kW: 2 - 1,30; 1, 3 – 1,35

The results obtained indicate that the use of amorphous boron additives in the sintering of impact diamond micpowder is effective to improve the physicomechanical properties of nanocomposites based on them.

References

[1] A. M. Mazurenko [et al.] Inorganic Materials. Vol 31 No 1 (1995) P. 51-54.

Hybrid nanocomposite coatings

N.Chekan[1], Y.Auchynnikau[2*], I.Akula[1], Y.Eisymont[2]
[1]*Physical-Technical Institute of the National Academy of Sciences of Belarus*
[2]*Yanka Kupala State University of Grodno*
e-mail: ovchin@grsu.by

The modes of processing in cryogenic liquids of superhard vacuum coatings are optimized to increase the wear resistance of metal-working tools made of high-speed steel. It is shown that the treatment of steel samples coated with titanium nitride in liquid nitrogen increases the adhesion interaction between the substrate and the coating. The effect of low temperatures has a positive effect on the tribotechnical characteristics of the investigated plasma-chemical coatings.

Resonant and nonresonant methods of nonstationary laser spectroscopy of nanocomposites

O.H. Khasanov[1]*, G.A. Rusetskiy[1], O. M. Fedotova[1], V.V. Samartsev[2]
[1.]*Scientific-practical materials research centre, 19 P. Brovky, Minsk, 220072, Belarus*
[2]*Zavoisky Physical-Technical Institute KSC RAS , Sibirsky tract 10/7, 420029, Kazan, Russia*
**corresponding author e-mail: olkhas@ mail.ru*

Methods of characterization of nanocomposites consisted of semiconductor quantum dots (QDs) incorporated into transparent nonlinear dielectric matrix are elaborated. Spectral composition, observation time, and phase-matching conditions for echo-responses excited by two noncollinear pulses are analysed. More specifically, spectral and spatial features of echo signals caused by permanent dipole moments (PDM) inherent to quantum dots, local field effects in them, as well as by angular distribution function of the PDM orientations, and spatial dispersion of transition dipole moments are considered. Applicability of methods based on non resonant four-wave mixing are also discussed.

Comparative study of structural, optical, dielectric and photocatalytic behavior of pure and doped Co-Zn spinel ferrites towards degradation of highly toxic Methylene blue dye

Deepika Chahar[1], Preeti Thakur[1], and Atul Thakur[2]*
[1]*Deparment of Physics, Amity School of Applied Sciences, Amity University Haryana, 122413 INDIA*
[2]*Centre for Nanotechnology, Amity University Haryana, 122413 INDIA*
**corresponding authore-mail: athakur1@ggn.amity.edu*

The nanoferrite samples having composition $Co_{0.5}Zn_{0.5}Fe_2O_4$, $Co_{0.5}Zn_{0.5}NiFeO_4$ and $Co_{0.5}Zn_{0.5}MgFeO_4$ were synthesized using citrate precursor method. The synthesized ferrites were characterized using XRD and FTIR for structural and optical investigations. The samples were found to have spinel structure with crystallite size values 36nm, 38nm and 48nm for Co-Zn, Ni-Co-Zn and Mg-Co-Zn respectively. Also, FTIR confirmed the formation of spinel structure. The samples were found to have very low values of dielectric loss at high frequency. The study of photocatalytic process was done to check the degradation of methylene blue dye using synthesized ferrites as catalysts. A significant degradation of methylene blue was observed using synthesized nanoferrites but Mg doped Co-Zn shows excellent degradation of dye with a degradation efficiency of almost 99%. All the observations revealed that these ferrites have potential applications in the field of high frequency devices and water purification.

Mössbauer spectroscopy and dielectric parameters of $SrFe_{12-x}Al_xO_{19}/\alpha\text{-}Fe_2O_3$ (x = 0; 0.5; 1; 1.5; 2) nanocomposites

A.V. Timofeev[1,*], V.G. Kostishin[1], V.V. Korovushkin[1], R.I. Shakirzyanov[1]
[1] *National University of Science and technology "MISIS", Leninsky Prospect, 4, 119049, Moscow, Russia, e-mail for the corresponding author*: andtim2011@gmail.com*

Recently, researchers are increasingly attracted by the material known for more than half a century - type M hexaferrite. This is confirmed by the fact that over the past 10-15 years the number of publications related to this material has increased. In addition, there is a very small number of works devoted to the preparation of composites based on hexaferrite in conjunction with hematite [1,2]. Specifically, in this work, a nanocomposite of the $SrFe_{12-x}Al_xO_{19}/\alpha\text{-}Fe_2O_3$ type (x = 0; 0.5; 1; 1.5; 2) was obtained, where the iron ion in strontium hexaferrite was replaced by an aluminum ion. In a number of works, it was noted that the substitution of this very element causes an increase in the coercive force in strontium hexaferrite, which can be useful, for example, for use in the field of permanent magnets [3,4].

The preparation of the desired nanocomposite was carried out simultaneously in a one-step process using the chemical coprecipitation method. The following reagents were used as precursors: strontium nitrate $Sr(NO_3)_2$, iron (III) nitrate nonahydrate $Fe(NO_3)_3 \cdot 9H_2O$, aluminum nitrate nonahydrate $Al(NO_3)_3 \cdot 9H_2O$.

The Mössbauer spectra of the obtained samples were recorded on Ms-104 Em spectrometer. The studies performed showed that the nanocomposites were indeed two-phase, where the spectra corresponded to strontium hexaferrite and hematite. In addition, it was found that the formation of the $\alpha\text{-}Fe_2O_3$ oxide mainly occurs due to the iron at the 12k position. At x = 0.5, the substitution with aluminum occurred only in the 12k position.

The dielectric characteristics of the nanocomposites were measured using E7-20 RLC meter in the frequency range 25 Hz – 10^5 Hz. The electrophysical parameters of the obtained samples were studied as a function of the degree of substitution by the Al^{3+} ion. The maximum dielectric constant with increasing frequency is characteristic of the degree of substitution x = 1.

References

[1] A. Author, B. Author, and C. Author, Journal Title Abbreviation Volume (Year) Pages.
[1] B. Belec, G. Dražić, S. Gyergyek, B. Podmiljšak, T. Goršak, M. Komelj, J. Noguése and D. Makovec // Nanoscale 9 (2017) 17551.
[2] Y.F. Xu, Y.Q. Ma, S.T. Xu, F.L. Zan, G.H. Zheng, Z.X. Dai // Materials Research Bulletin 57 (2014) 13–18.
[3] F. Rhein, R. Karmazin, M. Krispin, T. Reimann, O. Gutfleisch // Journal of Alloys and Compounds 690 (2017) 979–985.
[4] V. Barrera,I. Betancourt // Journal of Physics and Chemistry of Solids 93 (2016) 1–6.

Modified Stranski-Krastanov mechanism formation of GaN quantum dots in ammonia MBE

Y.E. Maidebura[1*], T.V. Malin[1], and K.S. Zhuravlev[1]
[1]*ISP SB RAS, 13 Lavrentiev aven., Novosibirsk, 630090, Russia,*
**e-mail for the corresponding author: hnxyr5@gmail.com*

In recent decades, semiconductors of III-N groups have attracted great interest of researchers due to the possibility of expanding the spectral range of operation of light-emitting and photodetectors from infrared to ultraviolet range due to the use of solid solutions of InN, GaN and AlN compounds. However, due to the high density of dislocations in the grown structures, which act as centers of nonradiative recombination, the creation of optoelectronic devices based on III-N semiconductors is a problem. A possible approach to overcome this problem is to use an active layer consisting of three-dimensional nanostructures known as quantum dots (QDs).

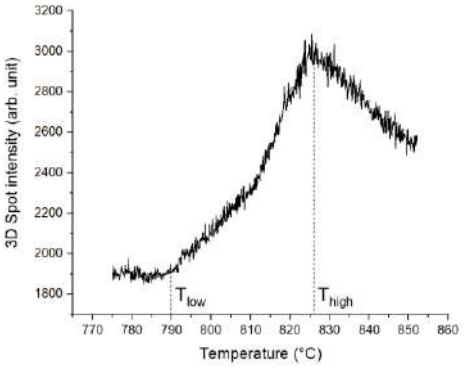

Evolution of the intensity of a 3D spot of a GaN layer with an increase in temperature in an ammonia flow of 15 sccm

The typical way of forming QDs is growth by the Stranski-Krastanov (S-K) mechanism. During the growth of GaN/AlN QDs by molecular beam epitaxy (MBE) with ammonia as a nitrogen source, a modified S–K mechanism is observed, in which a necessary condition is to stop the growth and turn off the ammonia flow. In this work, we studied the transformation of a two-dimensional (2D) GaN layer into three-dimensional (3D) islands (2D-3D transition) by the method of reflection high energy electron diffraction when the growth stopped and the temperature increased in a low flow of ammonia.

The experiment was carried out in an ammonia MBE machine, a 2 nm thick GaN layer was grown on an 885 nm thick AlN buffer layer, after which the growth was stopped, the ammonia flow decreased to 15 sccm, and the temperature increased from 775 to 850 °C.

As a result, it was found that the 2D-3D transition is reversible. Thus, with an increase in temperature, upon reaching T_{low}, 3D islands are formed, and with a further increase in temperature and reaching T_{high}, the reverse transformation of the islands into a 2D GaN layer is observed. To explain the experimental fact of the 2D-3D transition and its reversibility, a kinetic model was proposed in the form of a system of differential equations, in which a change in the surface energy is associated with a change in the surface concentration of particles. As a result, using the kinetic model, the total energies of 2D and 3D morphological states of the GaN layer were calculated. With an increase in temperature, the surface energy increases due to desorption processes and the 3D state of the surface becomes energetically favorable, and with further increase in temperature due to dissociation processes, the surface energy decreases and the 2D state of the surface becomes energetically favorable.

Fabrication and characterization of TiO_2 coral-like nanostructures decorated with Au nanoparticles

S.A. Khubezhov[1,2*], E. Yu. Ponkratova[2], M. E. Karsakova[2], I.V. Silaev[3], I.V. Tvauri[3], V.V. Prigodich[4], D.V. Yakimchuk[4], O.I. Il'in[1] and D.A. Zuev[2]
[1]*Southern Federal University, Research Laboratory of Functional Nanomaterials Technology, 2 St. Shevchenko 347922 Taganrog, Russian Federation*
[2]*School of Physics and Engineering, ITMO University, 9 St. Lomonosova 191002 St. Petersburg, Russian Federation*
[3]*Department of Physics, North Ossetian State University, 24 St. Markusa 362025 Vladikavkaz, Russian Federation*
[4]*Scientific-Practical Materials Research Center NAS of Belarus, 19 St. P.Brovka 220072 Minsk, Belarus*
**corresponding author e-mail: Soslan.khubezhov@gmail.com*

The paper presents a simple and fast method for the formation of coral nanostructures based on Au/TiO_2, which confirms a comprehensive analysis with high-resolution methods of surface investigation. The mechanisms of formation of oxide nanostructures in the course of thermoresistive oxidation of titanium foil are considered, in particular, it was found that in the temperature range T = 700 °C – 800 °C, coral-shaped TiO_2 nanostructures up to 2 μm long grow mainly along the [110] direction by merging smaller nanogranules.

According to the data obtained by SEM and XPS, it can be established that the surface of coral-like Au/TiO_2 nanostructures is a developed surface with a high density of separated gold nanoclusters.

The peculiarity of the morphology of the obtained coral-like Au/TiO_2 nanostructures confirms the high adsorption and plasmon activity of this material. In addition, the simplicity of the preparation method allows the development of real devices for wide use in sensorics, catalysis, etc.

Acknowledgment

The reported study was funded by RFBR (project number 20-52-04015) and BRFBR (project number Ф21РМ-054), and supported by the Ministry of Science and Higher Education of the Russian Federation; the state task in the field of scientific activity No. 0852-2020-0015. The synthesis of Au/TiO2 coral-like structers and XPS characterization were carried out within the framework of the project No. 20-52-04015 and Ф21РМ-054. Morphology (SEM) and structural (XRD) sudy of synthesized materials were carried out within the framework of the project No. 0852-2020-0015.

Laser-induced topological nanoclusters on solid surface with controlled functional characteristics: modeling and experiment

S. Arakelian*, D. Bukharov, T. Khudaiberganov and A. Kucherik
Stoletovs Vladimir State University, Vladimir, Russia
**corresponding author e-mail: arak@vlsu.ru*

The 4D-laser technology fabrication of new nanostructures of both different material composition and topology is considered based on advantages of quantum technologies and nonlinear dynamics. The functional characteristics of the cluster type and thin films nanostructures on the solid surface with controllable topology vs time are under study. The interaction effects of solid targets with laser pulses of different durations under first, ablation in liquid and second, the laser deposition procedure from the colloid on solid surface can be viewed as a possibility of synthesizing the complex topology objects. The result depends not only on the stationary processes in the system, but also on the dynamic interactions in the system leading to different final stable structures of required topology: from quantum dots (0D) to 3D nanoclusters. Both unusual electrophysics and optical prorerties of the objects were detected by controlled way.

Electronic properties of the phosphorene/MoS_2 heterostructure

A.V. Krivosheeva[1*], V.L. Shaposhnikov[1], V.E. Borisenko[1,2], J.-L. Lazzari[3]
[1]*Belarusian State University of Informatics and Radioelectronics, P. Browka 6, 220013 Minsk, Belarus*
[2]*National Research Nuclear University MEPhI, Kashirskoe Shosse 31, Moscow, 115409, Russia*
[3]*Aix-Marseille Univ, CNRS, CINaM, UMR 7325, Case 913, Campus de Luminy 13288, Marseille, France*
**corresponding author e-mail: krivosheeva@bsuir.by*

Stacking of different materials in monolayers opens new ways to novel applications for nanoelectronics. By means of first-principle methods we investigated electronic properties of an heterostructure composed of phosphorene and MoS_2 monolayers. It was found to be stable for an optimized interlayer distance of 3.52 Å while having an indirect electron energy gap of 0.5 eV.

Band structure of novel material C_3N_4

A.V. Krivosheeva[1], V.L. Shaposhnikov[1*], V.E. Borisenko[1,2]
[1]*Belarusian State University of Informatics and Radioelectronics, P. Browka 6, 220013 Minsk, Belarus*
[2]*National Research Nuclear University MEPhI, Kashirskoe Shosse 31, Moscow, 115409, Russia*
**corresponding author e-mail: krivosheeva@bsuir.by*

Computer simulation of atomic structure of several phases of novel graphite-like two-dimensional carbon nitride is performed, and the effect of combination of separate layers interacted by means of van der Waals forces is analyzed. All the phases show them to be either direct or indirect semiconductors. Layers of the materials demonstrate independent behavior without visible interaction. C_3N_4 semiconductor with hexagonal structure is proposed as a novel material suitable for nanoelectronic applications.

Electronic properties of lateral nanoheterostructures based on 2D dichalcogenides

V.L. Shaposhnikov[1*], A.V. Krivosheeva[1], V.E. Borisenko[1,2], J.-L. Lazzari[3]
[1]*Belarusian State University of Informatics and Radioelectronics, P. Browka 6, 220013 Minsk, Belarus*
[2]*National Research Nuclear University MEPhI, Kashirskoe Shosse 31, Moscow, 115409, Russia*
[3]*Aix-Marseille Univ, CNRS, CINaM, UMR 7325, Case 913, Campus de Luminy 13288, Marseille, France*
**corresponding author e-mail: shaposhnikov@bsuir.by*

The structural parameters and electronic properties of lateral nanostructures based on two-dimensional dichalcogenides (MoS_2, $MoSe_2$, WS_2, and WSe_2) have been estimated by *ab initio* calculations. All the systems analyzed were found to be stable and show semiconducting behavior with the band gap values in the range of 1.6–2.1 eV. The band spectra as well as densities of states show similar features. Some changes in the crystal structure as compared to binary dichalcogenides were noticed.

Investigation of the gas sensitivity of nanostructured zinc oxide films doped with aluminum

T. Svistova[1*], E.Rembeza[2], M.Belykh[1], A.Hanin[1]
[1]*Voronezh State Technical University*
20-letiya Octyabrya str., 84, Voronezh, 394006 Russia
[2]*Voronezh State University*
University sq., 1, Voronezh, 394006 Russia
**e-mail: svistamara@yandex.ru*

The work is devoted to the investigation of the gas sensitivity of zinc oxide films doped with aluminum to reducing gases and to oxidizing gases. It was found that the addition of aluminum lowers the temperature of the maximum gas sensitivity to vapors of the test gases and has an ambiguous effect on the value of the gas sensitivity.

Impact of the Carbon Nanomaterials on Structural and Magnetic Properties of the Ferrite-based Composites

S.V. Podgornaya[1*], M.A. Darwish[1,2], A.V. Timofeev[1], V.G. Kostishyn[1], S.V. Trukhanov[3] and A.V. Trukhanov[1,3*]
[1]*NUST MISiS, 119049, 4, Leninsky ave., Moscow, Russia, *e-mail kastor1986@yandex.ru*
[2]*Physics Department, Faculty of Science, Tanta University, 31527, Tanta, Egypt*
[3]*SSPA "Scientific and Practical Materials Research Center of NASB", 220072, 19 P. Brovki St., Minsk Belarus,*

Here, a polymer composites based on Al-substituted M-type hexaferrites (Al-HF) with carbon nanomaterials (carbon nanotubes or CNT and carbon nanoflakes or CNF) as fillers has been developed. For analysis of the carbon nanomaterials impact on structural and magnetic characteristics we produced 3 types of composites: 1. Al-substituted hexaferrite powders in PVDF - Al-HF/PVDF (without carbon); 2. The same mixture (Al-HF/PVDF) with quasi-one-dimensional carbon nanotubes - Al-HF/PVDF/CNT and 3. The same mixture (Al-HF/PVDF) with quasi-two-dimensional carbon nanoflakes Al-HF/PVDF/CNF. The ration between Al-HF:PVDF and Al-HF/PVDF:nanocarbon was fixed as 85:15 mass.% and 95:5 mass.% respectively. We have synthesized Al-HF by solid state reaction method [1]. CNT was commercially available product. CNF podwer was produced by our colleagues from Phys.-Chem. Tech. Lab. of S&P Materials Research Center [2]. Structural parameters (morphology) were estimated using scanning electron microscopy. It was concluded that the formation of the composites with various types of carbon carbon nanomaterials doesn't impact on the microstructure of the hexaferrite powder, while slightly changing the total density of the sample. Magnetic parameters (specific magnetization as function of the external magnetic field) were investigated in the +2T range at T=300K. It was observed that the addition of CNT or CNF leads to a decrease in Ms and Mr in CM. The main magnetic characteristics of the Al-HF/PVDF/CNT and Al-HF/PVDF/CNF are lower than those of the Al-HF/PVDF. Thus, for the Al-HF/PVDF the values of Ms (54.22 emu/g), Mr (27.79 emu/g) and Hc (0.31 T). It should be noted that the CM sample with CNT, in contrast to the sample with CNF, enters the state of magnetic saturation in fields up to 0.5 T. Al-HF/PVDF/CNF does not saturate even in fields up to 2 T, which may be due to the weakening of the dipole-dipole exchange interaction due to the influence of the type of carbon nanomaterial. On average, the magnetic characteristics for Al-HF/PVDF/CNT are noticeably lower than for Al-HF/PVDF/CNF. Thus, for Al-HF/PVDF/CNT, the values of Ms (42.04 emu/g) Mr (19.35 emu/g) differ from those for Al-HF/PVDF/CNF where Ms (48.77 emu/g) Mr (23.90 emu/g). The influence of the type of nanosized carbon on such CM characteristics as HC and Sq (Mr/Ms ratio) should be separately noted. It was observed impact of the type of the nanocarbon on such magnetic parameters as Ms, Mr, Hc and Sq.

Acknowledgement
The work was support by the Russian Science Foundation (Agreement No. 19-72-10071 from 06 Aug. 2019).

References

[1] M.A. Darwish, Asmaa I. Afifi, Anwer S. Abd El-Hameed, H.F. Abosheiasha, A.M. A. Henaish, D. Salogub, A.T. Morchenko, V.G. Kostishyn, V.A. Turchenko, A.V. Trukhanov, Can hexaferrite composites be used as a new artificial material for Antenna applications? Ceramics International 47(2), (2021) 2615-2623 https://doi.org/10.1016/j.ceramint.2020.09.108
[2] U. Novikau, I. Razanau, S. Filipovich, Novel Method of Graphite Exfoliation, MRS Adv. 1 (2016) 1395–1400. https://doi.org/10.1557/adv.2016.190.

Influence of synthesis conditions on composition, structure and mechanical properties of electrodeposited nanostructured Ni-Fe films

T. Zubar[1,2*], A. Trukhanov[1,2,3], D. Tishkevich[1,2], M. Panasiuk[1], V. Fedkin[1], V. Fedosyuk[1]
[1] *SSPA "Scientific and practical materials research centre of NAS of Belarus", 220072, Minsk, P. Brovki str., 19, Belarus, fix.tatyana@gmail.com*
[2] *South Ural State University, 454080, Chelyabinsk, Lenin Prospect, 76, Russia*
[3] *National University of Science and Technology MISiS, 119049, Moscow, Leninsky Prospekt, 4, Russia*

Nanostructured NiFe film was obtained on silicon with a thin gold sublayer via pulsed electrodeposition and annealed at a temperature from 100 to 400◦C in order to study the effect of synthesis conditions on the surface microstructure and mechanical properties. A nonlinear change in hardness was detected using nanoindentation. Explanation of the abnormal change in hardness was found in the nature of the relaxation method of elastoplastic energy under load. It is shown that the deformation of coatings with a grain size of 100 nm or more occurs due to dislocation slip. A decrease in grain size leads to the predominance of deformation due to rotations and sliding of grains, as well as surface and grain boundary diffusion. The effect of deformation mechanisms on the nanoscale hardness of Ni-Fe coatings was established. Full hardening of the coatings (both in the bulk and on the surface) was achieved while maintaining the balance of three mechanisms of elastoplastic deformation in the sample. Unique coatings consisting of two fractions of grains (nano-grains (about 70%) and their agglomerates (no more than 30%)) demonstrate high crack resistance and full-depth hardening due to the release of deformation energy for amorphization and agglomeration of nanograins.

High-resolution atomic force microscopy made it possible to trace stepwise evolving microstructure under the influence of heat treatment. It was found that NiFe film grains undergo coalescence twice - at ~100 and ~300 ◦C - in the process of a gradual increase in grain size. The mechanical properties of the Au/NiFe nanostructured system have been investigated by nanoindentation at two various indentation depths, 10 and 50 nm. The results showed the opposite effect of heat treatment on the mechanical properties in the near-surface layer and in the material volume. Surface homogenization in combination with oxidation activation leads to abnormal strengthening and hardening-up of the near-surface layer. At the same time, a nonlinear decrease in hardness and Young's modulus with increasing temperature of heat treatment characterizes the internal volume of nanostructured NiFe. An explanation of this phenomenon was found in the complex effect of changing the ratio of grain volume/grain boundaries and increasing the concentration of thermally activated diffuse gold atoms from the sublayer to the NiFe film.

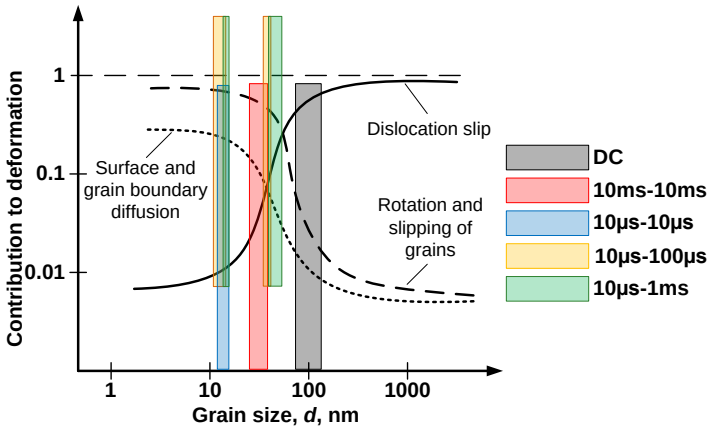

Contribution of different deformation mechanisms to the total deformation depending on the grain size of the Ni-Fe coating

Sintering of TiN/Si_3N_4 composites by SPS and HPHT methods and their properties

V. Urbanovich[1], T. Malikina[1], L. Jaworska[2], P. Klimczyk [2], M. Podsiadlo [2]
[1] *SSPA "Scientific and Practical Materials Research Center of NAS of Belarus", 19, P.Brovka St., 220072, Minsk, Belarus, e-mail: urban@physics.by*
[2] *The Institute of Advanced Manufacturing Technology, 37a, Wroclawskast, 30-011, Krakow, Poland*

Composites based on titanium and silicon nitrides are of interest and have great potential as cutting tools due to their high physical and mechanical properties. Usually, when sintering such ceramic materials, oxide activating additives are used [1-4].

The aim of this work was to obtain dense TiN/Si_3N_4 composites of various compositions without activating additives by the methods of spark plasma sintering SPS (60 MPa, 1600-1800 ^{o} C, 10 min) and sintering at high pressure and high temperature HPHT (7.8 GPa, 1400-1700 ^{o} C, 60 s), study of their microstructure, density, microhardness and crack resistance.

The starting powders were titanium nitride grade C (average particle size 0.8-1.2 μm) and nitride silicon α-modification produced by H. C. Starck (Germany) (average particle size up to 0.6 microns). The silicon nitride powder contained 5 % β-phase.

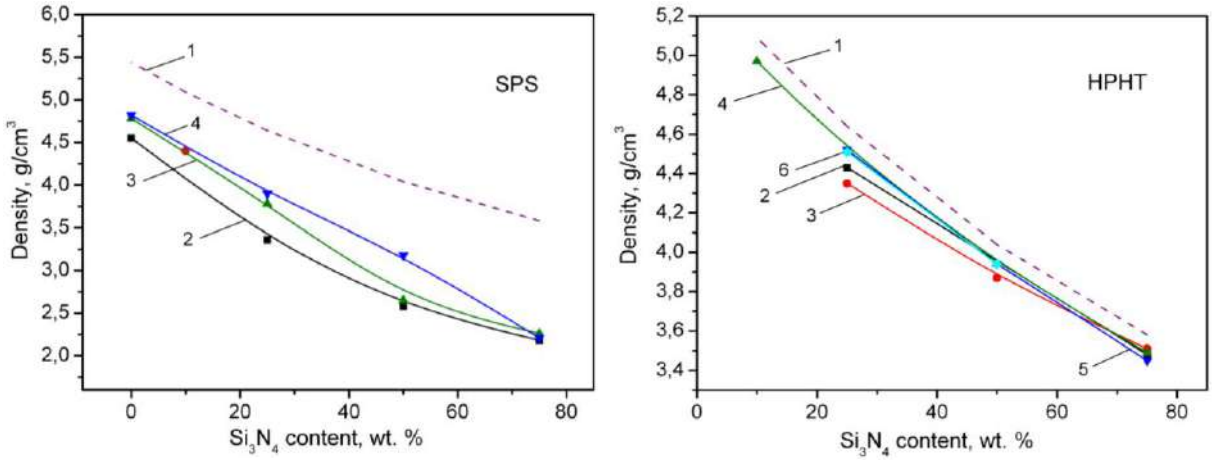

a b

Dependences of the density of TiN/Si_3N_4 composites on the Si_3N_4 content obtained by the method: a - SPS, 1 - calculation, 2 - 1600 ^{o} C, 3 - 1700 ^{o} C, 4 - 1800 ^{o} C; b - HPHT, 1 - calculation, 2 - 1400 ^{o} C, 3 - 1500 ^{o} C, 4 - 1600 ^{o} C, 5 - 1650 ^{o} C, 6 - 1700 ^{o} C

The results of compaction of composites TiN/Si_3N_4 are shown in the figure.

It was found that the advantage of HPHT sintering by the method is most significantly manifested in the TiN/Si_3N_4 composites with a higher content of 75 % Si_3N_4. Composites of the specified composition based on α-Si_3N_4 have the highest relative density of 97.8 %, microhardness of 21.3 GPa and fracture toughness of 6.18 MPa· $m^{1/2}$.

The study of the grain structure of the composites showed that with an increase in the sintering temperature, the grain size doubles in comparison with the particle size of the initial powder.

References

[1] H. Borodianska [et al.] Journal of Nanoscience and Nanotechnology Vol. 9 № 11 (2009) P. 6381-6389.
[2] N. Ahmad [et al.] Ceramics International Vol. 36 (2010) P. 491-496.
[3] N. Ahmad [et al.] Materials Research Bulletin Vol. 46 (2011) P. 460-463.
[4] L. Díaz [et al.] Journal of Nanomaterials, 2016, P. 68.

Effect of the neutron flux on thermal properties of nano silicon nitride

T.G. Naghiyev
[1]*Composite Materials Scientific Research Center at Azerbaiian State University of Economics, 6 Istiglaliyyat str., Baku, AZ1001 Azerbaijan*
[2]*Department of Nanotechnology and Radiation Material Science, National Nuclear Research Center, Gobu settlements, Baku-Shamakhi highway, Baku AZ1073, Azerbaijan*

The present work is devoted to study of free Gibbs energy, specific heat capacity, enthalpy, and entropy of nano Si_3N_4 particles in the temperature range of 300-1400K. All experiments were performed for before and after neutron irradiatiated Si_3N_4 nanoparticles and obtained result were comparatively analyzed. The enthalpy and entropy of Si_3N_4 nanoparticles have been studied as a function of temperature. The thermal stability of nanomaterial have been investigated by temperature dependencies of free Gibbs energy before and after neutron irradiation. The effect of neutron transformations on heat transfer in Si_3N_4 nanoparticles has been studied at temperatures up to 1400K.

Silicon, a group IV element in the periodic table, like other elements in that group, sits in favorable positions inside the crystal lattice in different matrices due to its favorable electronic configuration. As a result, it plays an important role in forming multifunctional physical properties as a key element of these matrices [1-7]. Due to their favorable physical properties, silicon compounds are used in optics, electronics, nuclear technology, etc. There are broad application perspectives [8-9].

Among silica compounds, the silicon nitride (Si_3N_4) is particularly important to note that it is in the spotlight due to its excellent physical and chemical properties. Silicon nitride combination increases its high physical and chemical stability, mechanical strength, high resistance to temperature, pressure, and other external influences, its application as an advanced ceramic material. Silicon nitride is successfully used as a ceramic material in electronics and optics with the perfect combination of different properties. In the present study, changes in the thermophysical properties of Si_3N_4 nanoparticles as a result of neutron irradiation were studied, specific heat capacity, Gibbs energy, enthalpy, and entropy of the system were compared comparatively before and after irradiation.

The nanomaterials used in the experiment are alpha Si_3N_4 nanoparticles (US Research Nanomaterials, Inc., TX, USA). All samples irradiated at full power (250 kW) and the central channel of TRIGA Mark II light water pool type research reactor at the Jozef Stefan Institute (IJS) in Slovenia. The parameters of the neutron flux available in full power mode in the central channel are $5.107 \cdot 10^{12}$ n/cm^2 sec (1 ± 0.0008, $E_n < 625$eV) for thermal neutrons, $6.502 \cdot 10^{12}$ n/cm^2·sec (1 ± 0.0008, $E_n \sim 625$eV ÷ 0.1 MeV) for epitermal neutrons, fast neutrons for $7.585 \cdot 10^{12}$ n/cm^2·sec (1 ± 0.0007, $E_n > 0.1$ MeV) and finally the flux density in the central channel for all neutrons is $1.920 \cdot 10^{13}$ n/cm^2·sec (1 ± 0.0005). The thermophysical parameters of Si_3N_4 nanoparticles before and after irradiation with neutron flux were studied in the "HITACHI STA 7300" device.

The thermal parameters of Si_3N_4 nanoparticles in the temperature range 300 K – 1400 K were compared comparatively before and after neutron irradiation. The specific heat capacity, Gibbs energy, enthalpy, and entropy of Si_3N_4 nanoparticles in the whole temperature range were calculated theoretically based on experimental results.

The analysis showed that the enthalpy and entropy of Si_3N_4 nanoparticles are stable at temperatures up to about 600 K. The oxidation rate is reduced due to the additionally formed trace elements as a result of the neutron transmutations. The effect of the P^{31} isotope obtained by neutron transmutations on temperature dependences of specific heat capacity on direct heat

transfer has been determined. It was found that the samples were more stable after neutron irradiation due to the temperature dependence of the free Gibbs energy of Si_3N_4 nanoparticles.

References

[1] Chenxing Liu et al. Study of high-alumina-silicon glass structure and performance modified by Li_2O replacing Na_2O. Journal of Non-Crystalline Solids **572** (2021) 121115.

[2] Hao Liu et al. Improved lithium storage performance by encapsulating silicon in free-standing 3D network structure carbon-based composite membranes as flexible anodes. Surface and Coatings Technology **423** (2021) 127606.

[3] T.G. Naghiyev. An investigation of silicon nitride (Si_3N_4) nanoparticles interaction with neutrons. Modern Physics Letters B **35**(6) (2021) 2150104.

[4] Elchin Huseynov, Adil Garibov and Ravan Mehdiyeva. Study of blend composition of nano silica under the influence of neutron flux. Nano Convergence (2014) 1:21.

[5] Yang Zhang et al. Molecular dynamics study of the mechanical properties of reinforced silicon structure with iron nanoparticles. Computational Materials Science **199** (2021) 110749.

[6] E.M. Huseynov, T.G. Naghiyev. (n, α) transmutation of AlN nanoparticles under the neutron flux. Advanced Physical Research **1**(2) (2019) 99-104.

[7] Yingjie Zhao et al. Recent progress in synthesis, growth mechanisms, properties, and applications of silicon nitride nanowires. Ceramics International **47**(11) (2021) 14944-14965.

[8] D. Birmpiliotis et al. A comparative study of nanostructured Silicon-Nitride electrical properties for potential application in RF-MEMS capacitive switches. Microelectronics Reliability **100–101** (2019) 113360.

[9] Elchin M. Huseynov, Tural G. Naghiyev. Study of thermal parameters of nanocrystalline silicon carbide (3C-SiC) using DSC spectroscopy. Applied Physics A **127** (2021) 267.

Hyperfine interactions in diamond with the NV centers: Quantum chemistry simulation vs. experiment

A. Nizovtsev[1,2*], S. Kilin[1], A. Pushkarchuk[2,3], S. Kuten[4] and F. Jelezko[5]

[1]*Institute of Physics, Nat. Acad. Sci., 220072 Minsk, Belarus.*
**e-mail: apniz@dragon.bas-net.by*
[2] *National Research Nuclear University "MEPhI", 115409, Moscow, Russia.*
[3]*Institute of Physical and Organic Chemistry, Nat. Acad. Sci., 220072 Minsk, Belarus.*
[4] *Institute for Nuclear Problems, Belarusian State University, 220006 Minsk, Belarus.*
[5] *Institute for Quantum Optics, Ulm University, 89069 Ulm, Germany*

Hybrid spin systems consisting of the electronic spin of single paramagnetic color centers in diamond and neighbor nuclear spins of isotopic ^{13}C atoms are now widely used to implement numerous applications in quantum information processing, quantum sensing and metrology. In these systems, the ^{13}C nuclear spins with their excellent coherence times serve as quantum memories accessed via the more easily controllable electronic spin of color centers. Historically first and most well-studied representative of such systems is the nitrogen-vacancy (NV^-) center hyperfine coupled to its intrinsic ^{14}N nuclear spin and, as well, to nuclear spins of ^{13}C atoms located in various sites of a diamond lattice including those disposed rather far from the NV^- center.

Key prerequisite for high-fidelity spin manipulation in the above systems with tailored control pulse sequences is a complete knowledge of hyperfine interactions (*hfi*) in them. Here we are presenting the review of our recent results on systematic computer simulation of spatial and hyperfine characteristics of various NV-^{13}C systems in the H-terminated NV-hosting diamond clusters $C_{291}[NV]H_{172}$ and $C_{510}[NV]H_{252}$ [1,2] as well as on the usage of the simulated *hfi* database not only to describe a wide range of available experiments but also to predict the characteristics of the NV-^{13}C systems, which are of particular interest for the emerging diamond-based quantum technologies. Using the simulated *hfi* database we also predicted i) optimal conditions for efficient coherent manipulation of the ^{13}C nuclear spin state in such systems with microwaves [3] and ii) the *hfi* characteristics of the NV-^{13}C systems in nanodiamonds grown from various isotopically substituted azaadamantane molecules differing in the ^{13}C position in the seed, as well as in the orientation of the NV center in the post-obtained diamond [4]. The data obtained in [4] can be used to identify (and correlate with the precursor used) the specific NV-^{13}C spin system by measuring the *hfi*-induced splitting in optically detected magnetic resonance spectra.

Acknowledgement

This work has been supported in part by Belarus state program of scientific investigations "Convergence-2025", by BRFFI, the project Φ18MC-036, and by National Research Nuclear University "MEPhI", the RSF-DFG project 21-42-04416.

References

[1] A.P. Nizovtsev et al. "Theoretical study of hyperfine interactions and optically detected magnetic resonance spectra by simulation of the $C_{291}[NV]^-H_{172}$ diamond cluster hosting NV center". New J. Phys.**16** (2014) 083014.
[2] A.P. Nizovtsev et al. "Non-flipping ^{13}C spins near NV center in diamond: Hyperfine and spatial characteristics by density functional theory simulation of the $C_{510}[NV]H_{252}$ cluster". New J. Phys. **20** (2018) 023022.
[3] A.P. Nizovtsev and S.Ya. Kilin, "Microwaves for Efficient Nuclear Spin Manipulation in NV–^{13}C Systems in Diamond". Bulletin of the Russian Academy of Sciences: Physics. **84** (2020*)* 235 *(*Izvestiya Rossiiskoi Akademii Nauk, Seriya Fizicheskaya. **84** (2020) 310).
[4] A.P. Nizovtsev et al. "Hyperfine interactions in the NV-^{13}C quantum registers in diamond grown from the azaadamantane seed". Nanomaterials. **11** (2021) 1303.

Simulation of the J_{CC} coupling in diamond clusters hosting the NV center

A. Nizovtsev[1,2*], S. Kilin[1], A. Pushkarchuk[2,3], S. Kuten[4],
D. Michels[5], D. Lyakhov[5], N. Kargin[2], A. Gusev[2], F. Jelezko[6]
[1]*Institute of Physics, Nat. Acad. Sci., 220072 Minsk, Belarus.*
**e-mail: apniz@dragon.bas-net.by*
[2] *National Research Nuclear University "MEPhI", 115409, Moscow, Russia.*
[3]*Institute of Physical and Organic Chemistry, Nat. Acad. Sci., 220072 Minsk, Belarus.*
[4] *Institute for Nuclear Problems, Belarusian State University, 220006 Minsk, Belarus.*
[5]*Computer, Electrical and Mathematical Science and Engineering Division, 4700 King Abdullah University of Science and Technology(KAUST),23955-6900,Thuwal, Saudi Arabia.*
[6]*Institute for Quantum Optics, Ulm University, 89069 Ulm, Germany.*

In the last decade there was rapid development of quntum magnetic sensing technology based on nitrogen-vacancy (NV) color centers in diamond (see, e.g. [1,2] for recent reviews), offering an unprecedented combination of high sensitivity and spatial resolution. Magnetometer based on single NV center can have nanometer-scale spatial resolution and exceptional sensitivity (up to ~Hz) allowing not only to detect target single nuclear spins (e.g. ^{13}C nuclear spins) located within the diamond but even to distinguish (by their chemical shifts) inequivalent nulear spins of molecules located at the diamond surface [3], thus enabling a new exciting research area of single-spin nuclear magnetic resonance (NMR) for investigating important issues ranging from determination of molecular structures of inorganic or biological compounds up to medical imaging for therapeutic matters. In this respect, finding out of the high-resolution NMR parameters is essential.

Among the NMR parameters, the indirect nuclear spin–spin coupling (the J-coupling), that arise due to second-order hyperfine interactions, is important. In this work, we present ***for a first time*** the calculation of the $J_{C\text{-}C}$ couplings in the H-terminated NV-hosting diamond clusters $C_{33}[NV]^{-}H_{36}$ and $C_{69}[NV]^{-}H_{84}$. We have optimized the cluster geometry using the Gaussian16 (revision B.01) software package with the DFT/B3LYP/CC-pVDZ (5D, 7F) theory level and then simulated the n-bond $^{n}J_{CC}$ coupling constants for all possible ^{13}C-^{13}C pairs in the clusters. The simulated constants for the cluster $C_{69}[NV]^{-}H_{84}$ are shown in the figure 1. The highest ones are those for neighboring ^{13}C: $^{1}J_{CC}$ were 50-65 Hz depending on the position of the ^{13}C pairs with respect to the NV center. The two-bond $^{2}J_{CC}$ constants were 1-5 Hz.

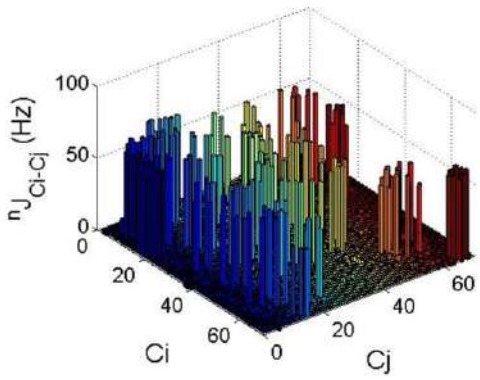

Fig.1. Simulated $^{n}J_{C\text{-}C}$ couplings for all possible ^{13}C nuclear spins pairs in the $C_{69}[NV]^{-}H_{84}$ cluster/

Acknowledgement

This work has been supported in part by BRFFI, the project Ф18MC-036, and by National Research Nuclear University "MEPhI", the RSF-DFG project 21-42-04416. The authors thank the KAUST Supercomputing Core Lab team for assistance with execution tasks on Skylake nodes.

References

[1] Schwartz I. et al. Blueprint for nanoscale NMR. Scientific Reports. 9 (2019) 6938.
[2] Barry J.F. et al. Sensitivity optimization for NV-diamond magnetometry. Rev. Mod. Phys. 92 (2020) 015004.
[3] Glenn D.R. et al. High-resolution magnetic resonance spectroscopy using a solid-state spin sensor. Nature. 555 (2018) 351.

Paramagnetic centers study of neutron-irradiated nanocrystalline boron nitride (h-BN) particles

Nicat R. Abbasov, Elchin M. Huseynov
National Nuclear Research Center, Inshaatchilar pr. 4, AZ 1073, Azerbaijan

It is clear that boron nitride has a specific properties at nano sizes resembling to other materials. Nanomaterials have various behaviour under the influence of ionizing environment and mechanical impacts. In general approach, the effects of neutron irradiation on nanomaterials from another class have been studied to some extent. Over the past few years, boron notride and its various types of composites are widely investigated by world scientists. BN has a wide range of applications in the extreme conditions due to attractive physical and chemical resistivity. EPR spectra of the nanocrystalline BN particles were compared before and after neutron irradiation in the different cases, such as "wide range", "selected range" and "saturation limit at selected range", etc.

EPR spectra of neutron irradiated BN nanoparticles, which intensify with increasing exposure time, can be well explained by the new isotopes formed as a result of neutron transmutations [1-3]. So that the B and N atoms in the nanocrystalline BN particles undergo isotope transmutations under the influence of neutron irradiation. Naturally, each of the B and N atoms has two stable isotopes. Each of these stable isotopes can form a different isotope by capturing a neutron. However, here the effective cross-section and absorption capacity of N isotopes is many times less than that of B atoms. As a result, we assume that the changes in N isotopes are sufficiently small and notenough to affect the spectrum. Two strong signal correponds to free electron of g factor in the EPR spectra of BN nanoparticles were observed as a results of the neutron irradiation.

[1] Elchin Huseynov, Anze Jazbec "EPR spectroscopic studies of neutron-irradiated nanocrystalline silicon carbide (3C-SiC)" Silicon 11/4, 1801–1807, 2019
[2] Elchin Huseynov, Anze Jazbec, Luka Snoj "Temperature vs. impedance dependencies of neutron-irradiated nanocrystalline silicon carbide (3C-SiC)" Applied Physics A 125, 91-98, 2019
[3] Elchin M. Huseynov, Tural G. Naghiyev, Adil A. Garibov, et al. "EPR spectroscopy of neutron irradiated nanocrystalline boron nitride (h-BN) particles" Ceramics International 47, 5, 7218-7223, 2021

Synthesis of nanocrystalline powders of complex cationic composition

N. Tereshko*, M. Bushinsky, R. Lanovsky, O. Mantytskaya,V. Fedotova, A. Nikitsin and A. Chobot
*Scientific-Practical Materials Research Centre NAS of Belarus, 220072 P. Brovki str. 19, Minsk, Belarus, tereshko@physics.by**

Among the methods of obtaining magnetic materials with a perovskite structure a special place is occupied by the sol-gel method which makes it possible to obtain nanomaterials with a narrow particle size distribution at relatively low temperatures using simple and inexpensive equipment. It was found that the optimal method for the formation of nanocrystalline powders of complex cationic composition, such as $LaMnO_3$ and $LaCoO_3$, doped with doubly charged Sr and Ni ions is a modified citrate sol-gel method. The synthesized samples were studied by the following methods: X-ray diffractometry, scanning electron microscopy, vibration magnetometry. The effect of doping with doubly charged cations on the particle size and structure of the samples has been studied.

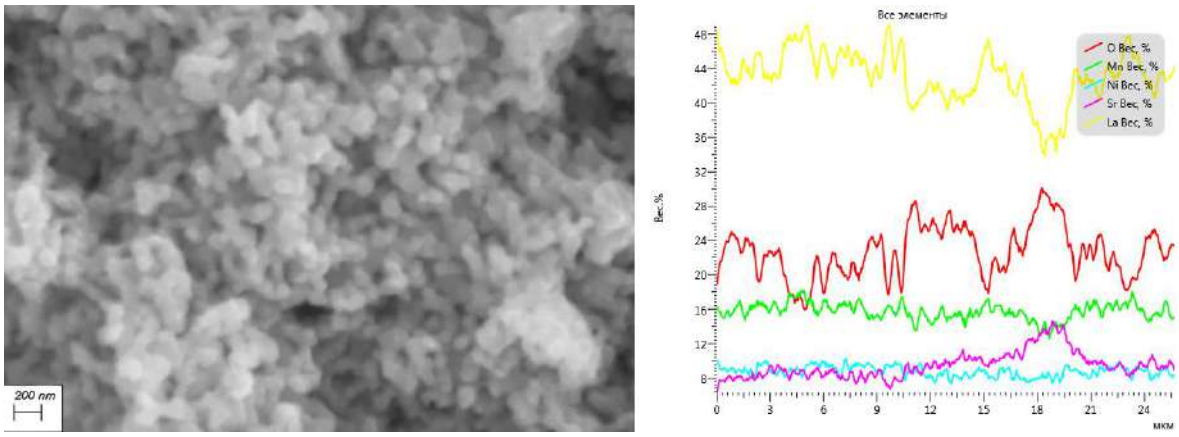

Figure 1 - SEM image and energy dispersive X-ray spectroscopy of the $La_{0.7}Sr_{0.3}Mn_{0.65}Ni_{0.35}O_3$ sample obtained by the sol-gel method

The results of energy dispersive X-ray spectroscopy showed that the content of components in the samples is consistent with the specified composition in the initial charge and also the homogeneity of the composition within separate grains. There is an insignificant change in the content of La, Sr, Mn, and Ni in different crystallites and an insignificant amount of grains with an impurity NiO phase. Therefore, the samples can be considered almost homogeneous in composition. The sample synthesized at 900^o C has a particle size of 100 - 150 nm (Fig. 1).

The developed technology for obtaining samples and experimental results of research can serve as the basis for both theoretical calculations of the physical properties of magnetic materials with the structure of perovskite and related compounds, and for the development of new functional materials with desired properties. The obtained patterns will make it possible to develop new magnetic, magnetoresistive and catalytic materials for use in the microelectronic and chemical industries and power engineering.

Acknowledgement
The authors would like to acknowledge the financial support from the State Scientific Research Programme “Condensed matter physics and creation of new functional materials and technologies for their production”, project 1.2.2.

Hydrophobization of PET TM-surfaces for oil/water emulsions separations

G.B. Melnikova[1*], A.E. Salamianski[2], I.V. Korolkov[3,4], T.N. Tolstaya[1], V.M. Akulova[2], I.B. Muslimova[3], A.R. Nurmukhamedova[3], S.A. Chizhik[1], M.V. Zdorovets [3,4]
[1]*A.V. Luikov Heat and Mass Transfer Institute of the National Academy of Sciences of Belarus, 220072, Belarus, Minsk, 15 Brovki Str.*
[1] *Institute of Chemistry of New Materials of the National Academy of Sciences of Belarus, 220141, Belarus, Minsk, 36 F. Skorina Str.*
[3]*L.N. Gumilyov Eurasian National University, 010008, Kazakhstan, Nur-Sultan, 5 Satpaev Str.*
[4]*The Institute of Nuclear Physics, 050032, Kazakhstan, Almaty, 1 Ibragimov Str.*
**corresponding author e-mail: galachkax@gmail.com*

According to the UNESCO data the pollution of wastewater with oil products is the ten numbers of dangerous. Traditional methods of wastewater purification, as flotation, coagulation, upholding do not satisfy the high purity degree requirements of water. The valuable impurities extraction allows theirs reusing by appointment. The oil/water emulsions filtration with using hydrophobic membranes allows to separate with high degree of purification. For water filtration, the ion track therephthalate) polyethyleneterephthalate track-etched membranes (PET TM) are often used. The modification of TM surfaces allows increace the hydrophobicity of membranes.

PET TM were prepared by irradiation of PET film (12 μm thickness) with Kr ions on accelerator DC-60 (Nur-Sultan, Kazakhstan) with an energy of 1.75 MeV/nucleon and ion fluence
of $1 \cdot 10^8$ ion/cm^2. Then membranes were processed by photosensitization for 30 min from each side and chemical treatment in 2.2 M NaOH at 85 °C to prepare membranes with pore sizes of 200 and 350 nm.

Octadecyltrichlorosilane (OTS, Sigma-Aldrich, 98% purity) was used without further purification. The OTS coating was formed on the surfaces of PET TM by spin-coating method. A solution of OTS in hexane with a concentration of 1 mM in a volume of 1 ml was applied to PET TM and they were rotated at a speed of 3000 rpm for 2 minutes.

The hydrophobic properties of the membrane surfaces after modification were measured on a DSA 100E device (KRUSS, Germany) accordingly values of the water contact angles (CA). The surface structures of the formed monolayers investigated by atomic force microscopy (AFM, NT-206, ALC “Microtestmaschines”, Gomel) using silicon cantilevers.

The flux of PET TM was measured at a pressure of 800 mbar with using water / chloroform emulsion. The emulsion was prepared by mixing 5 ml of water and 45 ml of chloroform using an IKA T 18 digital ULTRA-TURRAX disperser for 3-4 minutes.

As a result, after modification the pores diameters are increased on 50 and 15 % of PET TM-200 and PET TM-350, respectively. Accordingly of AFM-data of roughness the OTS layer form a uniform coating, and also envelop the boundaries of the membrane pores with a film of a modifier. The CA values of modified membranes are increased from 51° to 100°. The flux of modified membranes PET TM – 200 is of 17 ml/ (m^2·s), PET TM – 350 is of 124 ml/ (m^2·s), while using initial membranes the water / chloroform emulsion separation is not possible. The mofified membranes did not change properties during 5 filtration cycles.

Thus, the formed hydrophobic layers of OTS on the surface of PET TM can be used for filtration of emulsions of the water-in-oil type.

Acknowledgment

This research was funded by Belarusian Republican Foundation for Basic Research (contr. F20MS-025 of 04.06.2020) and the Science Committee of the Ministry of Education and Science of the Republic of Kazakhstan (Grant No. AP09057934).

Selection of tunneling barrier materials for spintronic devices based on strontium ferromolybdate

G. Suchaneck[1], E. Artiukh[2]*
[1]*TU Dresden, Solid State Electronics Laboratory, 01062 Dresden, Germany,*
[2]*SSPA "Scientific-Practical Materials Research Centre of NAS of Belarus", 220072 Minsk, Belarus*
**sirfranzferdinand@yandex.ru*

A main challenge of magnetic tunnel junction devices is the appropriate selection of a barrier material. Tunneling is sufficiently affected by the properties of the electrode/barrier interface. For instance, the interfacial spin polarization of $La_{2/3}Sr_{1/3}MnO_3$ deposited onto various barrier materials ($SrTiO_3$, TiO_2, $LaAlO_3$) depends significantly on the barrier material and is strongly different from the spin polarization of a free surface [1]. On the other hand, a suppression both in the Curie temperature T_C and in magnetization was observed in $La_{0.7}Ca_{0.3}MnO_3$/STO superlattice as the thickness of the $La_{0.7}Ca_{0.3}MnO_3$ layer decreased which was attributed to interfacial magnetic disorder [2].

Considering an ideal conductor-dielectric interface without surface- or adsorbate-induced states, a charge transfer occurs between the constituents creating an interface dipole which shifts the relative position of the metal Fermi level with respect to the conduction and valence bands of the dielectric. The magnitude of the interface dipole is defined by the strength of both interface constituents to attract electrons, i.e., by their effective electronegativities. The Pauling electronegativity scale X is based on the difference between the actual and the expected bond formation enthalpy in various A-B molecules. The difference is attributed to the partial ionic character of the A-B bond. To set up relative values for all of the elements, a value of X = 4.0 was assigned to the most electronegative element fluorine. Similarly, the displacement of the electron density at the interface might be defined by the difference of the effective electronegativity $\langle X \rangle$ of the interface constituents. An appropriate way to calculate the effective electronegativity of materials consisting of N components is the use the geometric mean of the electronegativity for the constituent elements.

Compound	Function	$\langle X \rangle$
Fe	Electrode	1.83
NiFe	Electrode	1.87
Co	Electrode	1.88
MgO	Barrier	2.12
La_2O_3	Barrier	2.18
$BaTiO_3$	Barrier	2.24
$SrTiO_3$	Barrier	2.26
$Ce_{0.69}La_{0.31}O_{1.845}$	Barrier	2.31
$La_{2/3}Sr_{1/3}MnO_3$	Electrode	2.31
$La_{0.7}Sr_{0.3}MnO_3$	Electrode	2.31
AlO	Barrier	2.35
$LaAlO_3$	Barrier	2.35
ZnO	Barrier	2.38
Sr_2FeMoO_6	Electrode	2.38
$Mg_3B_2O_6$	Barrier	2.40
$SrMoO_3$	Barrier	2.42
HfO_2	Barrier	2.49
Mn_2O_3	Barrier	2.50
Al_2O_3	Barrier	2.54
$SrMoO_4$	Barrier	2.57
Fe_3O_4	Electrode	2.62
TiO_2	Barrier	2.63
MnO_2	Barrier	2.64
Ta_2O_5	Barrier	2.71

Effective electronegativities of electrode materials and potential barrier materials

The effective electronegativity is correlated with the work function of metal, carbide, oxycarbide, nitride, oxynitride and LaB_6 electrodes on HfO_2 [3] proving its suitability to characterize the charge exchange at electrode-dielectric interfaces.

Calculated effective electronegativities of ferromagnetic and ferrimagnetic electrode materials as well as potential barrier materials are compiled in the table.

Acknowledgment
This work was supported by the EU project H2020-MSCA-RISE-2017-778308- SPINMULTIFILM.

References

[1] V. Garcia, M. Bibes, A. Barthélémy, M. Bowen, E. Jacquet, J.-P. Contour, and A. Fert, Phys. Rev. B 69 (2004) 052403.
[2] M.-H. Jo, M.N. Mathur, J.E. Evetts, M. Blamire, M. Bibe, and J. Fontcuberta, Appl. Phys. Lett. 75 (1999) 3689.
[3] J. K. Schaeffer, D. C. Gilmer, C. Capasso, S. Kalpat, B. Taylor, M. V. Raymond, D. Triyoso, R. Hegde, S. B. Samavedam, and B. E. White Jr, Microelectronic Engineering 84 (2007) 2196–2200.

Band structure investigation of ZrC nanoparticle using infrared spectroscopy

Gulnar I. Muradova
Institute of Radiation Problems of ANAS
AZ1143, B.Vahabzadeh 9, Baku, Azerbaijan gulnar-isgenderova@mail.ru

ZrC is a rare material with the potential to be used at ultra-high temperatures [1-5]. Due to the fact that ZrC is widely used in practice as a reactor material, the effect of ionizing radiation on its properties is of great interest. To date, enough experiments have been carried out with ZrC and other nanoparticles, and the results have been published in the form of relevant scientific articles. For studying structure of nano ZrC compound, researchs was on infrared region. As you know infrared spectrometry used to identify mixtures on materials and analyze the structure of the selected sample. The main goal of the IR analysis of ZrC nanoparticles is to easily observe the spatial vibrations of these samples in the initial approximation. As a result of the analysis of the spectra, it was found that the sample has seven peaks in the general approach. The peaks explaining the oscillations of the Zr-C bonds are explained by the corresponding wave numbers in the FTIR spectra. The same time the oscillations of the Zr-O-C bonds are explained by the corresponding wave numbers. It is assumed that the picker corresponds to the values of the wave number of 2190 cm-1 and 2360 cm-1 characterizes the C-OH groups and the C-O vibrations.

As a result of the analysis of the FTIR spectra of ZrC nanoparticles, it was identified that the peaks which explain the oscillations of the Zr-C bonds appeared only at the values of the wave number 1010cm^{-1} and 1380cm-1. On the other hand, it was found that the peaks which wave number 970cm^{-1} and 1600cm-1 explain the oscillations of the ZrO-C bonds. As with other nanomaterials, ZrC nanoparticles are superficially active, so there have been identified C-OH groups and infrared peaks which characterizing C-O oscillations.

[1] Yonggang Tong et al. "Carbon fiber reinforced ZrC based ultra-high temperature ceramic matrix composite subjected to laser ablation: Ablation resistance, microstructure and damage mechanism" Ceramics International 46, 2020, 14408-14415
[2] Yi Hou et al. "High temperature electromagnetic interference shielding of lightweight and flexible ZrC/SiC nanofiber mats" Chemical Engineering Journal 404, 2021, 126521
[3] G. Gutierrez et al. "Thermal behaviour of xenon in zirconium carbide at high temperature: Role of residual zirconia and free carbon" Journal of Nuclear Materials 416, 2011, 94-98
[4] G. Antou et al. "High temperature compressive creep of spark plasma sintered zirconium (oxy-)carbide" Materials Science and Engineering: A 612, 2014, 326-334
[5] M.M. Lo´pez Guerrero, A. Garcı´a de Torres et al "Quantitative determination of ZrC in new ceramic materials by Fourier transform infrared spectroscopy" Ceramics International 37 (2011) 607–613

Oxide removal mechanisms from the InP surface during annealing in As flux

D. Dmitriev*, D. Kolosovsky, A. Toropov, and K. Zhuravlev
Rzhanov Institute of Semiconductor Physics, Siberian Branch, Russian Academy of Sciences
Russia, 630090 Novosibirsk, Lavrentiev aven. 13, e-mail: ddmitriev@isp.nsc.ru

InP(001) substrates are actively used for the growth of heteroepitaxial structures of integrated microwave photonics systems [1]. Pre-epitaxial thermal cleaning of InP substrates in an ultrahigh vacuum of the growth chamber in an arsenic flux makes it possible to obtain a sharp layer/substrate heterointerface and to avoid uncontrolled embedding of phosphorus in InAlAs/InGaAs layers, lattice-matched with the InP(001) substrate [2]. When arsenic interacts with the oxidized InP surface, a solid solution $InP_{1-x}As_x$ is formed, the composition of which depends on the annealing temperature and the arsenic flux [3]. However, the mechanisms of oxide removal, surface transformation, and InPAs layer formation are not fully understood. It is obvious that understanding these processes is important for technologies for the growth of heteroepitaxial structures on InP. In this work, the mechanisms of oxide removal from the surface of an epi-ready InP(001) substrate in an arsenic flux are studied in situ by the method of reflection high-energy electron diffraction (RHEED).

The studies were carried out in a Compact-21T molecular beam epitaxy system from Riber, equipped with a RHEED system and a kSA 400 diffraction pattern analysis system. We used epi-ready InP(001) substrates from AXT.

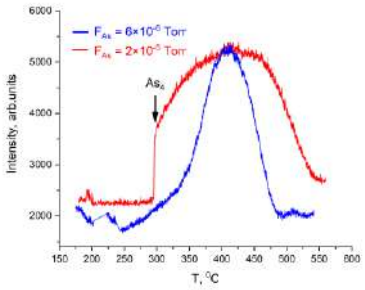

Intensity of (00) reflex in RHEED upon annealing InP in an As flux.

We observed a slow increase in the (00) reflex intensity at T>250 ℃ without an arsenic flux, which indicates thermal removal of the oxide. At the moment of switching on the arsenic flux $F_{As}=6\times10^{-6}$ Torr at T=300 ℃, there are no changes in the dependence of the (00) reflex intensity, i.e. the contribution of interaction with As to oxide thinning is insignificant. At T~350 ℃, the nature of the oxide removal process changes sharply, which is associated with the activation of the chemical reaction of the interaction of arsenic with oxide. Indeed, according to Van't Hoff law, an increase in temperature by 10 degrees leads to an increase in the reaction rate by 2-4 times. With a large flux $F_{As}=2\times10^{-5}$ Torr, a sharp thinning of the oxide layer occurs. This is due to the increased contribution of the chemical reactions of As and oxide, which is proportional to the concentration of As. However, as a result of these reactions, the oxide is not completely removed, and upon further heating, a slow thermal thinning of the oxide occurs. At a temperature of T~410 ℃, the maximum intensity of the (00) reflex is reached, which indicates the complete removal of the oxide layer, which no longer scatters the electron beam. The subsequent decrease (00) reflex intensity of the is associated with an increase in the surface roughness due to desorption of phosphorus and segregation of indium, but with a higher flux of arsenic, it occurs more slowly, since the flux of arsenic decreases the desorption of V-group elements from the surface.

I Thus, the oxide layer is likely to consist of two types of oxides, one of which actively interacts with As, and the other decomposes predominantly thermally.

Acknowledgement
The research was funded by RFBR and Novosibirsk region, project number 20-42-540009.

References

[1] M. Smit, K. Williams, and J. van der Tol, APL Photonics 4 (2019) 050901.
[2] D.V. Dmitriev, et al., IOP Conf. Ser.: Mater. Sci. Eng. 475 (2019) 012022.
[3] D.V. Dmitriev, et al. Surface Science 710 (2021) 121861.

Structural and luminescent properties of two-dimensional silicon layers epitaxially grown on dielectric calcium fluoride substrates

V.A. Zinovyev[1]*, V.A. A.V. Kacyuba[1], V.A. Volodin[1,2], A.F. Zinovieva[1,2], S.G. Cherkova[1], Zh.V. Smagina[1], A.V. Dvurechenskii[1,2], A.Y. Krupin[3], O.M. Borodavchenko[4], V.D. Zhivulko[4], A.V. Mudryi[4]

[1]*Rzhanov Institute of Semiconductor Physics, Siberian Branch of Russian Academy of Sciences, 630090 Novosibirsk, Russia, zinoviev@isp.nsc.ru**

[2]*Novosibirsk State University,63090 Novosibirsk, Russia*

[3]*Novosibirsk State Technical University, 630073 Novosibirsk, Russia*

[4]*Scietific Practical Materials Research Centre of National Academy of Sciences, P. Brovki str., 19, 220072 Minsk, Belarus*

At present, all over the world there is an increased interest in two-dimensional materials based on silicon and germanium [1]. This work is aimed at finding optimal conditions for the formation of two-dimensional Si layers embedded in a dielectric CaF_2 matrix, as well as studying their structural and optical properties.

The growth was carried out by molecular beam epitaxy on Si (111) substrates. Studies of the surface morphology of the grown structures made it possible to determine the conditions favorable for the formation of two-dimensional Si layers. The vibrational spectra of the created structures were studied by Raman spectroscopy. The Raman spectra of structures with one and ten Si bilayers embedded in CaF_2 exhibit a narrow peak at 418 cm^{-1}, which can be attributed to vibrations of Si – Si bonds in the plane of a two-dimensional Si layer intercalated in CaF_2 (curves 3 and 4 in figure 1). The results of studies performed for multilayer structures have demonstrated that under the chosen growth conditions, with an increase in the number of structure layers, the planarity of Si/CaF_2 heterointerfaces is preserved, which makes it possible to observe an enhanced total Raman signal from 10 two-dimensional Si layers of an atomic bilayer thick. Investigations by the photoluminescence (PL) method showed that the PL spectra from the created structures exhibit an emission band at 680 nm, which can be associated with radiative recombination of charge carriers in two-dimensional Si layers embedded in a dielectric matrix. The effect of hydrogenation on the optical properties of the grown structures with Si layers embedded in the CaF_2 matrix has been studied. The analysis of the PL spectra showed that the treatment in hydrogen plasma leads to a noticeable increase (by almost 4 times) in the integral intensity of the PL signal from a multilayer structure with two-dimensional Si layers in the spectral wavelength range from 400 to 800 nm.

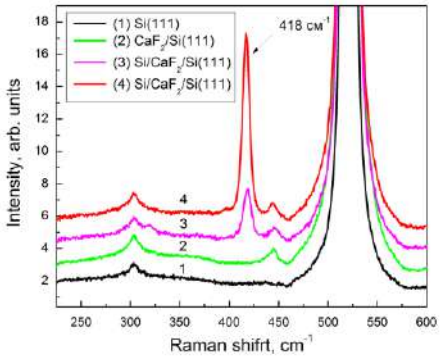

Fig.1. Raman spectra of the epitaxially grown structures with one (3) and ten (4) Si bilayers embedded in a dielectric CaF_2 matrix on Si(111) substrate. Raman spectra of Si(111) substrate (1) and epitaxially grown CaF_2 film (2).

Acknowledgement

This work was funded by the Russian Foundation for Basic Research (Grant No. 20-52-00016) and the Belarussian Republican Foundation for Fundamental Research (Grant No. F20R-092).

References

[1] M. Galbiati, N. Motta, M. De Crescenzi, and L. Camilli, Appl. Phys. Rev. 6 (2019) 041310.

Nanostructured silicon: from green hydrogen to nanomedicine

V. Sivakov
Leibniz Institute of Photonic Technology, Dept. Functional Interfaces, Albert-Einstein Str. 9, 07745 Jena, Germany
vladimir.sivakov@leibniz-ipht.de

The future of modern society is tied to the availability of sustainable energy resources and effective diseases diagnostics and therapy. However, among various sources of energy, sunlight is the most abundant and cleanest natural energy resource. It is presumed that the grid parity of solar cells can be reached by using nanostructured semiconductors or a new solar cell architectures that is most-likely based on nanotechnology. Over the last several years, wet chemically etched silicon nanowires have been favored in my group at Leibniz IPHT as a promising highly effective optoelectronic material due to a number of unique physical-chemical properties such the ability to tune the optical band gap and the absorption spectrum. Creation of one-dimensional silicon nanostructures has opened up a new area for device applications in electronics, optoelectronics, thermoelectronics, photocatalysis, photovoltaics, sensor, and bio-imaging. Hydrogen is regarded to be one of the most promising green energy source in the Industry 4.0. One promising approach to produce hydrogen is a photocatalytic water splitting. The high porosity leads to an increased active surface area and also to an enlarged optical band gap.

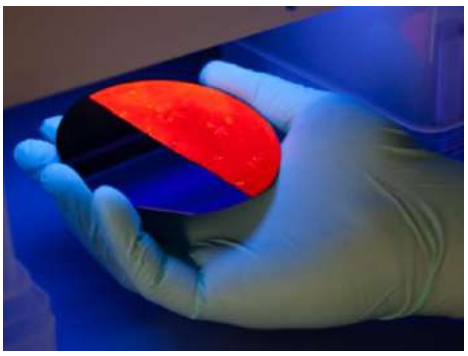

Digital image of nanostructured 4-inch single crystalline silicon wafer. (© Sven Döring)

Cancer diagnostic and therapy challenge the scientific community to design research addressing the urgency of ending cancer. These novel nanostructures are based on insights gained during the last years of research in my group and are expected to lead to significant progress steps, by which such material will be promoted from “promising material” to effective material for the biophotonic and biomedical applications. For all these reasons new labeling and drug delivery agents for bio-application are an important field of research with a growing potential for medical use.

Optical active modificated nanodiamond for ferroelectric LC

S. Adamchyk [1], A.A. Lugovski[1], V. Lapanik[2], G. Gusakov[2], G. Pitsevich[2],A.P. Lugovski[2]
[1] *Republican Scientific Center for Human Issues of Belarusian State University,220045 Minsk, Kurchatov st., 7, Belarus, Sergey.adamchik@gmail.com* *
[2] *A.N. Sevchenko Institute of Applied Physical Problems of Belarusian State University, 220045 Minsk, Kurchatov st., 7, Belarus*

New liquid crystal devices with improved electro-optical properties are being actively developed. In particular, one of the promising areas is ferroelectric liquid crystals. Earlier [1] we found that one of the group of compounds suitable for this purpose are chiral liquid crystals that form the smectic phase C.

At the same time, it is known that the addition of nanoparticles to a liquid crystal can cause a change in its orientation, a decrease in the phase delay, and an acceleration of the optical response of LCs with an increase in their concentration.

On this basis, we proposed to use ultradispersed detonation diamond covalently modified with a biphenyl fragment to improve the electro-optical properties of LCs.

Nanodiamond powder «UDA-SP» produced by «Sinta» (Minsk) were used in the present work. Prepurification of the UDD from non-diamond impurities was carried out by the treatment of the diamond blend with nitric acid at elevated temperature and pressure and then by acid-alkaline treatment of the powder, washing with distilled water and drying was carried out in two stages. In the second stage UDD samples were annealed for 1 hour at temperature 430^0C in air and were purified of metal impurities by ultrasonic treatment in hydrochloric acid. The final conjugate is (S)-oktan-2-yl-4'-hydroxy-[1,1'-diphenyl]-carboxylate attached to nanodiamond via ether linker. It was synthetized by the treatment of oxalyl chloride on the carboxyl groops of nanodiamond surface followed by their reaction with (S)-oktan-2-yl-4'-hydroxy-[1,1'-diphenyl]-carboxylate in the presence of a base [2].

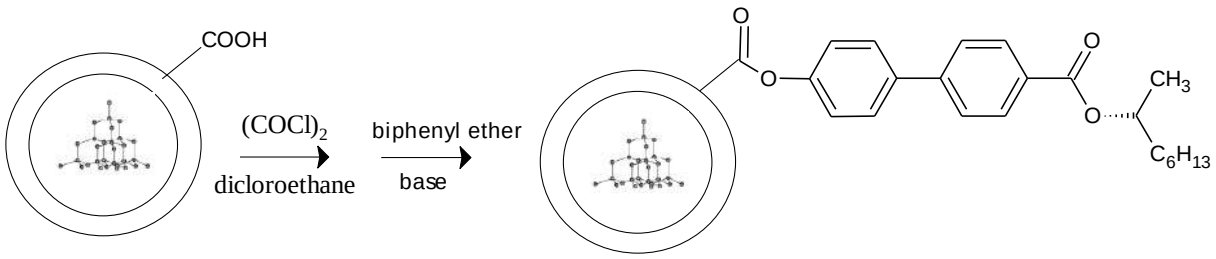

Figure

Covalent bonding of biphenyl has been proven by the IR absorption spectra. Compared with the initial spectrum of nanodiamond powder in the range 1000-1900 cm^{-1}, an intense band with maxima of 1683 cm^{-1} are observed. This band can be attributed to vibrations of the functional groups –C=O– in ethers. Another band in a range 1600-1605 cm^{-1} can be attributed to the –C–C– vibrations of the aromatic systems of biphenyl.

The influence of optical active modificated nanodiamondon on properties of ferroelectric LCs have been investigated. Doping such dopant leads to the increase of the spontaneous polarization by 25%, increase of the tilt angle by 15% and reduces the response time by 40%.

References

[1] V.Lapanik, A. Lugouskiy, S.Timofeev, W.Haase, Liquid Crystals. Volume 41, N 9 (2014) pp. 1391–1397.
[2] J. Clayden, Organic chemistry. Oxford: Oxf.ord University Press. (2001) pp. 276–296.

Hydrophobic coatings based on octadecyltrichlorosilane

V.M. Akulova [1*], A.E. Salamianski [1], A.A. Rogachev[1], I.G. Chishankov[1], G.B. Melnikova[2], To Thi Xuan Hang[3], Nguyen Thuy Duong[3], Vu Ke Oanh[3], Tran Dai Lam[3]
[1] *Institute of Chemistry of New Materials of the National Academy of Sciences of Belarus, 220141, Belarus, Minsk, 36 F. Skorina St., myfavoritecheese@mail.ru*
[2] *A.V. Luikov Heat and Mass Transfer Institute of the National Academy of Sciences of Belarus, 220072, Belarus, Minsk, 15 Brovki St.*
[3]*Institute for Tropical Technology, A13, 18 Hoang Quoc Viet, Cau Giay, Hanoi, Vietnam*

Reducing of friction and wear between contact silicon surfaces of micro-electro-mechanical systems (MEMS) is a significant problem in the field of microelectronics [1, 2]. Octadecyltrichlorosilane (OTS) is a good choice for creating hydrophobic self-assembled monolayers (SAMs), which eliminate friction and wear of silicon surfaces [2]. The goal of this work is to obtain the OTS layer on silicon surface by spin-coating method, and it's further investigation in comparison with SAMs.

Monolayer of OTS was formed on silicon by self-assembled process [2]. Coating of the OTS was fabricated from 1 mM OTS solution in hexane by spin-coating method during 2 min at a rotation speed of 3000 rpm. The contact angle of samples was measured by the "sessile" drop method, including deposition of 3 μL water drops on OTS coatings. Linear microtribometer was used for the tribotechnical testing [2]. Testing conditions were: normal load of 1.0 N, 3 mm diameter steel ball as indenter, 3 mm stroke, linear speed of 4 mm/s [2].

It was shown that the water contact angles of SAM and layer of OTS obtained by spin-coating method are ~105.6°±2.6° and 96.2°±4.0°, respectively. We guess that the difference in the water contact angle of both coatings is due to the fact that layers of OTS obtained by spin-coating method have less packing density of molecules as opposed to SAMs. Initial hydrophilic silicon wafers are destroyed during one sliding cycle at a normal load of 1.0 N, while modified by monomolecular OTS films silicon wafers are stable throughout 29.0±4.0 sliding cycles against a steel ball. Meanwhile, silicon surface modified OTS by spin-coating method is worn after 65.0±5.0 sliding cycles (Fig. 1). This result can be explained by increasing of amount of OTS in friction unit in case OTS layer formed by spin-coating method [2]. Moreover, molecules of OTS in SAM form strong covalent bonds with the surface of silicon wafers during the self-assembly process, and in the case of spin coating layers, the reason for adsorption of OTS molecules on silicon is Van der Waals forces [2]. Thus, OTS coatings obtained by self-assembled and spin-coating methods can be used as protective coatings in MEMS.

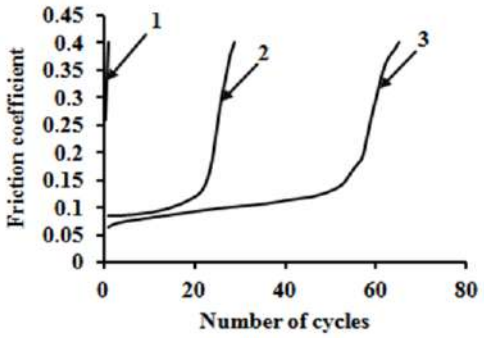

Fig.1. The friction coefficient as a function of nuber of sliding cycles: 1– unmodified silicon surface, 2 – SAM of OTS, 3 – layer of OTS obtained by spin-coating method

Acknowledgement
The work was supported by the Belarusian Republican Foundation for Fundamental Research – grant number X21BA-003.

References

[1] M. Li, B. Su, B. Zhou, H. Wanga, J. Meng, Appl.Surf.Sci. 508 (2020) 1-8. https://doi.org/10.1016/j.apsusc.2019.145187
[2] V. Akulova, A. Salamianski, I. Chishankov, V. Agabekov, Soft Materials (2021) 1-18. https://doi.org/10.1080/1539445X.2021.1933034

Chemical deposition of bismuthselenide thin films from aqueous media

M.D. Likhachev[1*], V.F. Markov[1,2] , A.V. Pozdin[1]
[1]*Ural Federal University named after the First President of Russia B.N. Yeltsin, Yekaterinburg, 620002 Russia, e-mail: matveilihachev123456789@gmail.com**
[2] *Ural Institute of State Fire Service, Emergency Ministry of Russia, Yekaterinburg, 620062 Russia.*

Narrowband Bi_2Se_3 (Eg ~ 0.3 eV) is considered one of the most important components in solar energy, in optical and photosensitive devices, in thermoelectric cooling devices and in infrared spectroscopy. The compound has a rhombohedral phase, the same crystal structure is observed for other compounds of groups V-VI, such as Bi_2Te_3 and Sb2Te_3, with the corresponding band gaps of 0.11 and 0.14 eV, respectively. Therefore, this work is aimed at studying the surface structure of the obtained films.

Thin Bi_2Se_3 films were synthesized by chemical deposition from aqueous solutions of bismuth nitrate $Bi(NO_3)_3$, triethanol $C_6H_{15}NO_3$, sodium selenosulfate Na_2SeSO_3, ammonium hydroxide NH_4OH. All films were applied onto previously degreased sitall substrates in a TS-TB-10 liquid thermostat for 150 min at a temperature of 353 K.

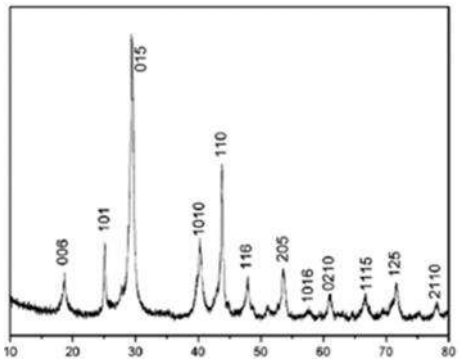

Figure 1 - X-ray diffraction pattern of a Bi2Se3 film obtained by hydrochemical deposition at a temperature of 353 K for 150 min.

X-ray diffraction analysis of Bi_2Se_3 thin films showed that the films are polycrystalline with a preferred orientation of crystallites (015) in the direction normal to the surface. They are characterized by a rhombohedral phase (space group R-3 2/m) with a Bi_2Se_3 crystal lattice constant equal to 0.41301 ± 0.00003 nm (Figure 1).

Bismuth selenide film materials grow in a forcedly oriented direction during synthesis, and this explains the needle-like state of the particles.

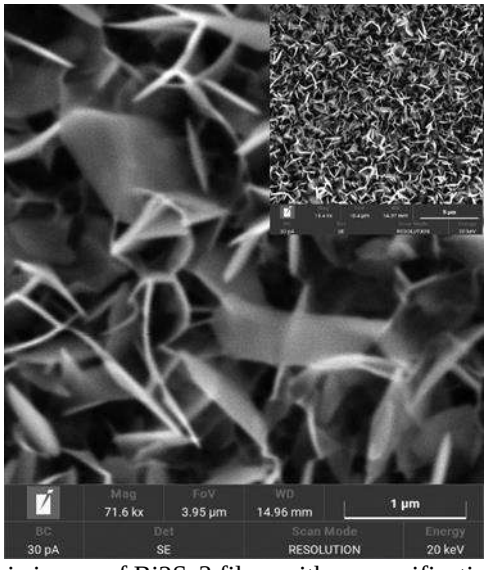

Figure 2 - Electron microscopic image of Bi2Se3 films with a magnification of 50,000X, obtained under thermostated conditions. The inset shows an image of the film surface with a magnification of 10,000X.

Electrophysical properties of cobalt-doped thin-film PbS

A.V. Pozdin[1*], L.N. Maskaeva[1,2], V.F. Markov[1,2]
[1]*Ural Federal University named after the First President of Russia B.N. Yeltsin, Yekaterinburg, 620002 Russia, e-mail: andrej.pozdin@yandex.ru**
[2] *Ural Institute of State Fire Service, Emergency Ministry of Russia, Yekaterinburg, 620062 Russia.*

Narrow-band PbS (Eg~0.4 eV) is widely used in optoelectronics as IR photodetectors, sensors, optical switches, efficient solar radiation conversion devices, sensors. To change the optical and functional properties of PbS films, doping with various metals playing the role of donors or acceptors is carried out, leading to changes in the zone structure, as well as optical and photoelectric properties. Therefore, this work is aimed at studying the effect of Co^{2+} ions on the photoelectric properties of PbS films.

Thin films of PbS were synthesized by chemical deposition from aqueous solutions of lead acetate $Pb(CH_3COO)_2$, sodium citrate $Na_3C_6H_5O_7$, ammonium hydroxide and iodide NH_4OH, NH_4I and thiourea $(NH_2)_2CS$. Alloying films Co^{2+} PbS was carried out during synthesis by introducing into the reactor at a salt $CoCl_2$ when they are deposited for 1.5 and 3.0 hours. All films were deposited on preliminarily degreased glass substrates in a «TS-TB-10» liquid thermostat at 353 K.

The photoelectric characteristics (dark resistance R_d, volt sensitivity U_s) of PbS(I,Co) films were measured on an installation K.54.410 with a 573K blackbody radiation source at a radiation modulation frequency of 800 Hz and an irradiance of $1 \cdot 10^{-4}$ W/cm^2. The type of conductivity of the films was determined from the sign of the thermopower when creating a temperature gradient in the region of probe contacts.

All films doped with cobalt and iodine retained the p-type of conductivity. The dynamics of changes in the photovoltaic properties (R_d,=*f*[$CoCl_2$] и U_s,=*f*[$CoCl_2$]) of elements (5×5) mm^2 based on PbS(I,Co) layers from the content of cobalt (II) chloride in the reaction bath is shown in the figure.

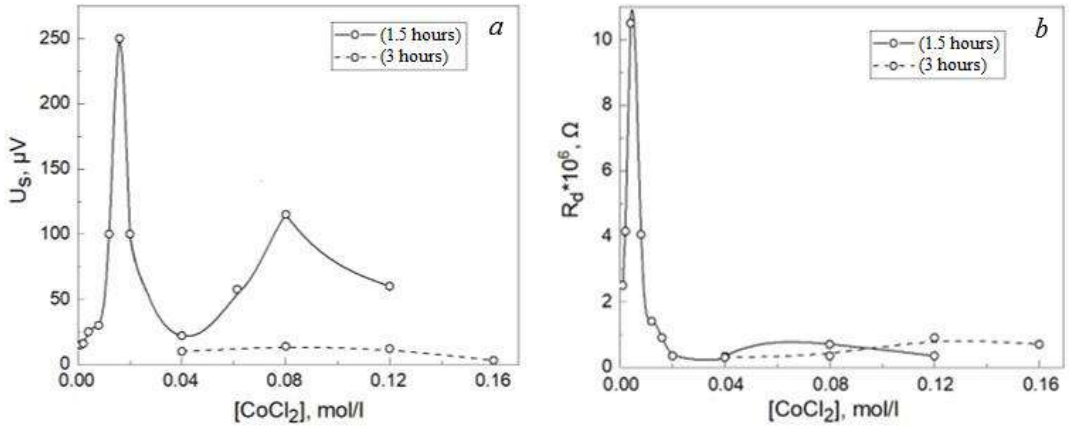

Figure. Changing the volt sensitivity U_S (*a*) and dark resistance R_d (*b*) of elements (5×5) mm^2 based on films PbS(I,Co) from the concentration of $CoCl_2$ in the reaction bath

On the dependence of the volt sensitivity Us as a function of the concentration of cobalt chloride $CoCl_2$ in the reaction bath of a PbS (I,Co) film, the chemical deposition of which lasted 1.5 hours, two maxima of 250 μV (0.016 mol/l) and 120 μV (0.08 mol/l) are observed. After a three-hour deposition, the PbS (I,Co) layers, the thickness of which exceeds the one-and-a-half-hour films by about 50-100 nm, have a weaker photoresponse.

Light transmission spectra of ZnS:Mn thin films

O.A. Lipina [1], A.N. Bezzabotnova[2*], L.N. Maskaeva[2,3]
[1]*Institute of Solid State Chemistry, Ural Branch of the Russian Academy of Sciences, Yekaterinburg, 620990 Russia.*
[2]*Ural Federal University named after the First President of Russia B.N. Yeltsin, Yekaterinburg, 620002 Russia, e-mail: bezzabotnova009@gmail.com**
[3]*Ural Institute of State Fire Service, Emergency Ministry of Russia, Yekaterinburg, 620062 Russia.*

Wide-band semiconductor ZnS (Eg~3.68 eV) is widely used in optoelectronic devices, lasers, solar cells, biosensors, electro-catholuminescent displays and fluorescent materials. The doping of ZnS films with different metals can change the optical, structural and functional properties. Therefore, the purpose of this work was to study the effect of manganese ions on the light transmission of ZnS films.

Preparation of thin films ZnS:Mn from the system "zinc chloride $ZnCl_2$ - manganese chloride $MnCl_2$ - ammonium hydroxide NH_4OH - thiocarbamide N_2H_4CS" was carried out by chemical deposition on preliminarily degreased glass substrates at 353 K during 120 min.

The light transmission spectra of the films discussed were taken on the UV-3600 spectrophotometer in the wavelength range of 200–1700 nm with a scanning step of 1 nm.

In Figure (a) it can be seen that in the spectra of all the samples obtained, a sufficiently long section is allocated, covering a wavelength range from 300 to 1000 nm (1.2–4.1 eV), in which there is a gradual decrease in the magnitude of light transmission T (λ). At the same time, for a film synthesized from a solution with 10^{-2} mol/L $MnCl_2$ was found a clear shift in the region of decline towards large wavelengths. At $\lambda < 300$ nm, there is a significant absorption of the transmitting radiation at $T \rightarrow 0$. This is due to the high probability of interband electron transitions in the precipitated layers of ZnS:Mn and in the substrate material.

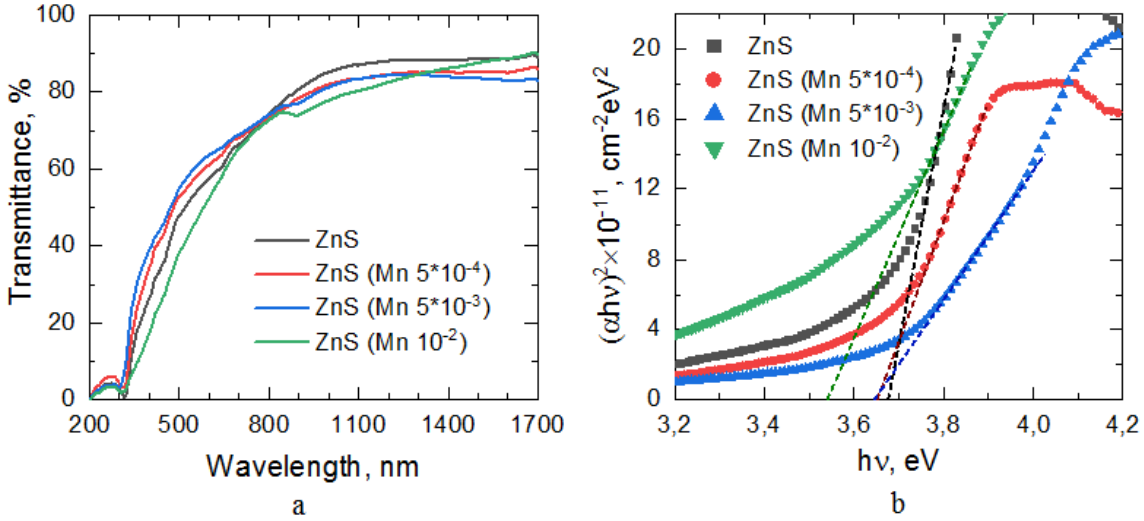

Figure. Light transmission (a) and graphical determination of the optical band gap (b) of ZnS: Mn films

According to the obtained data, the value of the the band gap E_g is graphically determined (Fig. b), which was 3.68 eV for the undoped layer of ZnS, which is consistent with the literature data. For ZnS:Mn films precipitated from solutions with concentrations of 0.0005, 0.005 and 0.01 mol/L $MnCl_2$, the band gap value takes smaller values equal to 3.65, 3.64 and 3.54 eV, due to the replacement of zinc ions (0.076 nm) by larger manganese ions (0.083 nm).

Chemical deposition of nickel-doped PbS(I) thin-films

Borisova E.S.[1], Pozdin A.V.[1], Maskaeva L.N.[1,2]

[1] Ural Federal University named after the First President of Russia B.N. Yeltsin, Yekaterinburg, 620002 Russia, e-mail: boris12221@yandex.ru
[2] Ural Institute of State Fire Service, Emergency Ministry of Russia, Yekaterinburg, 620062 Russia.

One of the representatives of the family of semiconducting chalcogenides $A^{IV}B^{VI}$ is the narrow-gap semiconductor PbS, which has unique electronic properties controlled by the interaction of the s-electrons of the cation with the valence p-electrons of the anion. At present, the possibility of creating materials with new luminescent, conducting and magnetic properties based on Ni^{2+} doped PbS deserves attention - a new direction of research, promising for optoelectronics and nanoelectronics, sensorics and voltaics [1].

To obtain nickel-doped PbS films, the method of chemical deposition from aqueous media has obvious advantages, the use of which makes it possible to reduce the cost of obtaining thin-film compounds using simple equipment and low-temperature conditions of the process.

Thin-film PbS layers were obtained by chemical deposition onto previously degreased glass substrates from aqueous solutions containing lead acetate $Pb(CH_3COO)_2$, thiourea $(NH_2)_2CS$, sodium citrate $Na_3C_6H_5O_7$, ammonium hydroxide NH_4OH and iodide NH_4I. The films were doped during chemical deposition by additionally introducing $NiCl_2$ from 0.0005 to 0.008 mol/l into the reactor. The synthesis of the films was carried out for 90 min at 353 K. As a result, light gray shiny PbS (I, Ni) films were obtained, the thickness of which decreased from 340 nm to 290 nm with an increase in the concentration of the dopant $NiCl_2$.

Electron microscopic studies indicate a change in the morphology of the films (Fig. 1). As a result of introducing a minimum concentration of $NiCl_2$ salt (0.0005 mol/l) into the reaction mixture, a PbS (I, Ni) film is formed with an average crystallite size of 100-150 nm of broken faceting, which are characterized by a fairly uniform microstructure. An increase in the concentration of nickel chloride to 0.004 mol/l is accompanied by an increase in the grain size up to 250-350 nm and secondary nucleation from the surface. The introduction of 0.008 mol/l $NiCl_2$ into the reaction mixture increases the uniformity of grains having a round shape with an average size of ~ 220-320 nm.

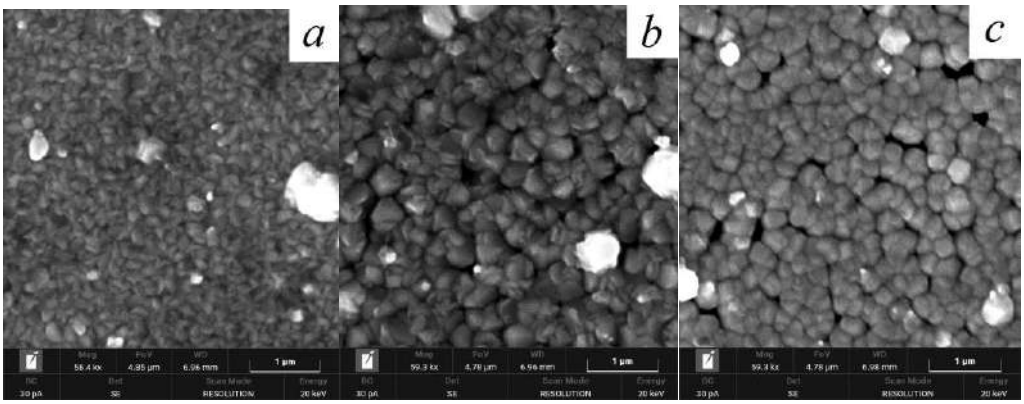

Figure 1. Micrographs of the PbS(I,Ni) thin-films scale 1.0 μm doped with $NiCl_2$ mol/l: 0.0005 (*a*), 0.004 (*b*), 0.008 (*c*).

References

[1] S. HOROZ , A. EKINCI , O. SAHIN, Journal of Ovonic Research Vol. 14, No. 3, 2018, P. 201 – 208

Photosensitive properties of $Cd_xPb_{1-x}S$ supersaturated solid solutions films

A.D. Selyanina[1]*, I.O. Selyanin[1,2], L.N. Maskaeva[1,3] and V.F. Markov[1,3]
[1]*Ural Federal University named after the first President of Russia B.N. Yeltsin, 28 Mira St., Yekaterinburg, 620002, Russia, n-kutyavina@mail.ru**
[2]*Institute of solid state chemistry of Ural Branch of Russian Academy of Sciences, 91 Pervomayskaya St., Yekaterinburg, 620990, Russia*
[3]*Ural State Fire Service Institute of Emergency Ministry of Russia, 22 Mira St., Yekaterinburg, 620137, Russia*

$Cd_xPb_{1-x}S$ solid solutions are well-studied materials for microelectronics with a variable bandgap (from 0.4 to 2.42 eV), which have found their application in various devices: from solar cells to infrared detectors. One of the simplest and most economical methods for the $Cd_xPb_{1-x}S$ thin films preparation is chemical bath deposition (CBD). This method assists in selecting the conditions for obtaining $Cd_xPb_{1-x}S$ films with optimal properties for specific devices. The advantage of chemically synthesized compounds based on the CdS - PbS system lies in the possibility of a wide variation of their functional properties depending on the composition, morphology, crystalline structure, the level of cadmium supersaturation of the solid solution, and the type of conductivity. All of the above parameters make it possible to "tune" the appearance of the photoemissive effect under illumination or a specific chemical activity to sensory processes in semiconductor layers.

Let us consider how the change in the reaction mixture composition of the studied films affected their photoelectric properties, in particular, on the dark resistance R_d and voltage sensitivity U_s under infrared irradiation. The volt photosensitivity of $Cd_xPb_{1-x}S$ solid solutions films deposited from reaction baths with concentrations from 0.01 to 0.04 mol/l $Cd(CH_3COO)_2$ increases approximately twofold according to the dependence in the figure. A further increase in the content of cadmium acetate to 0.08 mol/l in the reactor leads to a sharp drop in the voltage sensitivity of the studied layers. And it is absent in the film obtained at the maximal content of the cadmium salt (0.1 mol/l).

As for the dark resistance R_d, its dependence on the cadmium acetate content in the reaction bath is more complex: first, a monotonic increase from ~ 70 to ~ 350 MΩ per square is observed, and then it decreases to ~ 70 MΩ. A further sharp increase in Rd to 1000 MΩ per square of the film is associated with a significant content of the amorphous CdS phase besides the solid solution, according to the data of energy-dispersive and XRD analyzes.

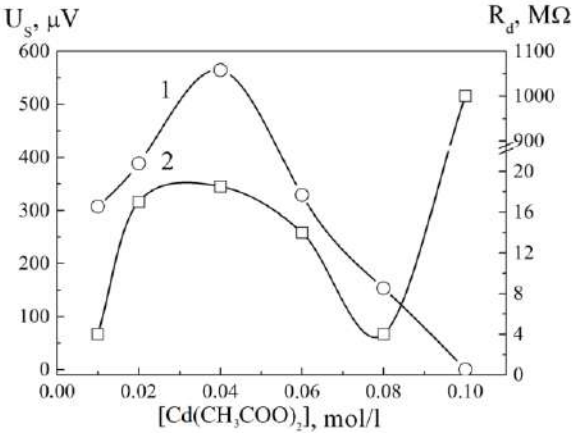

Dependence of voltage sensitivity U_s (1) and dark resistance R_d (2) of $Cd_xPb_{1-x}S$ solid solutions films on the $Cd(CH_3COO)_2$ content in the reaction bath

Acknowledgement

The research was carried out with the financial support of the Ministry of Science and Higher Education of the Russian Federation, project No FEUZ-2020-0058 (N687.42B.223/20) and RFBR grant 20-48-660041p_a.

INFLUENCE OF THE STRUCTURE AND PROPERTIES OF NANOMODIFIERS ON PHYSICAL AND MECHANICAL CHARACTERISTICS OF CORUNDUM CERAMICS

Shevchenok A.A.[1], Ulyanova T.M.[2], Bolodon V.N. [1] , Barayshuk S.M.[1], Kashaed E.A.[3], Kulbitskaya L.V.[2]
[1]*Belarusian State Agrarian Technical University, 99 Nezavisimosti Avenue. 220023, Minsk, Belarus,alexshev56@mail.ru*
[2]*Institute of General and Inorganic Chemistry of the National Academy of Sciences of Belarus, 9/1 Surganov str., 220072 Minsk, Belarus,*
[3]*Powder Metallurgy Institute of the National Academy of Sciences of Belarus, 41Platonov str. 220060 Minsk, Belarus*

Influence of high-disperse nanostructured modifiers of alumina - magnesia on processes of consolidation of the composite ceramics of industrial alumina oxide powders annealed at the temperature 1600-1700^{o}C, changes of its microstructure and physical-mechanical properties are investigated. The procedures of composite ceramics with improved physical-mechanical characteristics were developed.

The samples of ceramics have been prepared from micron alumina powder with nanostructured whiskers Al_2O_3 – MgO in ratio (wt.%) from 99.0:1.0 to 85.0:15.0 by mixing in planetary-type mill and static uniaxial pressing with the effort 500 MPa. Then the samples were annealed in the temperature region 1600-1700^{o}C. The nanostructured whiskers Al_2O_3 – MgO (99.5 : 0.5 mol.%) had 0.1-1.0 μm lengthwise and consisted of nanograins in 9-15 nm for θ-phase, and in 45-50 nm for α-corundum. The dependence of ceramics physical-mechanical properties on a content of modifying filler had parabolic character, and the sample with 10 wt. % nanostructured whiskers possessed higher level of properties in 1.5 – 2.0 times than ceramics from pure micron alumina powder.

It was established, that distribution of nanograins on borders of microparticles of alumina oxide powder arises due to the processes of self-diffusion of active modifiers. Moreover, nanostructured modifiers fill a pore space that causes both sliding of particles at mechanical and thermal loads of material and transfers the mechanism of fragile destruction to pseudo-plastic. The introduced nanostructured modifiers promote the process of lamellar zones formation in the volume of material and this in turn reinforces its mechanical properties.

Study of Transport Phenomenon in Amorphous Re_xSi_{1-x} Thin Films on the Both Sides of the Metal–Insulator Transition at Very Low Temperatures

A. El Oujdi[1], S. Dlimi[2], A. Echchelh[1], and A. El Kaaouachi[3],
[1] *Laboratory of Energetic Engineering and Materials, Faculty of Sciences Ibn Tofail, Kenitra, Morocco*
[2] *Physics department, Faculty of Sciences, Agadir, 80000 Morocco*
[3] *MPAC group, Faculty of Sciences, BP 8106, Agadir, 80000 Morocco*

In this work, we study the electrical conductivity behaviors on the both sides of the metal-insulator transition (MIT) in Re_xSi_{1-x} amorphous thin films at very low temperature. In fact, our investigation reanalyzed the experimental measurements of Re_xSi_{1-x} obtained by K.G. Lisunov et al. On the insulating side of the MIT, the electrical conductivity can be interpreted by the existence of the variable range-hopping regime. However, on the metallic side of the MIT, the electrical conductivity is mainly due to electron–electron interactions and low localization effects.

Keywords: transport phenomena, electrical conductivity, low temperatures, variable range hopping, metalinsulator transition

References

[1] A. Kawabata, solid state commun. 34, (1980) 431.
[2] L. Kleiman., Phys. Rev. 160, (1967) 585.
[3] D. G. Langreth, Phys Rev. 181, (1967) 753.
[4] A. El kaaouachi, R. Abdia, A. Nafidi, A. Zatni, H. Sahsah and G. Biskupski
Journal of American Institute of Physics USA, Vol 1219, Issue 1 (2010) pages 92-100.
[5] Mott. N. F, J. Non-Cryst. Solids 1 (1968) 1.
[6] Shklovskii. B.I., Efros. A.L., Electronic Properties of Doped Semiconductors, Springer, Berlin, (1984).
[7] L. R. Thoutam, J. Yue, P. Xu, and B. Jalan Phys. Rev. Materials 3, 065006 – Published 27 June 2019.
[8] Jin-XiaSui, Xiao-XiongWang, Xue-TongZhang, Wen-PengHan, ChaoSong, JingYu, Jia-qiChen, Huan-huanLiu, FengYuan, Yun-ZeLong, Journal of Magnetism and Magnetic Materials Vol 498, 15 March 2020, 166107
[9] T. Mori Journal of Solid State Chemistry Vol 275, July 2019, Pages 70-82
[10] P. R. Ghediya, T. K. Chaudhuri, and J. Ray Journal of Materials Science: Materials in Electronics vol 31, (2020) pages658–666.
[11] Altshuler B L and Aronov A G (1983) JETP Lett. 37 410
[12] B.L. Al'tshuler, A.G. Aronov, A.I. Larkin, D.E. Khmel'nitskii, Sov. Phys. JETP, vol 54, (1981) pp.411-419.

Positive magnetoconductivity and inelastic scattering time at low temperatures with magnetic field in InSb semiconductor

A. El oujdi[1], A. El kaaouachi[4,], S. Dlimi[2], L. Limouny[3] , B. Ait Hammou [d], M. El Hassan[1] , A. Echchelh[1], and J. Hemine[1]

In this work, we investigate the temperature dependence of the perpendicular electrical conductivity in presence of magnetic field of InSb sample measurements obtained by S. Abboudy [1]. First we determine the value of the critical magnetic field B_C for which the Metal Insulator Transition (MIT) occurs. On the metallic side of the MIT, we are interested in the study of positive magneto conductivity as a function of magnetic field by modeling it with complex theoretical models. The validity of these models is tested by calculating and comparing the inelastic scattering time τ_ε for each model used.

Keywords: Metal Insulator Transition, InSb, Positive magnetoconductivity, Inelastic scattering time, Magnetic field, Low temperatures.

References

[1] S. Abboudy, Journal of Philosophical Magazine B, Vol. 66, No.1, (1992) pp, 15-23.
[2] B. L. Altshuler, and A. G. Aronov, *JETP Lett.* 37 (1983) 410.
[3] Y. Isawa, J. Phys. Soc. Japan 53 (1984) 2865.
[4] A. Kawabata, Solid State Commun. 34 (1980) 432.
[5] A. Kawabata, Solid State Commun. 38 (1981) 823.
[6] P. A. Lee and Ramakrishnan, T V , Phys. Rev. B 26 (1982) 4009.
[7] A. El oujdi, S. Dlimi, A. Echchelh, and A. El kaaouachi, Journal of the Solid State, Vol. 62, No. 12, (2020) pp. 2445–2451.
[8] A. El kaaouachi, R. Abdia, A. Nafidi, A. Zatni, H. Sahsah and G. Biskupski
Journal of American Institute of Physics USA, Vol 1219, Issue 1 (2010) pages 92-100.
[9] A. Narjis, A.El kaaouachi, L.Limouny, S.Dlimi, A.Sybous, J.Hemine, R.Abdia,
G.Biskupski, Journal of Physica B Vol 406 (2011) pp 4155–4158.

Electrical transport phenomenon and Variable Range Hopping conduction in reduced graphene oxide/polystyrene composites

M. El Hassan[1*], A. El oujdi[1], A. El kaaouachi[2], S. Dlimi[3], L. Limouny[3], A.Echchelh[1] ,Asmaa Chakhmane[4], and B. ait Hammou[2]
[1]*Laboratory of Energetic Engineering and Materials, Faculty of Sciences Ibn Tofail, Kenitra, Morocco.*
[2]*MPAC group, Faculty of Sciences, BP 8106, 80000, Agadir, Morocco.*
[3]*Physics department, Faculty of Sciences, 80000, Agadir, Morocco.*
[4]*Electrical department, Faculty of Science and Technology Hassan II, Mohammedia, Morocco.*

In this work, we investigate the temperature dependence of the electrical conductivity of a two-dimensional reduced graphene oxide (RGO)/polystyrene (PS) composites. We re-analysed, in our investigation, the experimental measurements of RGO/PS composites with different RGO concentrations obtained by W. Park et al.[1]. We show using two different methods: the Zabrodskii method and a numerical method based on the calculation of the percentage deviation; that the electrical conductivity follows, at the beginning, the Efros-Shklovskii Variable Range Hopping regime (ES VRH) with $T^{-1/2}$. This behaviour showed that long range electron-electron interaction reduces the Density Of State of carriers (*DOS*) at the Fermi level and creates the Coulomb gap (CG). When the RGO concentration increases, we noticed that the temperature dependence of the electrical conductivity tends towards $T^{-1/3}$, which may suggest a possible crossover from ES VRH regime to the Mott VRH regime for high RGO concentration values. We also, calculated and represented the Density Of State (*DOS*) function $N(E)$ for each sample. We noted that the width of a parabolic function $N(E)$ and the parameter Δ representing the half of CG width increases by decreasing the RGO concentration.

Keywords Zabrodskii method · Density Of State · RGO/PS · Variable Range Hopping

References

[1] W. Park, J. Hu, L. A. Jauregui, X. Ruan, and Y. P. Chen, Journal of Applied Physics Letters 104, (2014) 113101.
[2] N.F. Mott, Journal of Non-Crystalline Solids 1 (1968) 1.
[3] N.F. Mott, Metal–Insulator Transitions, Taylor and Francis, London, (1974).
[4] B.I. Shklovskii, A.L. Efros, Electronic Properties of Doped Semiconductors, Springer, Berlin, (1984).
[5] A. El kaaouachi, A. Nafidi; G. Biskupski, Journal of Physica Status Solidi (b) (2004) vol. 241, N°1, 155-162
[6] Zabrodskii, A .G. and Zinoveva, K.N., "Low-temperature conductivity and metal insulator transition incompensate n-Ge,'' Sov. Phys. JETP 59, (1984) 425.
[7] Nguyen V. L., Phys. Lett. A, 207, (1995) 379.
[8] J. Liu, Q. Liu, W. Wang, Y. Liang, D. Lu, and P. Zhu, Journal of Physics and Chemistry of Solids, Vol :129, (2019). Pages 111-121.
[9] J. Xue, S. Huang, J. Y. Wang and H. Q. Xu , Journal of RSC Advances, 9, (2019). Pages 17885–17890 | 17885.
[10] H. Matsuura, A. Takeshita, T.Imamura, K. Takano, K. Okuda, A. Hidaka, S. Ji, K. Eto, K. Kojima, T. Kato, S. Yoshida and H. Okumura Japanese Journal of Applied Physics, Vol 58, N° :9, (2019) Pages 098004-1 : 098004-3.
[11] I. Rawal, and P. K.Goyal Journal of Solid State Sciences, Vol 99, (2020) Page 105984.
[12] A. El kaaouachi, R. Abdia, A. Nafidi, A. Zatni, H. Sahsah and G. Biskupski Journal of American Institute of Physics USA, Vol 1219, Issue 1 (2010) pages 92-100.

Study of electrical conductivity in metallic n-type InP semiconductor at low temperature in presence of strong magnetic field

D. Ennajih[1], A. El kaaouachi[2], A. Echchelh[1], A. El oujdi[1], E. Mounir[1], B. Ait Hammou [2], and S. Dlimi[3]
[1] *Laboratory of Energetic Engineering and Materials, Faculty of Sciences Ibn Tofail, Kenitra, Morocco.*
[2] *MPAC Team, Faculty of Sciences of Agadir, BP 8106, 80000 Agadir, Morocco.*
[3] *Physics Department, Faculty of Sciences of Agadir, BP 8106, 80000 Agadir, Morocco.*

We have studied the transport properties in metallic n-type InP semiconductor. We show that the dependence on temperature of metallic electrical conductivity obey to the law $\boldsymbol{\sigma = \sigma(T = 0) + mT^{1/2}}$. We have found that the coefficient of thermal variation *m* changes sign when the magnetic field increases. We have proposed several complex theories to provide a physical explanation for this sign change such as the Zeeman effect, the effects of weak localization and the effects of electron-electron interactions.

Keywords*:* Metal-Insulator Transition, low temperatures, strong magnetic fields, low localization effect, electron-electron interaction effects, metallic electrical conductivity, coefficient of thermal variation

References

[1] I. M. Percher, Y. Volotsenko, A. Frydman, B. I. Shklovskii, and A. M. Goldman, Phys. Rev. B **96**, (2017) 224511.
[2] H. K.Kyung, L. A. Samuel, H. Hans, K. Hojin, J. H. Sung, P. Min, E. Johnas, M. P Kasper, M. Satoshi, A. Kazuo, K. Sergey and W. P. Yung, Scientific Reports **8**(2018).
[3] S. Chaudhuri, P. A. Bhobe, and . A. K. Nigam, Journal of Physics: Condensed Matter **30**, Number 1 (2018).
[4] M. Pollak, and I. Riess, Journal of Physics C: Solid State Physics **9**, (2018) 12.
[5] O. Entin-Wohlman, Y. Gefen, and Y. Shapira, Journal of Physics C: Solid State Physics **16**, (2017) 7.
[6] N. F. Mott, Phil Mag **6**, (1961) 287.
[7] M. C. Maliepaard, M. Pepper and R. Newbury Phys. Rev. Lett. **61**, (1988) 369.
[8] P. A. Lee, T. V. Ramakrishman, Rev. Mod. Phys. 52 N(2) (1885) 287.
[9] B. L. Altshuler, A. G. Aronov, A. Larkin, and D. E. Khmelintski, Sov. Phys. J.E.T.P, 54, (2) (1981) p411.
[10] A. Kawabata, Solid. State. Commun, **34** (1980).
[11] Y. Isawa, J. Phys. Soc. Japan **53**, (1984) p 2856.
[12] D. G. Langreth, Phys. Review **181**, N°2, (1969) p 753.
[13] L. Kleinman, Phys. Review **160**, N°3, (1967) p 585.
[14] A. El Oujdi, S. Dlimi, A. Echchelh, and A. El Kaaouachi, Physics of the Solid State **62**, No. 12, (2020) pp. 2445–2451.
[15] A. El Oujdi, A. El Kaaouachi, A. Echchelh, B. Ait Hammou, R. Tiskatine and S. Dlimi, Physics of the Solid State **62**, No. 5, (2020) pp. 885–890.

Influence of magnetic field on transport phenomena and scale laws in metallic n-type InP

D. Ennajih[1*], A. El kaaouachi[2], A. Echchelh[1], A. El oujdi[1], and S. Dlimi[3]
[1] *Laboratory of Energetic Engineering and Materials, Faculty of Sciences Ibn Tofail, Kenitra, Morocco.*
[2] *MPAC Team, Faculty of Sciences of Agadir, BP 8106, 80000 Agadir, Morocco.*
[3] *Physics Department, Faculty of Sciences of Agadir, BP 8106, 80000 Agadir, Morocco.*

We have studied the transport properties in metallic n-type InP semiconductor. We show that the dependence on temperature of metallic electrical conductivity obey to the law $\sigma = \sigma(T = 0) + mT^{1/2}$. We highlight the absence of a minimum electrical conductivity σ_{min} proposed by Mott at the metal insulator transition (MIT). We show that the conductivity at temperature $T = 0K$, $\sigma(T = 0)$, follows a scaling law as a function of the effective parallel and perpendicular Bohr radii $a_{\parallel}$ and $a_{\perp}$.

Keywords*:* Metallic side of Metal-Insulator Transition, low temperatures, strong magnetic, scale theory, effective parallel and perpendicular Bohr radii $a_{\parallel}$ and $a_{\perp}$.

References

[1] Altshuler B L and Aronov A G JETP Lett. (1983) 37 410.
[2] Abrahams E., Anderson P. W., Lucciardelo D. C.; and Ramakrishnan T. V. Scaling Theory of Localization: Absence of Quantum Diffusion in Two Dimensions. Phys. Rev. Lett, 42 (1979). p 673.
[3] El oujdi A., Dlimi S., Echchelh A., and El kaaouachi A. Study of Transport Phenomenon in Amorphous RexSi1–x Thin Films on the Both Sides of the Metal–Insulator Transition at Very Low Temperatures. Physics of the solid state, Vol 62(12) (2020) 2445-2451.
[4] Mott, N. F. The transition to the metallic state. Phil Mag. Volume 6 (62) (1961) 287-309.
[5] Rosenbaum T. F., Andres K., Thomas G. A., and Bhatt R. N. Phys. Rev. Lett, Vol 45, N°21 (1980) p1723.

Morphological features of thin-film PbS (Mn) and PbS (Mn, I)

Beltseva A.V. [1*], Pozdin A.V. [1], Maskaeva L.N. [1,2]
[1]*Ural Federal University named after the First President of Russia B.N. Yeltsin, Yekaterinburg, 620002 Russia, e-mail: avbeltseva@mail.ru**
[2] *Ural Institute of State Fire Service, Emergency Ministry of Russia, Yekaterinburg, 620062 Russia.*

The nanoscale design of quantum dots and nanocrystals due to the controlled incorporation of dopants is an area of fundamental research, the interest in which is due to its potential application to numerous breakthrough technologies. In particular, ions of 3d transition metals (Mn, Fe, Co, Ni), due to the configuration of electronic d-shells, can provide PbS layers with magnetic properties that are relevant for innovative applications from bio-visualization [1] to spintronics [2]. Such additives can lead to a change in the physical properties due to a decrease in the size of lead sulfide particles to the nanoscale, since when the crystallite size approaches the exciton size (~ 18 nm) in PbS due to the size effect, a blue shift of the absorption edge occurs.

Therefore, in this work, the evolution of the morphology of thin-film PbS (Mn), PbS (Mn, I) layers obtained by introducing a donor in the form of Mn^{2+} ions into the reaction mixture is considered, and for comparison, simultaneously with manganese, an acceptor in the form of I deposition. The reaction mixture contained constant concentrations of lead acetate $Pb(CH3COO)_2$, sodium citrate $Na_3C_6H_5O_7$, ammonium hydroxide NH_4OH, thiocarbamide $(NH_2)_2CS$ with varying manganese chloride from 0.05 to 0.15 mol / l - PbS (Mn) films. For comparison, a fixed concentration of ammonium iodide NH_4I, PbS (Mn, I) films, was introduced into the discussed reaction mixture. In the synthesized PbS (Mn, I) films, nanoscale particles are predominant, the fraction of which sharply increases to 99 (0.05 mol/l) and 97 (0.1 mol/l), decreasing to 87% (0.015 mol/l). The fraction of nanodispersions in the structure of the discussed PbS (Mn,I) films is quite large.

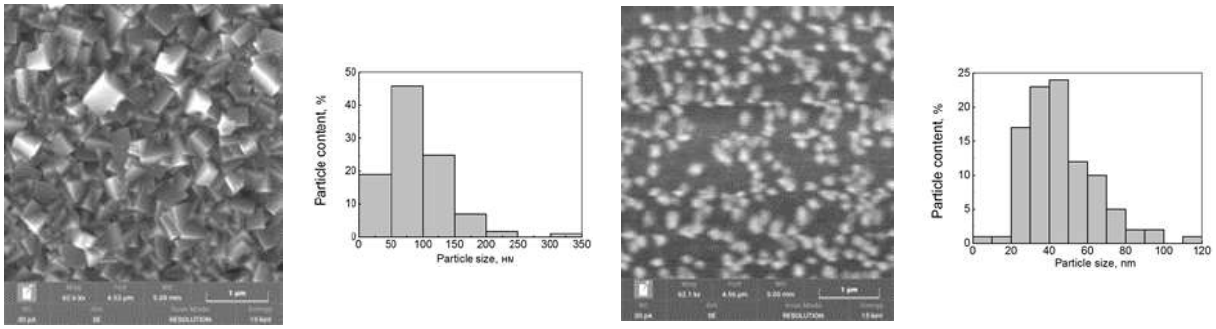

a b

Figure. Microimages of PbS (Mn) (a) and PbS (Mn, I) (b) films and histograms of particle size distribution

Thus, as a result of the introduction of an ammonium salt into the reaction mixture of iodide, nanoparticles appeared, and the introduction of $MnCl_2$ promotes an increase in nanodispersions to 87-99%, which should affect the optical and functional properties of the synthesized thin-film layers.

References

[1] J. Huang , X. Zhong , L. Wang , L. Yang , H. Mao , Theranostics 2012 , 2 ,86 .
[2] D. A. Bussian , S. A. Crooker , M. Yin , M. Brynda , A. L. Efros ,V. I. Klimov , Nat. Mater. 2009 , 8 , 35 .

Synthesis of water-dispersible metal sulfide nanoparticles by chemical bath deposition

N.S.Kozhevnikova[1,2]*
[1]*Institute of Solid State Chemistry, UB RAS, Pervomayskaya str., 91, Ekaterinburg, 620990, Russia, e-mail: kozhevnikova@ihim.uran.ru**
[2]*Ural Federal University of the first President of Russia B. N. Yeltsin. Mira St., 19, Ekaterinburg, 620002, Russia,*

During the past decade the synthesis of semiconductor nanoparticles has become a major field of research due to their unique chemical, optical and electronic properties. The quantum confinement provides molecular-like discrete energy levels, and the semiconductor band gap exhibits strong size dependence. Numerous methods have been developed for the production of M_xS_y nanoparticles (NPs) and quantum dots (QDs). The organometallic approach and its alternatives, based on the high temperature decomposition of organometallic precursors into well-stirred and hot organic solvents, generally provide the best quality QDs.[1] However, for many biological applications, the transfer of QDs to water through a capping ligand exchange is necessary. Some chemicals used in this route are extremely toxic, pyrophoric and/or expensive. In parallel with the success of organic synthetic routes, aqueous routes have also been developed. The problems associated with phase transfer could be avoided by direct synthesis in an aqueous medium.[2]

In this work, we developed a convenient one-pot method for the synthesis of M_xS_y NPs and QDs (CdS, PbS, Cu_2S, Ag_2S) directly in aqueous solution by simply mixing metal salt, sulfur agent, and capping ligand.

The synthetic parameters affecting the growth and the aggregation and sedimentation stability of M_xS_y NPs, such as the metal salt/sulfur and stabilizing agent/ligand ratios, precursor concentrations, and pH were established. The aggregate stability of hydrophobic CdS, PbS, and Ag_2S NPs in aqueous solutions was found to be determined by the adsorption-solvation stability factor. The coordination bonds between the stabilizing agent and the surface atoms of the colloidal NP prevent the process of particle aggregation in aqueous media. As shown in Fig., M_xS_y monomers are involved in the processes of M_xS_y QDs nucleation and growth. Ostwald ripening results in the growth of large particles from reactions among smaller particles, leaving the total number of particles the same. Ostwald ripening should result in a broadening of the nanoparticle distribution over time and an increase in the number of large particle at the expense of a decrease in the number of smaller particles. The present one-pot approach may provide a more simplified, environmental friendly and low-cost synthesis approach, which would have potential advantages in preparing high-quality semiconductor NPs with desired sizes for both fundamental research and industrial applications.

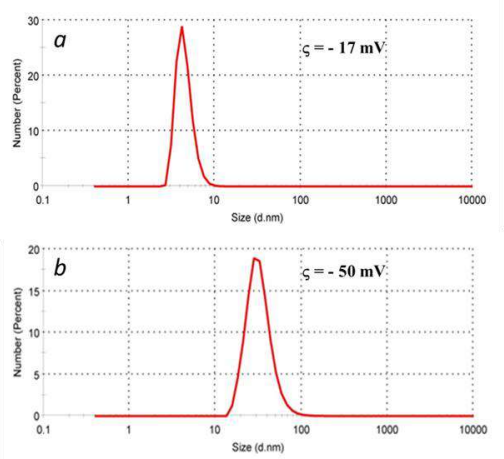

Fig. Size distribution of Ag_2S QDs in colloid solution at the first 2 days (a) and after 70 days after synthesis (b)

References

[1] X.Peng, J.Wickham, A.P.Alivisatos, J. Am. Chem. Soc. 120 (1998) 5343-5344.
[2] A. Aboulaich, D. Billaud, M. Abyan, L. Balan, J.-J. Gaumet, G. Medjadhi, J. Ghanbaja, R. Schneider, ACS Appl. Mater. Interfaces. 4 (2012) 2561−2569.

Formation regularities of the AlN crystalline phase on the sapphire surface by molecular beam epitaxy technique

D. Milakhin[1]*, T. Malin[1], V. Mansurov[1], Yu. Galitsyn[1], and K. Zhuravlev[1,2]
[1]*Rzhanov Institute of Semiconductor Physics of SB RAS, 13 Lavrentiev Aven., Novosibirsk, 630090, Russia, dmilakhin@isp.nsc.ru**
[2]*Novosibirsk State University, 1 Pirogova Str., Novosibirsk, 630090, Russia*

The problem of epitaxial growth of III-nitrides on a sapphire (Al_2O_3) substrates is associated with a number of technological difficulties due to the large mismatch of the lateral parameters of the crystal lattices of the grown AlN layer (a_{AlN} = 3.11Å) and the Al_2O_3 substrate (a_{Al2O3} = 4.76Å), equal to ~53%, as well as the thermal expansion coefficients of AlN ($4.2 \cdot 10^{-6} K^{-1}$) and sapphire ($7.0 \cdot 10^{-6}$ K^{-1}). To match the lattice parameters of III-nitrides and sapphire, a thin layer of crystalline AlN is formed by chemical transformation of the Al_2O_3 surface during exposure of the heated substrate to an active nitrogen flux. This process is called nitridation. The crystalline perfection of the AlN layer formed as a result of nitridation process affects the surface morphology, deformation and concentration of defects, and also sets the polarity of the subsequent epitaxial layers. Therefore, it can be concluded that the success of the implementation of the entire heteroepitaxial structure depends on such process. Thus, the sapphire nitridation process requires detailed study.

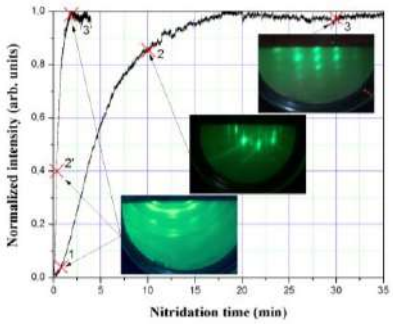

The formation of the AlN buffer layer at different degrees of nitridation process completeness

Although in recent years, active research has been carried out in this field of the initial stage of the AlN semiconductor structures formation on sapphire, namely: it was investigated at which form of sapphire surface (reconstructed ($\sqrt{31} \times \sqrt{31}$) R ± 9 ° or unreconstructed (1 × 1)) should be performed the nitridation process to obtain a AlN crystalline layer [1,2], the nitridation kinetics of the sapphire substrate under different initial conditions - the ammonia flux and the substrate temperature [3,4] and the influence of the reflection high energy electron diffraction technique (RHEED) on the nitridation process was explored [5], there are still many actual problems in this field.

In this work, using the RHEED technique, the completeness degree of sapphire nitridation was investigated, taking into account the electron beam influence on the sapphire nitridation process. It was found that ~ 85% completeness of the crystalline AlN phase formation on the sapphire surface promotes the growth of a two-dimensional AlN buffer layer with a smooth surface morphology and metallic polarity, in contrast to the AlN growth without nitridation or with excessive sapphire nitridation, in which polycrystalline and three-dimensional AlN structures are formed, respectively (figure). Independent methods of IR spectroscopy and X-ray photoelectron spectroscopy were used to determine the thickness of the AlN nucleation layer at ~ 85% completeness degree of nitridation process, wich was ~1 monolayer.

Acknowledgement
The work was carried out within the framework of the state assignment 0306-2019-00008 "Heterostructures based on A_3B_5 materials for microwave electronics and microwave photoelectronics".

References
[1] D. Milakhin, T. Malin, V. Mansurov, Yu. Galitsyn, A. Kozhukhov, D. Utkin, and K. Zhuravlev, Appl Surf Sci. 541 (2021) 148548.
[2] D. Milakhin, T. Malin, V. Mansurov, Yu. Galitsin, and K. Zhuravlev, Semiconductors 49 (2015) 905–910.

[3] D. Milakhin, T. Malin, V. Mansurov, Y. Galitsyn, and K. Zhuravlev, J. Therm. Anal. Calorim 133 (2018) 1099.
[4] D. Milakhin, T. Malin, V. Mansurov, Yu. Galitsyn, and K. Zhuravlev, J Phys Conf Ser. 1851 (2021) 012005.
[5] D. Milakhin, T. Malin, V. Mansurov, Yu. Galitsyn, and K. Zhuravlev, Phys. Status Solidi B 256 (2019) 1800516.

EFFECT OF BATH TEMPERATURE ON STRUCTURAL AND OPTICAL PROPERTIES OF PVA CAPPED SnS NANOCRYSTALLINE FILMS GROWN BY CBD PROCESS

P. Mallika Bramaramba Devi and K.T. Ramakrishna Reddy*
Solar Energy Laboratory, Department of Physics, Sri Venkateswara University, Tirupati 517502, India.
** Corresponding author mail id: ktrkreddy@gmail.com*

Polyvinyl alcohol (PVA) capped tin monosulphide (SnS) films were successfully deposited on glass substrates at four different bath temperatures varying from 50 °C to 80 °C using a simple and low-cost technique, chemical bath deposition (CBD). The precursors used to synthesize PVA capped SnS nanocrystalline layers were stannous chloride ($SnCl_2$, $2H_2O$) and thioacetamide (C_2H_5NS) with tartaric acid ($C_4H_6O_6$) as a complexing agent and polyvinyl alcohol $[-CH_2CHOH-]_n$ as a capping agent. The structural behaviour of the deposited layers was studied using Raman spectra, recorded at room temperature. Raman peaks observed at lower bath temperatures (< 70 °C), corresponds to SnS phase in addition to its secondary phases such as Sn_2S_3 and SnS_2. The Raman peaks observed for the layers deposited at higher bath temperatures (≥ 70 °C) had shown pure SnS phase without any secondary phases. Also, the intensity of Raman peaks is highest for the layers deposited at 80 °C, indicated high crystallinity related to the other layers. The optical investigations showed a higher optical absorption coefficient (~ 10^5 cm^{-1}) for the layers deposited at 80 °C than the other layers ($T_b \leq$ 70 °C). A blue shift in optical band gap values was observed, that varies from 1.92 eV to 1.55 eV with the increase of bath temperature, might be due to the existence of quantum confinement effect in the deposited layers. The average particle size estimated using Brus equation, varied slightly from 5 nm to 8 nm. The other optical parameters such as refractive index, extinction coefficient, high frequency dielectric constant, optical carrier concentration, relaxation time and optical conductivity were also determined. The layers deposited at 80 °C exhibited high optical conductivity (~ 10^{16} s^{-1}) compared to other deposited layers, hence, such layers might be useful as an absorber layer in solar cell development.

Thermodynamic assessment of the possibility of formation of $Cu_xPb_{1-x}S$ Solid Solutions by hydrochemical deposition and their application

A.V. Pyastolova[1*], A.V. Pozdin[1], L.N. Maskaeva[1,2]
[1]*Ural Federal University named after the First President of Russia B.N. Yeltsin, Yekaterinburg, 620002 Russia, e-mail: andrej.pozdin@yandex.ru**
[2] *Ural Institute of State Fire Service, Emergency Ministry of Russia, Yekaterinburg, 620062 Russia.*

Under normal conditions PbS - compound of $A^{IV}B^{VI}$ group is a direct narrow-gap semiconductor with bandgap width from 0.4 to 0.49 eV, therefore, it absorbs visible and near-infrared light. Cu_2S, a compound of group $A_2^{IV}B^{VI}$, is a degenerate p-type semiconductor with a significant fraction of ionic conductivity and with a bandgap from 1.2 eV to 2.5 eV.

Lead is partly replaced by copper in the PbS crystal lattice, allowing smooth adjustment of the parameters and spectral sensitivity range. PbS-Cu_2S thin films have a heterojunction in which a photon can be absorbed by both components of the system, which has a useful effect on the photovoltaic properties, which means that it appears possible to use these thin films effectively in solar cells. And also in displays, electronics, and optoelectronics.

To determine the concentration area of joint formation of lead and copper (I) sulfides, we calculated the boundary conditions of formation in the systems «$PbAc_2$ -CuCl - Na_3Cit- NH_4OH - CH_4N_2S» (Figure) by the method suggested in [1].

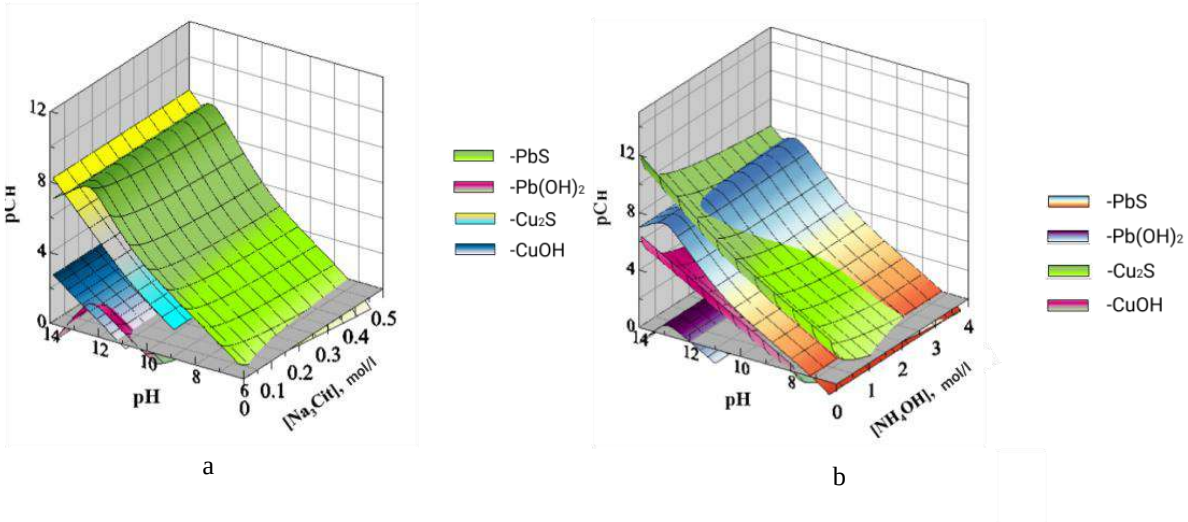

Figure. Boundary conditions of solid phase formation PbS, Cu_2S, $Pb(OH)_2$, CuOH in the system «$PbAc_2$ -CuCl - Na_3Cit- NH_4OH - CH_4N2S» from pH environment and concentration of ligands: citrate-ions (a) and ammonia-ions (b).

The concentration regions of the $Cu_xPb_{1-x}S$ solid solution formation are located below the Cu_2S plane at pH =10.1-13.5 (a) and pH = 8-11.5. (b). In these two systems there is a probability of formation of impurity phases $Pb(OH)_2$ and CuOH.

[1] L.N. Maskaeva, E.A. Fedorova and V.F. Markov, Thin Film and Coating Technology. Ural Federal University. - Yekaterinburg : Ural Federal University, 2019. - 236 c.

Laser spectroscopy of bio-suspensions

O. Khasanov[1], R. Rusetski[1], K. Pistsova[2], O. Fedotova[1*], A. Bugay[3], S. Nikolic[4], and A. Kovacevic[4]
[1]*SPMRC of NASB, P. Brouki 19, Minsk 220072, Belarus, <eowynknight@gmail.com>*
[2]*Belarusian State University, Nezalezhnasci Ave. 2, Minsk 220030, Belarus*
[3]*JINR, Joliot Curie 6, Dubna 141980, Moscow region, Moscow, Russia*
[4]*Institute of Physics, University of Belgrade, Pregrevica 118, 11080 Belgrade, Serbia*

Solution of challenge problem of laser pulse penetration into biological tissues and suspensions allows to elaborate reliable techniques of deep tissue imaging and noninvasive diagnostics including laser spectroscopy [1, 2]. The laser radiation acts on a microparticles with a gradient force directed along the gradient of the field intensity and moving them towards the high intensity area. Even if the refractive index of particles is slightly larger than the refractive index of the liquid, as in the case of a suspension of cyanobacteria [1], self-channeling of laser radiation in the suspension may occur. Dynamic equilibrium is achieved through the competition between optical pressure gradients and particle diffusion due to Brownian motion.

The gradient force originated from the interaction of the electrical component of light with the induced dipole moment of the bioparticle depends on particle polarizability, which can be complex quantity due to particle absorption ans may prevail over the Coulomb effect. Optical nonlinearity of biological suspensions mediated by optical forces is of a concentration origin and may focuse laser radiation like Kerr nonlinearity. The viscosity of liquid affects the particle movement and its mobility in the gradient force field. Another optical force responsible for laser radiation self-guiding in suspension is the scattering force (especially forward). It can also contribute to medium nonlinearity.

In this work we study laser beam propagation in biological suspensions mediated by optical forces, including light absorption. The model is based on modified nonlinear Schrödinger equation coupled with diffusion-convection equation. The parameters of suspension and radiation are altered in wide range. It was found that under the action of the transverse components of the gradient force, the bioparticles are aligned along the beam axis, moving along it under the action of the longitudinal component of the gradient force. The magnitude of the gradient force depends on the size of the microparticle, its polarizability, as well as on the radius and intensity of the laser beam. The magnitude of the forward scattering force depends on the laser intensity and wavelength, as well as on the polarizability of the particle. The particles move under the action of the scattering force, which leads to their movement into the field region with a higher intensity, where the pressure force is greater, which creates an additional acceleration of the particles. The combined action of the Brownian motion of microparticles and the scattering force prevents the accumulation of particles on the axis of the laser beam, contributing to their concentration near the beam axis. The width of this section grows with an increase in the intensity of Brownian motion. The combined effect of diffusion and light pressure forces leads to the formation of a waveguide for laser radiation in a suspension of microparticles.

Acknowledgement
This study was supported by the Belarusian Republican Foundation for Fundamental Research (project F20SRBG-007)

References
[1] A. Bezryadina et al. Phys. Rev. Lett. 119 (2017) 058101.
[2] R. Gautam et al. Nature, Light: Science and applications 8 (2019) 31

Effect of the chalcogenizer on the boundary conditions for the formation and micro- and nanostructured films of PbS

Pimina A.V[1], Markov E.[2], étudiante (2070035), Maskaeva L.N[1].
[1] *Federal State Autonomous Educational Institution of Higher Education «Ural Federal University named after the first President of Russia B.N.Yeltsin», Russia, Ekaterinburg, Mira 28, Anyapi1856@gmail.com*
[2] *Collège de Bois-de-Boulogne, Montréal, QC, Canada*

Thin films of PbS are narrow gap semiconductor of II-VI compounds with band gap E_g=0.41 эВ (400K) and high photosensitivity in near infrated region that allow to use it as colar energy converters, sensors, infrated detectors, fire detection sensors. Researchers prefer to obtain this compound by chemical bath deposition which has a significant advantages for industrial adaptation. Traditional chemical bath includes lead salt, complexing agent and chalcogenizer. Thiourea is used in most publications as chalcogen source, less often thioacetamide but there are other supplies of sulfur ions.

Therefore this is dedicated to thermodynamic assement of the possibility of obtaing a PbS films by chemical deposition using as chalcogenizer thiourea CH_4N_2S, thioacetamide C_2H_5NS, allylthiourea $C_4H_8N_2S$ and on based on analysis of ionic equilibria with experimental verification of the results. The deposition of PbS using thiourea as an example in alkaline solution in the presence of a ligand can be written as:

$$PbL^{2+} + N_2H_4CS + 2OH^- = PbS\downarrow + L + H_2CN_2 + 2H_2O$$

Thermodynamic assesment of the boundary conditions of deposition of solid phases of PbS and $Pb(OH)_2$ performed in the system «$PbAc_2$ – L – N_2H_4CS (C_2H_5NS, $C_4H_8N_2S$) – OH^- » is shown in the figure. Concentration area located between the planes of boundry formation of PbS and $Pb(OH)_2$ corresponds only to PbS. In the area below the surface responsible for the onset of $Pb(OH)_2$ deposition, it becomes possible to form also lead hydroxide.

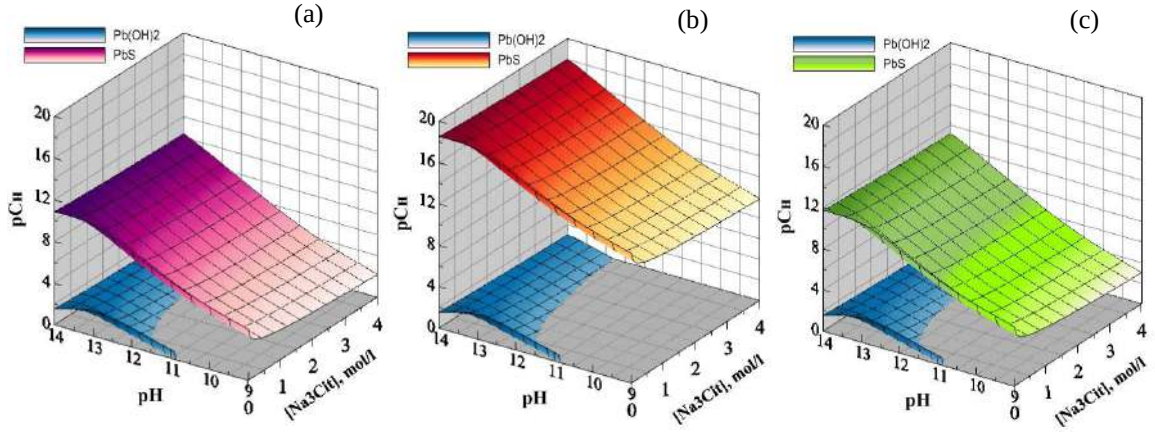

Figure. Boundary conditions for the formation of PbS and $Pb(OH)_2$ depending on the pH of the environment and concentration of CH_4N_2S(a), C_2H_5NS(b), $C_4H_8N_2S$(c). Based on calculations and preliminary experiments, reaction mixtures were formed to obtain micro- and nanostructed PbS.

Based on thermodynamic calculations and preliminary experiments on chemical deposition, reaction mixtures were formed to obtain micro- and nanostructed PbS using different chalcogenizer.

Upconversion nanoparticles for solution of optogenetics problems

D. Klezovich[1], K. Pistsova[1], A. Pashkevich[2], Ya. Gorbach[3],
O. Khasanov[4], O.Fedotova[4], D. Zharkov[5]
[1]*Belorusian State University, Nezavisimosti av. 4, 220030, Minsk, Belarus,*
[2]*Research Institute for Nuclear Problems of BSU, Bobruyskaya 11, 220030, Minsk, Belarus*
[3] *Grammar school 19, Zolotaya Gorka 18/2, Minsk. 220089, Belarus*
[4]*Scientific-practical materials research centre, 19 P. Brovky, Minsk, 220072, Belarus*
[5]*Zavoisky Physical-Technical Institute KSC RAS , Sibirsky tract 10/7, 420029, Kazan, Russia*

The use of upconversion nanoparticles for optogenetics is a new topical direction of research. Optogenetic technology is as follows: the required light-sensitive protein is selected and delivered to a specific group of cells. Then, it must be stimulated selectively using optical methods to treat non-invasively with its help these cells. Optogenetics opens up unique opportunities for studying neural networks and selectively affecting neural connections. Selectivity opens up possibilities for the treatment of still incurable diseases, such as Alzheimer's disease. However, there are still many unresolved problems. First, the use of visible light is necessary. Currently, the most common approach is the activation of the channel rhodopsin ChR2 by visible light [1]. However, stimulation of neurons in optically opaque living tissues is still an invasive method that requires the introduction of an optical fiber [2]. The need for non-invasive optical methods for stimulating nerve cells can be met by using upconversion biologically and chemically inert and non-toxic nanoparticles capable of realizing a safe and high-precision method for exciting ion channels of neurons. Thus, to improve the elemental base of optogenetics, not only a systematic search is required, but also the development of synthesis technology and methods for characterizing actual nanoparticles, as well as detailed studies of their upconversion and kinetic properties, which will enable neurons to be activated with minimal risk of unwanted side effects.

In this work, we discuss the results of the synthesis and the upconversion properties of yttrium orthovanadate nanocrystals doped with rare-earth ions Yb^3 and Er^{3+}. Within the framework of the Judd-Ofelt model, the intensities of transitions in the spectra of rare-earth ions are calculated. The mechanisms of energy transfer between impurity ions and their efficiency, as well as the effect of the matrix on the positions of the maxima of the luminescent lines are investigated. The dependence of the luminescence intensity on the method and temperature regime of synthesis, the composition of the matrix, the size and shape of nanoparticles, and also on the concentration of rare-earth ions is analyzed.

The paper also evaluates the prospects for using semiconductor quantum dots with a large intrinsic dipole moment. As shown earlier, in such materials, the intrinsic dipole moment can parametrically excite signals at multiple frequencies in the photon echo mode. The features of echo-responses at multiple frequencies, their phase-matching conditions, as well as the nature of the processes underlying the parametric generation of these signals are analyzed.

References

[1] M. Pochechuev et al.. Journal of biophotonics, Vol. 11 (2018), p. e201600203.
[2] M. Pochechuev, et al. Journal of biophotonics, Vol. 11 (2018), p. e201700106.

Calculation of the concentration of centers responsible for photoluminescence in the visible range in heavily doped AlGaN: Si layers

I. V. Osinnykh[1,2*], I. A. Aleksandrov[1], and K. S. Zhuravlev[1,2]
[1]*Rzhanov Institute of Semiconductor Physics of the Siberian Branch of the Russian Academy of Sciences, Novosibirsk, 630090, Russia, igor-osinnykh@isp.nsc.ru*
[2]*Novosibirsk State University, Novosibirsk, 630090, Russia*

$Al_xGa_{1-x}N$ alloys have emerged as important materials for high- power electronics and deep UV light sources (light emitting and laser diodes). The creation of effective light-emitting devices is impossible without doping the epitaxial layers. The formation of epitaxial *n*-GaN and Ga-rich $Al_xGa_{1-x}N$ layers using silicon (Si) as a donor does not cause significant difficulties. However, doping of $Al_xGa_{1-x}N$ becomes less efficient with an increase in Al content (x) higher than x>0.6. The electron concentration becomes significantly lower than the concentration of silicon atoms due to the self-compensation of Si donors. It is assumed that vacancies or their complexes also lead to the appearance of intense broadband photoluminescence (PL) in the visible spectral range, which was observed in $Al_xGa_{1-x}N$ epitaxial layers with a mass fraction of Al> 0.6 with strong doping with silicon [1]. The aim of this work was to establish the elemental composition of the centers of this luminescence in AlN.

The Si, C, and O impurity concentrations in Si doped AlN about 1.5×10^{20}, 8×10^{19}, and 4×10^{19}, cm^{-3}, respectively, were estimated by secondary-ion mass spectrometry (SIMS), using a IMS7f (CAMECA) setup with primary Cs^+ ions. The defect concentrations were calculated in the thermodynamic equilibrium model. The defect formation energies were calculated using the density functional theory (DFT) with hybrid functional HSE with modified fraction of Hartree-Fock exchange □=0.33 in Quantum ESPRESSO software package. Details of the DFT calculation of the formation energies are described in Ref [2].

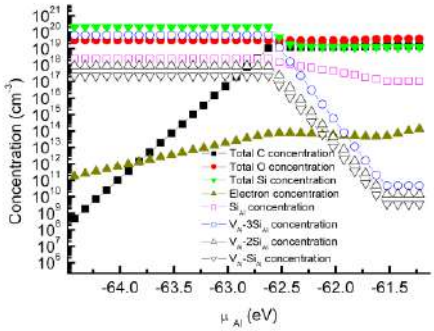

Calculated dependences of C, O, Si, V_{Al}-nSi_{Al} and electron concentrations on Al chemical potential

The defect types included in the calculation of the defect concentrations are intrinsic defects in AlN, C-, O- and Si- containing defects and complexes, which were considered in Ref [2]. The Al chemical potential was related to partial pressures. Chemical potentials of C, O, Si were obtained in such a way that the total concentrations of these elements corresponded to measured values. The concentration of V_{Al}-3Si_{Al} is 4×10^{19} cm^{-3} that an order of magnitude higher than concentration of donors Si_{Al}. According to calculations the luminescence maximum position for band to eA transitions for V_{Al}-3Si_{Al} should be about 3.56 eV that higher than the obsereved PL maximum position 3.0 eV. Another complexes V_{Al}-1Si_{Al} and V_{Al}-2Si_{Al} should have luminescence maximum positions close to 3.0 eV, but the concentration of V_{Al}-1Si_{Al} 2×10^{17} cm^{-3} is much lower than the concentration of V_{Al}-2Si_{Al} 9×10^{17} cm^{-3}. Therefore V_{Al}-2Si_{Al} is most likely candidate for the acceptor.

References

[1] P. A. Bokhan, P. P. Gugin, Dm. E. Zakrevsky, K. S. Zhuravlev, T. V. Malin, I. V. Osinnykh, V. I. Solomonov, and A. V. Spirina , J. Appl. Phys. 116 (2014) 113103.
[2] I.A. Aleksandrov, and K. S. Zhuravlev, J. Phys.: Condens. Matter 32 (2020) 435501.

Thermal annealing of germanium nanowires: structure and optical properties

A.Pavlikov[1,2,3]*, A.Sharafutdinova[2], I. Gavrilin[1,4], V. Zaytsev[2], A.Dronov[1,2]*, S. Gavrilov[1]
[1]*National Research University of Electronic Technology – MIET, Bld. 1, Shokin Square, Zelenograd, 124498, Russia, e-mail: dronov.alexey@org.miet.ru**
[2]*Faculty of Physics, M.V. Lomonosov Moscow State University, Leninskie Gory, Moscow 119991, Russia*
[3]*National Research Centre "Kurchatov Institute", Kurchatov sq., 1, Moscow, 123182, Russia*
[4]*Frumkin Institute of Physical Chemistry and Electrochemistry Russian Academy of Sciences, 31, bld.4, Leninsky prospect, Moscow, 119071, Russia*

Due to unique electrophysical and optical properties Germanium nanowires (Ge NW) have a wide range of application. Ge NW can be used in Li- and Na- ion batteries, thermoelectricity, photodetectors and sensors. Recently, the possibility of electrochemical deposition of Ge NW from aqueous solutionsusing particles of low- melting metals (Ga, In etc.) at nearly room temperature has been demonstrated. The structures obtained by this method showed excellent electrochemical characteristics in Li- and Na- ion batteries. Along with this, recent Raman spectroscopy studies of such Ge NW demonstrated irreversible changes in the spectral line shape, indicating a structural transformation due to intense exciting radiation.[1, 2] This structural change can be associated with strong heating of Ge NW due to their low thermal conductivity. In current study as-prepared amorphous Ge NW were crystallized under the action of probe laser radiation. The crystallization thresholds for the as-prepared sample were found to be 10 W/cm^2 at 633 nm and 375 2 W/cm^2 at 488 nm. Specular reffiection in the near IR and visible ranges decreases with decreasing wavelength were observed due to the increasing contribution of difiuse reffiection and absorption in the Ge NW layer. According to our estimates, the absorption coefficient of as-prepared sample at a wavelength of 488 nm is 1.7 times lower than at a wavelength of 633 nm. This results in stronger heating when excited with a He-Ne laser and a lower crystallization threshold. The estimated crystalline volume fraction demonstrate, that annealing in a vacuum oven at 300 ^{o}C and 600 ^{o}C leads to partial crystallization of Ge NW which retain their morphology. However, annealing at 600 ^{o}C made the studied nanostructures more resistant to the thermal effect of probe laser radiation. Annealing at a temperature of 600 ^{o}C also leads to lower red light absorption in Ge NW as compared to annealing at 300 ^{o}C, as a result of which the crystalline volume fraction practically does not change during the entire time of He-Ne laser probing. The heating of the Ge NW can lead to irreversible effects in the structure and, as a consequence, to a change of the electrochemical characteristics. In turn, annealing at 600 ^{o}C can make the studied nanostructures more resistant to heat.

Thus, the comparative study of the heat treatment effect on structural and optical properties of germanium nanowires obtained by electrochemical deposition from an aqueous solution are presented. The obtained results will be useful for the development of various devices (metal-ion batteries, photodetectors, sensors, etc.) based on Ge NW obtained by the ec-LLS method.

Acknowledgement
The work was supported by the Russian Science Foundation (project no. 20-19-00720).

References.

[1] S. Gavrilov, A. Dronov, I. Gavrilin, R. Volkov, N. Borgardt, A. Trifonov, A. Pavlikov, P. Forsh, P. Kashkarov, J Raman Spectrosc, 49, 5 (2018), 810–816
[2] A. Pavlikov, P. Forsh, P. Kashkarov, S. Gavrilov, A. Dronov, I. Gavrilin, R. Volkov, N. Borgardt, S. Bokova- Sirosh, E. Obraztsova, J Raman Spectrosc, 51, 4 (2020), 596–601.

AlSb/InAs heterostructures for HEMT transistors

M. Sukhanov[1*], K. Zhuravlev[1,2], A. Bakarov[1,2]
[1] *Rzhanov Institute for Semiconductor Physics, Siberian Branch, Russian Academy of Sciences, 630090, Novosibirsk, Russia* *
[2] *Novosibirsk State University, 630090, Novosibirsk, Russia*

At present time, InAs/AlSb HEMT transistors are promising for high-frequency, low power consumption and low noise applications. The value of conduction band discontinuity in InAs/AlSb (~1.35 eV) and high electron mobility in InAs channel make possible it to fabricate transistors with higher cut-off frequency and lower power consumption, then in other HEMT materials (e.g. InGaAs). This work describes the growth process of InAs/AlSb HEMT heterostructure and transistor fabrication and its characterization.

The HEMT InAs/AlSb heterostructure was grown by molecular-beam epitaxy on the GaAs substrate. The structure consists of: 1.7 µm AlSb buffer layer followed by 300 nm thick $Al_{0.7}Ga_{0.3}Sb$, 50 nm thick AlSb barrier layer, 15 nm thick InAs channel layer and 5 nm spacer AlSb, followed by 1.2 nm InAs with Si delta doping, the cap layer is InAs. For the investigation of quantum well interface influence on the electron mobility, several samples were grown with 0.5, 0,75 and 1 ML InSb-like interface at AlSb/InAs heterojunction because of higher electron mobility, then at AlAs interface [1], to form an InSb-like interface, the AlSb layer was exposed in the antimony flow for 5 s and, then, the antimony source was closed and indium monolayers (MLs) were deposited. The highest electron mobility was obtained for 0.75 ML InSb interface: the room temperature electron mobility was ~15000 $cm^2/(Vs)$ and electron concentration was $1.2 \cdot 10^{12}$ cm^{-2}, the measurements were done by Van der Pauw method with In contacts. The zone diagramm for the InAs/AlSb quantum well was calculated.

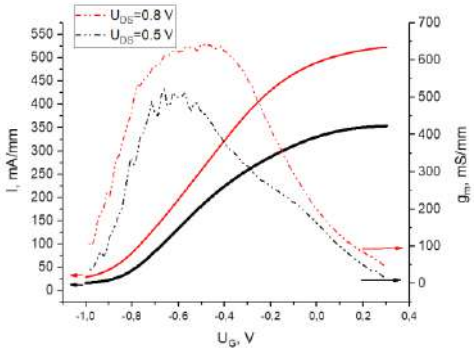

Drain–gate characteristic of the transistor and transconductance at U_{DS} = 0.8 V and 0.5 V.

After epitaxial growth, ohmic contacts Ge / Au / Ni / Au were formed by thermal annealing. For the formation of mesa structures and isolation of transistors different etching regimes were used, according to SEM images, during the liquid etching, lateral etching under metallization occurs, which creates leakage currents. The drain and drain-gate characteristics were measured. At the drain characteristics weak saturation was observed, which is related to the effect of impact ionization in InAs channel, such effect is typicaly observed for InAs/AlSb HEMT and associated with the generation of electron-hole pairs in the InAs channel, the holes due to the potential barrier absence, leave the channel and diffuse toward the gate or buffer. The drain-gate characteristics of the fabricated transistors are shown in Figure. The maximum of transconductance is 640 mS/mm at U_{DS} = 0.8 V and U_G = –0.55 V. The drain–gate characteristics show a current of tens of mA/mm at U_G = –1 V, which is indicative of the leakage currents in the structure, the origins of leakage is assosiated with the conductive layer between drain and source, which remains after etching and must be removed by combining different etching regimes.

References

[1] G. Tuttle, H. Kroemer, H. English, JAP 67 (1990) 3032-3037.

Structural and Thermal Properties of Novel TiO_2 doped Polymeric Chitosan-TPP@TiO_2 Core-Shell Nanoparticles

Angel Grace Raja[1], Kalai Arasi S. & Rajakumari R.*
PG and Research Department of Physics, Queen Mary's College, Chennai – 600004, Tamil Nadu, INDIA
[1]*Presenter. Email ID: angelgraceraja@gmail.com*
**Corresponding Author. Email ID: raj_mtwu30@yahoo.co.in*

Chitosan, the deacetylated form of Chitin, had been investigated in recent years and found to possess remarkable properties. It proved to be an inexpensive, non-toxic biopolymer which was biocompatible and biodegradable. In this study, Chitosan-TPP@TiO_2 core-shell nanoparticles were synthesized using the method of Ionic Gelation. Chitosan, a cationic biopolymer was reduced to nano scale by ionic crosslinking with the anionic compound Sodium Tripolyphosphate (TPP). Chitosan-TPP nanoparticles which were instantly formed were then coated with TiO_2. The structural properties of the Chitosan-TPP@TiO_2 core-shell nanoparticles were studied using X-ray Diffraction (XRD) and High Resolution Transmission Electron Microscopy (HRTEM). XRD analysis revealed that Chitosan-TPP nanoparticles which were amorphous in nature had become crystalline on account of the addition of TiO_2. It was also observed that the crystal structure formed was Tetragonal-BCC which could agree well with Selected Area Electron Diffraction (SAED) pattern and Lattice fringes from HRTEM images. HRTEM images clearly revealed the formation of single and multi-layered core-shell nanostructures having alternating Chitosan-TPP and TiO_2 layers. X-ray Photoelectron Spectroscopy (XPS) was employed to investigate the surface composition of Chitosan-TPP@TiO_2 core-shell nanoparticles. The Survey spectrum showed the existence of C, N, O and Ti thus confirming the presence of both Chitosan and TiO_2. XPS spectra of individual elements of the nanoparticles revealed that Nitrogen present in Chitosan had impregnated well into the TiO_2 crystal and there was good interaction between Chitosan matrix and TiO_2. The thermal properties of Chitosan-TPP@TiO_2 core-shell nanoparticles were assessed using Thermogravimetric Analysis/Differential Thermal Analysis (TGA/DTA) and Differential Scanning Calorimetry (DSC). TGA showed two-step mass reduction which was in good agreement with DTA and DSC thermograms. The sample proved to be stable up to 200℃. This study holds bright prospects for further application in Photocatalysis, Energy conversion and storage devices.

An Investigation on Thermal and Structural properties of TiO_2 encrusted over ZnO Core-Shell Nanoparticles.

Kalai Arasi S.[1], Angel Grace Raja & Rajakumari R.*
PG and Research Department of Physics, Queen Mary's College, Chennai – 600004, Tamil Nadu, INDIA
[1]*Presenter. Email ID: madhu091991@gmail.com*
**Corresponding Author. Email ID: raj_mtwu30@yahoo.co.in*

ZnO was encapsulated by TiO_2 for the formation of ZnO@TiO_2 Core-Shell nanostructures. The ZnO@TiO_2 Core-Shell nanostructures were synthesized at room temperature using Wet Chemical Method and their structural and thermal properties were investigated. The synthesized sample was characterized using X-ray Diffraction (XRD), High Resolution Transmission Electron Microscopy (HR-TEM), X-ray Photoelectron Spectroscopy (XPS), Thermogravimetric Analysis/Differential Thermal Analysis (TGA/DTA) and Differential Scanning Calorimetry (DSC) to explore their Core-Shell structure and thermal properties. X-ray Diffraction studies revealed that the synthesized material was crystalline in nature. The structures investigated from XRD for ZnO@TiO_2 consisted of both Hexagonal-Primitive lattice arrangement for ZnO and Tetragonal-BCC crystal lattice for TiO_2. The average crystallite size was found to be 25 nm. The Williamson-Hall (W-H) plot for ZnO@TiO_2 Nanoparticles showed anisotropy in X-ray line broadening. The average crystallite size calculated from Y-intercept was found to be 12 nm and the value of lattice strain from slope was obtained as -0.00491. HR-TEM analysis revealed that the structures of ZnO and TiO_2 analyzed from XRD were well correlated with the d-spacing obtained from (Selected Area Electron Diffraction) SAED pattern and lattice fringe images. The average particle size was observed to be in the range 50-85 nm. The elemental composition of the synthesized sample ZnO@TiO_2 was confirmed using XPS. XPS revealed that Zn^{2+} was bonded with oxygen for the formation of ZnO. Since no other Zn 2*p* peaks appeared, it confirmed the existence of ZnO nanoparticles and that the core nanoparticles did not enter the shell surface. The spectrum of Ti 2*p* showed two peaks at 458.44 eV and 464.30 eV which indicated the formation of Ti^{4+} on ZnO nanoparticles. TGA revealed two-step mass reduction. The exothermic and endothermic reaction peaks observed in DSC were in good agreement with DTA and the relative phase transitions in ZnO@TiO_2 were also observed. The synthesized sample ZnO@TiO_2 would be a promising candidate for photocatalytic activity. From thermal analysis, high residual mass was observed. The synthesized ZnO@TiO_2 nanoparticles could be a suitable candidate for sensing and storage applications as it could withstand high temperatures, even above 1000°C.

Synthesis of ZnO and Zn_2SiO_4 nanocrystals in SiO_2 by ion implantation with subsequent annealing

M. Makhavikou[1*], F. Komarov[1], L. Vlasukova[2], I. Parkhomenko[2], O. Milchanin[1], E. Wendler[3] and A. Mudryi[4]

[1] *A.N.Sevchenko Institute of Applied Physics Problems, Kurchatova Str. 7, 220045, Minsk, Belarus, e-mail: m.mohovikov@gmail.com*
[2]*Belarusian State University, Independence Ave. 4, 220030 Minsk, Belarus*
[3]*Friedrich-Schiller-University, Max-Wien-Platz 1, D-07743, Jena, Germany*
[4]*Scientific and Practical Materials Research Center, National Academy of Sciences of Belarus, P. Brovki Str. 17, 220072 Minsk, Belarus*

Zn_2SiO_4 and ZnO nanocrystals were fabricated in (600 nm) SiO_2 matrix by an implantation at room temperature of Zn^+ (130 keV) and Zn^+ (140 keV) + O^+ (50 keV) respectively. The ion energies for zinc and oxygen ions were chosen to achieve overlapping depth profiles. A fluence of $5 \cdot 10^{16}$ ions/cm^2 was used for all types of ions. After implantation samples were annealed at 750°C for 2 hour in air atmosphere. The combination of elemental analysis (RBS), structural (XTEM, HRTEM, SAED) and optical (PL) techniques have been used to identify the synthisezed phases and to find correlation between optical and structural properties of the Zn-based/SiO_2-nanocomposite.

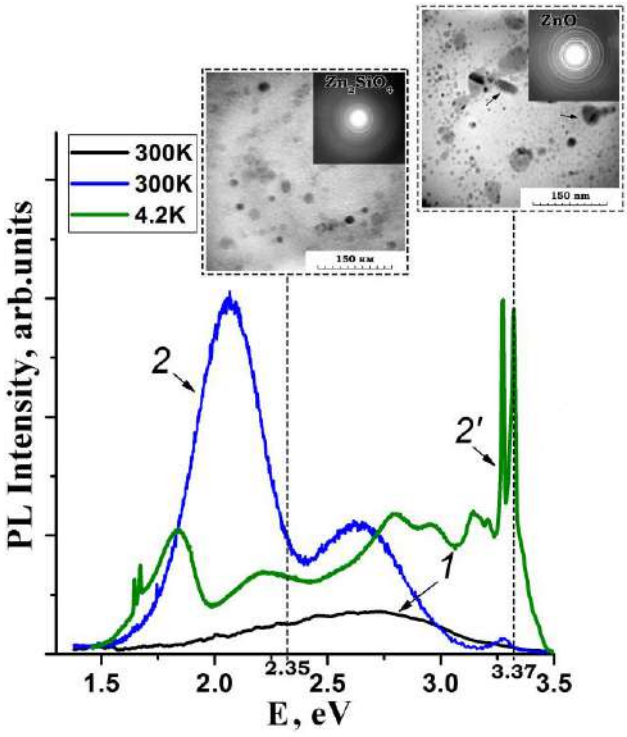

curve 1 – $Zn^+\downarrow$, curves 2, 2′ – $Zn^+\downarrow + O^+\downarrow$

Fig. 1 – PL spectra of the samples implanted with Zn (curve 1) and Zn+O (curves 2, 2′) after annealing. Curves 1 and 2 depict PL taken at room temperature, and curve 2′ depicts PL taken at 4.2 K.

Using RBS and TEM techniques it was shown the amount of implanted impurities affects elemental and structural properties of synthesized composition. Based on SAED data, it was found that implantation with Zn ions only followed by annealing results in the formation of orthorhombic Zn_2SiO_4 phase (space group $R\bar{3}$) [1], and the implantation with Zn and O ions with subsequent annealing results in the formation of zinc blende ZnO phase (space group $F\bar{4}3m$) [2]. Based on PL data, it has been shown, that the photoluminescence of as-implanted (SiO_2+Zn) and (SiO_2+Zn+O) nanocomposites is associated with the formation of radiative defects in SiO_2 matrix. Subsequent annealing results in a decrease of photoluminescence intensity for the samples implanted with zinc, and an increase of emission intensity for the double implanted samples. In the case of annealed nanocomposites, the observed luminescence at room and low temperature can be assigned to radiative defects as well as formation of crystalline phases of Zn_2SiO_4 and ZnO for the samples implanted with Zn ions only, and with Zn+O ions, respectively.

References

[1] H.E. Swanson [et al.] Standard x-ray diffraction powder patterns 539 (7) (1957) 62–64.

[2] I. Parkhomenko [et al.] J. of Phys. D: Appl. Phys. 54 (26) (2021) 265104-1–265104-9.

Formation of Copper Nanoparticles in Carbon Matrix by Solid-phase Pyrolysis of Copper Phthalocyanine

S. Pashayan[1*], H. Gyulasaryan[1], A. Manukyan[1], V. Anischik[2]
[1]*The Institute for Physical Research of NAS of Armenia, Ashtarak-2, 0203, Armenia*
[2]*Belarusian State University, Nezavisimosti Avenue, 4, 220030, Minsk, Belarus;*
*e-mail: stpashayan@gmail.com**

Nanostructured thin-film island-type coatings on sapphire and silicon substrates, consisting of copper nanoparticles dispersed in a carbon matrix, were obtained by solid-phase pyrolysis of copper phthalocyanine.

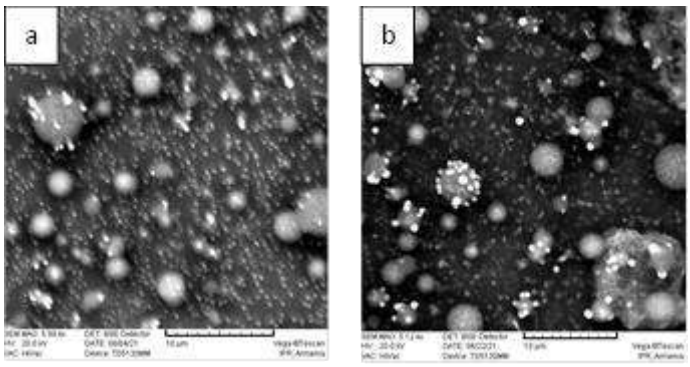

Fig. 1. SEM images of obtained films on sapphire substrate:
a - as-deposited (T_{pyr} = 900°C, t_{pyr} = 30 мин);
b – after annealing (T = 300 °C, t = 30 мин)

Some of the samples after pyrolysis were annealed in a muffle furnace. The elemental composition, structure and morphology of obtained samples were investigated by scanning electron microscopy, energy dispersive X-ray microanalysis and X-ray diffraction.

The sizes of the formed nanoparticles vary between 10 and 400 nm depending on the temperature and time of pyrolysis. It has been established that the structure, surface properties of the films obtained, as well as the structure of the carbon matrix, also vary according to pyrolysis and annealing conditions.

The study showed that this method allows to synthesize thin-film and composite materials with given properties.

Vibrational properties of irradiated Al nanoparticles by Raman spectroscopy method

S. Jabarov
Institute of Radiation Problems ANAS, B. Vahabzade, 9, AZ-1143, sakin@jinr.ru

The synthesis of nano-sized materials and the production of composite materials based on them, which is considered to be the main research area of condensed matter physics, is one of the most popular fields of physics today, and based on this, it was determined that a nano-sized oxide layer is formed on the surface of some materials, and this layer has different properties from the bulk material. The interest in metal nanoparticles is due to the fact that their synthesis is more practical and there is a wide range of applications of nanocomposite materials based on them, which in turn facilitates the study of external effects on composites. Although the effect of electron beam on the crystal structure of nano-sized Al particles has been studied, its effect on other physical and chemical properties has not been sufficiently studied. Since X-rays cannot accurately identify light element atoms such as hydrogen and oxygen, as well as aluminum, it is important to check the decomposition of $Al(OH)_3$ under the influence of electron beams. In this study conducted, the effects of the electron beam on the crystal structure and atomic dynamics of Al nanoparticles of size d = 40-60 nm up to 1.03×10^{18} cm^{-2} fluence were studied by Raman spectroscopy.

Raman spectroscopy measurements were carried out with "NT-MDT, NTEGRA Spectra" evolution spectrometer to reveal the lattice vibration bands of nano aluminum samples in the range 500-4500 cm^{-1}. The laser light wavelength was 633 nm of the He-Ne laser.

In order to study the effect of electron beam on nano-sized Al crystals, the atomic dynamics of non-irradiated and irradiated samples were studied by the Raman spectroscopy method in the frequency range ν = 500-3200 cm^{-1}. It can be seen from the spectra that 5 Raman modes are observed in Al crystals without radiation: 864, 1448, 1635, 1877 and 2990 cm^{-1}. Analysis of the obtained modes shows that ν_1, ν_4 and ν_5 correspond to the Al-Al bond. Modes ν_2 and ν_3 correspond to the oscillations of the bonds formed between the Al atoms and the O and H atoms.

5 Raman modes are also observed in the Raman spectrum of the 4.16×10^{16} cm^{-2} fluence irradiated sample: 855, 1406, 1621, 1875 and 2976 cm^{-1}. This indicates that the $Al(OH)_3$ groups do not completely decompose when irradiated at small fluences, and therefore the Al atoms in the spectra show similar oscillations corresponding to the O and H bonds. The formation of $Al(OH)_3$ in the X-ray diffraction spectra of a 4.16×10^{16} cm^{-2} fluence irradiated sample is not observed because the X-ray diffraction method is difficult to identify light element atoms. If the concentration of $Al(OH)_3$ in the sample is quite low, then this phase is not observed at all.

In the Raman spectrum of a 1.20×10^{17} cm^{-2} fluence irradiated sample, 3 Raman modes occur: 854, 1860 and 2959 cm^{-1}. This indicates that when irradiated at high fluences, the $Al(OH)_3$ groups are completely broken down, and therefore only oscillations corresponding to Al-Al bonds are observed in the spectra. Modes ν_2 and ν_3 corresponding to the oscillations of the bonds formed between the Al atoms, that similar the O and H atom bonds, does not appear. In the Raman spectrum of a 1.03×10^{18} cm^{-2} fluence irradiated sample, 3 Raman modes corresponding to Al-Al bonds: 830, 1824 and 2918 cm^{-1}.

The work was supported by the grant program of the МИЦНТ СНГ 2021, No. 21-105.

Radiation induced effects in CaF_2 films grown on Si by molecular beam epitaxy

A. Dvurechenskii[1,2*], Zh. Smagina[1], V. Volodin[1,2], A. Kacyuba[1], A. Zinovyev[1], G. Ivlev[3], S. Prakopyeu[3]
[1]*A.V. Rzhanov Institute of Semiconductor Physics, Siberian Branch of the Russian Academy of Science, Novosibirsk 630090, Lavrentev av.13, Russia, e-mail: dvurech@isp.nsc.ru**
[2]*Novosibirsk State University, 630090, Pirogova 1, Novosibirsk, Russia*
[3]*Belarusian State University, av Nezavisimosti, 4, 220030 Minsk, Belarus*

CaF_2 films characterized as insulator with a large bandgap (12.1 eV) and high dielectric permittivity. The small of the lattice constant mismatch with silicon provides the epitaxial growth of films with the high quality Si(111)/CaF_2 interface. The narrow defected layer at the interface with the Si substrate is attractive for growth heterostructures with ultrathin layered materials for advanced device applications. Thin films fluorides were used as barrier layers in resonant-tunnel diodes. Field-effect transistors of the standard architecture based on silicon, gallium arsenide and diamond, with calcium fluoride as a gate dielectric lead to significantly lower tunnel leaks, compared to oxide materials.

The aim of present experiments were to study the the electron and pulsed laser beam radiation-induced phase transformation and elemental content of CaF_2 films grown on Si(111). The epitaxial CaF_2 growth was carried out at the substrate temperature of 550°C, and the growth rate was 0.3 Å/s. The CaF_2 film thicknesses from 2 nm to 40 nm were studied in the experiments with atomic force microscopy, a Hitachi SU8220 scanning electron microscop with facilities to analyze the elemental composition by energy dispersive X-Ray spectroscopy from the area of the structure with dimensions up to 1 μm in the plane and the depth of 400 nm. The phase composition was determined on the base of Raman light scattering.

It was found that the electron irradiation during epitaxial growth of CaF_2 leads to radiation-induced phase transformation of CaF_2 into the $CaSi_2$ film of metallic conductivity (electron energy was 20 keV, current density 50 μA/cm^2) [1]. The same radiation induced phase transition takes during the electron irradiation at the substrate temperature above 300°C after complete the CaF_2 film growth.

The crystal structures of thin $CaSi_2$ films were found to depend on the deposited CaF_2 film thickness:

– it is the trigonal rhombohedral modification 3R for thin (<20 nm) CaF_2 films;
– and the trigonal rhombohedral modification 6R for thicker films.

Nanosecond time resolved reflectivity and transmission changes in CaF_2/Si(111) structures have been measured to study the phase transitions, surface modification and radiolysis induced by nanosecond ruby laser pulses. The Si lattice heating up to melting point leads to nanohills formation on surface of the structure, the height of which does not exceed 100 nm with the average base diameter 360 nm and the surface density $2 \cdot 10^8 cm^{-2}$. The Raman scattering and energy-dispersive X-ray spectroscopy data indicates that the nanohills contain cavities inside them, and they are filled with Si_2F_6 molecules gas. The shell of the nanohills, obviously, consists of calcium oxide.

Acknowledgement
The reported study was funded by RFBR and ROSATOM, project number 20-21-00028

References
[1] Kacyuba [et al.] Materials Letters, V.268, P.127554 (2020).

Structural analysis of Y_2O_3 nanoparticles

R. Rzayev
Azerbaijan State Pedagogical University, U. Hajibeyli, 68, AZ-1000, ravilrzayev@mail.ru

It is known that different physical and chemical properties of materials change in nanoscales. The size effect affects both the structural and physical properties of nanomaterials. It has been found that when nano-sized aluminum metal is irradiated by high-energy electrons, the values of the lattice parameters decrease. Under normal conditions, the hydroxide groups formed by Al atoms combined with water molecules decompose and pure aluminum nanoparticles are observed. Composite materials containing nanoparticles also have unique physical properties.

In this work, the crystal structure of a 20-40 nm nanoscale Y_2O_3 compound was studied by the X-ray diffraction method at room temperature. As a result of the analysis of the obtained spectra, the lattice parameters, atomic coordinates, space group and crystal syngony were determined. The morphology of the powdered research object was examined under a scanning electron microscope.

The crystal structure of Y_2O_3 nanoparticles was studied by X-ray diffraction method at room temperature (Bruker D8 Advance X-ray diffractometer. Parameters: 40 kV, 40 mA, Cu Kα, λ = 1.5406 Å). The obtained diffraction spectra were analyzed with the help of the Ritveld method in the program FullProf. Analysis of the surface morphology and microstructure of Y_2O_3 compounds was carried out on SEM (Scanning Electron Microscope, ZEISS, ΣIGMA VP) at room temperature.

The surface structure and size effect of Y_2O_3 nanoparticles have been studied. Studies on a scanning electron microscope at a scale of 100 nm have shown that the scale of nanoparticles varies in the range of d = 20–40 nm. It is known that the properties of materials vary in nanoscales (d = 1–100 nm). Therefore, it is important to find materials that can retain their nanoscales for a long time. As can be seen, yttrium oxide nanoparticles are a stable material and retain their nanoscales. This is due to the fact that oxidation, decomposition, and the formation of hydroxide groups by combining with water molecules do not occur.

The crystal structure of yttrium oxide nanoparticles at room temperature was studied by X-ray diffraction. The analysis revealed that the crystal structure of the Y_2O_3 compound has a cubic symmetry of the Ia-3 space group. The lattice parameters have the values: $a = b = c$ = 10.5958 Å. In a crystal lattice, trivalent yttrium atoms stand in two different positions. The first atom (Y1) is in the coordinates x = 1/4, y = 1/4 and z = 1/4, and the second atom (Y2) is in the coordinates x = −0.0165, y = 0 and z = 1/4. Bivalent oxygen atoms stand in one coordinate position: x = 0.3942, y = 0.1428 and z = 0.3825. Oxygen atoms form various bonds with yttrium atoms in the range $d_{O–Y}$ = 2.1628–2.4083 Å. The distances between the atoms of the same element are longer. Bonds between oxygen atoms: $d_{O–O}$ = 2.8207–3.7003 Å, and bonds between yttrium atoms: $d_{Y–Y}$ = 3.6416–3.8922 Å, forming bonds in the various range. This is because as the ionic radii of the atoms increase, they settle at greater distances from each other. Therefore, there is a difference in the lengths of the bonds they form. It is known that oxygen atoms, which are considered light elements, have smaller ionic radii. Yttrium atoms, which are considered heavier elements, have considerably smaller ionic radii than oxygen atoms.

Sr_2FeMoO_6 - based nanostructures prepared using ultrasound treatment

N. Kalanda[1], S. Demyanov [1], M. Yarmolich[1], A.Petrov[1]*, V. Prihodich[1] and N. Sobolev[2]
[1]*Scientific-Practical Materials Research Centre of the NAS of Belarus, 220072 Minsk, Belarus, petrov@physics.by*
[2]i3N, Departamento de Física, Universidade de Aveiro, 3810-193 Aveiro, Portugal

Due to their unique and extremely important magnetotransport and magnetic properties, metal oxide Sr_2FeMoO_6 systems with an ordered double perovskite structure are among the most promising materials for spintronic devices. Nanosized powders of strontium ferromolybdate are of particular interest.

Sr_2FeMoO_6 powder has been synthesized by a modified citrate-gel technique, the features of which are described in detail in [1-2]. Samples with different pH values were obtained by adding the required amount of ethylenediamine to the solution. Of these, only the material with pH = 4 was single-phase with an average grain size of ~ 240 nm and the degree of superstructural ordering of iron and molybdenum cations P = 65%, as a result of which it was used [1-2] to study the sequence of phase transformations during the crystallization of the single-phase Sr_2FeMoO_6 in order to obtain nanosized grains, stage-wise synthesis modes were used. At the first stage, preliminary synthesis was carried out in a polythermal mode at a heating rate ϑ = 2 deg / min to T = 893 K in a continuous flow of a gas mixture of 5% H_2/Ar, followed by holding for 1 hour. At the second stage, in order to decompose the intermediate $SrMoO_4$ phase as quickly as possible and achieve conversion values of α ~ 100% for SFMO, the temperature was raised to T = 1060 K, followed by holding for 1 hour. The final synthesis of $Sr_2FeMoO_{6-\delta}$ was carried out at T = 1220 K for 4 hours. As a result, a single-phase compound $Sr_2FeMoO_{6-\delta}$ with superstructural ordering of Fe / Mo cations P = 88% has been obtained.

Since agglomeration of grains up to 1450 nm in size was observed in strontium ferromolybdate nanopowder, ultrasonic dispersion was used to obtain highly dispersed particles with an average size d_{av} <100 nm. It was found that after ultrasonic action on a suspension of the composition 25 ml (C_2H_5OH) + 0.01g ($Sr_2FeMoO_{6-\delta}$) + 0.05 g (Tween 20), subjected to dispersion for 60 minutes, it was found that the agglomerates disappeared, and the grain size decreased from 240 nm to 70 nm (see Figure).

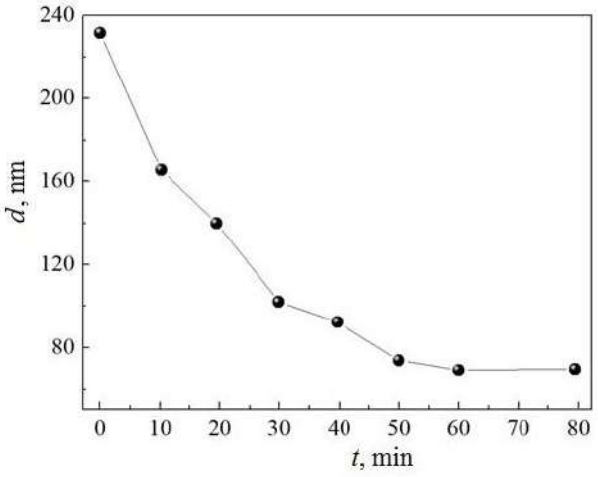

Dependence of the $Sr_2FeMoO_{6-\delta}$ particles dimension on the dispersion time

Acknowledgement
The work was supported by the European project H2020 –MSCA –RISE –2017 –778308 – SPINMULTIFILM.

References

[1] M.Yarmolich, N. Kalanda, S.Demyanov, H. Terryn, J. Ustarroz, M.Silibin, G.Gorokh, Beilstein J. Nanotechnol. 7 (2016) 1202–1207.
[2] M.Yarmolich, N. Kalanda, S.Demyanov, Ju.Fedotova, V. Bayev, N. Sobolev, Phys. Status Solidi B. 253 (2016) 2160–2166.

Effect of zinc doping on microstructural and electric properties of nickel nanoferrites

Pinki Punia[1], Manish Kumar Bharti[2], Rakesh Dhar[1], Preeti Thakur[3], Atul Thakur[4*]
[1] *Department of Physics, Guru Jambheshwar University of Science & Technology, Hisar, Haryana 125001, India*
[2] *Department of aerospace, Amity University Haryana, Gurugram, Haryana 122413, India*
[3] *Department of Physics, Amity University Haryana, Gurugram, Haryana 122413, India*
[4] *Amity Institute of Nanotechnology, Amity University Haryana, Gurugram, Haryana 122413, India*
**corresponding author e-mail: athakur1@ggn.amity.edu*

The nanoparticles of $Ni_{1-x}ZnxFe2O4$ (x=0 and 0.5) were successfully synthesized via citrate precursor method and sintered at 900 ^{o}C for 3 h. The structural and electrical properties of nickel ferrites before and after substitution of zinc ions were studied using X-ray diffraction method, Fourier transform infrared spectroscopy and two probe method. The crystallite size and porosity of $NiFe_2O_4$ (45 nm and 41%) were smaller for $Ni_{0.5}Zn_{0.5}Fe_2O_4$ (35 nm and 38%) nanoparticles. Electrical resistivity increased more than 10 times from 2.45×10^{8} Ωm and 1.8×10^{9} Ωm for $NiFe_2O_4$ and $Ni_{0.5}Zn_{0.5}Fe_2O_4$ respectively.

Yafet-Kittel Angles in Polycrystalline Cobalt Ferrite Nanoparticles

M. K. Bharti[1*], S. Chalia[1], P. Punia[2], P. Thakur[3], S. N. Sridhara[4], A. Thakur[5], P. B. Sharma[1]
[1]*Department of Aerospace Engineering, Amity University Haryana, Gurugram, Haryana 122413, India*
[2]*Department of Physics, Guru Jambheshwar University of Science and Technology, Hisar, Haryana 125001, India*
[3]*Department of Physics, Amity University Haryana, Gurugram, Haryana 122413, India*
[4]*Hindustan Institute of Technology and Science, Chennai, Tamil Nadu 603103, India*
[5]*Amity Institute of Nanotechnology, Amity University Haryana, Gurugram, Haryana 122413, India*
**Corresponding author e-mail: reachmkbharti@gmail.com*

Cobalt ferrite nanoparticles (CFNPs) of ~31 nm were prepared using citrate precursor method. XRD data confirmed the spinel structure, nanoscale size and phase purity of the prepared nanoparticles. SEM confirmed the formation of polycrystalline grains with clear and well-defined grain boundaries. The VSM data revealed that the as-prepared CFNPs exhibited moderate specific saturation magnetization (~59 emu/g), moderate specific remanent magnetization (~24 emu/g) and slightly higher coercivity (~601 Oe). The significant decrease observed in the specific saturation magnetization between the as-prepared CFNPs and their bulk counterparts was related to the presence of Yafet-Kittel type of magnetic order and corresponding Yafet-Kittel angles.

Structural studies of the sol-gel glasses with copper selenide nanoparticles by SANS technique

V.S. Gurin[1*], A.V. Rutkauskas[2], Yu.E. Gorshkova[2], S.E. Kichanov[2], A.A. Alexeenko[3], D.P. Kozlenko[2]
[1]*Research Institute for Physical Chemical Problems, Minsk, Belarus; gurin@bsu.by*
[2]*Joint Institute for Nuclear Research, Dubna, Russia*
[3]*Gomel State Technical University, Gomel, Belarus*

Copper chalcogenides, among many other perspective semiconductors, reveal novel properties combining both quantum confinement effects and the plasmon resonance phenomenon. The latter appeared due to elevated free carrier concentration (electrons or holes, depending type of compounds). These compounds possess variable composition and non-stoichiometry and include a number of stable and metastable phases, e.g. in $Cu_{2-x}Se$ for $1 \le x \le 2$. The value of x strongly affects the carrier concentration and all their properties. In optics, new absorption bands and IR luminescence were discovered for the chalcogenides and associated with the plasmon resonance. Research of last years has demonstrated very interesting interplay in the nanoscale effects inherent to both metals and semiconductors [1].

In the present work, we investigate the structural features of copper selenide nanoparticles embedded into amorphous (glass-like) silica matrix fabricated through the sol-gel technique [2] using small-angle neutron scattering (SANS). This technique allows address the structural data at different scale (1-1000 nm) with no material destruction.

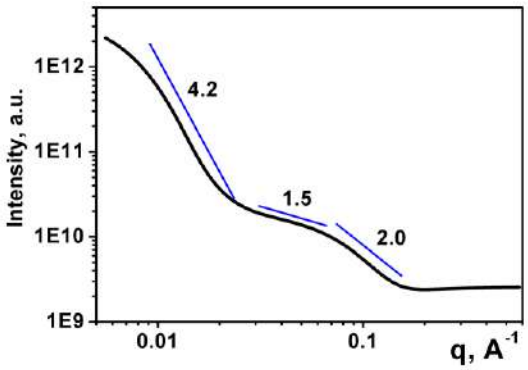

Fig. 1. Approximated data of SANS measurements for a glass with Cu_2Se nanoparticles. The numbers are α exponents for linear fitting of the corresponding parts of the curve.

Fig. 1 demonstrates the approximated SANS curve for a glass sample with copper selenide nanoparticles. The approximation of the raw SANS data was carried out on the basis of the exponential-power law approach which incorporates both Guinier and Porod dependencies for SANS with smooth matching [3]. The linear parts were fitted by the formula $I = Aq^{-\alpha}+B$, where A and B are fitting constants, to find the values of fractal dimensions for the whole structure.

The scattering objects assigned to Cu_2Se particles have the diameter about 57 nm and the size approximately larger on the order of magnitude can be found for other structural features. The latter may be associated with modifications in the glass matrix due to effects of particles formation (e.g. different volume contraction of silica and copper selenide under cooling).

Fractal properties of the stuctures under study appear to be more complicated, and at least three different exponents may be deduced from the SANS data. The maximum value of α (~4.2) is for the lower q range that corresponds to the larger scattering objects and α~2.2 is obtained for the q range around 0.1 $Å^{-1}$. Likely, these are nanoparticles and their comparatively low fractal dimension can mean the rough particle-matrix interface. The lower α for the intermediate q range and its significant growth further indicate possible variation of the glass structure within the considerable wide region around the particles.

References

[1] G. Xu, Sh. Zeng, B. Zhang, M.T. Swihart, K.-T. Yong, P. N. Prasad, Chem. Rev.116 (2016) 12234.
[2] V.S. Gurin, A.A. Alexeenko, S.A. Zolotovskaya, K.V. Yumashev, Mater. Sci. Eng. C 26 (2006) 952.
[3] G. Beaucage, J. Appl. Crystallogr. 28 (1995) 717.

MULTI-DISTIPLINARY

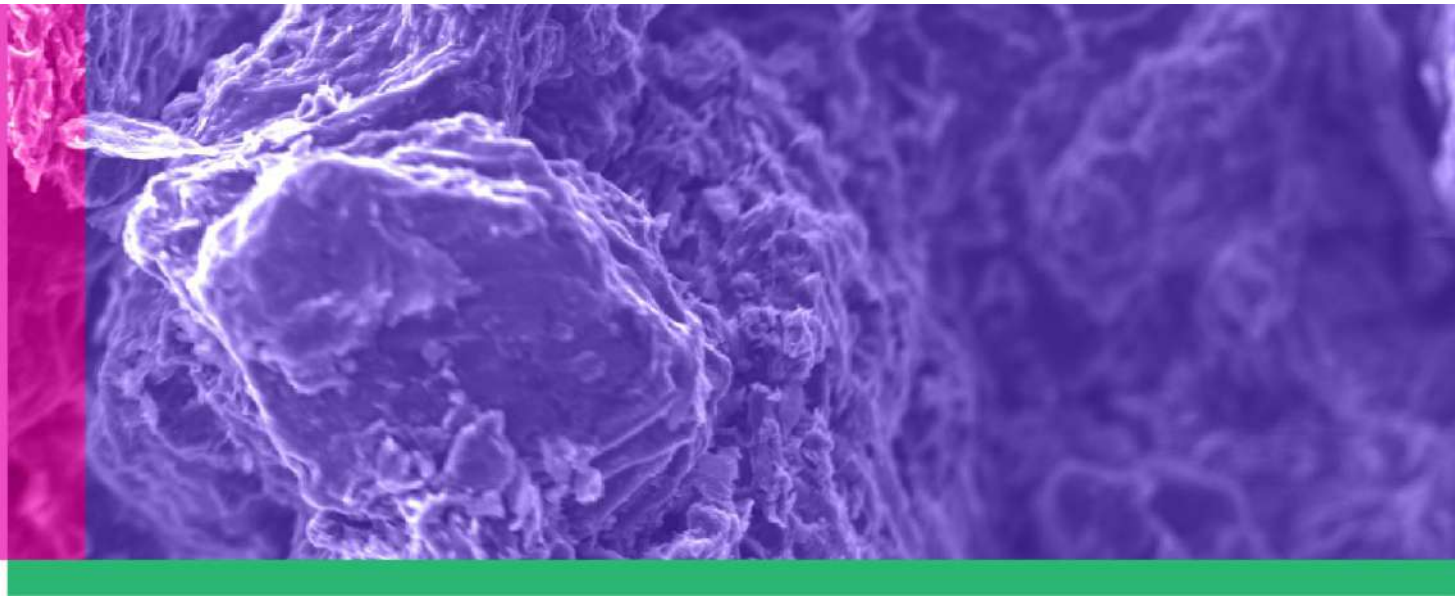

Multiferroic composites for sensing and energy harvesting applications

J. Vidal[1], A. Turutin [1,2], I. Kubasov [2], N. Sobolev [1,2], D. Malinkovich[2], A. Kholkin [1,2,3*]
[1] *University of Aveiro, 3810-193, Campus de Santiago, Aveiro, Portugal*
[2] *National University of Science & Technology MISiS, 119991, Leninskiy prospekt 4, Moscow, Russia*
[3]*National Research Tomsk Polytechnic University, 634050, prospect Lenina 30, Tomsk, Russia*
***corresponding author email: kholkin@ua.pt*

Magnetoelectric (ME) effect is defined as a linear coupling between polarization and magnetic field (direct effect) and vice a versa between magnetization and electric field (converse effect). This effect has been of immense interest in the scientific community over the past years. Unlike ME single-phase multiferroics, numerous ME composites, combining elastically coupled piezoelectric and magnetostrictive phases, have been shown to yield very strong ME effects even at room temperature. These structures also offer a great flexibility in the sense that a large number of parameters may be tuned independently including the materials properties of the constituent phases and the connectivity between them. Consequently, these composites are nowadays very close to a range of promising applications including: DC and AC magnetic vector field and electric current sensors, magneto-electro-elastic energy harvesters, multiple-state memory devices, micro-sensors in read heads, transformers, spinners, diodes, spin-wave generators, electrically tunable microwave filters, and various biomedical devices.

In this work, we report fabrication and investigation of a variety of different magnetoelectric composites made of magnetostrictive (metglas) and piezoelectric materials such as $LiNbO_3$ (LNO), $GaPO_4$ (GPO) and $PbMg_{1/3}Nb_{2/3}O_3$-$PbTiO_3$ (PMN-PT). ME measurements were performed as a function of the crystal cuts, magnitude and orientation of the magnetic bias field and frequency of the modulation field. Despite much weaker piezoelectric coefficients of LNO and GPO, direct ME effects were found to be competitive with PMN-PT as piezoelectric. Greatly enhanced ME coefficients in certain resonance modes were explored and their relations to the materials properties of piezoelectric materials and the geometry of the composites were investigated. We demonstrate that the orientational control of piezoelectric components can be used in order to obtain almost any desired quasi-static and resonant anisotropic ME properties for a given application. The anisotropic quasistatic ME coupling was generally found to be two times larger in bidomain LNO composites as compared to their monodomain counterparts. Large ME effects were obtained in low-frequency electromechanical resonance modes that are important for biomedical applications. Interestingly, the contour modes were strongly suppressed in bidomain systems, whereas bending modes were greatly enhanced in the studied composites. At a bending resonance frequency of 6862 Hz, we found a giant $|\alpha E31|$ value up to 1704 $V\cdot(cm\cdot Oe)^{-1}$ in laminate composites metglas/bidomain y+140°-cut LNO. Furthermore, the equivalent magnetic noise spectral density of these composites was as low as 92 $fT/(Hz^{1/2})$, a record value for such a low operation frequency. Therefore, we have shown that such composite systems may be used in simple and sensitive low-frequency magnetic and current sensing devices, including simultaneous magnetic/mechanical energy harvesting systems and magnetic field sensors. Biomedical applications of such composites will be considered as well.

References

[1] J. Vidal, A. Turutin, et al, IEEE Trans. Ultrason. Ferroelectr. & Freq. Control 67 (2020) 1219.
[2] A. Turutin , J. Vidal, et al, J. Magn. Magn. Matls 486 (2019) 185209.
[3] A. Turutin, J. Vidal et al, Appl. Phys. Lett. 112 (2018) 262906.

Solid state physics applications for teaching and research activity of mechanical engineering students

I. Tyukhov
Department of Mechanical Engineering, San Jose State University, One Washington Square San Jose, CA 95192-0087, USA, igor.tyukhov@sjsu.edu

Modern engineering students of San Jose State University, which is located in the heart of Silicon Valley, CA, study courses like Mechatronics, Solar Energy Engineering, Renewable Energy Engineering, related to electronic devices in mechanical systems, generation of green energy. Renewable energy is the new driver in our fast changing world, with electrical energy as their basis. Integrating mechanical design, energy conversion processes, electronic principles into a single device, mechanism, apparatus, or energy system is an urgent task. Bringing these different technologies together is not an easy task, but students should be prepared for new technology.

Taking into account the fast growing photovoltaic industry, decreasing price for solar cells [1, 2] and new job opportunities for this industry, a project was proposed by the author to create a photovoltaic (PV) stations lab for the Thermal engineering laboratory of the Mechanical Engineering Department of SJSU. The project was supported by California State University. Four lab stations (LS) were created: two to study fundamentals of photovoltaic energy conversion and the real size solar cells (SCs) of different types, and next two to study solar modules from mono- and poli-Si SCs with balance-of-system for practicing with design of small, but real size PV lighting system.

LS1 and LS2 design to teach the main characteristics and parameters of SCs (for teaching proficient consumer skills) and to teach how to find the equivalent circuit parameters such as shunt and series resistance, the saturation (reverse) current, ideality factor of the I-V characteristics of SCs from both light and dark I-V curves, the dependence of the open circuit voltage on the short circuit current (teaching research skills).

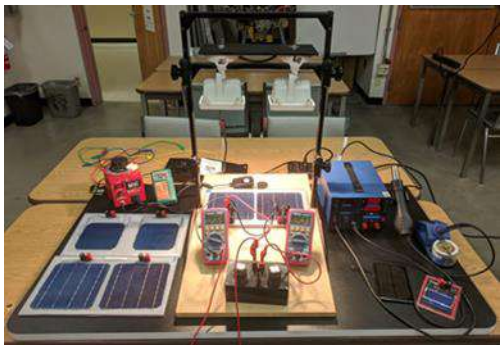

Lab station 1 for study solar cells.

LS3 and LS4 allows us to take measurements of illuminated and dark I-V characteristics, the main parameters of solar modules: short circuit current, open circuit voltage, maximum power, fill factor (for teaching proficient consumer skills), to study components of PV systems: batteries, charge controllers, inverters. maximum power point trackers, programmable battery power display, oscilloscope, DC and AC LED loads, illuminance meter (for teaching electrical engineering skills). Students practice with the design and simulating of autonomous PV systems and investigate their characteristics using different gadgets of BoS (for teaching design and engineering skills).

Lab stations demonstrate broad functionality with quite cheap and compact equipment based on Solid State Physics achievements with an opportunity to add new solar cells, modules, components, electronic gadgets and optical elements.

Acknowledgement
Autor thanks to Laboratory Innovation Technology Program and Prof. Nicole Okamoto for support this project.

References

[1] M. A. Green How Did Solar Cells Get So Cheap? Joule 3, 631–640, March 20, 2019.
[2] S.R. Kurtz, et al. “Revisiting the Terawatt Challenge" MRS Bulletin, pp 159-164, March 2020.

Application of the Prigogine-Flory-Patterson model for calculating the thermodynamic properties of binary liquid cyclohexane + *n*-propylbenzene and cyclohexane + cumene mixtures in a wide range of temperatures and pressures

A. Shchamialiou[1*], V. Samuilov[1], N. Holubeva[1], A. Paddubski[1], D. Drăgoescu[2], and F. Sîrbu[2]
[1]*Belarusian State University of Food and Chemical Technologies, Schmidt Avenue 3, 212027 Mogilev, Belarus, shche70@mail.ru**
[2]*"Ilie Murgulescu" Institute of Physical Chemistry, Splaiul Independentei 202, 12-194, Bucharest, Romania*

In this work, the thermodynamic properties of two binary liquid mixtures, as: cyclohexane + *n*-propylbenzene and cyclohexane + cumene have been calculated using the Prigogine-Flory-Patterson (PFP) model, at temperatures from (298.15 to 433.15) K and pressures up to 100.1 MPa

The calculated values of density, speed of sound, isentropic and isothermal compressibility, isobaric expandability, isobaric and isochoric heat capacity have been obtained for the two above mentioned studied binary liquid mixtures.

The possibilities of using the PFP model for calculating and predicting the thermodynamic properties of mixtures in a wide range of temperatures and pressures are estimated. The checking on the possibility of using the PFP model was carried out on the basis of the previously data obtained by us: the experimental results on the density and speed of sound for the above mentioned studied mixtures, in the temperature range from (298.15 to 433.15) K and at pressures up to 100.1 MPa. We also used the data on density, speed of sound, and isobaric heat capacity, reported by other authors [1, 2], for the same mixtures at atmospheric pressure.

The experimental data are in good agreement with the calculation results, when we used the differential relations of thermodynamics and the empirical Redlich-Kister equation and when using the PFP model with a contact interaction parameter, fitted by the empirical equation based on the experimental data. The standard deviations of the experimental data from those calculated by the PFP model with predicted contact interaction parameter are significantly higher than the expanded uncertainty of these data.

Thus it is shown that the simultaneous predicting the various thermodynamic properties using the PFP model, for the above mixtures in a wide range of temperatures and pressures has low accuracy. The calculation of thermodynamic properties based on the PFP model and on the density and speed of sound experimental data has an accuracy that is insignificantly worse than the accuracy of calculations using differential relations of thermodynamics and empirical equations.

Acknowledgement

The authors would like to acknowledge the support of the Belarusian Republican Foundation for Fundamental Research and the Romanian Academy for financial support in the framework of the joint project T20RA-002.

The Romanian authors want to express their acknowledgement to the Romanian Academy, for the financing the research program "Chemical thermodynamics and kinetics. Quantum chemistry" of the "Ilie Murgulescu" Institute of Physical Chemistry. The financial support of the EU (ERDF) and Romanian Government, which allowed for the acquisition of the research infrastructure under POS-CCE O 2.2.1 Project INFRANANOCHEM - Nr. 19/01.03.2009, is also acknowledged.

References

[1] S.L. Oswal [et al.] J. Mol. Liq. 109 (2004) 155–166.
[2] S. Fujii [et al.] J. Chem. Thermodyn. 27 (1995) 1319–1328.

Electric properties of the $ZnNb_2O_6$ ceramic matrix doped with TiO_2 studies for application as a dielectric resonator

T.H. de Vasconcelos[1*], D.X. Gouveia[1], H.O. Barros[2] and A.S.B. Sombra[2]
[1]*Federal Institute of Ceará, PPGET, Fortaleza, Ceará, 60040-531, Brazil, thiagohfisica@mail.com**
[2] *Federal University of Ceará (UFC) - LOCEM, Fortaleza - Ceará,60755-640, Brazil*

This work presents the dielectric properties studies of $ZnNb_2O_6$ matrix doped with (%)TiO_2. The complex permittivity ε*, tgδ, return loss of the pure and doped phases are studied in the microwave range. Experimental results and numerical simulation of the return loss and the Smith Chart are presented and compared in a good agreement. The simulated radiation patterns are also presented, indicating a possible application as dielectric resonator antenna (DRA).

Keywords: $ZnNb_2O_6$, dielectric properties, DRA.

SIMULATING OF CHARGE ACCUMULATION IN IRRADIATED SIPM CELL WITH METALLIZED DIVIDING TRENCHES

D.A. Aharodnikau
Scientific-Practical Materials Research Centre of NAS of Belarus, 19, P. Brovka Str., 220072, Minsk, Belarus, ogorodnikov@ifttp.bas-net.by

With the help of software complex «Silvaco» the change in distribution of electric fields and charge in the SiPM cells with metallized dividing trenches was considered. SiPM cells were irradiated with X-ray quanta with 10 keV energy up to a dose 10^5 rad. The cells represented itself optically isolated n^+-p-p^+-structures. The optical isolation of the cells was represented as trenches, which were filled with tungsten after passivation of the walls with a SiO_2 layer. The metal output of the trench was electrically connected to the n^+-region of the cell. The SiPMs were irradiated in the following electrical conditions: reverse bias U_b = -30 V (active mode) and U_b = 0 V (passive mode). It was shown that during the irradiation in the active mode the electric field intensity and charge accumulation near the SiO_2/p-Si interface significantly increases. The results can be explained by the influence of the electric field on the hole charge yield in SiO_2.

Keywords: SiPM; charge accumulation; Si/SiO_2 interface; X-ray quanta.

References

[1] Gulakov I.R. Fotopriemniki kvantovykh sistem [Photodetectors of quantum systems]. Minsk. 2012. (In Russian)
[2] Popova, E. The cross-talk problem in SiPMs and their use as light sensors for imaging atmospheric Cherenkov telescopes. / E. Popova, P. Buzhan, B. Dolgoshein, A. Ilyin, V. Kaplin, S. Klemin, R. Mirzoyan, M. Teshima // Nucl. Instr. Meth. Phys. Res. A610. –2009. –P. 131-134.
[3] Garutti E., Musienko Yu. Radiation damage of SiPMs. Nuclear Inst. and Methods in Physics Research, A. 2019; 926: 69–84.
[4] Tapero, K.I. Radiacionnye jeffekty v kremnievyh inte-gral'nyh shemah kosmicheskogo primenenija [Radiation effects in silicon integrated circuits for space applications] / K. I. Tapero, V. N. Ulimov, A.M. Chlenov // Vlijanie ionizirujushhih izluchenij na krem-nij, bipoljarnye pribornye struktury: ucheb. posobie [The Influence of ionizing radiation on silicon, bipolar devices: textbook] / K. I. Tapero, V. N. Ulimov, A.M. Chlenov. – Minsk, 2012. — P. 261–287. (In Russian)
[5] [SILVACO International. ATLAS User's Manual. Device Simulation Software. [Electronic resource]. URL: http: // www.silvaco.com. (Request date 13.05.2021)

Calculation of the verification interval for a tape feeder PLC-VD-2.5 / 10

L. Lobanovsky[1,2], S. Leonchik[1]*, A. Khomenya[2], I. Zyl[2], A. Poklonsky[2], V. Shambalev[2]
[1] *SSPA "Scientific-Practical Materials Research Centre of NAS of Belarus", P. Brovka str., 19, 220072, Minsk, Belarus*
[2] *The FERRIT enterprice, P. Brovka str., 19B, NAS of Belarus, 220072, Minsk, Belarus*
* *corresponding author e-mail: Leonchik@physics.by*

The article presents the calculations of verification intervals for the commissioned continuous weighing tape feeder PLC-VD-2.5 / 10, manufactured by the "Ferrit" enterprice (Minsk, Belarus). Possible values of verification intervals are shown for various parameters of the operating characteristics of the tape feeder.

Superconducting characteristics of niobium welded connections

S.E.Demyanov
SSPA "Scientific-Practical Materials Research Centre of NASB", Minsk, Belarus
e-mail: demyanov@physics.by

A comparison of the measurement results of of the electrical resistance of welded joints samples of superconducting niobium at the DESY scientific center, Germany and at the SRC of the NASB for materials was carried out. Critical analysis showed that DEZY measurements have drawbacks, which do not allow a complete assessment the superconducting properties of niobium. Our studies of the temperature and magnetic superconducting transitions, the widths of these transitions in welded samples indicate a slight deterioration in the superconducting properties of niobium during heat treatment. The reason for this is due to increase of impurity elements concentration in the welding zone.

Volumetric and acoustic properties for binary mixtures of cyclohexane and n-propylbenzene/izo-propylbenzene, at temperature of 298.15 K and normal pressure

F. Sirbu[1]*, D. Dragoescu[1] , A.P. Shchamialiou[2], V.S. Samuilov[2], N.V. Holubeva[2], A.G. Paddubski[2]
[1]*„Ilie Murgulescu" Institute of Physical Chemistry, Spl. Independentei 202, P.O.Box. 12-194 060021, Bucharest, Romania; e-mail adress: sflorinela@yahoo.com*
[2]*Belarusian State University of Food and Chemical Technologies, Schmidt Avenue 3, 212027, Mogilev, Belarus*

The thermophysical properties as densities and speeds of sound, for the two binary mixtures of cyclohexane with *n*-propylbenzene and *izo*-propylbenzene, were measured over the entire range of composition x_1 of aromatic hydrocarbons, at temperature of 298.15 K and atmospheric pressure P = 0.1 MPa.

The experimental values for densities and speeds of sound, for both systems were correlated by the Jouyban-Acree model with good accuracy.

From the experimental results, the excess molar volumes, the partial/apparent molar volumes, the isentropic compressibilities and the excess isentropic compressibilities, were calculated.

The experimental excess molar volumes values have been also used to test the applicability of the Prigogine-Flory-Patterson theory and the results were analyzed in terms of molecular interactions and structural effects, occurred between the components of the mixture.

A graphically comparison of the excess molar volumes, for both studied mixtures at T = 298.15 K, between our data and available literature data - Fujii et.al. (1995) [1] was made. This comparison gives acceptable results.

All the excess properties calculated for the mixtures, have been correlated with composition by the Redlich-Kister polinomial equation. The correlation parameters were estimated for both studied mixtures. The calculated excess quantities have been represented graphically at T = 298.15 K.

The experimental and calculated results concerning the relation to the molecular interactions and structural effects between components of mixtures are presented.

Acknowledgements

This research has been carried out in the framework of the joint project AR-FRBCF 2020-2021, with the financial support of the Romanian Academy and the Belarusian Republican Foundation for Fundamental Research.

The Romanian authors want to express their acknowledgement to the Romanian Academy, for the financing the research programme "Chemical thermodynamics and kinetics. Quantum chemistry" of the "Ilie Murgulescu" Institute of Physical Chemistry. The financial support of the EU (ERDF) and Romanian Government, which allowed for the acquisition of the research infrastructure under POS-CCE O 2.2.1 Project INFRANANOCHEM - Nr. 19/01.03.2009, is also acknowledged.

References

[1] S. Fujii [et al.] J. Chem. Thermodyn. 27 (1995) 1319-1328.

Pharmacological evaluation of N-(p-iodophenyl)-N'-(2-tenoil)-thiourea structure using computational means

A. Stefaniu[1*], C. Stoicescu[2], L. Pintilie[1], I. Gheorghe[2], and F. Sirbu[2]
[1]*National Institute for Chemical - Pharmaceutical Research and Development - Bucharest, 112 Vitan Av., 031299, Bucharest, Romania, e-mail: astefaniu@gmail.com*
[2]*Institute of Physical Chemistry Ilie Murgulescu of the Romanian Academy, e-mail: sflorinela@yahoo.com*

The paper presents the results of a computational analysis of molecular and QSAR properties using Spartan'14 software Wavefunction, Inc. Irvine CA U.S.A. [1], carried out on the lowest energy configuration of N-(p-iodophenyl)-N'-(2-tenoil)-thiourea. The investigated structure was previously suggested by literature data as potential antibacterial or antifungal agent [2]. Generally, the thiophene heterocycle is used as scaffold to design biologically active molecules with potential against various targets, including antitumor [3]. Based on structural data, the reactivity parameters at global-molecular level, were evaluated in terms of electron affinity, ionization potential and electronegativity, starting from the calculated energy levels of frontier molecular orbitals, obtained using DFT/B3LYP [4] level of theory. Local reactivity descriptors as Mulliken charges are also reported. Supplementary data regarding drug-likeness properties and bioactivity scores toward G protein-coupled receptor ligand, ion channel modulators, kinase inhibitors, nuclear receptor ligands, protease inhibitors and other enzym targets, were collected from computations using Molinspiration virtual screening platform. Oral bioavailability results togheter with electron density derived properties constitue the premises for further molecular docking simulations against several enzyme targets to identify the inhibition potentcy of such thiophene derivative, constitutant of a larger compound library.

References

[1] Y. Shao, L. F. Molnar, Y. Jung et al. Phys. Chem. Chem. Phys. 8:27 (2006) 3172-3191.
[2] C. Bădiceanu, A. Missir, C. Chifiriuc, O. Drăcea, I. Răut, C. Larion, L. Ditu, G. Mihăescu, Rom. Biotechnol. Lett. 15 (2010) 5545-5551.
[3] Y. L. Volodina, A. S. Tikhomirov, L. G. Dezhenkova et al. Eur. J. Med. Chem. 221 (2021) 113521.
[4] C. Lee, W. Yang, , R.G. Parr Phys. Rev. B 37 (1988) 785–789.

Analysis of Surface Graphitization and Transfer Layers in Friction of Cu-Doped Hydrogen-Free Diamond-Like Carbon Coatings

I. Razanau[1*], V. Kazachenko[2], and A. Dvorak[2]
[1]*Scientific-Practical Materials Research Centre of NAS of Belarus, 19 Brovki Str., 220072 Minsk, Belarus, razanau@physics.by**
[2]*Science and Technology Park of BNTU "Polytechnic," 37/1 Surganova Str., 220013 Minsk, Belarus*

Diamond-like carbon (DLC) possesses good biocompatibility, high mechanical and antifriction properties. DLC-based coatings are perspective for medical implant surface modification. Copper doping improves the antibacterial properties of the DLC coatings. On the other hand, copper also acts as a graphitization agent for DLC. This work aimed at studying the influence of low-content copper dopping of DLC on its tribological properties.

Thin composite DLC-Cu and non dopped DLC coatings were deposited using a physical vapor deposition (PVD) method: high-current pulsed cathodic vacuum arc discharge with a cathode made of graphite with or without copper insets. Tribological tests of the coatings were performed in dry conditions using a sphere-on-plane scheme of reciprocating friction with the counterbody of silicon nitride. Structural changes in the coatings on the friction tracks and the structure of the transfer layers on the counterbodies were studied using scanning electron microscopy and Raman spectrometry.

It is shown that 1% copper doping significantly changes DLC coating tribological properties. Initial stages of Cu-doped DLC coatings friction are characterized by intensive surface self-organization leading to substantial friction track graphitization, detectable by both Raman spectrometry and SEM. The transfer products on the counterbody have a nanographite structure. In contrast, no graphitization was detected for the non dopped DLC under the same conditions, and the transfer products on the counterbody have an amorphous carbon structure. As a result, copper doping leads to the change in the wear mechanism of the coating: no signs of fatigue wear are detected for the dopped DLC, whereas partial coating delamination is characteristic of the non dopped DLC. The results show that the low-content Cu-dopped DLC coatings are perspective not only as the antibacterial but also as the running-in tribotechnical layers.

Acknowledgment
The BRFFR grant T19KITG-014 financially supported the work.

Amplitude electro-optical modulator based on sequences of Fabry-Perot resonators

V. B. Zalessky, A. I. Konoiko, V. M. Kravchenko, A. S. Kuzmitskaya*
State Scientific and Production Association of Optics, Optoelectronics and Laser Technology; 68-1 Nezavisimosti avenue, Minsk, Belarus 220072; mickevichhanna@gmail.com

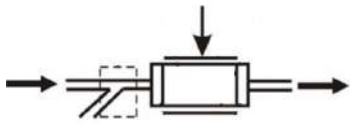

Fabry-Perot Electro-Optic Resonator

The speed of the existing electro-optical amplitude light modulators is determined by the frequency properties of the control signal supply channel, which are limited by the capacitive characteristics of the modulator electrical circuit and the mismatch between the electric (microwave) and light waves. The use of phase electro-optic modulation in multi-beam interference devices for amplitude modulation of light can significantly reduce the value of the control electric voltage due to multiple interactions of light with an electro-optical medium and, therefore, increase the operating frequency range of such modulators [1]. However, the existing methods do not fully take into account the effect on the efficiency of amplitude modulation of the features of devices based on multipath interference, which limits their operating frequency range [2, 3].

In this paper, we consider the features of electro-optical amplitude modulation of light radiation in a Fabry-Perot interferometer for a wide frequency spectral range of control electrical harmonic signals.

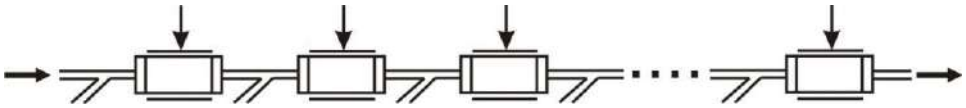

Electro-optic amplitude modulator with N Fabry-Perot resonators

According to calculations, in the absence of a control voltage, the time of generating the leading edge of the light signal of a modulator with nine resonators in 1.76 times as much as one resonator. When a control electric voltage is applied to the resonators, at the time when the amplitude of the optical signal at the output reaches the level of 90% of the incident radiation, a sharp drop in the light intensity occurs at the output of the modulators. Moreover, the decay time of the optical signal to a level of 2% in the case of a modulator with nine resonators is an order of magnitude shorter than that of a single one resonator. As a result, the duration of the optical signal at the output of the modulator with nine resonators is t1 = 1.314 t9, where t1 is the duration of the signal at the output of the modulator with one resonator. This means that it is possible, firstly, to raise the frequency of light signals by 30%, and secondly, to significantly reduce the value of the control voltage and, consequently, the electric power supplied to the resonators.

As a result, the development and study of systems of electro-optical modulators for high-speed optical communication lines based on controlled Fabry-Perot resonators was carried out, which allow both to significantly reduce the value of control voltages and to increase the frequency of modulated optical signals while increasing the stability of their amplitude-phase characteristics.

References

[1] A. Author, B. Author, and C. Author, Journal Title Abbreviation Volume (Year) Pages.
[1] V.A.Pilipovich and others, Reports of the National Academy of Sciences of Belarus, T. 59 No. 4 (2015) P. 41-46
[2] E. P. Mustel, V. N. Parygin, Light modulation and scanning techniques, 1970, 296 p.
[3] A. Yariv, Optical waves in crystals, 1987, 616 p.

Nonlinear dynamics of powerful femtosecond laser pulses in condensed matters

D. Klezovich[1*], O. Fedotova[2], O. Khasanov[2], G. Rusetsky[2] and T. Smirnova[3]
[1]*Belarusian State University, Nezavisimosti av. 4, 220030, Minsk, Belarus,*
e-mail: diestardom@gmail.com
[2]*Scientific-Practical Materials Research Centre of the NAS Belarus,*
19 P. Brovky, Minsk, 220072, Belarus
[3]*International Sakharov Environmental Institute BSU,*
Dolgobrodskaya. 23/1, 220070, Minsk, Belarus

In present work we study conditions of spatio-temporal localization of terawatt femtosecond vortex (doughnut) and vortex-less (Gaussian) laser pulsed beams in Kerr media in the light bullet (LB) form. As is known, in Kerr media the filamentation makes possible the spatial and temporal compression of pulses. The filament is a self-organized structure formed through the competition of underlying processes such as, for example, diffraction, Kerr nonlinearity, plasma photoinduced via multiphoton absorption or tunnel mechanisms, etc. Under anomalous group velocity dispersion (GVD) one of filamentation regimes may be realized, i.e. LB generation. As shown in experiment [1], the stability of the LB is due to their polychromatic Bessel-like structure consisting of a sharply localized high-intensity core and a weak, delocalized low-intensity periphery, which balances energy losses in the central core.

The system of nonlinear Schrödinger equation for the complex envelope of the electric field and kinetic equation for the electron plasma density is exploited. The Hamiltonian deduced on the base of this equation in approximation of negligible dissipation allowed us to obtain a potential function (Figure). In the frame of two-scale variation approach the system of motion equations for both temporal T(z) and spatial R(z) beam radii was found.

The solution of this system allowed to define the stability regions for LB. Solutions of the above equation system have been analyzed in broad spectral range of the anomalous GVD for fused silica and other Kerr solids at different values for topological charge *m* (0,1,2,3,4) and various ratios of input pulse power to critical one for self-focusing $\alpha>10$. Under suggestion that the multi-photon ionization mechanism is dominated, we deduced the expressions for stationary values T_0 and R_0 corresponding to the minimum of the potential function V(R,T) and estimated their values in dependence on medium and radiation parameters. The stability is originated from the complete balance of all underlying processes accompanying the pulsed beam spreading.

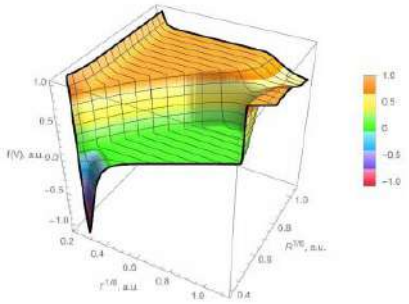

Figure. Potential energy surface as a function of temporal and spatial (transverse) beam radii.

For vortex beams the following threshold dependence of their possible input power on m is revealed: $\alpha > 2m/0.093$. Only pulsed beams obeying this condition may propagate in vortex LB regime. The Gaussian-type LBs are free of such conditions.

.

References

[1] D. Majus et al. Phys. Rev. Lett. Volume 112 (2014), pages 193901-1-5.

Li_2TiO_3-$BaMoO_4$ ceramic composite as device for microwave applications

F. A. C. Nobrega[1]*, R. F. Abreu[1], V. C. Martins[1], M. A. S. Silva[1], J. P. C. Nascimento[2], A. J. M. Sales[1,4], J. C. Sales[3] and A. S. B. Sombra[1,4]
[1]*Federal University of Ceara, Pici Campus, Fortaleza CE, Brazil,*
[2]*Ceara Federal Institute of Education, Science and Technology, Fortaleza Campus, Fortaleza CE, Brazil*
[3]*State University of the Valley of Acarau, Cidao Campus, Sobral CE, Brazil*
[4]*Telecommunication and materials science and engineering, Fortaleza CE, Brazil*
*aleksonnobrega@gmail.com**

Some ceramic composites synthesized by the solid-state reaction, from ceramic oxides, are used as filters and antennas in the microwave region. Ceramic composite antennas can operate at different frequencies and be applied as radar, satellite, and military use devices.The ceramic oxides exhibit dielectric properties (permittivity (ε) and dielectric loss (tan δ)), which allows its use as an antenna. Li_2TiO_3 (LTO) can form a ceramic composite by adding another oxide, as it exhibits ε = 17.65, tan δ = 5.40x10^{-3} and temperature coefficient at resonant frequency (τ_t) = + 19.92 ppm .°C^{-1}. An oxide that has a negative τ_t value is $BaMoO_4$ (BMO, ε = 9.84, tan δ = 5.00x10^{-3}), having τ_t = - 79.24 ppm.°C^{-1}, thus, the ceramic composite LTO - BMO it can form a ceramic composite with thermal stability. Thus, the objective of this work is to synthesize a ceramic composite based on LTO and BMO with good thermal stability. For this, ceramic oxides LTO and BMO were synthesized via solid-state reaction and characterized by X-ray diffraction. Then, the ceramic composite was synthesized with 60 wt % LTO and 40 wt % wt BMO in the mass and sintered at 900 °C. After synthesis, the sample was analyzed by the Hakki-Coleman technique and the SILVA-FERNADES-SOMBRA methods to evaluate its dielectric properties and its τ_f, respectively. After the analysis, it was observed that the sample operates at a frequency of 6.86 GHz, presents permittivity, and dielectric loss equal to 13.17 and 1.85x10^{-3}, respectively. The measured value of τ_f is + 1.35 ppm.°C^{-1}. With these results, the ceramic composite based on LTO-BMO and can be used an antenna.

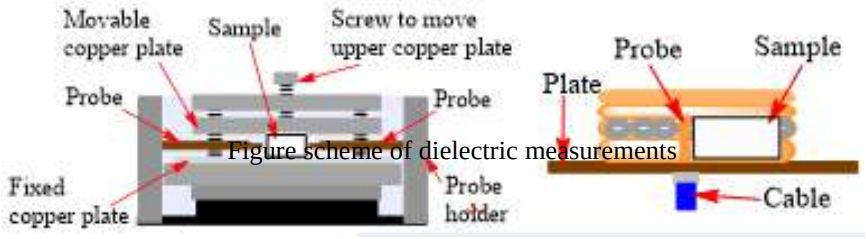

Figure scheme of dielectric measurements

Dielectric measure scheme and temperature coefficient at resonant frequency

Acknowledgement
This work was partly sponsored by the Brazilian Research Agencies FUNCAP-Cearense Foundation for Scientific and Technological Development Support, CNPq-National Council for Scientific and Technological, CAPES- Coordination for the Improvement of Higher Education Personnel.

References

[1] R. F. Abreu, T. O. Abreu, D. da M. Colares, S. O. Saturno, J. P. C. do Nascimento, F. A. C. Nobrega, A. Gosh, S. J. T. Vasconcelos, J. C. Sales, H. D. de Andrade, I. S. Queiroz, and A. S. B. Sombra, J. mater Sci: Mater Elec 32 (2021) 7034-7048;
[2] V. C. Martins, R. G. M. Oliveira, F. F. Carmo. M. A. S. Silva, S. A. Pereira. J. C. Goes. M. M. Costa. D. X. Gouveia, and A. S. B. Sombra, J. Phys and Chem Solids 125 (2019) 51-56;
[3] E. C. Xiao, J. Li, J. Wang, C. Xing, M. Guo, H. Qiao, Q. Wang, Z. M. Qi, G. Dou, F. Shi, J. Materiomics 4 (2018) 383-389;
[4] M. A. S. Silva, T. S. M. Fernandes, and A. S. B. Sombra et all, J. Appl. Phys. 112 (2012) 74-106;
[5] W. E. Courtney, IEEE Trans. Microw. Theory Tech 18 (1970) 476-485.

High-speed fiber communication photoreceiver module based on a partially-depleted InAlAs/InGaAs/InP photodiode

K.S. Zhuravlev[1,*], A.M. Gilinsky[1], I.B. Chistokhin[1], V.S. Arykov[2], I.V. Yunusov[2], N.A. Valisheva[1], and D.V. Dmitriev[1]
[1] *A.V. Rzhanov Institute of Semiconductor Physics, 630090 Novosibirsk, Russia. E-mail: zhur@isp.nsc.ru*
[2] *Infrared and Microwave Technologies LLC, 634041 Tomsk, Russia*

The transmission of analog high-frequency signals over optical links requires the application of wide bandwidth photoreceivers with a 5–10 A/W (or 250–500 V/W at a 50-Ohm load) or higher sensitivity and a low supply voltage. The design of a high speed photoreceiver module for optical link data and UHF signal transmission lines comprising a high speed pin-photodiode and a transimpedance amplifier for 2.5–10 GHz frequency ranges is considered in this work. The photodiode utilizes a partially-depleted absorber structure and is made of an InAlAs/InGaAs/InP heterostructure. The use of the partially-depleted absorber layer design allows one to improve the device bandwidth due to the minimization of the space charge effect. The heterostructures were grown by molecular beam epitaxy on semi-insulating InP substrates and consisted of the following layer sequence:

- A 300 nm thick n^+-InAlAs layer doped to a concentration of $5\cdot10^{18}$ cm^{-3},
- A 50 nm doped absorbing layer of n^+-InGaAs with a doping concentration of $5\cdot10^{18}$ cm^{-3},
- An undoped *i*-InGaAs absorbing layer of 220–800 nm thickness with a residual doping concentration of less that 10^{15} cm^{-3},
- A doped *p*-InGaAs absorbing layer of 100–220 nm thickness with a doping concentration of $1\cdot10^{18}$ cm^{-3},
- A doped wider bandgap p^+-InAlAs layer with a thickness of 300 nm and a doping concentration of $5\cdot10^{18}$ cm^{-3},
- A 30 nm thick contact p^+-InGaAs layer with a doping concentration of $2\cdot10^{19}$ cm^{-3}.

The heterostructures were processed to form round shape mesa structures with diameters of 20–40 μm, depending on the frequency range. An antireflection coating was deposited onto the thinned substrate before separation of the wafer into individual photodiode chips. Thick (up to 5 μm) golden layers formed by electroplating were employed to reduce the electric resistance of the contact leads. The input radiation is directed through the back (substrate) side of the chip. The sensitivity of the back-illuminated photodiodes spans the 1.0–1.7 μm wavelength range.

The photodiode output signal is amplified by a low-noise transimpedance amplifier chip produced by Elvees R&D Center. The amplifier chip is mounted close to the photodiode chip in a TO-8 size can. The input radiation can be fed via a fiber link or open space, depending on the mount version. The amplifier provides both symmetric as well asymmetric output transfer line options.

Shielding behaviors and mechanism of some boron containing resoureces for nuclear radiation protection

Mengge Dong[1,2]*, Suying Zhou[1], Xiangxin Xue[1,2], and Xiating Feng[3]
[1]*Department of Resource and Environment, School of Metallurgy, Northeastern University, Shenyang 110819, PR China, e-mail for the corresponding author*: mg_dong@163.com*
[2]*Key Laboratory of Metallurgical Resources Recycling Science, Liaoning Province, Shenyang 110819, PR China*
[3]*Key Laboratory of Ministry of Education on Safe Mining of Deep Metal Mines, Northeastern University, Shenyang 110819, China*

Boron containing resources of Liaoning Province, including Szaibelyite (B1), Ludwigite (B2), boron bearing iron concentrate (B3), boron concentrate (B4), boron rich slag (B5), boron mud (B6) are the research objects in the paper. The shielding behaviors and mechanism for neutron and gamma were investigated. It is found that the interactions of B1-B6 with gamma rays are different with each other because of the difference components, but the mainly interactions of B1-B6 are photoelectric absorption in the low energy region, incoherent scattering in the intermediate energy region and pair production in nuclear filed in the high energy region. The gamma ray shielding performance is B3, B2, B5, B4, B1, B6 in descending order, and better than ordinary concrete. Besides, the elements with high content and high atomic number in the boron containing resources have a large contribution to the shielding performance for gamma ray. Shielding property of B1-B6 for thermal neutrons is mainly based on the absorption cross section of B-10 isotope, and shielding performance is B1, B5, B3, B4, B2, B6 in descending order, which is positively correlated with boron content. Besides, the shielding ability of B1-B6 is better than ordinary concrete. Contribution of elements with high content or high cross section is relative high for fast neutron shielding. Shielding performance is B3, B5, B2, B4, B1, B6 in descending order, which is positively correlated with density. Morevoer, B1-B5 is better than ordinary concrete. Boron containing resource composite materials (BE1-BE6) were prepared by epoxy resin and B1-B6. It is found that the macroscopic cross section of BE1-BE6 are between 0.47-4 cm^{-1}, the shielding performance is relative high and is BE1, BE5, BE4, BE2, BE3, BE6 in descending order. Gamma ray shielding ability is BE3, BE4, BE5, BE1, BE2, BE6 in descending order, but are both general. All in all, the boron rich slag would be the best one for shielding both neutrons and gamma rays.

The dielectric properties of system $Ho_XMn_{1-X}Se$

M.N. Sitnikov*, A.M. Kharkov, O.B. Begisheva, N.A. Cheremnykh, E.O. Kriger, I.I. Dmitras
Reshetnev Siberian State University of Science and Technology31, Krasnoyarskii rabochiiprospekt, Krasnoyarsk, 660037, Russian Federation, kineru@mail.ru *

The study of systems with high degeneracy, for example, spin [1], dipole [2] glasses is of interest both from a fundamental point of view and from a practical point of view. The characteristics of spin and dipole glasses can be controlled by weak external magnetic and electric fields, which can be used as sensors for RAM in microelectronics. Electronic doping of manganese sulfide induces the degeneracy of t2g electronic states, which can be removed by the spin-orbit or Yang-Teller interaction.

In solid solutions of $Ho_XMn_{1-X}Se$, a charge ordering can occur, which can be controlled by both a magnetic and an electric field.

The $Ho_XMn_{1-X}Se$ samples were synthesized by the solid-state reaction. X-ray powder diffraction patterns of the compounds were carried out at room temperature on a DRON-3. The samples are single phase and have a NaCl-type cubic lattice [3].

The dielectric properties of $Ho_xMp_{1-x}S$ solid solutions were studied in the temperature range of 80K<T<380K without a field and in a magnetic field of H = 12 kE. With increasing temperature, the permittivity increases and has an inflection point in the range of 240 K-290 K. In a solid solution of $Ho_xMn_{1-x}S$, the temperatures of the maxima of dRe (ε) / dT coincide with the maxima of the imaginary part of the permittivity and shift to the high temperature region with increasing frequency and are described in the Debye model.

The value of the permittivity decreases with increasing frequency and increases in a magnetic field, which is typical for disordered systems, for example, in dipole glasses. The permittivity in the frequency range up to one megahertz during electron doping in $Ho_xMn_{1-x}S$ is due to the migration polarization of localized electrons and relaxation conductivity. In the Debye model, the relaxation time of electric polarization is found, which has an activation character and is described by the Arrhenius law. In the vicinity of the percolation concentration of holmium ions through the lattice, the contribution of migration polarization disappears and the dielectric characteristics are due to relaxation conductivity in the high frequency region.

Acknowledgement

The research was funded by RFBR, Krasnoyarsk Territory and Krasnoyarsk Regional Fund of Science, project number 20-42-243002

References

[1] S.S. Aplesnin. Pphysica status solidi (b), 149 (1), pp. 267-273, (1988)
[2] S.S. Aplesnin, L.V. Udod, M.N. Sitnikov, M.S. Molokeev, L.S. Tarasova, K.I. Yanushkevich. Physics of the Solid State, 59 (11), pp. 2268-2273. (2017)
[3] S.S. Aplesnin, A.M. Khar'Kov, M.N. Sitnikov, V.V. Sokolov. Journal of Magnetism and Magnetic Materials, 347, pp. 10-13. (2013)

Advanced Primary Aqueous Mg Batteries from Anode and Electrolyte Perspectives

M.L. Zheludkevich[1,2]*, Min Deng[1], Linqian Wang[1], Daniel Höche[1], Sviatlana V. Lamaka[1], Darya Snihirova[1]
[1] *Institute of Surface Science, Helmholtz-Zentrum Hereon, Max-Planck Strasse 1, 21502 Geesthacht, Germany, mikhail.zheludkevich@hereon.de**
[2] *Institute of Materials Science, Faculty of Engineering, Kiel University, 24143 Kiel, Germany*

Aqueous primary Mg-based batteries are a promising alternative to conventional energy storage devices, thanks to negative electrode potential and high volumetric capacity of metallic Mg. However, several critical factors decrease the efficiency of Mg batteries and limit their wider application — namely the self-corrosion of anodes and electrode blockage by the discharge products.

In this work, the discharge properties of Mg-based batteries were boosted through optimization of Mg-based anodes via Ca addition and designing the new electrolyte additives. It has been shown that the optimized Mg-Ca anode confers higher cell voltage and higher specific energy density than a high purity Mg and several commercial Mg alloys. The enhancement of Mg-based batteries' performance can also be achieved by adding organic additives into electrolyte, which can prevent the formation of insoluble precipitate on the electrode and accelerate the dissolution of magnesium anode. Therefore, it can increase the cell voltage and specific energy of Mg-Ca system battery.

Optical and viscometric properties for binary (cyclohexane + aromatic hydrocarbons) mixtures, at temperature of 298.15 K and atmospheric pressure

D. Dragoescu[1]*, F. Sirbu[1], A.P. Shchamialiou[2], V.S. Samuilov[2], N.V. Holubeva[2], A.G. Paddubski[2]

[1]*„Ilie Murgulescu" Institute of Physical Chemistry, Spl. Independentei 202, P.O.Box. 12-194 060021, Bucharest, Romania; e-mail adress: ddragoescu@icf.ro*

[2]*Belarusian State University of Food and Chemical Technologies, Schmidt Avenue 3, 212027, Mogilev, Belarus*

The optical and viscometric data for two binary mixtures of cyclohexane with aromatic hydrocarbons, were measured versus molar fraction x_1 of *n*-propylbenzene/*izo*-propylbenzene at temperature of 298.15 K and atmospheric pressure.

The experimental values for refractive indices, n_D, and viscosities, η, for both systems were correlated by the Jouyban-Acree model with good accuracy.

The deviation in refractive indices, the excess molar refractions, and the deviation in viscosities, based on the obtained experimental results, were calculated in this work.

In order to predict the refractive index on mixing, the theoretical Lorentz-Lorenz (n,ρ) mixing rule was used.

From the viscosity experimental values, the molar enthalpy of activation and the molar entropy of activation for viscous flow, as well as the excess Gibbs energy of activation for viscous flow, were calculated for both studied binary mixtures.

The Redlich−Kister polynomial equation was applied in order to correlate all the excess properties of the binary mixtures with composition. The correlation parameters were estimated for both mixtures. The calculated excess and deviation quantities have been represented graphically at T = 298.15 K.

The experimental and calculated results concerning the relation to the molecular interactions and structural effects between components of mixtures are presented.

Acknowledgements

This research has been carried out in the framework of the joint project AR-FRBCF 2020-2021, with the financial support of the Romanian Academy and the Belarusian Republican Foundation for Fundamental Research.

The Romanian authors want to express their acknowledgement to the Romanian Academy, for the financing the research programme "Chemical thermodynamics and kinetics. Quantum chemistry" of the "Ilie Murgulescu" Institute of Physical Chemistry. The financial support of the EU (ERDF) and Romanian Government, which allowed for the acquisition of the research infrastructure under POS-CCE O 2.2.1 Project INFRANANOCHEM - Nr. 19/01.03.2009, is also acknowledged.

Structural Dynamics of SARS-CoV-2 Spike Protein-Angiotensin-Converting Enzyme 2 Complex as Key Panoply for Medical Countermeasures

Harsh Sharma[1], Raghukul Chaudhary[1], Deepa Suhag[2*], Ravi Datta Sharma[2]* and Amresh Prakash[1]*
[1]*Amity Institute of Integrative Sciences and Health, Amity University Haryana, Manesar (Gurugram), Haryana 122413, India*
[2]*Amity Centre for Nanotechnology, Amity University Haryana, Manesar (Gurugram), Haryana 122413, India*
** corresponding author e-mails: deepasuhag@gmail.com; rdsharma@ggn.amity.edu; and amreshprakash@jnu.ac.in*

We report the model structure of SARS-CoV-2's S protein and the dynamics governing its molecular interaction with ACE2. Plausibly, N-terminal attachment of myristoyl lipid anchors to glycine residue confers flexibility to the backbone and directs reversible S protein-membrane and protein-protein interactions, thereby building highly stable S-ACE2 complex for aggravated host tropism. Thus, interfacial hydrophobic residues involved in cellular attachment may be explored as potential targets for therapeutic interventions of COVID-19.

WORKSHOP ADVANCED TECHNIQUES FOR MATERIALS SCIENCE

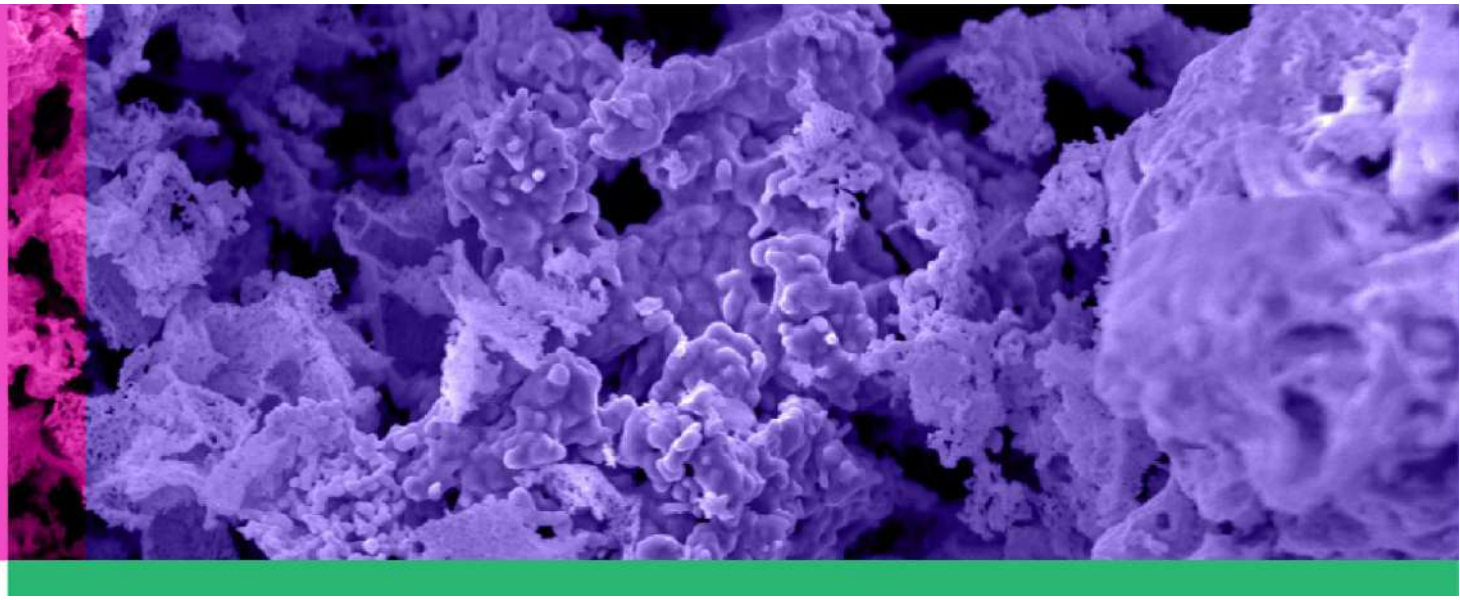

Charge-Sensitive Techniques in Solid State Research

A. Zharin*, K. Pantsialeyeu, V. Mikitsevich, A. Svistun
Belarusian National Technical University, Nezavisimosty Ave., 65, 220013, Minsk, Belarus
** corresponding author e-mail: anatoly.zharin@gmail.com*

New methods of surface analysis based on charge-sensitive techniques, namely Kelvin probe, non-vibrating probe, ionization probe, surface photovoltage probe, as well as their digital modifications, are described, as well as examples of their use.

Evaluation of Li_2TiO_3 – $BaMoO_4$ ceramic composite: Dielectric characterization and numerical investigation for microwave applications

Francisco Alekson Chaves Nobrega[1,5], Roterdan Fernandes Abreu[2,5], Vitor Carvalho Martins[1,5], João Paulo Costa do Nascimento[3,5], Marcelo Antonio Santos da Silva[5], Antonio Jefferson Mangueira Sales[5], Tallison Oliveira Abreu[1,5], Juscelino Chaves Sales[4], e Antônio Sérgio Bezerra Sombra[1,2,5]

[1]*Department of Organic and Inorganic Chemistry, Science Center, Federal University of Ceará (UFC), Brazil;*

[2]*Telecommunication Engineering Department, Federal University of Ceará (UFC), Fortaleza, Brazil;*

[3]*Federal Institute of Education, Science and Technology of Ceará, PPGET, Fortaleza, Ceará, Brazil;*

[4]*State University of the Valley of Acarau, Cidao Campus, Sobral CE, Brazil*

[5] *Telecommunication and Materials Science and Engineering of Laboratory (LOCEM)*

** corresponding author e-mail: aleksonnobrega@gmail.com*

This work presents the dielectric properties of a ceramic composite with 95 wt% of Li_2TiO_3 and 5 wt% $BaMoO_4$ (LTO95) for applications in the microwave region. Dielectric properties in the microwave region (MW) was obtained using the Hakki-Coleman method and thermal stability of the sample was experimentally obtained by the temperature coefficient of resonant frequency (t_f). Finally, a numerical simulation was performed to obtain far-field parameters. Resultts obtained demonstrate that the composite could be applied in devices operating in the microwave region.

Impedance study of the ceramic composite Li_2TiO_3-Al_2O_3

V.C.Martins[1,3], F.F.Carmo[3], M.A.S.Silva[3], J.C.Goes[3], A.S.B.Sombra[2,3*]
[1]*Organic and Inorganic Chemistry Department, Federal University of Ceará, UFC, 60455-760, Fortaleza, CE, Brazil*
[2]*Telecommunication Engineering Department, Federal University of Ceará (UFC), P.O. Box 6007, Fortaleza, Ceará, 60755-640, Brazil*
[3]*Physics Department – Telecommunication, Materials Science and Engineering of Laboratory (LOCEM), P.O. Box 6030, Fortaleza, Ceará, 60455-760, Brazil*

In recent years, technological development in the area of ceramic materials has attracted the attention of the scientific community due to applications in radiofrequency (RF) devices.

The present work shows the electric and dielectric study of ceramic composite made from lithium titanate (Li_2TiO_3) and aluminum oxide (Al_2O_3), by complex impedance spectroscopy. This work aims to characterize the ceramics of lithium titanate with addition of 5% by weight of aluminum oxide, examining which modifications occur in the dielectric properties of the material. The composite ceramic was produced by the solid-state reaction method using a planetary mill and post-grinding calcination. The structural and morphological characterization was performed using X-Ray Diffraction (XRD) techniques, and Scanning Electron Microscopy (SEM). The electric and dielectric study to possible applications in radio frequency was made by measurements analysis of impedance spectroscopy with temperature variation. The analysis of the diffractogram of the Li_2TiO_3 synthesis showed the formation of only a single phase. The Li_2TiO_3 study showed the electrical and dielectric properties of impedance (Z′), dielectric permittivity (ε′), and Temperature coefficient of capacitance (TCC), where they were studied in the frequency range from 1 Hz to 1 MHz and temperature (200–440 °C). The results indicate that electroceramics and composite ceramic presented a colossal dielectric permittivity ($\varepsilon' > 10^3$), stable thermical in the studied temperature range and the electrical results were modeled through equivalent circuit configurations composed of two associations in parallel with R-CPE, representing the electric responses of the grain, grain boundary presented by the studied electroceramics.

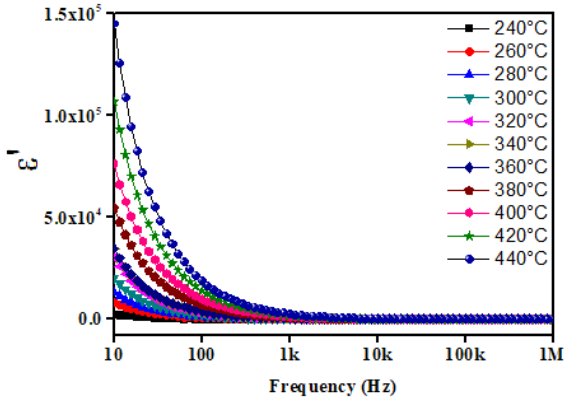

Figure 1. Dielectric permittivity (ε') x Frequency (Hz) with temperature variation (240 – 440 °C)

Study of the dielectric properties of the ceramic matrix La_2ZnTiO_6 – TiO_2 the microwave region.

F. E. A. Nogueira[1,3], T. O. Abreu[2,3], V. C. Martins[2,3], F. A. C. Nobrega, K. J. A. Gurgel[1,3] A. S. B. Sombra [3]
[1]*Telecommunication Engineering Department (UFC), P.O. Box 6007, Fortaleza, Ceará, 60755-640, Brazil,*
[2] *Department of Organic and Inorganic Chemistry, Federal University of Ceará (UFC), Campus do Pici, Science Center, 6040, Fortaleza, CE, Brazi,*
[3]*Laboratório de Telecomunicações e Ciências e Engenharia dos Materiais (LOCEM), Campus do Pici, Centro de Ciências, P.O. Box 6030, Fortaleza, CE, Brasil, fenilton@gmail.com*

Studies of new ceramic materials with electrical properties have grown in recent years, being of great interest for the development of projects in the field of engineering and materials science, advanced ceramics prove to be promising materials, especially for applications in devices operating in the range of microwave (MW). In this work, the structural and dielectric properties of the ceramic matrix La_2ZnTiO_6 belonging to the double perovskite family with addition of TiO_2 in a molar proportion of 6% were investigated. The solid state reaction method was used to prepare the powders, followed by calcination at a temperature of 1150°C. After calcination, the samples were pressed into cylinders and sintered at 1300°C, the ceramic pieces obtained were characterized as to their structure and morphology through X-ray diffraction, confirmed by Rieteveld refinement. With the analysis of the results, it was observed that the composite $(0.94)La_2ZnTiO_6$-$(0.06)TiO_2$ presents its dielectric properties different from the La_2ZnTiO_6 matrix, because its resonant frequency is 4.43 GHz, its temperature coefficient of the resonant frequency (τf) is –56.77 ppm/K, its electrical permittivity (εr) is 46.33, and its loss tangent (tg δ)) is $1.69.10^{-2}$. From these results it was observed that the composite formed by the addition of TiO_2 in the La_2ZnTiO_6 matrix can operate in the microwave region and can be a dielectric resonator antenna.

Solid state physics research on modern photon sources

V. M. Haramus
Helmholtz-Zentrum Hereon, Max-Planck-Straße 1, 21502 Geesthacht, Germany,
vasyl.haramus@hereon.de

A huge number of new materials has been developed in few last decades. X-ray research has played an important role in many of these developments. Experiments at the free-lectron lasers and the 3rd and 4th synchrotons which measure structural and dynamic properties of materials simultaneously, can help to improve known materials and develop new ones with revolutionary characteristics. Extremal high photon flux of new generation photon sources requires superconductive insertion devices which operate at helium temperature. Registration of photons after interaction with probe is frequently performed via cryogenic X-ray detectors with working temperature below 1 K. Different types of cryostats belong to standard equipment of almost every material science beamline which gives an opportunities in precise structure and dynamic studies varying other parameters such as pressure, magnetic and electrical field et. al. Status of current research with photons on solid state physics in Helmholtz-Zentrum Hereon will be presented.

Acknowledgement
The author tanks a financial support from project TransFerr. This project has received funding from the European Union's Horizon 2020 research and innovation programme under the Marie Skłodowska-Curie grant agreement No 778070.

UNALLOCATED

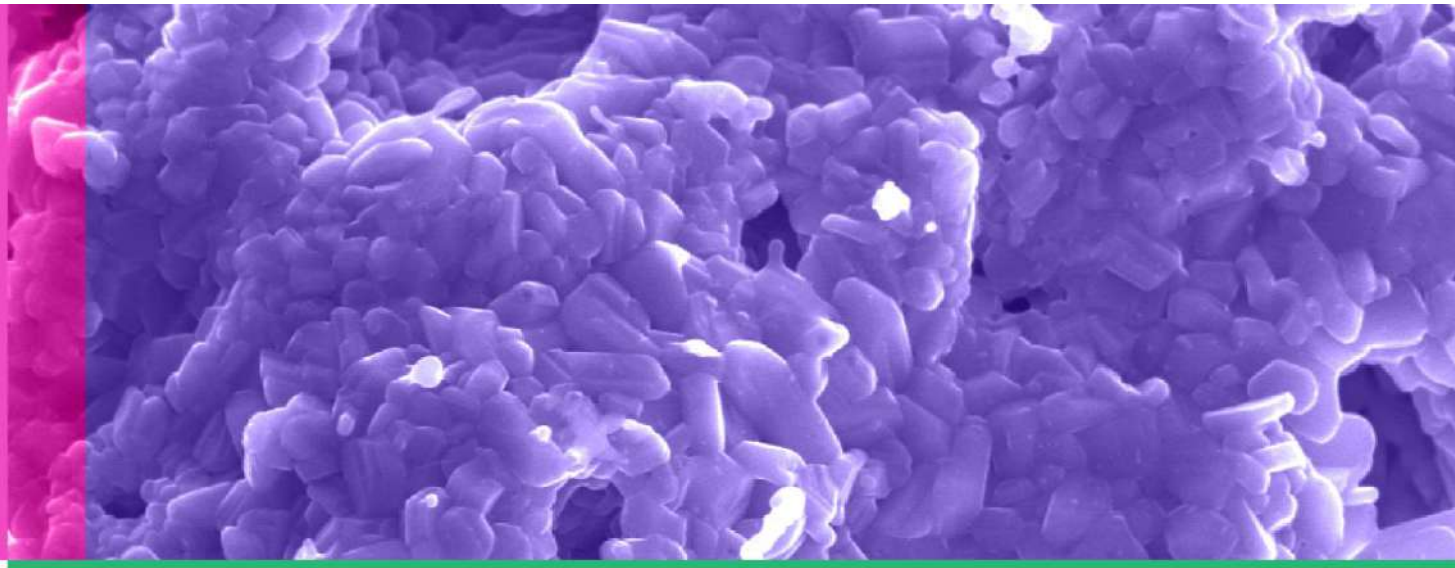

Work function monitoring to determine surface quality after diamond nanomachining

K. Pantsialeyeu, V. Mikitsevich, A. Svistun, A. Zharin
[1] *Belarusian National Technical University, Nezavisimosty Ave., 65, 220013, Minsk, Belarus, nil_pt@bntu.by**

The electon work function (EWF) is a sensitive parameter to characterize the metal surface (chemical impurities and inclusions, internal stresses and dislocations, atomic and monoxide heterogeneity and more) [1]. The Kelvin Probe is most convenient as a means of measuring the EWF, including in scanning mode (Scanning Kelvin Probe). The basis of the method is to use a vibrating capacitor to determine the contact potential difference between measured surface and a surface of reference electrode. The value of the EWF of measured surface is determined relatively to the EWF of reference electrode.

For these studies, the Digital Scanning Kelvin Probe was developed [1, 2]. The main parameters: the probe diameter is 1 mm; the linear dimensions of a sample are 200x200 mm, the measurement range of the contact potential difference is ± 5 V and the resolution is 250 μm.

An aluminum alloys processed by diamond nanomachining were studied. Such a processing provide to ensure the surface roughness of non-ferrous metals at the level of Ra ≤ 0.005 microns. The technological action of the cutter leads to oxidation processes on a surface and changes in the physicochemical parameters. Control of geometric parameters only turns out to be incorrect.

The research shows that the EWF is a highly sensitive parameter for characterizing the quality of the machining of the aluminum alloys surface. For example, the results of mapping of the EWF distribution are shown in the figure. The relative changes of the EWF (ΔΦ) at a surfaces with 10, 12, and 14 roughness classes was estimated 80 meV, 65 meV and 5 meV, respectively.

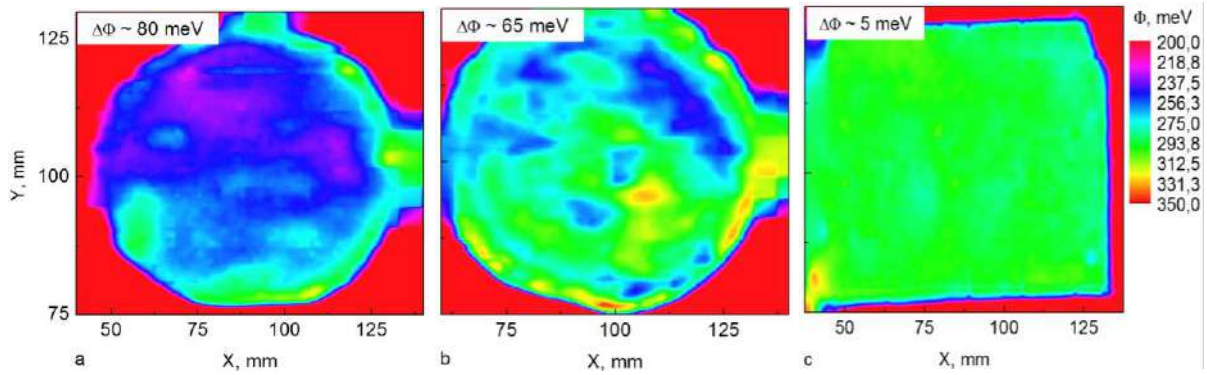

The work function distribution maps of aluminum alloy AMg2 (analog ENAW5251) with surface roughness class: a –10 class; b – 12 class; c – 14 class

The EWF monitoring in conjunction with geometric characteristics of a surface, especially roughness, can be used for definition and optimization of technological modes for optical surfaces and precision parts made of non-ferrous metals and alloys [3].

References

[1] Pantsialeyeu K., Zharin A., Gusev O., Vorobey R., Tyavlovsky A., Tyavlovsky K. and Svistun A. Digital contact potential probe in studying the deformation of dielectric materials. IAPGOS (2020). Volum 4. № 10. Pages 57–60.
[2] Pantsialeyeu K., Zharin A., Mikitsevich V. and Gusev, O. Semiconductor wafers testing based on electron work function of surface. Euroasian Journal of Semiconductors Science and Engineering (2020). Volume 2. Iss. 5. Article 2. Pages. 11–15.

[3] Pantsialeyeu K., Zharin A. and Kierczynski K. Charge sensitive techniques in control of the homogeneity of optical metallic surfaces. Przeglad Elektrotechniczny (2016). R. 92, №8. Pages 190 – 193.

Physicochemical study for host-guest type molecular recognition in cyclodextrin complexes of thiourea derivatives

A. Neacsu[1], I. L. Gheorghe[1], C. Stoicescu[1*]
[1*] *„Ilie Murgulescu" Institute of Physical Chemistry, Spl. Independentei 202, P.O.Box. 12-194 060021, Bucharest, Romania; e-mail adress: cristina.silvia.stoicescu@gmail.com*

In the present work it was demonstrated the formation of the nanotubular structure between 2-thiophenecarboxylic acid thiourea derivative drugs: N-(p-chlorophenyl)-N'-(2-thenoil)-thiourea (1), N-(p-iodophenyl)-N'-(2-thenoil)-thiourea (2), N-(p-bromophenyl)-N'-(2-thenoil)- thiourea (3), N-(p-methoxyphenyl)-N'-(2-thenoil)-thiourea (4), N-(p-methylphenyl)-N'-(2-thienyl)-thiourea (5), N-(p-methylphenyl)-N'-(2-thenoil)-thiourea (6), N-(p-methylphenyl)-N'- (3-thenoil)-thiourea (7) and 2-hydroxypropyl-β-cyclodextrin (HPβCD).

The complexes between HP-β-CD and thioureides with two different molar ratio (thioureide:HP-β-CD = 1:1 and 1:2) were obtained by both physical mixing and co-precipitation methods. Differential scanning calorimetry (DSC), thermogravimetry (TG), Fourier transform-infrared spectroscopy (FTIR), UV-Vis spectroscopy and scanning electron microscopy (SEM) methods were used to characterize the pure substances and the complexes. It was observed that two cyclodextrins can accommodate one long enough guest molecule (the case of the 2-thiophenecarboxylic acid thioureas drugs) [1, 2]. The obtained results has shown that there is the possibility of 1:2 drug/HPβCD complex formation.

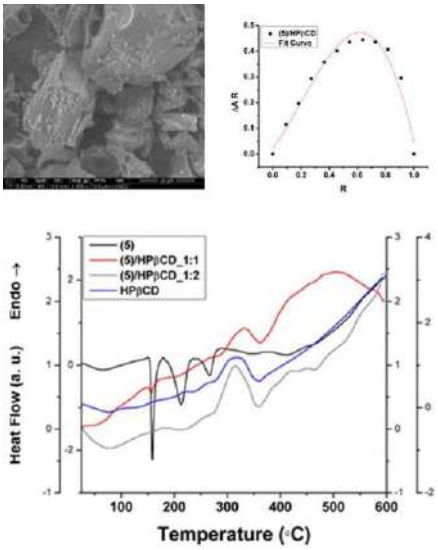

The SEM image (the left side up of the plot) and the Job's plot graph (the right side up of the plot) of the (5)/HPβCD complex. The DSC curves of the pure drug (5) and for different (5)/HPβCD molar ratios.

Acknowledgement

Authors are grateful to Romanian Academy as well as E.U. (ERDF) and Romanian Government support for acquisition of the research infrastructure under POS – CEE 2.2.1 Project INFRANANOCHEM/2007 - 2010, is also acknowledged. Authors also would like to thank Dr. Cornel Munteanu for help with SEM acquisition data.

References

[1]. S. S. Jaffer [et al.] J. Colloid Interface Sci. 337 (2009) 294–299
[2]. X. Wen [et al.] Bioorg. Chem. 32 (2004) 223–233

Properties of Barium titanat with additives of nicel ferrite

Laletin V.M., Poddubnaya N.N.
Institute of Technical Acoustics of the National Academy of Sciences of Belarus, 210009, Vitebsk, Belarus, e-mail: laletin57@rambler.ru

Currently barium titanate is one of the most used materials in modern electronic and technical devices. Since its dielectric characteristics substantially depend on the production technology, it is of interest to study the effect of modifying additives on its properties. We used nickel ferrite as an additive. The choice was due to the fact that the interaction of barium titanate and nickel ferrite is eutectic. The aim of this work is to study the effect of nickel ferrite additives and sintering temperature on the physical characteristics of barium titanate ceramics.

Barium titanate doped with nickel ferrite was obtained by sintering mixtures of single-phase components. The powder mixtures of 7 compositions were prepared with the following weight ratios of ferrite to piezoelectric: 0:100, 0.05:99.95, 0.1:99.9, 0.15:99.85, 0.2:99.8, 0.3:99.7, 0.5:99.5. Nickel ferrite $NiFe_2O_4$ was synthesized from nickel oxide (NiO) and iron oxide (Fe_2O_3) at a temperature of 1100°C. It was used as a magnetic phase. The ferroelectric was barium titanate $BaTiO_3$, synthesized from titanium oxide (TiO_2) and barium carbonate ($BaCO_3$) at a temperature of 1150°C. Dielectric characteristics were studied using an E7 - 8 device. The antiresonance - resonance method was used to find the piezomodule d_{31} and the electromechanical coupling coefficient for radial oscillations. The samples were sintered in air at temperatures of 1200, 1220, 1240, 1260, 1280 and 1300°C. The ceramic disks were subjected to plane-parallel grinding. The electrodes were made by burning silver paste at a temperature of 700°C for 0.5 hour.

Figure 1 shows the results of the effect of the composition of the ceramics on the density of the samples obtained at sintering temperatures of 1200°C and 1300°C. A characteristic feature of the curves is the presence of a jump in density, when, with an increase in the ferrite content, the density first increases and then sharply decreases. Moreover, if for the curve obtained at a sintering temperature of 1200°C, the density drops at a ferrite concentration above 0.05 wt.%, then for a curve obtained at a sintering temperature of 1300°C, a drop in density is observed at a ferrite concentration above 0.1 wt.%. Such an anomalous dependence of the density of ceramics on the additives of ferrite indicates the eutectic nature of the interaction between barium titanate and nickel ferrite. The increased reactivity of the mixture in the region of small additives of ferrite (0.05–0.1 wt.%) is apparently due to an increase in the diffusion rate due to the appearance of internal surfaces during the rupture of crystallites due to the stresses created by the new phase [1]. The formation of new crystallites leads to the dispersion of the sintering activator at the atomic level. In this case, the upper limit of the concentration of the activator is determined by the degree of solubility of the additive in the main component. With an increase in the sintering temperature of ceramics, the degree of solubility increases, as a result of which the density maximum shifts to the region of increasing ferrite concentration. Thus, in the process of eutectic doping, the total effect of solid-phase and eutectic liquid-phase activation takes place, leading to a sharp increase in the sintering capacity of the dispersed system [2]. When the concentration of the additive exceeds its solubility in the main component, a second phase is formed. This leads to a loosening of the structure and a sharp decrease in density. Note also that ceramic samples containing 0.3 wt.% or more of nickel ferrite exhibit ferromagnetic properties, which confirms the presence of a nickel ferrite phase.

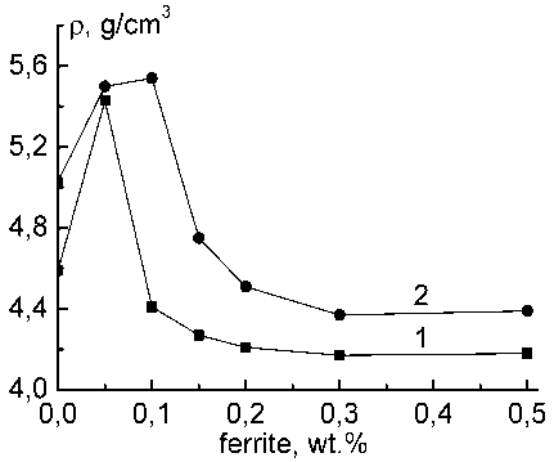

Figure 1 - Dependence of the density of barium titanate ceramics on the content of nickel ferrite. 1 - sintering temperature 1200°C. 2 - sintering temperature 1300°C

Let us consider the effect of the sintering temperature on the density of pure barium titanate and on the density of barium titanate doped with 0.05 wt.% and 0.1 wt.% nickel ferrite (Figure 2). The density of pure barium titanate increases with an increase of sintering temperature from 4.6 g/cm^3 (1200°C) to 5.0 g/cm^3 (1300°C). The density of barium titanate doped with 0.05 wt.% ferrite in the studied sintering temperature range remains constant and amounts to approximately 5.5 g/cm^3. In the case of barium titanate doped with 0.1 wt.% ferrite we observe a density jump in the sintering temperature range 1240°C - 1260°C caused by the transition of the structure from two-phase to single-phase and intensification of the sintering process. It should be noted that the introduction of 0.05 wt.% nickel ferrite into barium titanate can significantly lower the sintering temperature of pure barium titanate. The indicated density value of 5.5 g/cm^3 for barium titanate ceramics can be obtained only by sintering at a temperature of ~1360°C [3].

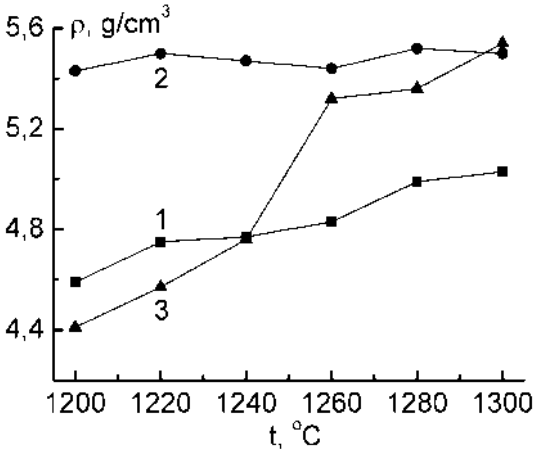

Figure 2 - Dependence of density on the sintering temperature of ceramics. 1 - pure barium titanate, 2 - barium titanate doped with 0.05 wt.% ferrite, 3 - barium titanate doped with 0.1 wt.% ferrite

Figure 3 shows the dependences of the dielectric constant on the sintering temperature of the ceramics of pure barium titanate and barium titanate doped with 0.05 wt.% ferrite and 0.1 wt.% ferrite. In the case of pure barium titanate, the dielectric constant with an increase of the sintering temperature increases from 914 (1200°C) to 1034 (1300°C). This is due to an increase in the density of the ceramic. For barium titanate doped with 0.05 wt.% ferrite an inverse relationship is observed. The dielectric constant decreases from 1480 (1200°C) to 1290 (1300°C) with an increase of the sintering temperature. This is caused by an increase in

grain size [4]. The dependence of the dielectric constant of barium titanate doped with 0.1 wt.% ferrite qualitatively reflects the dependence of the density on the sintering temperature.

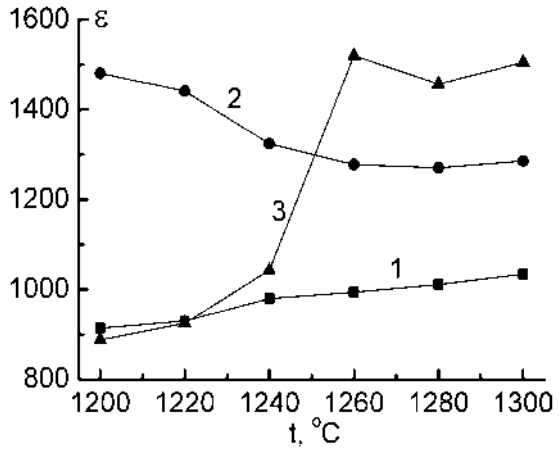

Figure 3 - Dependence of the dielectric constant on the sintering temperature of the ceramic.
1 - pure barium titanate, 2 - barium titanate doped with 0.05 wt.% ferrite, 3 - barium titanate doped with 0.1 wt.% ferrite

Figure 4 shows the dependences of the piezomodule d_{31} and the electromechanical coupling coefficient of barium titanate doped with 0.05 wt.% ferrite on the sintering temperature of the ceramic. With an increase in the sintering temperature of the ceramics, an increase in the parameters is observed. The magnitude of the piezomodule varies from 26 pC/N (1200°C) to 68 pC/N (1300°C), the electromechanical coupling coefficient - from 11 to 32. The electromechanical coupling coefficient qualitatively reflects the behavior of the piezomodule, that confirms its dependence on the polarization of the ceramics. This is caused by a decrease in the dielectric constant and an increase in the grain size of the ceramics [4].

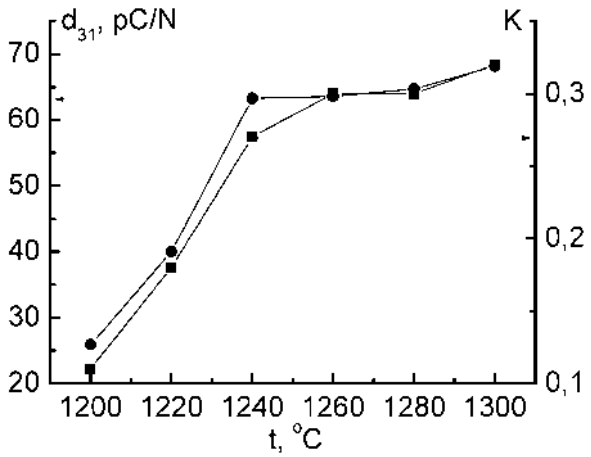

Figure 4 - Dependence of the piezomodule d_{31} and the electromechanical coupling coefficient on the sintering temperature of barium titanate doped with 0.05 wt.% ferrite

Thus, eutectic doping of barium titanate ceramics is observed in the case of small quantity of nickel ferrite (0.05-0.1 wt.%) that leads to an increase in density, dielectric constant, piezomodule d_{31}, electromechanical coupling coefficient and a decrease in the sintering temperature. When nickel ferrite is added over 0.1 wt.% to barium titanate the formation of a two-phase structure is observed accompanied by a sharp decrease in the density of the ceramic.

This work was supported by the Belarusian Republican Foundation for Fundamental Research (Grant No. F21VA-006).

References

[1] Kroeger F. Chemistry of imperfect crystals (1969).
[2] Spitsyn V.I. and other Reports of the USSR Academy of Sciences V. 273. No. 1. (1983), Pages 153-156.
[3] Okazaki K. Technology of ceramic dielectrics (1976).
[4] Smazhevskaya E.G., Feldman N.B. Piezoelectric ceramics (1971).

CONTENT

PHYSICAL AND CHEMICAL TECHNOLOGIES

FUNCTIONAL MATERIALS & APPLICATIONS

THEORY & MODELING IN MATERIAL SCIENCE

NANOMATERIALS & NANOTECHNOLOGIES

MULTI-DISTIPLINARY

WORKSHOP ADVANCED TECHNIQUES FOR MATERIALS SCIENCE

UNALLOCATED